The Erosion of Pipe Bends in Pneumatic Conveying Systems

by

Kap Ngam TONG

Thesis submitted for the degree of Doctor of Philosophy
under the conditions for the award of higher degrees
of the Council for National Academic Awards

School of Mechanical Engineering
Thames Polytechnic
London

August - 1981

Abstract

The main objective of this work is to determine the various fundamental parameters involved in the erosive wear process in 90^{o} pipe bends, by a stream of pneumatically conveyed suspensions of solid particles. From appropriate analysis of the test data, a basis of correlation in terms of the respective parameters has been established, from which the likelihood of erosion can be predicted.

In order to extend the potential range of variables involved in the mechanics of the erosion process, and to present results of practical value to industry, two full scale pneumatic conveying test rigs were ultilised. A low pressure test rig enabled detailed tests to be carried out in the dilute phase range, whilst a high pressure test rig allowed tests well into the medium phase range. The potential range of variables investigated in this work was planned within the limits of each test rig.

The main variables investigated were: the inter-relating effect of particle size on phase density, particle hardness, bend to pipe diameter ratio, effect of phase density above a value of 8, and the corresponding inter-relating effects of velocity and bend radius.

In all cases, the specific effect of each variable was analysed in terms of the two primary erosion descriptors, viz mass eroded and depth of penetration. The overall magnitude of these individual variables was separately evaluated on the basis of bend performance, i.e. in terms of conveying capacity and service life of the bends, from which the potential influence of each variable, based on actual test conditions, could be assessed and compared.

Whilst the premature failure of some of the bends tested was a recurring feature throughout this work, a more significant feature, which hitherto has not been reported elsewhere, is the phenomenon of rapid failure of replacement bends. A number of potential factors have been identified. In addition, the effect of particle degradation has been briefly considered, and a number of definitive trends with regard to all the variables investigated in this work, have been established.

Acknowledgements

The author would particularly like to thank his two Programme Supervisors, Dr. D. Mills and Dr. J. S. Mason, for their guidance and encouragement throughout the programme of work.

Sincere gratitude is also extended to Mr. R. B. Stacey, Technical Director of Mucon Engineering Co., Ltd., Basingstoke, who is the author's Industrial Supervisor, for his support.

The School's technicians, under the supervision of Mr. W. S. Churchill, provided invaluable assistance in maintaining and supporting the author's test programmes. Mr. S. Curtiss and Mr. L. Gray deserve special mention.

The author would also like to thank the staff from the Central Service Unit for providing much of the photographic work. The support given by the various members of the Bulk Solids Handling Unit of Thames Polytechnic, is gratefully acknowledged.

Last, but not least, the author wishes to express his gratitude to Mrs. A. Follis for patiently typing the text of this thesis.

Author's Note

All the work in this thesis is the sole and original work of the author, except where stated otherwise by acknowledgement or reference.

A large part of this thesis has already been presented at conferences or prepared for publication at the time of binding. Details are given in Appendix C.

Contents

Abstract i

Acknowledgements ii

Author's Note iii

List of Tables x

List of Figures xi

Chapter 1 - Introduction to Pneumatic Conveying

1.1 Introduction 1

1.2 Advantages 1

1.3 Disadvantages 2

1.4 Scope of Work 3

1.5 Publication Policy 4

Chapter 2 - A Literature Survey on Solid Particle Erosion

2.1 Introduction 5

2.2 The Mechanics of Erosion 6

2.2.1 Impacting Particle Parameters 8

2.2.2 Impact Parameters 10

2.2.3 Target Material Surface Parameters 17

2.3 The Mechanisms of Erosion 21

2.3.1 Mechanical Theories 23

2.3.2 Thermal Mechanisms 27

2.4 Conclusions 28

Chapter 3 - A Literature Survey on Pipe Bend Erosion

3.1 Introduction 29

3.2 The Factors Involved in Bend Erosion 29

3.2.1 Kinematic Factors 29

3.2.2 Material Factors 30

3.2.3 Bend Geometry Factors 30

3.3 Full Scale Erosion Tests 30
3.3.1 Review of Experimental Studies 31
3.3.2 Review of Industrial Studies 34
3.3.2.1 Bend Geometry 34
3.3.2.2 Bend Liners 36
3.3.3 Theoretical Investigations 37
3.4 The Work of Mills and Mason 42
3.4.1 Effects of Phase Density 42
3.4.2 Effects of Conveying Velocity 44
3.4.3 Effects of Particle Size 47
3.4.4 Premature Failure of Bends 47
3.4.5 Influence of Other Variables 49
3.5 Conclusions 49

Chapter 4 - Experimental Research Plants and Equipment

4.1 Introduction 51
4.2 Low Pressure Rig 51
4.2.1 Operation and Control 51
4.3 High Pressure Rig 51
4.3.1 Operation and Control 54
4.4 Test Loops 54
4.4.1 Low Pressure Rig 54
4.4.2 High Pressure Rig 58
4.5 Test Bends 58
4.6 Erosion Measurement Procedure 62
4.7 The Test Materials 68

Chapter 5 - Experimental Programmes

5.1 Introduction 71
5.2 Low Pressure Rig Experimental Programmes 71
5.3 High Pressure Rig Experimental Programme 73
5.4 Test Data 74

Chapter 6 - The Influence of Phase Density - I

6.1 Introduction 78
6.2 Review of Previous Work 78
6.3 Experimental Plan 80
6.4 Bend Wear Results and Discussion 80
6.4.1 Specific Erosion Analysis 83
6.4.2 Penetration Rate Analysis 92
6.4.3 Surface Erosion Profiles 96
6.5 Bend Life Analysis 98
6.6 Conclusions 106

Chapter 7 - The Influence of Particle Hardness

7.1 Introduction 108
7.2 Review of Previous Work 108
7.3 Experimental Plan 111
7.4 Particle Characteristics 112
7.4.1 Test Materials 112
7.4.2 Particle Size 123
7.4.3 Particle Shape 124
7.4.4 Particle Hardness 124
7.4.5 Moisture Effects 128
7.5 Velocity Effects 129
7.6 Bend Wear Results and Discussion 131
7.6.1 Introduction 131
7.6.2 Specific Erosion Analysis 132
7.6.3 Penetration Rate Analysis 141
7.6.4 Bend Life Analysis 147
7.6.4.1 Calculation Procedure 147
7.6.4.2 Influence of Other Variables 153
7.6.5 Surface Erosion Patterns 153
7.7 Effect of Particle Degradation 158
7.7.1 Introduction 158
7.7.2 Review of Previous Work 159
7.7.3 Effect on Erosion and Penetration Results 160
7.8 Conclusions 164

Chapter 8 - The Influence of Pipe Bend Diameter Ratio

8.1 Introduction 166

8.2 Review of Previous Work 166

8.2.1 Effect of Impact Angle 167

8.2.2 Location of Maximum Wear 169

8.2.3 Effect on Penetration 169

8.2.4 Effect on Velocity 170

8.2.5 Effect on Bend Life 171

8.3 Experimental Plan 171

8.3.1 Introduction 171

8.3.2 Test Bends 172

8.3.3 Control of Variables 173

8.3.4 Test Programmes 173

8.4 Bend Wear Results and Discussion 175

8.4.1 Introduction 175

8.4.2 Presentation of Results 179

8.4.3 Specific Erosion Analysis 180

8.4.3.1 Scatter of Results 180

8.4.3.2 Effect of Bend Radius 184

8.4.4 Penetration Wear Analysis 188

8.4.5 Inter-relating Effects of Bend Radius and Effective Impact Angle 196

8.4.6 Effect of D/d in terms of Impact Angle 203

8.4.7 Surface Erosion Profiles 213

8.5 Conclusions 220

Chapter 9 - Erosion of Replacement Bends

9.1 Introduction 221

9.2 Factors Involved 221

9.2.1 Effectsof Particle Size and Shape 222

9.2.2 Effect of Bend Position 224

9.2.3 Effect of Secondary Flows 225

9.2.4 Effect of Effective Impact Angle 227

9.2.5 Other Factors 228

9.3 Effect on Bend Wear Results 229

9.3.1 Specific Erosion Results 234

9.3.2 Penetration Wear Rate Results 234

9.4 Bend Life Analysis 235
9.4.1 Data based on Original Test Bends 236
9.4.2 Data based on All Test Bends 241
9.4.3 Discussion 243
9.5 Conclusions 244

Chapter 10 - The Influence of Phase Density - II

10.1 Introduction 246
10.2 Review of Previous Work 246
10.3 Experimental Plan 250
10.3.1 Introduction 250
10.3.2 Powder Considerations 251
10.3.3 Velocity Considerations 254
10.3.4 Test Programmes 256
10.4 Bend Wear Results and Discussion 257
10.4.1 Introduction 257
10.4.1.1 Particle Concentration Effects 261
10.4.1.2 Transitional Velocity Effects 262
10.4.2 Specific Erosion Analysis 264
10.4.2.1 Scatter of Results 264
10.4.2.2 Phase Density Effects 269
10.4.2.3 Velocity Effects 277
10.4.2.4 Comparison with Dilute Phase Test Data 281
10.4.3 Penetration Rate Analysis 286
10.4.3.1 Introduction 286
10.4.3.2 Phase Density Effects 287
10.4.3.3 Velocity Effects 294
10.4.3.4 Comparison with Dilute Phase Test Data 302
10.4.4 Bend Life Analysis 310
10.4.4.1 Introduction 310
10.4.4.2 Analysis based on Mass Eroded 311
10.4.4.3 Analysis based on Depth of Penetration 315
10.4.4.4 Discussion 318
10.5 Surface Erosion Profiles 323
10.6 Conclusions 332
10.6.1 Phase Density 332
10.6.2 Velocity 334

Chapter 11 - Conclusions

Conclusions 337

Appendices

A Nomenclature A1-2

B References B1-15

C Publications C1-2

List of Tables

Table	Title	Page
3.1	Details of Empirical Data on Bend Erosion	32
4.1	Material Bulk Properties	70
5.1	Details of Test Programmes	75
5.2	Erosion Data on All Test Bends	76
5.3	Erosion Data on Bends which Failed	77
8.1	Erosion Data for Original Bends Tested 176-178	
8.2	Influence of Effective Impact Angle on Specific Erosion and Penetration Wear Rate	199
9.1	Comparisons between the Prematurely Failed Bends and Replacement Bends	223
9.2	Influence of the Erosion and Penetration Rates of Replacement Bends on the Overall Results .	230
10.1	Individual Test Data	258-260

List of Figures

Figure	Title	Page
2.1	Influence of Particle Size and Velocity on the Erosion of an 11% Cr Steel by Quartz Particles	9
2.2	Influence of Particle Size on Strike Efficiency of a Nominal Velocity of 100 m/s	9
2.3	Influence of Particle Hardness on the Erosion of a C60H Steel at Normal Angle of Impact.....	9
2.4	Influence of Initial Particle Size on the Degree of Fragmentation of Quartz for 90^{o} Impacts	11
2.5	Variation of Weight Change with Mass of Particle Impacted	11
2.6	Variation of Erosion with Impact Angle for Ductile and Brittle Materials by 100 μm Silicon Carbide Particles at 156 m/s	13
2.7	Variation of Erosion with Impact Angle and Particle Size for Plate Glass	13
2.8	Influence of Velocity on Erosion for Different Materials	15
2.9	Variation of Volume Removed with Indentation Hardness of Different Metals	18
2.10	Variation of Resistance to Erosion with Indentation Hardness of Different Metals	18
2.11	Variation of Volume Removed with Indentation Hardness of Annealed and Work-hardened surface of Different Metals .	18
2.12	Variation of Erosion with Steel Alloys of Different Hardness	20
2.13	Volumetric Erosion as a Function of a Thermal Product ..	20
2.14	Depth of Erosion as a Function of Modulus of Elasticity of a Variety of Materials	22
2.15	Reciprocal Rate of Volume Loss as a Function of Strain Energy of Different Materials	22
2.16	Effect of Erosion with Impingement Angle for 300 μm Cast Iron Pellets against Aluminium at 10 m/s	24
2.17	Effect of Erosion with Impact Angle for 135 μm Quartz against H46 Steel at 365 m/s	24

Figure	Title	Page
2.18	Modes of Material Removal according to Hutchings.....	26
3.1	Effect of Diameter Ratio on Penetration Rate in Pneumatic Transport	33
3.2	Effect of Diameter Ratio on Penetration Rate in Hydraulic Transport	33
3.3	Influence of Bend Angle on Penetration Rate	33
3.4	Influence of Particle Velocity and Phase Density on Bend Wear Profile	35
3.5	Bend Erosion Pattern - After Some Wear	35
3.6	Variation of Impact Angle with Time	38
3.7	Relation Between Angle of Fracture and Critical Impact Angle	38
3.8	Influence of D/d on the Variation of Angle of Fracture with Bend Angle	38
3.9	Variation of Non-dimensional Volume Loss with Particle Velocity	40
3.10	Influence of D/d on Service Life of Bends in Terms of Non-dimensional Time	40
3.11	Variation of Erosion with Phase Density	43
3.12	Variation of Penetration Rate with Phase Density	43
3.13	Influence of Phase Density on Pipe Wear Profile	45
3.14	Influence of Phase Density on Bend Wear Profile	45
3.15	Variation of Specific Erosion with Velocity	46
3.16	Variation of Individual Specific Erosion Values with Mean Particle Size	46
3.17	Influence of Particle Size on Rate of Penetration	48
3.18	Influence of Particle Size on Pipe Section Wear Profile	48
3.19	Influence of Product Condition on Penetration Rate	50
4.1	Low Pressure Rig Plant	52
4.2	Low Pressure Rig Layout	53
4.3	High Pressure Rig Plant	55
4.4	High Pressure Rig Layout	56

Figure	Title	Page
4.5	A Typical Conveying Cycle Trace	57
4.6	Test Loop Configuration	59
4.7	New Test Loop Configuration	60
4.8	High Pressure Rig Test Loop Configurations	61
4.9	Test Bends	63
4.10	Schematic Diagram of Booth Bend	64
4.11	Surface Erosion Patterns	65
4.12	Cross-section Profile of Booth Bend	66
4.13	Bend Wall Thickness Measuring Instruments	67
4.14	Test Materials	69
5.1	Conveying Characteristics of Pulverised Fly Ash	72
6.1	Photomicrograph of Sand	81
6.2	Particle Size Distribution of Sand	82
6.3	Variation of Erosion with Mass Conveyed at a Phase Density of 1	84
6.4	Variation of Erosion with Mass Conveyed at a Phase Density of 3	85
6.5	Variation of Erosion with Mass Conveyed at a Phase Density of 5	86
6.6	Variation of Erosion with Mass Conveyed at a Phase Density of 7	87
6.7	Influence of Particle Size on Phase Density in terms of the Variation of Erosion with Mass Conveyed	90
6.8	Variation of Erosion with Phase Density	91
6.9	Influence of Particle Size on Phase Density in terms of Penetration Rate	93
6.10	Influence of Particle Size on the Variation of Penetration Rate with Phase Density	95
6.11	Surface Erosion Patterns of Test Bends	97
6.12	Influence of Particle Size on Phase Density in terms of Bend Wear Profile	99
6.13	Influence of Particle Size on Phase Density in terms of Pipe Wear Profile	100

Figure	Title	Page
6.14	Influence of Particle Size on the Variation of Mass Eroded to Cause Bend Failure with Phase Density	102
6.15	Influence of Phase Density on the Conveying Capacity of Bends	104
6.16	Influence of Phase Density on the Service Life of Bends	105
7.1	Influence of Particle Hardness on the Erosive Wear of a Number of Materials	109
7.2	Effect of Particle Hardness on the Erosion of an 11% chromium steel at 130 m/s and normal impact	109
7.3	Photomicrograph of Sand	113
7.4	Photomicrograph of Pulverised Fly Ash	114
7.5	Photomicrograph of Calcined Alumina	115
7.6	Photomicrograph of Hydrate Alumina	116
7.7	Photomicrograph of Fluidised Bed Ash	117
7.8	Particle Size Distribution of Sand	118
7.9	Particle Size Distribution of Pulverised Fly Ash	119
7.10	Particle Size Distribution of Calcined Alumina	120
7.11	Particle Size Distribution of Hydrate Alumina	121
7.12	Particle Size Distribution of Fluidised Bed Ash	122
7.13	Particle Shape Classification Diagram	125
7.14	Comparison between Published and Measured Particle Hardness Values	127
7.15	Variation of Erosion with Mass Conveyed for Individual Bends Eroded by Sand	133
7.16	Variation of Erosion with Mass Conveyed for Individual Bends Eroded by Fluidised Bed Ash and Pulverised Fuel Ash	134
7.17	Variation of Erosion with Mass Conveyed for Individual Bends Eroded by Calcined Alumina	135
7.18	Variation of Particle Size Distribution of Fluidised Bed Ash	138
7.19	Variation of Specific Erosion with Particle Hardness ..	139
7.20	Penetration Data for Bends Eroded by Sand	142
7.21	Penetration Data for Bends Eroded by Fluidised Bed Ash	143
7.22	Penetration Data for Bends Eroded by Calcined Alumina	144

Figure	Title	Page
7.23	Influence of Particle Hardness on Rate of Penetration . . .	145
7.24	Variation of Penetration Wear Rate with Particle Hardness	146
7.25	Variation of Erosion with Particle Hardness	148
7.26	Influence of Particle Hardness on the Conveying Capacity of Bends	151
7.27	Influence of Particle Hardness on the Service Life of Bends	152
7.28	Typical Surface Erosion Patterns	154
7.29	Influence of Particle Hardness on Bend Wear Profile ..	156
7.30	Influence of Particle Hardness on Pipe Wear Profile ..	157
7.31	Influence of Particle Recirculation on Mass Eroded from the Bends	161
7.32	Influence of Initial Mean Particle Size on Erosion ...	162
7.33	Influence of Change in Initial Mean Particle Size on Change in Erosion and Penetration	163
8.1	Location of Maximum Wear and Site of Impact in a Bend .	167
8.2	Particle Size Distribution of Sand	174
8.3	Variation of Erosion with Mass Conveyed for Individual Bends with D/d of 4	181
8.4	Variation of Erosion with Mass Conveyed for Individual Bends with D/d of 5.6	182
8.5	Variation of Erosion with Mass Conveyed for Individual Bends with D/d of 12	183
8.6	Variation of Individual Specific Erosion with Diameter Ratio	185
8.7	Variation of Specific Erosion with Diameter Ratio	187
8.8	Penetration Data for Bends with D/d of 4	189
8.9	Penetration Data for Bends with D/d of 5.6	190
8.10	Penetration Data for Bends with D/d of 12	191
8.11	Influence of Diameter Ratio on Rate of Penetration ...	193
8.12	Variation of Penetration Wear Rate with Diameter Ratio	194
8.13	Variation of Individual Penetration Wear Rate with Diameter Ratio	195

Figure	Title	Page
8.14	Influence of Bend Geometry on Bend Wear Profile	198
8.15	Influence of Bend Geometry on Pipe Section Wear Profile	200
8.16	Influence of Bend Geometry and Effective Impact Angle on Specific Erosion and Penetration Wear Rate	201
8.17	Influence of Bend Geometry and Particle Trajectory on the Location of Maximum Wear and Failure	205
8.18	Variation of Impact Bend Angle with D/d for Different Particle Trajectories	206
8.19	Variation of Relative Erosion with Impact Angle	208
8.20	Comparison between Actual and Predicted Data on the Effect of D/d on Erosion	209
8.21	Variation of Relative Penetration with Impact Angle ..	211
8.22	Comparison between Actual and Predicted Data on the Effect of D/d on Penetration	212
8.23	Surface Erosion Patterns of Elbows	214
8.24	Surface Erosion Patterns of Bends with D/d of 5.6	215
8.25	Surface Erosion Patterns of Bends with D/d of 12	216
8.26	Influence of Diameter Ratio on Bend Wear Profile	218
8.27	Influence of Diameter Ratio on Pipe Wear Profile	219
9.1	Typical Surface Erosion Patterns	226
9.2	Influence of Replacement Bends on the Variation of Specific Erosion with Diameter Ratio	232
9.3	Influence of Replacement Bends on the Variation of Penetration Wear Rate with Diameter Ratio	233
9.4	Variation of Specific Erosion with Diameter Ratio ...	237
9.5	Variation of Mass Eroded at Failure with Diameter Ratio	239
9.6	Influence of Diameter Ratio on the Conveying Capacity of Bends	240
9.7	Influence of Diameter Ratio on the Service Life of Bends	242
10.1	Effect of Particle Concentration on Ersoion and Relative Wear	248
10.2	Particle Size Distribution of Sand	252

Figure	Title	Page
10.3	Variation of Erosion with Mass Conveyed at a Phase Density of 10	265
10.4	Variation of Erosion with Mass Conveyed at a Phase Density of 17	266
10.5	Variation of Erosion with Mass Conveyed at a Phase Density of 22	267
10.6	Influence of Phase Density on the Variation of Erosion with Mass Conveyed	270
10.7	Variation of Specific Erosion with Phase Density	272
10.8	Variation of Specific Erosion with Phase Density	273
10.9	Variation of Specific Erosion with Phase Density	275
10.10	Variation of Accumulative Erosion with Velocity	278
10.11	Variation of Accumulative Erosion with Velocity	279
10.12	Influence of Phase Density on Specific Erosion	283
10.13	Influence of Diameter Ratio on the Variation of Phase Density with Mass Eroded	285
10.14	Penetration Data for Individual Bends Tested at a Phase Density of 10	288
10.15	Penetration Data for Individual Bends Tested at a Phase Density of 17	289
10.16	Penetration Data for Individual Bends Tested at a Phase Density of 22	290
10.17	Influence of Phase Density on Penetration Rate	293
10.18	Variation of Maximum Depth of Penetration with Mass Eroded for a Number of Selected Test Bends	296
10.19	Influence of Velocity on Penetration in terms of Mass Eroded	297
10.20 a	Effect of Velocity on Maximum Depth of Penetration at a Phase Density of 10	299
b	at a Phase Density of 17	300
c	at a Phase Density of 22	300
10.21	Effect of Velocity on Maximum Depth of Penetration ...	301
10.22	Influence of Phase Density on Penetration Rate	304
10.23	Influence of Phase Density on Depth of Penetration for a Constant Mass Eroded	305

Figure	Title	Page
10.24	Influence of Diameter Ratio on the Variation of Phase Density with Penetration Rate	308
10.25	Influence of Phase Density on the Conveying Capacity of Bends	312
10.26	Influence of Phase Density on the Service Life of Bends	313
10.27	Variation of Penetration Wear Rate with Phase Density .	316
10.28	Influence of Phase Density on the Conveying Capacity of Bends	319
10.29	Influence of Phase Density on the Service Life of Bends	320
10.30	Surface Erosion Patterns of Bends with D/d of 5.6	324
10.31	Surface Erosion Patterns of Bends with D/d of 24	325
10.32	Influence of Phase Density on Bend Wear Profile	327
10.33	Influence of Phase Density on Pipe Wear Profile	328
10.34	Influence of Phase Density on Bend Wear Profile	329
10.35	Influence of Phase Density on Pipe Wear Profile	330

Chapter 1

Introduction to Pneumatic Conveying

1.1 INTRODUCTION

Of all the various forms of bulk handling, the transport of dry bulk materials in a gas suspension through a pipeline, normally termed pneumatic conveying, is now widely accepted as a viable means of handling a wide range of bulk solids. In the chemical industry, pneumatic conveying is in fact the only acceptable means of handling toxic and hazardous materials, particularly with regard to the recent introduction of the Health and Safety at Work Act.

Since the first commercial application of pneumatic transport was introduced in grain handling in 1892 (Bannister 1959), several different systems have been developed and are now well established in a number of industries such as mining, dredging, paper mills, flour milling, and petrochemical (Zenz and Othmer 1960). New fields of applications now include solid waste collection and disposal (Hayden and Breidenbach 1971), construction industry (Jones 1971), capsule transport (Simper and Baker 1973), tunnelling (Faddick and Martin 1978), sewage engineering (Maule et al 1978), and fluidised combustion of coal (Thurlow 1978).

Whilst much has been written on the theory of gas-solid suspension flow in a pipeline, and despite numerous correlations which have been produced for predicting the behaviour of two phase gas-solid suspension flow, particularly pressure drop which is the most fundamental parameter for design and operation purposes, no universally acceptable formulae have yet been produced. This is primarily due to the complex mechanics involved in particle-particle, particle-gas, particle-pipe interactions which are difficult to isolate experimentally (Yang and Keairns 1976). Thus, to arrive at an optimal design of a pneumatic conveying system, the design approach is still largely based upon practical experience, and in this respect, is an art rather than a science (Kraus 1965, Stoess 1970, Mason and Stacey 1975, Scott 1978, Mason 1980).

1.2 ADVANTAGES

The principal reasons for selecting pneumatic conveying systems over other forms of mechanical handling are briefly :

1.2.1 Flexibility of application and installation.

The pneumatic conveying pipeline is compact, and can be quickly and easily installed along walls, ceilings or underground in existing buildings. The system can be designed to convey materials from and to any number of feed points and can subsequently be modified or extended to cater for changes in production requirements.

1.2.2 Comparatively reduced maintenance and labour costs.

A typical pneumatic conveying system contains few working parts in continuous operation and, together with valves and filter units, they can be concentrated at a convenient position where they can be easily serviced, thus reducing maintenance and labour costs.

1.2.3 Cleanliness and safety.

The material is transported in a totally enclosed, airtight pipe. This means that the system can be self-cleaning and so it can be used again for different materials, without risk of contamination. There is no wastage or spillage, thus health hazards due to dusty or toxic pollutants are eliminated.

1.2.4 Relatively low capital costs and increased automation.

Whilst early pneumatic conveyors consumed more power than conventional mechanical conveyors, there are now several efficient and advanced systems which reduce power costs considerably. By incorporating pneumatically operated control valves and various signalling devices, the conveying systems can be designed to operate automatically, with no manual intervention and only limited surveillance.

1.3 DISADVANTAGES

In any pneumatic conveying system, however, there are three main problems which must be taken into account regarding the material to be conveyed:

1.3.1 Plant erosion.

The erosion of pipelines, particularly at pipe bends, is a major disadvantage when conveying abrasive products. In industrial applications, wear in bends can be several times greater than in straight pipes. Erosion is a major problem in the design and operation of equipment, particularly in the petrochemical industry, as well as in the pneumatic stowing in coal mines and in the pulverised fuel feed lines to boilers.

1.3.2 Product degradation.

Particle degradation can present a major problem when conveying certain materials. In extreme cases, degradation may be so severe that its flow characteristics are totally changed. Certain friable materials can not be pneumatically transported, unless the partial degradation of the material is inconsequential to the end use of the product.

1.3.3 Explosion and fire hazard.

Some materials, when mixed with air, are potentially explosive and can be ignited due to the electrostatic charge induced during conveying. This hazard can be reduced considerably by ensuring that all piping connections are properly earthed and explosion vents provided in the system. However, it has been reported (Stoess 1970) that certain combustible materials have been conveyed safely, and tests have shown that a local explosion would not necessarily propagate through the entire length of the system.

1.4 SCOPE OF WORK

The erosion of pipe bends, which is perhaps the dominant factor which makes industry reluctant to install pneumatic conveying systems for handling abrasive materials, is the main aim of this investigation. The objective is to analyse the effects of the parameters associated with actual pipe bend erosion, in order to establish a correlation from which the likelihood of erosion, and its extent, can be predicted.

Although the general problem of erosion has been investigated with specially developed bench-type rigs (Chapter Two), very little work has been carried out on actual pipe bends. Whilst Mills and Mason (1976 to 1977, Chapter Three), have probably carried out and published more work on the problem of erosion in pneumatic conveying systems than any other workers in this field, their research has been limited to a very narrow range of variables, using a low pressure conveying rig. This current programme is aimed at extending their work and considering other variables which have not been investigated and which are of direct relevance to industry.

Two existing full-scale pneumatic conveying plants have been used in this work. One is a conventional low pressure rig which has seven 90^{o} bends in the 54 m long, 50 mm bore test section. This rig was used to investigate the influence of particle hardness and the effect of particle degradation caused by continuous recirculation of the material. An entirely new test loop was incorporated into this plant and, together with the existing test loops, the influence of bend radius was also investigated. An entirely unexpected phenomenon of the rapid failure of replacement bends in the course of this test series was observed, and the causes analysed. This effect has hitherto never been reported and the results obtained are of direct importance to industry, with regard to replacing worn bends with new ones.

A high pressure conveying rig, which could be linked up with three existing different test loop configurations, was also utilised. With high pressure air available, conveying was possible in a totally different mode. Tests were carried out to investigate the influence of higher phase densities, and correspondingly lower air velocities, using this rig.

1.5 PUBLICATION POLICY

It has been the author's intention to publish the work reported in this thesis which are of direct relevance to industry. For this purpose, some of the work presented here has already been presented at various conferences, and further work will be offered for publication in the near future.

A paper, based on Chapters One, Two and Three, entitled "The Erosion of Pipe Bends in Pneumatic Conveying Systems" was presented at an Institution of Mechanical Engineers Conference on 'New Developments in the Transport of Particulate Solids' (1979). Full details of all the papers presented are given in Appendix C.

Chapter 2

A Literature Survey on Solid Particle Erosion

2.1 INTRODUCTION

Solid particles, entrained in a moving fluid, are a common occurrence in many industrial processes. The impact of these particles, often at high velocities, on a surface leads to a form of wear categorised as 'solid particle erosion', or generally, 'erosion'.

Apart from pneumatic conveying systems, erosion also occurs in many industrial operations. In the chemical process industry erosion is particularly severe in the equipment used for the catalytic cracking of oil (Stoker 1949, Finnie 1959), and in coal gasification plants (Hall 1974, Dapkunas 1979).

In power plants erosion frequently occurs in boiler tubes exposed to pulverised fuel ash (Sterens 1949, Raask 1969), and on heat transfer tubes resulting from jet impingement in fluidised bed steam generators (Vaux and Newby 1978, Wood and Woodford 1979).

In turbomachinery erosion occurs in the compressor blades of gas turbine engines in helicopters, hovercraft and VSTOL aircraft due to dust ingestion (Montgomery and Clark 1962, Goodwin et al 1969), and in turbine blades due to the presence of fly ash, which is formed as a by-product in the combustion process (Grant and Tabakoff 1975, Tabakoff et al 1979).

Erosion is also a problem in industrial fan equipment, particularly in the mining industry, due to abrasive dust particles in the environment (Wallis 1975).

In the aerospace industry erosion is particularly serious in rocket motor tail nozzles, due to solid propellants (Neilson and Gilchrist 1968b, de Morton 1977), and on missiles and rockets due to atmospheric particles and rain droplet impacts encountered in hypersonic flight (Lorenz 1970, Siegelman and Pallone 1978, Letson 1979).

On the credit side, erosion can be harnessed usefully, as in sandblasting, shot peening, rock drilling (Finnie and Oh 1966), ultrasonic cleaning, sputtering, spark machining (Preece and Macmillan 1977), and ion implantation (Dearnaley 1980). Recently, a new technique of cutting steel by adding abrasives to the high pressure water jets, has been reported (Anon. 1980).

The common occurrence of erosion in such a wide and diverse range of industrial situations is a matter of considerable engineering and economic importance. Erosion is a very expensive problem. About 8% of wear encountered in industry is due to erosion (Eyre 1978), and wear as a whole is perhaps the most predominant cause for maintenance breakdowns in industry (Bahadur 1978).

Thus, it was the economic importance of wear in general, and erosion in particular, that led to numerous studies of the mechanisms of erosion from specially developed erosion testing apparatus during the past two decades. These rigs were designed to simulate erosion of a target surface material by a stream of solid particles. Tests were carried out under controlled conditions and the respective effects and influences of the various particles and target materials over a range of particle velocities and impingement angles were analysed. From these observations several theoretical models were postulated, and empirical mathematical expressions developed.

A survey of solid particle erosion literature by the author has revealed that the erosion process had been studied from several points of view by different investigators. Some have been of a general nature, with a view to gaining a better understanding of the basic operative mechanisms of erosion, whilst others have been undertaken to satisfy a very specific need for a particular application.

2.2 THE MECHANICS OF EROSION

Solid particle erosion is a highly complex process. To date, there is still no general agreement concerning the number and relative importance of the various parameters, and to what extent each affects erosion. This is due to the many interdependent variables which restrict any precise, quantitative analysis, and the resultant experimental data does not permit any valid comparison and correlation between the data reported from various sources.

However, considerable progress had been made in recent years in gaining a basic understanding of the mechanics of the erosion process. The parameters of significance involved in solid particle erosion, determined from analytical studies and bench type erosion tests (Tilly 1969, 1979, Finnie 1972, Uuemois and Kleis 1975, Ruff and Weiderhorn 1979), are also

of importance in the erosive wear process in pneumatic conveying (Mills and Mason 1975). They have also been shown to be of importance in hydraulic conveying (Truscott 1975). These factors can be generally summarised into three broad categories :-

2.2.1 Impacting Particle Parameters

- 2.2.1.1 Particle size,
- 2.2.1.2 Particle shape,
- 2.2.1.3 Particle hardness,
- 2.2.1.4 Particle friability,

2.2.2 Impact Parameters

- 2.2.2.1 Angle of impact,
- 2.2.2.2 Particle velocity at impact,
- 2.2.2.3 Particle rotation at impact,
- 2.2.2.4 Particle concentration,
- 2.2.2.5 Properties of the carrier gas,
- 2.2.2.6 Test temperature,
- 2.2.2.7 Duration of exposure.

2.2.3 Target Material Surface Parameters

- 2.2.3.1 Surface properties,
- 2.2.3.2 Surface hardness,
- 2.2.3.3 Surface thermal properties,
- 2.2.3.4 Surface strain rate sensitivity,
- 2.2.3.5 Surface stress level.

With such an extensive range of potential variables, many of which are inter-related, it is extremely difficult to isolate and investigate the individual effects in detail experimentally. In most cases, only a few parameters were considered, and others neglected. This probably explains why many investigations contain general conclusions, based either on limited research materials, or without considering all the factors involved (Finnie 1972, Uuemois and Kleis 1975, Adler 1979).

Reviews of the current state of information on solid particle erosion have appeared recently in several sources (Finnie 1972, Uuemois and Kleis 1975, Engel 1976, Preece and Macmillan 1977, Hutchings 1979b, Tilly 1979, Ruff and Weiderhorn 1979, Adler 1979), and on erosive wear in pneumatic conveying by Mills and Mason (1975). Together with earlier sources (Finnie 1960, Wellinger and Uetz 1963, Finnie et al 1967, Tilly 1969), the state of understanding on solid particle erosion has been adequately

reviewed. In this section, therefore, only the central features of the respective influences of the various parameters which are likely to be applicable to the erosion process in pneumatic conveying, are discussed.

2.2.1 Impacting Particle Parameters

Properties of the impacting particle, such as size, shape and hardness, are major indicators of the potential erosiveness of the material to be conveyed.

Tilly and co-workers (Goodwin et al 1969, Sage and Tilly 1969, Tilly 1969 and Tilly and Sage 1970) found that a critical particle size exists, above which erosion is not influenced by size, and this value appears to increase linearly with velocity (Fig. 2.1). Kleis (1969) also found a similar dependence with larger particles . In addition, different materials were also found to exhibit different types of size dependence. However, Tilly (1969) pointed out that there is also an aerodynamic effect, where particles less than 20 μm may be deflected around the target without impacting (Fig. 2.2).

Particle shape and hardness are closely related. Sharp, angular particles are potentially more erosive than rounded or spherical particles (Finnie 1960, Tilly 1969) , and the hardest particles tend to have the sharpest profiles. In tests on mild steel at low velocities, 100 μm quartz was about ten times more erosive than similarly sized glass spheres (Raask 1969). Tests carried out on 11% chromium steel with sand at 130 m/s and 90^{o} impact angle by Goodwin et al (1969) confirm that erosiveness is dependent upon hardness and, by inference, on sharpness. Mills and Mason (1975) pointed out that sharpness can also vary with the history of the product in pneumatic conveying. A recirculated or used material will have a more rounded profile than a freshly prepared material of the same composition. Wellinger and Uetz (1963) also found a strong dependence of erosion on both particle hardness and sharpness. Fig 2.3 shows that there is also a similar critical particle hardness value above which erosion is not dependent on particle hardness. A similar trend in the field of abrasive wear, which is closely related to erosive wear (Mills and Mason 1975) is also reported by Khruschov (1974) and, in terms of a critical particle size, by Rabinowicz et al (1961) and Nathan and Jones (1966),

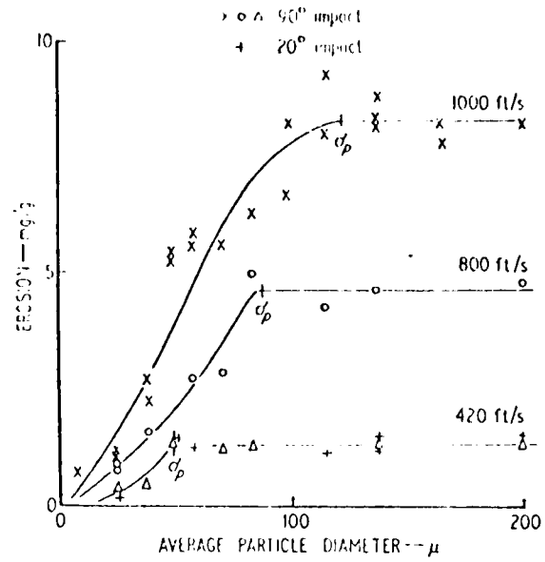

FIG. 2.1 Influence of Particle Size and Velocity on the Erosion of an 11% Cr Steel by Quartz Particles

(Goodwin et al 1969)

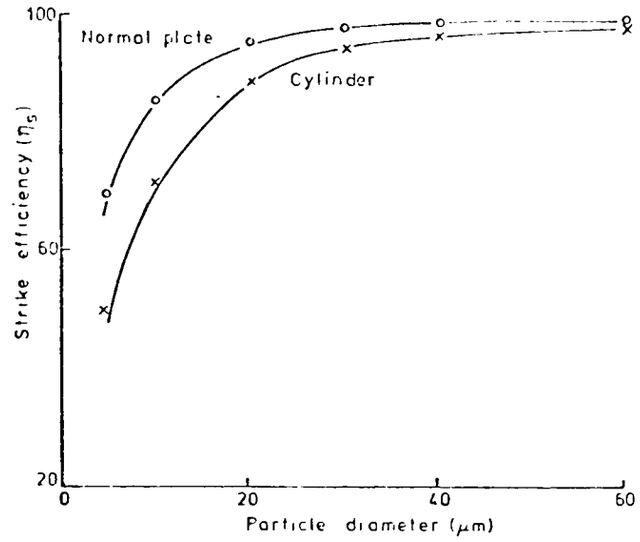

FIG. 2.2 Influence of Particle Size on Strike Efficiency at a Nominal Velocity of 100 m/s.

(Tilly 1969)

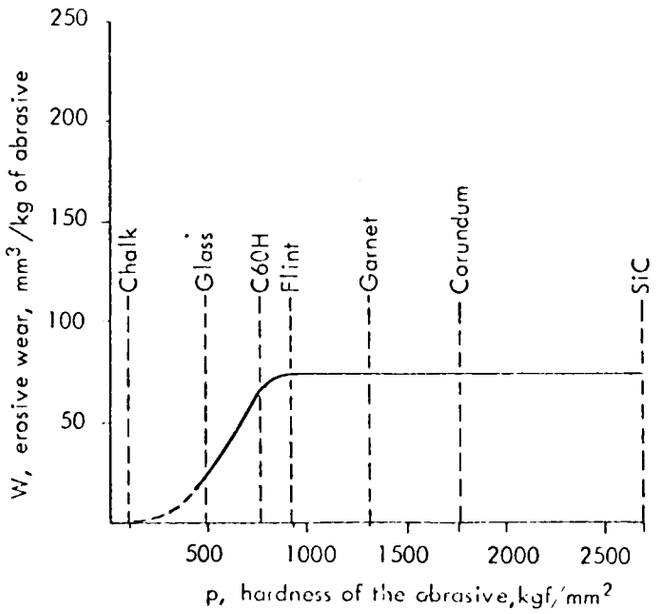

FIG. 2.3 Influence of Particle Hardness on the Erosion of a C60 H Steel at Normal Angle of Impact

(Wellinger and Uetz 1963)

using a range of abrasive grits on various metals and alloys.

The effect of particle fragmentation, and hence the degree of degradation, has received little attention apart from Tilly (1973), who found that a major role in the erosion process is played by particle fragmentation. This process involves a threshold velocity and particle size below which damage does not occur, and that it is also dependent on the surface material. Fig. 2.4 (Tilly and Sage 1970) shows that surface material could be an important factor with regard to reducing particle degradation, particularly at pipe bends in pneumatic conveying systems. This is important because particle degradation can cause serious problems in pneumatic conveying by virtue of the changes in particle shape and particle size distribution. Apart from quality control with friable materials, the increase in 'fines' can affect the flow characteristics of a product. Degradation can change a free-flowing powder into one which can only be handled with difficulty, and is also shown to be a factor in the premature failure in pipe bends (Mills and Mason 1976c). Uuemois and Kleis (1975) found that the abrasiveness of the particles also depends to a considerable extent on the impurity and water content.

Recent studies (Ives and Ruff 1978) have focussed attention on the effect of particles embedding into surfaces due to particle fragmentation upon impact during erosion. Examination of the target material subsurface microstructure has revealed a significant amount of particle embedding. This results in an initial 'incubation' period before steady state erosion rate develops, and confirms the incubation effect reported previously by Neilson and Gilchrist (1968a), Behrendt (1970)(Fig. 2.5), and Tilly and Sage (1970).

2.2.2 Impact Parameters

The primary impact parameters which strongly influence the erosion process are angle of impact and velocity. Comparatively small changes in these parameters can produce significant variations in the magnitude of erosion, whilst the other secondary parameters such as temperature, properties of the carrier gas, etc., have little effect.

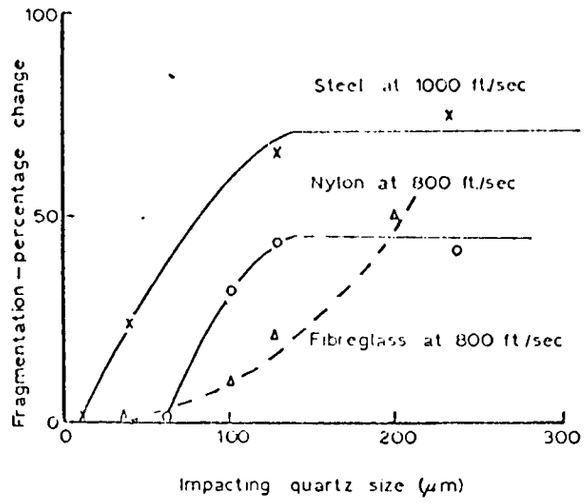

FIG. 2.4 Influence of Initial Particle Size on the Degree of Fragmentation of Quartz at Normal Impacts.

(Tilly and Sage 1970)

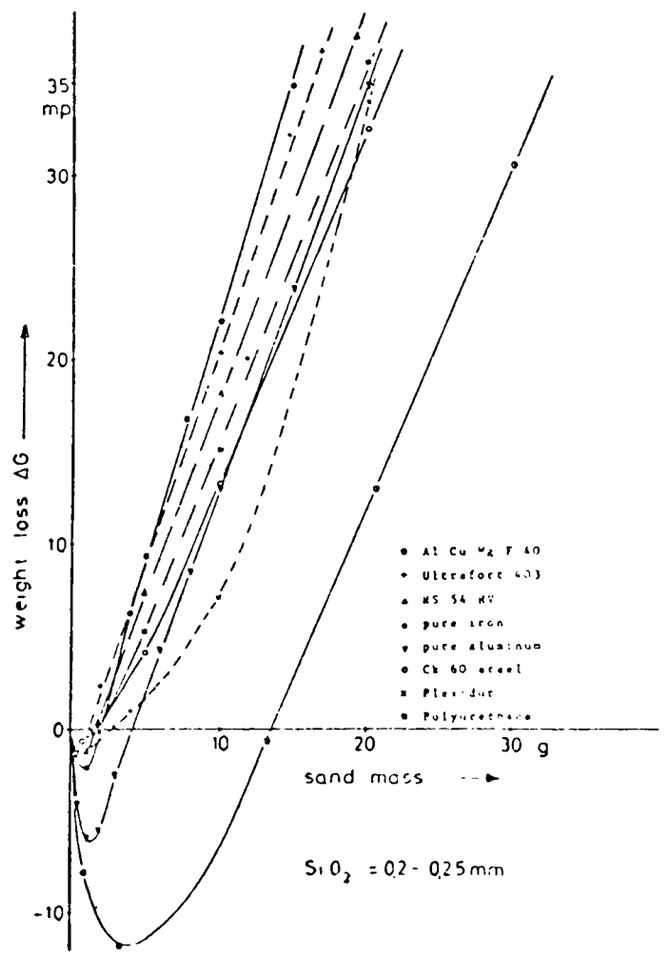

FIG. 2.5 Variation of Weight Change with Mass of of Particle Impacted. (Behrendt 1970)

The variation of erosion with impact angle is perhaps the best starting point to an understanding of the mechanics of the erosion process. Fig. 2.6 shows the effects of impact angle and surface material. Maximum erosion for aluminium occurs at around 20^{o} and then falls to about one third of this value at normal impact. For aluminium oxide, erosion rises monotonically to a maximum at 90^{o} impact. The behaviour of aluminium is typical of ductile metal and that of aluminium oxide of a brittle material. These characteristic ductile and brittle modes of erosion are well recognised in solid particle erosion literature. However, not all materials strictly conform to these patterns; for example, highly hardened carbon steels (Finnie 1960) and certain alloy steels (Gulden 1979) may exhibit both types of behaviour. Also, under certain conditions, a nominally brittle material may erode in a characteristically ductile manner due to the particle size effect, (Fig. 2.7) (Sheldon and Finnie 1966a).

The sharp distinction between these two different modes of erosion indicates distinctly separate mechanisms of material removal in each case. For ductile erosion the process is predominantly due to plastic deformation, and for brittle erosion it is mainly due to the propagation of fractures into the material surface. A characteristic feature of ductile erosion is the presence of ripples on the surface erosion pattern at low angles of impact (Finnie and Kabil 1965, Sheldon and Finnie 1966b).

In pipe bend erosion the magnitude of the influence of impact angle is determined by the intersection of the path of the particle trajectory preceding from the straight pipe to the outer bend wall surface. This is, in turn, determined by the bend geometry, usually defined in terms of bend to pipe diameter (D/d) ratio. The influence of D/d on impact angle has been extensively investigated by Brauer and Kriegel (1964, 1965a,b), Kriegel (1970) and Glatzel (1977), and will be discussed in detail in Chapters Three and Eight.

Of all the parameters involved in the erosion process, velocity is probably the most important. Numerous investigations have been carried out on the effects of velocity, and over a range of velocities the results can be expressed in the form -

$$\text{erosion} = \text{constant } V^{n}$$

where V is the particle velocity. The exponent, n, has been found

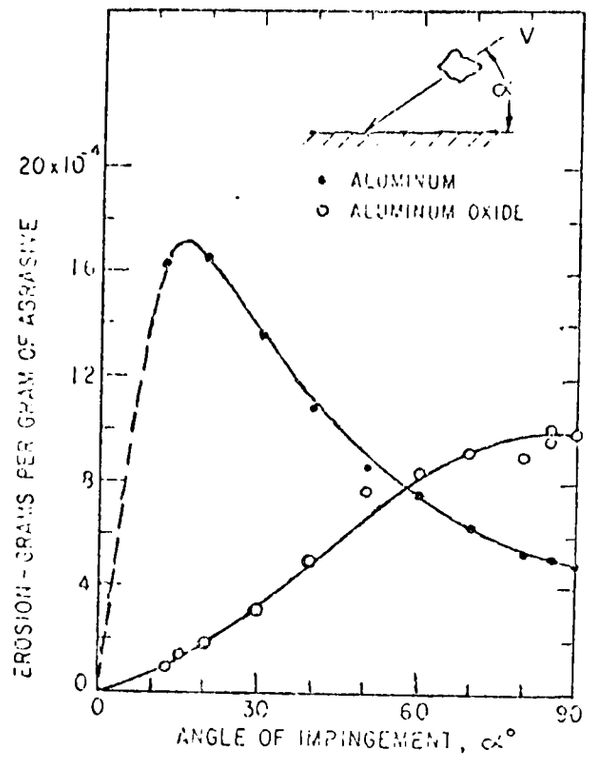

FIG. 2.6 Variation of Erosion with Impact Angle for Ductile and Brittle Materials by 100 μm SiC particles at 156 m/s. (Finnie et al 1967)

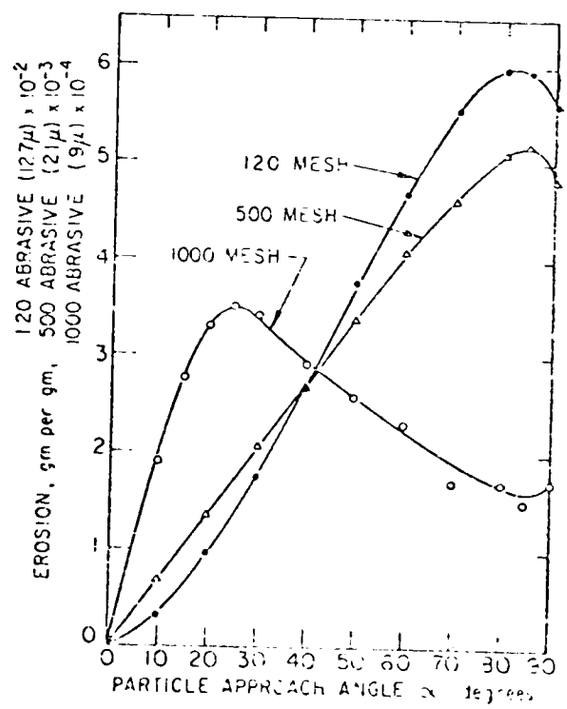

FIG. 2.7 Variation of Erosion with Impact Angle and Particle Size for Plate Glass.
(Sheldon and Finnie 1966 a)

to vary from 2.0 to 3.4 for ductile metals, and from 2.0 to 6.5 for brittle materials. The substantial variation in the velocity exponent is attributed to the wide variety of experimental conditions under which they were obtained (Preece and Macmillan 1977) and also due to the accuracy of the testing facilities themselves (Wolak et al 1977, Adler 1979). However, the general consensus of opinion is that, for ductile materials the exponent, n, lies between 2.3 and 2.4 (Tilly 1979) and is shown to be independent of the type of material (Fig. 2.8).

However, detailed studies have found some dependence of the velocity exponent on other inter-relating parameters. Sheldon (1970) reported that the velocity exponent for steel seemed to exhibit a size effect, whilst copper and aluminium seemed to be independent of particle size. Goodwin et al (1969) found that, for small particles, n is equal to 2.0, but for sizes above 100 μm it is around 2.3, and this increase is attributed to the degree of fragmentation.

From single particle impact studies, Sheldon and Kanhere (1972) found a small difference in the velocity dependence of erosion between uneroded and previously eroded surfaces. Hutchings and co-workers (Winter and Hutchings 1974, Hutchings and Winter 1974, 1975) reported that a threshold velocity is required before material is removed from the surface, and the mechanism of the removal process itself is dependent on the particle shape, particle rake angle and particle rotation at impact. The threshold velocity is also substantiated by Ives and Ruff (1978) based on scanning and transmission electron microscopy methods on stainless steel and copper specimens subjected to erosion by 50 μm angular Al_2O_3 and glass particles at 59 m/s. Ruff and Weiderhorn (1979) also reported that the velocity exponent is dependent, to some degree, on impact angle and temperature.

The range of velocities used in these solid particle erosion tests, generally within 35 to 600 m/s, is well above the low range of around 5 to 30 m/s encountered in typical pneumatic conveying situations. A more suitable and convenient parameter for pneumatic conveying is the conveying air velocity, rather than the particle velocity. Particle velocity is essential in solid particle erosion tests but, provided that for a given air velocity the particles are accelerated to their terminal velocities, conveying air velocity is a satisfactory substitute parameter (Mills and Mason 1975).

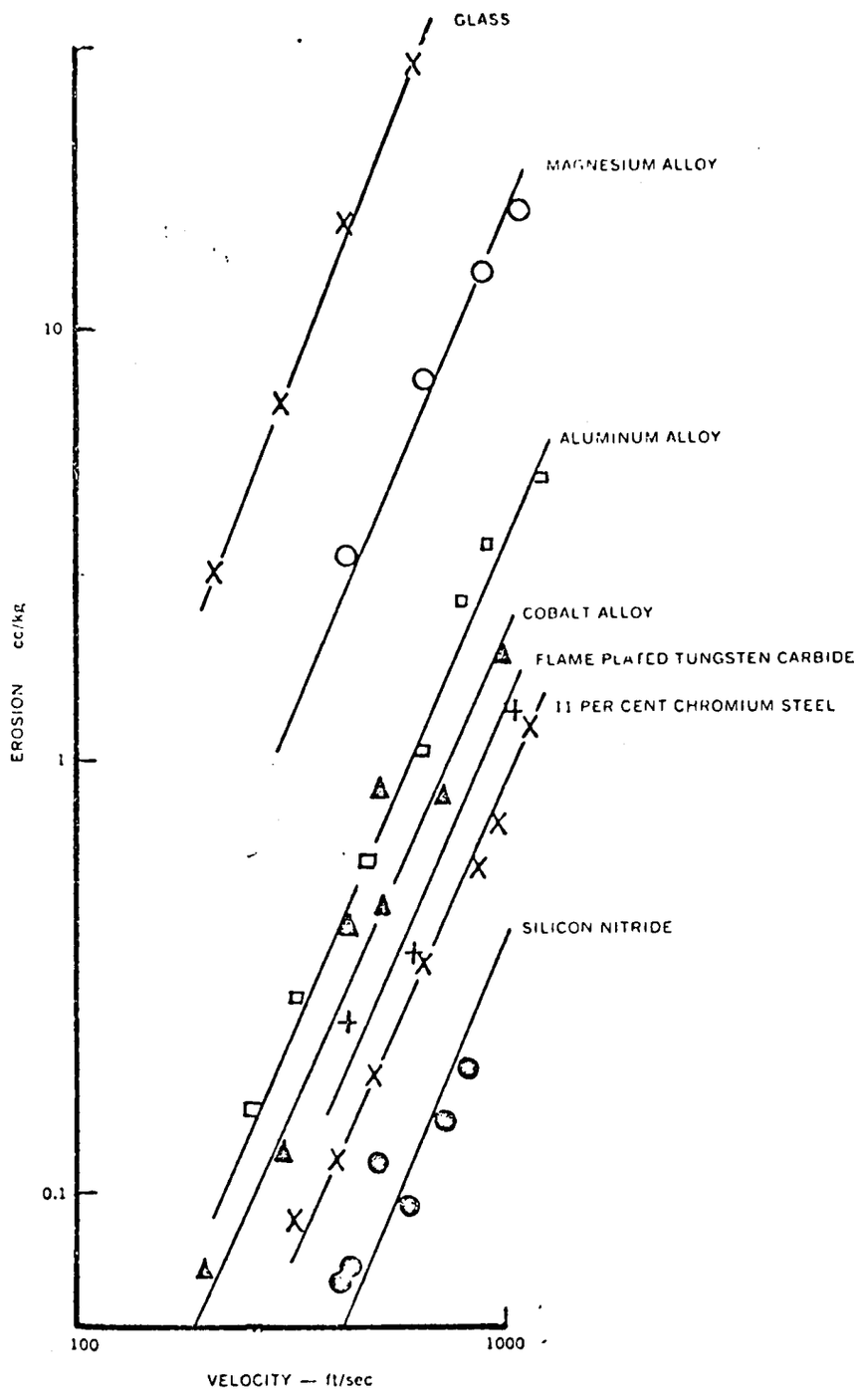

FIG. 2.8 Influence of Velocity on Erosion for Different Materials
(Tilly and Sage 1970)

Finnie (1962) reported that the erosion in a pipe is observed to increase considerably with only a slight increase in fluid velocity, and predicted that the velocity exponent in terms of fluid velocity, is equal to four. This exponent is substantiated by Grant and Tabakoff (1975) using quartz particles on an aluminium target, but only at normal impacts, by taking the aerodynamic effects into consideration. Laitone (1979) found the increase in the velocity exponent is a direct result of aerodynamic effects due to the deflection of the particles around the target, as reported earlier by Tilly (1969).

The effect of particle concentration has received little attention apart from limited studies specifically carried out on gas turbine and aero engine erosion by Montgomery and Clark (1962), Wood and Espenchade (1964) and Tilly and Sage (1970). In these studies, particle concentration is expressed as mass of dust per unit volume of suspension, or per unit area per second (Tilly and Sage 1970). Conflicting results were reported and, as these were either due to the narrow limits of particle concentration studied or within the ranges of concentration, the concentration effect is negligible (Uuemois and Kleis 1975). The effect of particle concentration is closely related to the velocity, particle size and impact angle and, in general, erosion is reduced as particle concentration is increased (Tilly 1979).

In pneumatic conveying Mills and Mason (1975) reported that particle concentration is an important variable in the erosive process in pipe bends and it is more convenient to use the term 'phase density', which is the ratio of mass flow rate of material conveyed to the mass flow rate of air. This is more appropriate to pneumatic conveying situations, for it is a dimensionless quantity and its value remains constant at any section of a pipeline, unlike particle concentration which varies with density, and hence with air pressure.

Mason and Smith (1972) were probably the first to carry out industrially orientated tests on pipe bend erosion to assess the relative effects of velocity and phase density. 25mm and 50mm square section perspex bends were subjected to erosion by a stream of pneumatically conveyed suspensions of 63 μm alumina particles. The flow and wear patterns around the bend were visually observed and, instead of the usual convention of measuring erosion in terms of mass or volume removed,

they expressed erosive wear rate in terms of mass conveyed per unit depth eroded. They found that, over the range of velocities investigated from 29 to 85 m/s, the erosive wear rate could be expressed in the form -

$$\text{erosion} \propto \text{velocity}^{2.25} \times \text{phase density}^{-1.36}$$

This expression clearly showed that velocity and phase density are inter-related parameters.

Mills and Mason (1976 to 1977) investigated the erosion of pipe bends using a full scale test rig. Tests were carried out over a range of air velocities from 15 to 32 m/s, and phase densities from 0.5 to 8.0. They found that the velocity exponent, in terms of mass eroded, was consistently at 2.65 over this range of velocities. However, in terms of conveying capacity, the exponent, based on depth of penetration, is 3.5. Since mass flow rate is directly proportional to velocity, the exponent in terms of bend life is even higher, at 4.5. The influence of phase density on erosion was found to be considerably affected by the condition of the conveyed material. The overall results of their work are discussed in detail in the next chapter.

Apart from these major parameters, which play a significant role in the erosive wear process in pneumatic conveying, the other impact parameters, such as properties of the carrier gas, temperature and duration of exposure, have received little attention. Finnie (1972), however, commented that these parameters have little significant effect on the overall erosion process.

2.2.3 Target Material Surface Parameters

The effects of material properties on erosion have also been studied by numerous investigators in order to provide a basis of correlation between the erosion resistance of a material to some form of material property such as hardness or modulus of elasticity.

In Finnie's theoretical analysis of ductile erosion(Finnie 1958, 1960), he predicts that the erosion resistance is inversely proportional to the flow stress of the material, which is directly related to its indentation hardness. Experimental results (Finnie et al 1967) for a wide variety of technically pure metals and heat treated steels were given (Fig. 2.9). For pure metals, the volume removed was

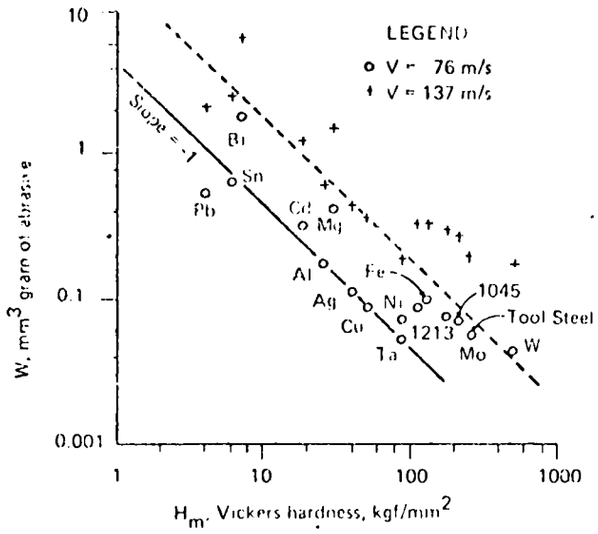

FIG. 2.9 Variation of Volume Removed with Indentation Hardness of Different Metals. (Finnie et al 1967)

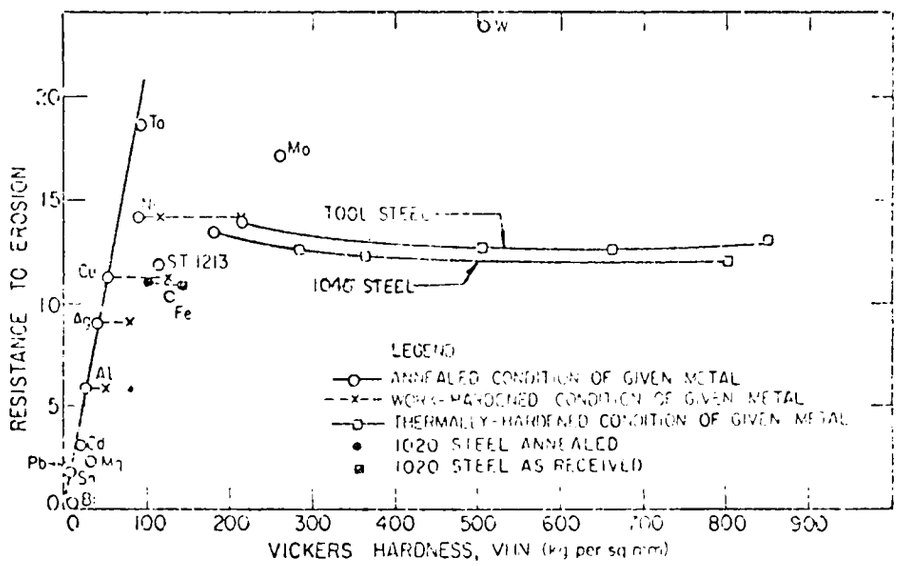

FIG. 2.10 Variation of Resistance to Erosion with Indentation Hardness of Different Metals. (Finnie et al 1967)

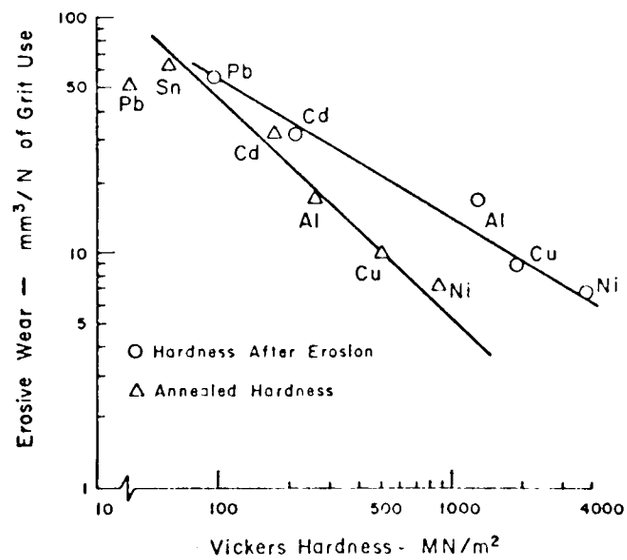

FIG. 2.11 Variation of Volume Removed with Indentation Hardness of the Annealed and Work-hardened Surface of Different Metals. (Sheldon 1977)

inversely proportional to the annealed surface hardness, and the bcc metals (Fe, Mo and steels) typically erode two to three times more rapidly than fcc metals of similar hardness. This was attributed to the presence of small amounts of impurities which raise the initial yield stress, and thus the hardness, of bcc metals. No increase in the resistance to erosion was found when the steels were heat treated or by raising the hardness of fcc metals (Ni, Cu, Ag and Al) by cold working (Fig. 2.10). This is in contrast to the work by Khruschov (1957, 1962) on abrasion tests who showed that, whilst work hardening had no effect on abrasion resistance, heat treatment of steels did increase the resistance to some degree. However, the lack of improved erosion resistance through cold working and heat treatment of alloys was also substantiated by Smeltzer et al (1970).

Further work by Sheldon (1977) on other pure metals, aluminium and copper-nickel alloys, found that a better correlation to erosion resistance is the micro-indentation hardness based on fully work hardened surfaces rather than on annealed hardness (Fig. 2.11). However, Ruff and Weiderhorn (1979) suggest a more suitable quantity would be based on dynamic hardness, which is a more appropriate variable for characterising the erosion of either ductile or brittle materials.

Recent work by Raask (1979) on a range of commercially available steels found that, for steel alloys, there was a non-linear inverse relationship between the erosion wear rate and hardness (Fig. 2.12). He suggested the use of refractory materials with low porosity and strong grain to grain bond properties, to reduce erosion at oblique angles of impact. A similar non-linear relationship for steels was also reported earlier by Wood and Espenschade (1964).

In pneumatic conveying pipelines information of this nature, on the hardness of materials, should provide a reliable guide to the relative erosion resistance of bend materials for the conveying of abrasive products.

Other attempts to correlate erosion resistance have been based on the thermal-mechanical properties of the materials. Smeltzer et al (1970) reported metallographic evidence of local melting at the surface during erosion, and correlated erosion as a function of melting temperature of the material. Ascarelli (1971) introduced a thermal pressure quantity, being the product of thermal expansion

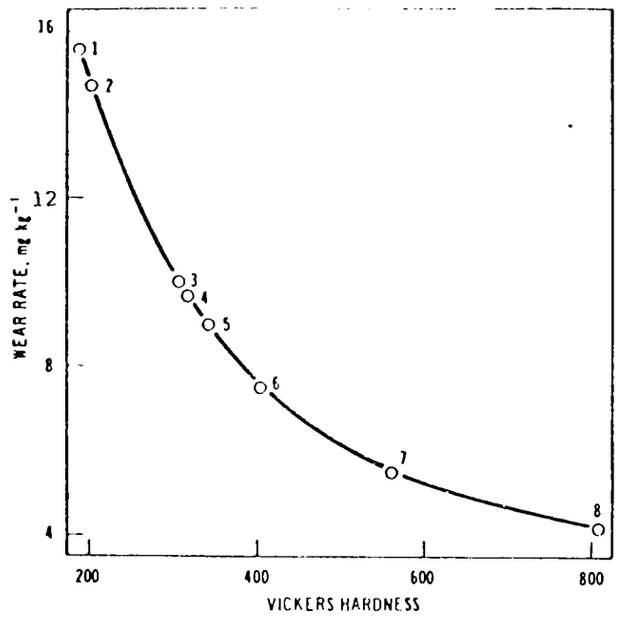

Quartz impaction; velocity 27.5 m^{-1}
1-Mild Steel 3,4,5,6 7-CrB-steel
2-Austenitic Hardened steels 8-Ni-hard.

FIG. 2.12 Variation of Erosion with Steel Alloys of Different Hardness. (Raask 1979)

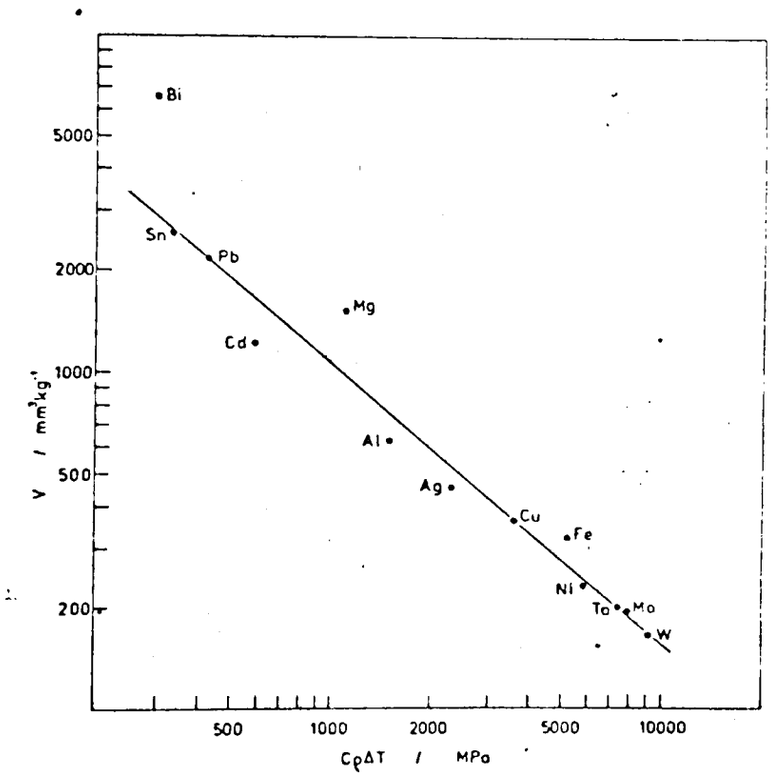

FIG. 2.13 Volumetric Erosion as a function of a Thermal Product. (Hutchings 1975)

coefficient, melting point of the material and bulk modulus, and correlated this quantity with the erosion data produced by Finnie et al (1967). Hutchings (1975) proposed that an improved correlation could be obtained by correlating volumetric erosion with the product of specific heat of the eroded surface, its density and the temperature rise required for melting, and also replotted Finnie's data to support his contention (Fig 2.13). Vijh (1976, 1978) postulated that an even better correlation would be one based on the interatomic bond energy. However, whilst there is some success with these correlations based on pure metals, the predictive ability of these parameters for alloys has yet to be investigated.

Brauer and Kriegel (1965a) investigated the erosion of a variety of ductile and brittle materials, and found that erosive wear can be correlated to the elastic modulus of the materials (Fig. 2.14). Other investigators proposed that the material behaviour during erosion is unique, and that there exists no common material property such as hardness or modulus of elasticity that can be used to describe the erosion process. Thus, Thiruvengadam (1966) introduced the concept of erosion strength to relate the erosion resistance of a variety of engineering materials to the strain energy of the material (Fig. 2.15), although the basis of his experimental evidence was based on cavitation erosion. Kriegel (1968) proposed a quantity called 'wear stress', which is not entirely unique but is a function of yield strength and fracture strength of the material. However, Sheldon (1970) pointed out that these correlations, which are essentially based on strain energy, are only valid for comparing ductile or brittle materials, but not one with the other.

Other material properties such as strain rate sensitivity and stress level have received little attention, but Finnie (1972) reported that residual stresses had no effect on erosion, and Ruff and Weiderhorn (1979) stated that strain rate effects need further study.

2.3 THE MECHANISMS OF EROSION

To date several theories on the mechanisms of ductile erosion have been proposed. These can be broadly classified (Hutchings 1979b) into those which are 'mechanical', in which impact stresses lead to deformation or fracture of the material and its consequent removal, and 'thermal', in which surface melting is postulated as a result of localised energy

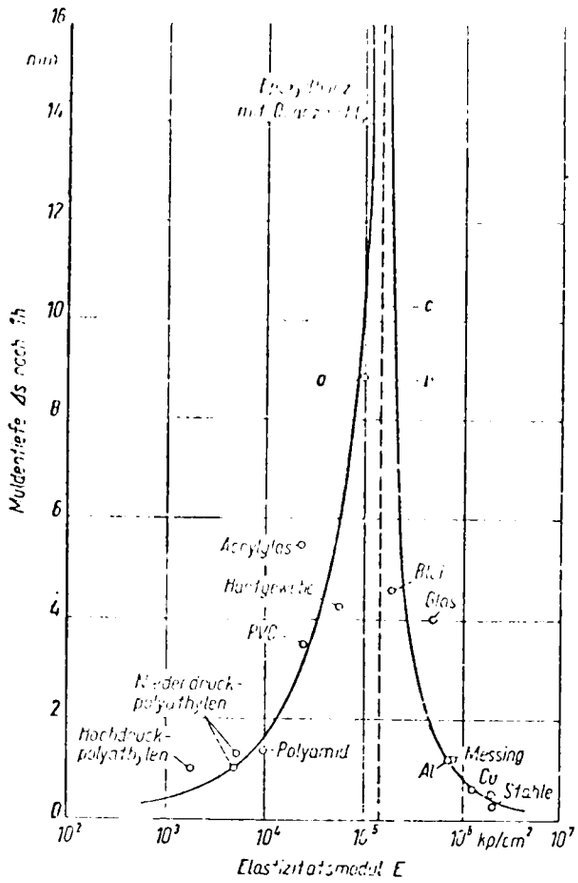

FIG. 2.14 Depth of Erosion as a function of Modulus of Elasticity of a variety of Materials. (Brauer and Kriegel 1965 a)

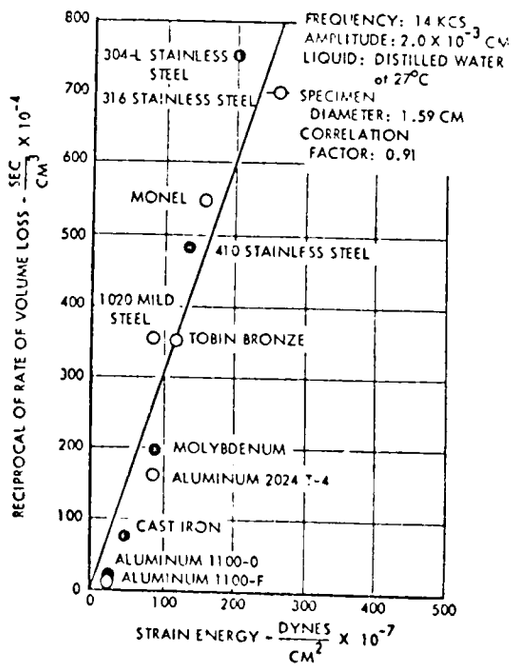

FIG. 2.15 Reciprocal Rate of Volume Loss as a function of Strain Energy of Different Materials. (Thiruvengadam 1966)

released on impact, with metal being removed in the form of molten droplets.

2.3.1 Mechanical Theories

Foremost amongst the proponents of mechanical theories is that of Finnie (1958, 1960, 1972), who developed semi-empirical models based on the concept that a significant proportion of the kinetic energy of each impacting particle will be absorbed by the target material, resulting in surface material removal as a cutting or micro-machining process. Whilst his theory successfully accounts for brittle erosion (Sheldon and Finnie 1966b), his predictive model for ductile erosion is valid for rigid particles greater than 100 μm and only at oblique angles of impact, since his model postulated that no material removal would occur at normal impact. This was contrary to experimental evidence and empirical correction factors were proposed to improve the predictive ability of the model. Furthermore, his model predicts that the velocity exponent is equal to 2, which is again contrary to experimental results. A modification of his original analysis for a velocity exponent greater than 2 and variable with respect to impact angle, was recently provided (Finnie and McFadden 1978).

Bitter (1963a, b) modified Finnie's analysis to account for the erosion at normal impact. He hypothesised that an additional mechanism apart from cutting wear was operative during erosion at high impact angles (Fig. 2.16). This was termed deformation wear, which is a process of strain hardening and subsequent embrittlement of the ductile target. However, his model contains two important wear descriptors which must be obtained experimentally. Neilson and Gilchrist (1968a) further simplified Bitter's analysis and provided a purely empirical scheme for fitting the experimental data. Again, erosion tests must be performed to determine some of the parameters involved in the models.

In contrast to Finnie's single stage micro-machining model, Tilly (1973) proposed a two-stage erosion process based on single particle impact studies. The first stage is the formation of an indentation and possibly the removal of a chip of metal. The second stage is the fragmentation of the particles upon impact, causing further material removal by the scouring action of these fragments. Tilly found that, although secondary erosion caused by these fragments was at a minimum at low impact angles and maximum at normal impact (Fig. 2.17), it does not fully account for the target volume loss at normal impact.

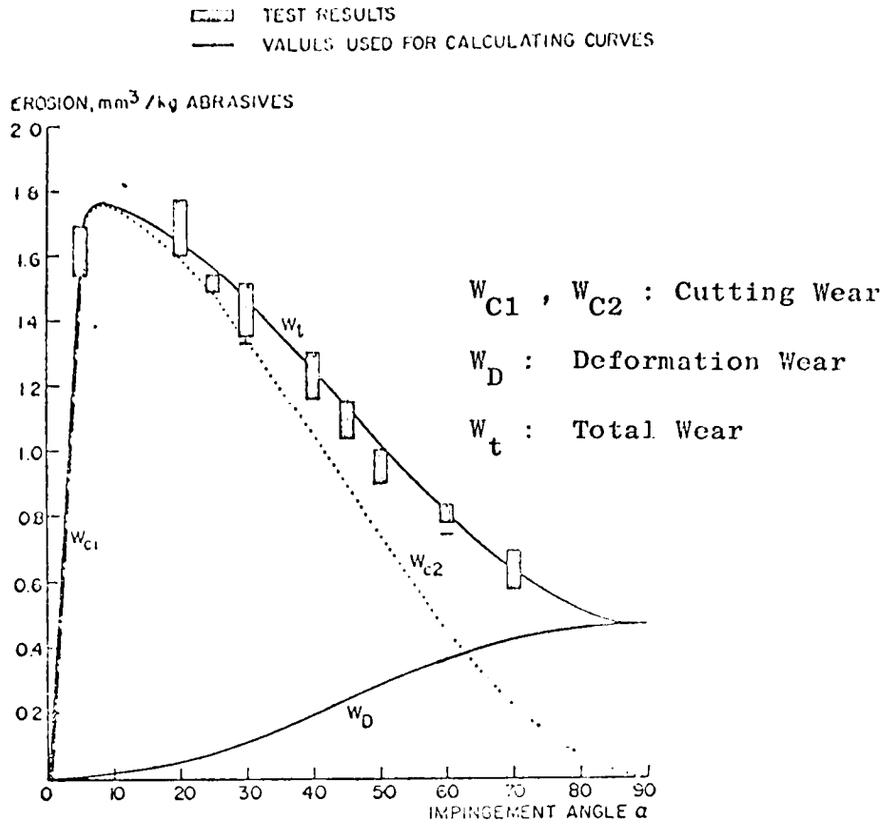

FIG. 2.16 Effect of Erosion with Impingement Angle for 300 μm Cast Iron Pellets against Aluminium at 10 m/s. (van Riemsdijk and Bitter 1959)

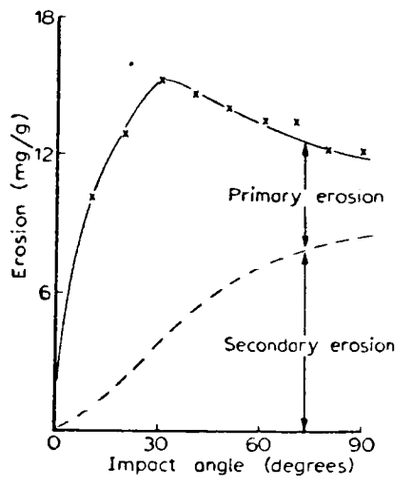

FIG. 2.17 Effect of Erosion with Impact Angle for 135 μm Quartz against H46 Steel at 135 m/s. (Tilly 1973)

Recent single particle impact studies by Hutchings and co-workers (Hutchings 1974, 1977, Hutchings and Winter 1974, 1975, Winter and Hutchings 1975), have provided detailed insights into the mechanism of material removal. Using relatively large steel balls and various irregular projectiles on a variety of ductile metals, they identified two mechanisms of material removal, depending on the particle shape and particle rotation. Ploughing deformation has been observed at oblique angles of impact by spherical or angular particles which can lead to material removal. Cutting deformation is exemplified only by the impact of angular particles and is further categorised into Type I or Type II cutting (Fig. 2.18). Type I cutting occurs when a forward rotation is imparted to the particle upon impact and Type II cutting when backward rotation occurred. Type I cutting plays a predominant role compared to Type II cutting which is a true machining process, and occurs only at a narrow range of rake angle from 0 to -17^{o}. Based on metallographic studies of the impact crater sites caused by ploughing and Type I cutting mechanisms, they found that in both processes an overhanging lip (Fig.2.18) is produced at impact and is subsequently removed by a process of adiabatic shear. Finnie's analysis did not allow for particle rotation and the conceptual model in his analysis would be based on Type I cutting as defined by Hutchings. Hutchings pointed out that all three forms of deformation are operative in multiple particle impact erosion at low impact angles. However, Adler (1979) commented that Hutchings' models are highly idealised and require further modifications before they may adequately reproduce the volume removal rates as obtained in practice.

Head and Harr (1970) employed statistical techniques in their development of predictive models of erosion. Dimensional analysis was used to identify the physical variables involved and empirical models, based on their experimental data, were postulated. However, its predictive ability under untried conditions is limited. Head et al (1973) later modified the original model and introduced another empirical variable but, due to the large number of parameters involved, its application is relatively limited. Moreover, the model proposed is simply a statistical correlation of experimental data obtained without any provision for the mechanism of material removal involved.

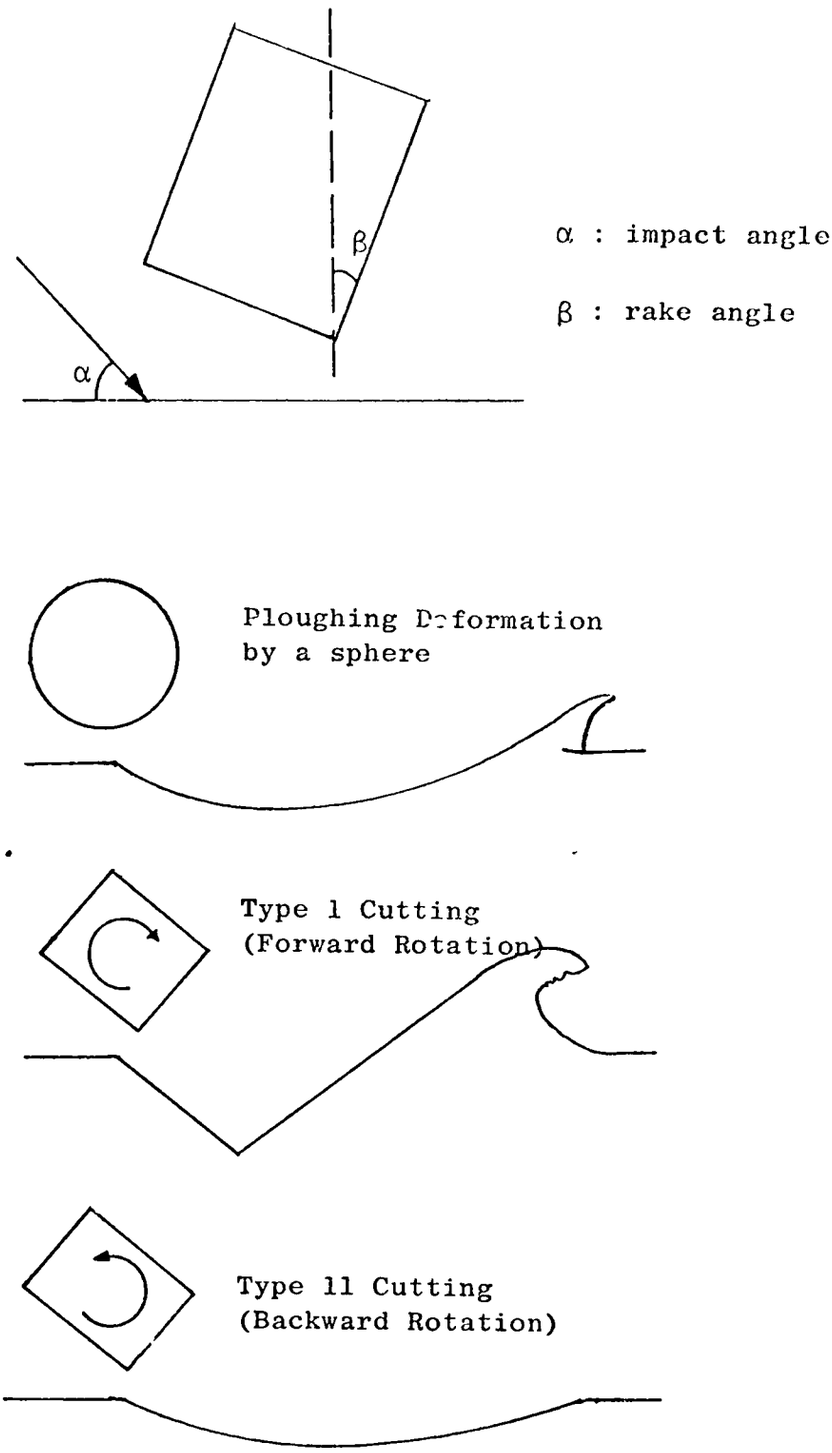

FIG. 2.18 Modes of Material Removal according to Hutchings and co-workers.

2.3.2 Thermal Mechanisms

Proponents of thermal mechanisms of erosion tend to emphasise the correlations observed between erosion rates and thermal properties of the material.

Smeltzer et al (1970) were amongst the first investigators to propose predictive erosion models based on changes in the thermal regime of the target material. Based on purportedly metallographic evidence of the local melting point of several alloys at the target surface during impact, they postulated that, in a general deformation process, up to 95% of the external energy was dissipated by heating and melting at impact, whilst the remaining energy produced mechanical work. In addition, they estimated that the available kinetic energy per impacting particle was sufficiently high to melt the volume of material removed per impacting particle. Thus, on this basis, they proposed two mechanisms of material removal; melting of the surface followed by splattering of the molten material, and bonding of solidified material to embedded particles which are removed by subsequent impacting particles. Predictive models were developed based on these thermal mechanisms, but erosion tests must be performed to evaluate certain parameters involved in these models. Although evidence of target melting was also reported by Jennings et al (1976), they found that, in addition to thermal mechanisms, mechanical mechanisms in terms of kinetic energy input are also operative in the erosion process, although the relative contribution of each class of mechanism to the total volume removal is unknown.

Ascarelli (1971) also introduced the concept of target melting as suggested by Smeltzer et al (1970), but no specific mechanism of material removal is postulated in his correlations, except that the melted material is removed by a stream of impinging particles.

Hutchings (1979b) commented that whilst some temperature rise in the target material adjacent to the impacting particle must be expected, he estimated that, if 80% of the kinetic energy of a 3.5g projectile at 100 m/s is dissipated at impact on a mild steel target, the temperature rise of the target would be about 500^{o}K. This rise is high, but not great enough to cause local surface melting. Thus, he postulated that the fundamental mechanism operative in ductile erosion is primarily mechanical, with melting playing only a subsidiary role in aiding the material removal process.

2.4 CONCLUSIONS

This brief literature survey on solid particle erosion clearly shows that the mechanics of the erosion process are highly complex. The majority of these studies either seek to relate erosion, in terms of mass or volume loss, to some particle and environmental parameters, or seek to relate erosion resistance of various materials to some simple material property of the target material itself. Consequently, several mechanisms of erosion have been postulated. It is obvious that there is no single or universal mechanism of erosion which can adequately explain the phenomena of material removal, and it is probable that several mechanisms are operative simultaneously in the erosion process.

Whilst much useful information has been obtained from these studies, their applicability to predicting the erosion of pipe bends in pneumatic conveying is strictly limited. Thus, there is a need for tests to be carried out with an actual pneumatic conveying rig in order to investigate the erosive wear process in pipe bends.

Some general tests on pipe bend erosion have been reported, but the results obtained are restricted to specific purposes. Recently Mills and Mason have carried out extensive tests on pipe bend erosion and their results, together with the results of others in this field, are reviewed in the next chapter.

Chapter 3

A Literature Survey on Pipe Bend Erosion

3.1 INTRODUCTION

In the erosive wear process in pneumatic conveying, a considerable number of variables are involved. Whilst most of these variables are similar to those involved in general solid particle erosion, there are considerable differences between the importance and magnitude of the relative effects of these variables in both processes. As mentioned in the preceding chapter, some parameters are not applicable to pneumatic conveying whilst others, which have little effect in other solid particle erosion situations, play an important role in the erosive wear process in pneumatic conveying. In addition, there is a group of variables specifically associated with bend geometry and these have not been investigated in the more general solid particle erosion studies.

Whilst information from general solid particle erosion studies helps in the understanding of the erosion process, the mechanics of the erosive wear process in pneumatic conveying is quite different. Thus, it is appropriate to emphasise once again the factors which are primarily involved in the pneumatic conveying erosion process in the following section.

3.2 THE FACTORS INVOLVED IN BEND EROSION

Erosion in pneumatic conveying systems occurs predominantly in pipe bends. Mills and Mason (1975), in a comprehensive review of literature on erosive wear in pipelines, have grouped these factors involved into three broad categories. These are associated with the kinematic impact variables of the impacting particles, properties of the surface material, and the geometry of the bend.

3.2.1 Kinematic Factors

These are associated with the erosive action of the particles, which depends upon :

3.2.1.1 Hardness and strength of the particles,

3.2.1.2 Particle size and shape,

3.2.1.3 Velocity of the particles,

3.2.1.4 Solids to gas ratio or phase density.

3.2.2 Material Factors

These are associated with the erosion of a surface by the particles, which depends upon:

3.2.2.1 Nature of surface,

3.2.2.2 Direction of the particle relative to impact.

3.2.3 Bend Geometry Factors

These are associated with the geometry of the bend, which can be varied in terms of:

3.2.3.1 Shape and size of the pipe,

3.2.3.2 Bend radius,

3.2.3.3 Bend angle,

3.2.3.4 Orientation of the bend.

The relative effects of the variables in the first two categories have been investigated in detail from simulative studies carried out with bench type erosion apparatus. Those associated with bend geometry can only be satisfactorily studied from an actual pneumatic conveying test rig. Whilst several predictive models have been postulated from numerous solid particle erosion studies, there is relatively little information regarding actual pipe bend erosion models. This lack of information is primarily due to the inherent difficulty of obtaining sufficiently accurate quantitiative data from industrial plants (Mills and Mason 1975, Truscott 1975). Although some studies have been carried out in the past, there are still no general predictive bend erosion formulae available for design purposes.

3.3 FULL SCALE EROSION TESTS

The transport of solids by means of pipelines is usually economical if large quantities of materials are conveyed continuously. To a large extent the continuous flow of materials is highly dependent upon the service life of the pipelines. Apart from the operational costs of running the system, one of the major costs involved is the replacement of worn pipes and bends, which may necessitate a partial or even complete shutdown of the whole plant. As bends are a common feature of both pneumatic and hydraulic conveying systems, and are particularly vulnerable to erosion, a number of studies have been carried out recently on the mechanics of bend erosion using full scale test rigs.

Most of the early work on erosion was on hydraulic conveying, particularly with regard to the transportation of abrasive slurries(Worster and Denny 1955, Turcaninov 1962, Brauer and Kriegel 1964). Apart from the problem of bends and pumps (Truscott 1972), there is also considerable wear in the pipeline itself, due to the enormous lengths and capacities of the installations. Marcus (1980) reported that pipelines up to 1000 miles for transporting coal, with a capacity of 25 million tons per year in a 38 inch pipe, are presently being built in the United States. Although the flow velocity in hydraulic conveying is generally not more than 3 m/s, which is low compared to the range from 5 to 30 m/s in pneumatic conveying, the erosion processes in both systems are closely related (Mills and Mason 1975).

3.3.1 Review of Experimental Studies

Apart from the recent work of Mills and Mason (1976 to 1977) which is considered in detail in a later section, information regarding experimental work on bend erosion in pneumatic conveying is relatively limited. Table 3.1 lists the essential data obtained by some of these investigators.

Dolganov and Stejnberg (1966) reported the wear of 45^{o} and 90^{o} bends by a stream of highly abrasive ferrovanadium concentrates. They found that, for the two phase densities considered, the specific erosion, in terms of mass loss per unit mass of material conveyed, was approximately double in 90^{o} bends compared with those in 45^{o} bends.

Kriegel (1970) carried out a series of tests on perspex pipe bends and elbows. Steel sand was used as the conveyed material and the relative effects of diameter ratios and bend angles were investigated. In terms of diameter ratios (D/d), a maximum penetration rate was found to exist at a D/d of 6.5 (Fig. 3.1). This is comparable to the results reported earlier by Brauer and Kriegel (1964) on hydraulic transport of ore, where a pronounced maximum occurred at a D/d of 5.6, although the bends were of mild steel (Fig. 3.2). In both cases either elbows or long radius bends were recommended in order to avoid the rapid wear of bends with D/ds in this region. Kriegel (1970) also substantiated the results reported by Dolganov and Stejnberg (1966) on the influence of bend angle on erosion (Fig. 3.3).

Bikbaev et al (1972, 1973) reported a series of tests carried out over a range of particle velocities and phase densities, on the effect of bend radii on penetration rate. For a constant D/d particle

TABLE 3.1 Details of Empirical Data on Bend Erosion

Source	*Dolganov and Stejnberg (1966)	*Kriegel (1970)	Bikbaev et al. (1972,1973)	Mason and Smith (1972)	Mills and Mason (1975to1977)	*Glatzel (1977)
Pipe diameter (d) - mm	50	?	50	25;50	50	34
Diameter Ratio (D/d)	7.2	0;4 to 13	4.8 to 18	20;12	5.6	0;3.7to17
Bend Angle (γ) - deg.	45;90	15 to 180	90	90	90	90
Bend Wall Thickness (s_w) - mm	?	4.5	?	?	4.0	3.0
Bend Material	steel	perspex	alloys	perspex	mild steel	perspex
Particle	FeV Concentrates	steel sand	quartz	alumina	sand	cast shot
Particle Shape	?	(round)	angular	angular	angular	round
Particle Size (d_p)-μm	20 to 200	?	295	63	70 to 280	440
Particle Density (ρ_p)-kg/m^3	4800	(7600)	2600	(4000)	(2400 to 2800)	7570
Phase Density	5.5;10	?	0.57 to 4.35	0.5;3.8	0.5 to 8.0	0.5 to 3.0
Conveying air velocity (c_a) - m/s	28	?	30.4to54.8	30;100	15 to 32	10 to 65

*Source: Glatzel (1977)

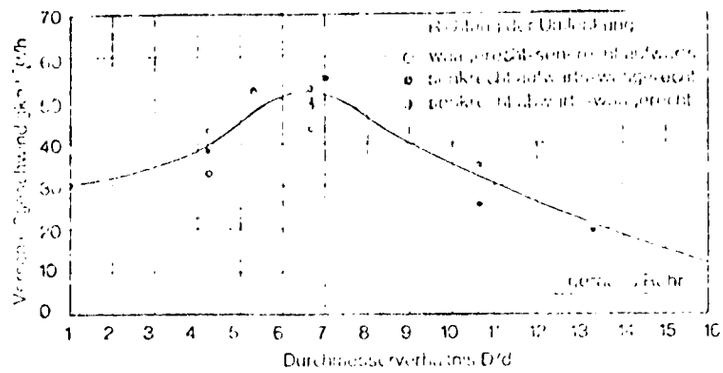

FIG. 3.1 Effect of Diameter Ratio (D/d) on Penetration Rate in Pneumatic Transport. (Kriegel 1970)

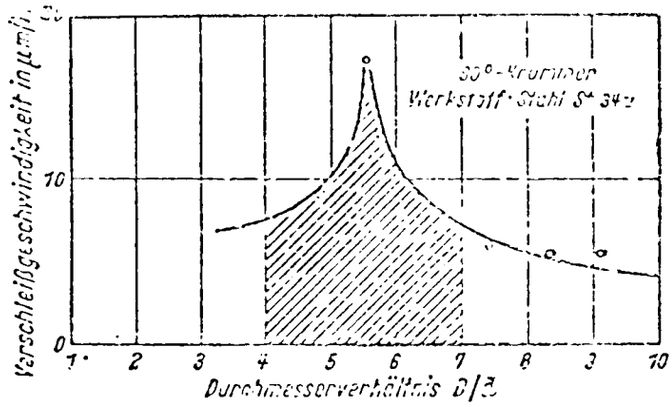

FIG.3.2 Effect of Diameter Ratio (D/d) on Penetration Rate in Hydraulic Transport. (Brauer and Kriegel 1964)

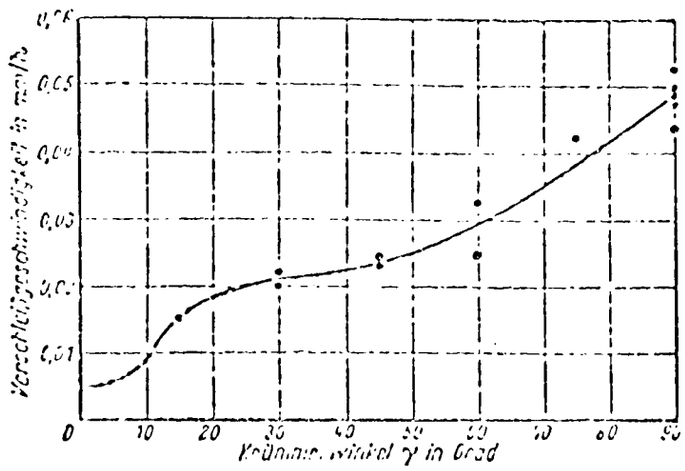

FIG. 3.3 Influence of Bend Angle (γ) on Penetration Rate. (Brauer and Kriegel 1964)

velocity was found to have a dominant effect on penetration rate (Fig. 3.4). A formula for determining the site of maximum wear, which was found to be independent of phase density and particle velocity, was also given.

Mason and Smith (1972), in contrast, reported the formation of primary and secondary wear craters along the outer bend wall surface and that deflection of the particles by these wear pockets could cause erosion of the inner bend wall surface (Fig. 3.5). They also found that the mean wear rate is influenced by phase density and velocity. In a later paper (Arundel et al 1973), it was reported that a critical phase density, in terms of relative wear rate, exists at a phase density of 24, based on information obtained from industrial data.

Glatzel (1977) investigated the erosion of perspex pipe bends with a view to developing a semi-empirical model for predicting the service life of pipe bends. Two series of tests were carried out using cast steel shot as the conveyed material. The first series of tests consisted of determining the fundamental erosion quantities from impact erosion of flat perspex specimens, such as depth of crater and volume loss at various impact angles and particle velocities. In the second series of tests, the erosion of perspex pipe bends with a range of diameter ratios was investigated. The relative effects of particle velocity and particle concentration profiles in the bend were determined. From both sets of results non-dimensional erosion quantities were determined and, from these quantities, a non-dimensional parameter for predicting the service life of pipe bends was developed.

3.3.2 Review of Industrial Studies

In this section some of the recent studies which have been carried out in industry, although for a specific purpose, are briefly reviewed.

3.3.2.1 Bend Geometry

As early as 1938, Schmidt suggested the use of elliptic bends, with a long sweep at the upstream end and a short radius at the downstream end, for minimising bend erosion. From observations on bend wear profiles, Schmidt postulated that such a design would ensure an elliptical erosion pattern, distributed over a wider surface area than in a conventional bend, thus reducing erosion per unit surface.

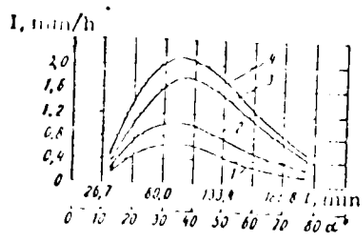

FIG. 3.4 Influence of Particle Velocity and Phase Density on Bend Wear Profile.

Curve	Velocity	Phase Density
1	33.1	4.35
2	39.2	3.01
3	50.0	2.93
4	54.8	2.10

(Bikbaev et al 1973)

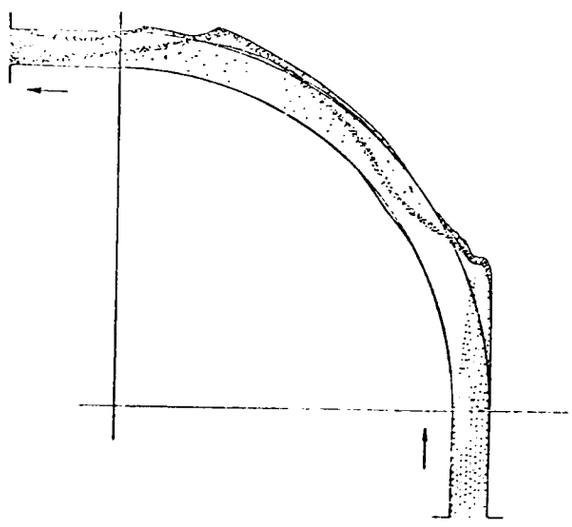

FIG. 3.5 Bend Erosion Pattern - After Some Wear

(Mason and Smith 1972)

Zenz (Zenz & Othmer 1960) suggested a more practical solution would be the use of 'square' elbows or "Tees". Some of the impacting particles would fill up the blanked arm of the bend and form a natural curvature, thereby shielding the bend against the impinging action of the following particles. Should blockage occur, a plug in the blanked arm could be removed to facilitate clearing.

Solt (1977) carried out a series of tests to investigate the wear resistance of a variety of bend designs, using different particles and a range of velocities. All the bends were of aluminium in order to reduce the time required for failure. "Tee" bends were found to have a longer service life than all the other bends.

The author has also tested a commercially available, proprietary "Tee" bend with a recess in one end, and the results are presented in the relevant chapters of this work.

3.3.2.2 Bend Liners

The recent development of a variety of commercially available wear resistant lining materials has led to several reports on their relative merits and applications in both pneumatic and hydraulic transport systems.

Kut (1971) described the economic advantages of applying epoxy coatings for protection against wear in pipelines, both internally and externally.

Lehrke and Nonnen (1975) reported the considerable reduction of wear by applying fused-cast-basalt linings into the pipelines, and quoted several successful industrial applications.

Olsen (1976) reported the superiority of fused-ceramic linings as a wear resistant material compared to ordinary materials.

Yang et al (1979) reported tests on a variety of refractory materials in a specially built, high temperature, dilute phase conveying test rig. The relative wear resistance of these materials was assessed in order of merit over a range of test conditions.

Several reports have appeared recently on industrial tests carried out on different proprietary bends which have been installed in the mining industry :-

Kostka (1978) and Faddick and Martin (1978) both described tests on several 'Radmark' flatback and 'Esser' circular segmented bends, with a variety of replacable lining materials such as Nihard and rubber, in the pneumatic conveying of coarse gravel and tunnel muck respectively. Firstbrook (1980) also reported tests on similar bends in a coal transport plant, whilst Marcus et al (1980) reported similar tests in the pneumatic stowing of waste rock in a gold mine.

In some of the above tests a special 'Radmark' dirt box bend, which is a bend-within-a-bend, has also been evaluated. The relative merits of the various lining materials and the different bend designs, however, are by no means conclusive yet and further tests are currently in progress. An interesting feature is that the authors all reported on the comparative ease of replacing liners in the flatback bends compared to circular bends.

3.3.3 Theoretical Investigations

Brauer and Kriegel (1964, 1965a, b) extensively investigated the influence of diameter ratio (D/d) on erosion by using both hydraulic and pneumatic test rigs. From detailed experimental studies of particle trajectories, they found that the angle of impact (β) is determined primarily by D/d. This is not to be confused with the angle of attack (α), which is defined as the inclination between the particle trajectory and the original flat surface, which remains constant. The angle of impact (β) which is defined as the inclination between the particle trajectory and the eroded material surface, will, over a period of time, vary from $\beta = \alpha$ to 90^{o} (Fig. 3.6). For 90^{o} bends the critical impact angle (δ_A) is given by

$$\cos(\delta_A) = \frac{D/d - 1}{D/d + 1} \qquad (3.1)$$

This is applicable for a range of D/d where the angle of fracture (δ_g) coincides with critical impact angle (δ_A). Within this range of D/d the authors suggest that δ_g should be determined by the path

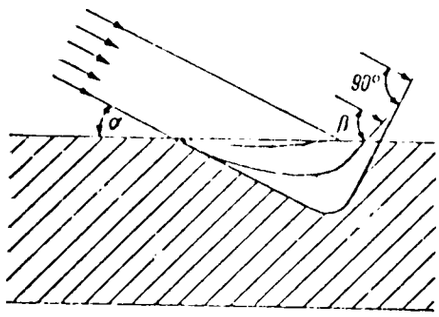

FIG. 3.6 Variation of Impact Angle with Time.

α : original impact angle

β : effective impact angle after some wear

(Brauer and Kriegel 1965 a)

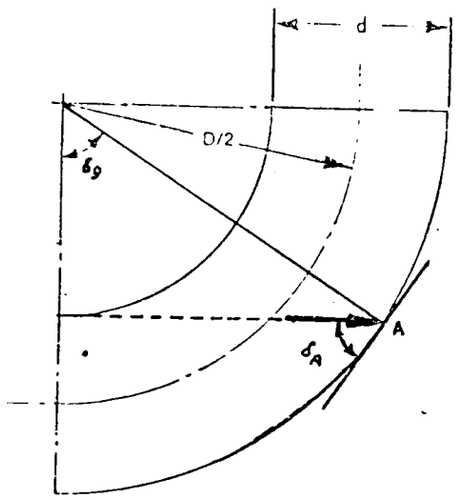

FIG. 3.7 Relation between Angle of Fracture (δ_g) and Critical Impact Angle (δ_A).

(Kriegel 1970)

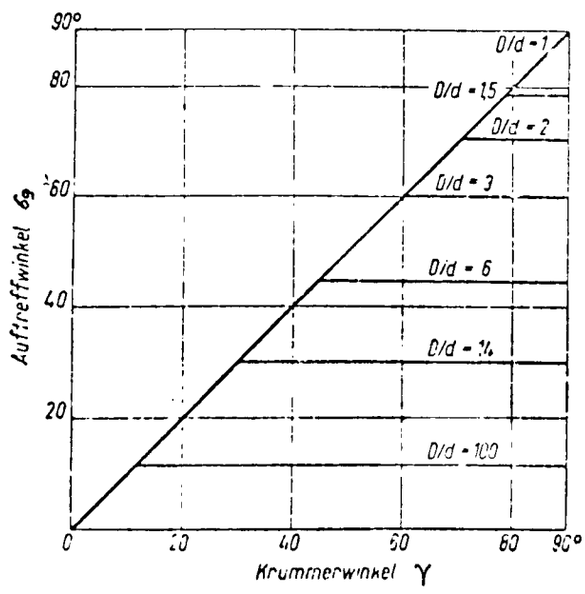

FIG. 3.8 Influence of (D/d) on the variation of angle of fracture (δ_g) with bend angle (γ).

The horizontal lines indicate the 'wear free' bend angle range for the stated values of D/d.

(Brauer and Kriegel 1965 a)

of the particle trajectory along the boundary of the inner bend radius as shown in Fig. 3.7.

For D/d greater than one, δ_g is less than 90^o. The influence of D/d in terms of δ_g and bend angle (γ) is shown in Fig. 3.8. This figure shows the extent of the 'wear free' range of bend angle for each D/d. without any effect on the estimated angle of fracture (δ_g).

Glatzel (1977) also investigated the influence of D/d and found that δ_g coincides with δ_A for D/d between 4 and 16. Glatzel was able to determine the particle velocity (w_p) in his test rig by means of high speed photography. Tests were carried out over a range of velocities from 3.9 to 28 m/s, and D/d from 0 (pipe elbows) to 17. In terms of non-dimensional volume erosion, the velocity exponent varied from 3.1 for pipe elbows to a constant 2.3 for a range of D/ds. In all cases these exponents are only valid for particle velocities greater than 6 m/s (Fig. 3.9).

A semi-empirical model for determining the service life of pipe bends is given by

$$t_B^* = \frac{1}{(C_{Rr}^* \; w_{pr}^{*4} \; \Delta s_w^* \; \sin\beta)_{max}} \qquad (3.2)$$

where t_B^* is the non-dimensional service life of bends, w_{pr}^* and C_{Rr}^* are the non-dimensional particle velocity and concentration profiles across the cross sectional area of the bend respectively, Δs_w^* is the non-dimensional depth of erosion obtained from a flat plate specimen under otherwise identical experimental conditions, and sin β is the angle of impact, defined by the bend geometry.

Equation (3.2) can be rewritten mathematically into

$$t_B^* = \frac{4 t_B \dot{M}_p}{\pi d^2 \rho_p s_w} \qquad (3.3)$$

where

$$t_B = \frac{\rho_p \; s_w \; F_s}{\dot{M}_p} \cdot \frac{1}{(C_{Rr}^* \; w_{pr}^{*4} \; \Delta s_w^* \; \sin\beta)_{max}} \qquad (3.4)$$

Fig. 3.10 shows the results predicted by the model in equation (3.4) for a range of bend materials. Although the models provide satisfactory agreement between calculated and experimental values, they involve rigorous mathematical treatment of the particle concentration

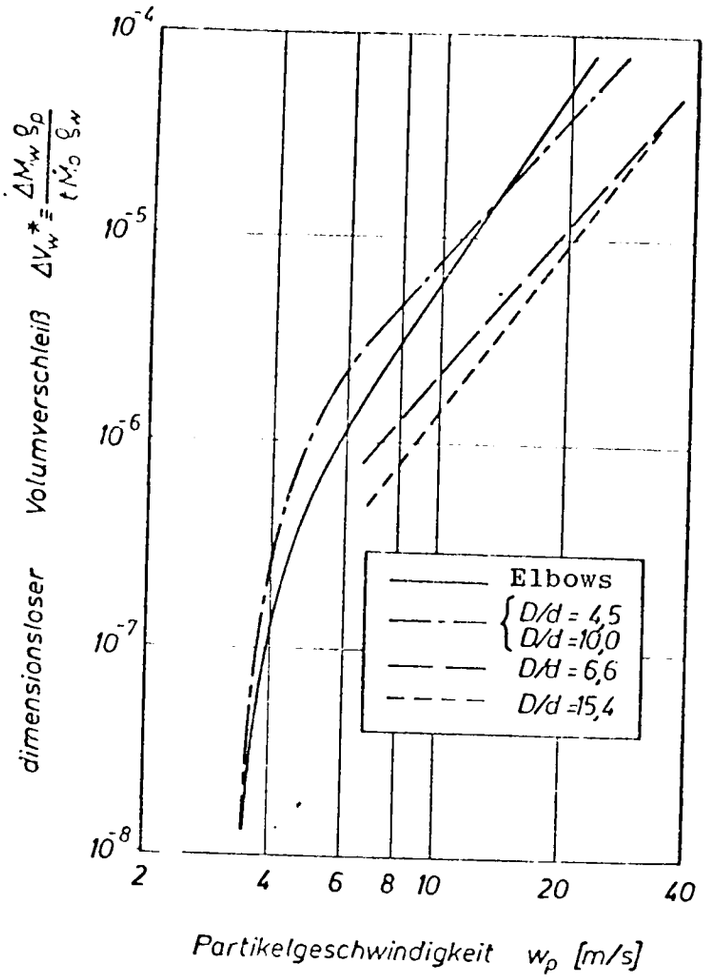

FIG. 3.9 Variation of Non-dimensional Volume Loss with Particle Velocity. (Glatzel 1977)

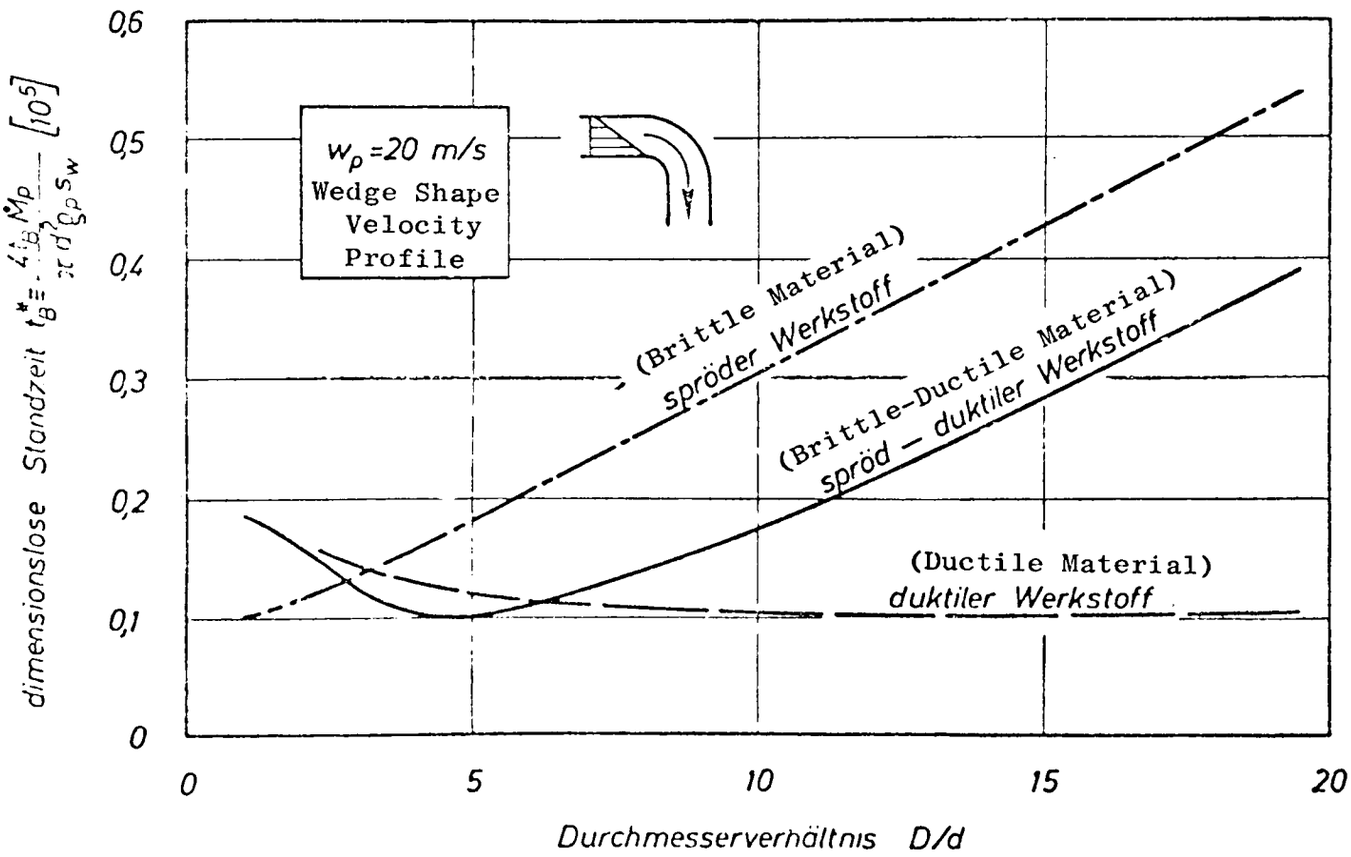

FIG. 3.10 Influence of D/d on Service Life of Bends in Terms of Non-dimensional Time. (Glatzel 1977)

and velocity profile terms. Furthermore, the predictive ability of the model is restricted to large spherical particles greater than 100μm conveyed at low phase densities and high velocities.

Ryabov (1978) reported a formula for determining the service life of pipe bends, based on information obtained from pneumatic sand feeding rigs in locomotive service facilities. The formula is given by

$$t_B = \frac{h}{10 \times 10^{-8} \mu\, k_\mu\, V\, k_w\, k_p\, k_r\, k_\phi\, A} \qquad (3.5)$$

where h is the bend thickness, μ is the material concentration by weight, V is the conveying air velocity, and k_μ, k_w, k_p, k_r and k_ϕ are the respective coefficients of concentration, wear factor, bend orientation, bend radius, and bend angle, and A is the coefficient of abrasiveness and particle size. However, no experimental evidence regarding its predictive ability is mentioned by the author.

Krasnov and Sharafiev (1978) reported industrial tests carried out to investigate the erosion of an inclined, descending, 200 mm pipeline, which was being used to convey a 3.2 mm aluminosilicate catalyst. A simplified semi-empirical expression for predicting the probability of 'failure free' operation of inclined pipelines, in terms of penetration rate as a function of 'wear macrowaves' or surface ripples, was given.

Soo (1977, 1980) in a theoretical treatment of erosion proposed several mathematical models, in terms of dimensionless erosion energy quantities, which involve several energy and material property parameters which must be experimentally determined.

Yeung (1979) proposed that the relative erosion rate (E_{max}) can be expressed by

$$E_{max} \propto w^3 Z_L \qquad \text{for large W,} \qquad (3.6)$$

$$E_{max} = w^{3.93} Z_L \qquad \text{for small W} \qquad (3.7)$$

where W is the initial flow velocity of the mixture, and Z_L is the phase density.

While his models are in agreement with the experimental results obtained by Mason and Smith (1972), the theory and analysis behind the models also involves a rigorous mathematical treatment of the fluid dynamics of gas-solid flow in a curved pipe, together with

certain highly idealised assumptions. Furthermore, the models are only valid for dilute phase suspension flows.

3.4 THE WORK OF MILLS AND MASON (1976 to 1977)

In recent years Mills and Mason have carried out a major series of tests on a full scale pneumatic conveying rig to investigate the various parameters involved in the erosive wear of pipe bends. Sand of different particle sizes was conveyed on a batch type basis, at a range of conveying air velocities and phase densities, through two horizontal loops in a rectangular configuration. The 90° bends tested at the corner of each loop were all of mild steel, 140 mm bend radius and 50 mm bore.

3.4.1 Effects of Phase Density

Their first series of tests was carried out to investigate the influence of phase density (the dimensionless ratio of the mass flow rate of solids conveyed to the mass flow rate of air used) on specific erosion (the mass eroded from a bend per unit mass of material conveyed). 70 μm sand was conveyed at a constant velocity of about 25 m/s at a range of phase densities from 0.5 to 8. Their results are presented in Fig. 3.11. Whilst this shows a definite trend towards a slight decrease in specific erosion rate with increasing phase density, the authors noticed that there was considerable variation in bend wear profiles over this range.

Further tests were carried out to investigate this aspect of the erosion process and the results are presented in Fig. 3.12. For a given mass eroded, the depth of wear was found to increase quite considerably with increase in phase density. Penetration rate was shown to have an over-riding influence on erosion, over that of mass eroded, in respect of the phase density of the conveyed product. The net effect is that the mass of product which can be conveyed through a bend before failure occurs actually decreases with increase in phase density. An analysis for evaluating the potential conveying capacity and service life of the bends in the form of a series of graphs was presented, based on empirical data for specific erosion and mass eroded to failure.

The authors also showed that increasing phase density has the effect of progressively increasing the pipe angle at which maximum erosion

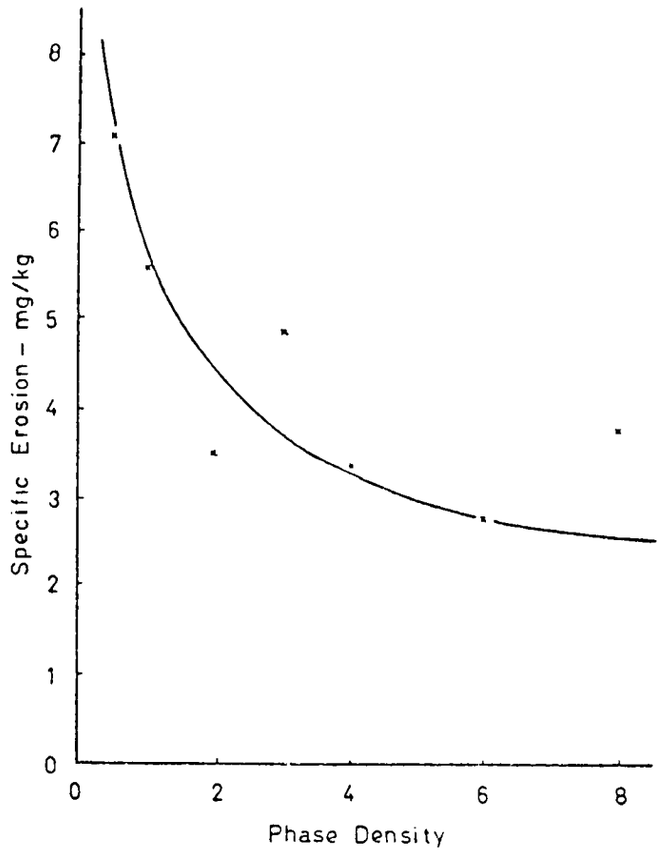

FIG. 3.11 Variation of Erosion with Phase Density

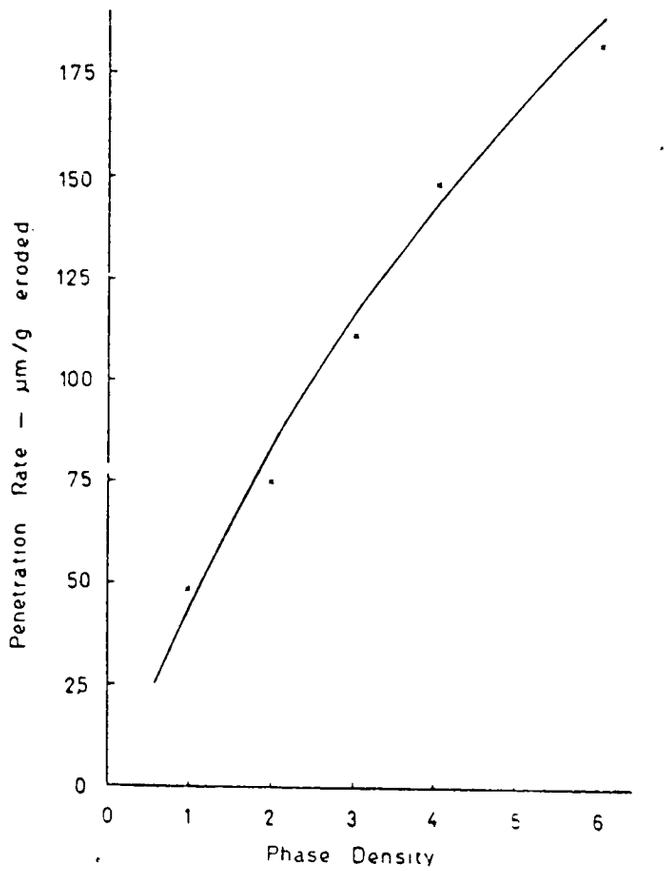

FIG. 3.12 Variation of Penetration Rate with Phase Density

occurs (Fig. 3.13), and that a progressively narrower path cuts through the bend (Fig. 3.14). A log plot of Fig. 3.11 indicated that the variation of erosion with phase density could be modelled as

$$\text{erosion} \propto \text{phase density}^{-0.37}$$

However, further analysis based on 230 μm sand suggested that the phase density exponent is considerably affected by the condition of the conveyed product. It varies from -0.16 when fresh to -0.38 for the worn and degraded sand at the end of the test programme. In terms of individual values, plotted on the same basis, the exponent showed an even more dramatic change from -0.16 to -0.73. The authors suggested that particle shape or sharpness might be responsible for this uncertainty regarding the actual value.

3.4.2 Effects of Conveying Velocity

In their second series of tests to investigate the influence of conveying velocity, 230 μm and 70 μm sand was conveyed at a range of velocities from 15 to 31 m/s and 25 to 31 m/s respectively, both at a constant phase density of 2 throughout the series.

In terms of the mass eroded from the bends, the authors found that the variation of specific erosion with velocity could be expressed by

$$\text{specific erosion} \propto \text{velocity}^{2.65}$$

and the same velocity exponent was obtained with recirculated sand, as shown in Fig. 3.15. Further tests by the authors showed that, for a given mass eroded, the depth of penetration of the particles into the bend wall surface also increased as the conveying velocity increased. As a result, less mass is required to be eroded before failure occurs. Consequently, bends will fail in an even shorter time than that predicted by specific erosion rates alone.

The authors suggested a modified power law relationship, in terms of actual pipe bend failure, in which the erosion rate is given by :

$$\text{pipe bend erosion} \propto \text{velocity}^{4.5}$$

Curves for evaluating the conveying capacity and service life of the bends with respect to velocity for a given set of conditions were also presented.

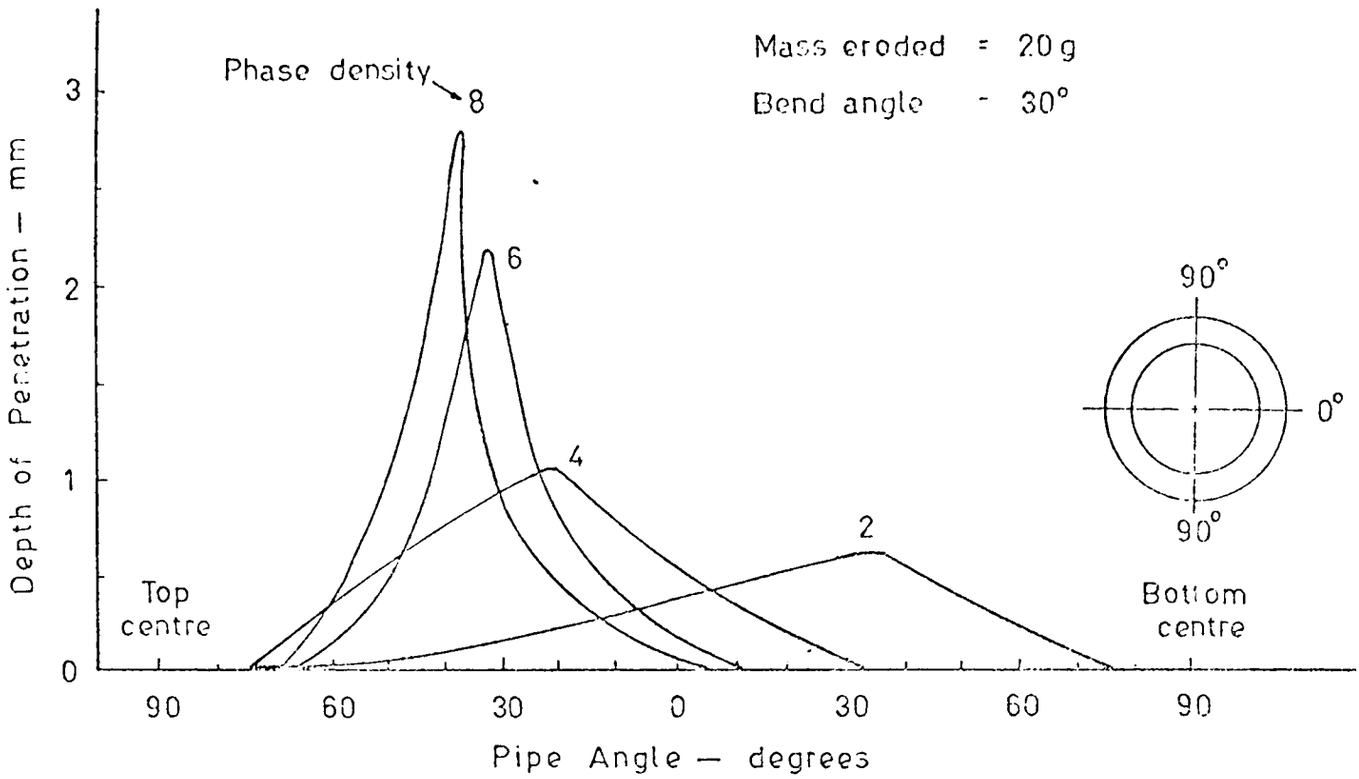

FIG. 3.13 Influence of Phase Density on Pipe Wear Profile

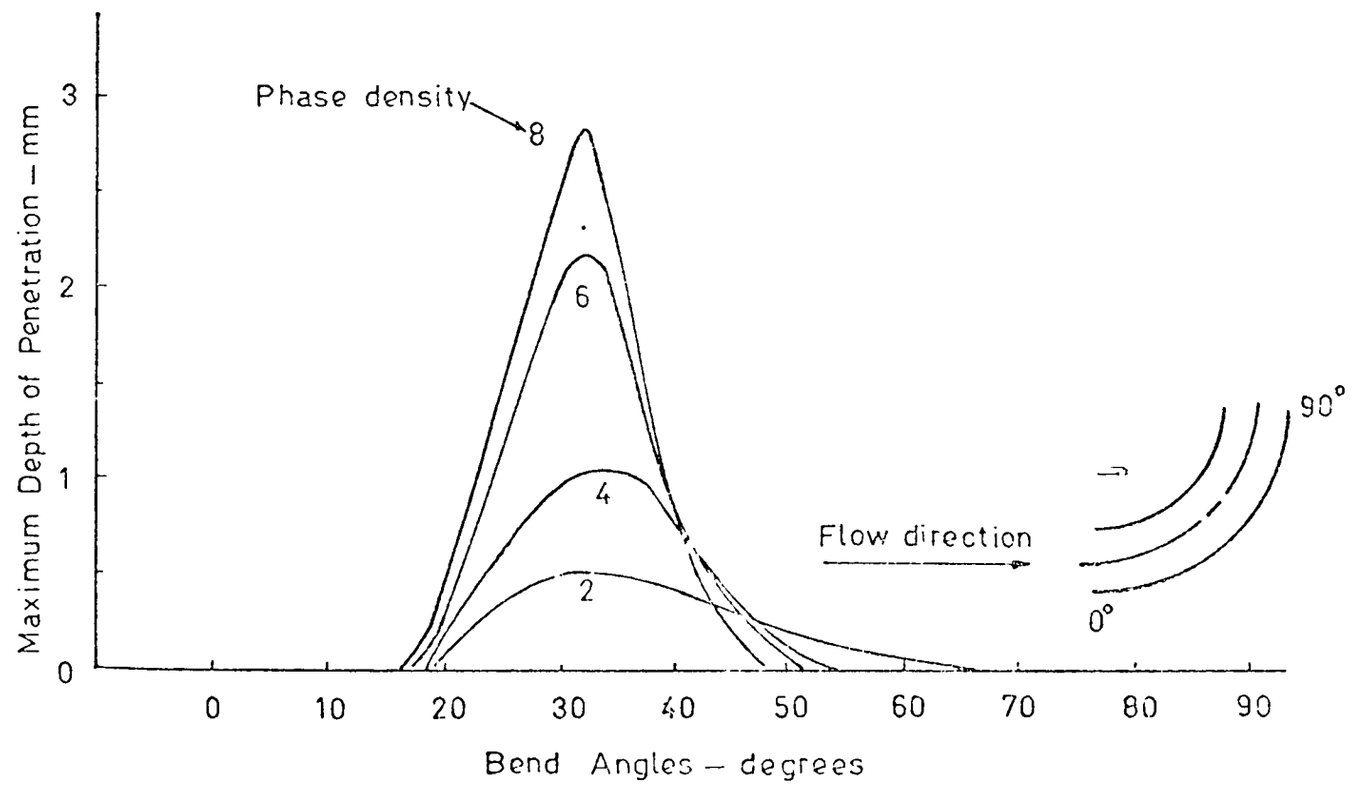

FIG. 3.14 Influence of Phase Density on Bend Wear Profile

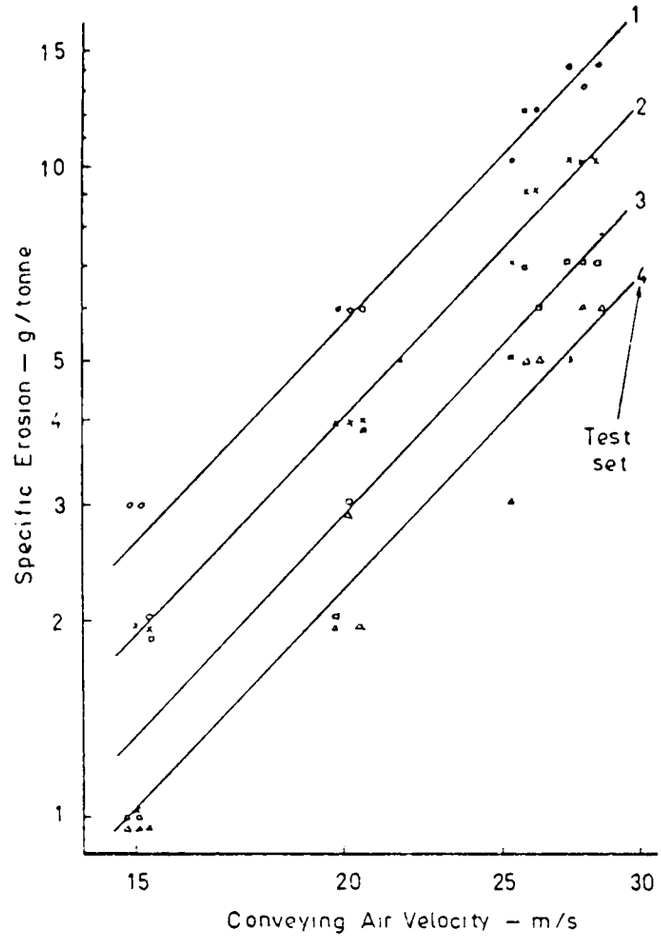

FIG. 3.15 Variation of Specific Erosion with Velocity

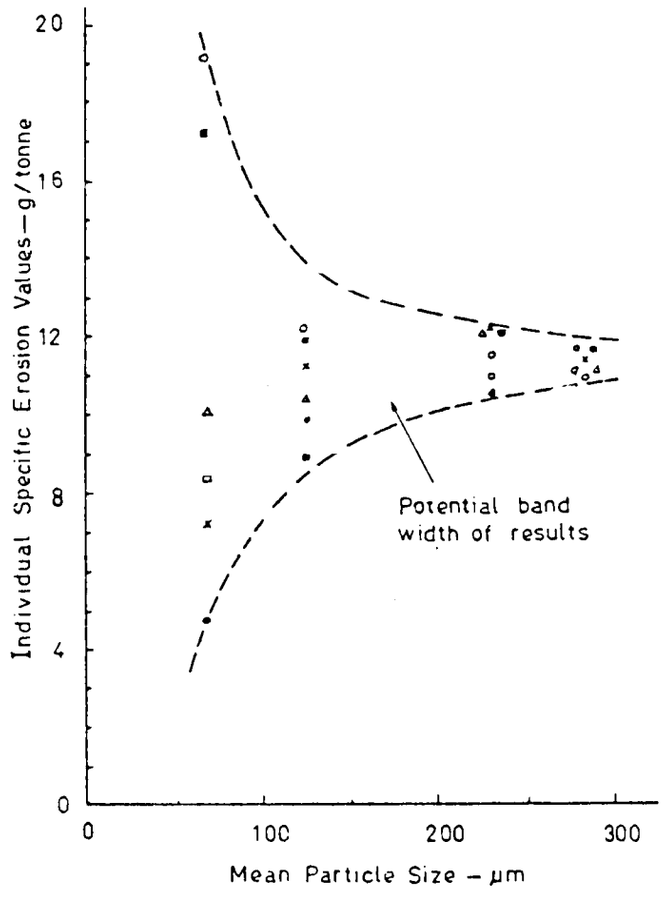

FIG. 3.16 Variation of Individual Specific Erosion Values with Mean Particle Size

3.4.3 Effects of Particle Size

For this investigation four batches of sand of different mean particle size were conveyed at a constant velocity of about 26 m/s and phase density of 2 throughout.

The mean specific erosion values obtained by the authors were found to be remarkably consistent for each of the four different particle size batches tested. However, in terms of individual results, there was considerable scatter with the 70 μm sand as compared with the 280 μm sand (Fig. 3.16). This degree of scatter was attributed by the authors to be a contributing factor in the premature failure of bends.

In terms of penetration rate, particle size was shown to have a significant effect (Fig. 3.17). Observation of the bend wear profiles by the authors indicated that the increase in penetration rate with smaller particle sizes was due to a much narrower cut through the bend (Fig. 3.18), resulting in a lower mass eroded at the point of failure than with larger size particles.

From an analysis of the influence of particle size on bend life the authors suggested conveying materials of large particle size from an erosion point of view. It was shown that a four-fold reduction in bend life and conveying capacity could result when conveying 70 μm sand compared with 280 μm sand.

Particle size was also shown to have a marked effect on the appearance of the eroded surfaces as well as an important factor in particle wear and degradation.

3.4.4 Premature Failure of Bends

An analysis of the factors influencing the premature failure of a number of pipe bends was discussed by the authors and was reported to be dependent upon a number of combinations of variables. Low conveying velocity, high phase density, fine powders and worn or rounded particles were considered to be the most significant factors. However, the authors also mentioned that there was a considerable element of unpredictability which must be taken into account regarding the effect of these combined variables.

The sources of these premature bend failures were attributed by the authors to the combined effects of the fine powders being influenced

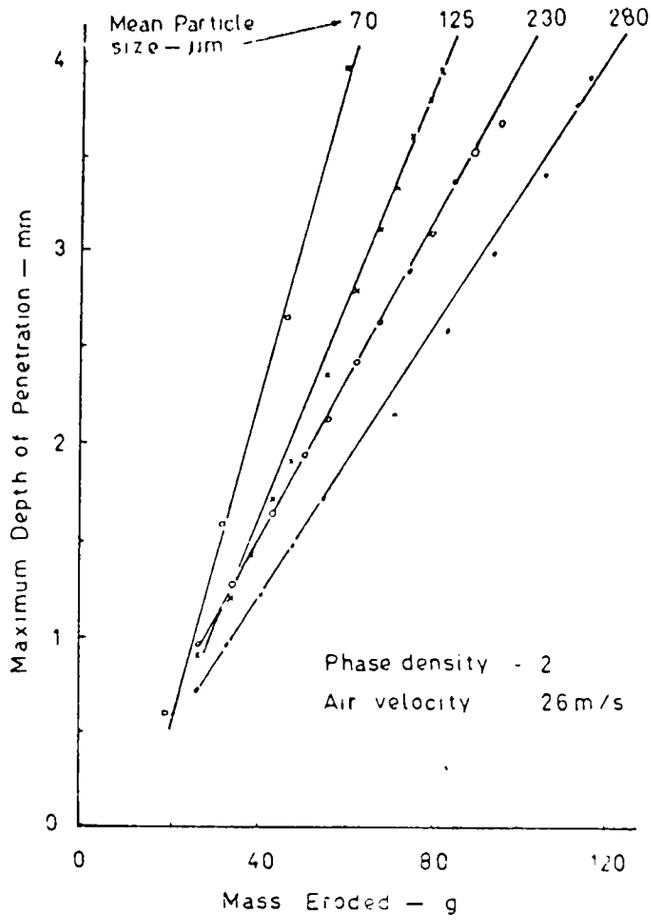

FIG. 3.17 Influence of Particle Size on Rate of Penetration

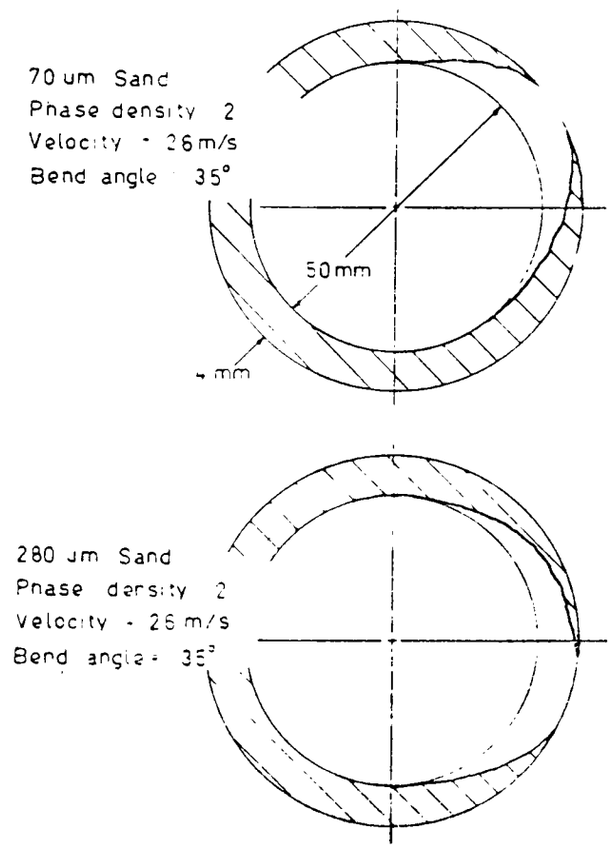

FIG. 3.18 Influence of Particle Size on Pipe Section Wear Profiles

considerably by the secondary flows induced by the bends, and the resulting impact angle of the particles in terms of maximum penetration and maximum mass eroded.

3.4.5 Influence of Other Variables

In the work carried out by the authors, a single batch of sand was used for a series of tests. With constant recirculation, some of the results obtained were considerably influenced by the subsequent change in particle shape, due to wear and degradation of the conveyed product.

Although, in terms of specific erosion, less mass was eroded with worn and degraded sand than with fresh angular sand, in terms of penetration rate, the situation was markedly reversed (Fig. 3.19). The large degree of scatter for the worn sand was considered to be partly responsible for the premature failure of some of the bends.

The influence of particle shape was closely related to velocity. Bends were observed to fail relatively rapidly when worn sand was conveyed even at low velocities. This was attributed to a change in the nature of the erosion process, below a certain transition velocity, as a result of the change in particle shape.

The degradation of the particles was considered to be mainly caused by the bends, whilst the magnitude of the problem was mainly influenced by the conveying velocity. The authors suggested the problem could be overcome considerably by using a dense phase conveying system.

3.5 CONCLUSIONS

The limited predictive ability of erosion in actual pipe bends, based on information obtained from numerous solid particle erosion studies, has led several recent investigations using full scale test rigs. These were used to provide a more realistic evaluation of the study of the mechanics of the bend erosion process.

Tests have also been carried out on a variety of proprietary bends, and with a range of lining materials. Although these may have solved specific erosion problems, they have contributed little to a better understanding of the erosion problem. Industrial data has also proved to be of limited value, for little correlation has been obtained between service data and experimental test results.

While a number of semi-empirical and theoretical bend erosion models have been postulated, their predictive ability is only applicable to specific conditions. This is primarily due to a certain number of highly idealised assumptions involved in the analysis.

Recently, Mills and Mason have published a major series of papers on the erosive wear of pipe bends, but their results have been limited to the effects of phase density, conveying velocity and particle size, and to relatively narrow ranges of these variables. Furthermore, their work has been based only on one particular material conveyed, i.e. sand, and on bends with a single diameter ratio of 5.6. Whilst their work has considerably contributed to our knowledge of the erosion process in pipe bends, further work is still necessary. On the basis of their work, another major programme of tests was undertaken to investigate the influence of other variables involved, for a better understanding of the mechanics of bend erosion process, and to present results of practical value to industry.

****

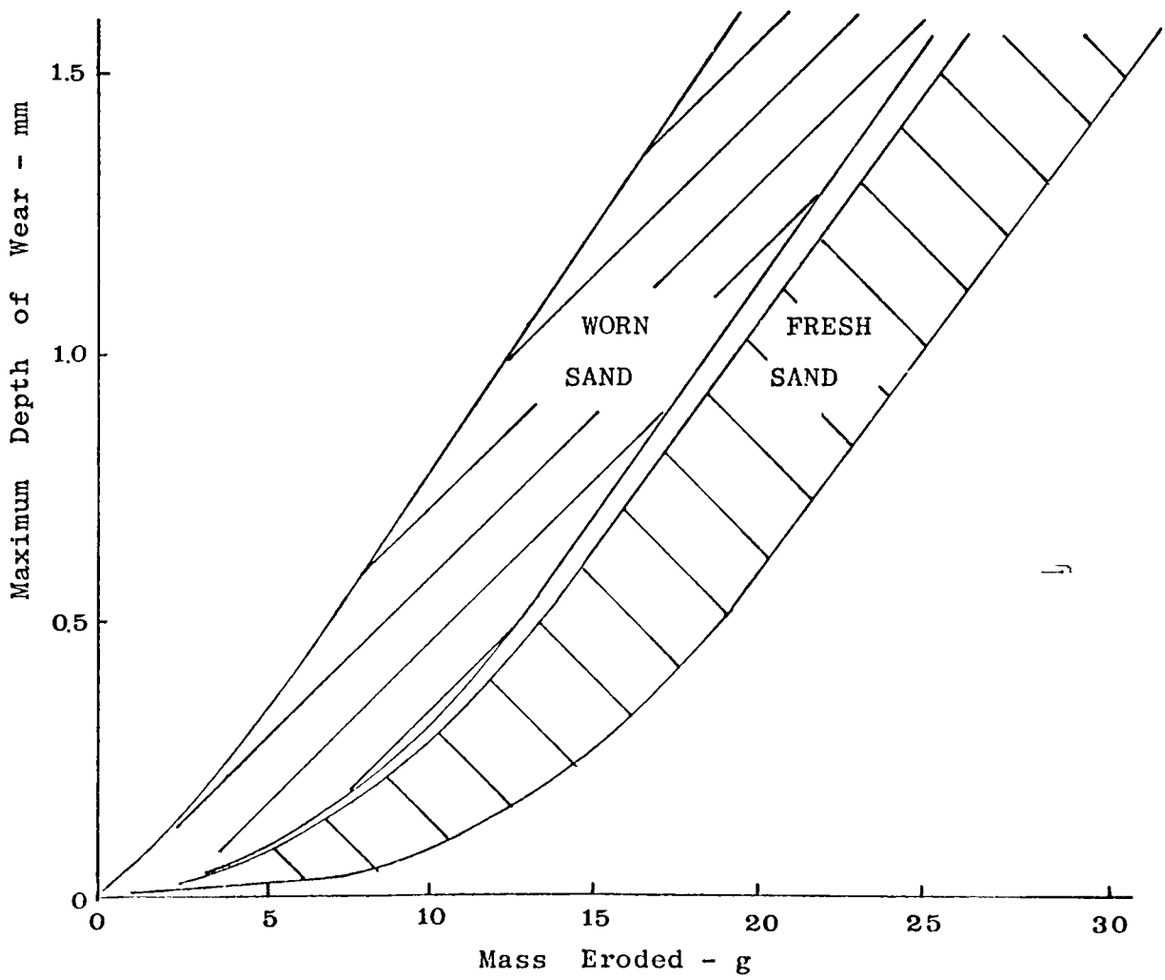

FIG. 3.19 Influence of Product Condition on Penetration Rate

Chapter 4

Experimental Research Plants and Equipment

4.1 INTRODUCTION

The need for full scale tests, in order to provide a better understanding of the mechanics of the bend erosion process in pneumatic conveying, and to present results of practical value to industry, has been clearly demonstrated by the work presented in the preceding chapters. Thus, in the work carried out by the author, two existing, separate full scale test rigs were utilised. Each of these rigs, because of its design capability, was used separately for a specific programme of tests, and the respective function and operation of both rigs is briefly described below.

4.2 LOW PRESSURE RIG

This consisted of a blow tank of about 1 m^3 capacity, with a similarly sized hopper mounted on load cells vertically above. Air was supplied by a Roots type blower capable of delivering about 0.07 m^3/s at a pressure of 2 bar absolute. A smaller sized blow tank was incorporated as a loading facility for charging the rig with new material, which could be discharged later via a short conveying line into an off-loading hopper. Fig. 4.1 is a photograph of this plant, and Fig. 4.2 shows its diagrammatic layout. A full description of this rig, including plant operation, control and instrumentation, is given in Mills (1977).

4.2.1 Operation and Control

Briefly, it was a batch type system with the material being conveyed from the blow tank, through the test loops and into the receiving hopper. With a capacity of about 1 m^3, it allowed up to 1.5 tonnes of material to be conveyed in one cycle. For each test run, the powder mass flow rate was continuously monitored by a recording instrument via the load cells. The conveying air mass flow rates were metered by two rotameters in the inlet line to the blower, and another rotameter in the off-take to atmosphere line. Thus, both phase density and conveying air velocity could be quickly and easily obtained, and start-up and shut-down transient effects were limited to a few seconds.

4.3 HIGH PRESSURE RIG

This consisted of a 1.13 m^3 blow tank capable of working up to a maximum pressure of 7 bar absolute. Oil-free air was supplied by a reciprocating

FIG. 4.1 Low Pressure Rig Plant

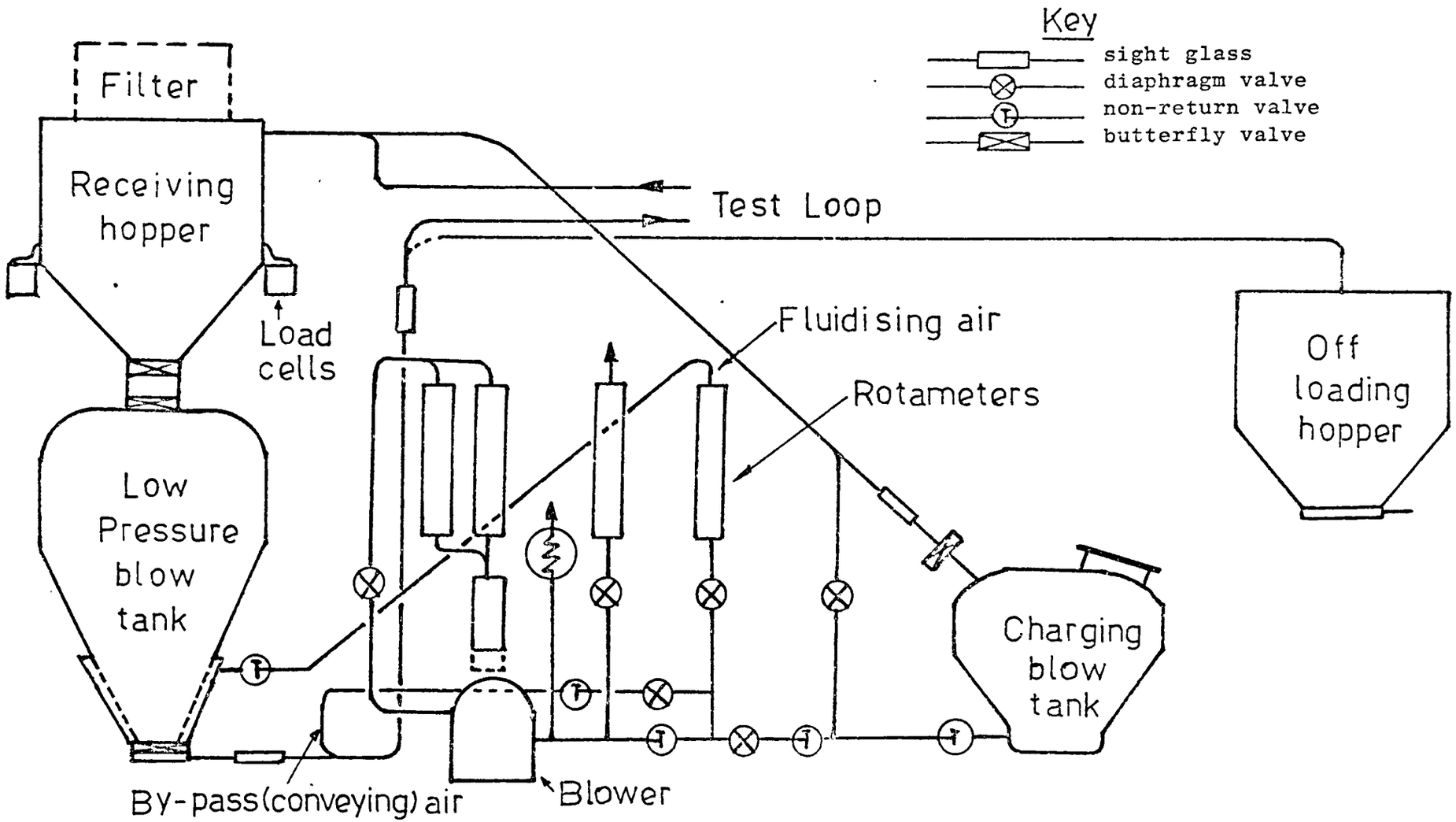

FIG. 4.2 Low Pressure Rig Layout

compressor to the bottom plenum chamber, and the material was conveyed via a discharge pipe passing through an aperture at the top dished end of the blow tank, and into the test loops. A similarly sized hopper, mounted on load cells, was located vertically above the blow tank. The material could also be loaded and discharged by using the charge/discharge facilities as in the low pressure rig. Fig. 4.3 is a photograph of this plant, and Fig. 4.4 shows its diagrammatic layout. A full description of this plant, including operation, control and instrumentation, is given in Waghorn (1977).

4.3.1 Operation and Control

This was also a batch type system, with the material being discharged directly into the test loops and returning to the hopper. The powder mass flow rate was obtained from the integrated outputs of the load cells, whilst the air mass flow rates to the blow tank (fluidising air) and conveying line (supplementary air) were metered by calibrated choked flow nozzles, in order to avoid flow measurement errors due to pulsations in the flow. By selecting the appropriate flow nozzles, and by presetting the upstream air pressure by simply adjusting a valve in the off-take air in the air receiver, the total air mass flow could thus be predetermined. A range of total of air mass flow rates, from a minimum of about 0.0060 kg/s (2.5 m/s) to a maximum compressor output capacity of about 0.1100 kg/s (45 m/s) could be achieved. The mass input into the hopper and the pressure in the blow tank could also be monitored by a UV recorder. This was done by feeding the output signals from the load cells and a calibrated pressure transducer in the blow tank to the UV recorder. Thus, a complete record of the blow tank pressure and the powder mass flow rate over a conveying cycle could be obtained. A sample trace is shown in Fig. 4.5. The two traces in this figure show the blow tank pressure (P_{BT}) rising to a steady state, whilst the mass of solids (m_s) into the hopper increases steadily until all the material in the blow tank has been fully discharged. At this stage the blow tank pressure rapidly reduces to its original pre-conveying value, and the conveying cycle is completed.

4.4 TEST LOOPS

4.4.1 Low Pressure Rig

The test section consisted of two horizontal loops in a rectangular

FIG. 4.3 High Pressure Rig Plant

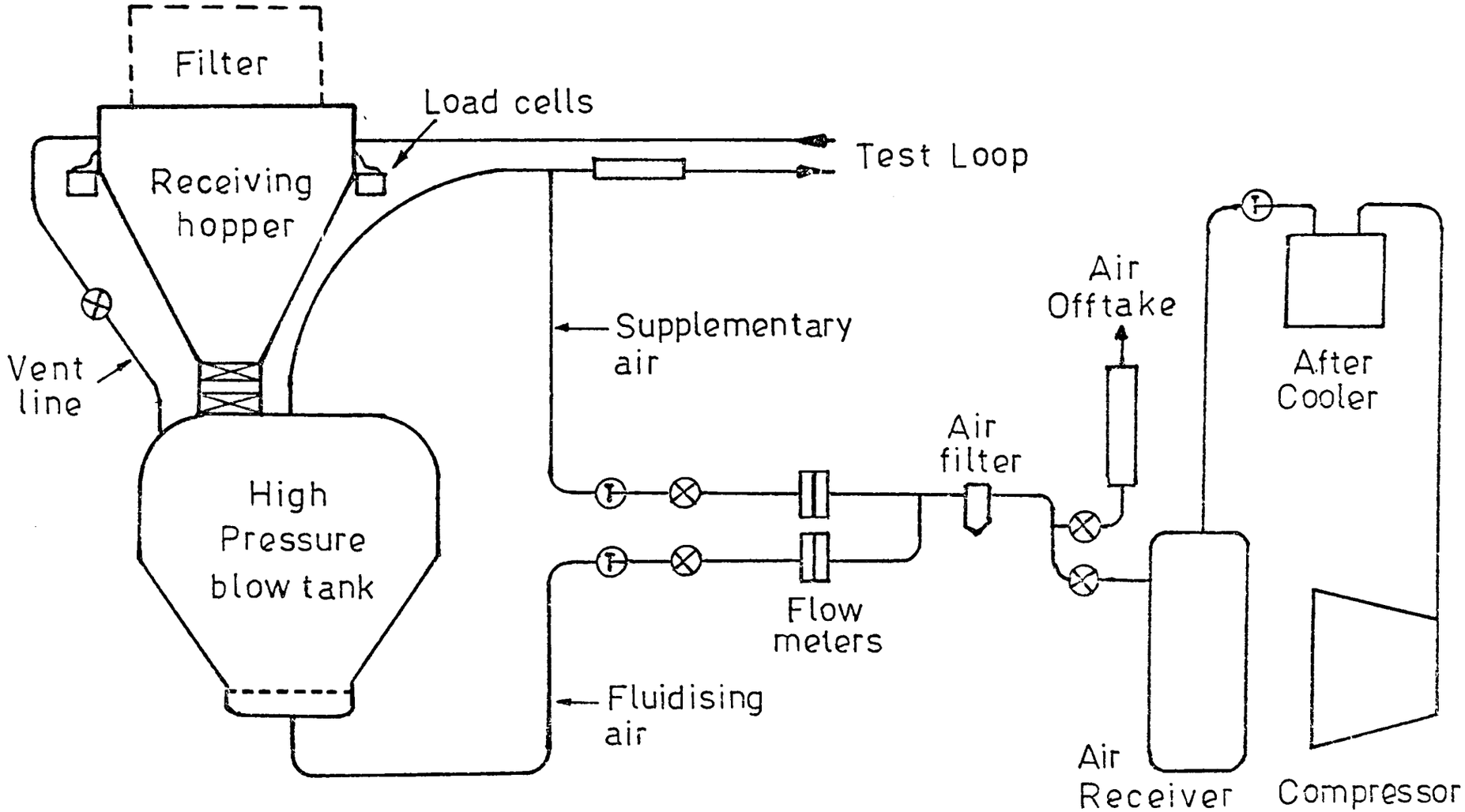

FIG. 4.4 High Pressure Rig Layout

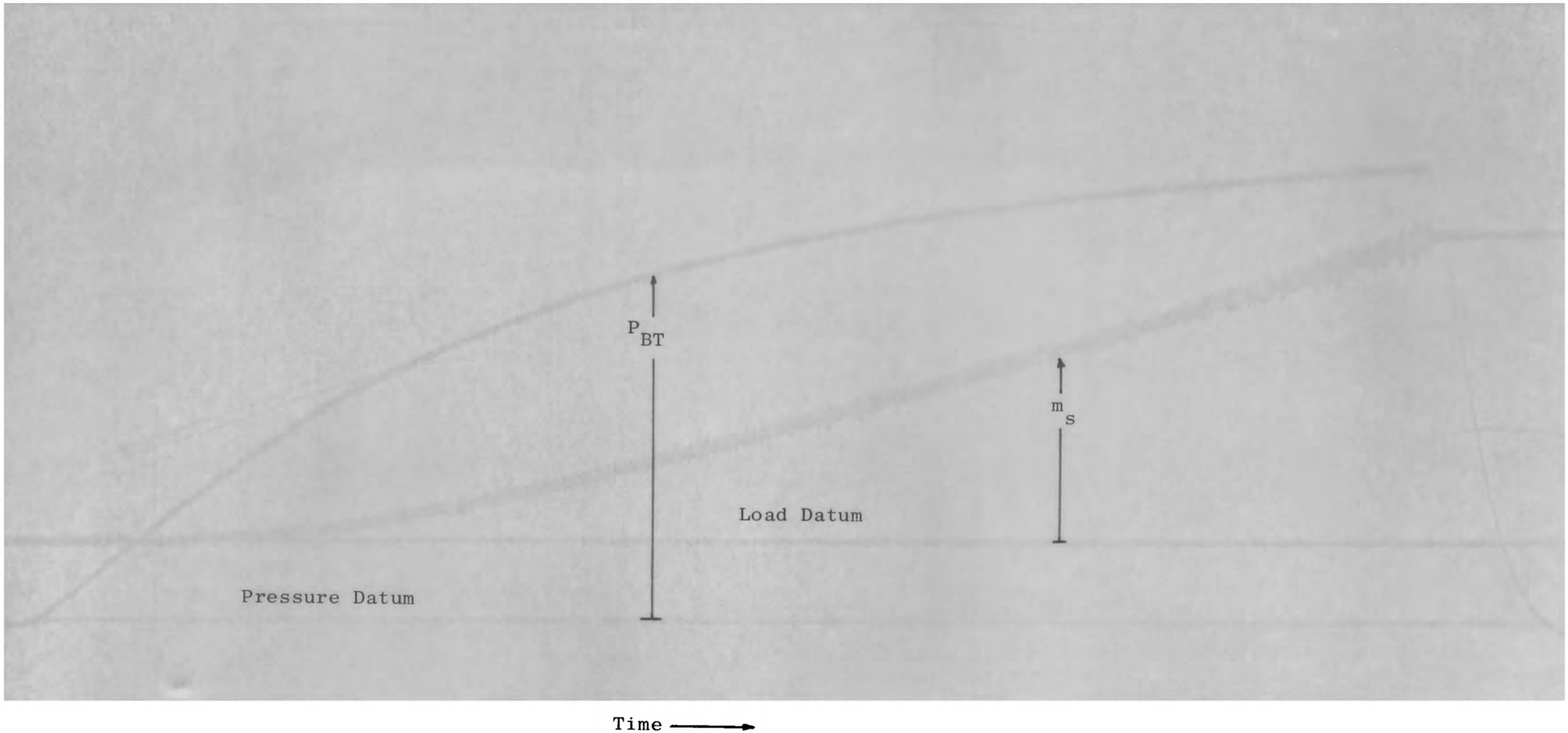

FIG. 4.5 A Typical Conveying Cycle Trace

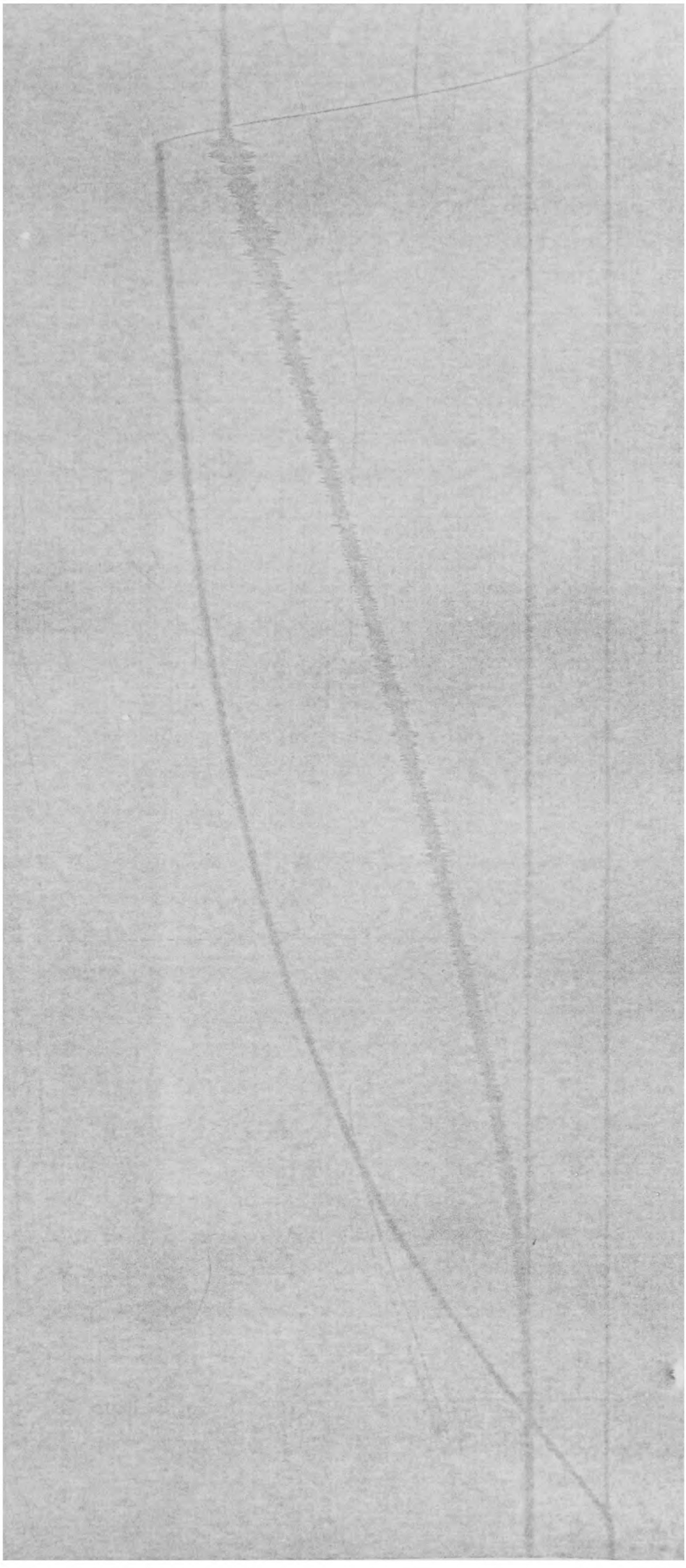

configuration, with a 90° bend at each corner. This allowed a set of seven identical bends to be tested simultaneously (Fig. 4.6). Each loop consisted of two 5.4 m pipe runs and two 8.2m pipe runs, giving a total of 27.2 m per loop. A 50 mm bore pipeline was used for the test loops, and the test bends were easily fitted and removed from the loops by means of screwed union couplings.

This particular test section, however, was only suitable for testing bends with diameter ratios (D/d) of 5.6 and 4. In order to test bends with a larger D/d, a new separate test line faciltiy was especially designed by the author to be incorporated into this rig (Fig. 4.7). This new test section also consisted of a double loop, but in a figure of eight configuration, with a 90° bend at each corner. Due to the limited laboratory space available, the length of each pipe run was severely restricted, but the minimum length was not less than 3 m, which is an adequate acceleration length for fully established flow to be achieved from one bend to the other (Rose and Duckworth 1969). The total length of this test section was 37 m and bends with a D/d of 12 were tested in this configuration.

4.4.2 High Pressure Rig

The test section consisted of a single loop of 42 m total length, having three identical 90° bends with a D/d of 24 at each corner. The possibility of incorporating either one or both loops in the low pressure rig to this single loop, enabled up to 11 bends, with a range of D/d, to be simultaneously tested over a range of phase densities and velocities. Fig. 4.8 shows the possible test loop configurations and the location of individual test bends in the respective test sections. Thus, the first test section consists of the original single loop, with bends 1, 2 and 11 only. The second test section consists of bends 1,2,3,4,5, 10 and 11 in that order with a total length of 69 m. The third test section consists of all the bends from 1 to 11, with a total length of 96 m. Bend number 10 was a proprietary 90° 'Booth' bend.

4.5 TEST BENDS

All the bends tested in this work were 90° bends and of 50 mm bore. The commercially available bends, with D/d of 5.6 and the two larger, specially pulled bends with D/ds of 12 and 24, were of mild steel. The two smaller bends, with D/ds of 4 (elbows) and 2.4 (Booth bend), were of cast iron.

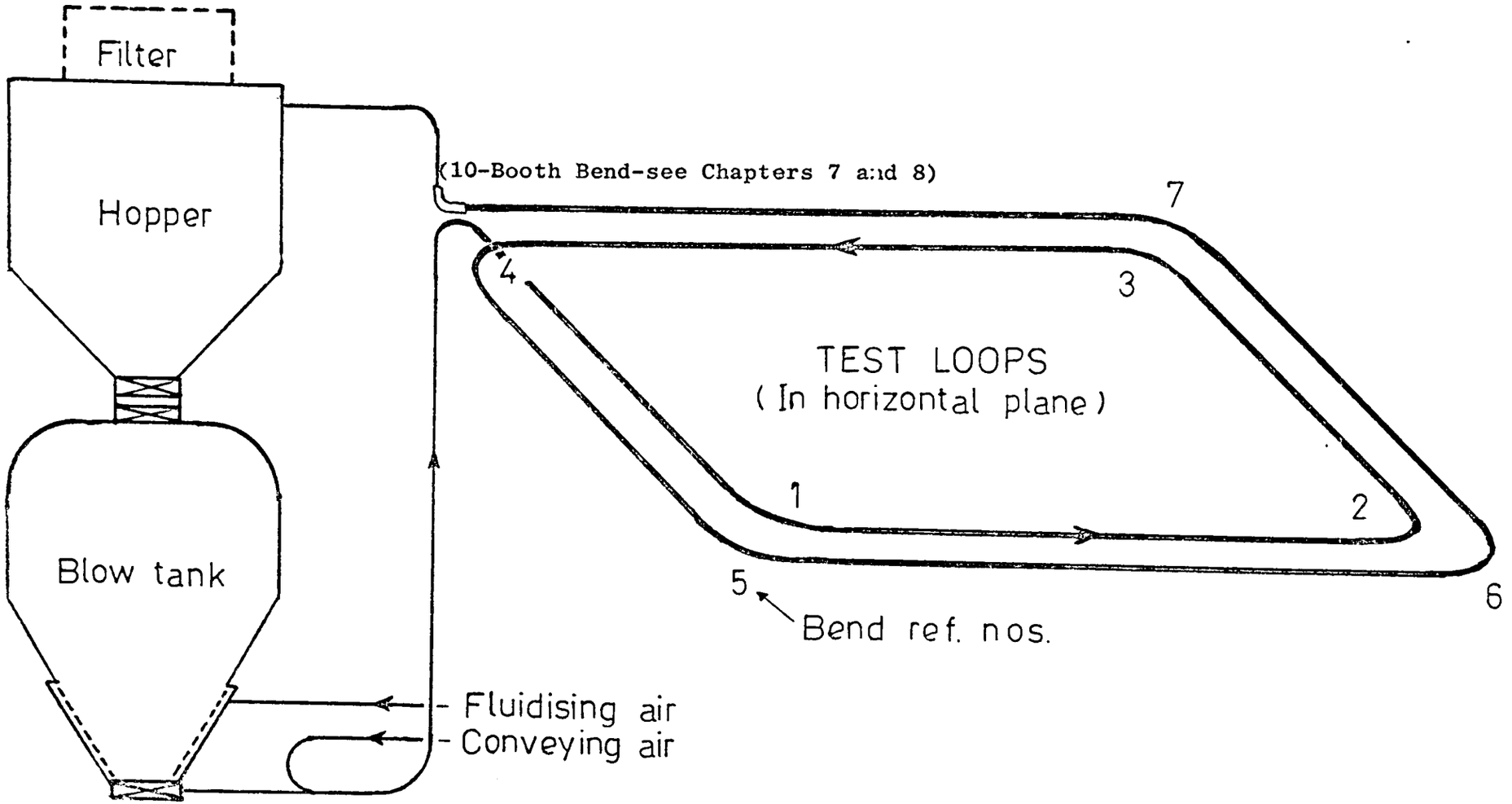

FIG. 4.6 Test Loop Configuration

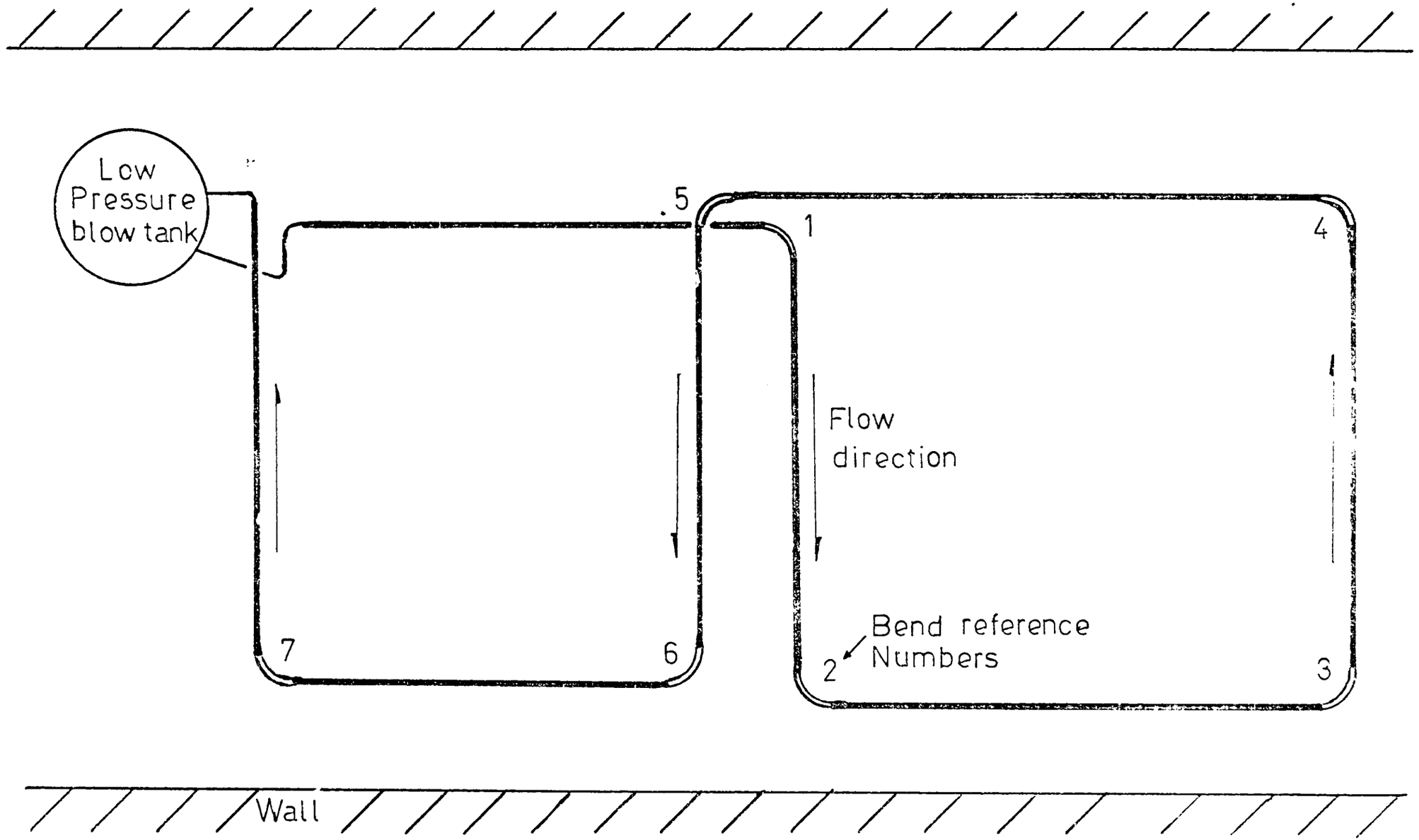

FIG. 4.7 New Test Loop Configuration

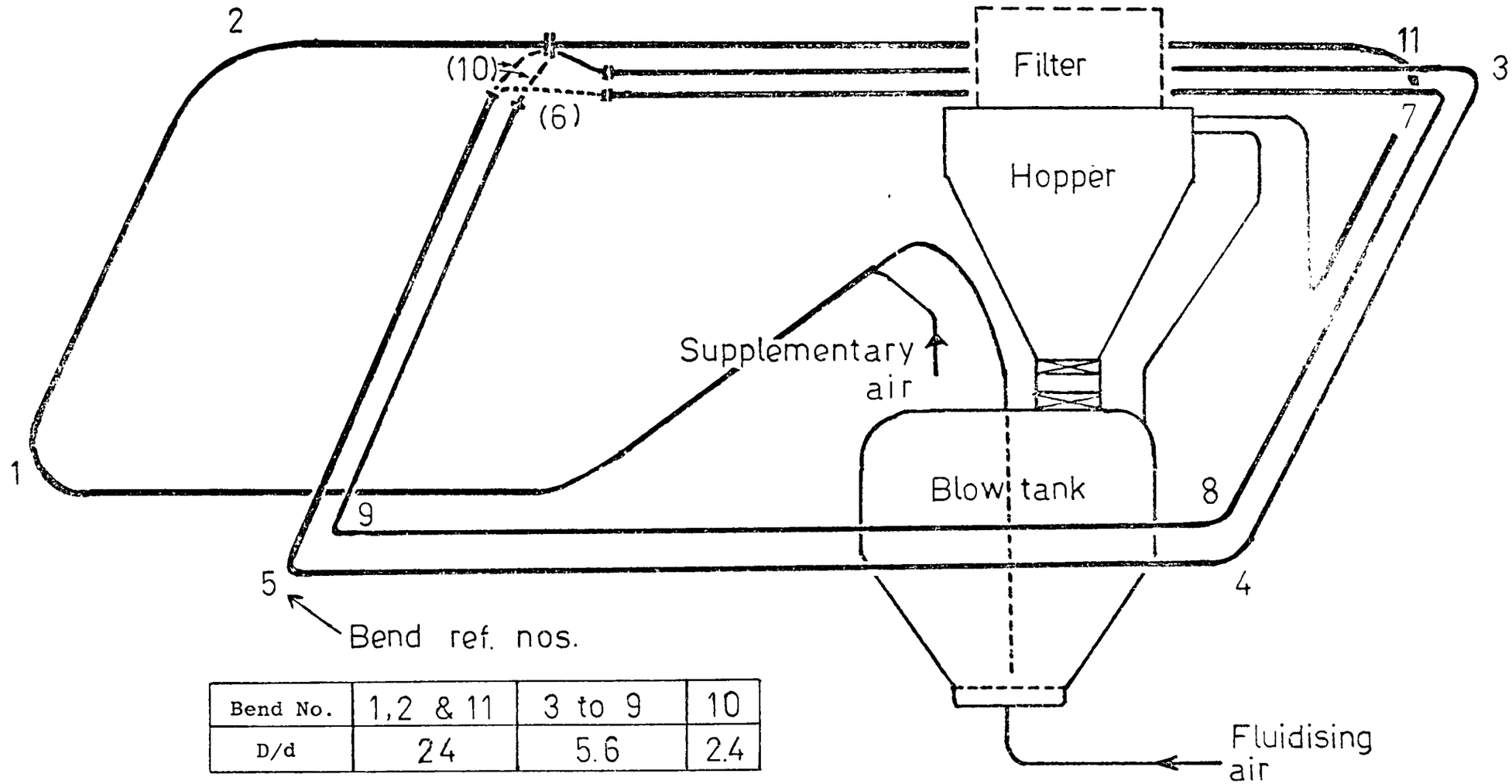

Bend No.	1,2 & 11	3 to 9	10
D/d	24	5.6	2.4

FIG. 4.8 High Pressure Rig Test Loop Configurations

The material hardness of these bends were very similar, with 158 kg/mm^2 for the mild steel bends and 154 kg/mm^2 for the cast iron bends. Fig. 4.9 shows the test bends whilst Fig. 4.10 is a schematic diagram of the Booth bend.

The surface erosion patterns of some of these test bends, which have been holed in the course of the investigations, are shown in Fig. 4.11. Included in this figure are some of the reinforced bends which were not monitored in the erosion studies. These had a 12 mm backing plate welded to the outer bend and have also been holed during the work carried out by the author. Fig. 4.12 shows the erosion pattern of the Booth bend after some 75 tonnes of various materials had been conveyed over a range of test conditions.

4.6 EROSION MEASUREMENT PROCEDURE

Prior to the start of each test programme, all the bends were painted with a reference number, corresponding to those indicated in Figs. 4.6, 4.7 and 4.8, and a reference letter indicating a particular test set. After each individual or a set of test runs, the bends were removed, cleaned and inspected visually for any sign of wear being established along the outer bend wall. The bends were then weighed individually on a beam balance to determine the mass of metal eroded. The use of this particular beam balance, however, was limited by its maximum capacity of 2 kilograms and was thus restricted to bends with D/ds of 5.6 and 4 only. For the larger and other heavier bends, a more versatile digital measuring instrument was obtained and utilised. The mass loss, over a total amount of material conveyed per run, gives the specific erosion in terms of mg/kg or g/tonne of the particular bend.

The variation of penetration rate, in terms of depth of penetration per unit time or mass conveyed, is also an important parameter in bend erosion. This quantity is primarily determined by measurements of the bend wall thickness. Fig. 4.13 shows the three bend wall thickness measuring devices used by the author in this work. The two dial gauge calipers, A and B, were specially designed to record the outer bend wall profiles of bends with D/ds of 5.6 and 4 respectively. For measurements of the two long radius bends and the Booth bend an ultrasonic digital thickness meter was specially acquired by the author for this purpose. This was due to the impracticability of using a dial gauge caliper for these bends

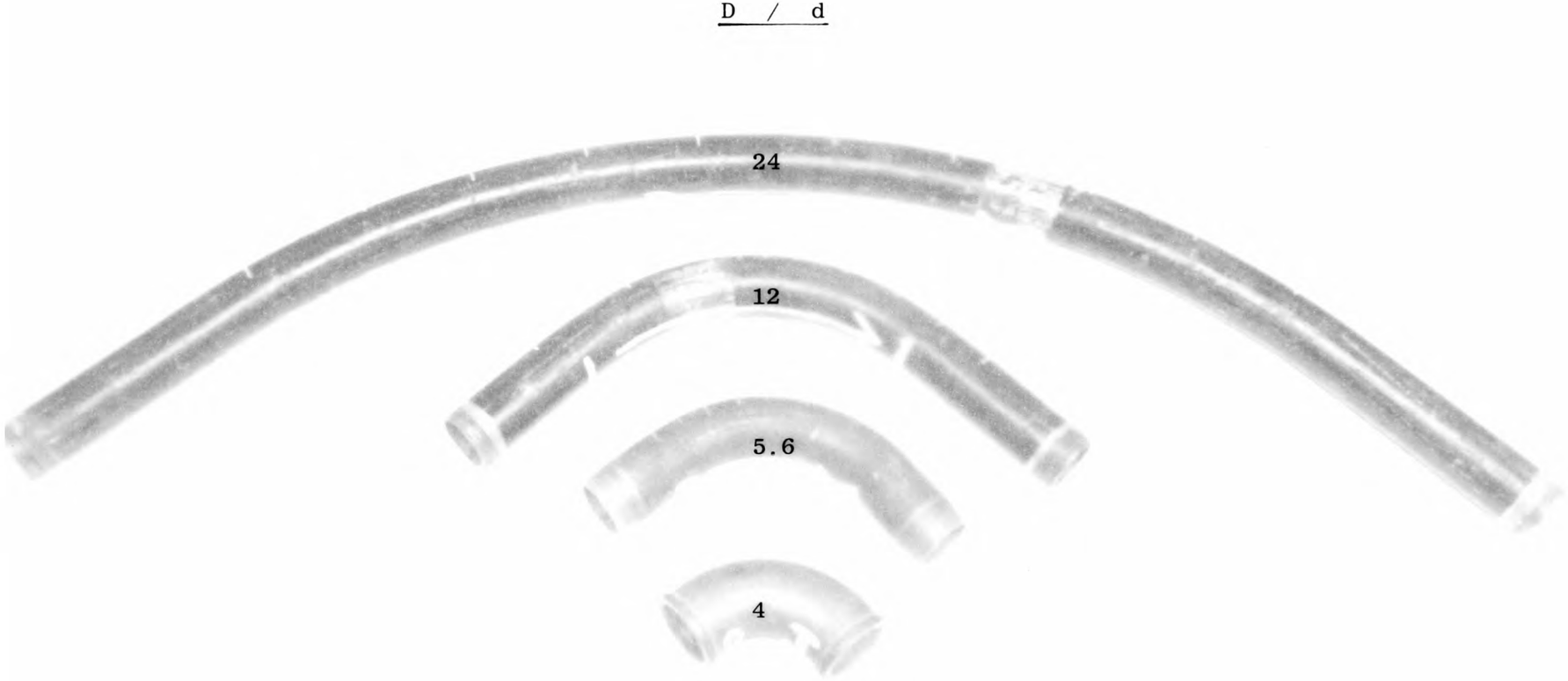

FIG. 4.9 Test Bends

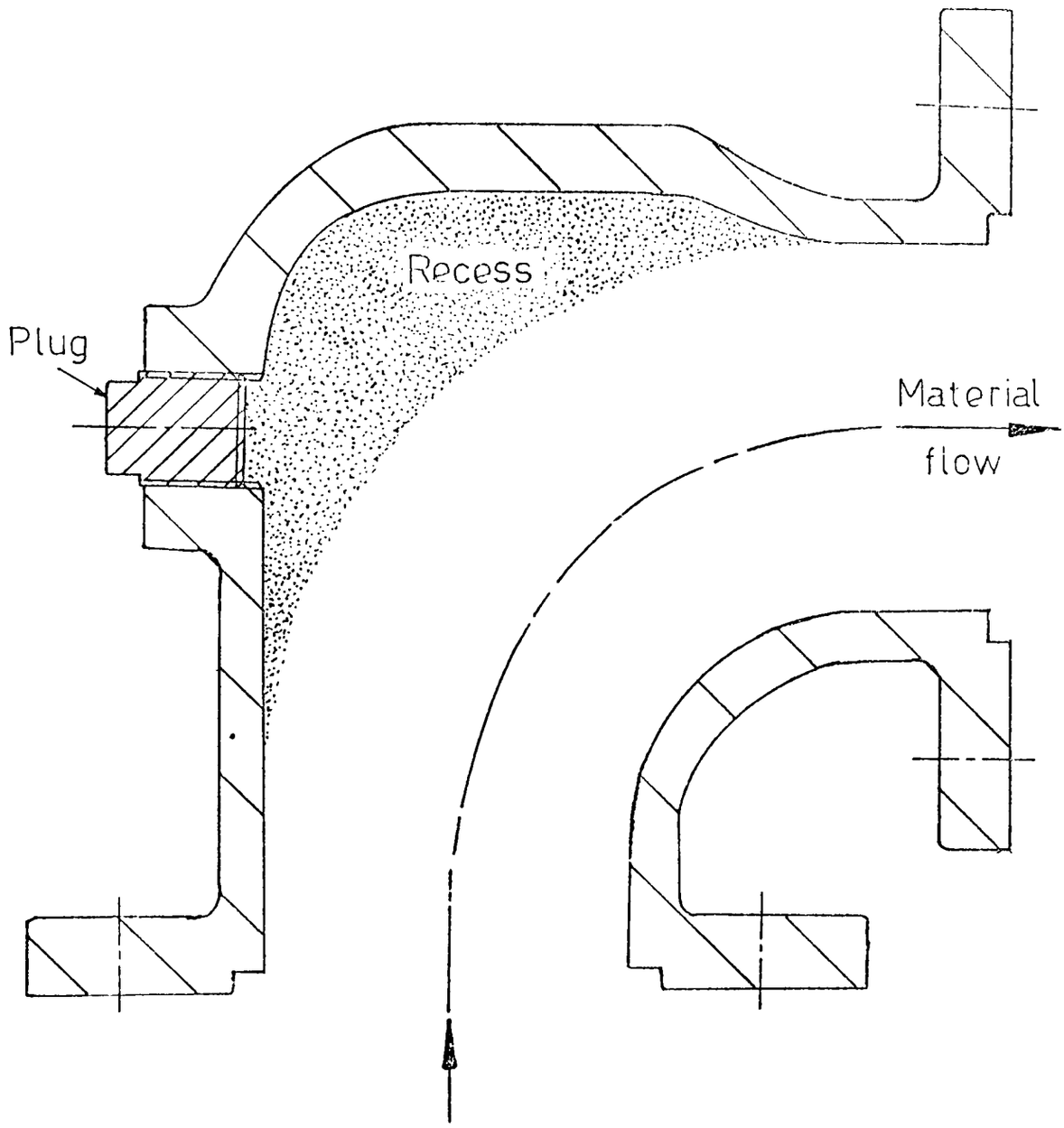

FIG. 4.10 Schematic Diagram of Booth Bend

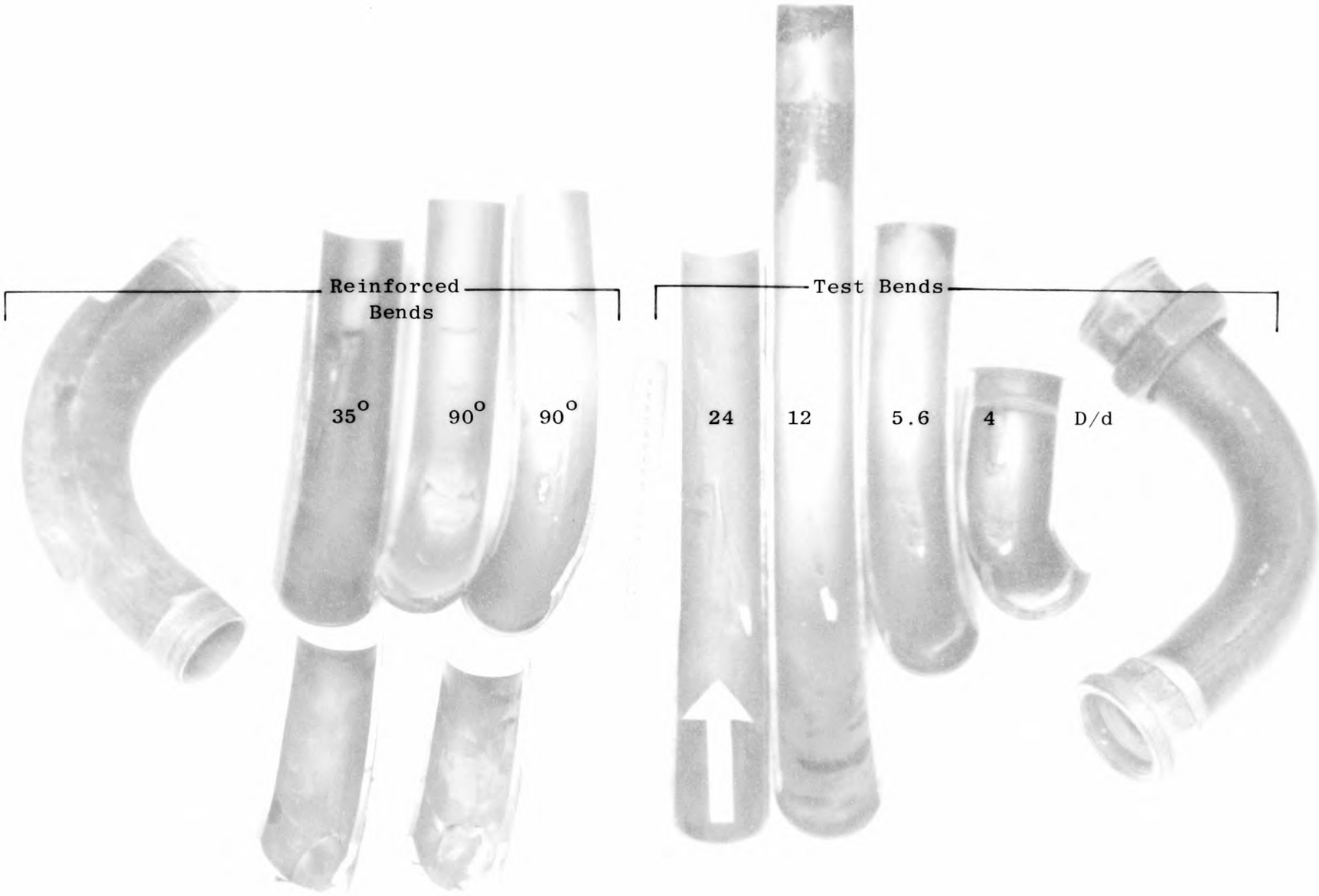

FIG. 4.11 Surface Erosion Patterns

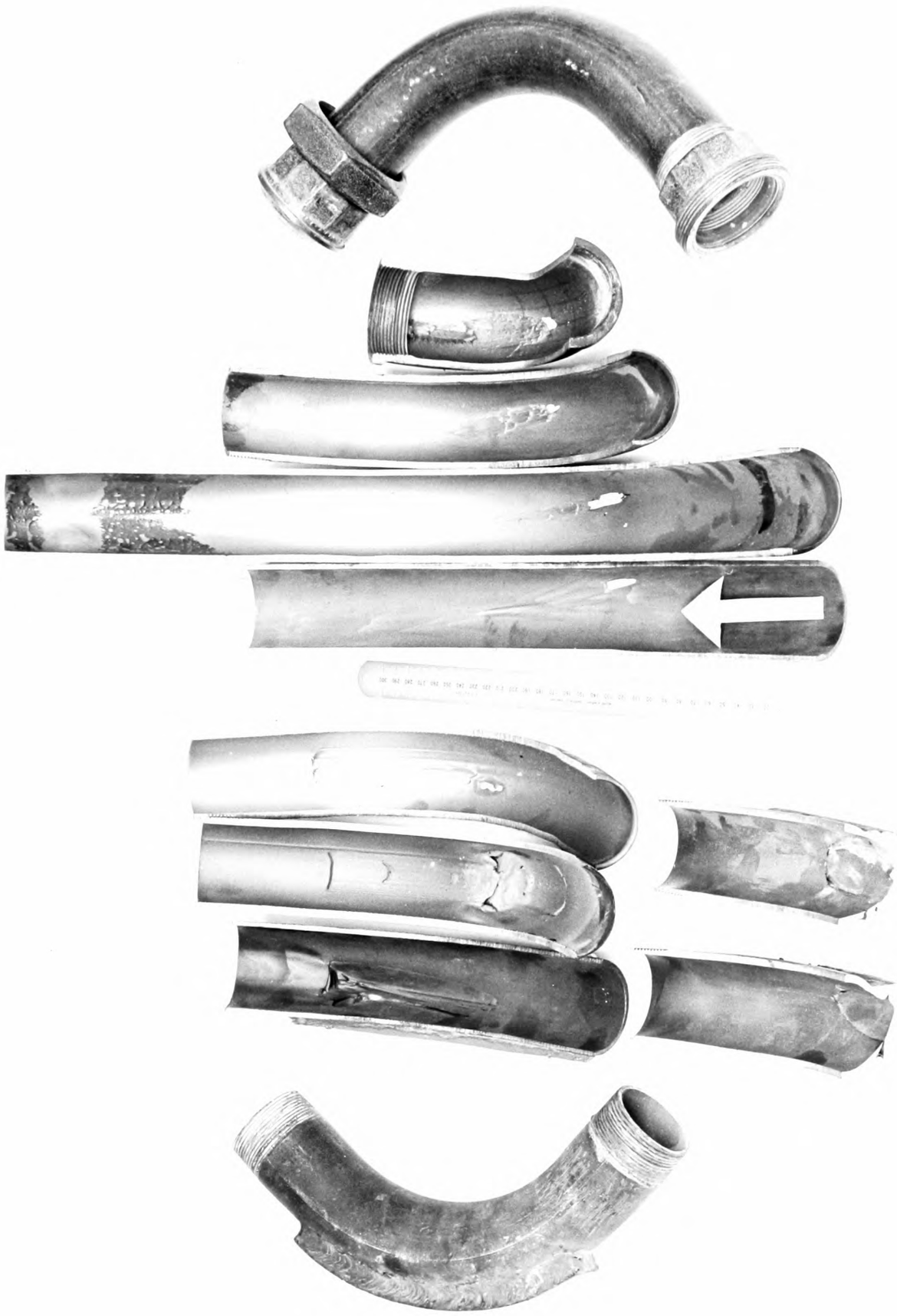

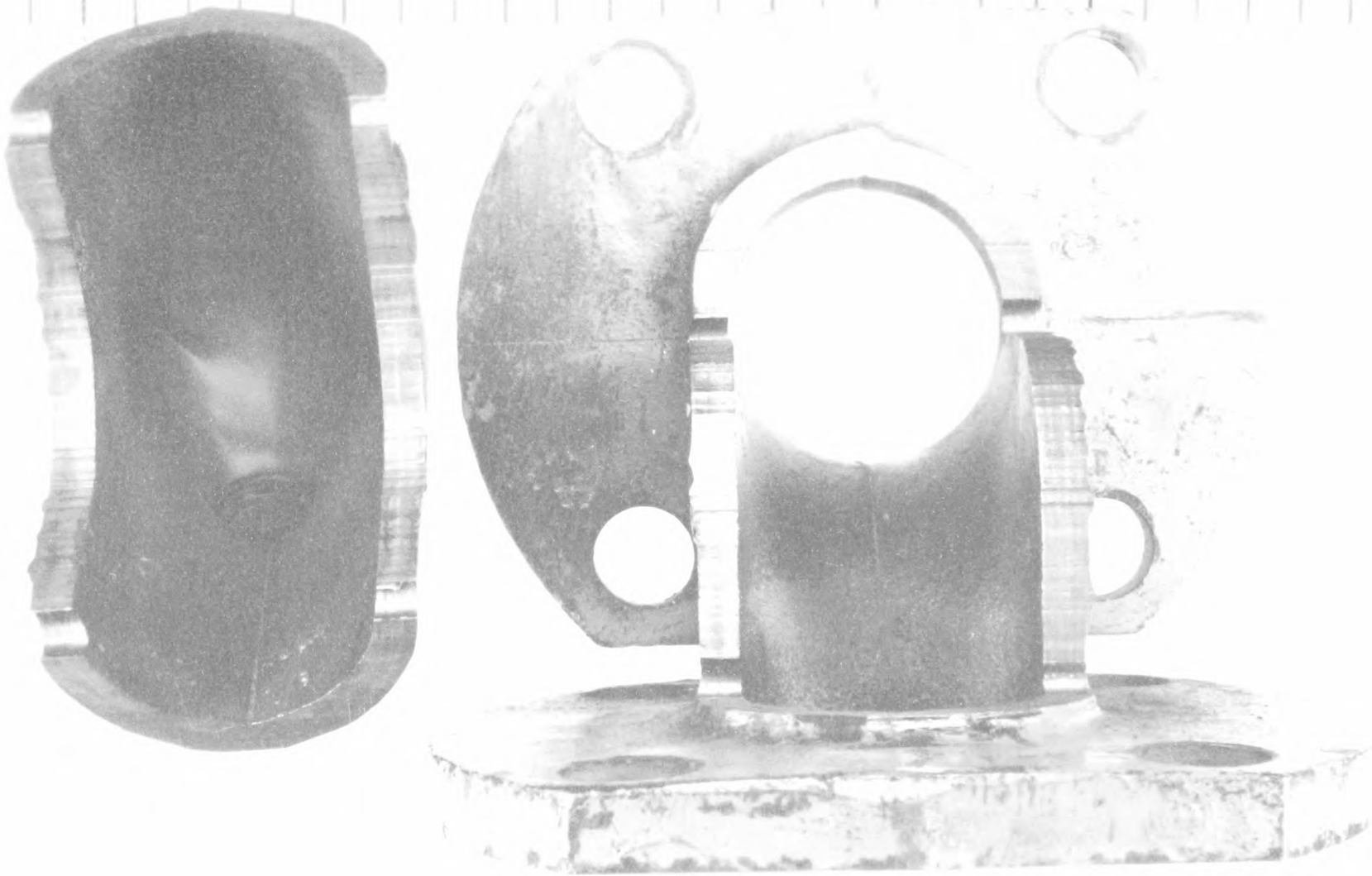

FIG. 4.12 Cross section Profile of Booth Bend

cms

FIG. 4.13 Bend Wall Thickness Measuring Instruments

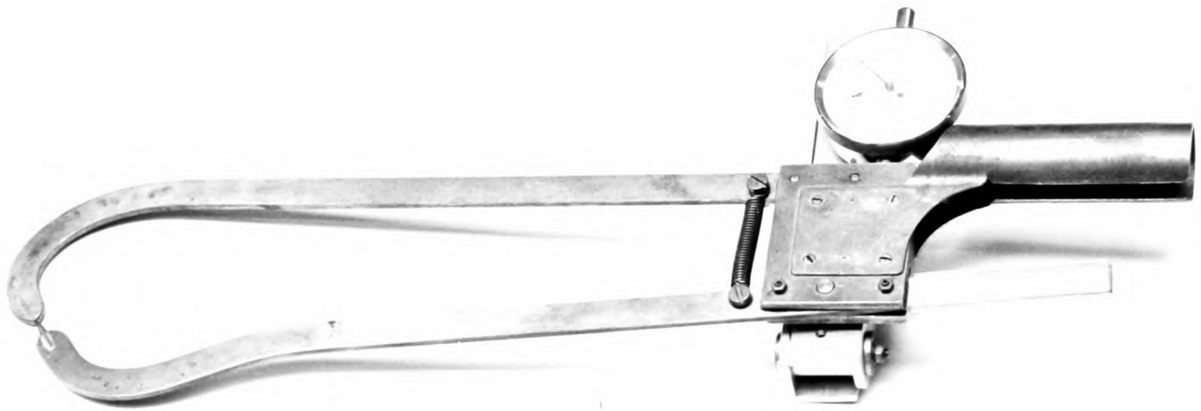

DIAL GAUGE CALIPER - A

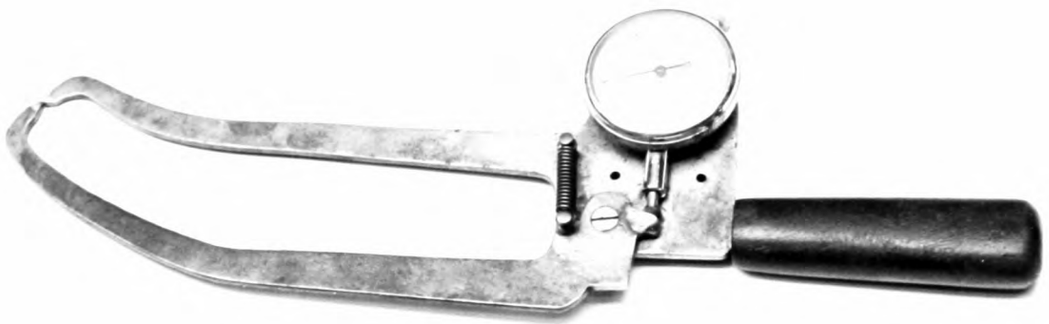

DIAL GAUGE CALIPER - A

ULTRASONIC THICKNESS METER

in contrast to the accuracy and versatility of using the ultrasonic thickness meter, with a simple probe, for determining the wall thickness of such bends.

At the end of each test series some of the bends, including those which failed, were cut into two. This enabled a more detailed inspection of the wear profiles to be made, and also the position of maximum wear to be accurately determined. The wall thickness of these 'cut' bends could also be cross-checked by means of a micrometer.

4.7 THE TEST MATERIALS

Five different materials were used in this investigation. These were two grades of sand, hydrate alumina, calcined alumina, pulverised fly ash, and fluidised bed ash (Fig. 4.14). The bulk properties of these materials are presented in Table 4.1 and further details of these material properties are given in the relevant chapters. These materials were all used in the investigations carried out in the low pressure rig. For tests carried out with the high pressure rig, pulverised fly ash was the material primarily used to establish the range of conveying capacities of this particular rig. In the test programme itself, however, sand with a similar mean particle size was used in the investigation.

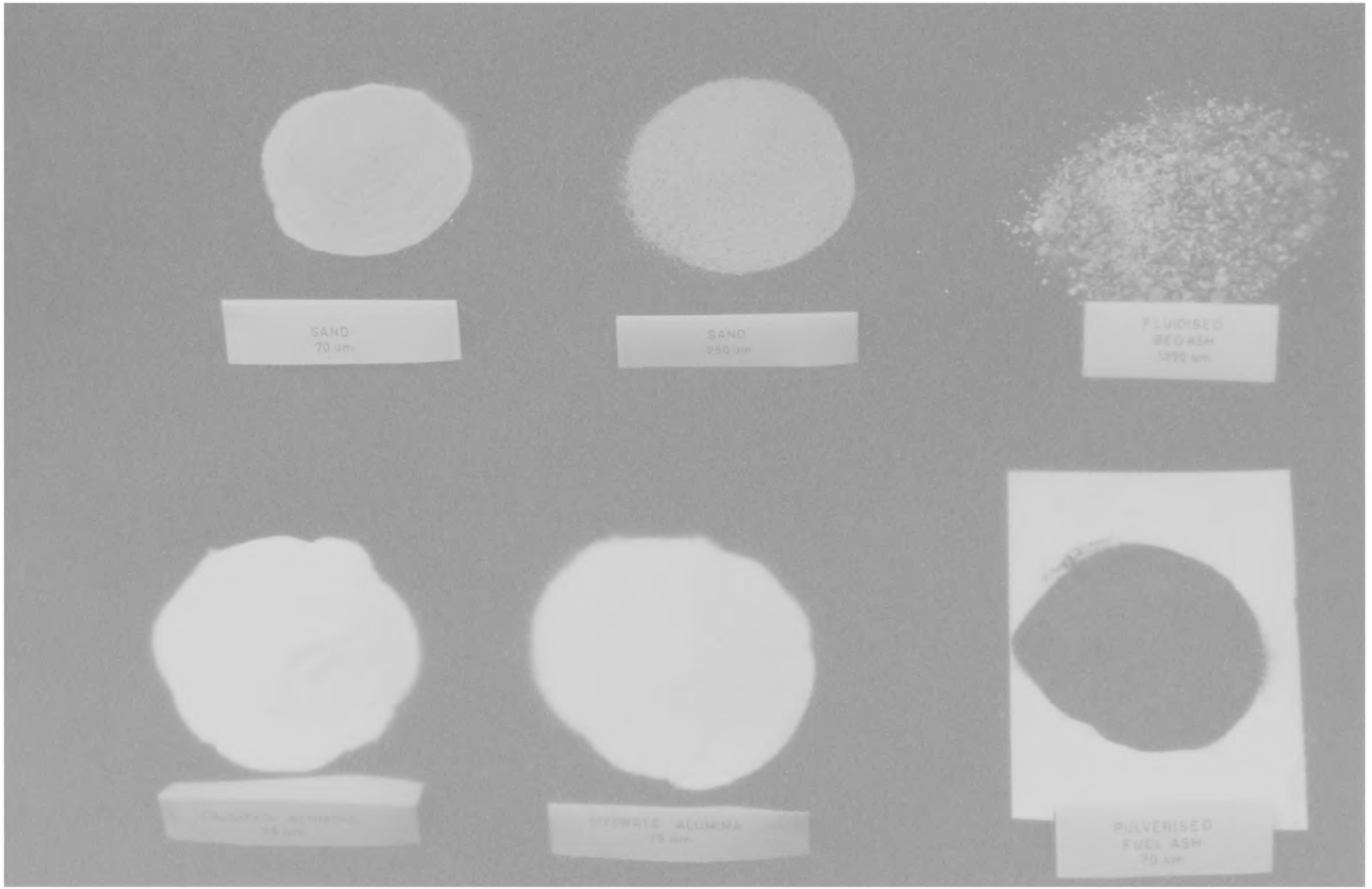

FIG. 4.14 Test Materials

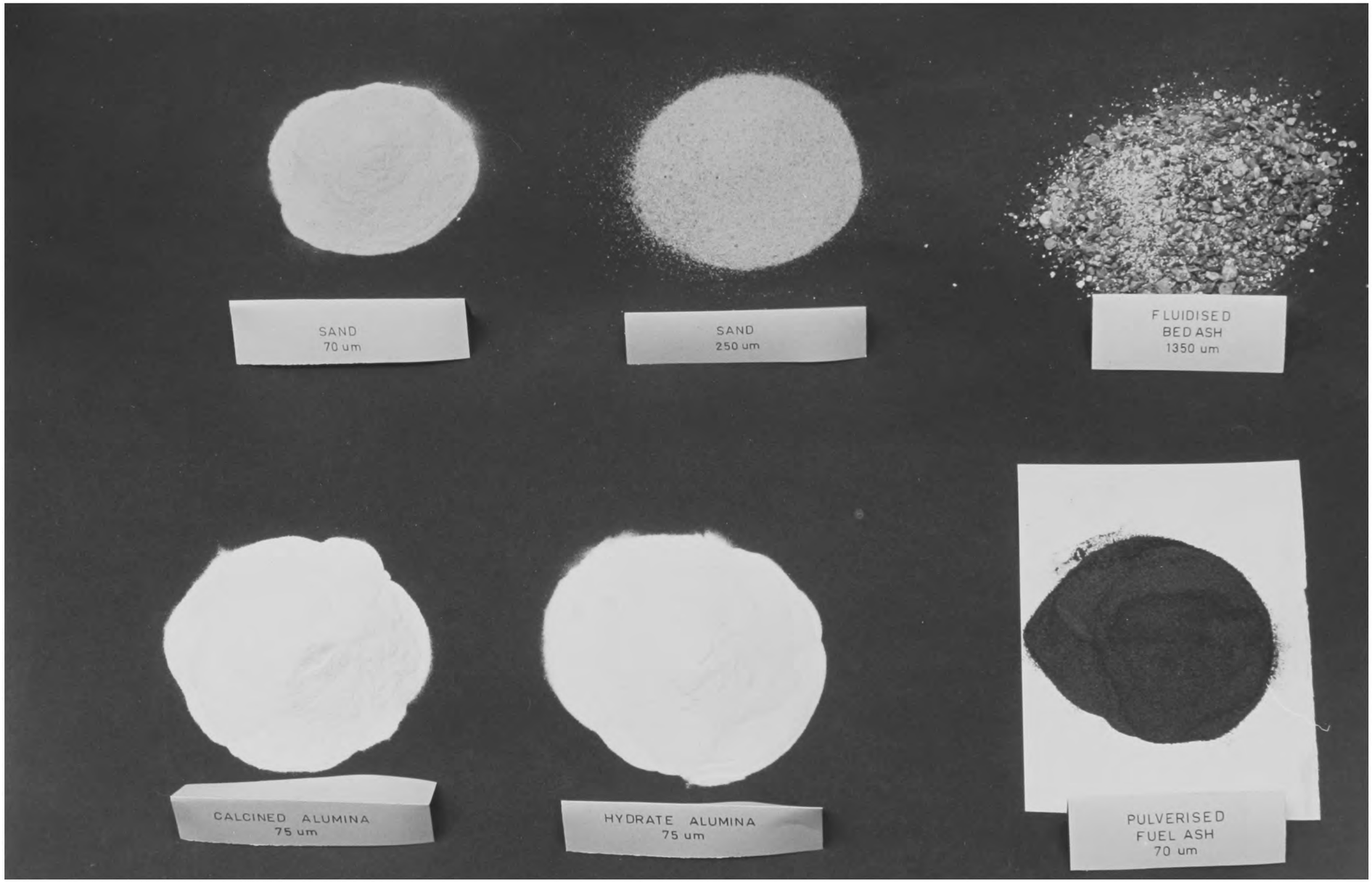
SAND
70 um
SAND
250 um
FLUIDISED
BED ASH
1350 um
CALCINED ALUMINA
75 um
HYDRATE ALUMINA
75 um
PULVERISED
FUEL ASH
70 um

TABLE 4.1 Material Bulk Properties

Material	Mean Particle Size d_p - μm	Particle Density kg/m^3	Bulk Density kg/m^3	*Particle Hardness kg/mm^2	*Particle Shape
Sand	250	2600	1400	1200	Angular
Sand	70	2472	1242	1200	"
Pulverised Fly Ash	70	1726	708	480	Spherical
Calcined Alumina	75	3342	831	2100	"
Hydrate Alumina	75	2450	1275	150	"
Fluidised Bed Ash	1350	2470	1390	2030	Irregular

* See Chapter 7 for details

Chapter 5

Experimental Programmes

5.1 INTRODUCTION

The two test rigs used by the author in this work were designed to operate under quite separate conveying conditions. The low pressure rig was essentially designed to convey material in a dilute phase mode, whilst the high pressure rig, with a much higher pressure available, was designed for dense phase conveying. Fig. 5.1 shows the conveying characteristics of pulverised fly ash obtained from these two rigs. The data in the lower half of this figure was based on results obtained with the low pressure rig whilst those in the upper half were from the high pressure rig. Thus, it can be clearly seen that, whilst the low pressure rig can only operate in the dilute phase regime, with a maximum density of about 10, it is possible to convey materials in the dense phase regime, with phase densities of over 100, with the high pressure rig. As the pneumatic conveying potential of a product in a pipeline is given by the conveying characteristics for a given product/pipeline situations, the experimental programmes in this work, were accordingly based on the ultilisation of these two separate test rigs. Further details with regard to the operational range of these two systems are given in Mills and Mason (1979 b, 1980).

5.2 LOW PRESSURE RIG EXPERIMENTAL PROGRAMMES

The first series of tests, which was basically introductory, was to investigate in more detail some of the results obtained by Mills and Mason (1976 to 1977), particularly with regard to the effects of phase density and particle size. In the tests carried out by these authors, 70 μm sand was used as the conveyed material and an analysis of bend life was produced. In order to examine the validity of their analysis and to establish its applicability for a range of particle sizes, 250 μm sand was conveyed over a similar range of phase densities and the experimental results obtained were compared (Chapter 6).

The second programme of tests was concerned with the influence of particle hardness on erosion. Although several studies have been carried out on the effect of material hardness, little information was available regarding the effect of particle hardness on pipe bend erosion. Four materials apart from sand were freely available to the author and an analysis of the data of this investigation is given in Chapter 7.

The next programme of tests was to investigate the influence of bend geometry, which is primarily the bend to pipe diameter ratio (D/d) parameter. Since erosion occurs predominantly in pipe bends, bend radius is a factor that is usually taken into account when designing systems for conveying

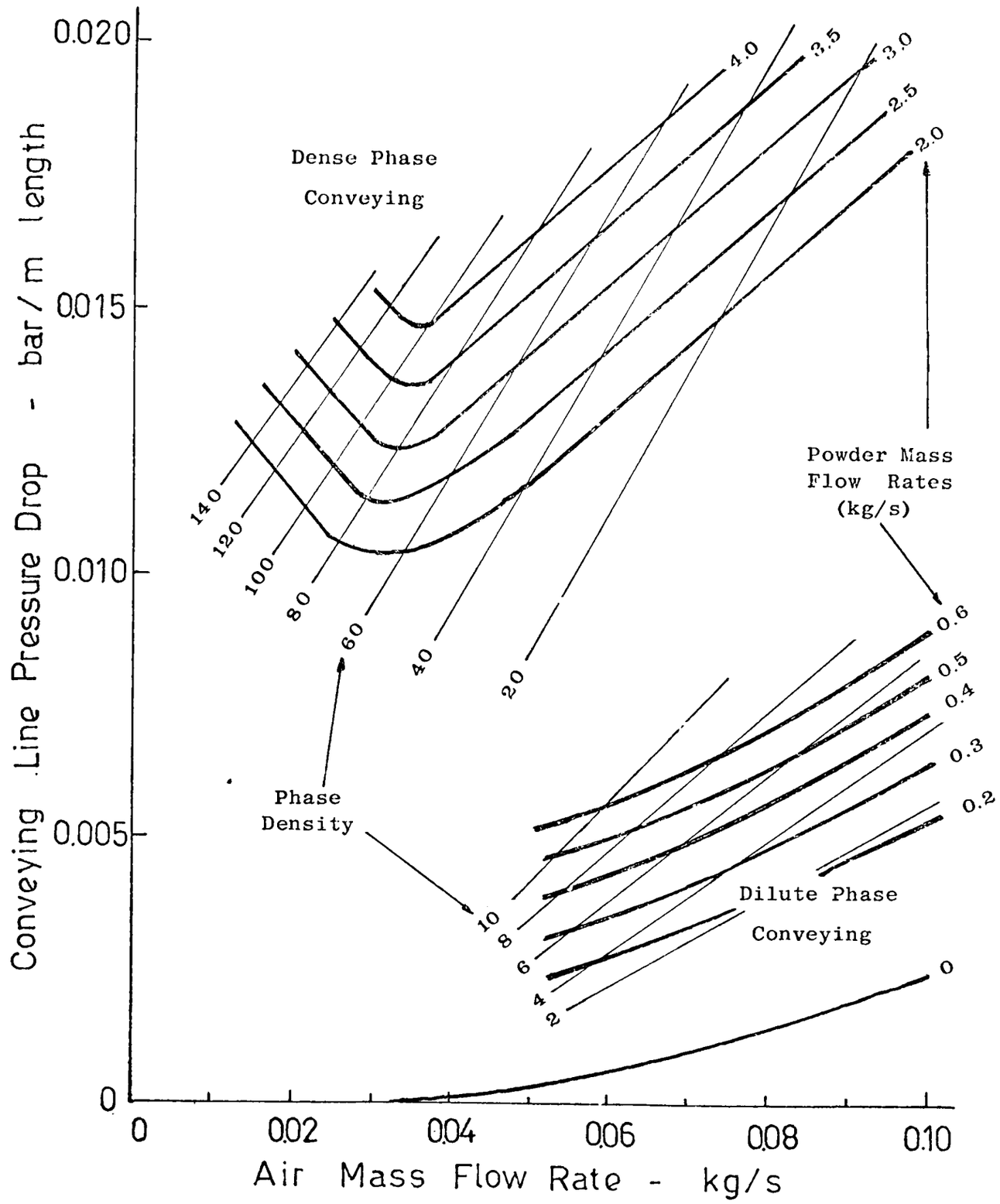

FIG. 5.1 Conveying Characteristics of Pulverised Fly Ash

abrasive products. However, little information is available for design purposes regarding the influence of D/d on erosion. To help rectify this situation a programme of tests was carried out. In order to extend the range of D/ds, a new test loop for accommodating bends with a larger D/d was specially constructed. An analysis of the influence of D/d on bend erosion is presented in Chapter 8.

In the course of this particular investigation an entirely unexpected phenomenon of the rapid failure of replacement bends was observed by the author. It was found that, when the failed bends were replaced by new bends, these new bends failed in a shorter period of time than the original bends that they were replacing, and by sand which had already been recirculated many times. This was even more interesting as the other remaining, unreplaced, original bends were still in service. The causes of this rapid failure of the replacement bends were investigated and are reported in Chapter 9.

5.3 HIGH PRESSURE RIG EXPERIMENTAL PROGRAMME

With the availability of a very much higher air supply pressure with this rig, it was proposed that a programme of tests should be carried out to investigate the effect of dense phase conveying on erosion. This particular work on the dense phase regime would considerably extend the work on the influence of phase density carried out with the low pressure dilute phase blow tank system presented in Chapter 6.

Conveying at a much lower velocity is also possible at higher phase densities and so it was proposed to investigate the influence of conveying air velocity over a much wider range. To a large extent this would automatically be achieved with this rig, for with high pressure or dense phase conveying over a long line in three loops (Fig. 4.8),the total pressure drop would be such that a large variation in velocity would be obtained.

Furthermore, with the possibility of incorporating the two loops in the low pressure rig to the existing single loop in this rig, the influence of a range of D/ds could also be assessed.

Whilst a maximum phase density of about 140 was possible with pulverised fly ash (Fig. 5.1), only a limited amount of erosion was measurable with this particular material. Thus, it was proposed to use similar sized sand, because of its availability and abrasiveness, for this programme of tests.

From preliminary conveying characteristic tests of sand in this particular system, it was found that its conveying behaviour was completely different from that of pulverised fly ash. For sand, a minimum conveying velocity of about 15 m/s was necessary in order to prevent saltation and consequently blockages, irrespective of the total length of pipeline. This meant that the conveying line pressure drop for this particular system could not be less than about 0.8 bar.

Thus, this particular requirement restricted any possibility of conveying sand in a dense phase mode. In fact, a maximum phase density of only about 22 was achieved and this programme was modified accordingly. A series of tests was then proposed at constant phase densities of 10, 17 and 22 and the results over this restricted range of phase densities was analysed and presented in Chapter 10. In terms of penetration rate, however, it was found that this range of phase densities was adequate, for the results showed that the penetration rate reaches a maximum at a phase density of less than 10 for this particular conveyed material, i.e. sand.

5.4 TEST DATA

Over the period of investigations carried out by the author, some 250 test runs were made, covering a range of test conditions. A list of all the tests is given in Table 5.1. All the particular conveying conditions, such as material used, its mean particle size, phase density, conveying velocity, etc., are given. This table serves as a reference to the work carried out, in chronological order, and gives some idea of the range of tests and scope of the work.

Table 5.2 gives a complete list of the erosion data of all the bends tested, in terms of mass eroded, at the end of each programme of tests. Table 5.3 is basically a further extension of Table 5.2 and gives the data of bends which failed in the course of each test programme in more detail. This table, for reference purposes, lists the particular bend number, its conveying conditions, mass eroded and the position of failure. Further details of all the bend tests in each respective test programme are given in the relevant chapters.

D/d	Bend Set Reference	Material	Phase Density	Conveying Velocity (m/s)	Run Numbers	Total Number of Runs	Mass Conveyed per run (tonne)	Average Conveying Time per run (h-min)	Test Rig
5.6	A	Sand (250 µm)	1	25	1---10	10	0.750	3-14	Low Pressure Rig
"	B	" "	3	26	11---40	30	"	1-00	
"	C	" "	5	26	41---57	17	"	0-35	
"	D	" "	7	25	61---79	19	0.730	0-25	
5.6	E	Sand (70 µm)	3	26	81---93	13	0.750	1-05	
*5.6	F	P.F.Ash (70 µm)	3	25	100--117	18	0.500	0-42	
5.6	G	Cal.Alumina(75µm)	3	25	120--129	10	0.670	0-56	
*5.6	H	Hyd.Alumina(75µm)	3	25	130--139	10	0.625	0-50	
* 4	J	Sand (70 µm)	3	25	140--165	26	0.750	1-04	
12	L	Sand (70 µm)	3	25	170--189	20	0.750	1-00	
*5.6	M	F.B.Ash (1350µm)	3	25	190--210	21	0.709	0-57	
*5.6;24	N	Sand (65 µm)	10	15 to 26	221--244	24	0.750	0-18	High Pressure Rig
5.6;24	P	" "	17	15 to 27	251--274	24	0.750	0-11	
*5.6;24	Q	Sand (60 µm)	22	14 to 31	281--310	30	0.750	0-07	

* includes Booth bend (D/d = 2.4)

TABLE 5.1 Details of Test Programmes

Bend Set Reference	Total Mass Eroded - g										
	Bend Number										
	1	2	3	4	5	6	7	8	9	**10	11
A	77	*90	*85	89	*94	*93	*95	-	-	-	-
B	66	80	81	*90	99	*96	114	-	-	-	-
C	60	*72	67	-	-	-	-	-	-	-	-
D	46	*62	51	-	-	-	-	-	-	-	-
E	26	39	*58; *47;34	47	*70	63	*66; *48	-	-	-	-
F	3	3	2	4	3	6	3	-	-	0	-
G	24	43	45	52	42	54	42	-	-	-	-
H	+7	+7	+4	+7	+6	+2	+1	-	-	0	-
J	21	15	21	36	*37	32	*42	-	-	5	-
L	45	*90; 36	60	*91; *74; 23	68	*85; *65; 44	*79; 66	-	-	-	-
M	55	63	54	*67	68	*80	75	-	-	27	-
N	17	45	7	16	17	16	17	22	25	5	48
P	33	55	8	17	20	-	-	-	-	-	56
Q	29	32	10	14	18	-	-	-	-	1	50

*Mass Eroded at Failure

**Booth bend

TABLE 5.2 Erosion Data on all Test Bends

Bend Reference	Phase Density	Velocity at Bend (m/s)	Mass Eroded - g		Conveying Details		Number of Batches	Position of Failure - deg.	
			at Failure	Total	Mass conveyed (tonne)	Conveying time (h-min)		Bend Angle	Pipe Angle
A6	1	26.7	90	93	6.71	28-05	9	40-44	C.L.
A5	"	26.5	90	94	6.91	30-08	10	40-45	"
A7	"	27.1	92	95	7.00	30-36	10	42-47	-15
A3	"	26.0	85	85	7.49	32-28	10	45-47	C.L.
A2	"	25.6	90	90	7.49	32-29	10	44-46	"
B6	3	27.7	96	96	17.91	23-56	24	40	-20
B4	"	25.5	90	90	20.50	27-33	28	37	-15
C2	5	25.4	68	72	12.00	9-25	16	35	-30
D2	7	23.7	60	62	13.14	7-35	18	35	-32
E3	3	24.4	51	58	4.10	5-20	6	32-40	15→35
E7	"	27.3	58	66	5.62	8-00	8	35-40	20→40
E3R	"	24.4	45	47	2.72	3-56	4	32-37	15→30
E7R	"	27.3	42	48	3.37	4-58	5	28-38	15→40
E5	"	25.8	70	70	9.37	13-27	13	25-32	10→30
J7	3	26.1	42	42	8.93	12-15	12	38	15
J5	"	24.6	36	37	18.23	25-49	25	33-37	0→15
L7	3	27.1	73	79	4.60	6-23	7	29-32	15→30
L4	"	24.9	81	91	9.09	13-23	14	30-35	5→25
L6	"	26.4	80	85	10.35	13-53	14	36	20
L2	"	23.7	88	90	12.50	16-45	17	34-37	30
L6R	"	26.4	60	65	2.55	3-23	4	28-35	15→45
L4R	"	24.9	62	74	3.63	4-11	5	27-33	15→45
M6	3	26.8	79	80	13.95	17-00	19	30	-45
M4	"	25.3	66	67	14.44	19-35	20	38	-45

R indicates Replacement Bend

C.L. : Horizontal Centre Line

Chapter 6

The Influence of Phase Density - I

6.1 INTRODUCTION

The first investigation carried out in this work was on the influence of phase density on erosion. In the work carried out by Mills and Mason (1976 to 1977), phase density was found to be one of the more important parameters in the erosive wear process of pipe bends in pneumatic conveying. Whilst some important trends regarding the effect of this parameter, particularly with regard to specific erosion and depth of penetration, were observed by the authors, definitive conclusions remained to be drawn. This was primarily due to their limited experimental data. In order to extend and substantiate their work further, and to provide a correlation of their analysis with regard to particle size, a programme of tests was carried out by the author. Sand with a mean particle size of 250 μm was conveyed over a similar range of phase densities at a constant inlet velocity of about 25 m/s, and the experimental results obtained are analysed and presented in this chapter.

6.2 REVIEW OF PREVIOUS WORK

The effect of phase density on erosion has received comparatively little attention until recently. From the general solid particle erosion studies, particle concentration, which is similar to phase density, has been found to have relatively little effect. The general consensus of opinion from these studies is that erosion is only very slightly reduced as particle concentration is increased.

From full-scale experimental studies, Mason and Smith (1972) found that phase density and velocity are inter-related parameters, whilst Bikbaev et al (1972, 1973) reported that a predominant effect on penetration rate was primarily due to velocity. Glatzel (1977) carried out a series of tests over a relatively narrow range of phase densities, but the specific effect of phase density was not investigated. Instead, his primary objective was to determine the particle concentration profiles over this range of phase densities, which were essential elements in his predictive bend erosion model.

Mills and Mason (1976 to 1977) are probably the only researchers who have specifically investigated the influence of phase density in detail. Their results were briefly reviewed in Chapter 3 and so, in this section, only their more relevant findings are discussed in detail.

In their first series of tests (1976a), about 0.750 tonnes of 70 μm sand was conveyed over a range of phase densities from 0.5 to 8. The conveying air at inlet to the pipeline was maintained at a constant value of about 25 m/s throughout the test series. In terms of specific erosion for this range of phase densities they found that

$$\text{erosion} \propto \text{phase density}^{-0.37}$$

This was determined at the end of a long programme of tests. In a further series of tests carried out with 230 μm sand at phase densities of 1, 2 and 4 (1976b), however, they analysed the data during the course of the tests and found that on an accumulative basis the phase density exponent varied from -0.16 to -0.38. In terms of individual test values the exponent showed an even more dramatic change, from -0.16 to -0.73. In both cases the magnitude of the effect of phase density was attributed to the condition of the conveyed product. The authors suggested that, although particle size appeared to have little effect on the variation of specific erosion (1977b), particle shape or sharpness was a more likely cause of the exponent variation.

The authors also found that the mass eroded was not proportional to the depth of wear over this range of phase densities (1977a, b). Although, in terms of specific erosion, less mass was eroded as phase density was increased, in terms of depth of wear, penetration rate was found to increase correspondingly. Thus, in terms of bend life, the combined net effect was that increased phase densities would result in a decrease in the mass of sand that could be conveyed before bend failure occurred (1977c).

However, the magnitude of this effect was considerably influenced by the reliability of their experimental data. In both programmes of tests the authors noticed that there was a considerable degree of scatter, particularly with respect to the specific erosion values. This scatter increased as the phase density was increased (1977a, b) and was considerably greater for the 70 μm sand than for the 230 μm sand. It was this degree of scatter which was primarily responsible for premature failure of bends (1976 c).

Furthermore, the same batch of sand was conveyed over the whole range of phase densities without any systematic chronological order in terms of a

particular phase density. In the tests carried out with the 230 μm sand the effects of velocity and phase density were both investigated in the same programme. Thus, this lack of systematic testing probably accounts for the wide variation of the phase density exponent obtained in their work.

6.3 EXPERIMENTAL PLAN

In order to avoid the problems of premature bend failure associated with the finer 70 μm sand, 250 μm sand (Fig. 6.1) was used in this programme. The particle size distribution of this sand, before and after each test series, is shown in Fig. 6.2. The use of this larger size sand, which is essentially conveyed over a similar range of phase densities, would also enable the author to correlate any inter-relating effects of particle size with respect to phase density.

About 0.750 tonnes of sand was used for each test series at a given phase density and the sand was recirculated within each test series. To ensure a uniform set of test conditions, and in order to provide reliability of the test data, a fresh batch of similar sized sand was used for each series of tests.

Four series of tests were carried out, corresponding to the four test phase densities of 1, 3, 5 and 7. A similar constant inlet conveying air velocity of about 25 m/s was maintained throughout the test series, thus providing a basis for direct comparison with the results obtained by Mills and Mason (1976a, b). The sequence of tests was carried out in a chronological order as tabulated in Table 5.1. At phase densities of 1 and 3 both test loops with seven test bends were utilised, and at phase densities of 5 and 7 a single loop with three test bends was used. In all cases the test bends were of mild steel with a constant diameter ratio of 5.6.

6.4 BEND WEAR RESULTS AND DISCUSSION

After each test run, all the bends were removed and the relevant measurements were recorded. This process was generally repeated until at least two of the seven test bends in the double loop failed, and one in the case of the single loop. In pipe bend erosion situations, the

FIG. 6.1 Photomicrograph of Sand


200 µm

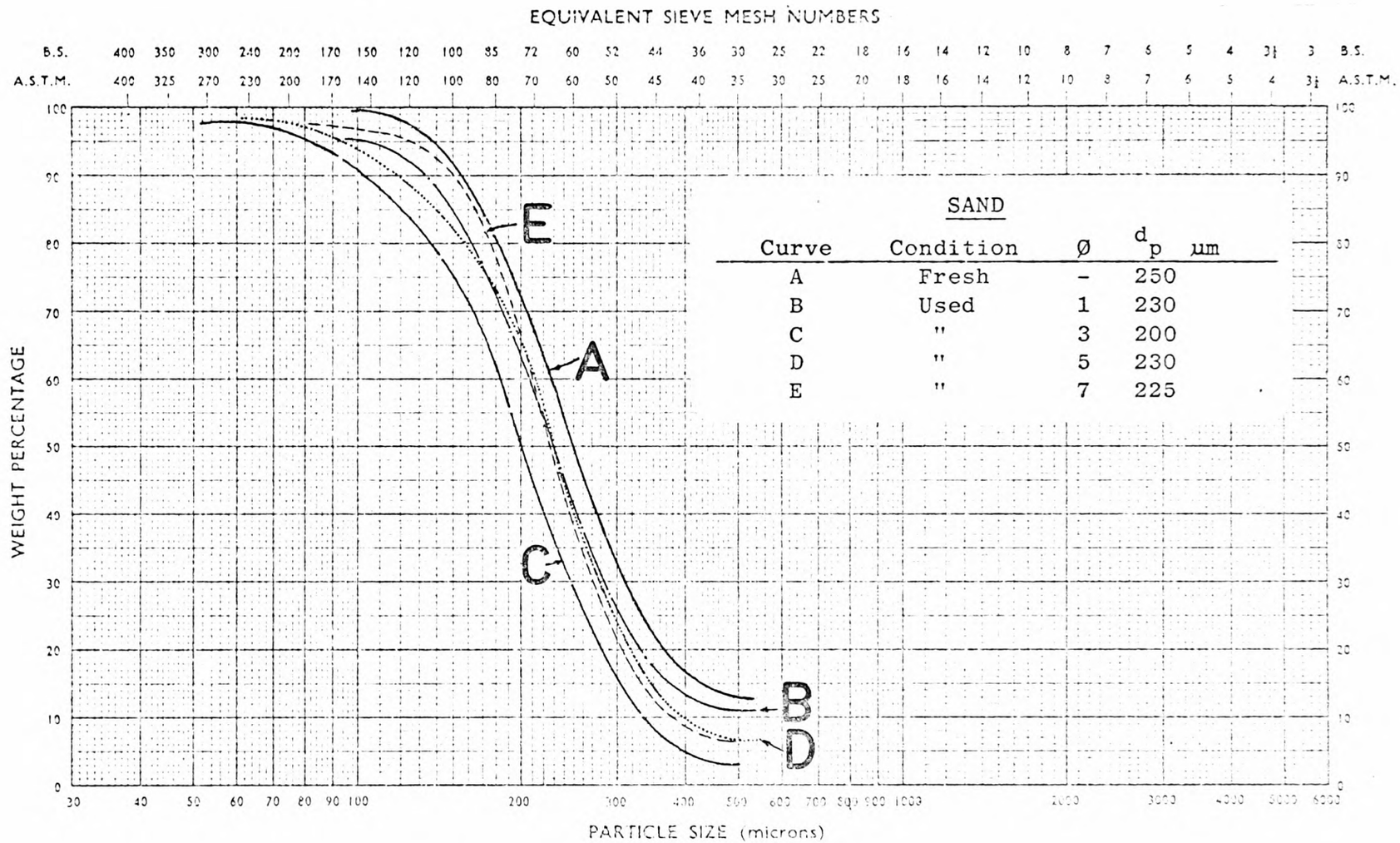

FIG. 6.2 Particle Size Distribution of Sand

service life of a bend is determined by the time required for the conveyed material to penetrate the thickness of the bend and so it is the penetration rate, rather than the specific erosion, which is the dominant factor. Thus, in this programme of tests the depth of wear of all the bends was carefully monitored. Since mass eroded is not proportional to the depth of penetration (Mills and Mason 1977a), analysis based solely on mass eroded can produce totally misleading results.

In the following analysis the two important bend erosion descriptors, viz. mass eroded in terms of specific erosion and depth of wear in terms of penetration rate, are discussed separately. The comparative experimental data obtained by Mills and Mason (1976a, b, c, 1977a, b, c) is also discussed, together with the author's work, in the following sections.

6.4.1 Specific Erosion Analysis

The experimental results, in terms of mass eroded for all the test bends, are presented graphically in Figs. 6.3 to 6.6. These are plots of erosion, on an accumulative basis, against mass conveyed for each bend tested at a given phase density, and show how the erosion varied with each batch of sand conveyed, and hence with respect to time.

An interesting feature of these curves, with the exception of those at a phase density of 3, is the small degree of scatter over this range of phase densities. This observation is in direct contrast to that reported by Mills and Mason (1976b, c) based on 70 μm sand results, which showed that the degree of scatter increased as phase density was increased. They attributed this phenomenon partly to the velocity effect in the test loop and partly to the fact that small particles will be influenced by the turbulence and eddies generated by bends in the pipeline. As phase density is increased there is a corresponding increase in pressure drop which causes a variation of velocity from bend to bend. Although part of the scatter of results shown in Figs. 6.3 to 6.6 can be attributed to this velocity effect, part is also due to some other cause, and the author considers particle degradation to be responsible. The effect of velocity was reviewed in Chapter 3 and from this it is assessed that at phase densities of 1, 5 and 7, the scatter of the results in excess of the velocity effect is ±9%, 16% and 17% respectively, but at a phase density of 3 it is ±28%. Thus, by

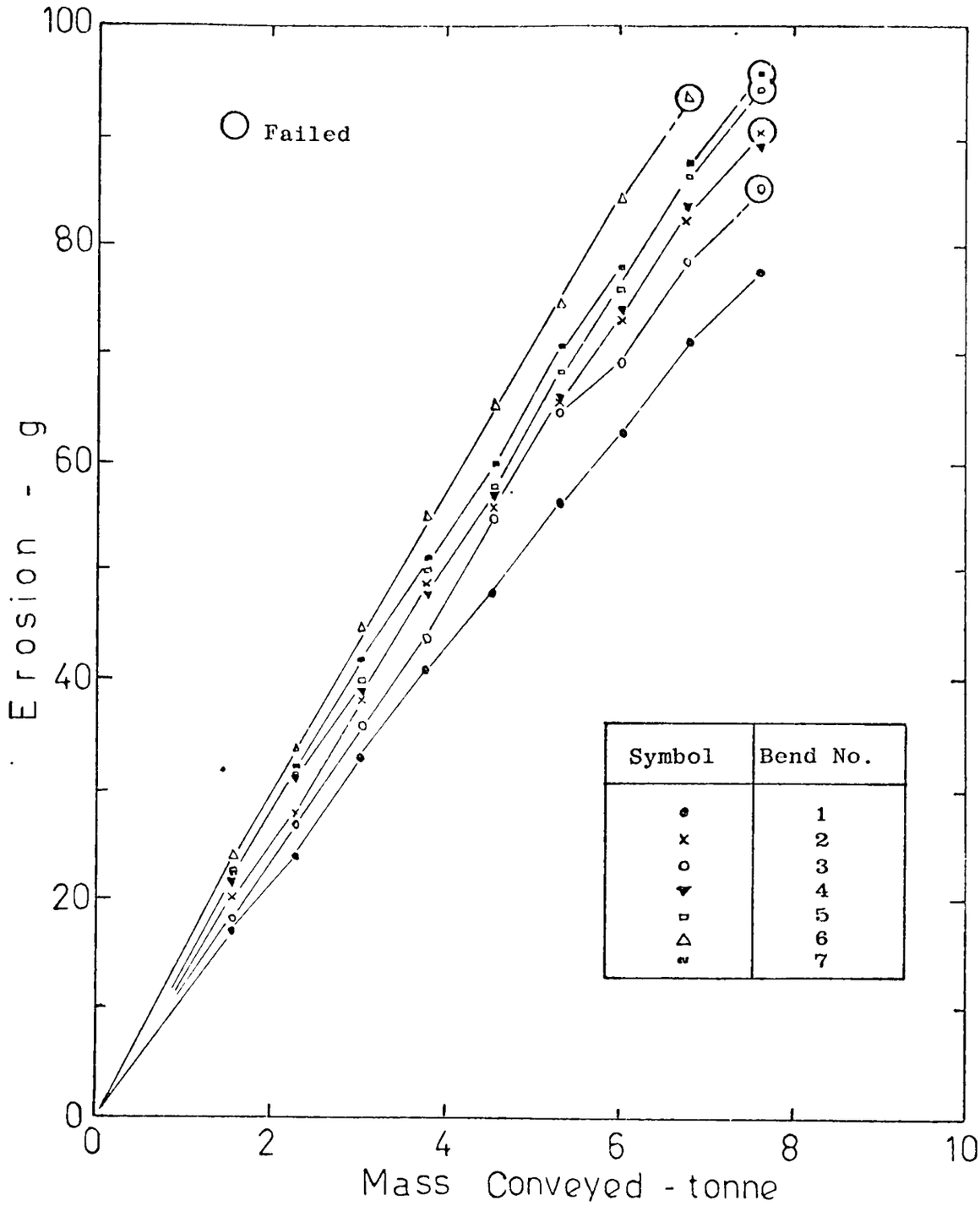

FIG. 6.3 Variation of Erosion with Mass Conveyed at a Phase Density of 1.

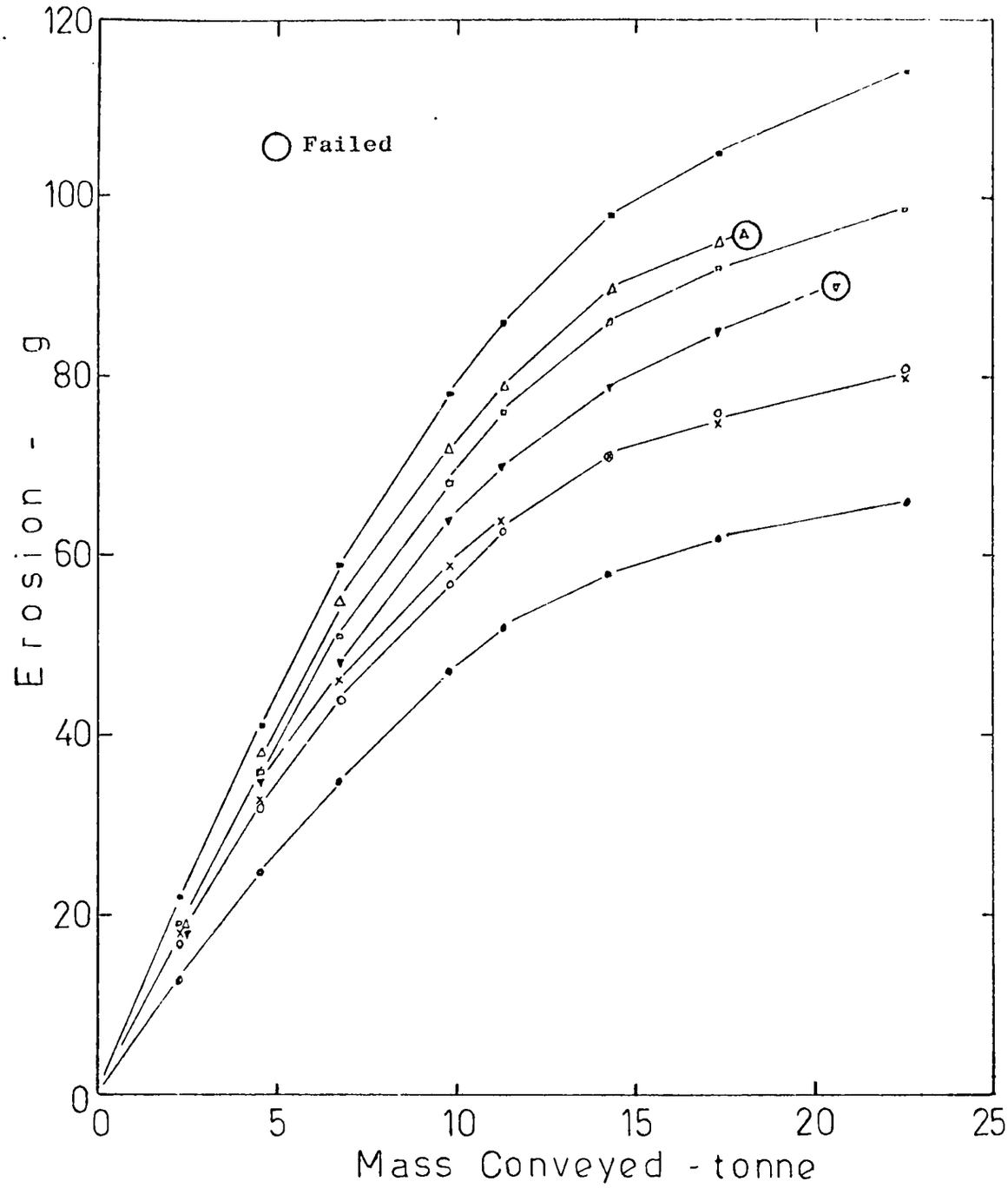

FIG. 6.4 Variation of Erosion with Mass Conveyed at a Phase Density of 3.

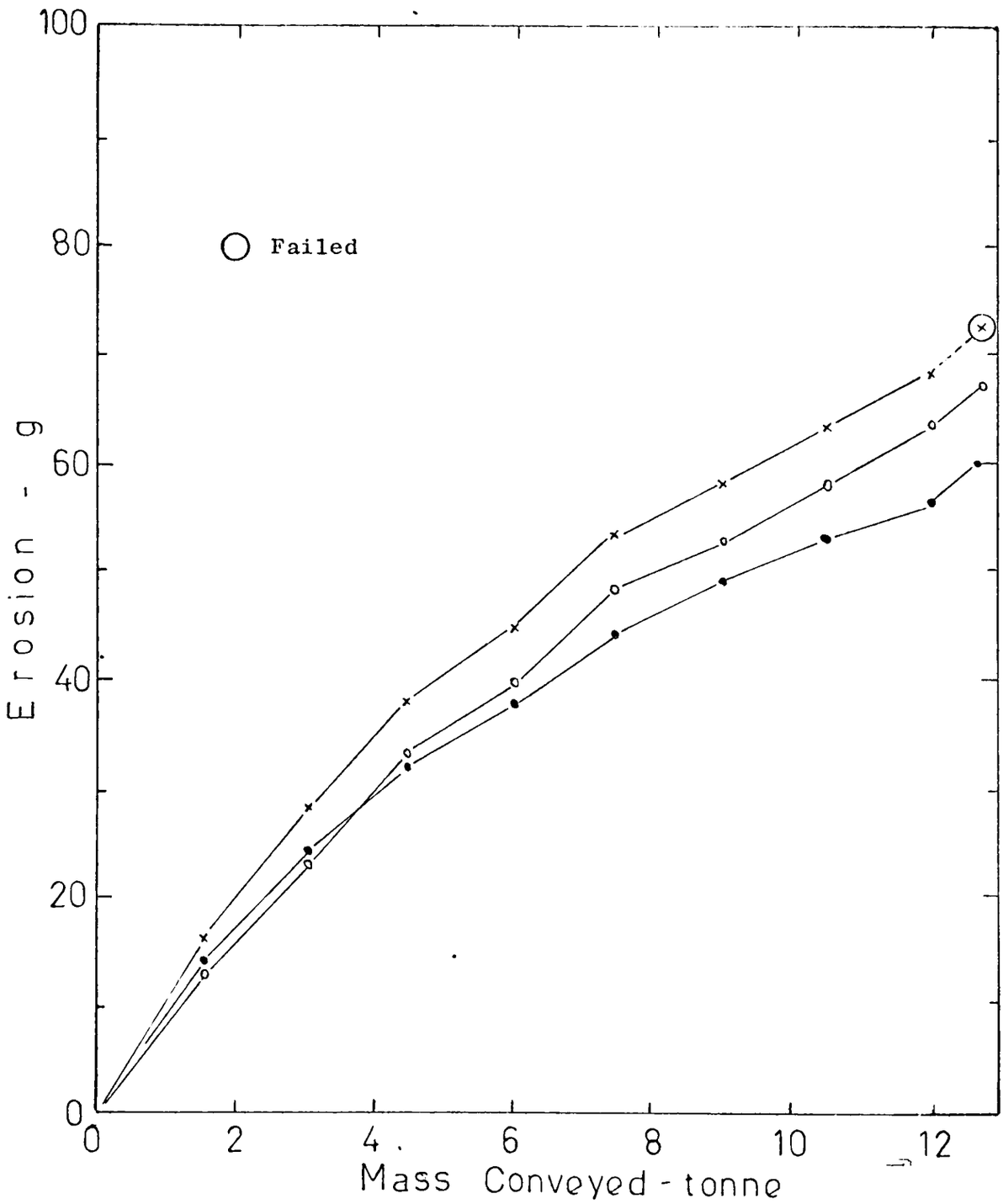

FIG. 6.5 Variation of Erosion with Mass Conveyed at a Phase Density of 5.

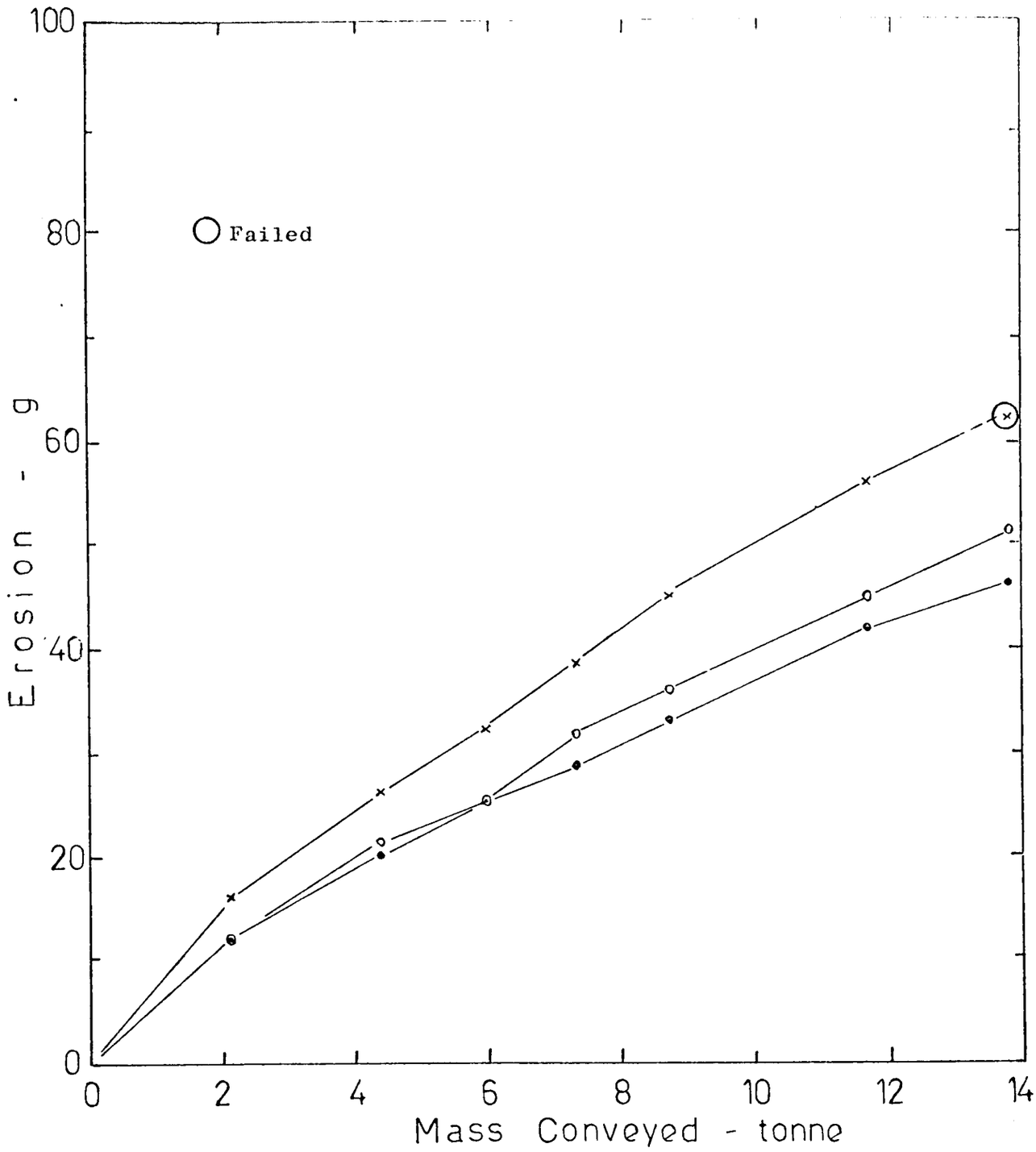

FIG. 6.6 Variation of Erosion with Mass Conveyed at a Phase Density of 7.

superimposing the scatter of results in Figs. 6.3 to 6.6 and by isolating the velocity effect from particle degradation effect for the 250 μm sand, it can be seen that the degree of scatter, particularly at a phase density of 3, is largely due to particle recirculation.

The first bend to fail at this phase density of 3 was after some 18 tonnes of sand had been conveyed, compared with 7, 12 and 13 tonnes at phase densities of 1, 5 and 7 respectively. From Fig. 6.4 it can be clearly seen that there was already a marked scatter of results after only 10 tonnes of sand had passed through the bends, and this scatter of results continued to increase to the end of this test series. From the particle size analysis (Fig. 6.2), the mean particle size at a phase density of 3 (curve C) was reduced by some 50 μm to about 200 μm . This reduction was some 10% greater than those at the other phase densities. In addition, there was a 15% increase in the 'fines' produced at the end of the test series for a phase density of 3, compared with only 7% at the other phase densities. Thus, it is probably this increase in 'fines' due to particle recirculation, combined with the velocity effect, that accounts for the scatter of results at the phase density of 3.

This large degree of scatter and consequent premature bend failure, both of which are primarily associated with the finer sand, will be examined further in Chapters 8 and 9, when 70 μm sand will be used in the investigations. The magnitude of the influence of particle degradation on erosion is also considered in more detail in Chapter 7, when fluidised bed ash with a mean particle size of 1350 μm was reduced by 50% to 650 μm after 21 runs and had only been conveyed a distance of about 1100 m.

Hence, in this work, with respect to particle size effects for the range of phase densities considered, no appreciable increase in the scatter of results was observed as phase density was increased when larger size particles were conveyed. The degree of scatter in the experimental results and consequent premature bend failure, is primarily attributed to the presence of 'fines' which are particularly associated with smaller particles, as suggested by Mills and Mason (1976c).

Since there was a considerable variation in the total number of runs, from 10 to 30 over the range of phase densities tested, there is a

need to evaluate the erosion data based on a common factor. It was decided to use the erosion values, in terms of both mass eroded and depth of penetration, from all the bends based on the first six batches conveyed. This would also provide a direct basis for comparison with the experimental results presented by Mills and Mason (1976a, b, 1977a).

Fig. 6.7 shows the influence of particle size on phase density in terms of erosion with respect to time. Whilst the rate of erosion for the 70 μm sand clearly tended to decrease with respect to time, for the 250 μm sand this appears to be to the contrary. However, for both particle sizes a definite trend towards decrease in erosion with increase in phase density is clearly shown. In terms of particle size effect the erosion rate for the 250 μm sand was approximately double that for the 70 μm sand, corresponding to the same phase density.

A log plot of the specific erosion results is presented in Fig. 6.8. Also included in this figure are the slopes obtained by Mills and Mason (1976a, b) from their work with 230 μm (-0.16) and 70 μm (-0.37) sand. In order to fully evaluate the influence of phase density on specific erosion, and to assess the effects of particle recirculation in this analysis, the experimental results of five test sets, corresponding to the first ten runs at each particular phase density tested in this work, are presented. These slopes clearly show that specific erosion decreases as phase density is increased, but for the 250 μm sand, although the slopes indicate that there is a definite trend towards a change from -0.33 to -0.47 due to particle recirculation, this change is not as dramatic as that reported by Mills and Mason for their 230 μm sand (1976b). In fact, in terms of individual values, the slopes for the 250 μm sand remained remarkably consistent at around -0.42 compared with a change from -0.16 to -0.73 for the 230 μm sand! The discrepancy between the slopes obtained for the 250 and 230 μm sand, which were essentially within the same particle size range, is explained by the fact that the slopes for the 230 μm sand were based on results which were obtained over a range of test conditions, i.e over different combinations of velocity and phase density, and so proper comparison between the slopes of these two materials are not appropriate.

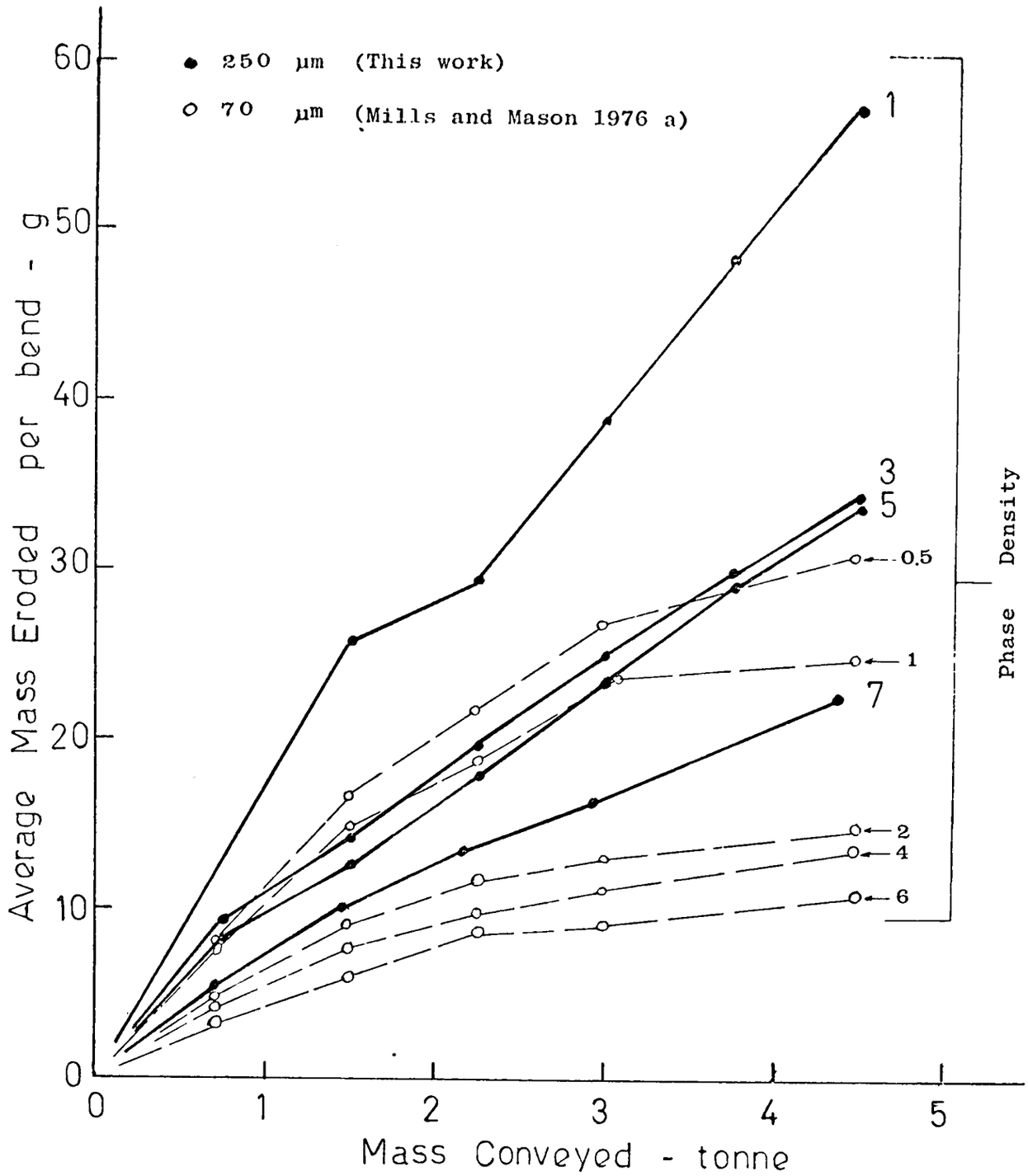

FIG. 6.7 Influence of Particle Size on Phase Density in terms of the Variation of Erosion with Mass Conveyed.

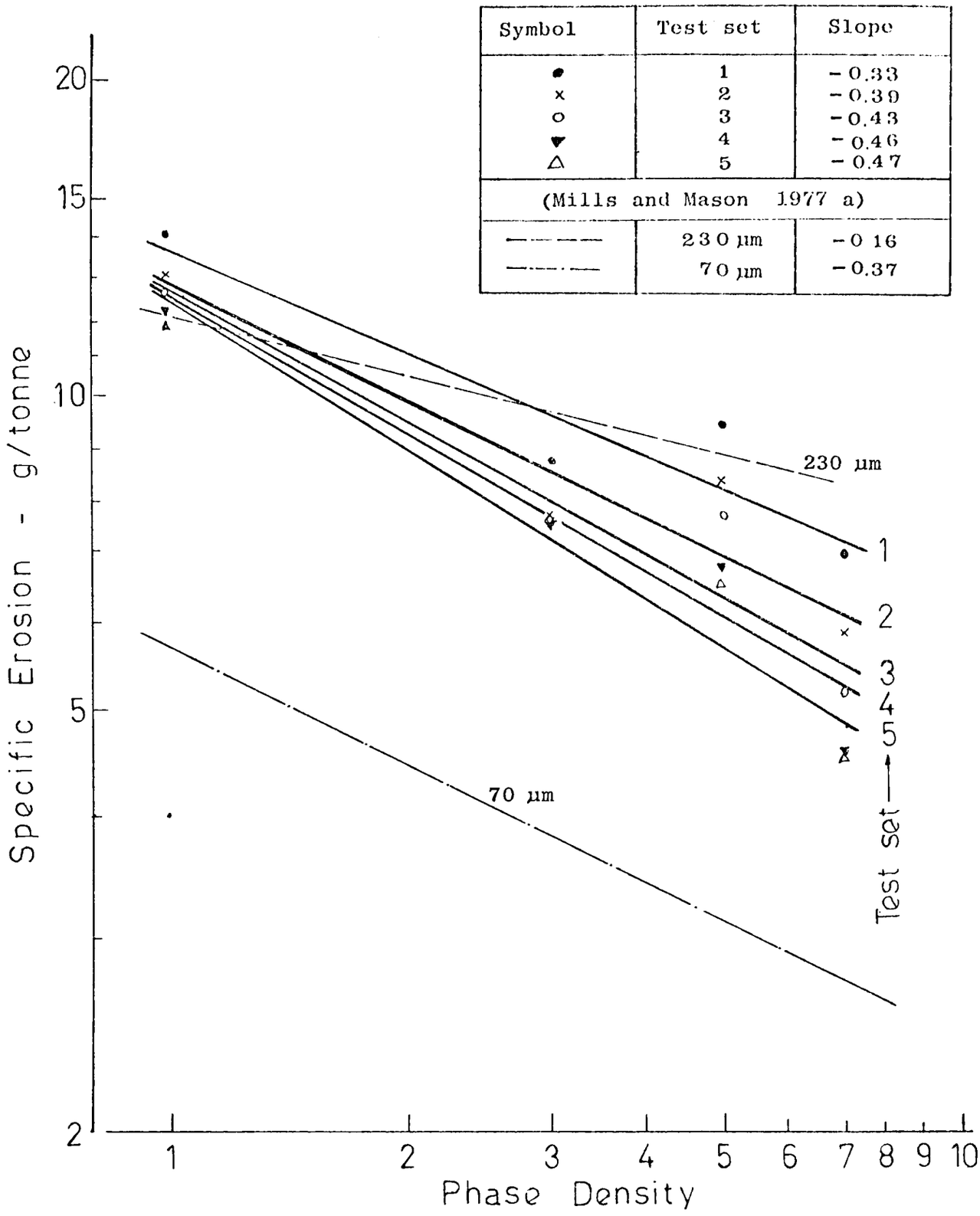

FIG. 6.8 Variation of Erosion with Phase Density

Whilst the slope for the 70 um sand (-0.37) was within the range of values for the 250 um sand, correlation in terms of phase density with respect to particle size based on these two materials is not reliable. This was due to the considerable degree of scatter in the results for the 70 um sand and so the accuracy of this slope is questionable. Further work is necessary with a wider range of particle sizes over this range of phase densities before any definitive influence of the inter-relating effect of particle size on phase density can be assessed.

On the basis of results obtained in this work (Fig. 6.8), the influence of phase density on specific erosion is given by :-

$$\text{erosion} \propto \text{phase density}^{-0.33}$$

for reasonably fresh sand. The actual value of the exponent is dependent to some degree on the condition of the product, as was also previously observed by Mills and Mason (1976b).

6.4.2 Penetration Rate Analysis

After each test run the wear profile along the outer wall of each test bend was recorded by measuring the minimum wall thickness every five degrees around the bend. In this way the point of maximum wear, which will ultimately determine the point of failure of the bend, could be located and monitored continuously over the entire test series.

Thus, for each test phase density, a set of results in terms of the variation of minimum bend wall thickness against the mass eroded from the bends, corresponding to each particular test run, was obtained. However, presentation of data in this form could give misleading impressions. This was due to the slight deviation of the initial bend wall thicknesses, caused by the extrusion process in manufacturing the bends. Hence, the experimental data was replotted by taking a datum of zero wear and expressing the results in terms of maximum depth of penetration instead, as shown in Fig. 6.9.

The four heavy lines represent the mean slopes of the experimental results at each phase density in this work. The six light lines included in this figure were replotted from data based on 70 μm sand obtained by Mills and Mason (1977a).

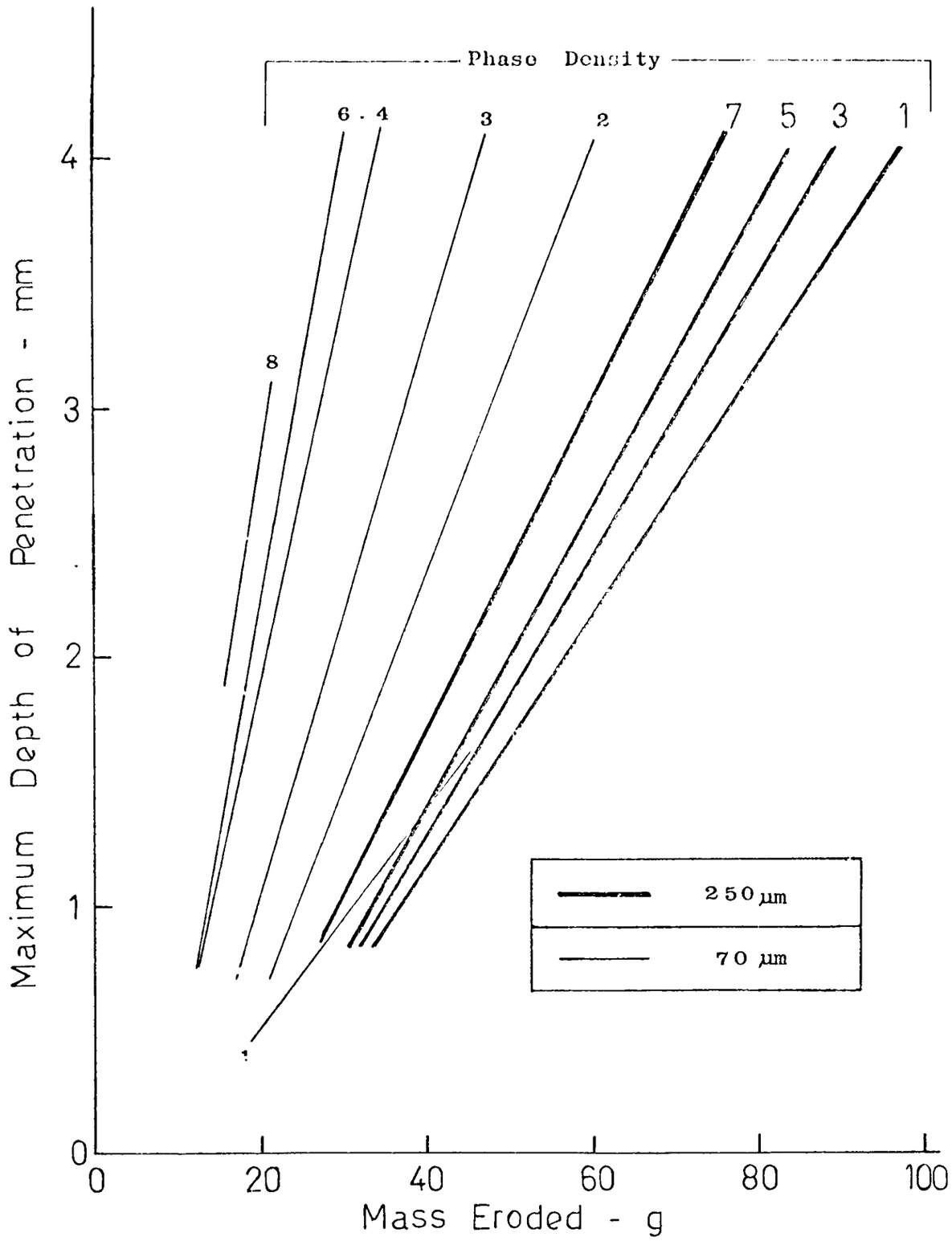

FIG. 6.9 Influence of Particle Size on Phase Density in terms of Penetration Rate.

Comparison of the slopes between these two sets of data clearly shows the marked influence of particle size as well as phase density, on penetration rate. The depth of wear is clearly not proportional to mass eroded, particularly for the finer sand. In order to examine the penetration rate effects in more detail, the gradients of all the slopes in this figure were determined and the penetration rates, in terms of maximum depth of wear per unit mass eroded, are presented in Fig. 6.10.

This figure clearly shows the magnitude of the influence of particle size on phase density with respect to penetration rate. Whilst the 70 μm sand shows a marked increase in penetration rate as phase density is increased, the 250μm sand hardly shows any significant increase over a similar range of phase densities. At a phase density of 1, both showed a similar penetration rate of about 50 μm/g, but as the phase density is increased to 7 they differ by a factor of about 4.

An interesting feature in this figure is the trend of the curves, particularly for the 250 μm sand, below the range of phase densities investigated. For the 70 μm sand extrapolation of the curve clearly shows that there would be no penetration rate when no material is conveyed, as expected. However, for the 250 μm sand there appears to be a threshold phase density below which penetration rate increases rapidly to a value of about 50 μm/g as phase density is increased to 1, and the penetration rate value remains relatively constant beyond this range of phase densities. Thus, it would appear that there is a transition effect with regard to particle size in terms of phase density on penetration rate. This is an interesting aspect of the inter-relating effect of particle size on phase density that warrants further investigation with a range of particle sizes conveyed over a wider range of phase densities, in order to determine the transition effect fully. Similar transition effects with regard to certain variables have also been reported by Goodwin et al (1969) on the inter-relating effect of velocity and particle size, and by Mills and Mason (1976b, 1977c) on the inter-relating effect of velocity and particle shape.

Although the penetration rate is expressed in terms of the mass eroded, this figure would also show a very similar relationship in terms of mass conveyed over this range of phase densities. Thus, in terms of

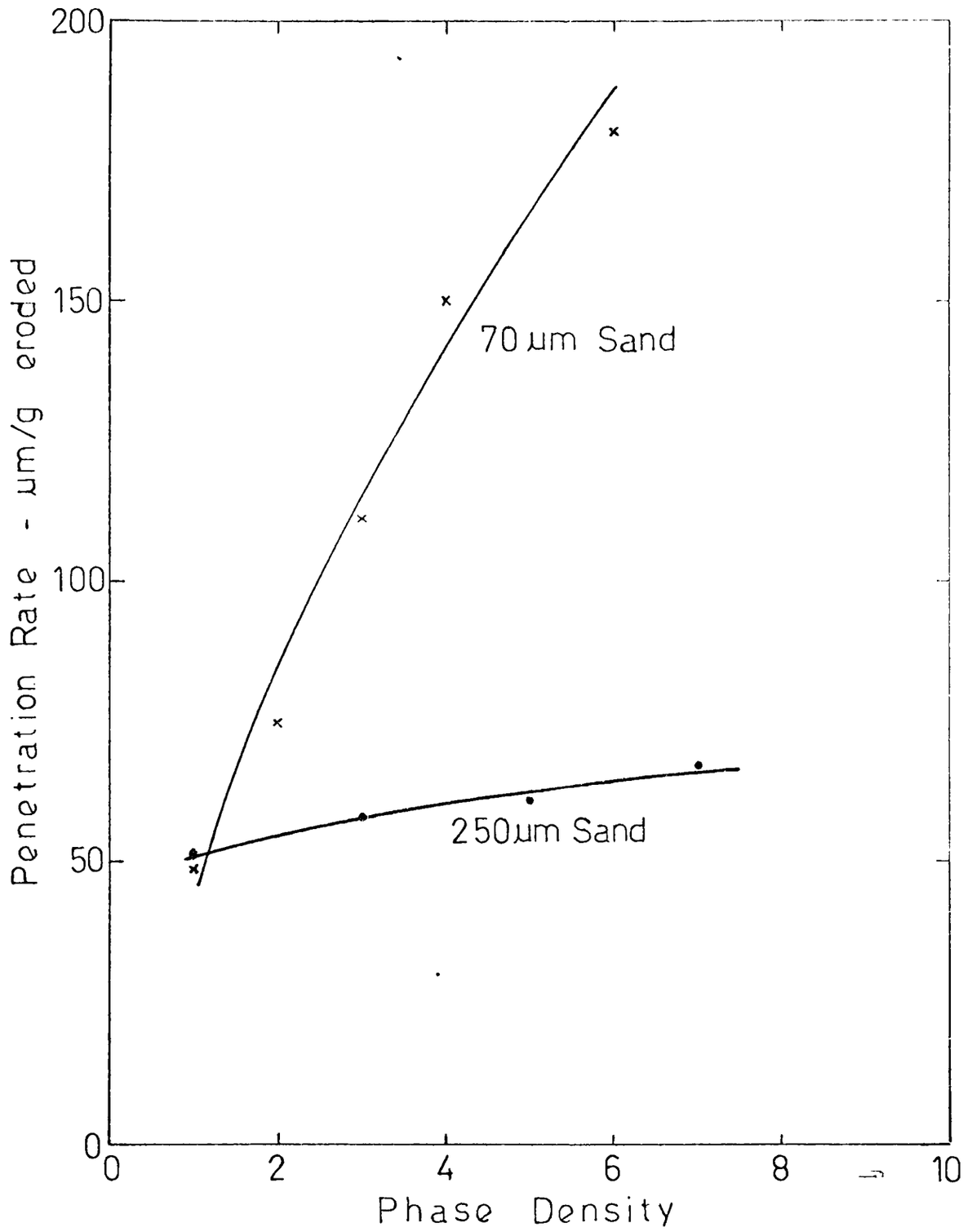

FIG. 6.10 Influence of Particle Size on the Variation of Penetration Rate with Phase Density.

potential service life, the influence of particle size over this range of phase densities is clearly evident. Bends will fail faster at higher phase densities when smaller particle sized products are conveyed, and also fail after a much lower tonnage had been conveyed compared with larger sized materials of similar particle hardness conveyed under essentially similar conditions. This aspect of the problem will be considered later in this Chapter.

6.4.3 Surface Erosion Profiles

The large difference in rates of penetration within a range of particle sizes has been explained previously by Mills and Mason (1977a, b), in terms of impact angle effects. Three basic stages of erosion, based on observations of the surface erosion patterns and wear profiles of bends eroded by 70 μm and 230 μm sand, were found to be dependent upon the impact angle. Briefly, for maximum volume removal, the impact angle at which this occurs is about 20^{o}, for maximum depth of wear it is about 55^{o}, and both are at a minimum at normal impact. The occurrence of the particular stages of erosion was primarily related to the erosive wear process in the bend itself. For bends eroded by the 70 μm sand a stepped erosion pattern was observed, compared with a fine rippled pattern produced by the 230 μm sand. The increase in penetration rate as phase density is increased for the 70 μm sand was attributed by these authors to the formation of steps, which rapidly increase the effective impact angle from about 20^{o} initially to about 45^{o}, which corresponds to an increased penetration rate. For the 230 μm sand, in the absence of any such steps the impact angle remains unchanged at about 25^{o}, which corresponds to a region of maximum erosion rate, but little significant increase in penetration. Examination of the surface erosion patterns of the bends eroded by 250 μm sand in this work largely confirms these observations. Fig. 6.11 shows the erosion pattern of one of the bends which failed at each particular test phase density. At the two lower phase densities, ripple patterns which are characteristic of ductile material erosion are clearly observed. At the two higher phase densities, some form of stepped pattern is observed. However, this was not prominent compared with a depth of some 2mm in the steps which was commonly observed in the 70 μm sand erosion patterns (Mills and Mason 1977b).

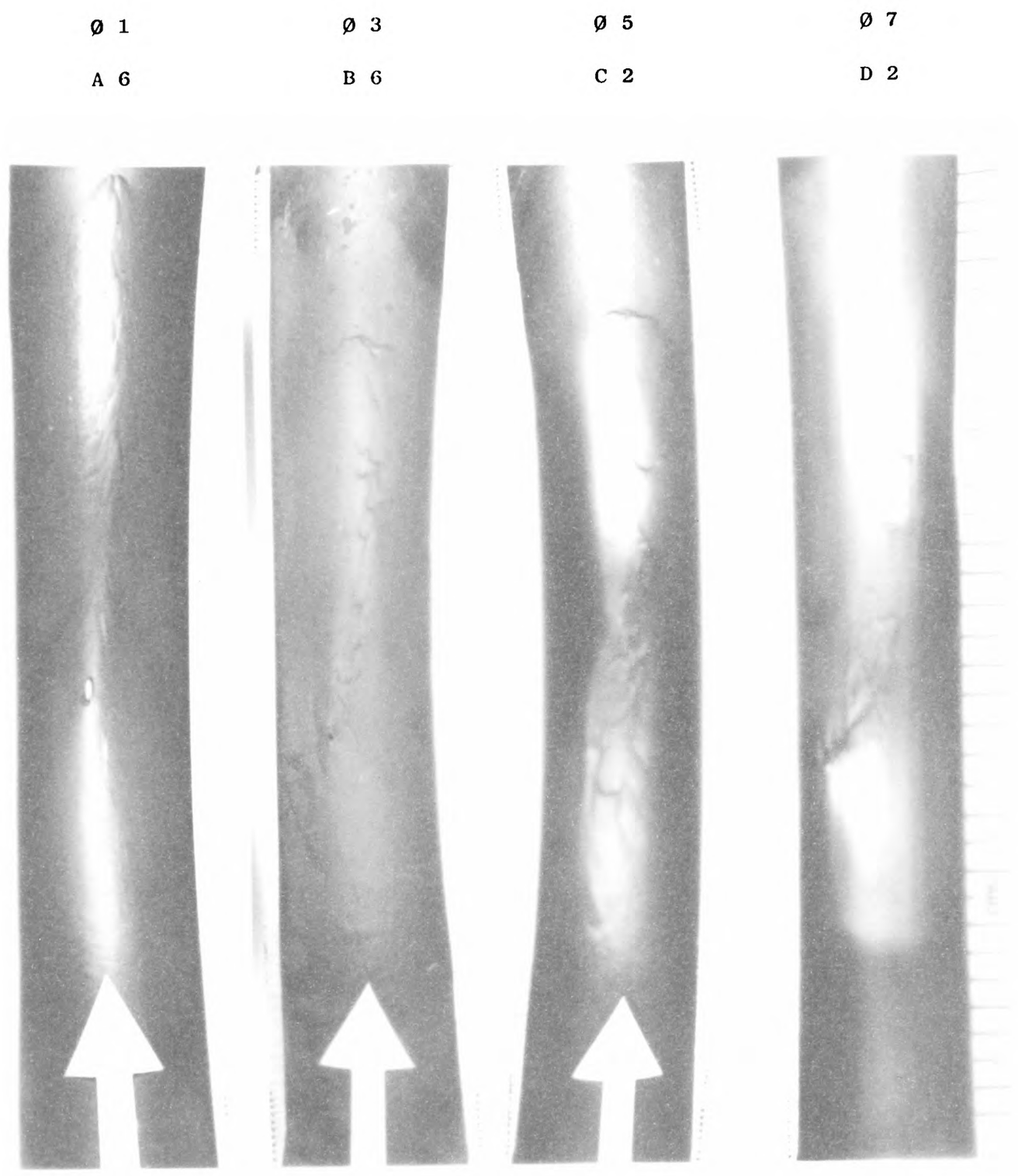

FIG. 6.11 Surface Erosion Patterns of Test Bends

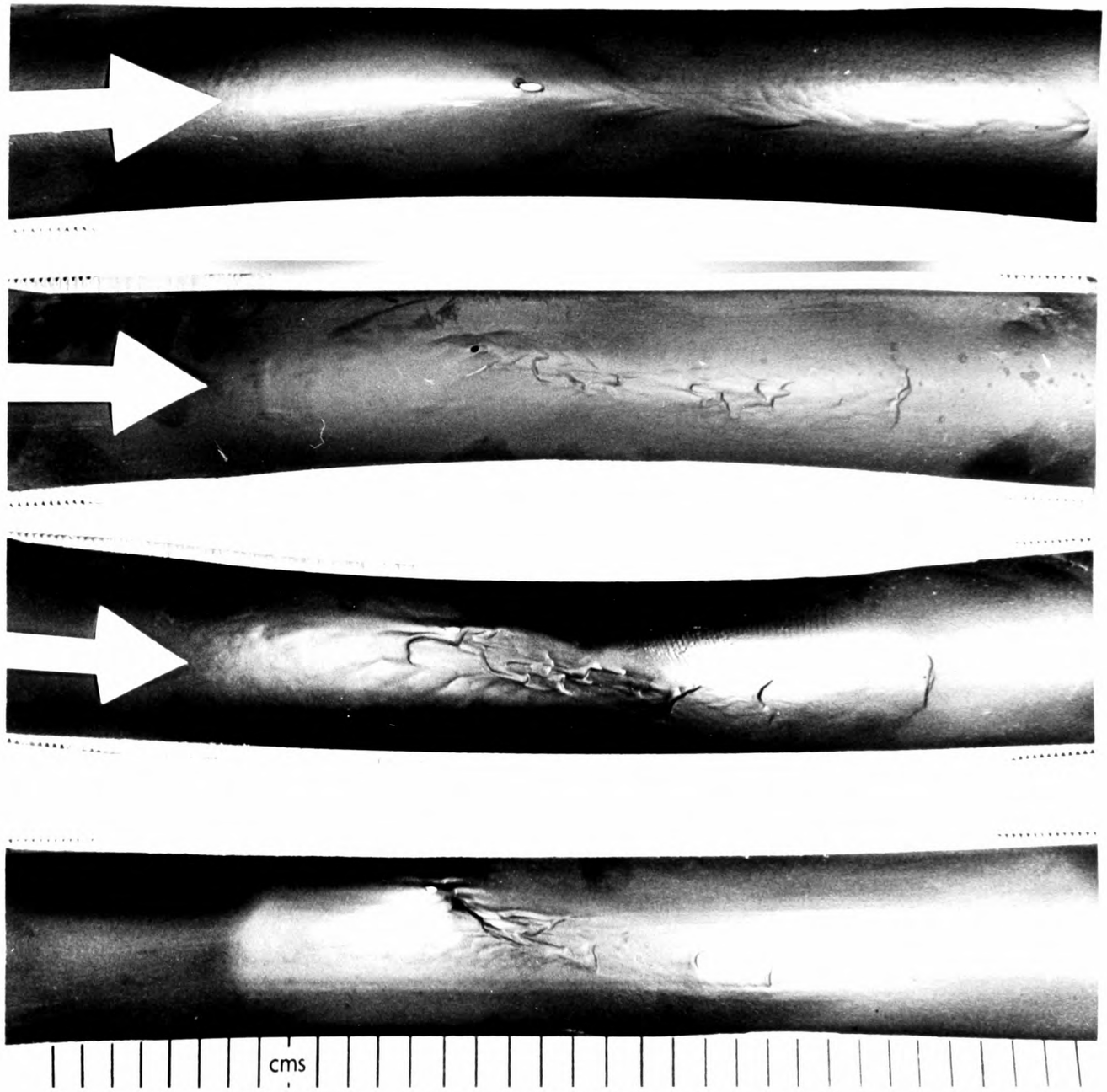
cms

The pronounced tracking of the erosion pattern across the bend, particularly at the higher phase densities, indicated considerable swirling flow in the bend. Mills and Mason (1976c) reported that these erosion tracks were a characteristic feature of premature bend failure when 70 μm sand was used. However, in this work these erosion tracks were probably due to the misalignment of the particular bend in the test loop.

The relatively limited increase in penetration rate as phase density was increased for the 250 μm sand (Fig. 6.10) can be further explained by comparing the bend and pipe wear profiles presented in Figs. 6.12 and 6.13. Both figures clearly show that, for a constant mass of 20 g eroded from each bend, there is a considerable increase in the depth of wear over this range of phase densities for the 70 μm sand compared with the 250 μm sand. Whilst the position of maximum wear in terms of bend angle remains fairly constant at 33^{o} and 42^{o} for the 70 and 250 μm sand respectively, there is a significant difference in terms of pipe angle. For the 70 μm sand the pipe angle at which maximum erosion occurs progressively increases above the centre line of the pipe (Fig. 6.13), whilst for the 250 μm sand it appears to remain fairly constant at about 30^{o} below the centre line.

These respective bend and pipe wear profiles also serve to explain the particle size effect on phase density with respect to both mass eroded and depth of wear. For the finer 70 μm sand, erosion occurs over a concentrated region and, as phase density is increased, this eroded region turns into a shallow valley which gets progressively steeper and consequently erodes to a greater depth in the process. However, for the larger sand erosion is spread over a wider range of both bend and pipe angle, and this erosion crater appears to increase as phase density is increased, thereby limiting any corresponding increase in depth of wear, as shown in Fig. 6.10.

6.5 BEND LIFE ANALYSIS

In order to determine the influence of phase density on bend life, the experimental data presented in both specific erosion and penetration rate analyses must be incorporated with the actual erosion results obtained from a pneumatic conveying system. Mills and Mason (1977a) have presented an analysis of bend life in terms of phase density, and

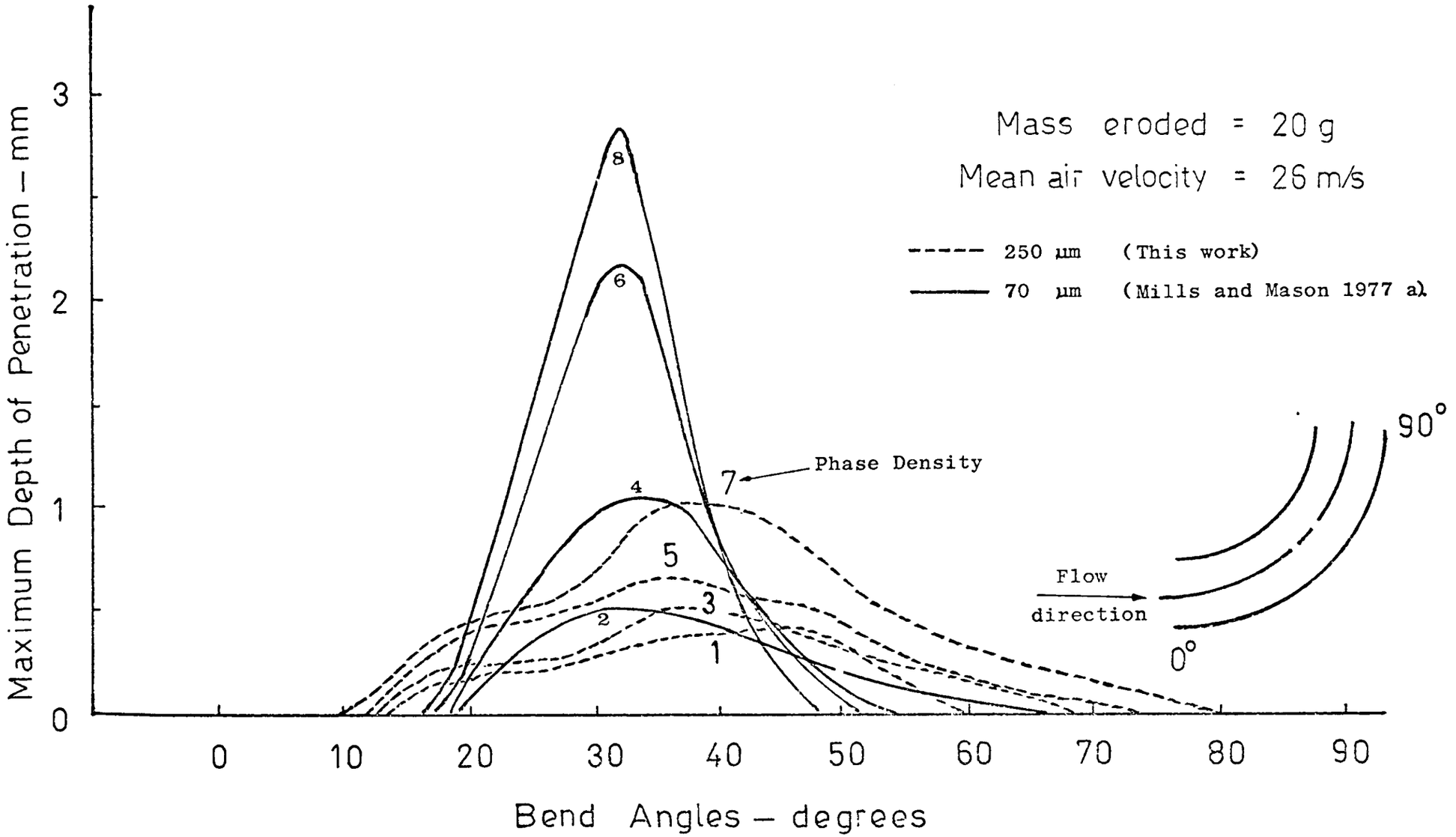

FIG. 6.12 Influence of Particle Size on Phase Density in terms of Bend Wear Profile.

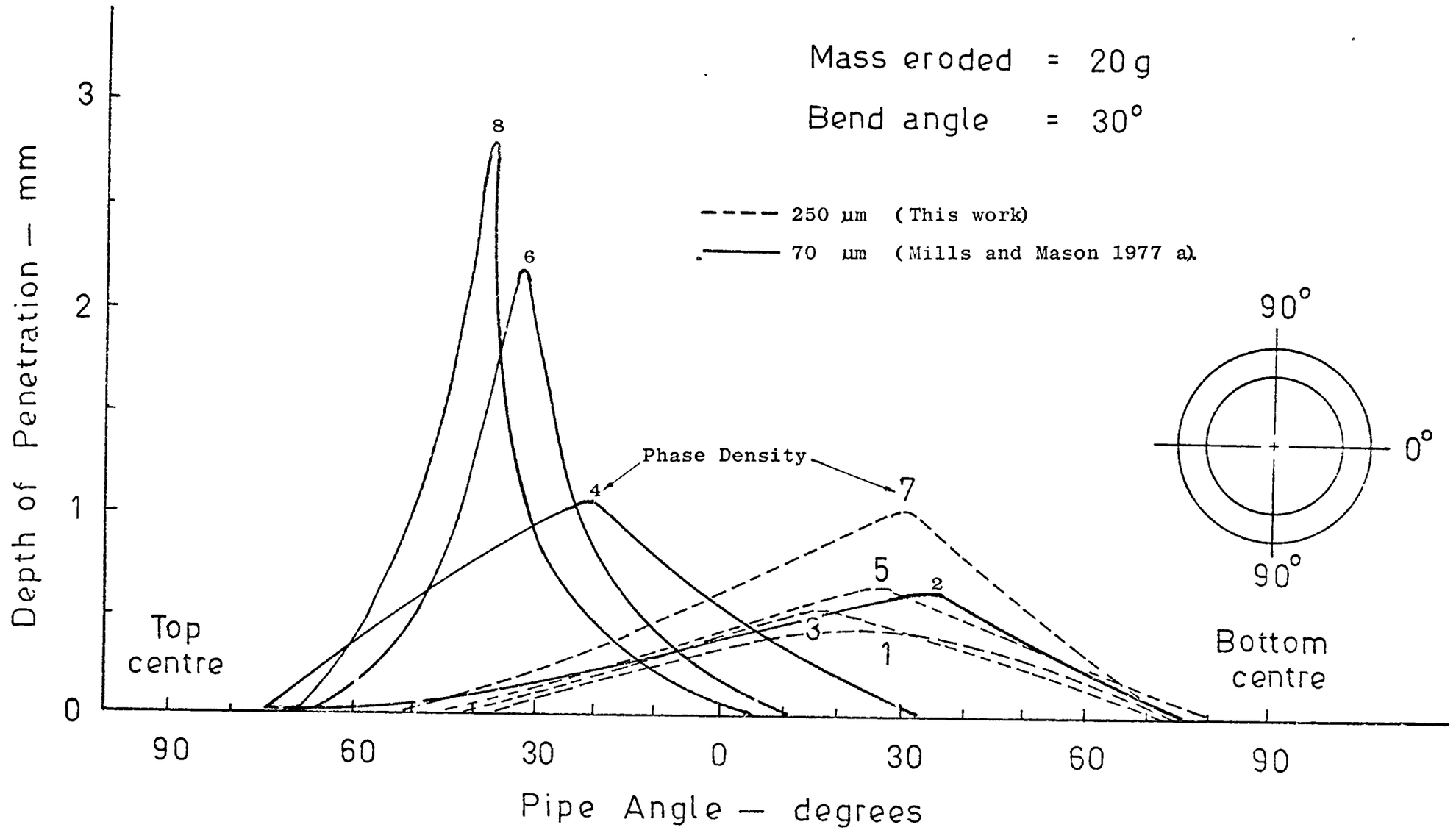

FIG. 6.13 Influence of Particle Size on Phase Density in terms of Pipe Wear Profile

in this section a similar procedure is adopted. For comparison purposes the results of their analysis, based on 70 μm sand, are also included.

For the purpose of determining the conveying capacity and service life of bends it is necessary to obtain a relationship between the actual mass eroded at time of failure (E_{bf}), and phase density (ϕ). This particular relationship for the 250 μmsand used in this work is given in Fig. 6.14. This graph shows the ultimate effect of phase density on the erosive wear of pipe bends and, together with the results for the 70 μm sand, the influence of particle size over this range of phase densities can also be seen. The two curves clearly show a definite trend towards a decrease in the mass of metal eroded from the bends at the time of failure as phase density is increased. A log. plot of the results for the 250 μm sand in this figure indicated that, over this range of phase densities, the erosive wear of bends with this particular sand can be represented by :

$$\text{Mass eroded at failure} \propto (\text{Phase density})^{-x}$$

From a linear regression analysis of the relevant experimental results, the above expression can be given by :-

$$E_{bf} = 95.5\ (\phi)^{-0.20} g \qquad (6.1)$$

From Fig. 6.8 the variation of specific erosion (ε) with phase density (ϕ) is given by :-

$$\text{Specific erosion} \propto (\text{Phase density})^{-y}$$

The phase density exponent was shown to be dependent upon the condition of the product, and this varies from -0.33 to -0.47 for the 250 μm sand. In order to present a more representative set of evaluations it was decided to use the exponent based on Test Set 3, i.e. -0.43. This decision was largely due to a very similar exponent of -0.42 which was consistently obtained in terms of individual test values. Thus, from a similar linear regression analysis of the relevant experimental data, the above expression can be given by :-

$$(\varepsilon) = 12.9\ (\phi)^{-0.43}\ \text{g/tonne} \qquad (6.2)$$

In the analysis given by Mills and Mason (1977a), they chose an exponent based on the results with 230 μm sand rather than from the 70 μm sand,

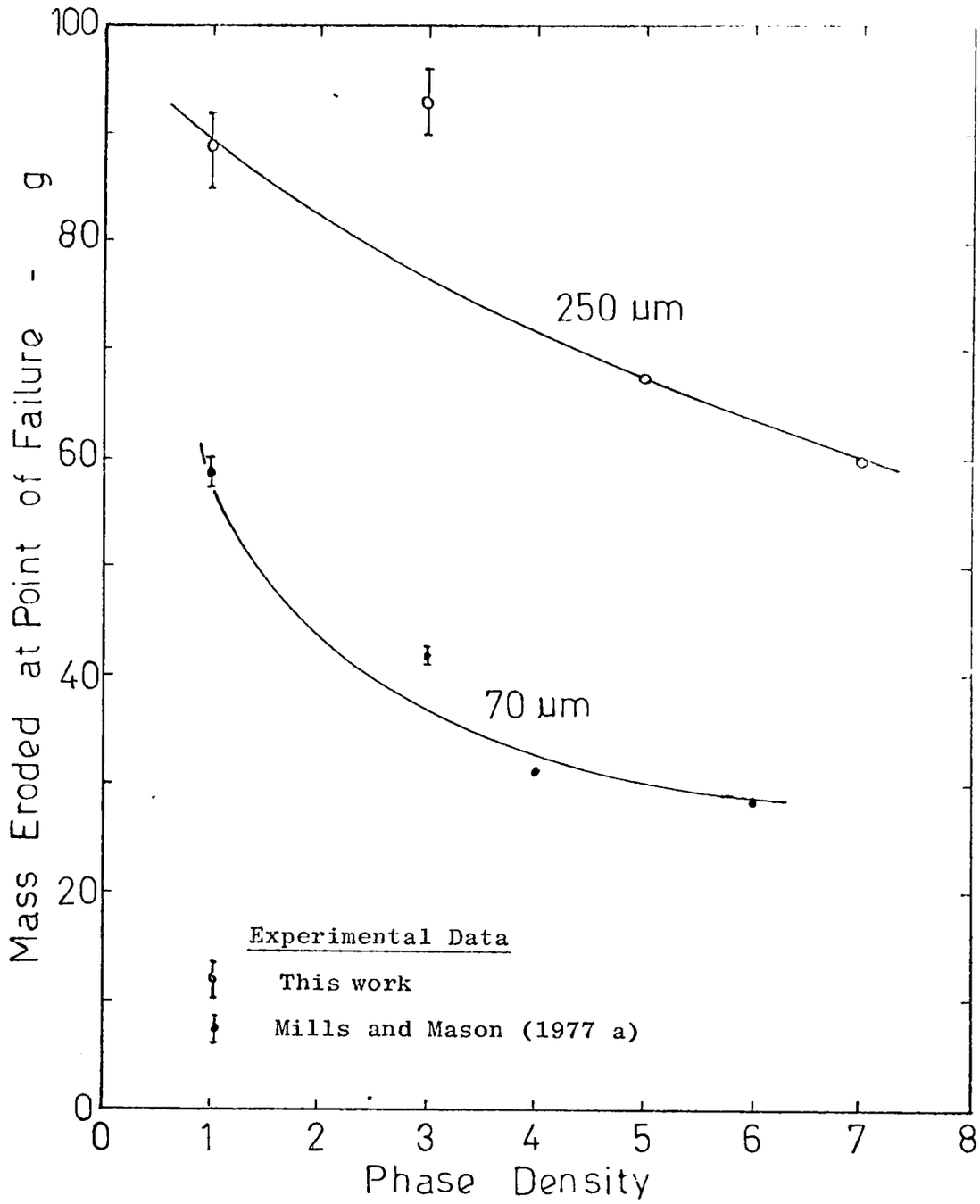

FIG. 6.14 Influence of Particle Size on the Variation of Mass Eroded to cause Bend Failure with Phase Density

due to the uncertainty with regard to its actual exponent. Furthermore, they showed that particle size had little effect on the variation of specific erosion (1976c, 1977b), thus justifying their selection of the particular exponent of -0.16 compared with -0.37 for the 70 μm sand. However, their observation was based on the results of a range of particle sizes at a phase density of 2 only. From Fig. 6.8 it can be seen that, at higher phase densities, there is a considerable increase in the variation of the specific erosion with respect to particle size. Thus, the reliability of their analysis, based solely on the exponent obtained from the 230 μm sand results, is questionable.

The mass of sand that can be conveyed through these bends before failure occurs (M_s), is given by :-

$$M_s = \frac{E_{bf}}{\epsilon}$$

Substituting the appropriate equations into this expression gives :-

$$M_s = 7.40\ (\phi)^{0.23} \qquad (6.3)$$

A graphical representation of this equation is given in Fig. 6.15.

For the service life of the bends, the conveying time to bend failure ($\Delta\tau_{bf}$) is given by :-

$$\Delta\tau_{bf} = \frac{M_s}{\dot{m}_s} = \frac{M_s}{\phi \dot{m}_a}$$

An air mass flow rate of 0.071 kg/s was required in order to achieve an air velocity of 25 m/s in the 50 mm bore pipeline in this work. Thus, substituting the appropriate values into the above expression gives :-

$$\Delta\tau_{bf} = 28.95\ (\phi)^{-0.77}\ \text{h} \qquad (6.4)$$

A graphical representation of this equation is given in Fig. 6.16.

The sets of curves in Figs. 6.15 and 6.16 clearly show that the influence of particle size on phase density is considerable. In Fig. 6.15, for the 70 μm sand, the overriding influence of penetration rate over that of mass eroded, as phase density is increased, results in a definite decrease in the amount of sand that can be conveyed through the bends before failure occurs. However, for the 250 μm sand, due to the relatively

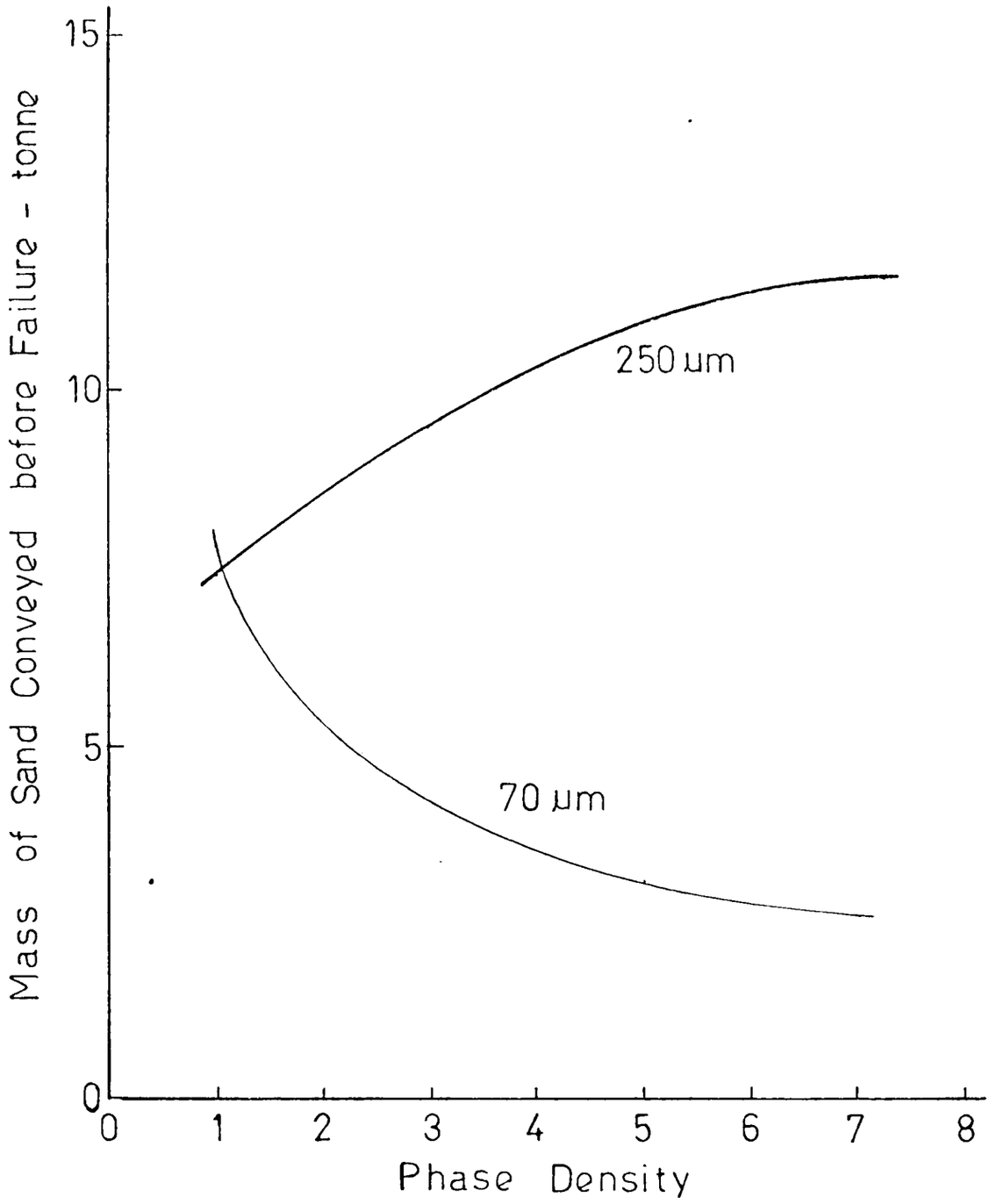

FIG. 6.15 Influence of Phase Density on the Conveying Conveying Capacity of Bends

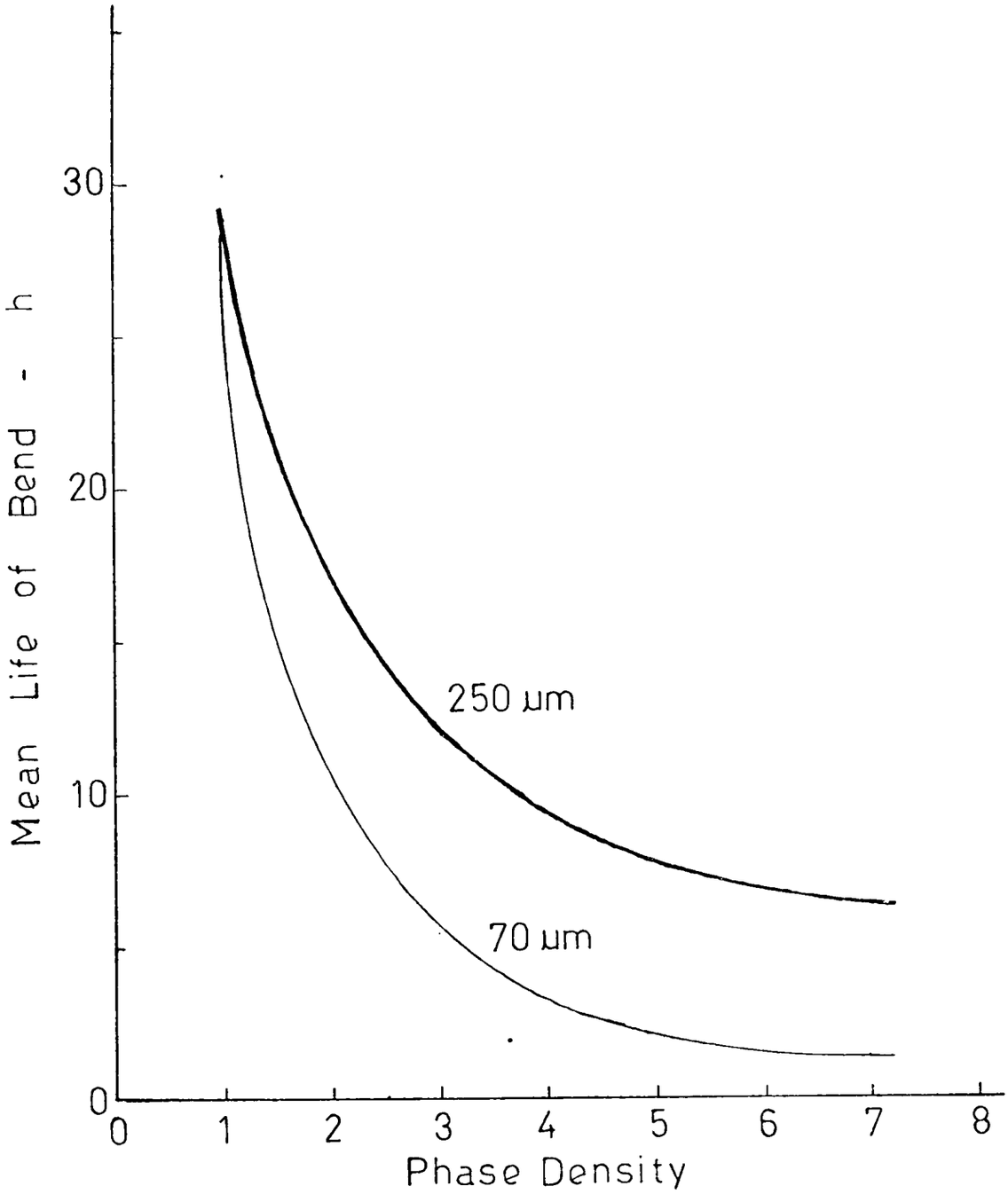

FIG. 6.16 Influence of Phase Density on the Service Life of Bends

insignificant increase in penetration rate over a similar range of phase densities, no such overriding effect was observed. Thus, as specific erosion decreases as phase density is increased, there is a corresponding increase in the amount of sand that can be conveyed before failure occurs. Experimental data given in Table 5.3 confirms the curve obtained in Fig. 6.15 for the 250 μm sand.

In Fig. 6.16 the influence of phase density on the service life of bends is represented. The information in this figure is particularly useful for the pneumatic conveying engineer with regard to the influence of particle size on phase density when designing systems for conveying a variety of different sized products. Since the mass conveyed is directly proportional to phase density, a decrease in the service life of bends with increase in phase density is expected. However, the particle size effect on phase density clearly shows that, at higher phase densities, up to a fourfold increase in bend life is obtained when larger sized material is conveyed, compared with a smaller sized similar material.

6.6 CONCLUSIONS

The main feature of this work on the influence of phase density on erosion is in highlighting the significant inter-relating effect of particle size on phase density. From the analyses of erosion in terms of both specific erosion and penetration rate, definitive trends with regard to particle size effect have been established. The magnitude of this particle size effect on phase density is clearly demonstrated in the bend life analysis.

It has also been shown that particle degradation, due to the continuous recirculation of the product, has a marked influence on erosion over this range of phase densities. The influence of particle degradation will be considered in more detail in the next chapter. Although in this work the only substantial degradation of the particles occurred at a phase density of 3, there was a matching increase in the scatter of the results. The degree of scatter has been reported to cause premature bend failures when finer particles are conveyed, and this is an area that is further examined in Chapters 8 and 9, when 70 μm sand is used.

Whilst it has been reported that, in order to reduce erosion, abrasive materials should be conveyed at higher phase densities, the results in this work clearly show that particle size effects should be fully taken into account before making such a decision. Although the finer 70 μm

sand results clearly show an overriding effect of penetration rate as phase density is increased, this is not the case for the larger 250 μm sand. It appears, therefore, that it may not be necessary to convey certain large particle sized abrasive materials in the dense phase mode only in order to reduce erosion.

It is obvious that much further work is needed in order to investigate the overall influence of particle size on phase density. In this work the velocity was essentially held constant and, since velocity is an important parameter in terms of both specific erosion and penetration rate, it is necessary to carry out a series of tests with a range of particle sizes and velocities,in order to determine the extent of the influence of particle size on phase density.

Chapter 7

The Influence of Particle Hardness

7.1 INTRODUCTION

The hardness of particles is a major factor in determining the potential erosiveness of a particular conveyed product. From the review of the general solid particle erosion literature in Chapter Two, however, it is clear that the specific influence of particle hardness has received relatively little attention. This lack of consideration of the particle hardness effect is perhaps not surprising, since in most of these studies usually only one type of particle, chosen for its abrasiveness, is used as the conveyed material in investigations on the effects of other variables.

In the full scale pipe bend erosion studies a lack of information on particle hardness also exists. Whilst dilute phase conveying systems are generally designed to handle non-abrasive products, dense phase systems allow the possibility of conveying a wide range of abrasive materials. With such a variety of products, ranging from non-abrasive grass seeds to highly abrasive alumina powders, which can now be successfully transported pneumatically in pipelines, there is a need for information regarding the influence of particle hardness on erosion. This information is necessary because a knowledge of its effect on erosion is essential, particularly at the design stage of a system, since it provides an indication of the need to take steps to avoid excessive abrasion and erosion of key system components apart from pipe bends. Thus, a programme of tests was specifically carried out by the author to investigate the influence of particle hardness on erosion and the results are reported in this chapter.

7.2 REVIEW OF PREVIOUS WORK

Wellinger and Uetz (1963) carried out a series of tests to investigate some of the general aspects of both abrasion and erosion. A sand-blast type tester was used to study the erosive wear process of a number of materials, each subjected to erosion by a stream of particles, ranging from chalk to silicon carbide. They found a strong dependence of erosion upon the hardness of the target materials in relation to the hardness of the impacting particles (Fig. 7.1). Apart from the size and shape of the particle itself and impact angle, the magnitude of erosion also depends to a large extent on the difference between the hardness values of the material and particle. The curves in Fig. 7.1 for steels clearly show that there is a threshold value of particle hardness beyond which erosion is decreased or remains relatively constant.

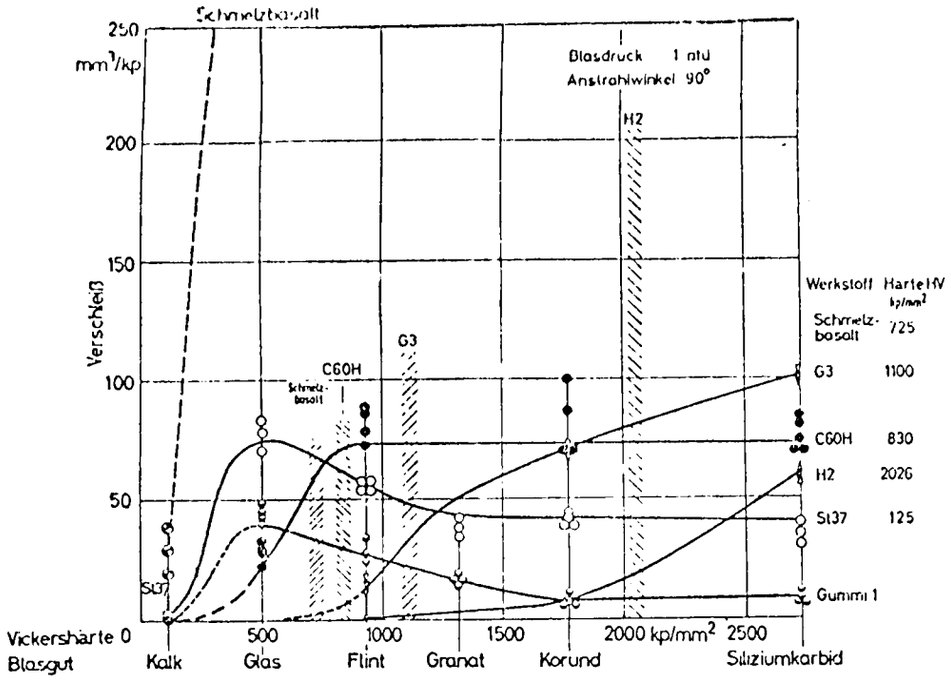

FIG. 7.1 Influence of Particle Hardness on the Erosive Wear of a number of Materials. Impact Angle-90° (Wellinger and Uetz 1963)

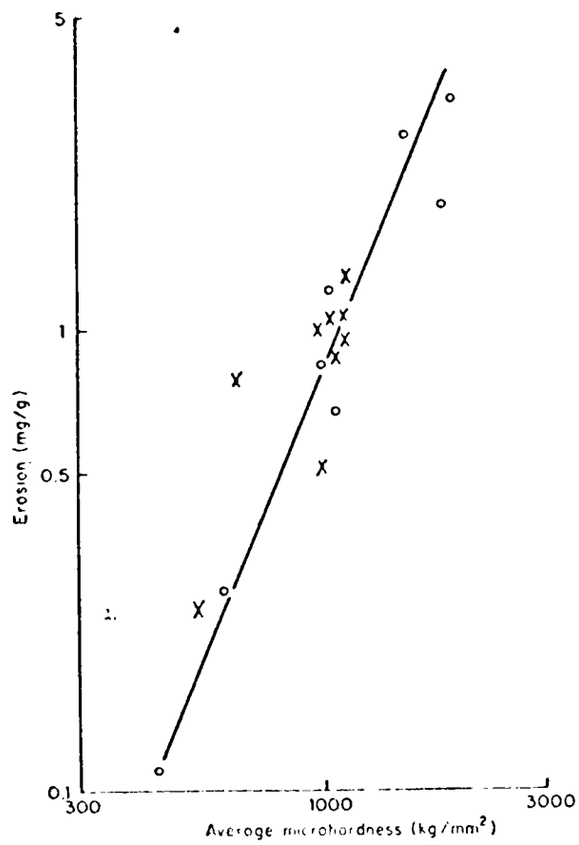

o Industrial sand

x Natural sand

FIG. 7.2 Effect of Particle Hardness on the Erosion of an 11% chromium steel at 130 m/s and normal impact. (Goodwin et al 1969)

Tilly and co-workers (Goodwin et al 1969, Tilly and Sage 1970) used a whirling arm erosion rig to investigate the effects of particle hardness. The particles used were natural and industrial sand with varying degrees of hardness depending upon the quartz content, all within a similar particle size range of between 125 to 150 μm. The erosiveness of these particles was measured by testing an 11% chromium steel plate at a constant velocity of 130 m/s. The results (Fig 7.2) showed that erosion is related to particle hardness by a simple powerlaw relation :-

$$\text{specific erosion} = \text{constant } (H_p)^{2 \cdot 3} \qquad (7.1)$$

where H_p = particle hardness in kg/mm^2.

Whilst this confirms that erosiveness is dependent upon hardness, and by inference on sharpness, it is also closely related to particle shape which can also vary with the history of the particle.

Mills and Mason (1977c) have investigated the influence of particle shape using similar sized 70 μm fresh and worn sand of a constant hardness value and confirmed that the degree of erosiveness also depends to a large extent upon the shape. Whilst sharp, angular, fresh sand was more erosive than the smooth, rounded, worn sand, in terms of depth of wear, the penetration rate for worn sand is much greater. Combined with the inter-relating effects of secondary flows and other variables, premature bend failures were found to occur more readily with worn sand. However, the magnitude of the effect of particle shape on erosion has not been assessed due to the difficulty of quantifying a precise shape factor value for these particles.

Apart from these relatively limited erosion studies on the effect of particle hardness, Khruschov (1957, 1962, 1974) also obtained comparatively similar curves to those shown in Fig. 7.1 in the field of abrasive wear. His experimental data was based on a range of metallic and non-metallic materials abraded by a variety of abrasives of varying hardness. It was found that the relative wear, defined as the ratio between the linear wear of a test specimen to that of a standard material, is dependent upon the correlation between the hardness of the abrasive (H_a) and the hardness of the test material (H_m). If H_a is less than or equal to H_m, no wear was observed. If H_a is more than 1.7 times H_m, the amount of wear is not influenced by the value of H_a. If H_a lies between the above ranges of values, wear is then found to be linearly proportional to H_a. In terms of relative wear resistance, which is the reciprocal of relative wear, Khruschov found that there is a correlation not only between the hardness values of the abrasive and surface material,

but also between the physical properties of the material and the abrasive. However, Richardson (1967, 1968), from similar abrasive tests on a wider range of metals and abrasives, discovered that the relative wear resistance for hard abrasives, defined when its hardness value (H_a) exceeds its maximum strained hardness value (H_u), is not a general property of the material itself, but is specific to the particular material only. Angus (1979) reported that in the case of metals, an important factor in determining the abrasion wear resistance is the work hardenability of the metal itself, rather than the initial hardness.

7.3 EXPERIMENTAL PLAN

The expression in equation 7.1 on the relation between erosion and particle hardness was based on results obtained from a bench type erosion testing apparatus. As mentioned in Chapter Three, the erosive wear process generated in these bench type rigs does not fully simulate the conditions encountered in an actual pipe bend. Therefore, the applicability of this particular expression to model bend erosion is strictly limited. Furthermore, the experimental data shown in Fig. 7.2 was only based on one particular type of particle, with a narrow range of hardness values and particle size, as well as at a test velocity which is well beyond the range normally encountered in a typical pneumatic conveying situation.

Thus, in order to carry out a thorough investigation into the effects of particle hardness on bend erosion, a programme of tests was specifically planned for this purpose. Five batches of materials with a range of hardness values, viz. sand, calcined and hydrate alumina, pulverised fly ash (p.f.ash) and fluidised bed ash (f.b. ash) were used. The sequence of test programmes was carried out in a chronological order as presented in Table 5.1. In order to maintain uniformity of the test conditions for comparison purposes, and to provide proper control of other variables associated in this work, it was decided to convey the materials at a constant phase density of 3 and to maintain a mean conveying air velocity in the test loops of about 25 m/s throughout the entire test programme. Each test material was then recirculated batchwise under similar conveying conditions within each test series. The variables associated with the bends were all held constant. For tests with p.f. ash, hydrate alumina and f.b. ash, the elbow bend at the end of the outer loop preceded by bend number 7, was replaced by a special Booth bend (D/d of 2.4) which is designated as bend number 10 as shown in Fig. 4.6. No erosion was found in this particular bend in tests with p.f. ash and hydrate alumina, and the only significant erosion

occurred when f.b. ash was used (Table 5.2). The limited erosion results of this particular bend are discussed in relation to the effect of diameter ratio on phase density in Chapter Ten.

7.4 PARTICLE CHARACTERISTICS

Although it is the effect of particle hardness that is investigated in this work, it is difficult to isolate this particular variable completely from other variables associated with the particles, such as size, shape, frangibility, moisture content and velocity. Whilst velocity is relatively easy to isolate and control as a separate variable, as discussed in the next section, the other particle variables are virtually impossible to isolate in tests of this magnitude, particularly when up to three-quarter tonnes of a material is used.

7.4.1 Test Materials

The general bulk properties of the test materials were presented in Table 4.1. Photomicrographs of these materials, before and after each test series, are shown in Figs. 7.3 to 7.7, and the corresponding particle size distributions are presented in Figs. 7.8 to 7.12.

The various batches of sand used in this work were obtained from British Industrial Sand at Redhill, Surrey. For this particular programme Grade HH sand was used, which was stated as being fine but with no quoted mean particle size value. This was obtained by the author by means of sieve analysis and was found to be 70 μm. The two grades of alumina powders were obtained from BA Chemicals Limited of Gerrards Cross, Buckinghamshire. The calcined alumina is produced by calcining aluminium hydroxide at temperatures above 1200°C to produce alpha alumina (Al_2O_3) which is the stable form of anhydrous alumina. It has a crystalline structure and occurs naturally as corundum which is primarily used as an abrasive, due to its extreme hardness and resistance to wear and abrasion. It is also used as refractory material and a ceramic due to its outstanding electrical and electronic properties. The dried hydrate of alumina is produced from bauxite by the Bayer process. It also has a crystalline structure and is chemically known as aluminium trihydrate ($Al_2O_3\ 3H_2O$) or more commonly aluminium hydroxide ($Al(OH)_3$). It is primarily used in the manufacture of aluminium sulphate or other aluminium compounds and in the production of catalysts. Hydrate alumina occurs naturally as gibbsite, which is the principal alumina constituent in tropical bauxites and has a very low hardness value.

(a) Fresh

(b) Used

FIG. 7.3 Photomicrograph of Sand

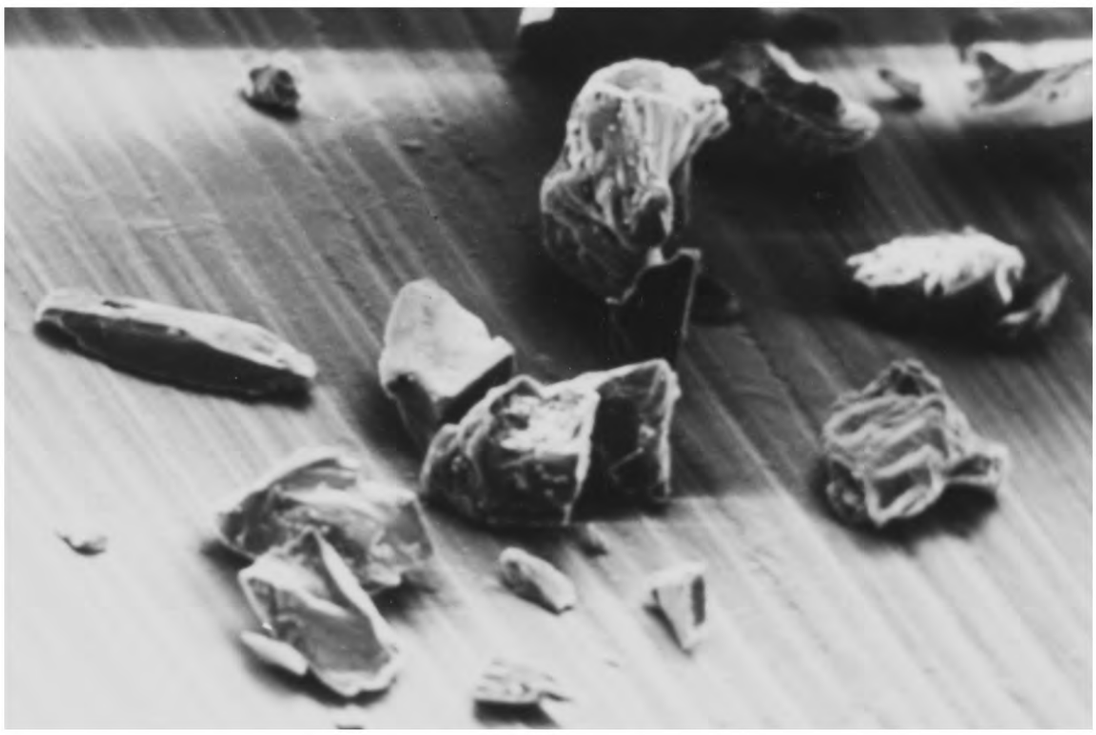
40µm

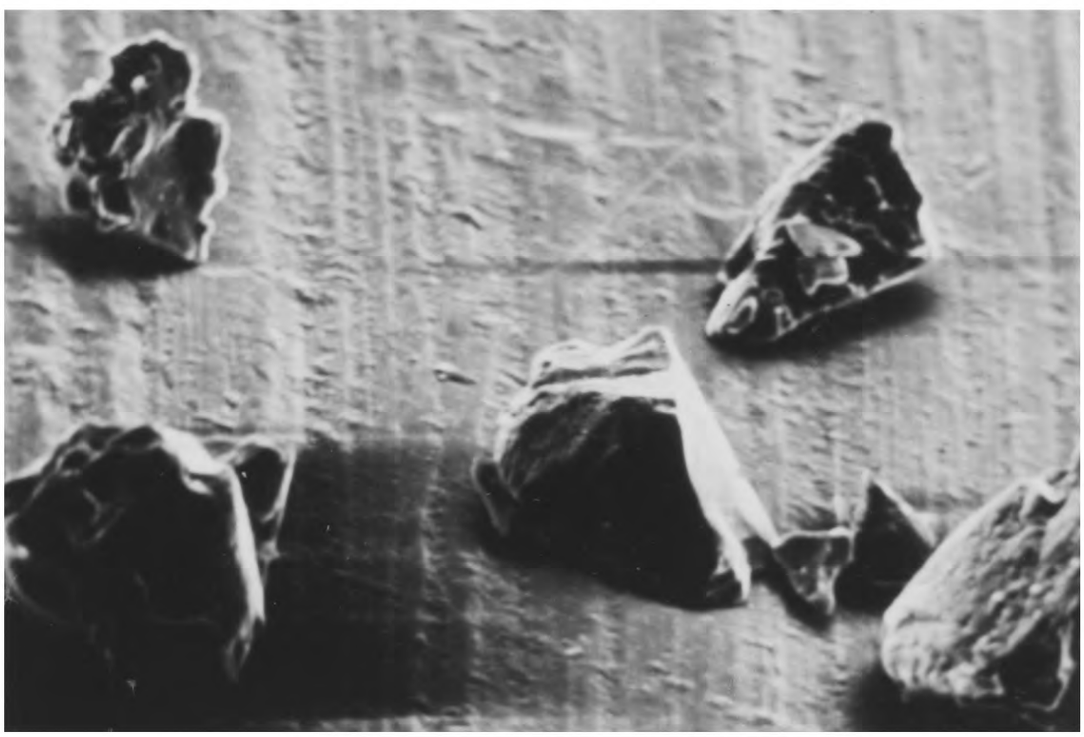
20µm

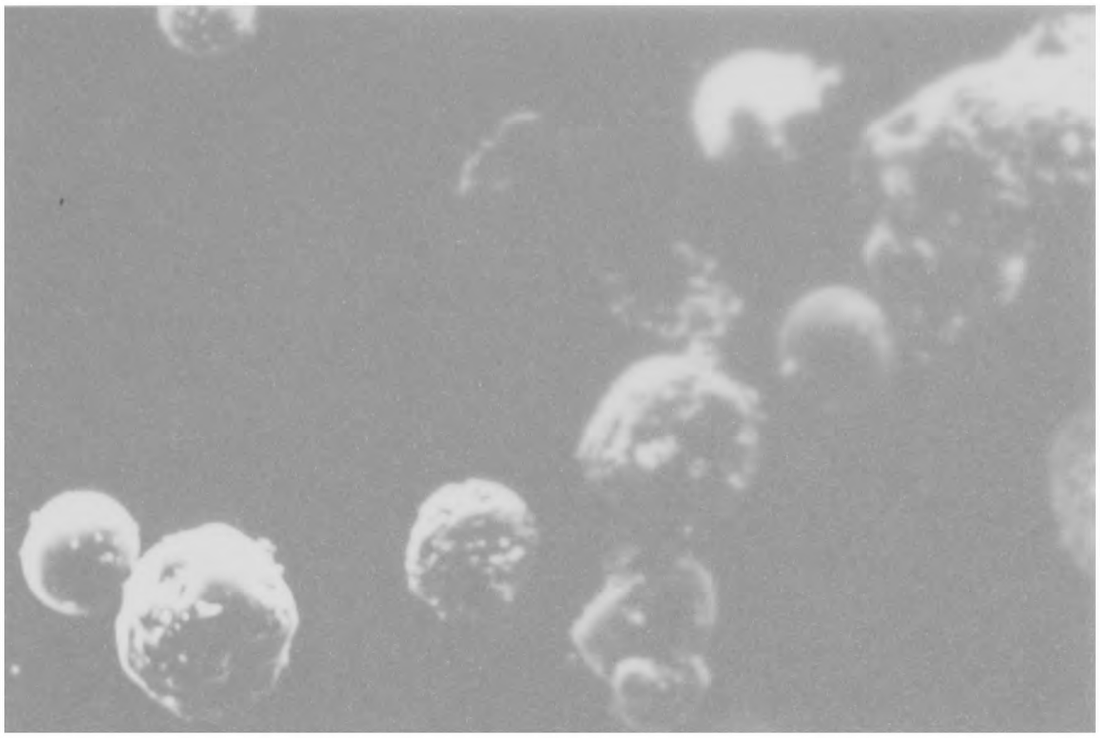

(a) Fresh

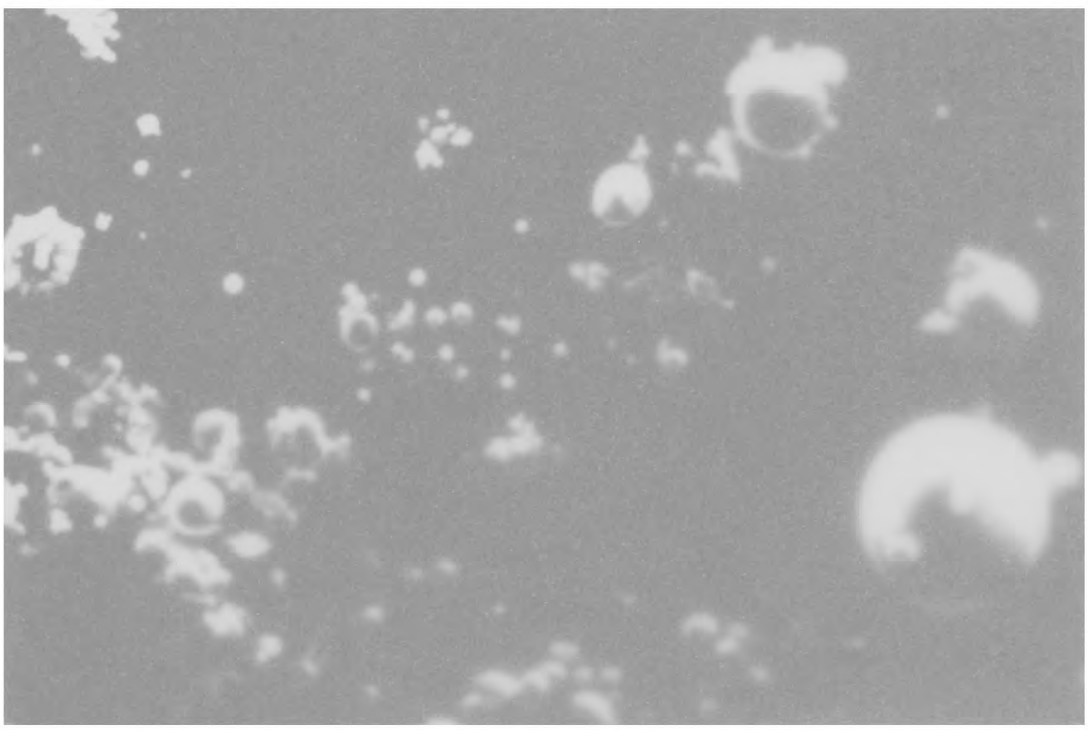

(b) Used

FIG. 7.4 Photomicrograph of Pulverised Fly Ash

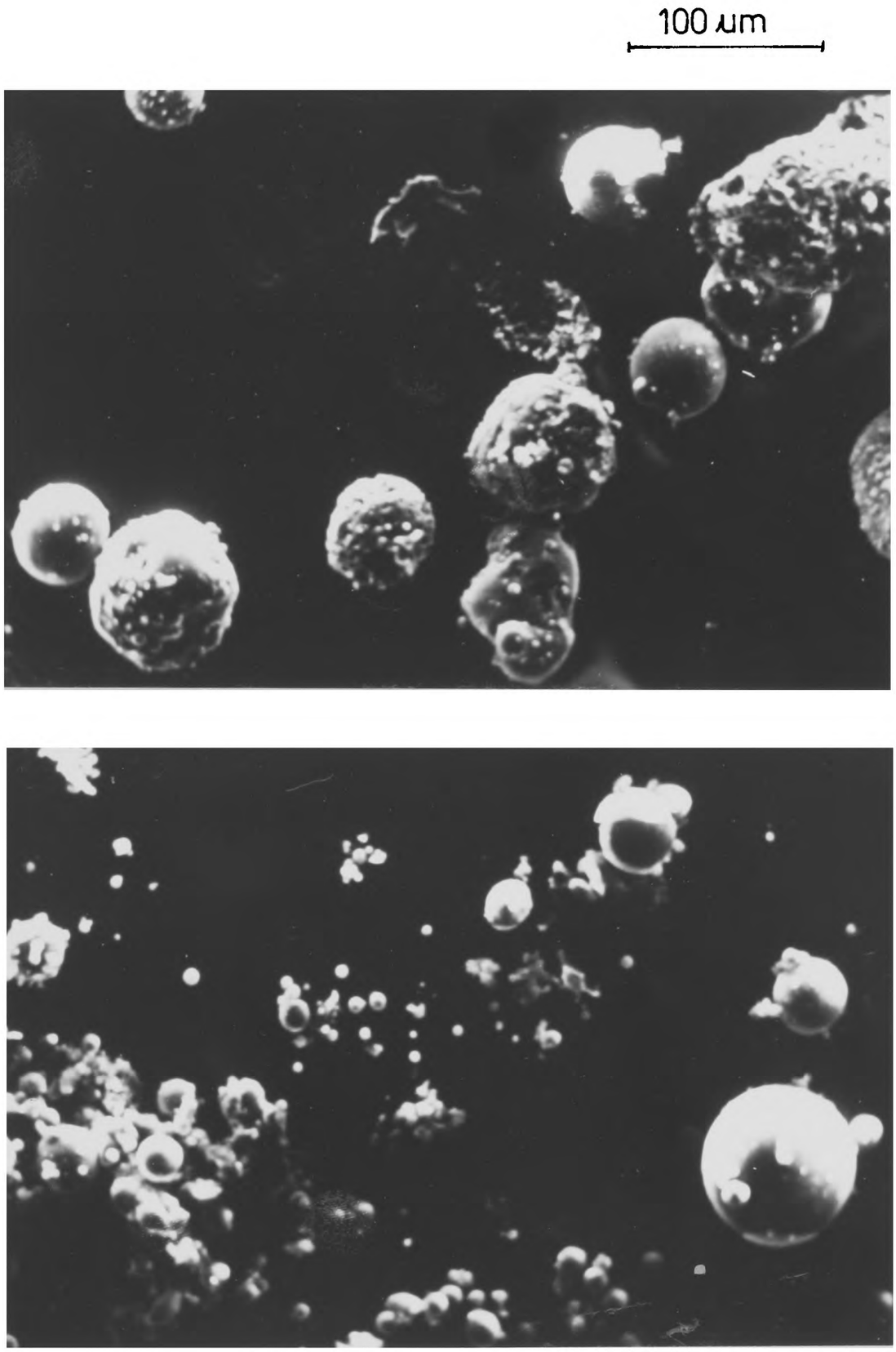
100 µm
40 µm

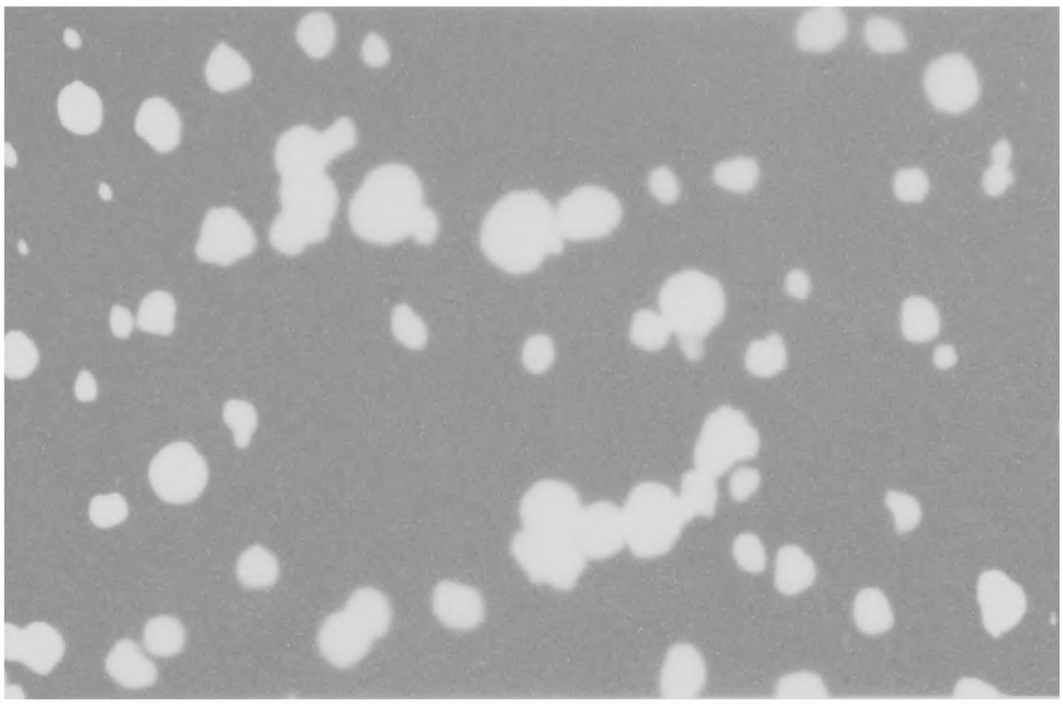

(a) Fresh

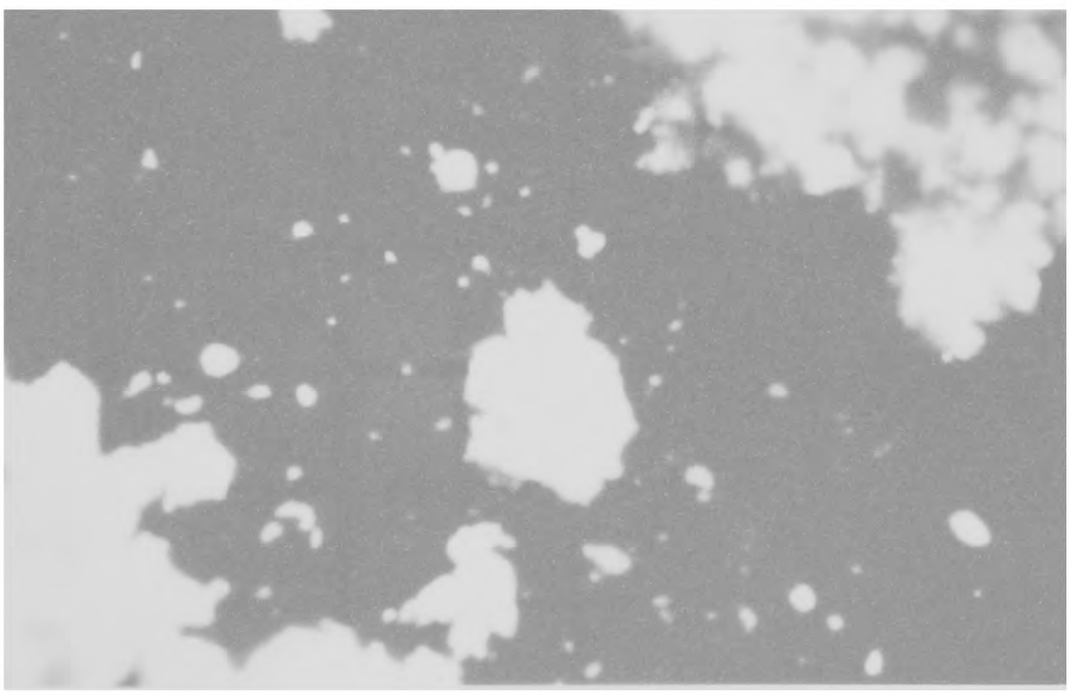

(b) Used

FIG. 7.5 Photomicrograph of Calcined Alumina
Magnification x 45

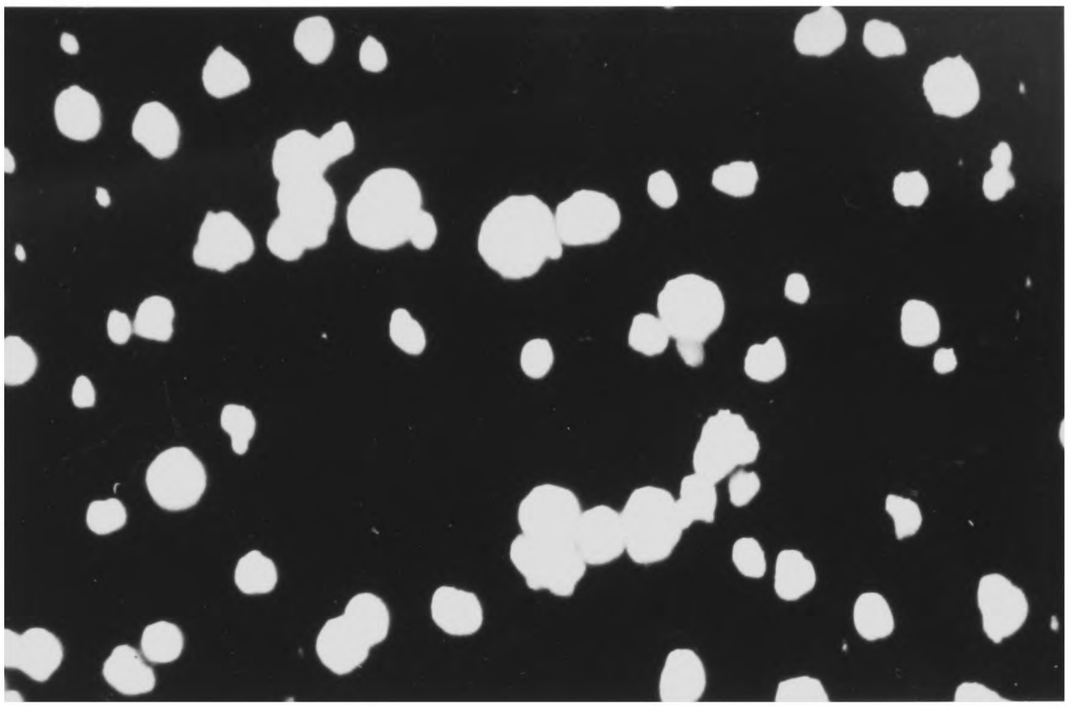

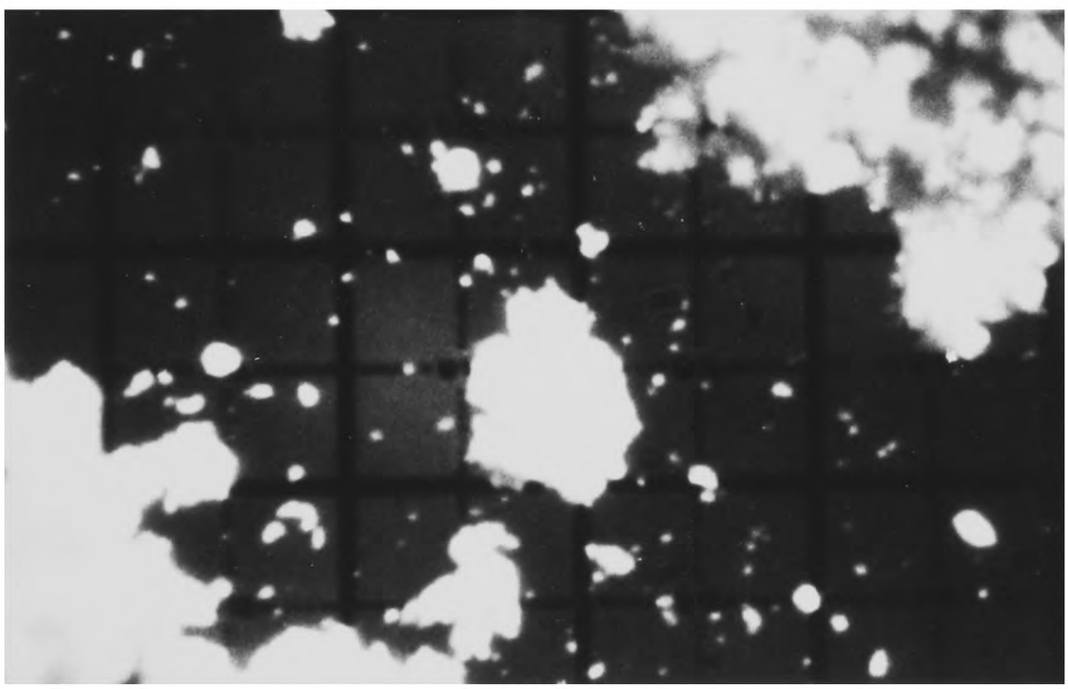

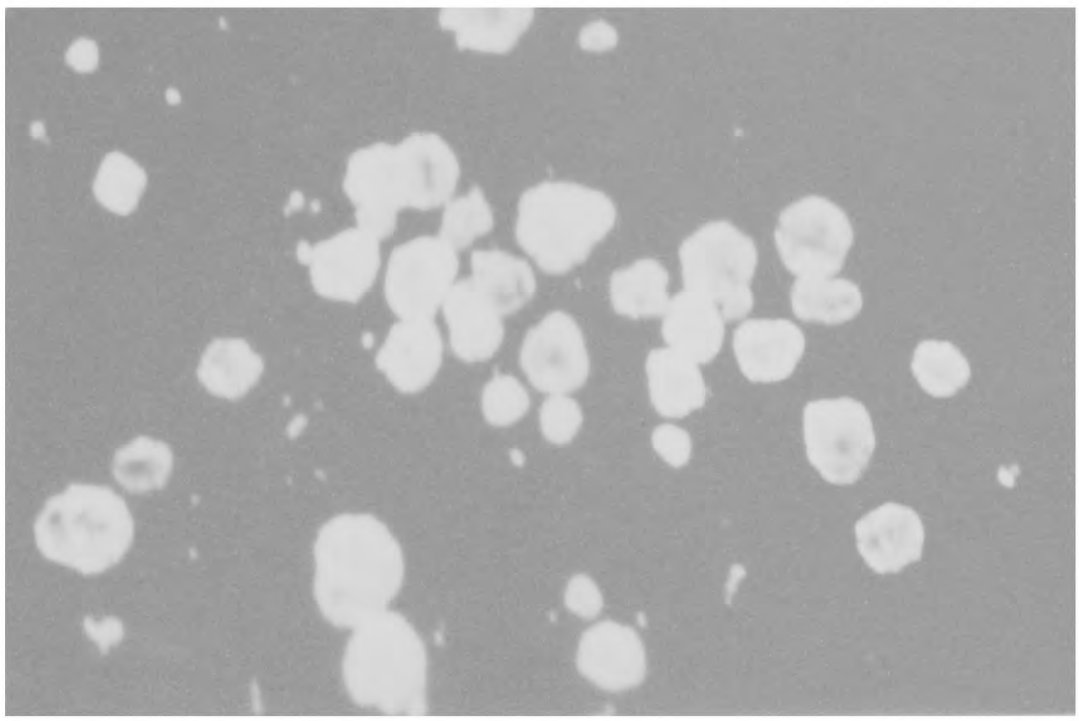

(a) Fresh

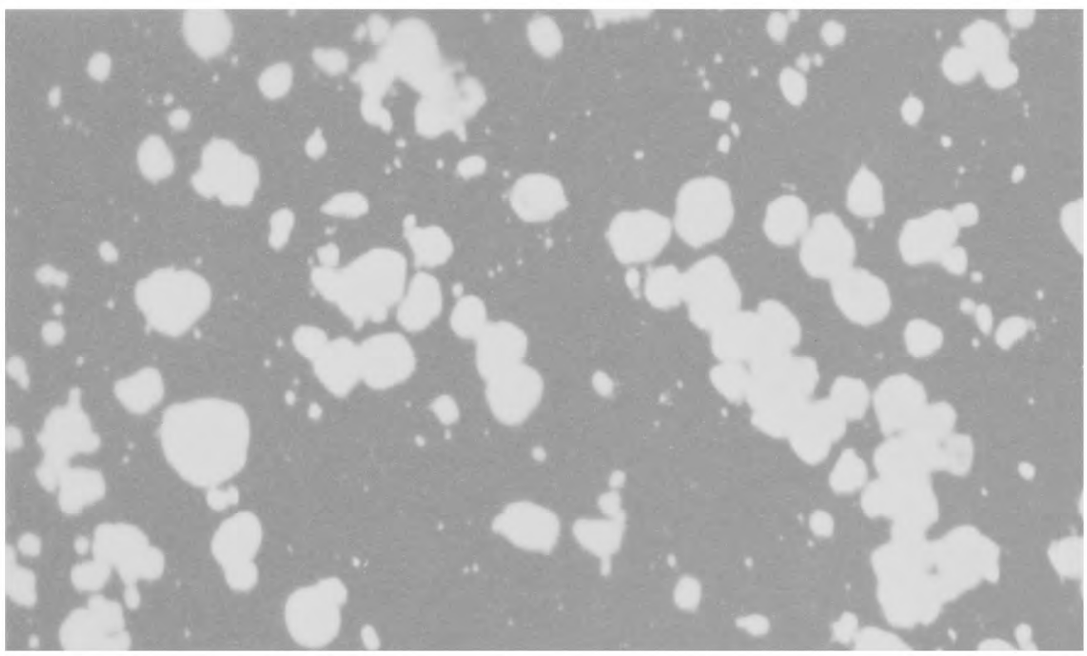

(b) Used

FIG.7.6 Photomicrograph of Hydrate Alumina
Magnification x 45

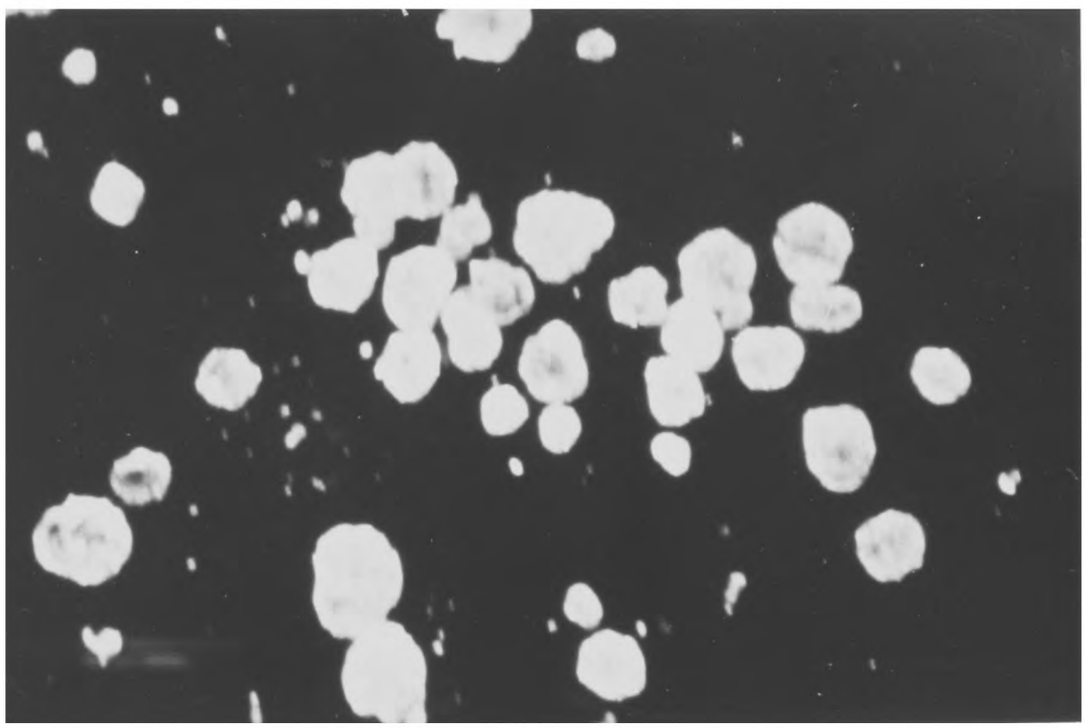

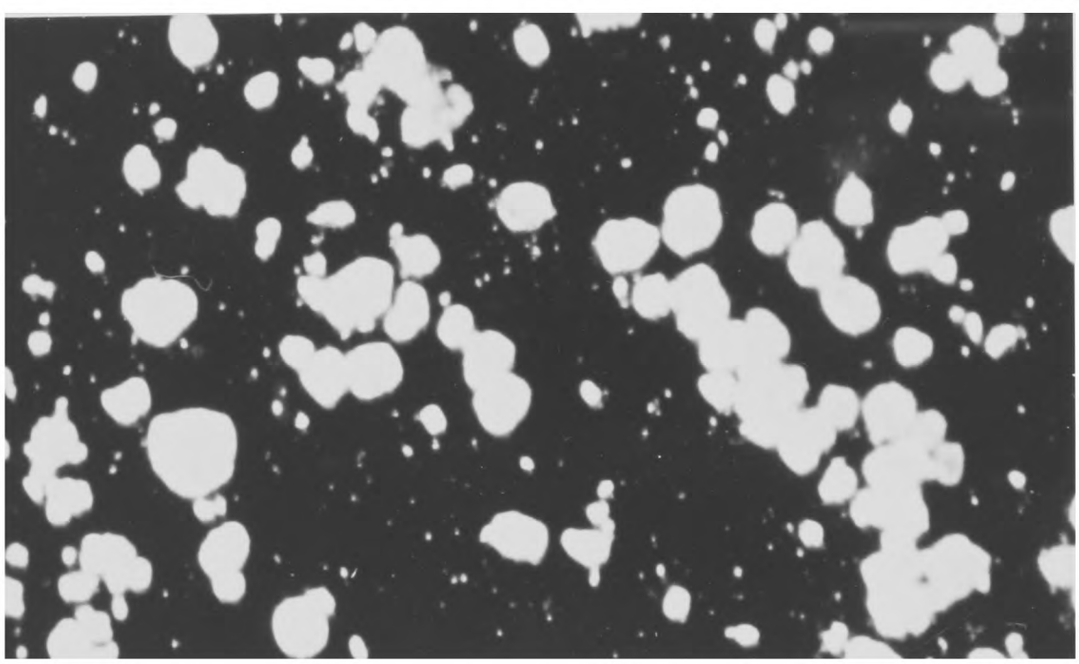

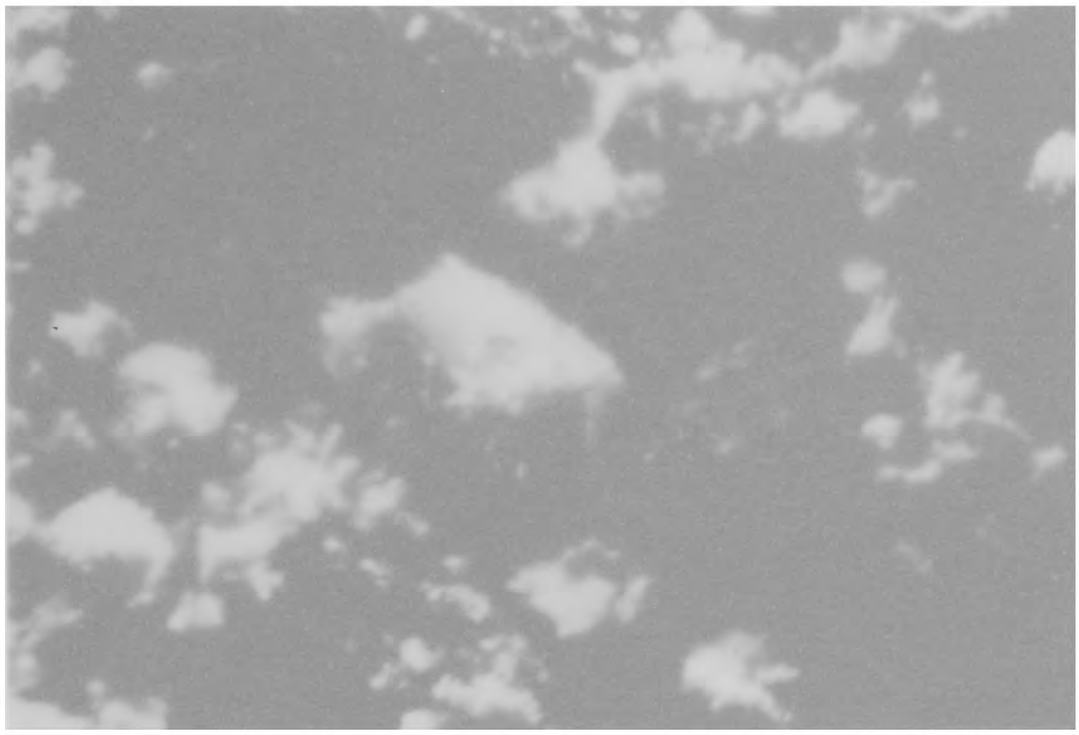

(a) Fresh

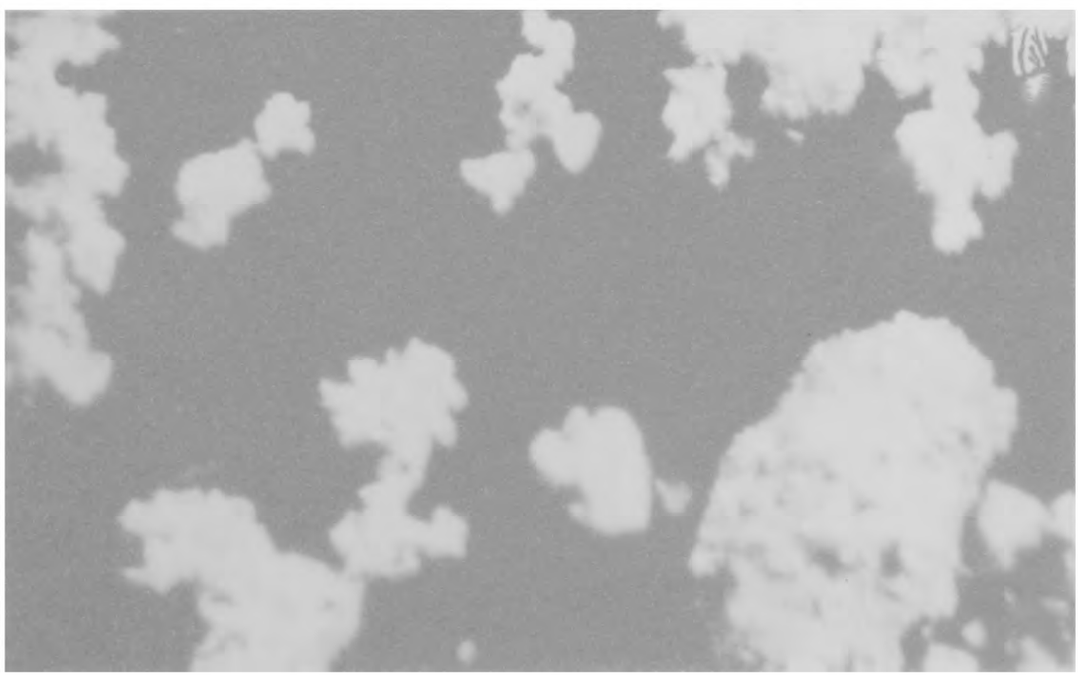

(b) Used

FIG. 7.7 Photomicrograph of Fluidised Bed Ash
Magnification x 25

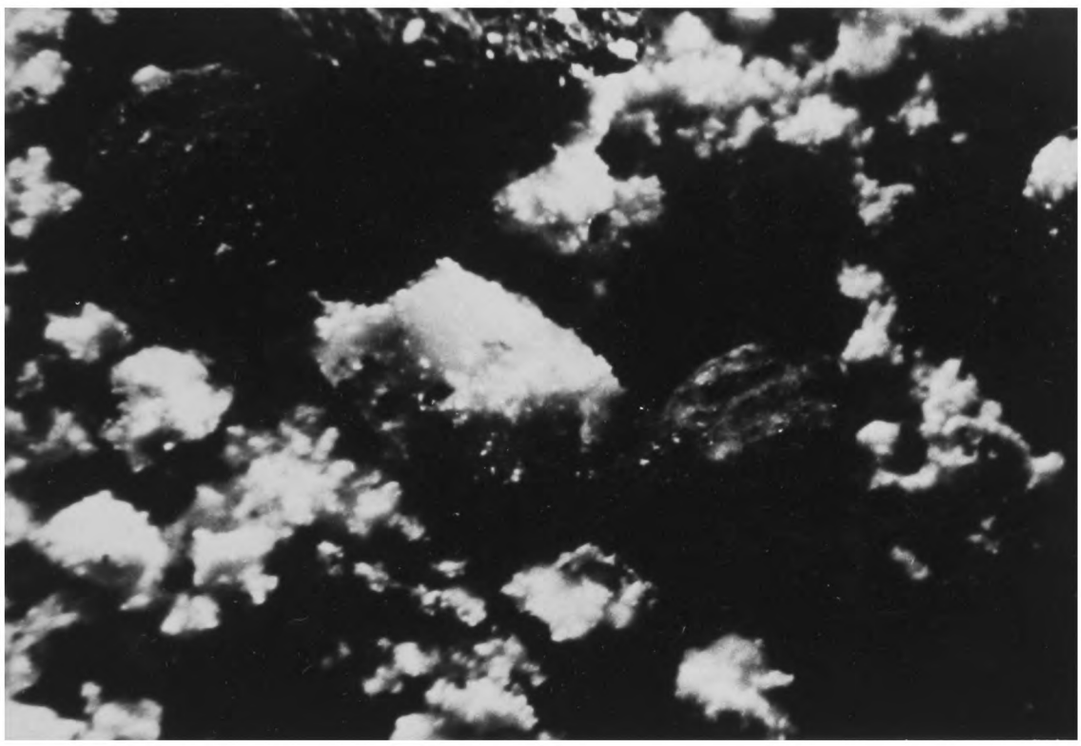

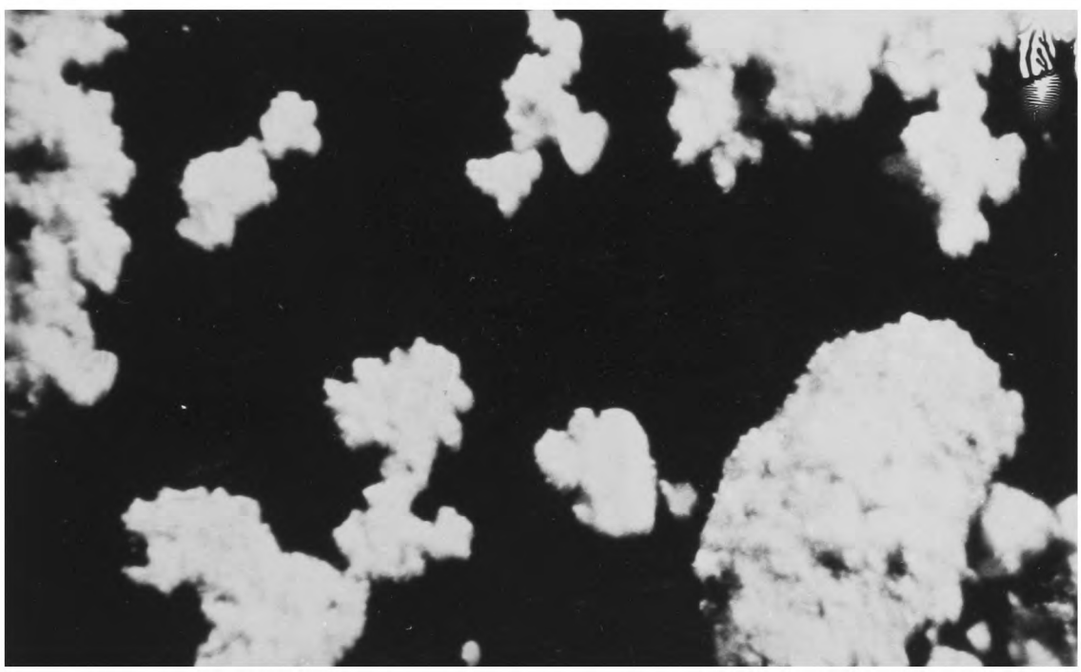

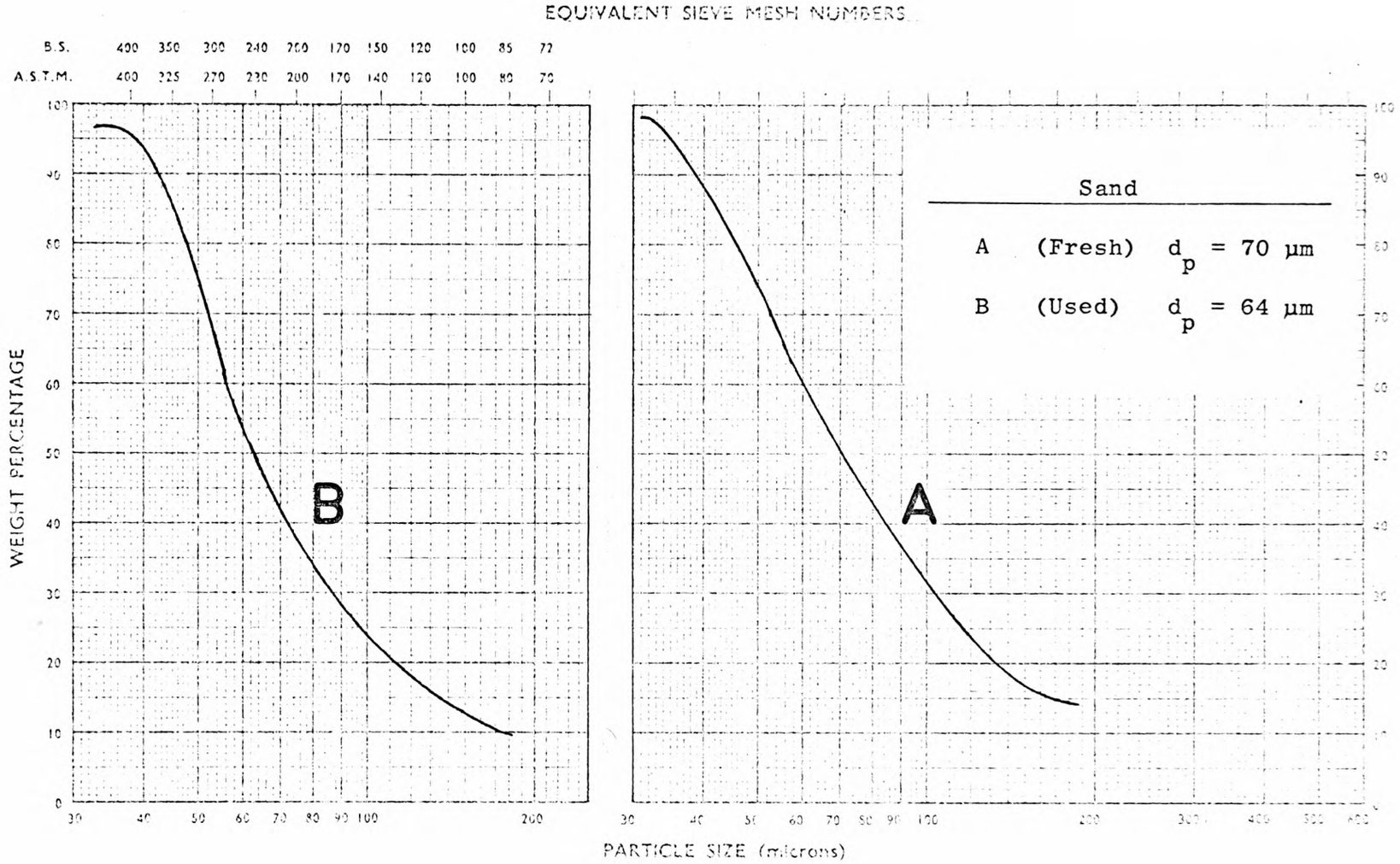

FIG. 7.8 Particle Size Distribution of Sand

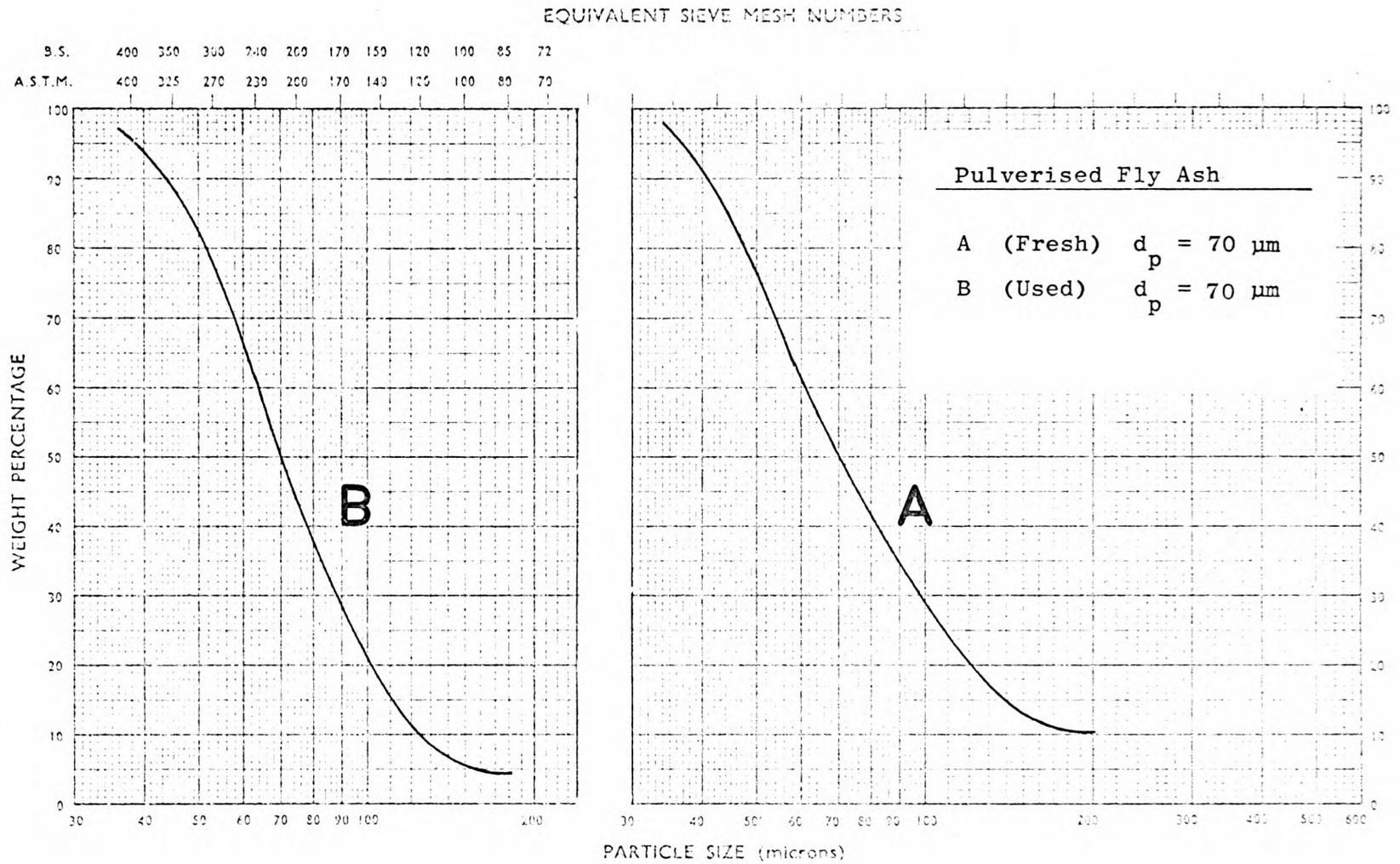

FIG. 7.9 Particle Size Distribution of Pulverised Fly Ash

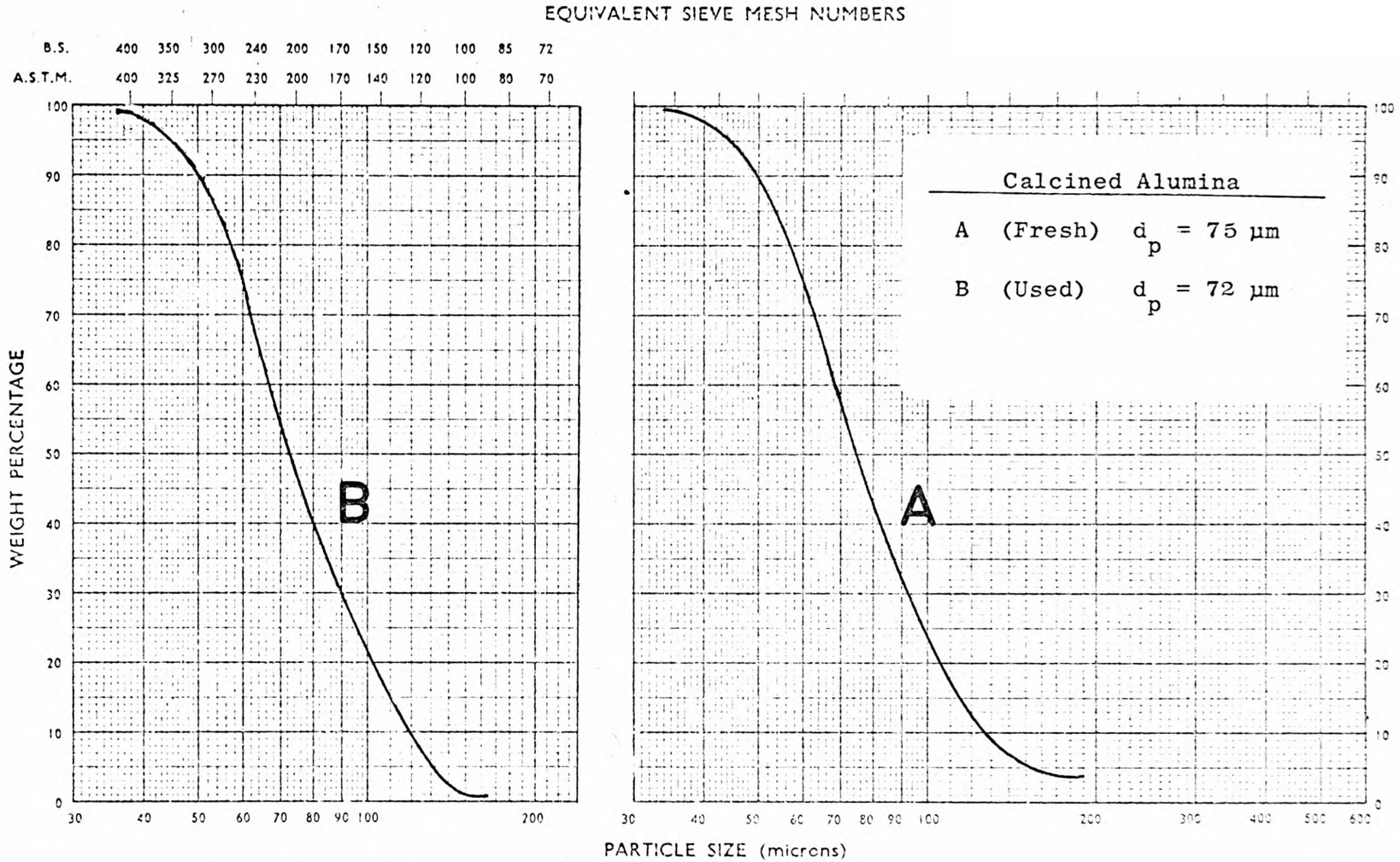

FIG. 7.10 Particle Size Distribution of Calcined Alumina

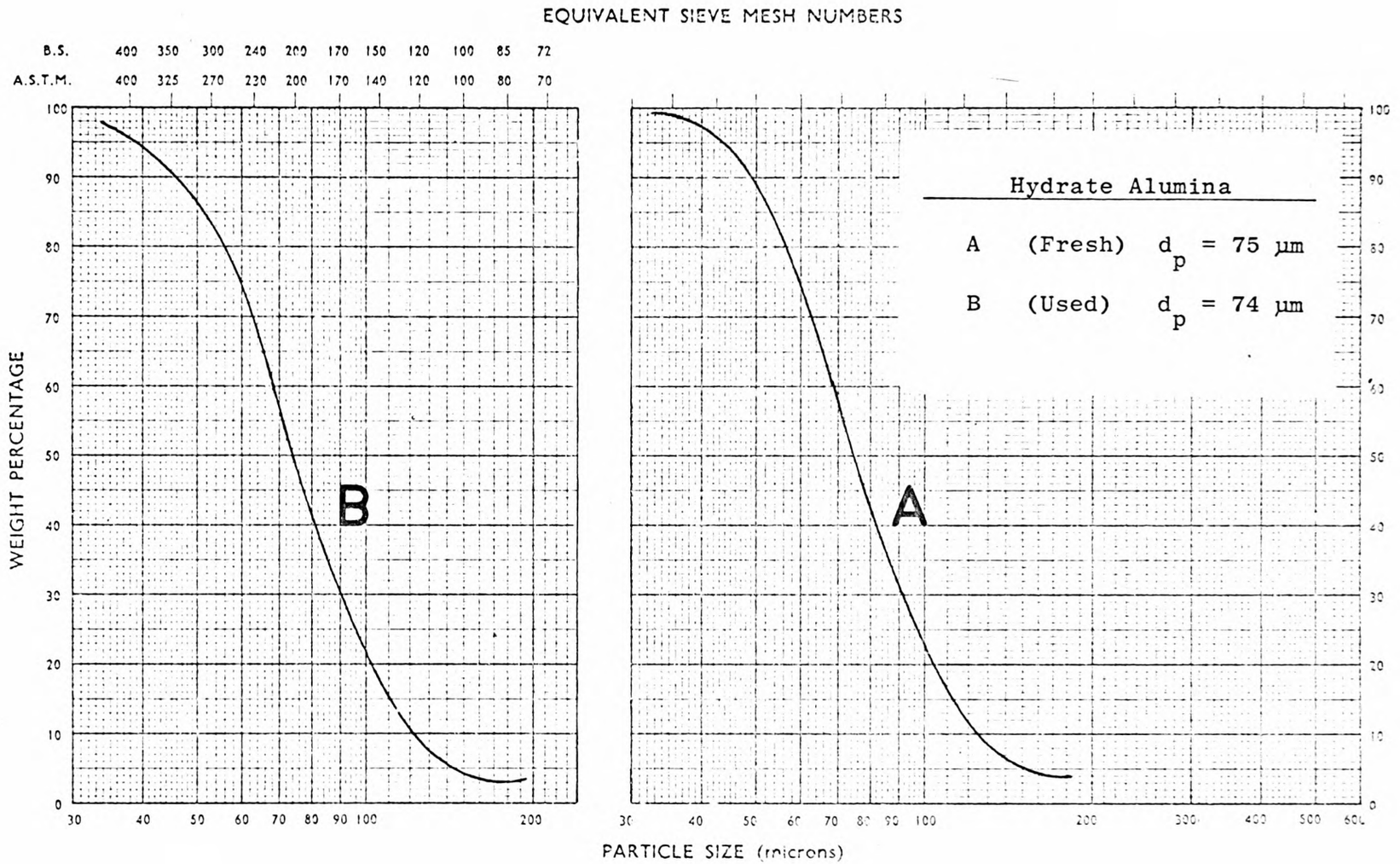

FIG. 7.11 Particle Size Distribution of Hydrate Alumina

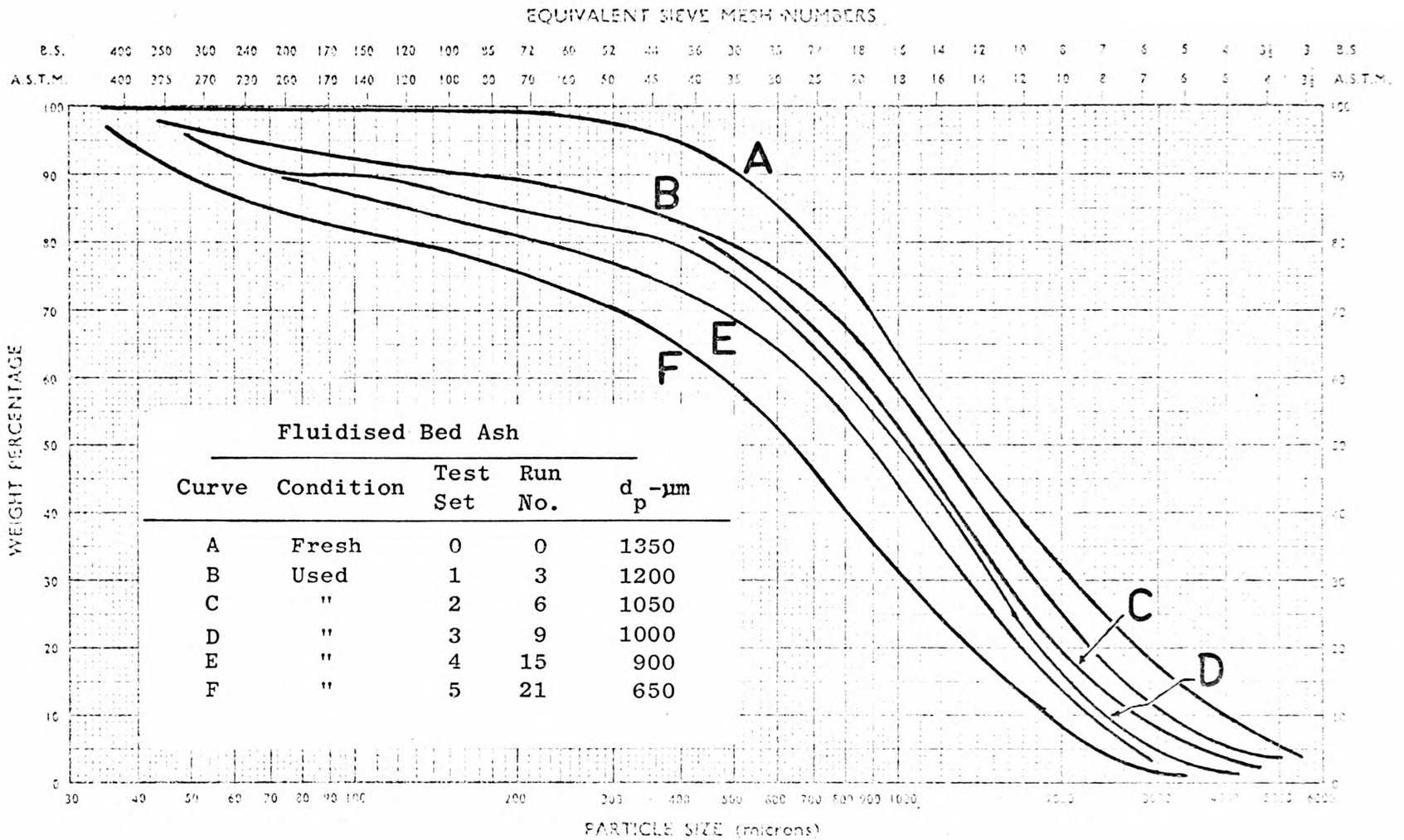

FIG. 7.12 Particle Size Distribution of Fluidised Bed Ash

The p.f. ash was obtained from a local coal-fired power station and the f.b. ash was obtained from an experimental plant in Scotland.

7.4.2 Particle Size

In Figs. 7.8 to 7.12 the particle size distributions of the respective test materials are presented. These were obtained by sieving a 50 g sample of the material taken before and after each test series, or test set in the case of f.b. ash, from the receiving and off-loading hoppers. Although the recognised method of obtaining truly representative samples is from a moving stream of particles (Allen 1975), this was not possible, for a sampling device was not incorporated into the test loop. Thus considerable care was taken to ensure that proper representative samples were obtained. Apart from f.b. ash, the size distribution of these fresh powders were comparatively similar, with about 20% greater than 100 μm and about 20% less than 45 μm, and a mean particle size between 70 and 75 μm. The size distribution of p.f. ash and the alumina powders were further analysed by means of a wide angle photosedimentometer, and the resulting respective mean particle sizes, in terms of Stoke's diameters, were comparable to those obtained by sieving.

Whilst there was no appreciable decrease in the mean particle size of these fine materials, there was a considerable increase in the 'fines' in tests with sand. The percentage of particles below 45 μm rose from less than 20% to over 35% in this particular test series. As explained earlier in the previous chapter, it was the presence of 'fines', together with the effect of secondary flows in the bend, that are largely responsible for the scatter of results, and consequently premature bend failure. Two bends failed prematurely in tests with sand and this aspect of premature bend failure will be discussed in more detail in Chapters Eight and Nine when similar sized sand is used in the investigation of the influence of bend radius.

The fresh f.b. ash encompassed a wide range of size distribution, with about 10% greater than 4mm and 10% less than 500 μm. This large size distribution, however, did not present any operational problems with regard to conveying. The inclusion of f.b. ash in this programme of tests was primarily to provide some erosion data on the secondary effect of particle degradation. As can be seen from Fig. 7.12, the mean particle size of this material progressively reduced to about 650 μm in the course of this test series. This reduction was regularly monitored and the

effect of particle degradation on erosion is discussed separately in a later section in this chapter.

7.4.3 Particle Shape

From the photomicrographs in Figs. 7.3 to 7.7, it can be seen that the sand particles are basically angular, whilst p.f. ash and the two grades of alumina are spherical , and the f.b. ash irregular. Apart from this simple visual particle shape classification, a more detailed classification based on a simple technique given by Riley (1977) is presented in Fig. 7.13. Briefly, about 4×10^{-3} mm^3 of the particles were weighed and poured into a measuring cylinder and filled with water to a certain level. After mixing, the particles were allowed to settle out for about 30 minutes, and the sedimentation volume (V_s) was then accurately measured. The measuring cylinder was then dropped 100 times from a height of 10 mm and the tapped sedimentation volume (V_t) measured. The plot of the change in volume against the ratio of the change in volume (Fig. 7.13) shows the variation of shape of these particles. For the p.f. ash and the two grades of alumina, ethylene glycol was used as the liquid medium. For f.b. ash the particles were obtained from the sample at the end of the test series. This was mainly due to the presence of large size particles in the other samples which will not settle uniformly, thus making accurate readings difficult. The results in this figure experimentally confirm the visual observations of the shapes of these test materials. Apart from this simple categorisation of particle shapes, no attempt has been made to quantify a specific shape factor value for these particles. This was due to the difficulty of selecting a true standard sample against which the shapes of the other samples could be compared, particularly from a batch of over 500 kg.

7.4.4 Particle Hardness

The hardness value of particles is usually expressed as a Moh's number obtained by scratch tests, or in terms of kg/mm^2 based on Vickers diamond pyramid micro-indentation tests. For comparison purposes, the hardness values of the test materials in this work are expressed in Vickers units.

While the hardness values of calcined alumina (corundum), hydrate alumina (gibbsite) and quartz/sand are easily obtained from standard

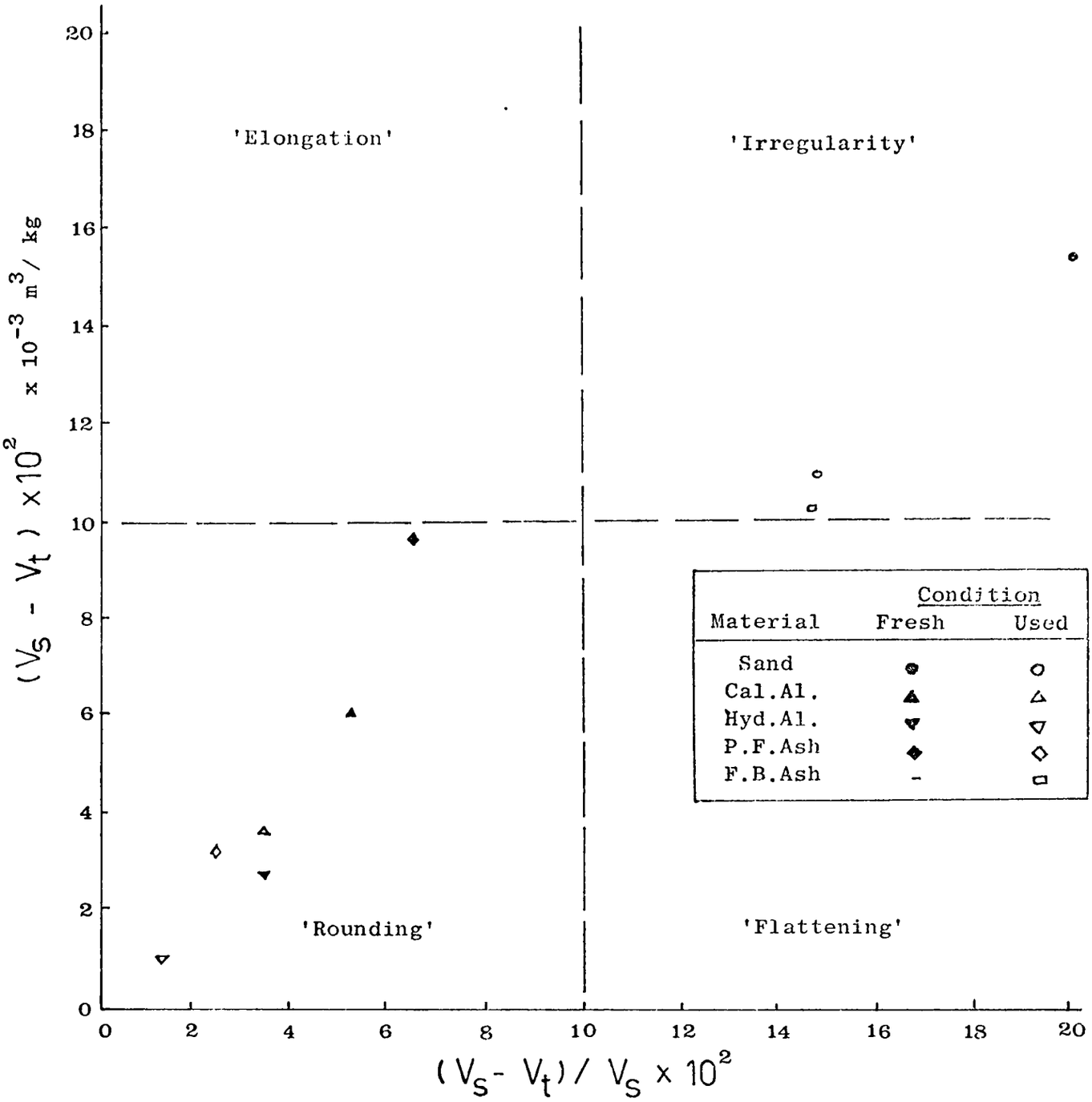

FIG. 7.13 Particle Shape Classification Diagram
(According to Riley 1977)

reference materials handbooks, those of p.f. ash and f.b. ash must be obtained empirically. Briefly, five bakelite moulds were all drilled to a depth of 10 mm and all the test materials were carefully compacted into each mould. A layer of wax was smeared onto the top of the moulds, and polished in the normal manner as for metallographic examination. These were then placed in a Vickers microindentation testing instrument and the resulting measured hardness readings recorded. To a large extent the accuracy and reliability of the hardness readings was considerably influenced by the degree of compaction (Hirschhorn 1969), and care was taken to ensure that all the specimens were equally compacted by applying a similar constant pressure. For calibration purposes, the two grades of alumina and sand, with a known hardness value, were also similarly tested and the resulting measured values compared, as shown in Fig. 7.14. By comparing these measured and actual hardness values the actual hardnesses of the other materials was thus obtained. It should be noted that all these hardness values are nominal and are subject to a large degree of deviation. Even amongst the published data there is a wide variation of the values obtained and Cooling (1965) has summarised the various sources of discrepancy into those due to instrumental errors and those due to specific properties of the material itself.

In the calibration graph in Fig. 7.14, reference values of 150 and 2100 kg/mm^2 for hydrate alumina and calcined alumina was decided upon by the author. The hardness value for gibbsite varies slightly from about 100 to 200 kg/mm^2 (Kretz 1973), but for corundum it varies from as low as 1765 (Wellinger and Uetz 1963) to over 2750 kg/mm^2 (Young and Millman 1964). However, a mean value of about 2100 kg/mm^2 has been reported by several sources (Tabor 1951, Mott 1956, Cooling 1965, Rabinowicz 1966) for corundum.

For sand the actual hardness depends upon the quartz content. Goodwin et al (1969) found that it varied from about 450 to 2000 kg/mm^2, whilst Rabinowicz (1966) quoted a value of 800 kg/mm^2. The hardness of quartz itself varies from 800 (Tabor 1951) to 1560 kg/mm^2 (Young and Millman 1964), and for quartz sand Wellinger and Uetz (1963) and Khruschov (1974) both reported that it varied from about 1000 to 1250 kg/mm^2. It was decided by the author to select a value of 1200 kg/mm^2 for the sand particles used in this work because of its high degree of erosiveness.

The use of pulverised coal as fuel in the power industry has led to several recent erosion studies due to p.f. ash (Sterens 1949, Fisher and Davies 1949, Raask 1969, 1979, Tabakoff et al 1979). Raask reported

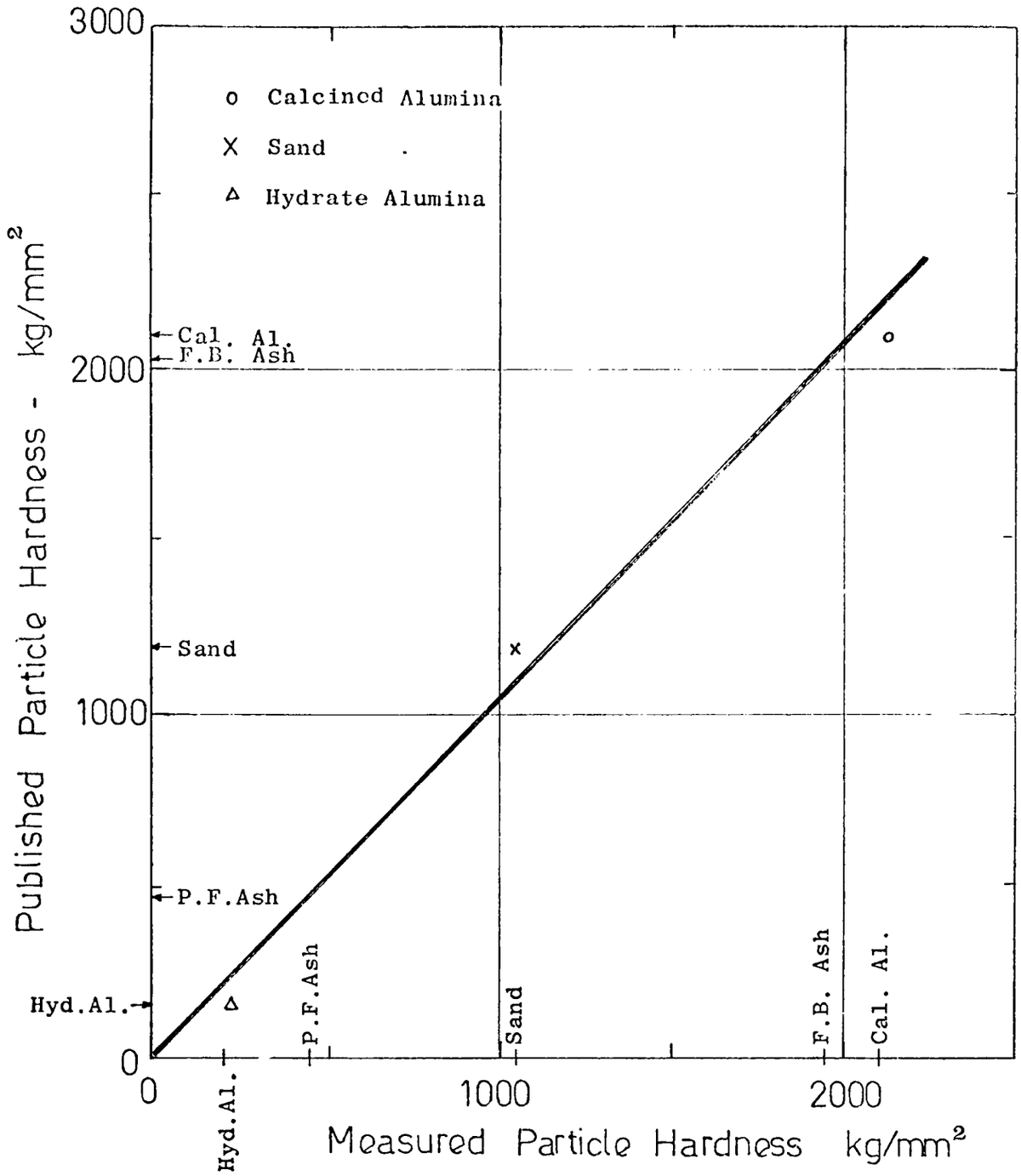

FIG. 7.14 Comparison between Published and Measured Particle Hardness Values

tests on the erosion of boiler tubes and in pneumatic feedlines transporting pulverised coal and ash. He found that whilst the bulk of p.f. ash consists of spherical glassy particles similar to those shown in Fig. 7.4, which causes comparatively little erosion, the erosiveness of p.f. ash is predominantly due to the presence of small quantities of unfused quartz and other irregularly shaped agglomerates of sintered ash particles. The hardness value of these glassy particles was estimated to lie between 550 to 600 kg/mm^2 which was comparable to the value of about 500 kg/mm^2 obtained by the author. The f.b. ash also consists of a variety of mineral matter, ranging from millimeter sized clinker to fine ash particles (Fig. 7.7). No published hardness value of f.b. ash is available in the literature, but from the hardness measurements made by the author, it was estimated to have a mean value of about 2000 kg/mm^2.

7.4.5 Moisture Effects

In tests with the highly abrasive calcined alumina material the test series had to be terminated after only ten batches had been conveyed through the test bends. This abrupt stoppage was primarily due to the effect of moisture on this particular batch of calcined alumina powder. After ten runs its moisture content was found to be over 5%, compared to less than 0.5% for the other test materials, including hydrate alumina. This tenfold increase had a dramatic effect on its flow properties. After the tenth run, the material was completely unable to flow out of the blow tank, despite repeated attempts to force it out by pressurising the blow tank to over 1 bar compared to a normal pressure of about 0.4 bar.

Stepanoff (1969) reported that the presence of moisture leads to cohesion between the particles and adhesion between the particles and the container walls or ducts, which may retard or stop the flow of materials under certain conditions. These forces cause the particles in the material to bind together to form a 'cake', thereby preventing any flow out of a container.

The hygroscopic nature of this particular batch of calcined alumina was primarily due to the presence of transition alumina elements. These were produced as a result of calcining aluminium hydroxide at temperatures of about 1000^{o}C, which is insufficiently high to give complete transformation to the inert stable alpha form. These transition aluminas are hygroscopic and can absorb up to 6% moisture in free air

(Craig 1980). However, sufficient erosion data had been obtained with this material and the results are evaluated together with those from the other test materials.

7.5 VELOCITY EFFECTS

As mentioned in Chapter 4, fine control of velocity in the low pressure rig was achieved by regulating the off-take to atmosphere valve to ensure the required volumetric air mass flow in the test loops. The velocity estimated in this case, as in all the analyses reported in this work, was that of the conveying air and not that of the particles. In full scale pipe bend erosion investigations of this nature, and also similarly in industrial plant pipeline situations, considerable difficulty, particularly with regard to instrumentation, would be encountered in measuring particle velocity. Provided that, for a given air velocity, the particles are accelerated to their terminal velocity, air velocity is a suitable substitute parameter for the purpose of analysis (Mills and Mason 1975). In all cases the test bends followed sufficiently long straight pipe runs to ensure that even the largest particles were accelerated to their terminal velocity.

However, it should be noted that in a gas-solid suspension flow, since the particles are carried through the pipe by a stream of gas, the solid particle velocity (U_p) is always less than the carrier gas velocity (U_g), and U_p will only approach U_g under certain conditions (Goldberg and Boothroyd 1969). Furthermore, in a horizontal pipe flow, the solid particles, depending on the particle properties, the fluid properties and the conveying velocity, may bounce between the pipe walls, roll or slide at the bottom of the pipe, or be suspended completely in the conveying fluid medium (Boothroyd 1971, Yang et al 1973). In addition, in the bend the particles may be deflected from the outer to the inner bend wall due to the formation of an erosion crater and proceed in a zig-zag pattern in the bend (Mason and Smith 1972), thereby experiencing acceleration and deceleration forces which are difficult to quantify due to the change in particle direction (Yang and Keairns 1976). Thus, precise measurement of particle velocity is extremely difficult when, in addition, parameters such as an appropriate shape factor and the coefficients of friction and restitution are not readily available (Scott 1978), particularly the coefficient of restitution which has been shown to be of paramount importance in determining particle velocity accurately (Wheeldon and Williams 1980).

Furthermore, in a gas-solid suspension flow there will be a drop in pressure and hence a variation in velocity along the length of the conveying pipe. In a constant bore pipeline velocity will increase due to the expansion of air as a result of this gradual pressure loss. However, in the measurements obtained in this work the maximum and minimum velocity values were within ±10% of the mean of about 25 m/s for all the bends tested in both loops.

For the sand, p.f. ash and the two grades of alumina, it has been estimated by the author, based on a semi-empirical correlation given by Leva (1959), that the slip velocity ratio (U_p/U_g) is consistently around 0.8. Thus, in view of the accuracy of the correlation which is subject to wide variation, it is reasonable to consider the air velocity value as a satisfactory substitute parameter.

In the case of f.b. ash, a similar estimation showed that the slip velocity ratio corresponding to the mean particle size of 1350 μm in the first test run was 0.56. However, due to its large mixed sized distribution, ranging from 10% over 4000 and 10% below 500 μm, the corresponding ratios were 0.40 to 0.68. Thus, not only is the mean particle velocity considerably less for these coarse particles, as would be expected, but there is also a considerable variation with regard to the individual particles within this size distribution. At the end of this test series after 21 runs, the mean particle size had been reduced to 650 μm , with about 15% greater than 1400 and 15% less than 45 μm. The corresponding slip velocity ratios were 0.65 for the mean and 0.56 and 0.84 for the upper and lower sized particles. With such a large variation in the slip velocity ratios there would also be a similar variation in terms of individual particle terminal and saltation velocities. From correlations given by Leva (1959), the terminal velocity for the largest particle (5600 μm) was about 18 m/s and its corresponding saltation velocity given by Matsumoto(1977) was about 11 m/s. Zenz (1964) is the only investigator to provide an empirical method by which the saltation velocity of a mixed particle sized distribution could be estimated. However, from his analysis, the saltation velocity for the largest particle was about 4 m/s, which is some 60% less than that predicted by Matsumoto's correlation. It should be noted that this apparently large difference is hardly surprising since these values were obtained from one of a number of velocity correlations. Accurate determination of the saltation and other particle velocity values is extremely

difficult and often conflicting, due to the presence of a variety of correlations which are currently available in gas-solid suspension flow literature (Duckworth 1971, Yang et al 1973, Jones and Leung 1978, Wheeldon and Williams 1980). However, in this work, with a conveying air velocity of about 25 m/s, it is reasonably safe to assume that all the individual particles are being accelerated to their terminal velocities. Thus, for comparison and analysis purposes it is reasonably valid to consider the conveying air velocity value only.

7.6 BEND WEAR RESULTS AND DISCUSSION

7.6.1 Introduction

In this programme of work, with the exception of hydrate alumina, both the specific erosion rate and penetration rate have been recorded for each of the test materials. In the case of hydrate alumina no erosion was observed in any of the seven test bends. In fact, there was an appreciable increase in the weight of each test bend (Table 5.2). This increase was due to the deposition of the hydrate alumina particles onto the surface of the outer bend wall (see Fig. 7.27a). A similar situation has also been observed in some of the general solid particle erosion studies (Chapter 2), but these studies showed that, after an initial 'incubation' period, during which the mass of the specimen increased slightly due to particle impaction, erosion then proceeded normally (see Fig. 2.5). However, in this work, after some 6 tonnes of hydrate alumina had been conveyed through the bends, there was still no erosion. This lack of erosion is primarily attributed by the author to its low hardenss value of 150 kg/mm^2, which is comparable to the surface hardness of the test bend material itself, which is 158 kg/mm^2. As mentioned in the brief literature review earlier, Khruschov (1957) found that from abrasive wear tests there would be no wear if the hardness of the abrasive particles is equal to or less than the hardness of the surface material. It appears, therefore, that a similar situation also exists in erosion tests. Hence, in the following sections, no further reference is made to this particular test material.

7.6.2 Specific Erosion Analysis

The experimental erosion data for all the individual bends tested in this programme of work are given in Tables 5.2 and 5.3. These were the total mass eroded at the end of each test series, and the corresponding erosion data, on an accumulative basis, is presented graphically in Figs. 7.15 to 7.17.

As mentioned earlier, two bends failed prematurely in tests with sand. These were bends 3 and 7 as shown in Fig. 7.15. Bend 3 failed after only 4.1 tonnes had passed through and bend 7 after a further 1.5 tonnes. These failed bends were immediately replaced by new, unworn bends which, in fact, failed in an even shorter time than the original bends that they were replacing, whilst the rest of the original bends were still in service. This rapid failure of replacement bends has a considerable effect on erosion analysis and will be discussed in the next two chapters. In this work, for comparison purposes with the other test materials, only the erosion data based on the original seven bends is considered, and for the sake of clarity the curves for the replacement bends are omitted from this figure. Since the first two bends failed prematurely, this series of tests was continued until a further bend failed. This was bend 5 which failed after some 9 tonnes had been conveyed.

In Fig. 7.16 the experimental erosion data of both p.f. ash and f.b. ash is presented. The set of curves along the abscissa were from tests with p.f. ash and these hardly showed any significant erosion compared with those of f.b. ash. This limited erosion is expected, due to the relatively low hardness value of p.f. ash (480 kg/mm^2), compared to f.b. ash (2030 kg/mm^2). Apart from the relative inter-relating effects of size and shape, the two sets of curves in this figure clearly demonstrate the specific influence of particle hardness on the magnitude of erosion.

In Fig. 7.17 the curves for calcined alumina clearly show a distinct trend towards an increase in erosion rate, compared to a gradual decrease in erosion rate observed for the other test materials over a similar range of tests. Apart from the hardness, size and shape effects, this increase in erosion rate is apparently due to the specific effect of moisture, which was found to increase tenfold to over 5% in the course of this particular test series. Whilst the

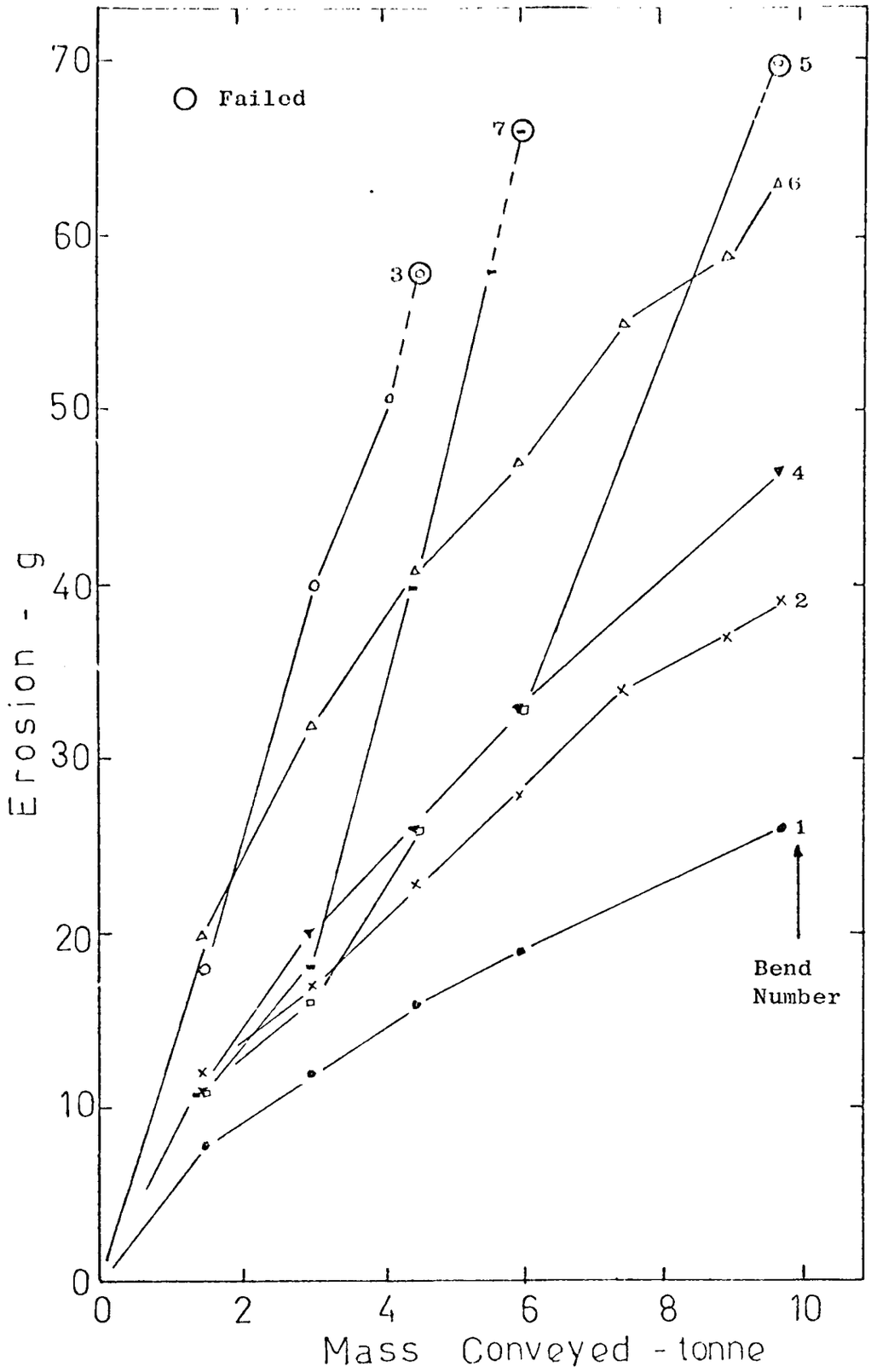

FIG. 7.15 Variation of Erosion with Mass Conveyed for Individual Bends Eroded by Sand (H_p=1200 kg/mm^2).

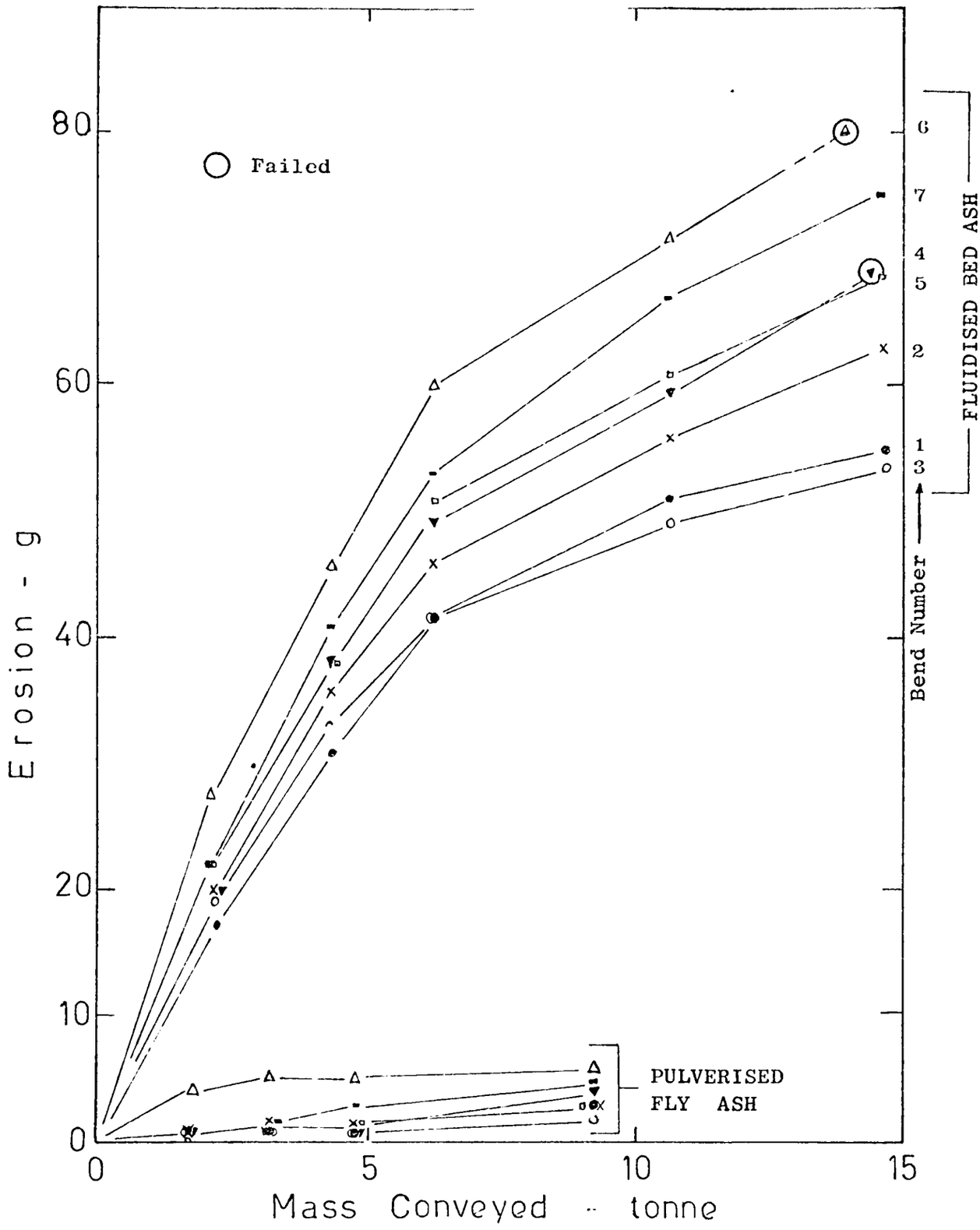

FIG. 7.16 Variation of Erosion with Mass Conveyed for Individual Bends Eroded by Fluidised Bed Ash (H_p=2030 kg/mm^2) and Pulverised Fly Ash (H_p=480 kg/mm^2).

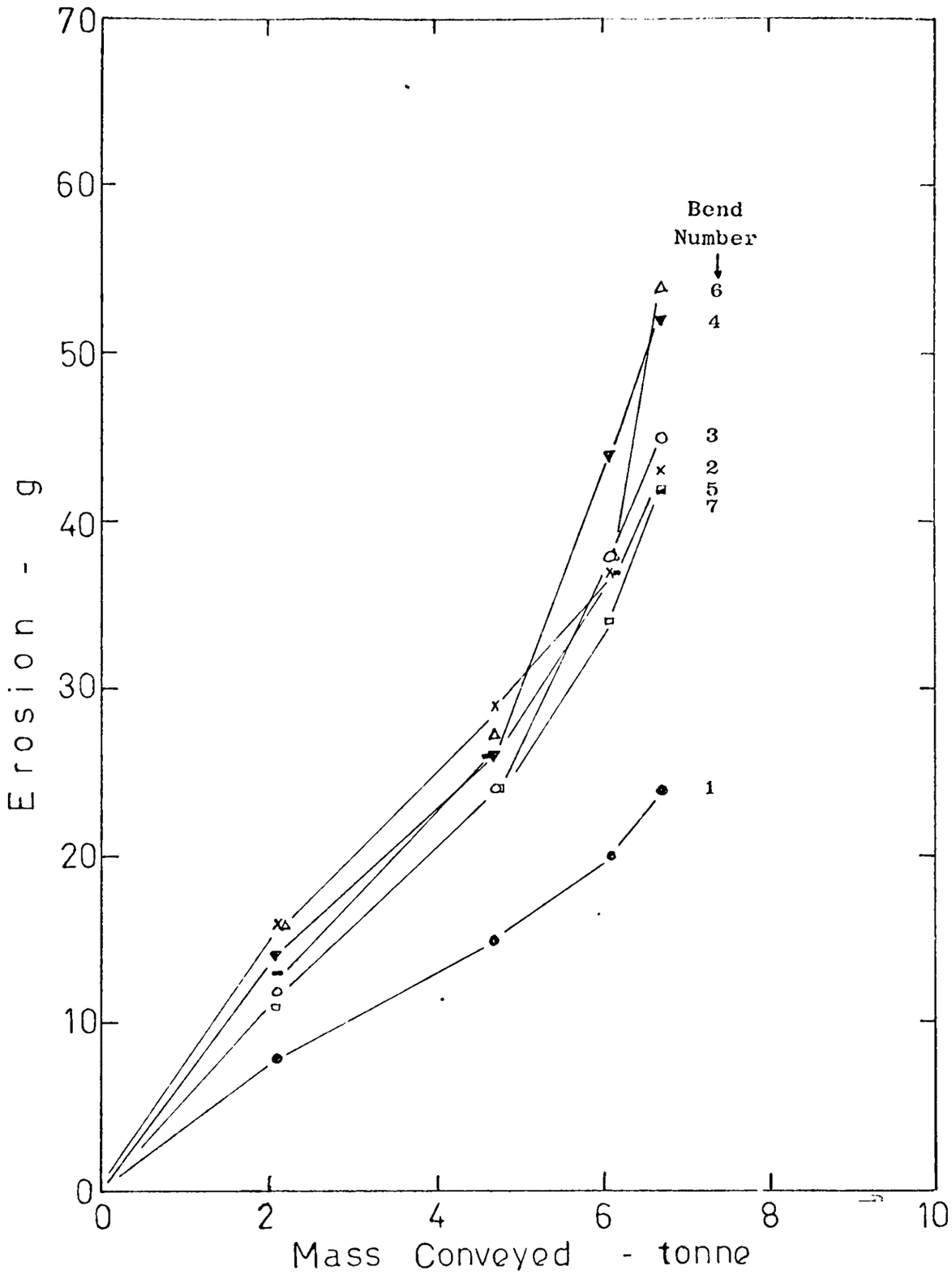

FIG. 7.17 Variation of Erosion with Mass Conveyed for Individual Bends Eroded by Calcined Alumina (H_p=2100 kg/mm^2).

effect of moisture has received relatively little attention in the general solid particle erosion literature, it has been reported by Wellinger and Uetz (1963) and Kleis (1969) that erosion increases as moisture is increased and a similar effect has also been reported in the field of abrasion studies by Rabinowicz (1966) and Lassen-Basse (1975). As mentioned earlier, this increase in moisture also led to an unexpected stoppage of this particular test series and no further tests were carried out after some 6.7 tonnes of calcined alumina had been conveyed through the bends.

A common feature of the curves in these figures is again the scatter of results. Whilst the magnitude of the degree of scatter gives an indication of the repeatability of the erosion data, it also provides an indication of an element of unpredictability in the erosive wear process in pipe bends. With such a large number of bends, the scatter of results is unavoidable and in an industrial plant situation this scatter of results clearly demonstrates the limitations of predicting precisely which bend will fail, except that it will fail randomly.

As mentioned in the preceding chapter, the causes of the scatter of results were partly attributed to particle degradation and partly to velocity effects around the bends. The velocity effect has been shown to a certain extent to be predictable and in this work, since all the tests were carried out at a constant phase density of 3, the pressure drop, and hence velocity, in the bends were approximately the same for every test. Therefore, it is possible to isolate the scatter of results due to velocity affect in each test series without the need to normalise the results in Figs. 7.15 to 7.17.

However, the effect of particle degradation on the scatter of results is not so predictable. For sand, although the mean particle size was reduced slightly from 70 to 64 μm, the percentage of 'fines' below 45 μm increased by a factor of about 1.5 to over 30% after only 6 runs. This increase in the 'fines', combined with the influence of secondary flows, has been shown to be predominantly responsible for premature bend failures. In the case with sand, without considering the two premature bend failure results, after 13 runs there is a variation in the scatter of results by a factor of 3:1.

For calcined alumina there was also a slight decrease in the mean particle size, with a corresponding increase from 17 to 21% in the 'fines' below 45 μm. However, apart from the result of bend 1, the scatter of results is very much less compared to those of sand over a similar number of runs.

For p.f. ash there was virtually no change in its particle size distribution after 18 runs and the results are fairly consistent. In the case of f.b. ash however, the effect of particle recirculation on the scatter of results is clearly evident as shown in Fig. 7.16. Prior to the start of this test series, sieve analysis (Fig. 7.18) showed that only 1.4% of the particles were less than 45 μm. At the end of this test series, after 21 runs, this had risen to over 14%. However, this dramatic increase in the 'fines' produced a variation in the scatter of results by a factor of only 1.5:1. This apparently limited scatter of results, despite the increase in 'fines' is largely attributed to the presence of a considerable number of large sized particles. Whilst the mean particle size had been reduced from 1350 to 650 μm, over 70% of the size distribution at the end of this test series was still over 300 μm, and it is the presence of these relatively large particles that limits any potential increase in the scatter of results due to the 'fines'. A similar effect has also been reported by Mills and Mason (1977 b, c, 1979 a), who showed that the scatter of results decreased as particle size was increased.

Apart from the scatter of results predominantly due to the presence of 'fines' in the test materials, the variation in the value of particle hardness does not appear to have any significant effect in this respect.

In order to evaluate specific erosion values, and for comparison purposes, the values of the total mass eroded from each test set were determined. Each test set consisted of 3 test runs and therefore the values for each test set have the accumulative value of 3 consecutive test runs. In Fig. 7.19 the specific erosion values of 3 test sets, comprising the first 9 test runs, are presented. These values correspond to the particle hardnesses of the four test materials respectively. The vertical line of values indicates the upper and lower estimations within each test set, and the location of the symbol indicates the mean. In all cases the limit of the values in each

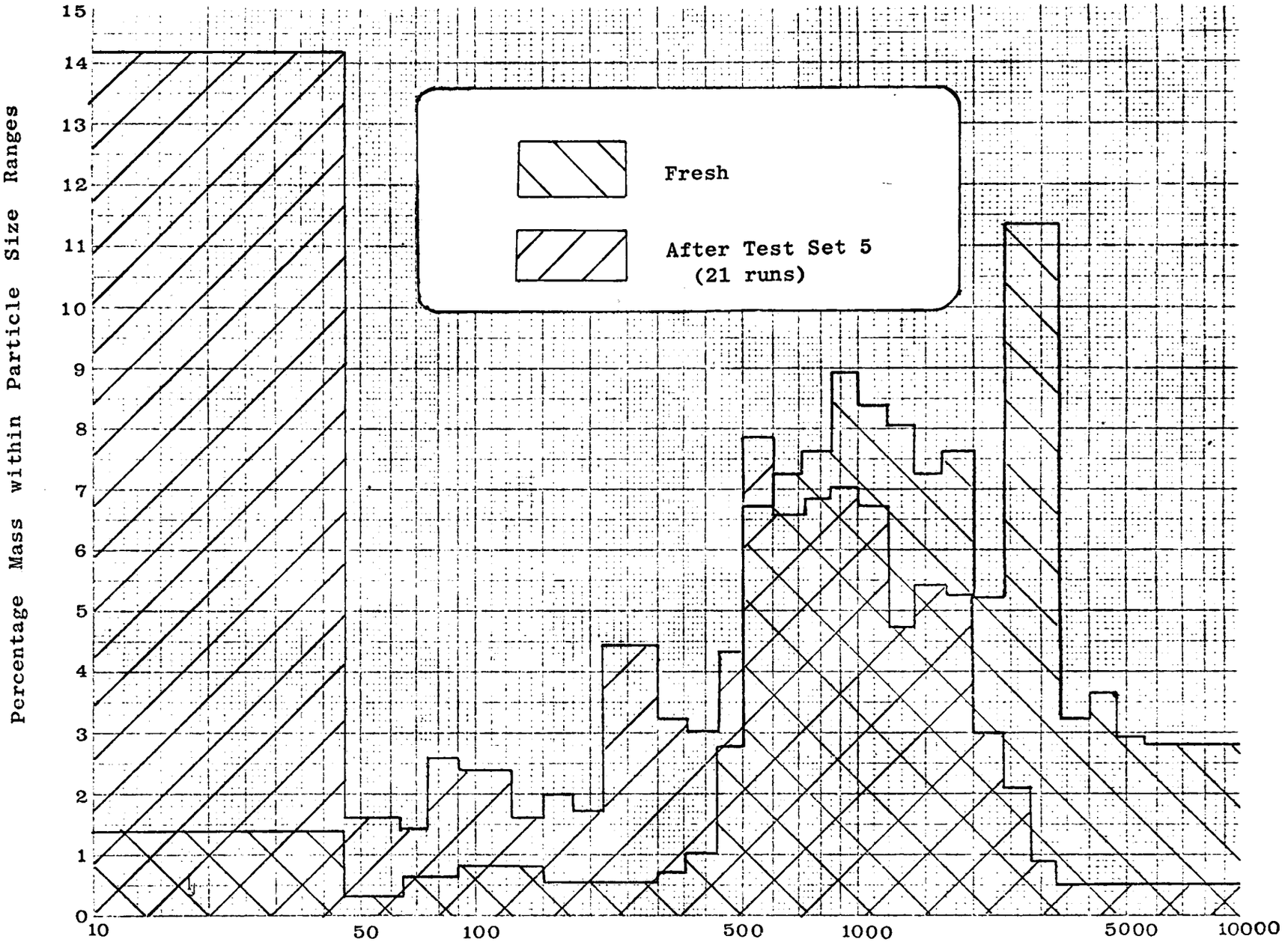

FIG. 7.18 Variation of Particle Size Distribution of Fluidised Bed Ash - Before and After End of Test Series.

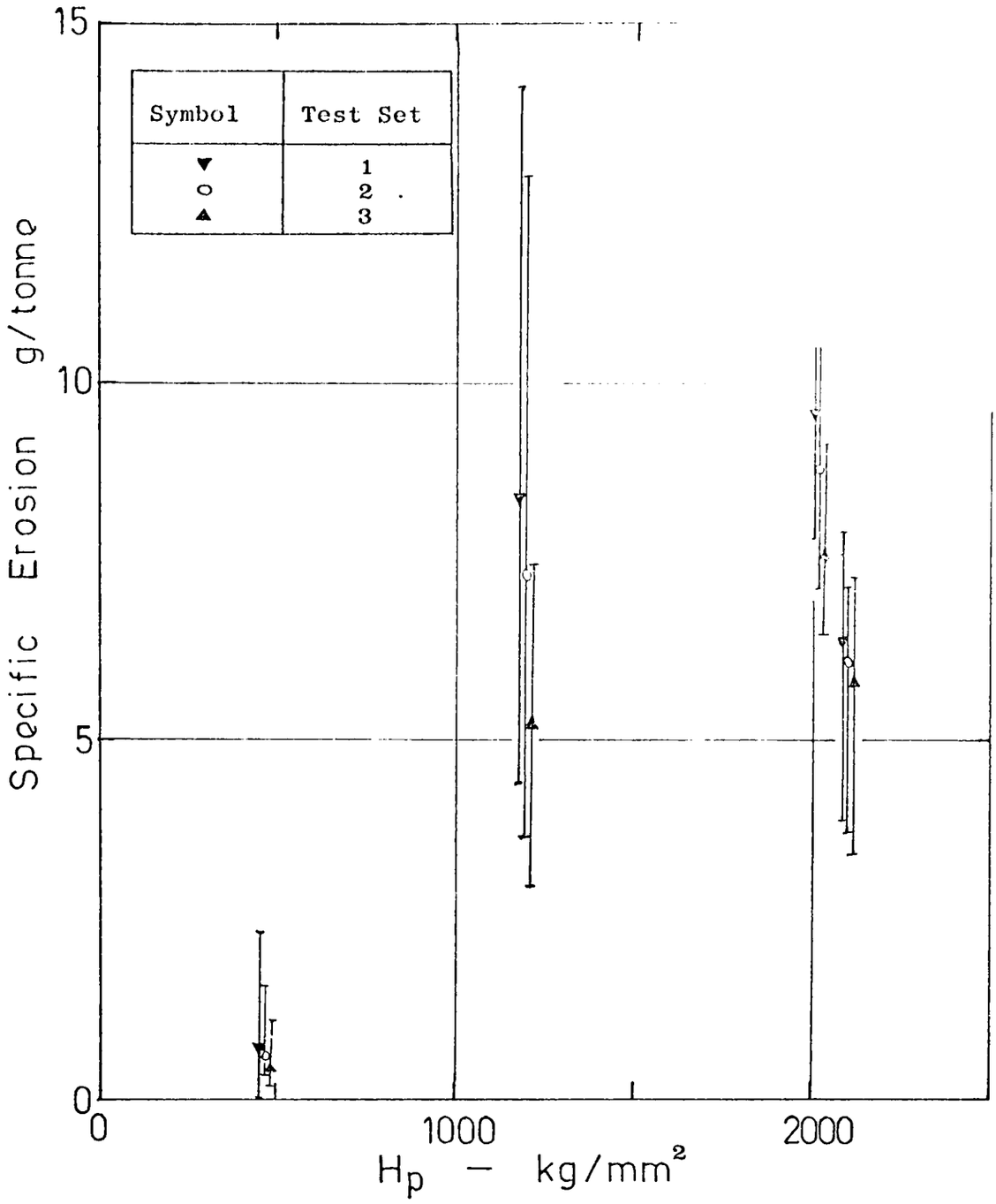

FIG. 7.19 Variation of Specific Erosion with Particle Hardness

vertical line clearly reflects the scatter of results shown earlier, particularly for sand.

However, in terms of particle hardness effects, the results in Fig. 7.19 clearly show that there is a threshold value of particle hardness, above which erosion is not influenced by the hardness of the conveyed material. Whilst no attempt has been made to join the mean values in this figure, it can be clearly seen that the trend of the results is similar to that shown in Fig. 7.1, obtained from erosion rig studies. From the data in this figure it appears that, in terms of specific erosion, materials with hardnesses greater than about 1000 kg/mm^2, would not be substantially more erosive than the sand particles. Comparison of the erosion results between p.f. ash (480 kg/mm^2), sand (1200 kg/mm^2) and calcined alumina (2100 kg/mm^2) clearly confirms that, since size distributions and test conditions are essentially identical, hardness is closely inter-related with shape, and the magnitude of erosion is considerably influenced by both as reported earlier by Goodwin et al (1969) and Mills and Mason (1977 c).

Apart from demonstrating the inter-relating influence of particle hardness and shape on erosion, the results in Fig. 7.19 also show the effect of particle size, particularly with regard to f.b. ash. While the mean particle size of fresh f.b. ash was 1350 μm, it reduced to 1200, 1050 and 1000 μm corresponding to test sets 1, 2 and 3 (Fig. 7.12) respectively. This reduction obviously has a significant effect on erosion, but over this range of tests the overall mean specific erosion values (see Fig. 7.31) are still comparable to those of sand and calcined alumina. Mills and Mason (1979a) reported that, in tests carried out at a constant phase density of 2, the results for sand with a range of particle sizes, show that erosion is essentially constant. The erosion data in this work (Fig. 7.19) from tests carried out at a constant phase density of 3, also confirms that at low phase densities erosion is substantially independent of particle size. In Chapter 6, however, the results obtained by the author show that there is a considerable variation in erosion with respect to particle size at higher phase densities.

A continuing feature of the work on erosion is the transitional effects with regard to certain inter-relating variables. The results in

Fig. 7.19 were based on the erosion of mild steel bends with a constant material hardness. In Fig. 7.1 the curves clearly show the inter-relating effect of surface material and particle hardnesses on the magnitude of erosion. Apart from the dependence of a critical hardness value on this inter-relating hardness effect, the threshold value also depends considerably on velocity. Although the results in Fig. 7.19 were from tests at a mean conveying air velocity of about 25 m/s, it appears that there is a transition effect with regard to velocity on the critical particle hardness value in terms of specific erosion, and further tests with a range of velocities would be necessary in order to determine the magnitude of this transition effect on critical particle hardness.

7.6.3 Penetration Rate Analysis

In contrast to the scatter of erosion results in Figs. 7.15 to 7.17, the corresponding data in Figs. 7. 20 to 7.22, in terms of the variation of maximum depth of penetration with mass eroded, shows a remarkable degree of consistency in comparison. No attempt has been made to draw lines through the points plotted in these figures since there is little scatter in the data, and all the results clearly fall within a band. The individual experimental points for each bend tested within each test series are identified by the same symbols as used in the previous figures and so these plots show the penetration history of each individual bend in terms of the maximum depth of penetration by the particles into each bend. The experimental results of p.f. ash are not included in any of these figures due to the small depth of penetration in relation to the scale of those of the other test materials.

For comparison purposes the mean slopes of the experimental data in Figs. 7.20 to 7.22 are given in Fig. 7.23. The gradients of these slopes clearly show that, apart from the relatively limited effect of particle hardness, the magnitude of penetration rate in terms of μm/g eroded, is substantially influenced by the shape and size of the particles.

Perhaps more useful representations of penetration data are those given in Fig. 7.24, which show the variation of penetration wear rate in terms of mm/tonne, with the hardness values of the test materials, including p.f. ash. These are the results of the first three test

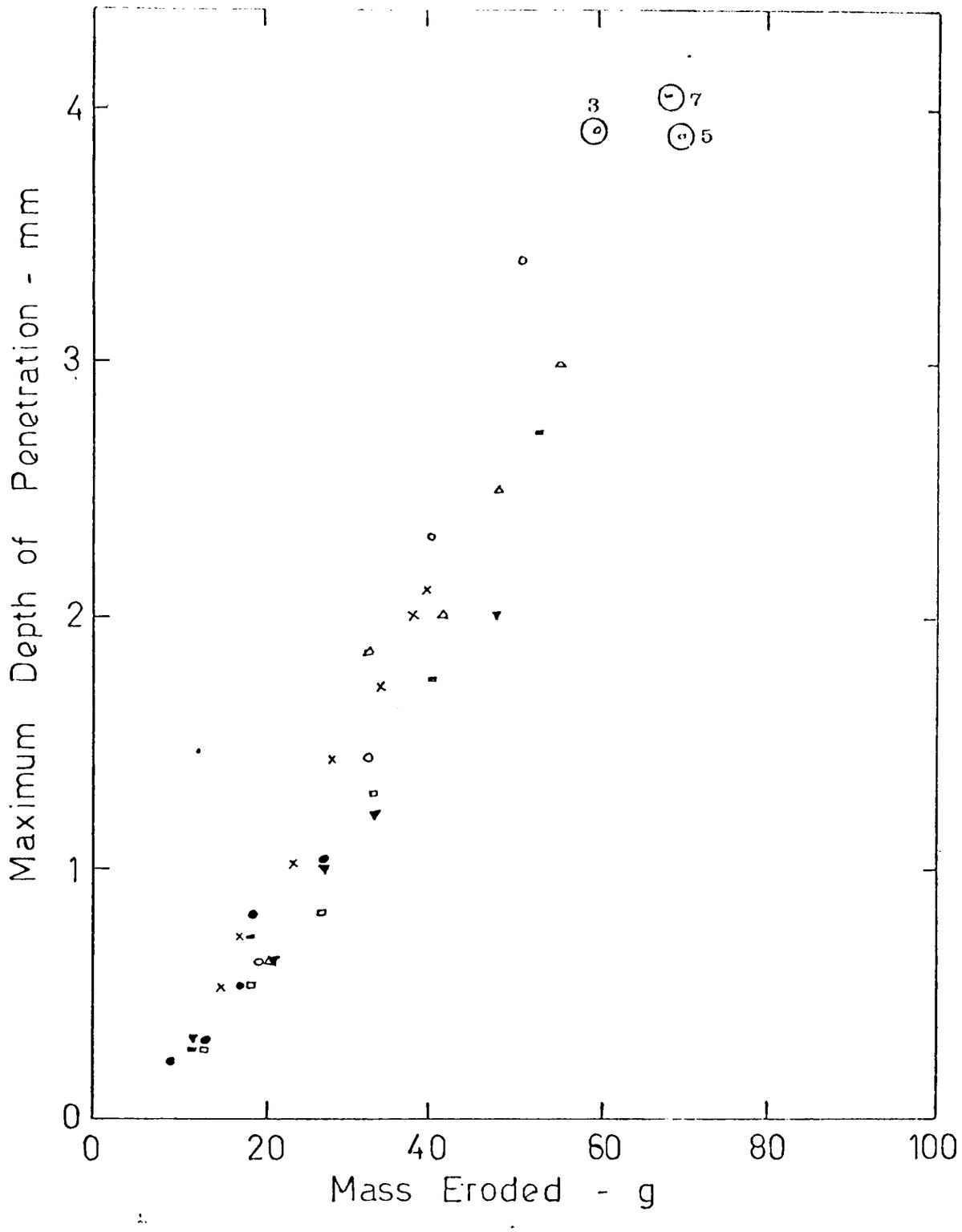

FIG. 7.20 Penetration Data for Bends Eroded by Sand

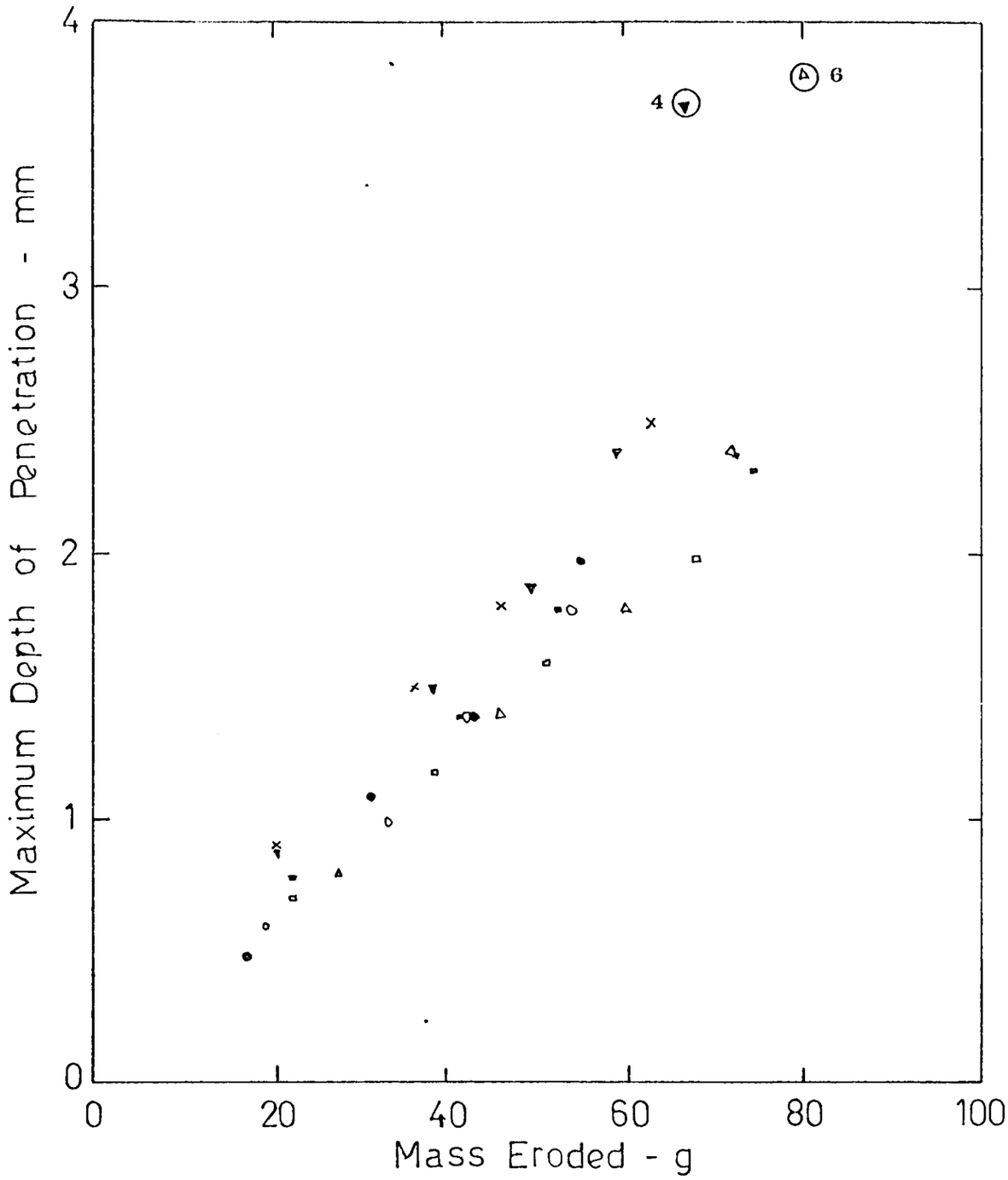

FIG. 7.21 Penetration Data for Bends Eroded by Fluidised Bed Ash

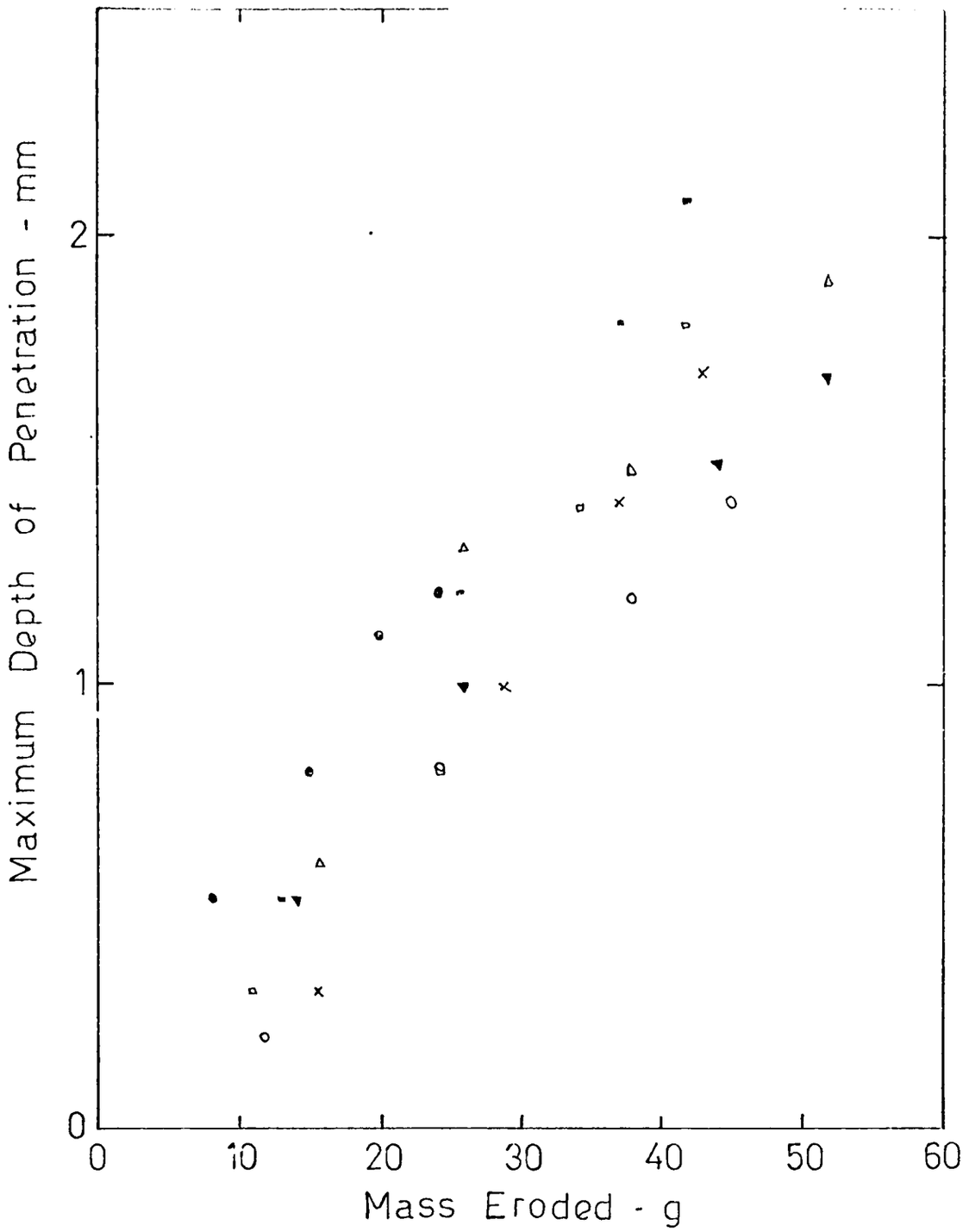

FIG. 7.22 Penetration Data for Bends Eroded by Calcined Alumina

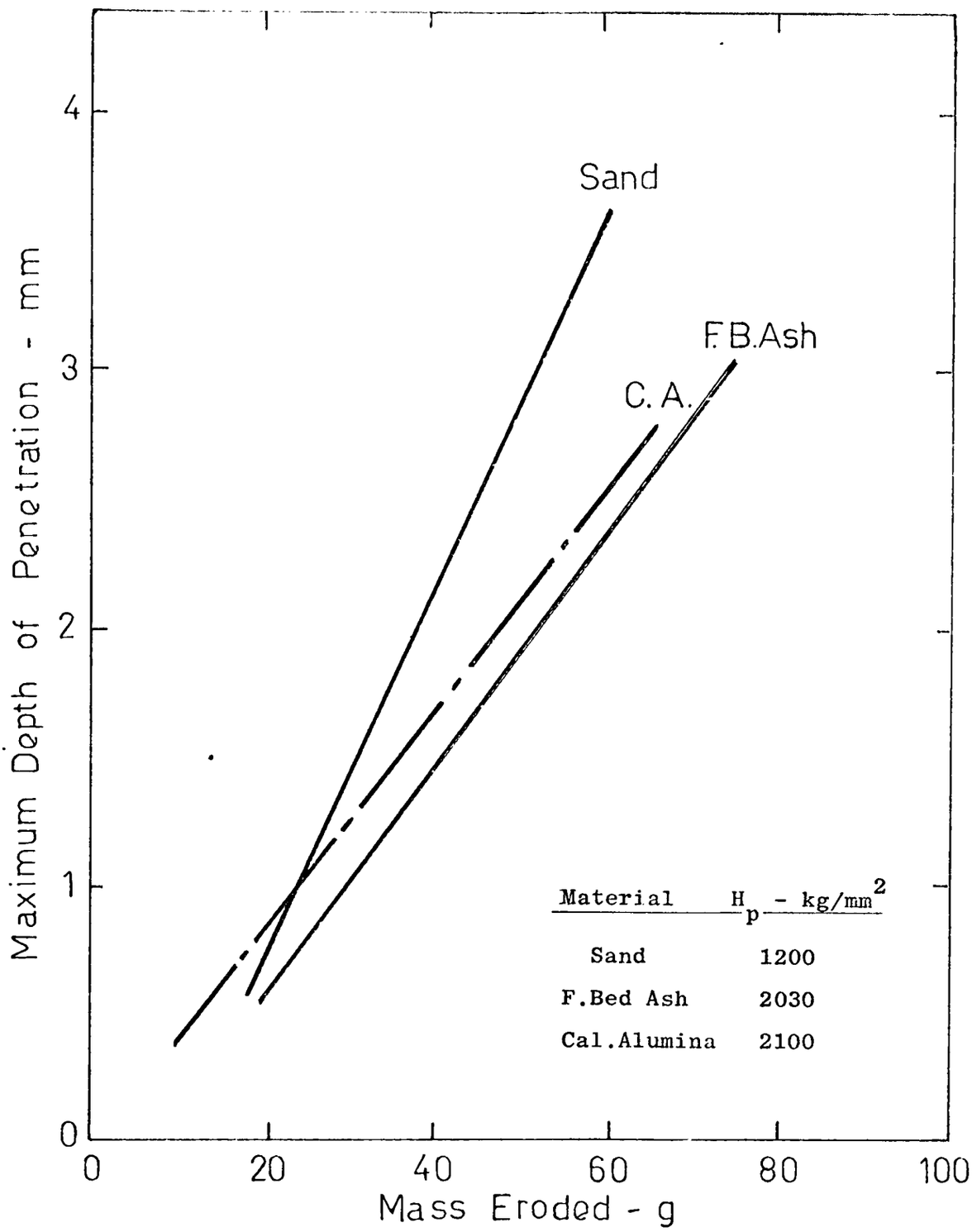

FIG. 7.23 Influence of Particle Hardness on Rate of Penetration.

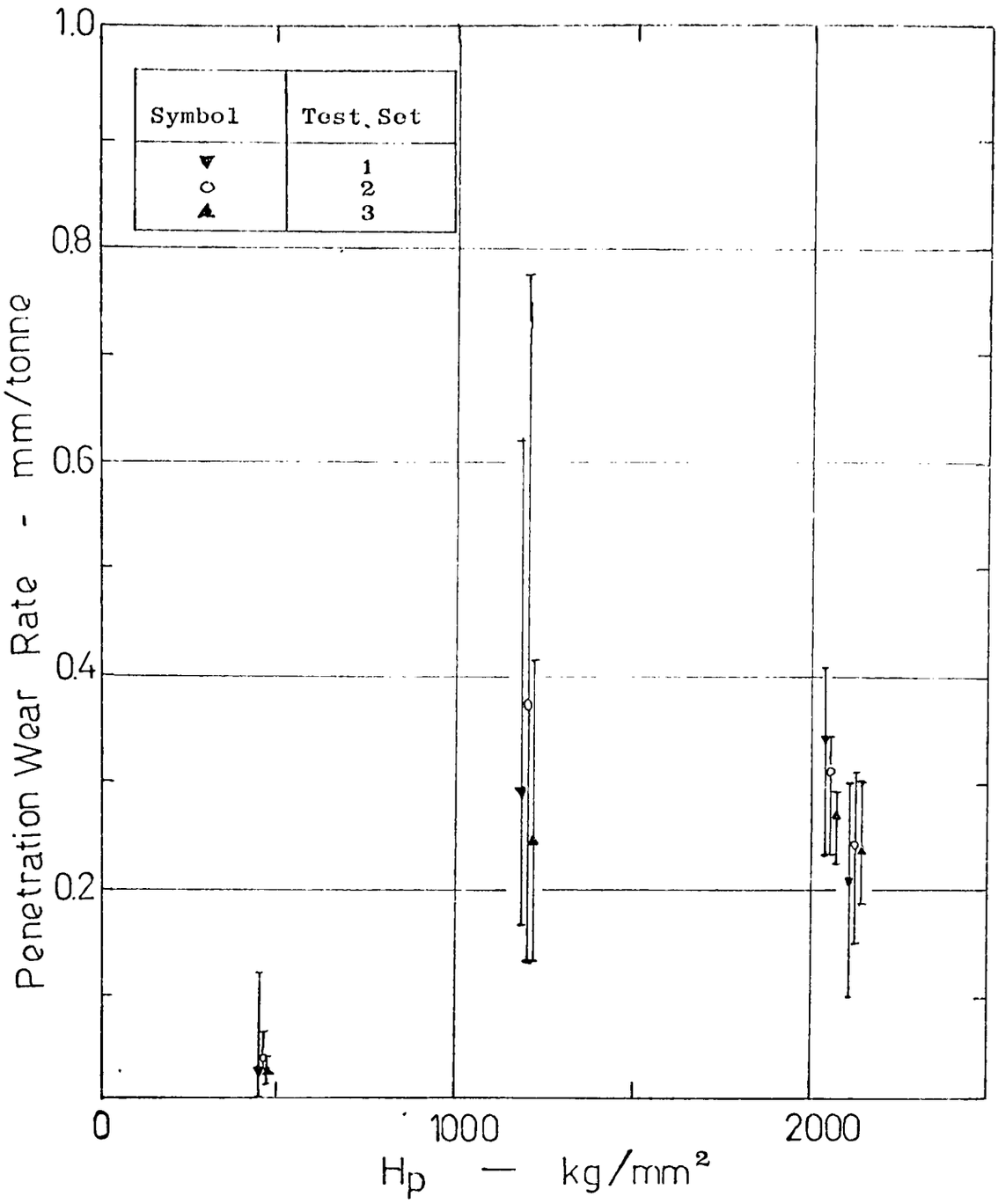

FIG. 7.24 Variation of Penetration Wear Rate with Particle Hardness

sets, and again, as in Fig. 7.19, no attempt has been made to join the mean values of each test set. The trends of these mean values also show that there is a threshold value of particle hardness above which penetration is not influenced by hardness. The similarity of results in Figs. 7.19 and 7.24 clearly has important implications for the pneumatic conveying engineer. Both figures show that there is a definite trend towards a critical hardness value beyond which both erosion and penetration are relatively independent of particle hardness and the magnitude of this value is considerably influenced by the inter-relating effects of shape, size and velocity of the particles as well as the hardness of the bend material itself.

7.6.4 Bend Life Analysis

A prime objective of the investigation in this work was to provide an analysis from which the likelihood of erosion could be predicted from the results of certain variables and, in this section, the specific influence of particle hardness on erosion is considered.

As explained in the preceding chapter, it is possible to determine a relationship in terms of conveying capacity and potential service life of bends by combining the experimental data on both specific erosion and depth of wear.

7.6.4.1 Calculation Procedure

A log plot of specific erosion results in Fig. 7.19 shows that, over this range of hardness values considered, from 500 to 2100 kg/mm^2, particle hardness (H_p) is related to specific erosion (ε) by a simple power law relationship:-

$$\varepsilon \propto (H_p)^y$$

From Fig. 7.25, the hardness exponent corresponding to the experimental data in test sets 1, 2 and 3 is 1.57, 1.59 and 1.84 respectively. The slight variation in the value of the exponent clearly indicates the influence of product condition to a certain extent on the magnitude of erosion. Since in most industrial plant operation situations it is unlikely that the material is conveyed more than once through the pipelines, it can be seen from Fig. 7.24 that

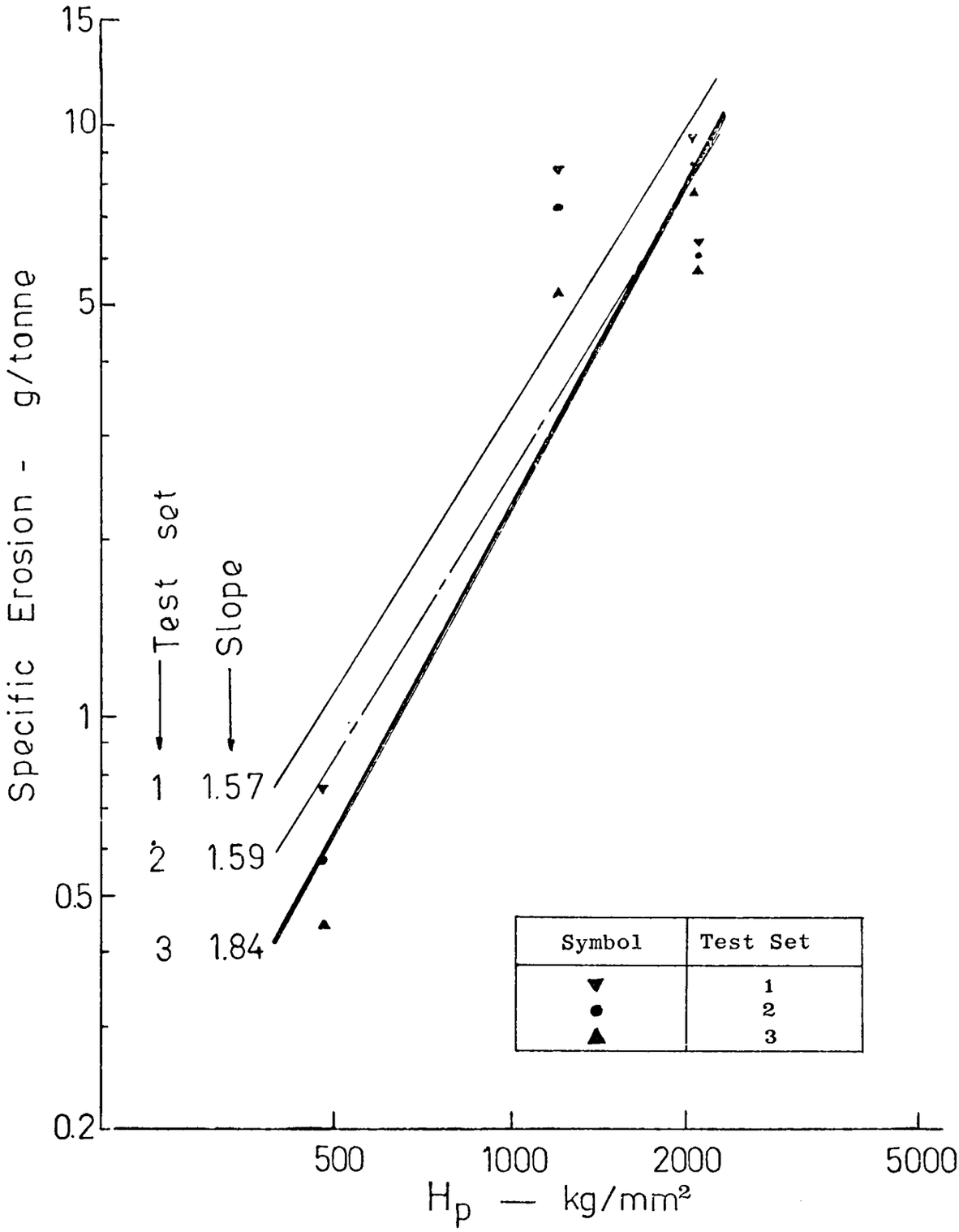

FIG. 7.25 Variation of Erosion with Particle Hardness

the exponent is fairly constant, and for the purpose of this analysis it was decided by the author to consider the value of 1.57 corresponding to test set 1, which is based on the results of a relatively fresh set of materials.

Hence, from a linear regression analysis of the relevant data, the above expression can be given by :-

$$\varepsilon = 6.25 \times 10^{-5} \ (H_p)^{1.57} \text{ g/tonne} \qquad (7.2)$$

In order to determine the conveying capacity of bends, the variation of mass eroded at the time of failure (E_{bf}) with respect to particle hardness (H_p) is required. In tests with sand three bends failed with a mean value of 60 g, and with f.b. ash two bends failed with a mean value of 73 g. Substituting the appropriate values, the relationship between E_{bf} and H_p can be expressed by:-

$$E_{bf} = 4.27 \ (H_p)^{0.37} \text{ g} \qquad (7.3)$$

It should be noted that the accuracy of the numerical values in the above expression is subject to some variation. Two of the three bends which failed in tests with sand, as mentioned before, failed prematurely. The rapid failure of these bends, with corresponding lower values of mass eroded at point of failure (Table 5.3), has a consequent effect on the overall mean value. Furthermore, in tests with f.b. ash the overall mean value at failure is also affected, to some extent, by the size effect, although it has been shown that at low phase densities there is no significant variation in terms of specific erosion. In tests with p.f. ash and calcined alumina, no bends failed. Although the relationship between E_{bf} and H_p is determined on the basis of the limited experimental results of two materials only, it is unlikely that there will be any significant variation of the numerical values in the above expressions, such that it would alter the magnitude of these expressions completely.

The conveying capacity of bends, in terms of the mass of material that can be conveyed through the bends before failure

(M_s), is given by :-

$$M_s = \frac{E_{bf}}{\varepsilon} \text{ tonne}$$

Substituting the appropriate equations into this expression yields :-

$$M_s = 0.68 \times 10^5 (H_p)^{-1.20} \text{ tonne} \qquad (7.4)$$

A graphical representation of this expression is given in Fig. 7.26.

In terms of bend life, using the relationship

$$\Delta\tau_{bf} = \frac{M_s}{\phi \dot{m}_a} \text{ h}$$

where $\Delta\tau_{bf}$ = the conveying time to bend failure, and substituting the appropriate values into this equation gives :-

$$\Delta\tau_{bf} = 2.78 \times 10^5 (H_p)^{-1.20} \text{ h} \qquad (7.5)$$

A graphical representation of this expression is given in Fig. 7.27.

The set of curves in Figs. 7.26 and 7.27 shows the influence of particle hardness on the conveying capacity and service life of bends in an actual pneumatic conveying situation. Both curves provide a real basis on which the performance of bends, under otherwise identical conveying conditions, in respect of particle hardness, should be compared.

The trend of the curves in both figures definitely indicates the existence of a critical hardness value in which there is a significant change in the performance of bends over the range of particle hardnesses considered.

For materials with a hardness value less than about 1000 kg/mm^2 there is a definite increase in the amount of material that can be conveyed through the bends before failure occurs, and this increases exponentially as the hardness of the material is decreased. In contrast, for materials with hardness values above this critical value bends will not fail as rapidly as the hardness values of the materials are increased progressively. The apparent lack of deterioration of the performance of bends as the hardness of the material is increased well beyond this critical

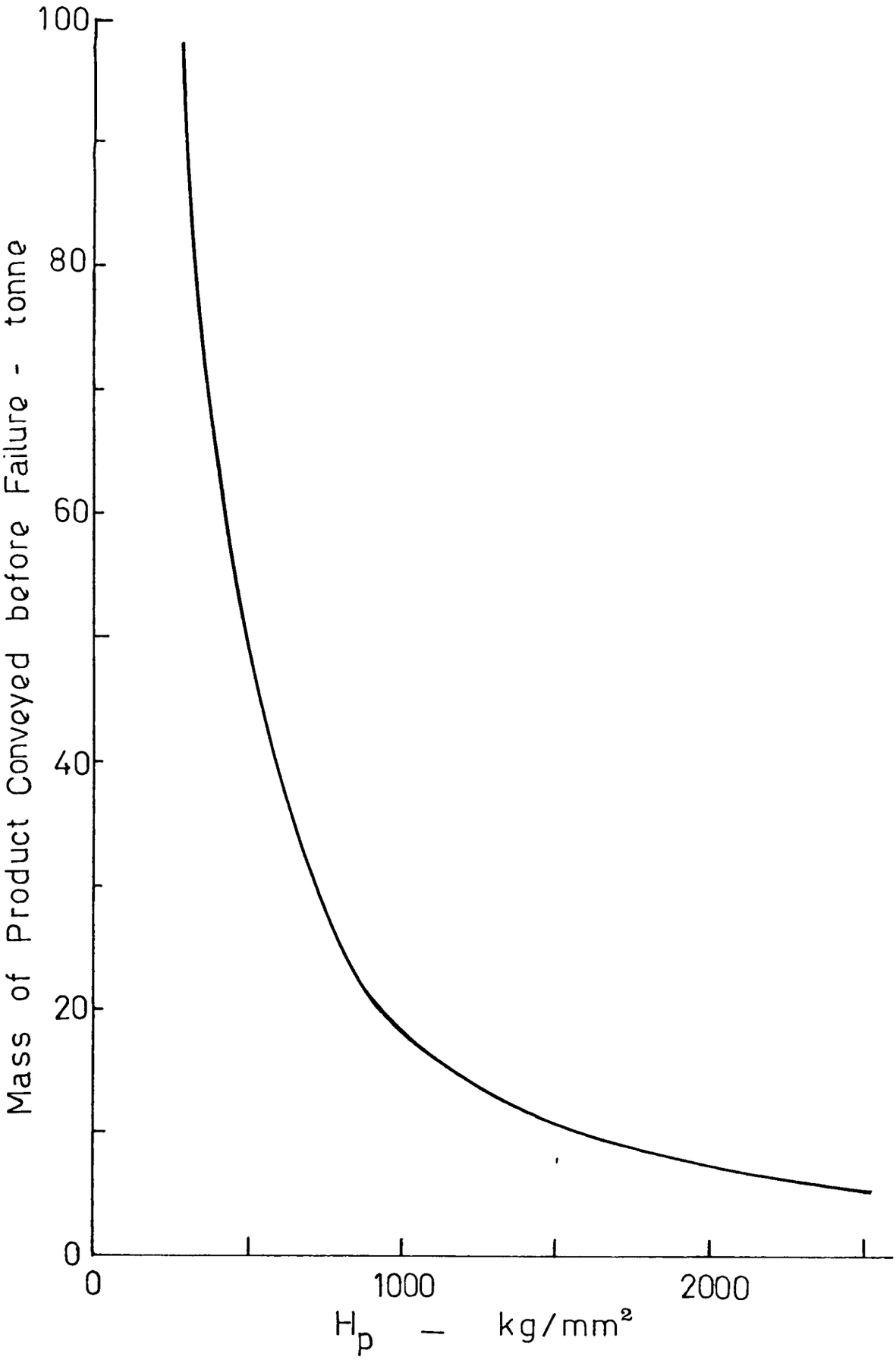

FIG. 7.26 Influence of Particle Hardness on the Conveying Capacity of Bends.

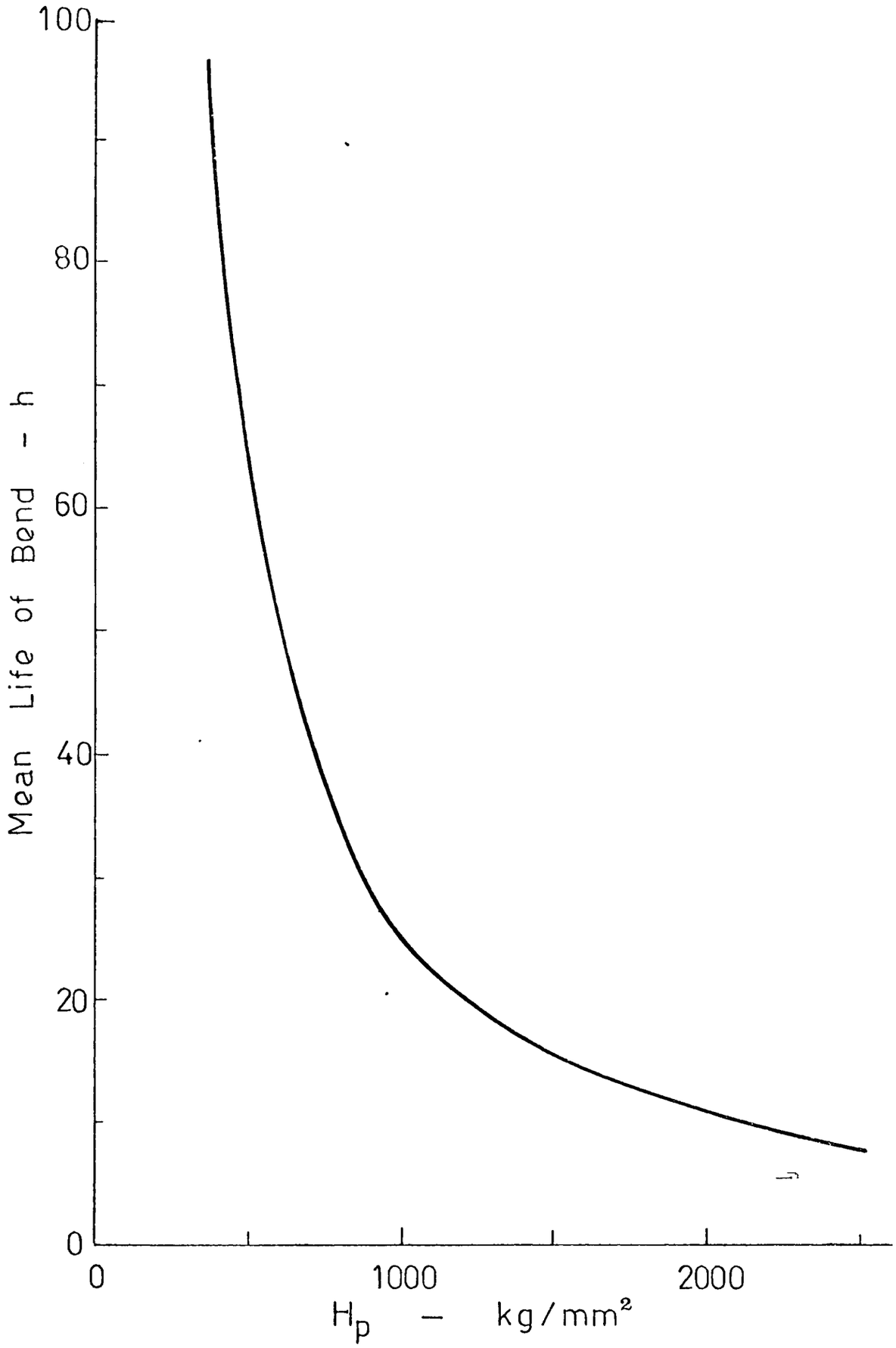

FIG. 7.27 Influence of Particle Hardness on the Service Life of Bends.

hardness value clearly reflects the trend of the results in Figs. 7.19 and 7.24 on the influence of particle hardness on both erosion and penetration.

7.6.4.2 Influence of Other Variables

As mentioned earlier, apart from the difficulty of isolating the inter-relating effects of shape and size from hardness, the magnitude of erosion is also considerably influenced by velocity and the hardness of the bend material itself.

To a certain extent, however, the inter-relating effects of these variables are predictable. Apart from the obvious change in the magnitude of the values in Figs. 7.26 and 7.27, the shape of the curves would not be significantly altered and both would still indicate a critical hardness value which, of course, will vary with the magnitude of the effect of both velocity and hardness of the bend material. Further work over a range of velocities and bend materials with different hardnesses, possibly incorporating various bend lining materials, is required in order to establish the range of transitional values with respect to particle hardness, and this is an area that warrants further investigation.

7.6.5 Surface Erosion Patterns

Fig. 7.28 (a to e) shows typical erosion patterns of one of the bends eroded by each respective test material. The five bends in this figure correspond to bend 6 as indicated in Fig. 4.6, so the conveying conditions in each of these bends are identical.

The lack of erosion due to hydrate alumina is clearly shown by the deposition of these particles onto the surface of the bend (a). The smooth profile and the absence of any noticeable erosion scouring marks in the bend eroded by p.f. ash (d) reflect the very limited erosion and penetration data of this particular test material. By contrast, the characteristic stepped erosion patterns, although not so pronounced in this particular bend, are clearly visible in the bend eroded by sand (c), and a similar pattern is observed more clearly in the bend eroded by calcined alumina (b), particularly the appearance of erosion ridges. The absence of any such erosion patterns in the bend eroded by f.b. ash (e) clearly reflects the characteristic size

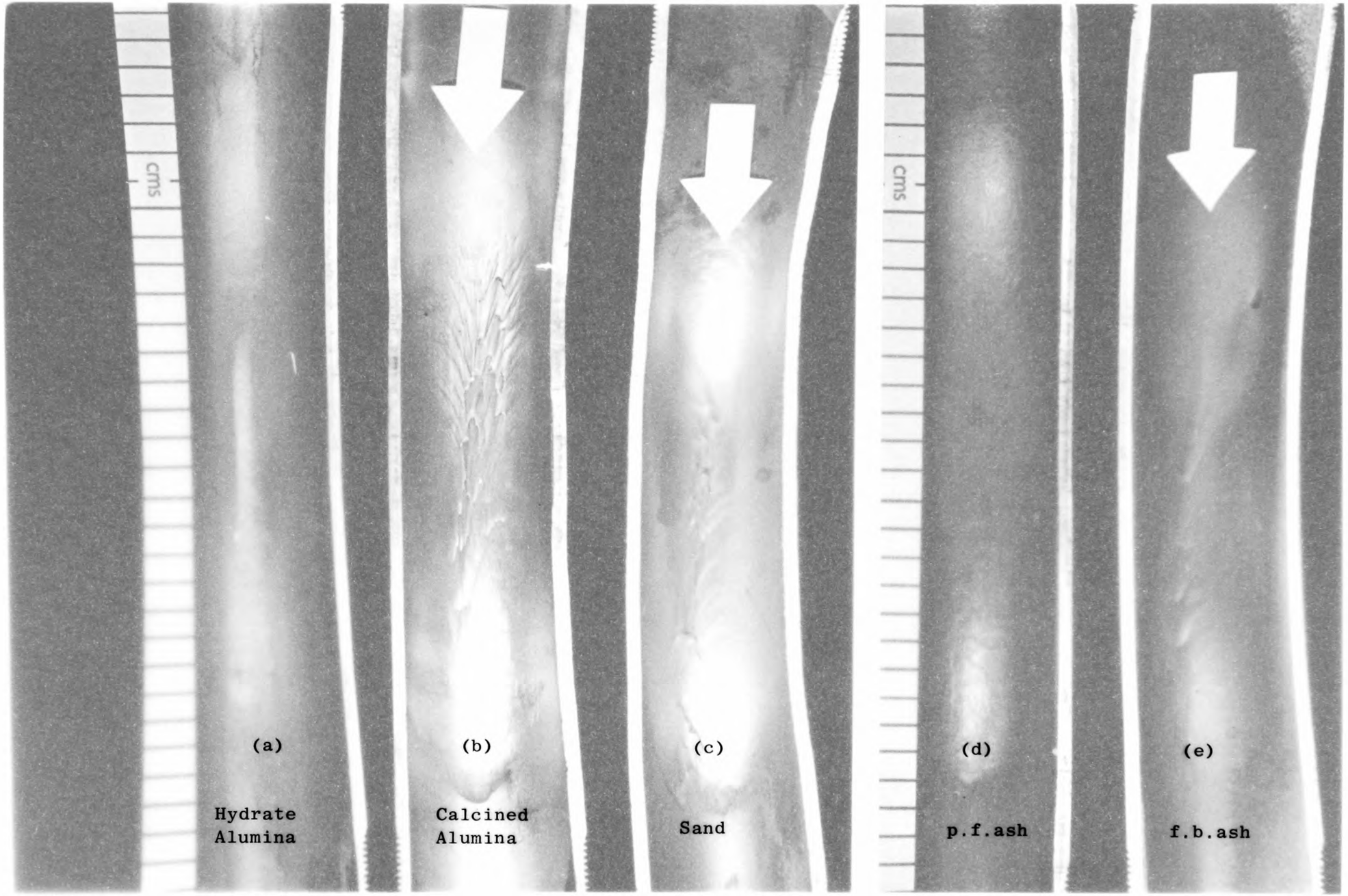

FIG.7.28 Typical Surface Erosion Patterns

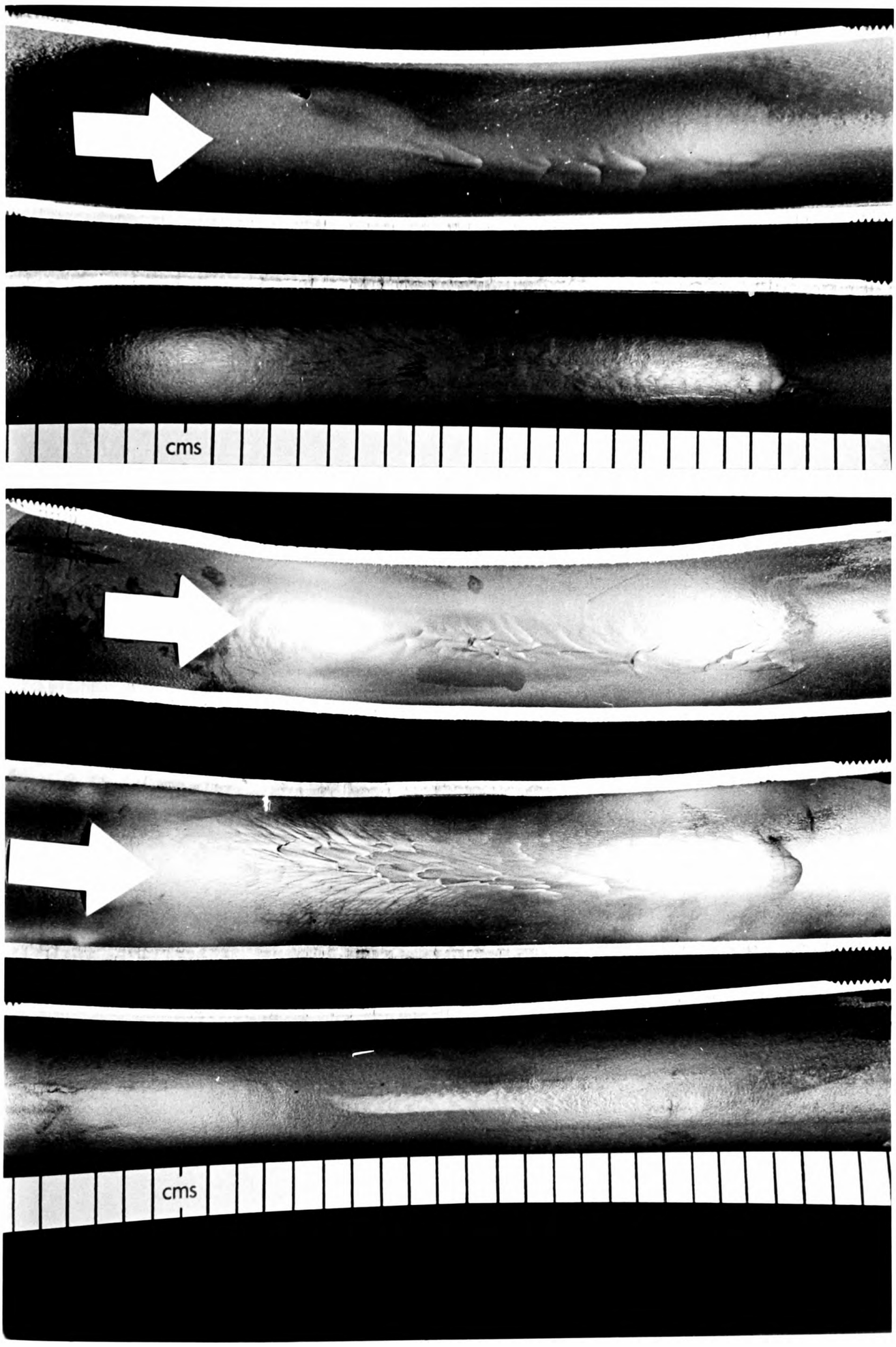
cms
cms

effect, and the tracking of the erosion patterns across this bend indicates the considerable presence of 'fines' in association with swirling flows.

The influence of particle hardness on mass eroded and depth of wear can be observed more clearly in Figs. 7.29 and 7.30 in terms of bend and pipe wear profiles. Once again, owing to the lack of any comparable data in tests with p.f. ash, only the respective wear profiles of sand, calcined alumina and f.b. ash are shown.

For a constant mass eroded from each bend of about 27 g, the curves in both figures clearly show the limited effect of hardness in terms of depth of penetration. Whilst there is some 75% difference between the hardnesses of sand and calcined alumina, there is hardly any appreciable difference in the depth of penetration between these two materials. With a higher hardness value, combined with the effects of moisture and shape, the curves for calcined alumina should show a greater depth of penetration compared to those for sand. However, the similarity of results in terms of depth of penetration for these two materials clearly shows the limited effect of particle hardness over the range of hardnesses considered.

In the case of f.b. ash the shape of the wear profile curves in both figures clearly demonstrates the over-riding effect of particle size over that of particle hardness. Furthermore, the position of maximum wear in terms of pipe angle substantiates further the size effect, which shows that as particle size is increased, the position of maximum wear and hence failure progressively decreases below the centre line of the pipe due to the increasing gravitational effect.

However, to a large extent the wear profiles in these figures are quite misleading, since they correspond to a certain constant amount of mass eroded. A more representative comparison of the penetration data over a range of constant mass eroded would be from the slopes presented earlier in Fig. 7.23. The slopes in this figure incorporate the individual wear profiles in Fig. 7.29 and clearly show that the depth of penetration is not proportional to mass eroded and, in terms of particle hardness, confirm the existence of a critical hardness value beyond which both erosion and penetration are relatively independent of particle hardness, as shown in Figs. 7.19 and 7.24.

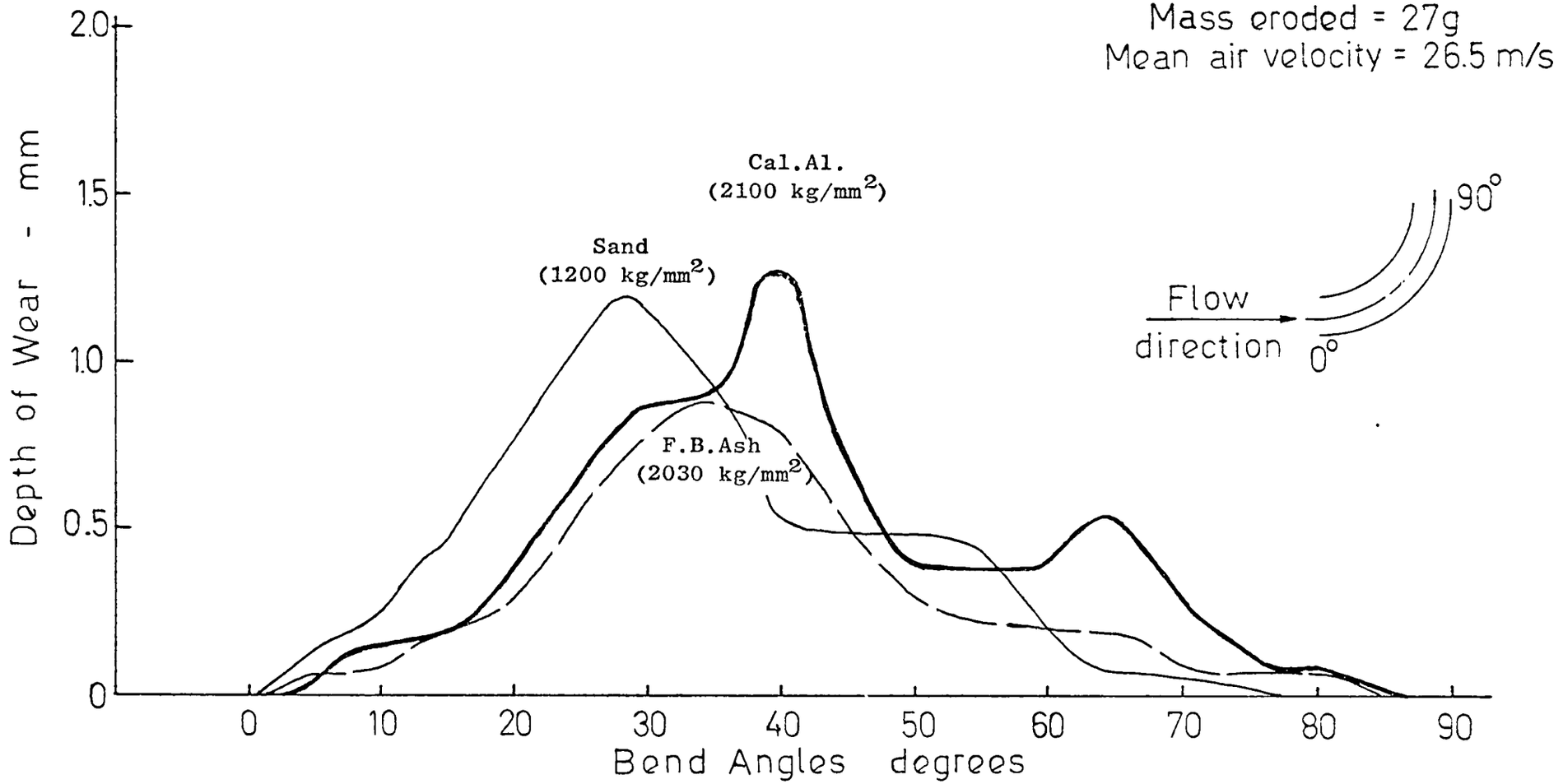

FIG. 7.29 Influence of Particle Hardness on Bend Wear Profile

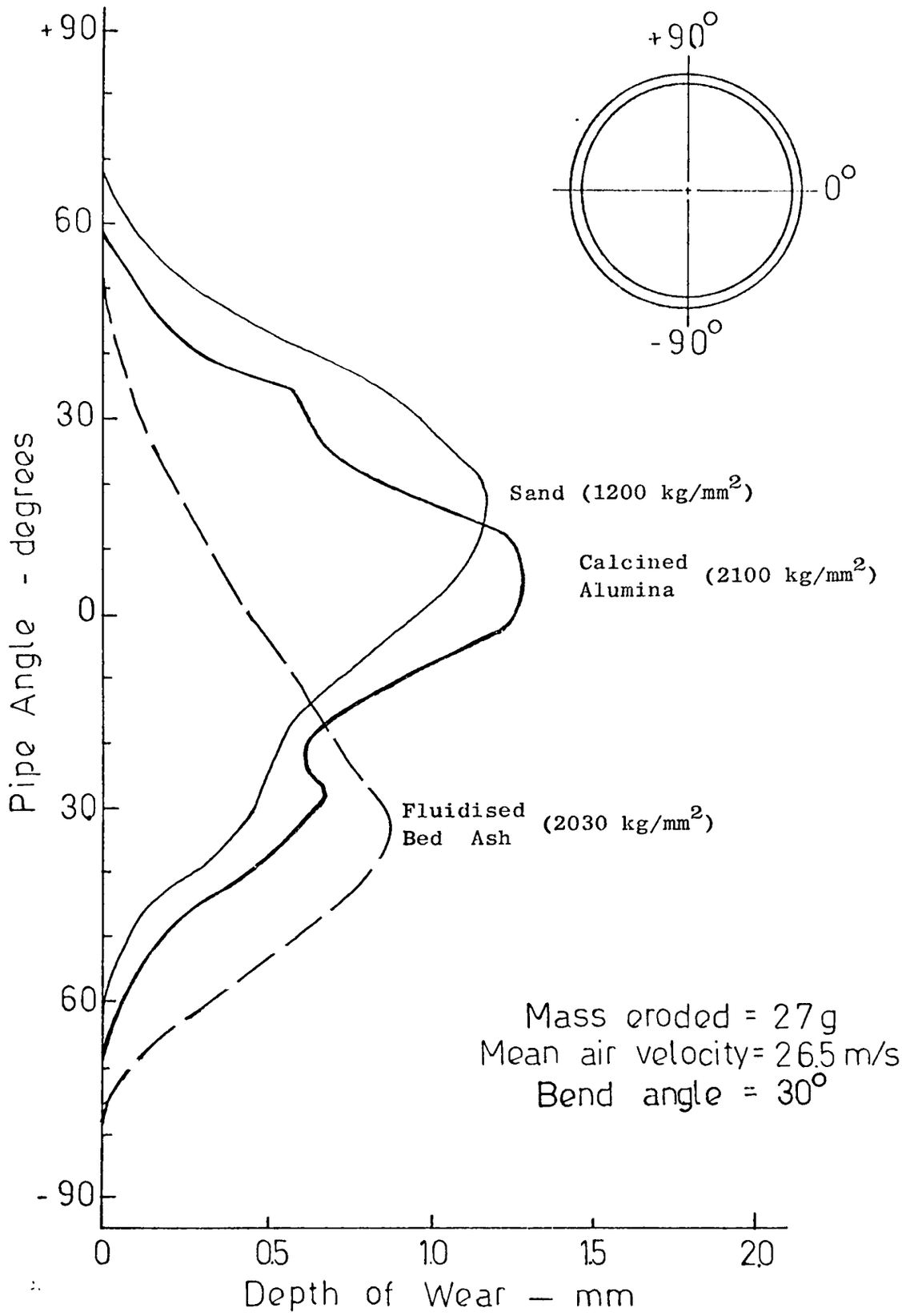

FIG. 7.30 Influence of Particle Hardness on Pipe Wear Profile

7.7 EFFECT OF PARTICLE DEGRADATION

7.7.1 Introduction

When a single batch of material is recirculated continuously through a pipeline there will inevitably be some degradation of the particles. To a certain extent the degree of degradation, when accompanied by a substantial change in the overall size distribution, can present difficulties in defining the characteristics of the gas-solid flow and predicting the pressure drop.

Whilst it has been generally well recognised that there is a distinct difference between the transport characteristics of coarse and fine particles (Boothroyd 1971), there are some conflicting observations on the relative effect of particle size on pressure drop. Pinkus (1952), from tests with 240 and 440 μm sand particles, found that pressure drop increases as particle size is increased and a similar observation has also been reported by Rao and Ghosh (1967) from tests with a variety of different sized seed grains. However, a majority of the more recent studies (Chari 1971, Mason and Boothroyd 1971, Scott 1978, Wheeldon and Williams 1980) reported that, under certain conveying conditions, pressure drop increases as particle size decreases. A general explanation of this behaviour, according to Velayudhan et al (1970), is that as particle size is decreased there is a corresponding increase in particle velocity. As frictional loss may be represented by an equivalent coefficient of friction term, it has been reported by Clark et al (1952), that the coefficient of friction is related to particle velocity by a parabolic function. From this it follows that, when particle velocity is increased, the equivalent friction coefficient increases, which results in a corresponding increase in pressure drop. Furthermore, it has been reported by several sources (Richardson and McLeman 1960, Doig and Roper 1963, Boothroyd 1971, Duckworth and Chan 1973) that finer particles are more susceptible to electrostatic charge and, consequently, increase in pressure drop. This whole picture is further confused by the drag reduction generated by very small particles, as reported by some authors. However, Huff and Holden (1965), from tests with a range of coal particles from 50 to 250 μm, found that at sufficiently high velocity, pressure drop remains constant, irrespective of particle size, although as pipe diameter is increased, the pressure drop for the larger particles is correspondingly much higher than for the smaller particles. Chowdhury et al (1967), from similar tests, although with a wider range of coal

particles from 100 to 500 μm, found that at a constant velocity and phase density, pressure drop is initially independent of size up to about 250 μm, beyond which it varies directly with particle size. In this work with fluidised bed ash, apart from the velocity effect, there was no significant increase in the conveying line pressure drop over the range of tests, despite a reduction in the mean particle size of some 50%. The lack of any increase in pressure drop is probably related in some way to the overall effect of the wide spectrum of size distribution of this f.b.ash material.

7.7.2 Review of Previous Work

Apart from some general limited studies on the breakage of coal (Hunter 1975, Sproson et al 1976), information on the specific subject of particle degradation of pneumatically conveyed materials is very limited. In the field of the general solid particle erosion studies, Tilly and co-workers (Goodwin et al 1969, Tilly and Sage 1970) are probably the only researchers who have investigated the effect of particle degradation on erosion in detail. Their results appear to show that it is necessary to exceed threshold conditions for fragmentation to occur (see Fig. 2.4), and the degree of fragmentation is dependent upon the type of target material as well as velocity.

Mills and Mason (1976b, 1978) have carried out limited studies on the effect of particle degradation on bend erosion. They reported that, apart from the difficulty of isolating a number of variables involved in the mechanics of product degradation, it can be essentially reduced to those associated with pipe bends and conveying distance. From their limited experimental results on 70 and 230 μm sand particles, they found that in both cases there is an initial high erosion rate followed by a gradual reduction and then a steady slow decrease in the mass eroded per batch conveyed (see Fig. 7.31 for the 230 μm sand results). Apart from a marked increase in the 'fines', they commented that the magnitude of degradation is likely to be considerably influenced by both particle velocity and phase density.

The experimental results obtained from the tests with f.b. ash in this work provide an opportunity for a more complete analysis of the effect of particle degradation on both erosion and penetration and, in the following section, the relative effects of these two parameters are discussed.

7.7.3 Effect on Erosion and Penetration Results

Fig 7.31 shows the influence of continuous recirculation of f.b. ash on the mass eroded from the bends. Also included on this figure, for comparison purposes, are the results for 70 μm sand from this work and 230 μm sand from the data of Mills and Mason (1977c). Apart from the marked effect of particle recirculation on erosion, the curves in this figure also show, more importantly, the additional inter-relating effects of particle size and hardness.

A feature of these curves is the initial high value of erosion, which shows a remarkable degree of consistency irrespective of particle size or hardness. However, as particle recirculation is increased there is a steady, progressive increase in the variation of erosion between these different sized materials. The trend of these curves clearly shows that, over a number of runs erosion is only relatively independent of both size and hardness when the material is relatively fresh, and care must be taken when attempting to apply the various erosion expressions available, which are usually only applicable under certain conditions.

The effect of particle degradation on the magnitude of specific erosion is demonstrated in Fig. 7.32. The two curves represent the plots of the mean values of erosion in terms of g/tonne, which corresponds to the respective initial value of mean particle size obtained in Fig. 7.12. The upper curve refers to the variation of accumulative erosion values, whilst the lower curve refers to the corresponding individual values per test set and the vertical line indicates the extent of maximum and minimum range of values per test set. In both cases the trend of the curves definitely shows that there is an initial rapid decrease in erosion from test sets 1 to 4, corresponding to a reduction in the initial mean particle size from 1200 to 900 μm, and then followed by a gradual rate of decrease. Although this particular test series was terminated after 21 runs, the slopes of the curves appear to indicate that any further reduction in particle size of this test material would have no further effect on specific erosion. A similar trend is also observed with regard to penetration in terms of mm/tonne.

Perhaps a more useful representation of the data on the effect of particle degradation is shown in Fig. 7.33. The plots in this figure are obtained by taking the accumulative values of both erosion and penetration at test set 1, corresponding to a mean particle size of 1200 μm, as the datum. By subtracting these values from the following consecutive

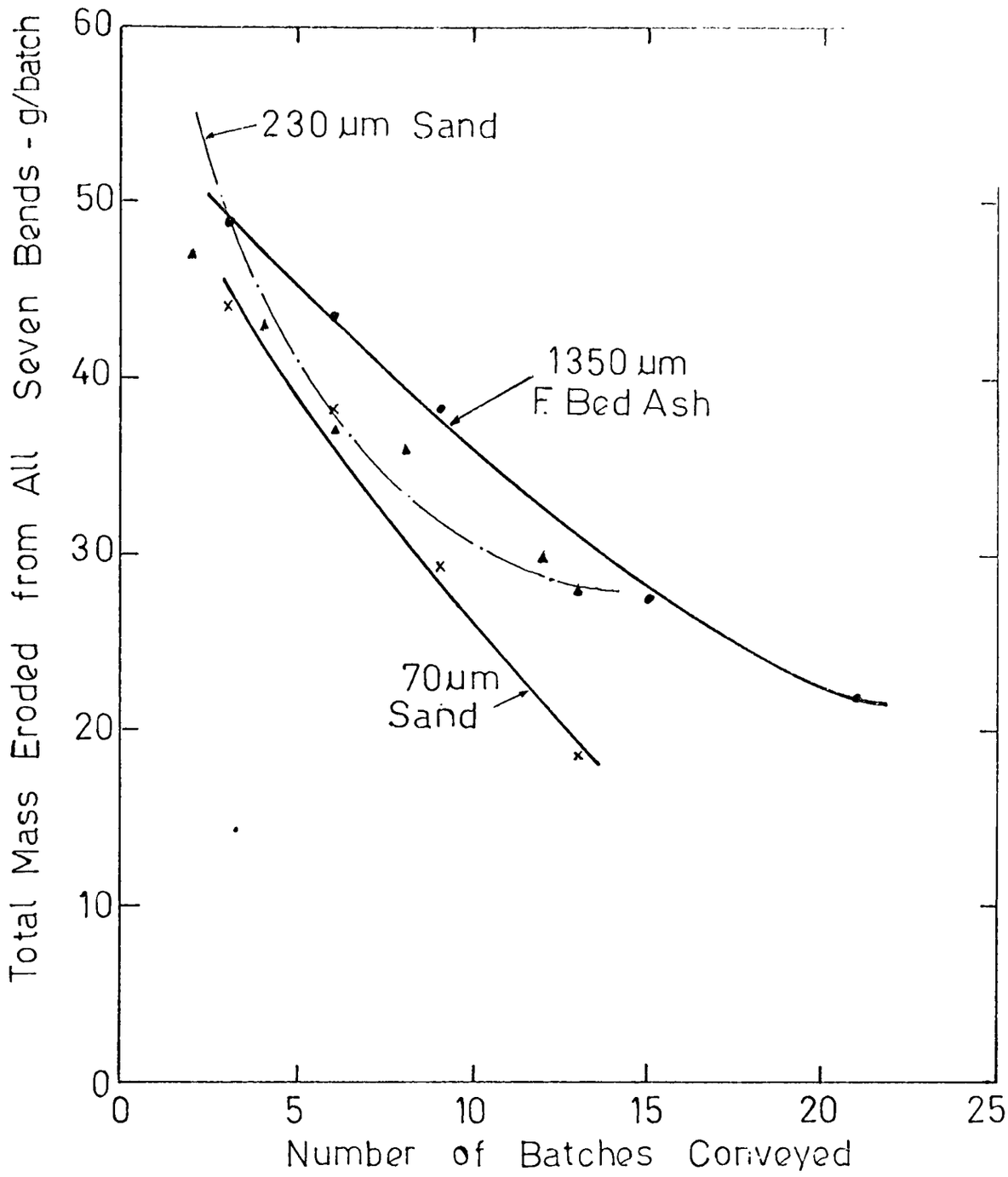

FIG. 7.31 Influence of Particle Recirculation on Mass Eroded from the Bends

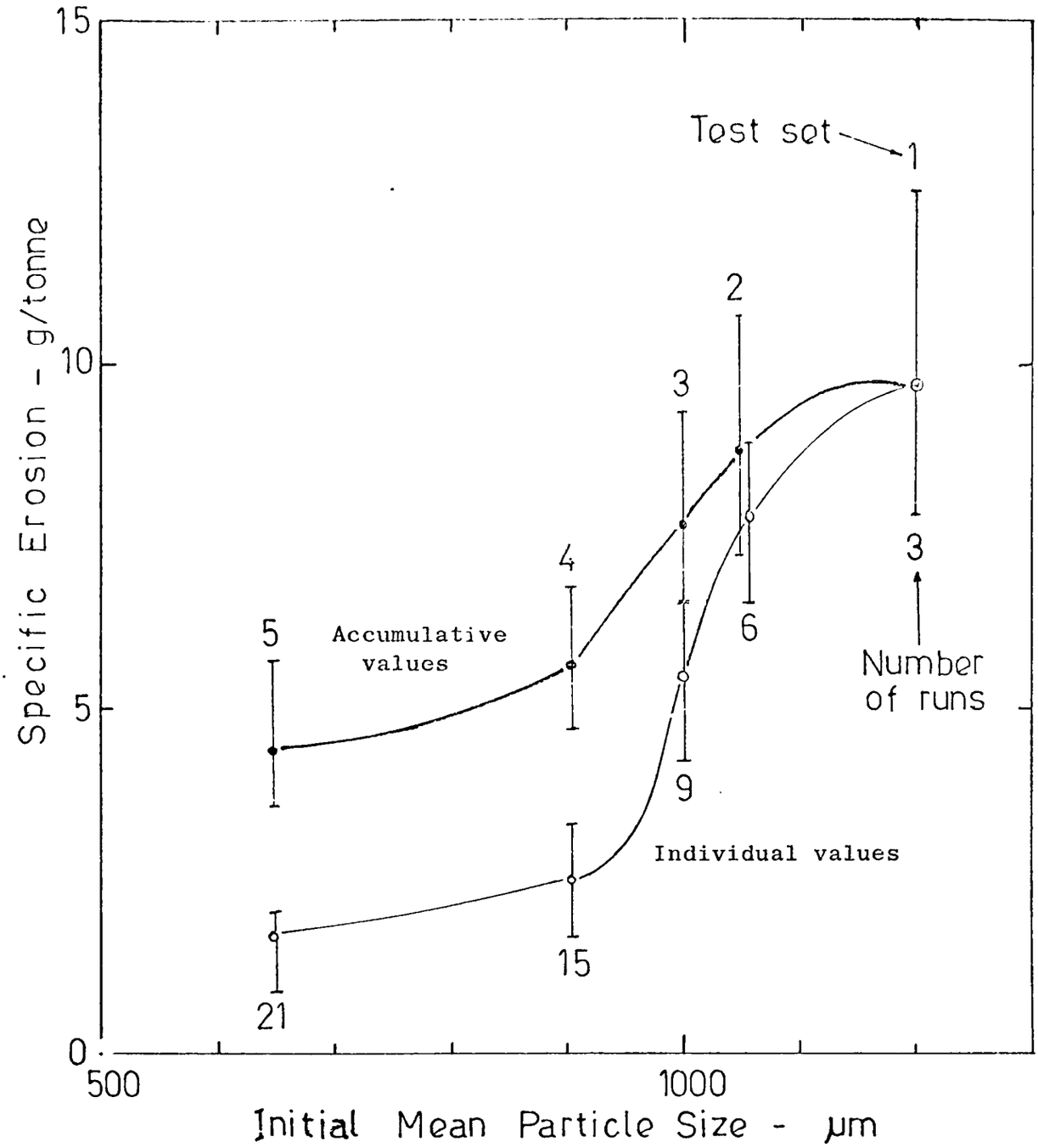

FIG. 7.32 Influence of Initial Mean Particle Size on Erosion

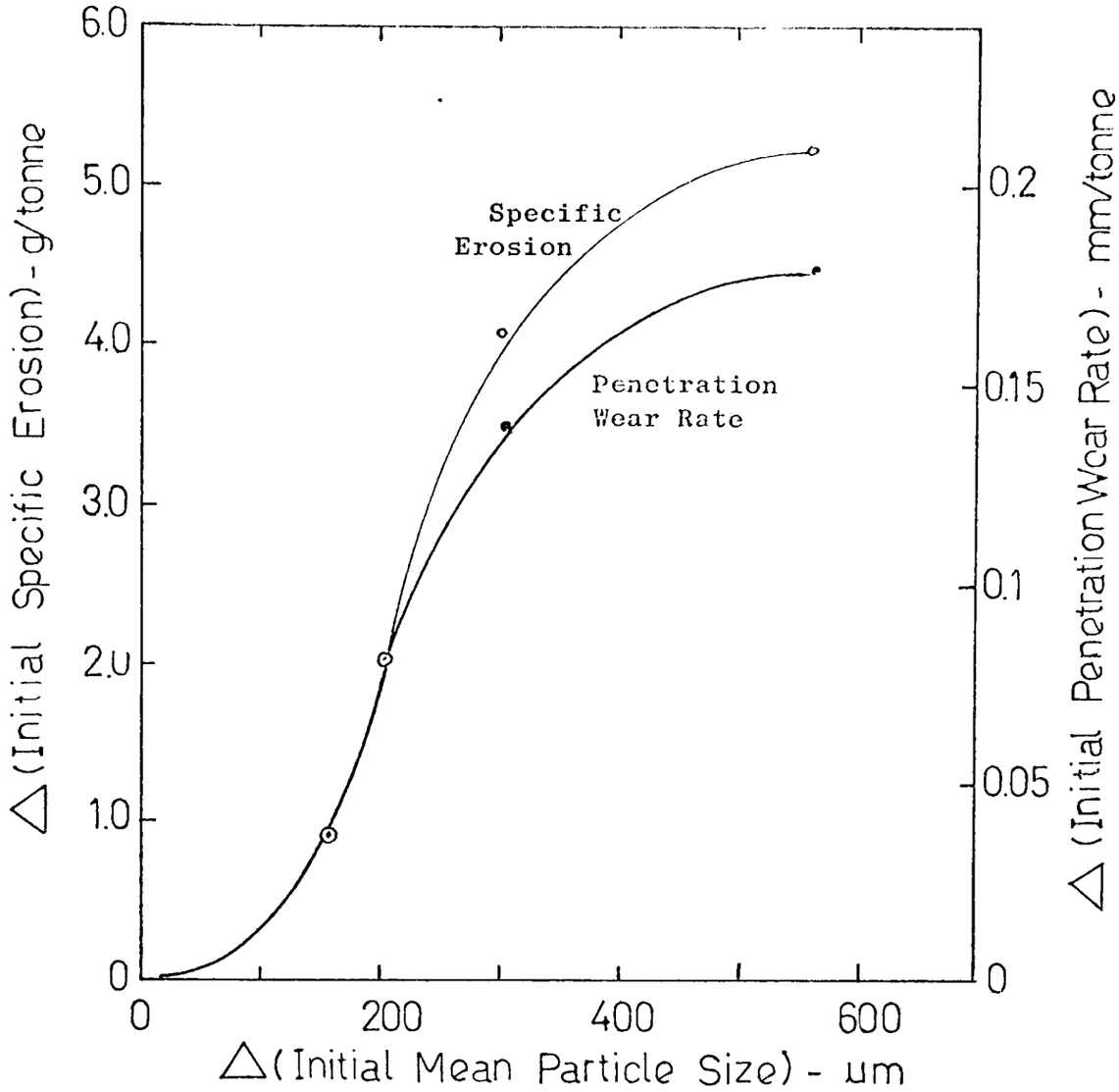

FIG. 7.33 Influence of Change in Initial Mean Particle Size on Change in Erosion and Penetration

accumulative values in test sets 2 to 5, the respective changes in the specific erosion and penetrative wear rate values are obtained, as shown in Fig. 7.32. The two curves in this figure, therefore, refer to the variation of a change in the value of erosion and penetration corresponding to a similar change in the initial mean particle size.

In both cases the curves clearly show that over this range of initial mean particle sizes there is a dramatic increase in the rate of change in both erosion and penetration, and this rate of increase is initially proportional to the rate of particle degradation. It appears that there is a certain threshold value of initial mean particle size beyond which both erosion and penetration remain relatively constant and are unaffected by any further degradation of the particles. Apart from the inter-relating effects of velocity and bend material, the results on Fig. 7.33 show that there is a direct relationship between mass eroded and depth of wear to the amount of particle degradation, particularly in the early stages of recirculation.

To a large extent the data in Figs. 7.32 and 7.33 incorporates the subsidiary effect of 'fines' and it is not possible to determine directly the effect of 'fines' on the magnitude of either erosion or penetration due to the large mixed size spectrum of this material. Further work is obviously necessary, preferably with a narrow range of particle sizes, in order to determine the effect of particle degradation in terms of the percentage of 'fines' on both erosion and penetration.

7.8 CONCLUSIONS

From the experimental results on the influence of particle hardness presented in this chapter,it has been established that there is a definite trend towards a critical hardness value beyond which both erosion and penetration remain relatively independent of particle hardness. To a certain extent this critical hardness value is considerably influenced by the inter-relating effect of velocity, but it is unlikely to vary very much from a value of about 1000 kg/mm^2.

Whilst the value of particle hardness is shown to be a major factor in determining the potential erosiveness of a particular conveyed product, the magnitude of the degree of erosiveness is also dependent upon the shape and size of the particles. To a certain extent, the magnitude of erosion also depends upon the difference between the hardness values of the conveyed product and the bend surface material, as well as upon the conveying air

velocity itself.

On the basis of the results of the material used in this work it has been shown that, under similar conveying conditions, the results with sand represent the critical maximum limit in terms of both erosion and penetration, and therefore, in terms of plant life. Materials with hardness values well beyond that of sand would not necessarily be more erosive.

The effect of particle degradation on erosion has been tentatively considered in tests with f.b. ash material. It has been shown that there is an initial direct relationship between specific erosion and penetration wear rate to the degree of degradation, until a stage is reached beyond which both erosion and penetration remain relatively constant, irrespective of any further degradation of the product.

Apart from an increase in 'fines' further work is necessary in order to fully establish the extent of the effect of 'fines' on erosion.

Chapter 8

The Influence of Pipe Bend Diameter Ratio (D/d)

8.1 INTRODUCTION

In the majority of bend erosion studies the groups of variables associated with the kinematic properties of the impacting particles and the properties of the surface materials have been extensively investigated. The group of variables associated with bend geometry has, however, received comparatively little attention.

Of all the variables involved in bend geometry, such as bend orientation, bend angle, and diameter ratio (D/d), it is the last variable that is the most important factor. As reported in Chapters 2 and 3, apart from velocity, the magnitude of erosion is predominantly influenced by the angle of impact. In a pipe bend this impact angle is determined primarily by its diameter ratio, and hence can be varied by bend radius.

Whilst bend radius is usually taken into account when designing systems for conveying abrasive products, only limited quantitative data regarding its influence on bend erosion is currently available. Therefore, in order to provide additional practical information of direct relevance to industry, a test programme was specifically carried out to investigate the influence of bend radius in terms of the D/d parameter, and the results obtained are analysed and discussed in this chapter.

8.2 REVIEW OF PREVIOUS WORK

Apart from the work of German investigators (Brauer and Kriegel 1964, 1965a,b, Kriegel 1968, 1970, Glatzel 1977, Glatzel and Brauer 1978), other sources of experimental information on the specific influence of D/d on bend erosion in pneumatic transport are relatively limited (Bikbaev et al 1972, 1973, Mason and Smith 1972). In Chapter 3 the work of these investigators was briefly reviewed and in this section the various effects associated with the specific influence of D/d are discussed in more detail.

8.2.1 Effect of Impact Angle

As mentioned in section 3.3.3, the angle of impact in bend erosion does not remain constant, but is variable over a period of time, corresponding to the rate of formation of an erosion crater. At any stage of the erosive wear process this angle of impact is referred to as the 'effective impact angle' or (β_B) where the subscript B identifies the particular site of erosion, as shown in Fig. 8.1. The effective impact angle should not be confused with the 'impact bend angle' or (δ_B) which is measured along the radius of the bend to the point of

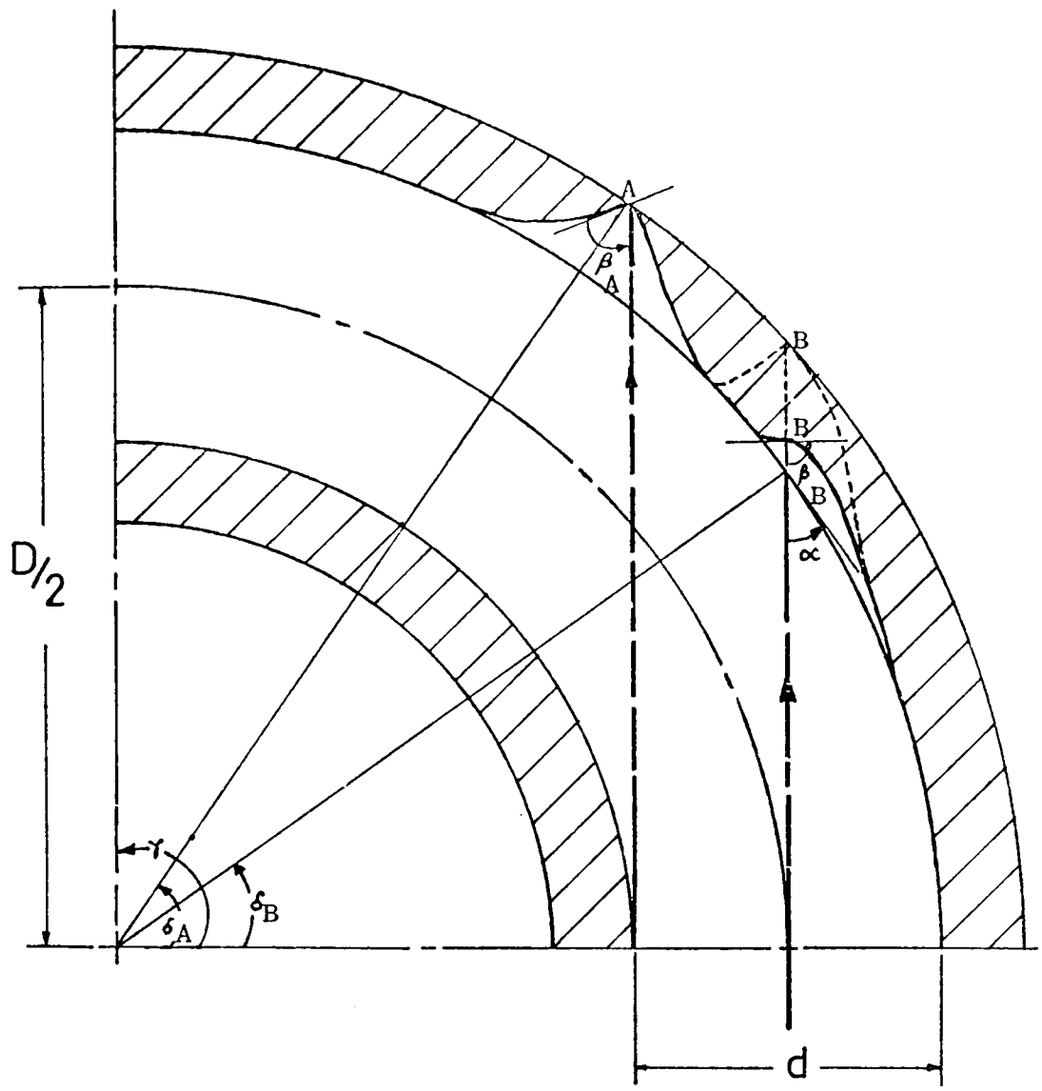

FIG. 8.1 Location of Maximum Wear and Site of Impact in a Bend.

impact, B. This impact bend angle is identical to the particle impact angle (α) which is defined as the inclination between the tangent to the bend surface and the particle trajectory. The location of maximum wear and subsequent position of failure is determined by the intersection of the projected path of the particle trajectory preceding from the straight pipe run to the outer bend radius. The location of this intersection is, in turn, dependent upon bend geometry. The effect of this variation of effective impact angle over a period of time has been clearly demonstrated by the work of Mason and Smith (1972) (see Fig. 3.5). They showed that in a bend with a large D/d, erosion first occurred at a low impact bend angle of about 20^{o}. As an erosion crater is gradually established the effective impact angle increases correspondingly and consequently leads to a deflection of the particles in a zig-zag pattern in the bend. As a result, secondary and tertiary wear craters may be created in the inner and outer bend surfaces, and may also lead to erosion in the following straight pipe run before the particles are properly re-entrained in the gas stream. However, apart from these visual observations, no attempt was made to assess the influence of the variation of effective impact angle on the magnitude of erosion.

Mills and Mason (1977 b) have provided an explanation for the differing rates and patterns of penetration, in terms of three basic stages of erosion which are dependent upon the effective impact angle (see also section 6.4.3.). Briefly, in a new unworn bend, initially the effective angle of impact is low and erosion, in terms of mass eroded, is relatively high. This is referred to as primary wear stage, which takes place over a wide range of bend angles. As the effective impact angle is gradually increased due to the formation of a stepped erosion crater, the rate of erosion is decreased, corresponding to an increase in penetration rate. This stage is referred to as secondary wear, and takes place over a relatively narrow range of bend angles. From the work of Brauer and Kriegel (1963) and Krasnov and Zhilinskii (1973), the effective impact angle for maximum penetration is about 55^{o}. For a reinforced bend, or a bend with a very thick wall, secondary wear will phase itself out when the effective impact angle reaches 80 to 90^{o}, at which both erosion and penetration rates are at a minimum, and this stage is referred to as tertiary wear. In all cases the magnitude of both erosion and penetration is shown to be directly influenced by effective impact

angle. However, apart from this explanation, experimental evidence on the variation of effective impact angle with both erosion and penetration rates has not been provided.

8.2.2 Location of Maximum Wear

From detailed experimental studies of particle trajectories in a bend, Brauer and Kriegel (1965 a,b) found that the location of maximum wear, and ultimately position of failure, is at a point A as shown in Fig. 8.1. The site of failure is described by the impact bend angle, and at this particular point is referred to as the 'critical impact angle' or (δ_A). In terms of bend geometry, this angle is given by equation 3.1, which can be alternatively expressed as :-

$$\sin\ (\delta_A) = \sqrt{1 - \left[\frac{D/d - 1}{D/d + 1}\right]^2} \qquad (8.1)$$

Glatzel (1977) found that the curve in the above expression is applicable for bends with a range of D/ds from 4 to 16 only. This was based on a series of tests on perspex bends eroded by 440 μm cast shot particles over a range of phase densities and velocities and substantiates the results of Bikbaev and co-workers (1972, 1973) who earlier reported that the position of maximum wear is independent of both of these parameters from tests with 295 μm quartz particles on various alloy bends with a range of D/d from 4.8 to 18. An expression for locating the position of maximum wear in terms of bend geometry has also been provided by these workers, and this expression is essentially similar to equation 8.1.

The experimental data of Mills and Mason (1976d, 1977 a,b), although based on mild steel bends with a single D/d of 5.6, also confirmed that the position of maximum wear and failure in relatively independent of phase density, velocity and particle size, but only in terms of impact bend angle. The position of maximum wear was found to lie consistently between an impact bend angle of about 30 to 40°. In terms of pipe angle, however, the position of maximum wear varies considerably over this range of parameters.

8.2.3 Effect on Penetration

The influence of D/d on penetration rate, in terms of μm/h, has been investigated by Brauer and Kriegel (1964). Mild steel bends with a range of D/ds from 3.3 to 9.1, were subjected to erosion by the

hydraulic transport of 110 μm iron ore concentrates. In terms of D/d a pronounced maximum penetration rate was observed at a value of 5.6 (see Fig. 3.2). Kriegel (1970) also reported that a similar relationship exists in pneumatic conveying. From tests with a range of perspex bends eroded by steel sand particles, he found that maximum penetration occurred at a D/d of 6.5 (see Fig. 3.1). Glatzel (1977), however, reported that a maximum exists at a D/d of 4 from tests with a similar range of perspex bends, but eroded by 440 μm cast shot particles. He commented that the difference in the critical value of D/d was largely attributed to different test conditions.

In order to avoid this rapid wear situation, either long radius bends or elbows are recommended. Mehring (1971), from industrial data, suggested that bends with D/d in excess of 24 are desirable in practice for handling abrasives. However, the work of Mason and Smith (1972) clearly cautioned against the use of bends with too large values of D/d, due to the possibility of the formation of several wear craters caused by the deflection of particles in a long radius bend.

8.2.4 Effect of Velocity

The specific influence of velocity on D/d has also been investigated by Glatzel (1977). As he was able to determine the velocity of particles accurately in his test rig, tests were carried out over a range of particle velocities and D/ds. In terms of non-dimensional volumetric erosion, a velocity exponent of 3.1 for pipe elbows, and a constant 2.3 for other bends was obtained (see Fig. 3.9). The difference in value between these two exponents was attributed to the higher angle of impact in elbows. Since perspex exhibits a semi-ductile brittle behvaiour, it was found from bench tests on flat plate perspex specimens that maximum erosion occurred at an impact angle of about 45^{o}. The corresponding angle of impact in elbows was about 50^{o}, which explained the higher exponent value for elbows. However, to a first approximation, Glatzel showed that the mean velocity exponent over this range of D/ds is 2.9, and could be considered as independent of D/d.

Mason and Smith (1972) obtained a value of 2.25 from tests on perspex bends with D/ds of 12 and 20, subjected to erosion by fine alumina particles. Mills and Mason (1976 b) obtained a value of 2.65 from tests with mild steel bends with a single D/d of 5.6 and sand over

a much wider range of test conditions. Whilst quantitative comparison between these exponent values is not possible, since the values obtained by Mason and co-workers were based on conveying air velocities, the velocity exponent values from these sources appear to lie within a similar range. Hence, it appears that velocity has no substantial effect on the magnitude of erosion in terms of D/d.

8.2.5 Effect on Bend Life

Glatzel (1977) has provided semi-empirical models for determining the service life of pipe bends. These models include the specific effect of bend geometry in terms of impact angle (β) (see equations 3.2 to 3.4). Although satisfactory agreement between calculated and experimental values was provided by these models, they involved rigorous iterative mathematical computation of the other inter-related terms which must be evaluated corresponding to each value of β. Furthermore, these models were based on certain highly idealised assumptions and consequently are only applicable under certain conveying conditions, such as for particles over 100 μm conveyed at low phase densities and high velocities.

Ryabov (1978) has also reported a formula for determining the service life of pipe bends (see equation 3.5). It includes the various parameters associated with bend geometry such as bend angle, bend orientation and bend radius in terms of the appropriate coefficient factors. However, no experimental evidence regarding its predictive ability is given and, in addition, no information on how to determine these bend geometry coefficients or other coefficients in this formula is provided.

8.3 EXPERIMENTAL PLAN

8.3.1 Introduction

Although it has been clearly shown that bend radius, in terms of the D/d parameter, is also an important factor in bend erosion, the magnitude of this influence is, to a considerable extent, directly associated with the inter-relating effect of effective impact angle. Whilst the dependence of erosion upon impact angle is well recognised, the corresponding dependence of erosion and penetration upon the variation of impact angle over a period of time has received very little attention.

While a few models have been developed from these experimental studies, the specific influence of bend radius on bend performance cannot be evaluated directly. The D/d parameter in these models is represented by some other related quantity, which cannot be isolated and considered separately from the other inter-relating variables. In addition, the applicability of these models is strictly limited to certain test conditions.

Therefore, in order to provide additional experimental information regarding the specific influence of D/d in terms of bend life analysis, and to investigate in more detail the variation of effective impact angle upon the magnitude of both erosion and penetration rates, a programme of tests was specially planned for this purpose.

8.3.2 Test Bends

Three sets of bends with D/d of 4, 5.6 and 12 were used in this investigation (see Fig. 4.9). The bends with D/d of 4 were cast iron elbows and the others were mild steel. The material hardness of these bends was comparable, with 154 kg/mm^2 for the iron elbows and 158 kg/mm^2 for the mild steel bends.

The selection of the range of D/d to be investigated in this work was largely dependent upon the existing test facility and laboratory space considerations. As explained in Chapter 4, the existing test section was designed for testing seven identical bends with D/d of 5.6. Whilst these bends can be easily removed and replaced with the same number of elbows, by means of fitting a short stub at each end of the elbow, for bends with a larger D/d ratio a new test section had to be constructed. The dimensions of this new test section, and consequently the possible range of D/ds, were primarily determined by both minimum acceleration length requirements and available laboratory space limitations. In order to provide as wide a test range of D/ds as possible, this new test section was specially designed by the author to accommodate seven identical bends with D/d of 12 in a figure of eight configuration (see Fig. 4.7).

It was felt that this limited range of test D/ds from 4 to 12 would be adequate, since experimental results from Brauer and Kriegel (1964) and Kriegel (1970) have shown that maximum penetration occurs at a D/d of between 5 and 7. Therefore, it was not necessary to consider

bends with a value of D/d well beyond the range tested. However, in tests with elbows, a special Booth bend with D/d of 2.4 was also included and later, in tests using the high pressure rig, the experimental data of the three large radius bends with D/d of 24 can also be incorporated into this work for comparison purposes. Therefore, provisions were made by the author to extend the range of D/d investigated in this work if warranted.

8.3.3 Control of Variables

As the variable investigated in this work is the D/d parameter, and in order to isolate the influence of this parameter from the other erosion parameters, it was necessary to maintain uniformity of test conditions throughout these test programmes.

About 750 kg of sand, with a mean particle size of 70 μm was used as the conveyed material. Its particle size distribution, before and after each test series, is presented in Fig. 8.2. The same batch of sand was recirculated batchwise until at least two of the test bends failed. This was then replaced by an equivalent batch of similar sized fresh sand prior to the next test series. For comparison purposes, and to provide proper control of the other variables associated in this work, it was decided to convey sand at a constant phase density of 3 and to maintain a mean conveying air velocity in the test loops of about 25 m/s for each set of D/d tested. As explained in the previous chapters, the velocity recorded throughout this work is the conveying air velocity. As air is not incompressible there will be an expansion of air as pressure drops along the conveying line, but the maximum and minimum estimated velocity between the first and last bend in each test section was within ± 10% of the mean of about 25 m/s for each set of test D/d.

8.3.4 Test Programmes

Three sets of tests, corresponding to each set of D/d tested, were carried out in a chronological sequence as presented in Table 5.1.

The first test series was on bends with D/d of 5.6. A large part of the experimental results has already been presented and discussed in the preceding chapter in terms of particle hardness effects. Some of this information, with specific reference to D/d effects, will

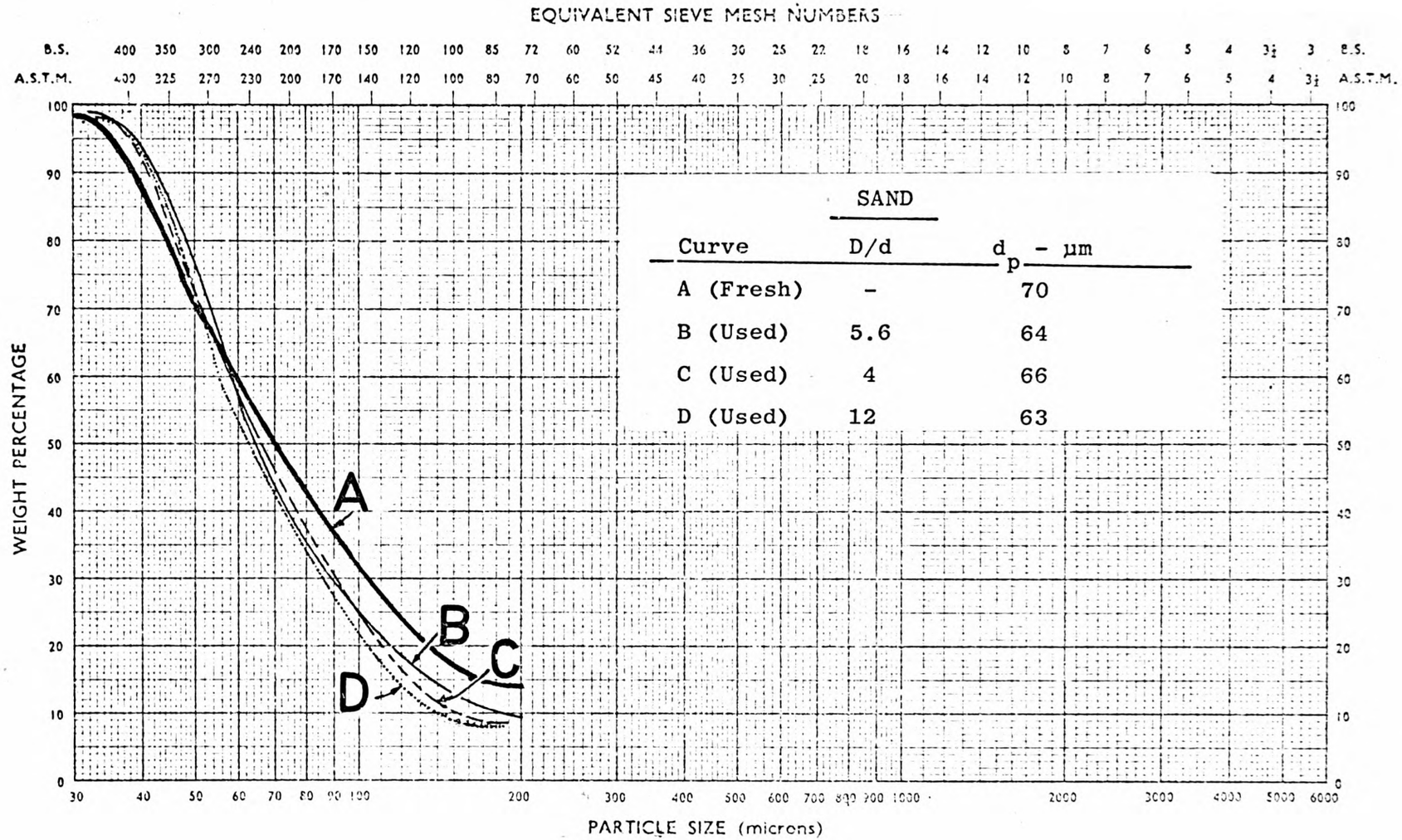

FIG. 8.2 Particle Size Distribution of Sand

again be reproduced in this chapter for comparison purposes.

The second test series was on elbows with D/d of 4. As mentioned earlier, a proprietary Booth bend with D/d of 2.4 was also included and designated as test bend number 10 (see Fig. 4.6). Twenty-six test runs were carried out within this test series. As no appreciable erosion was observed for this Booth bend, compared to the elbows (Table 5.2), the limited results of this particular bend will be discussed in Chapter 10 in terms of the effect of D/d on phase density.

The third and last series of tests was on the long radius bends with D/d of 12. These were specially pulled bends from standard 50 mm bore straight pipe runs. As a result, the mean thickness of these bends was only about 3.2 mm compared to 4.0 mm for the other two commercially available test bends and elbows.

As mentioned in section 4.6, the mass eroded from these different bends is readily obtained by means of an electronic balance. However, because of the different bend radii, the wear profiles of these bends can only be determined with special instruments. For bends with D/d of 4 and 5.6, the wear profiles were recorded by specially designed dial gauge calipers. For the larger bends with D/d of 12, and for the Booth bend, an ultrasonic thickness meter was used.

8.4 BEND WEAR RESULTS AND DISCUSSION

8.4.1 Introduction

A continuing feature throughout this work is the premature failure of bends. Mills and Mason (1976 c) have analysed some of the factors involved and concluded that the primary source of these premature bend failures can be directly attributed to the combined effects of fine powders being influenced considerably by secondary flows induced in the bends. The magnitude of rapid and premature bend failure was shown to be dependent upon a critical combination of certain variables, but an element of unpredictability must also be taken into consideration.

In this programme of tests a similar situation was also observed. A number of bends with D/ds of 5.6 and 12 failed prematurely compared to a solitary elbow (Table 8.1 and Figs. 8.3 to 8.5). With the exception of the failed elbow which was replaced by an ordinary bend with D/d of 5.6, the prematurely failed bends in the other two test

TABLE 8.1 Erosion Data for Original Bends Tested

	Bend Number						
	1	2	3	4	*5	6	*7
D/d = 4							
Total Mass Eroded (g)	21	15	21	36	⌇36	32	⌇42
Number of Batches	26	26	26	26	25	26	12
Mass Conveyed (tonne)	19.43	19.43	19.43	19.43	18.23	19.43	8.93
Conveying Time (h)	27.62	27.62	27.62	27.62	25.82	27.62	12.25
Specific Erosion (g/tonne)	1.08	0.77	1.08	1.85	2.03	1.65	4.70
Erosion Rate (g/h)	0.76	0.54	0.76	1.30	1.39	1.16	3.43
Maximum Depth of Penetration (mm)	1.5	1.3	1.8	1.7	4.0	3.0	4.5
Penetration Wear Rate (mm/tonne)	0.08	0.07	0.09	0.09	0.22	0.15	0.50
Penetration Rate (mm/h)	0.05	0.05	0.07	0.06	0.15	0.11	0.37
Velocity at Bend (m/s)	22.2	22.8	23.4	24.0	24.6	25.5	26.1
Pressure at Bend (bar abs)	1.28	1.25	1.21	1.18	1.15	1.11	1.08

* Failed bends ⌇Mass Eroded at Failure

TABLE 8.1 Continued

	Bend Number						
	1	2	+*3	4	*5	6	+*7
D/d = 5.6							
Total Mass Eroded (g)	26	39	≀51	47	≀70	63	≀58
Number of Batches	13	13	6	13	13	13	8
Mass Conveyed (tonne)	9.75	9.75	4.10	9.75	9.37	9.75	5.62
Conveying Time (h)	14.08	14.08	5.33	14.08	13.45	14.08	8.00
Specific Erosion (g/tonne)	2.67	4.00	12.44	4.82	7.47	6.46	10.32
Erosion Rate (g/h)	1.85	2.77	9.57	3.34	5.20	4.47	7.25
Maximum Depth of Penetration (mm)	1.2	1.8	3.9	2.1	3.9	3.1	4.0
Penetration Wear Rate (mm/tonne)	0.12	0.18	0.95	0.22	0.42	0.32	0.71
Penetration Rate (mm/h)	0.09	0.13	0.73	0.15	0.29	0.22	0.50
Velocity at Bend (m/s)	23.3	23.7	24.4	25.0	25.8	26.4	27.3
Pressure at Bend (bar abs)	1.28	1.25	1.21	1.18	1.14	1.11	1.07

* Failed bends
+ Replacement bend also failed
≀Mass Eroded at Failure

TABLE 8.1 Continued

	Bend Number						
	1	*2	3	+*4	5	+*6	*7
D/d = 12							
Total Mass Eroded (g)	45	≀88	60	≀81	68	≀80	≀73
Number of Batches	20	17	20	14	20	14	7
Mass Conveyed (tonne)	15.00	12.50	15.00	9.99	15.00	10.35	4.60
Conveying Time (h)	20.00	16.75	20.00	13.48	20.00	13.88	6.38
Specific Erosion (g/tonne)	3.00	7.02	4.00	8.11	4.53	7.73	15.97
Erosion Rate (g/h)	2.25	5.25	3.00	6.05	3.40	5.76	11.44
Maximum Depth of Penetration (mm)	2.1	3.3	2.1	3.2	2.2	3.4	3.2
Penetration Wear Rate (mm/tonne)	0.14	0.26	0.14	0.32	0.15	0.33	0.70
Penetration Rate (mm/h)	0.11	0.20	0.11	0.24	0.11	0.24	0.50
Velocity at Bend (m/s)	23.2	23.7	24.3	24.9	25.8	26.4	27.1
Pressure at Bend (bar abs)	1.27	1.24	1.21	1.18	1.14	1.11	1.08

* Failed bends
+ Replacement bend also failed
≀ Mass Eroded at Failure

D/ds were immediately replaced with new, similar sized bends. These new replacement bends in fact failed even more rapidly, whilst the remaining worn, original bends were still in service. Up to a two-fold increase in both erosion and penetration rates was obtained from replacement bends with D/d of 12, and about one and a half fold similar increase in the case of replacement bends with D/d of 5.6. These rapid rates of both erosion and penetration obviously have a dramatic effect on the overall results. Hence for comparison purposes, and unless otherwise stated, the analyses in the following sections will be restricted to the experimental results of the original seven test bends for each set of D/d tested. The specific effect of replacement bends will be examined in more detail in the next chapter, from which the causes of this rapid failure and its effect in terms of bend life evaluation will be presented.

8.4.2 Presentation of Results

For each set of D/d tested, the test bends were removed after a batch of sand had been conveyed through the bends. The mass eroded and wear profiles of each individual bend were recorded. From this regular monitoring procedure the erosion history of each individual bend, in terms of specific erosion and bend wall penetration rates, was obtained. Apart from providing information on depth of penetration, the variation of impact angle at various stages of erosion could also be determined from the respective bend wear profile measurements, from which its effect on erosion could be assessed.

As mentioned earlier, a number of bends which failed prematurely were immediately replaced with similar sized new, unworn bends. The rapid erosive wear rate of these replacement bends was also regularly monitored. Comparisons between the experimental results of the prematurely failed bends and their corresponding replacement bends will be presented and discussed in more detail in the next chapter. In order to obtain sufficient experimental data for the original test bends for comparison purposes, tests were carried out until one of the remaining original bends failed. In this way at least two of the original seven test bends were tested to failure, thereby providing a basis for proper comparison in terms of both erosion and penetration rates over the range of D/ds considered.

The essential erosion data for the range of D/d investigated has already been presented in Tables 5.2 and 5.3. Further details of the original seven test bends at each set of D/d tested are presented in Table 8.1.

8.4.3 Specific Erosion Analysis

The erosion history of all the bends tested at each set of D/d is presented graphically in Figs. 8.3 to 8.5. For comparison purposes the results of the respective replacement bends are also included. These are identified by the letter 'R' beside the particular bend number. Some of these replacement bends also failed and were replaced, and these are identified by the letters 'RR'.

The experimental data in these figures has not been normalised since all the tests were carried out under similar conveying conditions. The conveying line pressure drop at each set of D/d tested was found to be comparable and estimations of the velocity at each bend were therefore similar (Table 8.1). Hence, it was not necessary to normalise the results and, for the purpose of evaluating the specific erosion rates, it is adequate to consider the mean values of these measured results only.

8.4.3.1 Scatter of Results

A common feature of the curves in these figures is the large degree of scatter of the results. As has been reported in the previous chapters, premature failure of bends is directly attributed to the degree of scatter and to a certain extent the scatter of results in this programme of tests is therefore anticipated. Furthermore, since the results are not normalised to a constant velocity value of 25 m/s, there will be a slight variation of erosion from bend 1 to bend 7 in each set of D/d tested due to a variation of velocity in the bends. However, the lack of any systematic order of erosion in this respect for each set of D/ds tested, clearly demonstrates the limitations of predicting the erosive wear process in pipe bends based on well established observations, except that bends will fail randomly.

Apart from the likely sources of the scatter of results such as those attributed to velocity, phase density, and particle size effects, another contributing factor to the scatter of

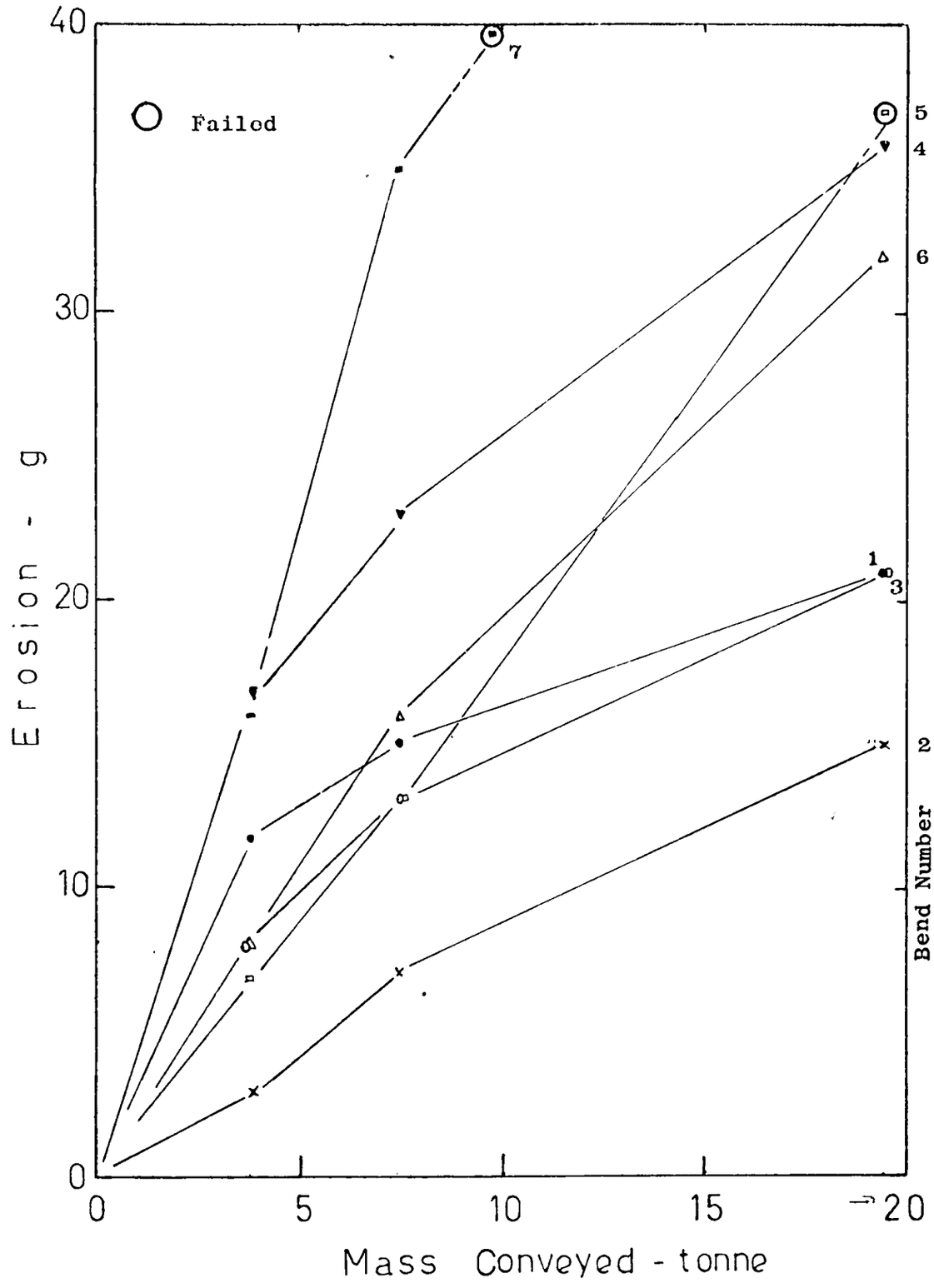

FIG. 8.3 Variation of Erosion with Mass Conveyed for Individual Bends with D/d of 4

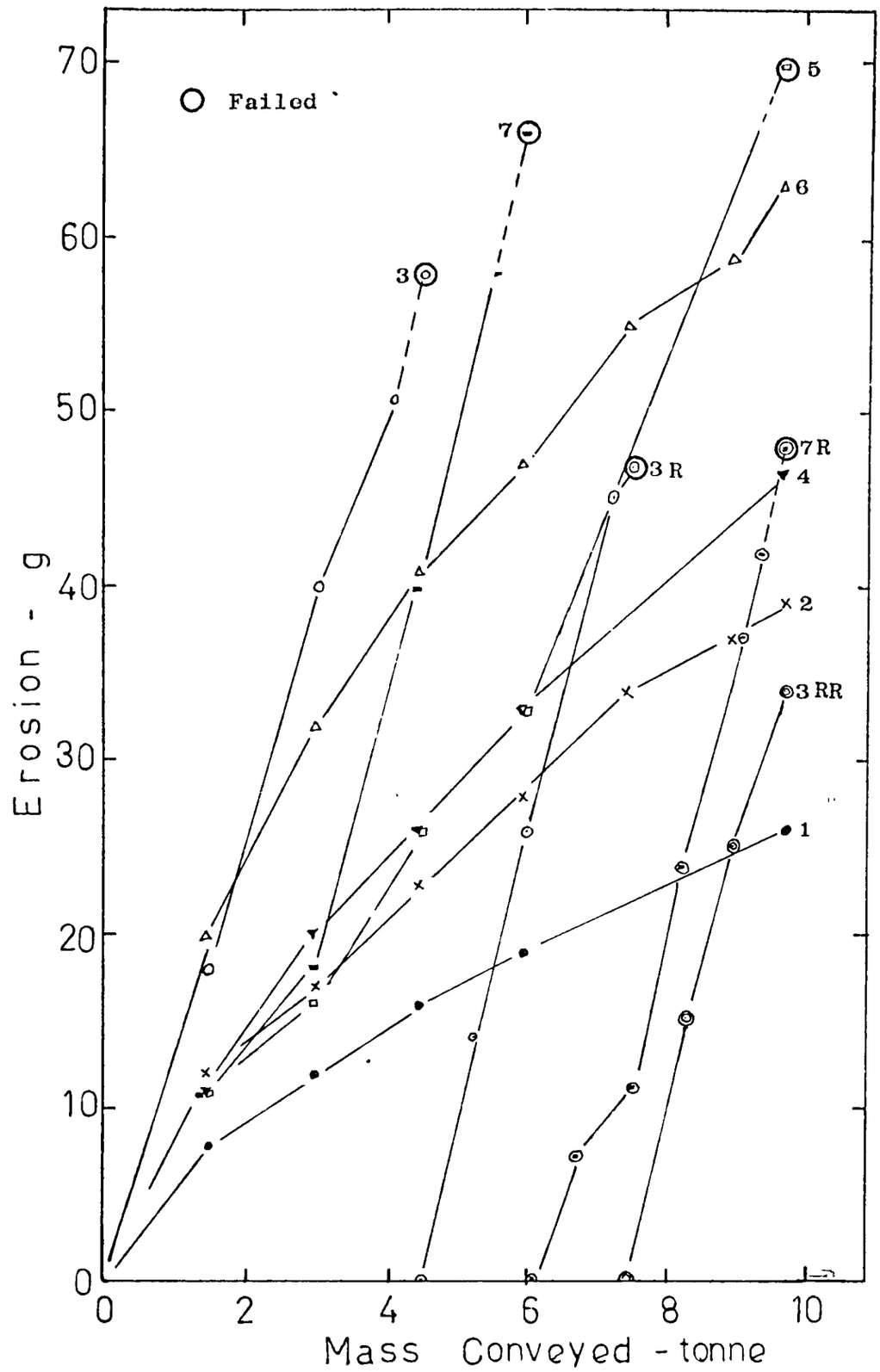

FIG. 8.4 Variation of Erosion with Mass Conveyed for Individual Bends with D/d of 5.6

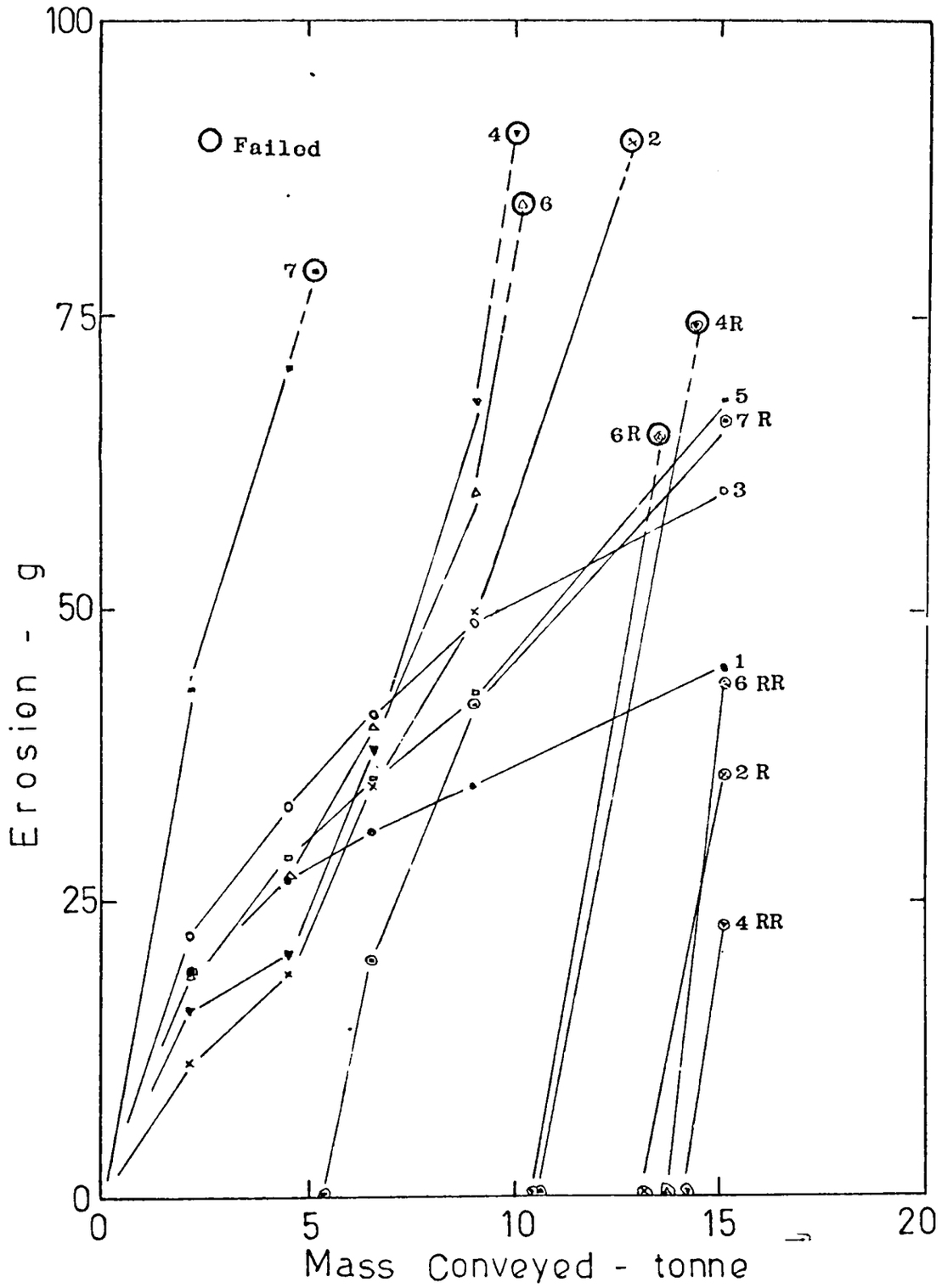

FIG. 8.5 Variation of Erosion with Mass Conveyed for Individual Bends with D/d of 12

results in Figs. 8.3 to 8.5 is the bend radius. Mills and Mason (1976 c) have analysed some of the factors involved in premature bend failures, but concluded that bend radius was not likely to have an additional effect. The experimental evidence in these figures in terms of D/d effect clearly demonstrates otherwise. Excluding the results of those bends which failed prematurely, the degree of scatter between the maximum and minimum values at the end of each test series differs by a factor of about 2.5:1 for the elbows and the intermediate radius bends, and about 1.5:1 for the long radius bends.

Since there is a large variation in the total number of runs at each set of D/d, a more representative basis of comparison would be to consider the first six runs. Over this number of runs the results of all the original seven test bends at each set of D/d tested will therefore be included. The degree of scatter for the elbows, after some 4.5 tonnes of sand had been conveyed, is of the order of about 6.7, compared to about 3.7 for the two sets of bends.

In both cases the variation in the order of scatter over the limited range of D/ds tested clearly demonstrates that bend radius is also an important factor, although it is not possible to quantify to precisely what extent. This is primarily due to the difficulty of isolating the specific effect of bend radius from the other inter-relating factors such as bend position, percentage of 'fines', secondary flows, particle shapes, etc.. In the next chapter the specific effect of these inter-related factors, which may be responsible for the scatter of results at each set of D/d tested, will be considered in more detail.

8.4.3.2 Effect of Bend Radius

The effect of bend radius, in terms of D/d, on specific erosion is presented in Fig. 8.6. Individual results for each of the original seven bends tested are plotted, and the line drawn represents the mean value at each set of D/d tested. The scatter of results is again reflected by the variation of individual plots in this figure. The magnitude of scatter between the

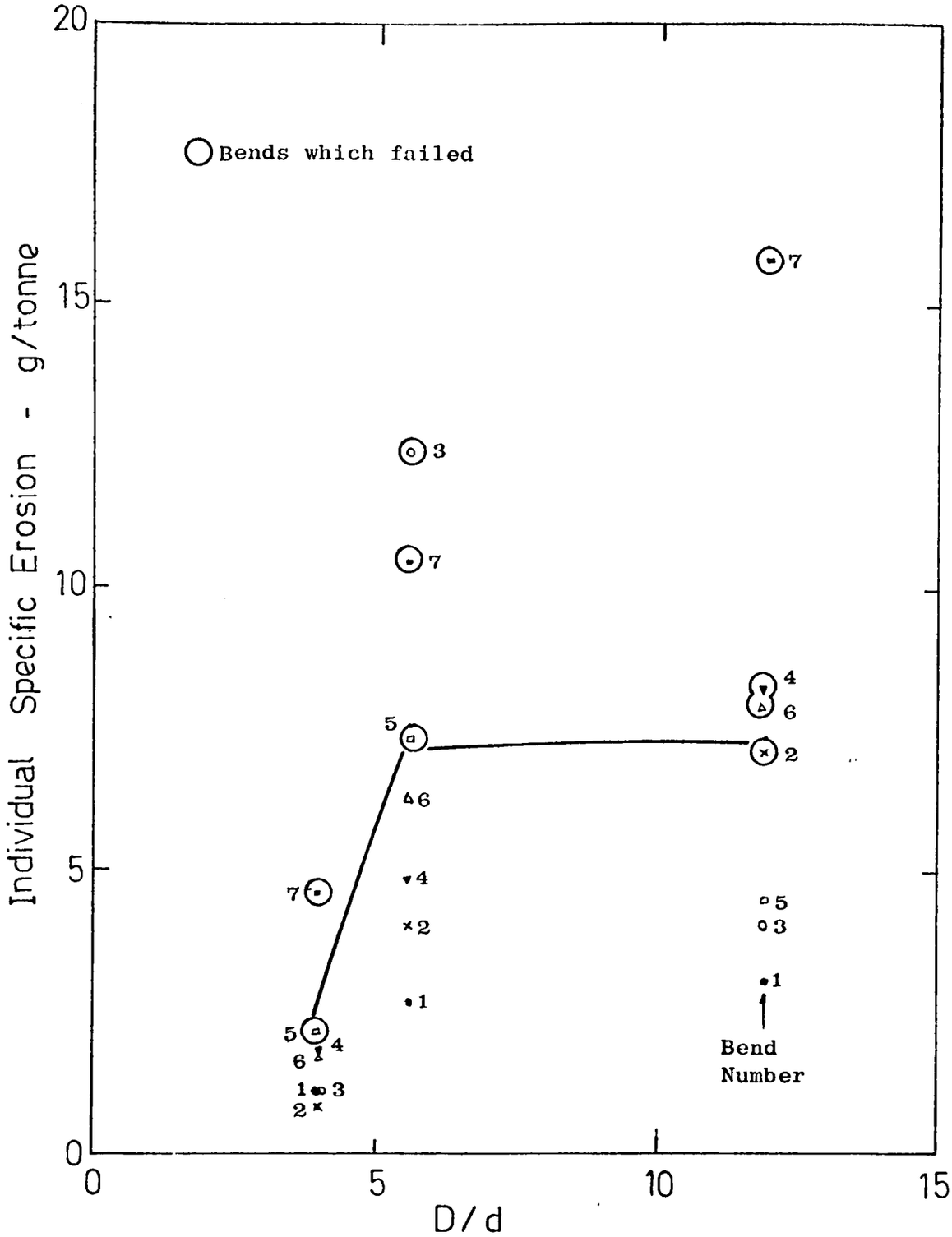

FIG. 8.6 Variation of Individual Specific Erosion with Diameter Ratio

maximum and minimum individual values is of the order of about 6.1 for the elbows, 4.7 for the intermediate bends, and 5.3 for the long radius bends. However, in terms of bend radius, the degree of scatter and hence the potential for premature failure of bends, appears to increase as bend radius is increased.

A more representative basis for comparison purposes would be from the data presented in Fig. 8.7. The four sets of results plotted in this figure represent the accummulative erosion values of three consecutive test runs per set. The limits of each vertical line indicate the upper and lower individual values, and lines drawn through the respective symbols locate the corresponding mean value within each test set. The influence of bend radius on the rate of erosion is clearly demonstrated by the trend of the curves. From test sets 1 to 3 a gradual reduction of the mean values over this number of runs is particularly observed for the intermediate and long radius bends. However, no further reduction is observed at test set 4; in fact, the mean values between test sets 3 and 4 are comparable.

This lack of any further decrease after nine runs is related to a corresponding change in the 'effective' impact angle in the bends, which was observed to increase only slightly over this period. This aspect will be discussed in more detail in section 8.4.5.

Another interesting feature of the results in this figure is with regard to the magnitude of the degree of scatter per test set. For the two sets of bends there is a gradual reduction in the scatter of individual results over this range of test sets, whereas no significant change is observed for the elbows. The marked decrease in the scatter for the bends, particularly after test set 2, is due to the premature failure of bends which occurs after 6 and 8 runs, corresponding to bends 3 and 7 for the intermediate bends, and after 7 runs, corresponding to bend 7 for the long radius bends. The absence of these high rates of erosion due to rapid premature bend failures is clearly reflected by the reduction in the scatter of results in test sets 3 and 4.

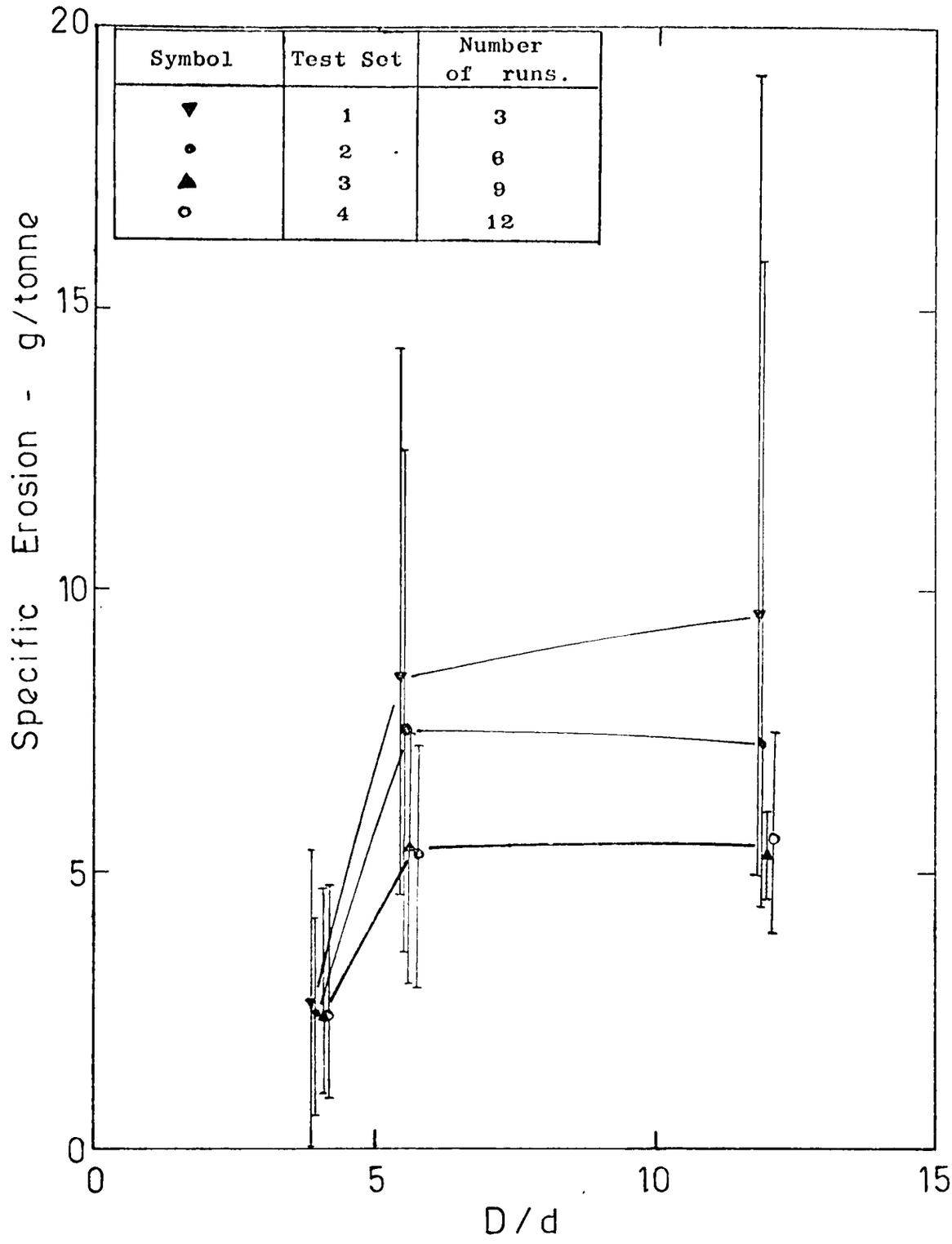

FIG. 8.7 Variation of Specific Erosion with Diameter Ratio

In all cases the trend of the curves over the range of D/ds investigated clearly shows that there is a threshold value of D/d beyond which erosion is not influenced by bend radius. In terms of specific erosion results the critical value of D/d appears to lie between 4 and 5.6. Although the conveying runs in this programme of tests were carried out at a constant phase density and velocity, it is unlikely that the threshold value of D/d will vary from this range of values at other test conditions, since it has been reported by other workers that velocity and phase density have no effect on erosion in terms of D/d. A similar trend in terms of erosion rate is also observed over the range of D/d tested. Whilst specific erosion data provides a direct comparison in terms of unit mass of conveyed product, the erosion rate gives an indication of the potential service life of a bend for given conveying conditions. The similarity of the trend of the results, both of which show a threshold value in terms of D/d of between 4 and 5.6, clearly has important implications for the pneumatic conveying designer.

8.4.4 Penetration Wear Analysis

In Figs. 8.8 to 8.10 the corresponding sets of experimental results, in terms of the variation of maximum depth of penetration with mass eroded, are presented. Although the wear profile along the circumference of the outer bend wall was recorded for each individual bend, only the one reading which indicates the position of maximum depth of wear into the bend is plotted in these figures. As in previous presentations, the same symbols are used to identify each individual bend and so, from these figures, the various specific rates of penetration at each set of bends tested can be determined.

With so much data available for these plots, and since the degree of scatter is small, it was not necessary to draw lines through the points plotted. With the exception of a few isolated points, all the plots appear to be remarkably consistent and fall within a band.

In Figs. 8.9 and 8.10 the corresponding plots of the respective replacement bends are also included for comparison purposes only. These plots clearly demonstrate the potential for rapid failure of these replacement bends, as indicated by their higher rates of penet-

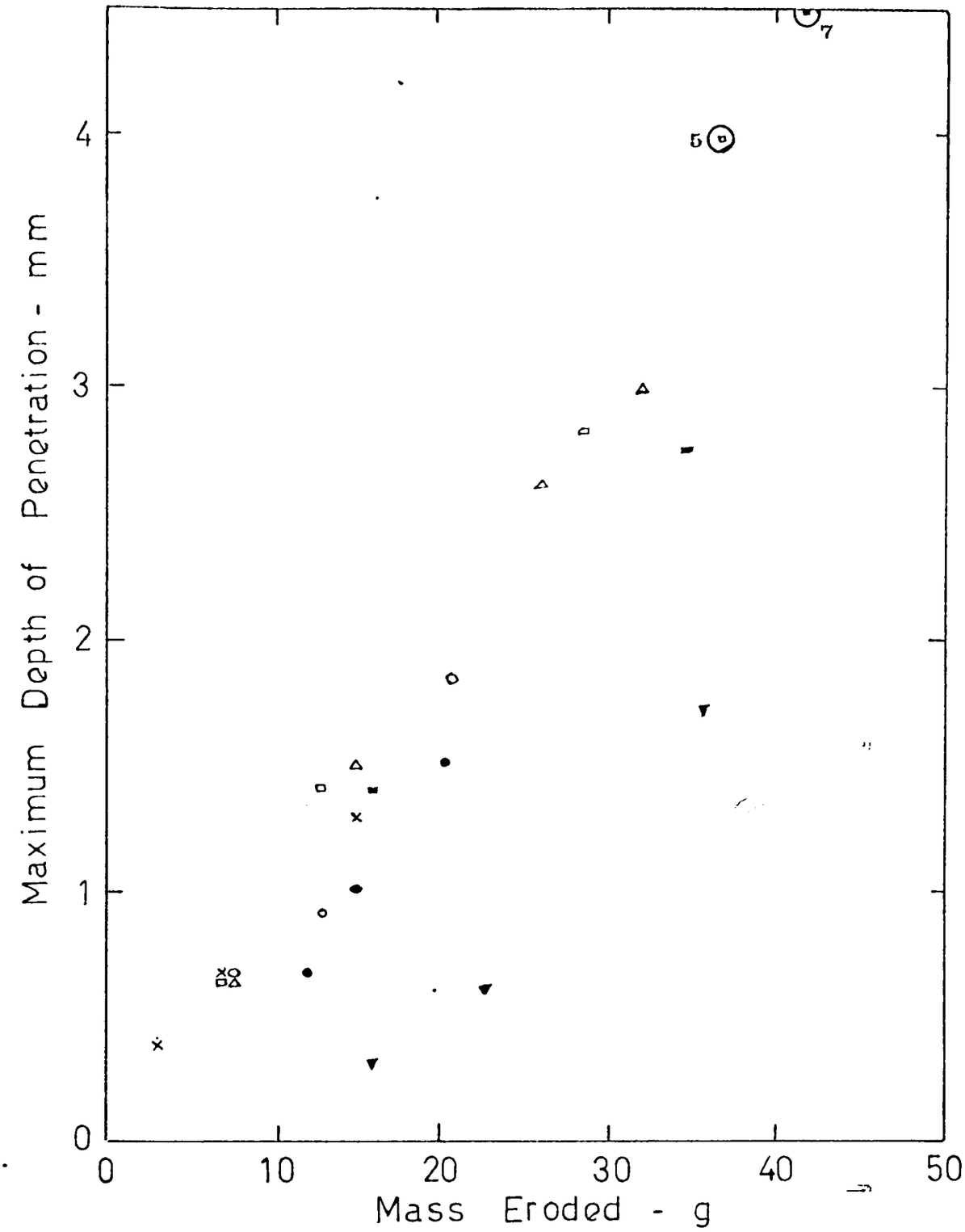

FIG. 8.8 Penetration Data for Bends with D/d of 4

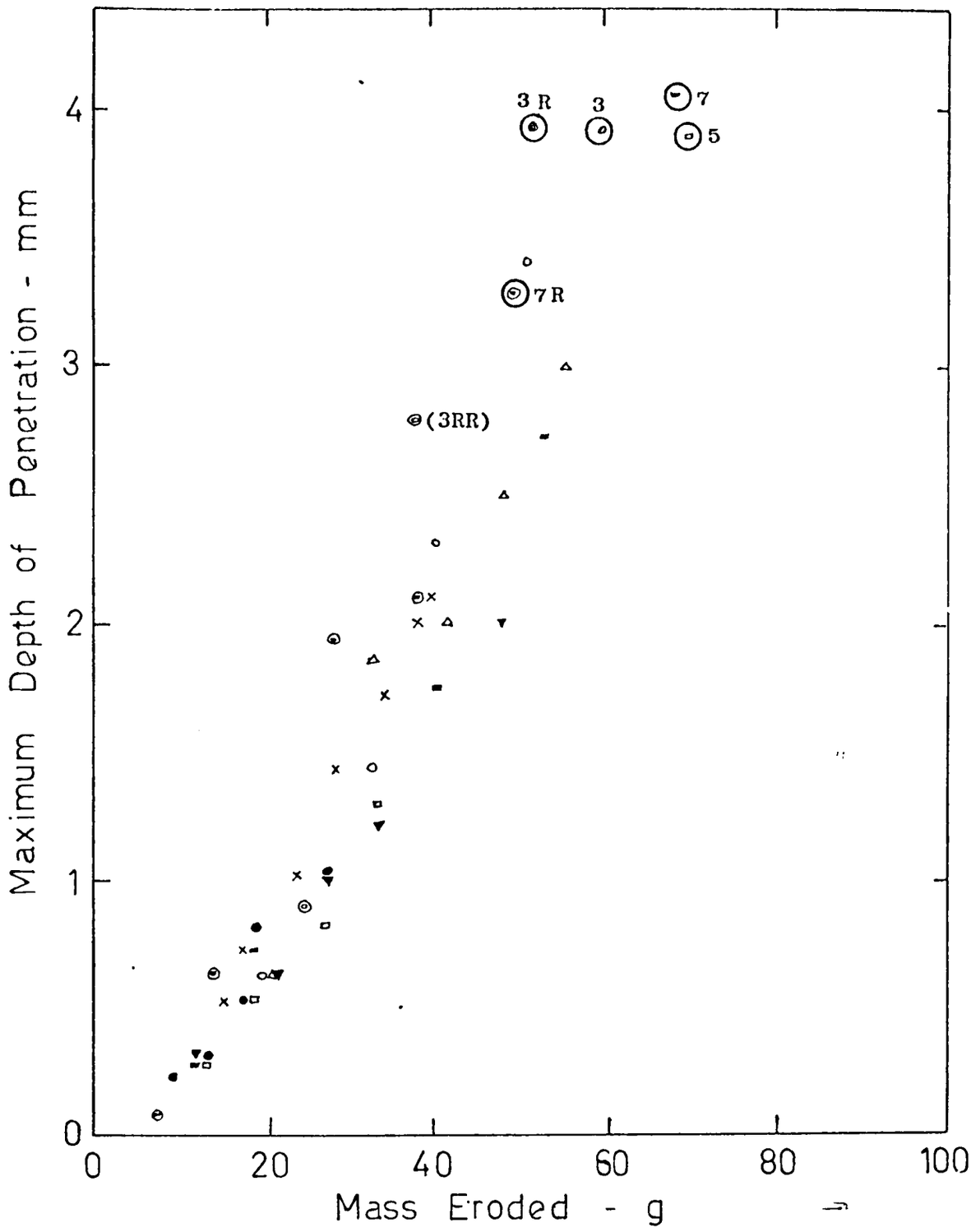

FIG. 8.9 Penetration Data for Bends with D/d of 5.6

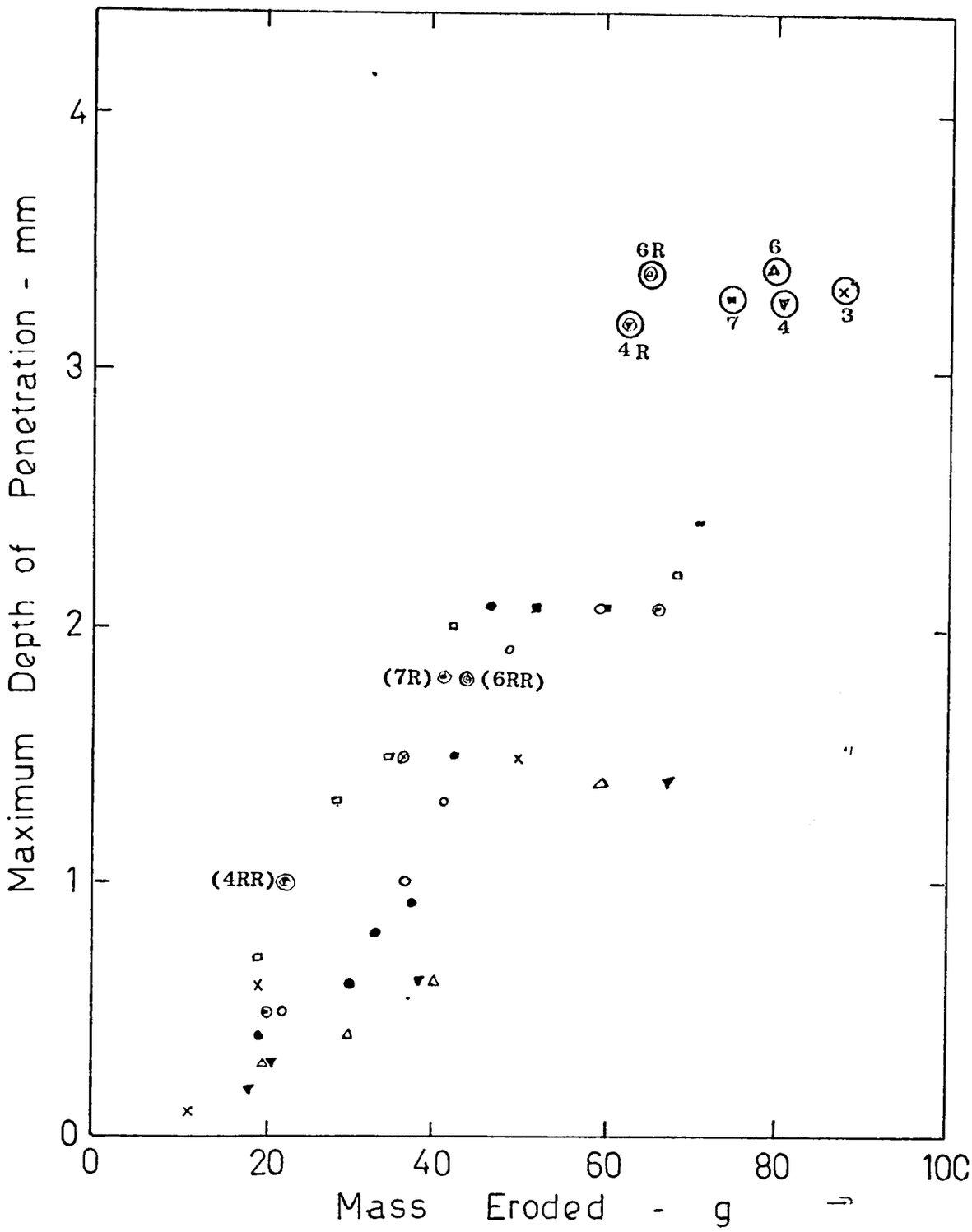

FIG. 8.10 Penetration Data for Bends with D/d of 12

ration which are consistently greater than the other bends. To a large extent this can be explained by the inter-relating effects of impact angle and particle shape and these will be discussed in more detail in the next chapter.

To show the effect of bend radius, the mean slopes of the results in Figs. 8.8 to 8.10 were determined and these are presented in Fig. 8.11. Apart from the initial transition section, these slopes are remarkably straight and beyond a given depth of penetration they are clearly separated. In terms of μm/g eroded from the bend, the gradients of these slopes clearly show that D/d has a marked effect. For a given depth of penetration the mass eroded decreases as bend radius is decreased, i.e. the rate of penetration increases as D/d is decreased. However, this information is misleading since it appears that elbows will fail more rapidly than ordinary bends. Since the thickness of a bend is finite, it is the rate of the depth of penetration by the particles into the bend wall, in terms of either penetration rate (mm/h) or penetration wear rate (mm/tonne), that is the criterion for bend performance and hence the mass eroded is only of secondary importance.

Fig. 8.12 shows the effect of D/d on penetration wear rate. The four lines correspond to the four test sets, as in Fig. 8.7, with the same symbols representing each respective set of tests. The trend of these curves clearly shows that a pronounced maximum occurs at a D/d of 5.6. In terms of penetration rate a similar trend is also observed and, in terms of individual values, Fig. 8.13 shows the overall equivalent results with a line joining the mean values. The critical value of D/d obtained from this work appears to substantiate Kriegel's data rather than Glatzel's, and is comparable to the value of about 6.5 reported by Brauer and Kriegel based on hydraulic tests.

Although the corresponding penetration wear rates for the elbows and long radius bends are comparable, for a constant thickness of 4 mm, the mean rates of penetration excluding the results of bend 7 were 0.12 mm/tonne or 0.08 mm/h for the elbows. These were respectively half of those for the long radius bends. In other words, the elbows lasted twice as long as bends with a D/d of 12. The values for the long radius bends were, in fact, comparable to the intermediate bends if the results of bends 3 and 7 are excluded. In practice, however,

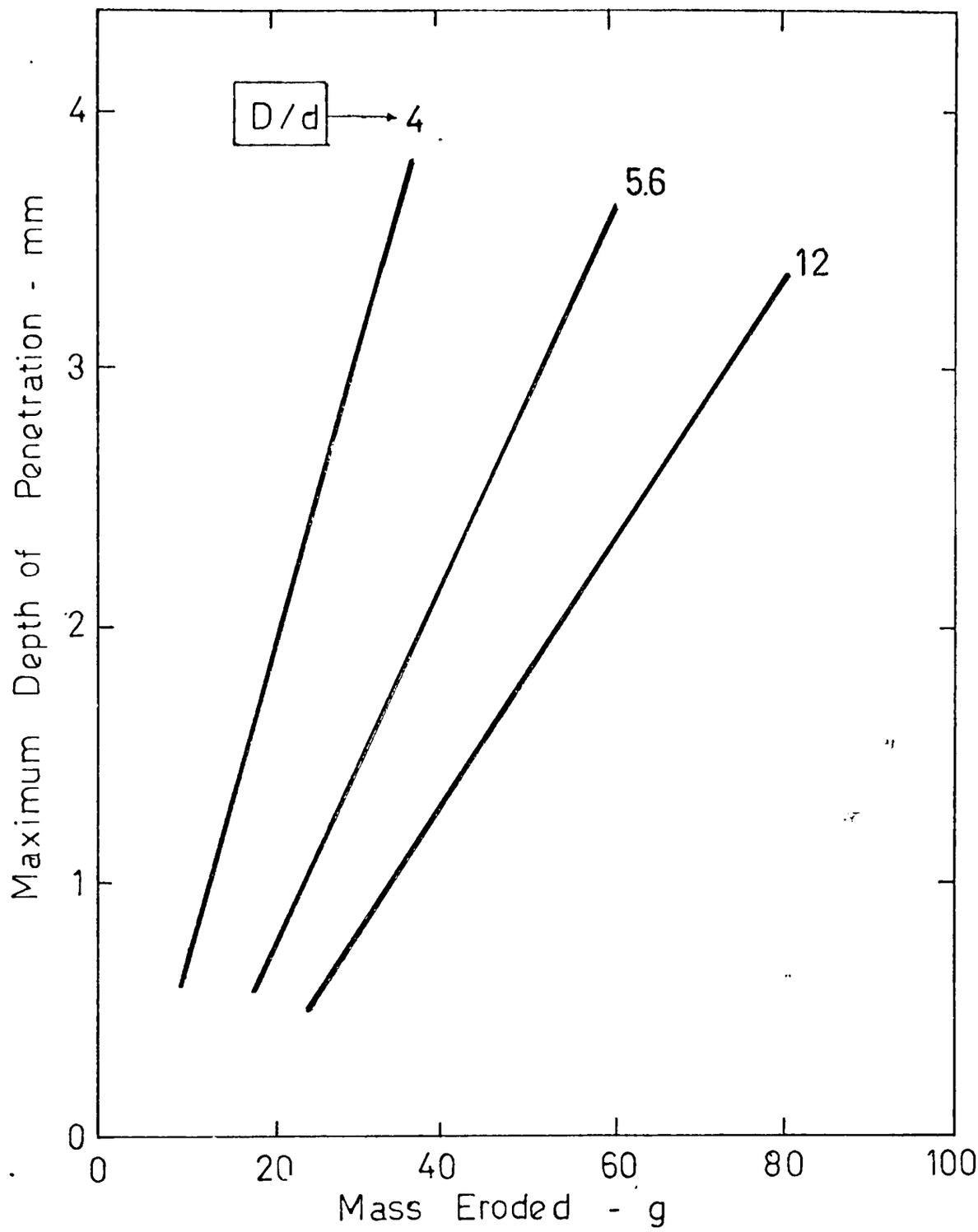

FIG. 8.11 Influence of Diameter Ratio on Rate of Penetration

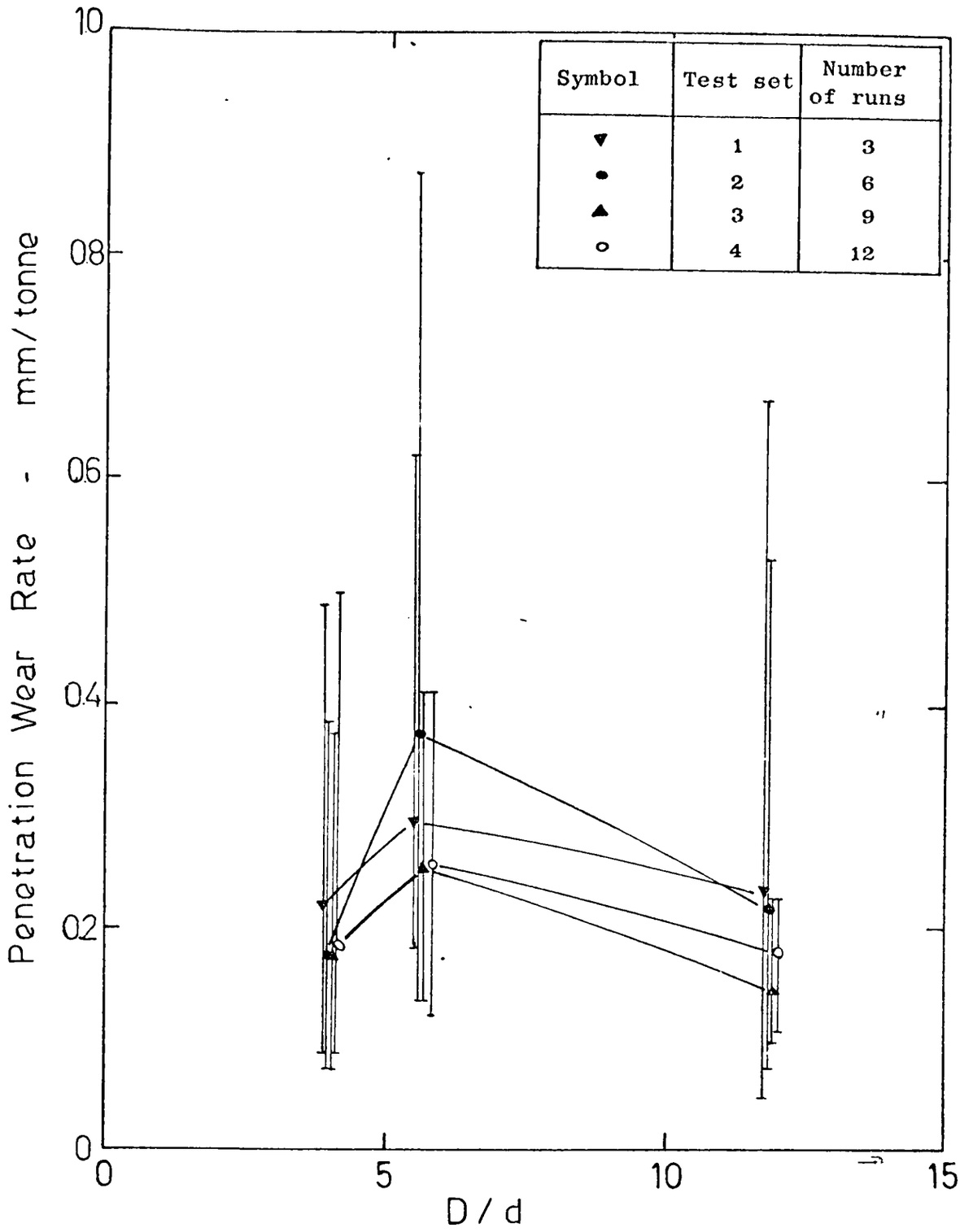

FIG. 8.12 Variation of Penetration Wear Rate with Diameter Ratio

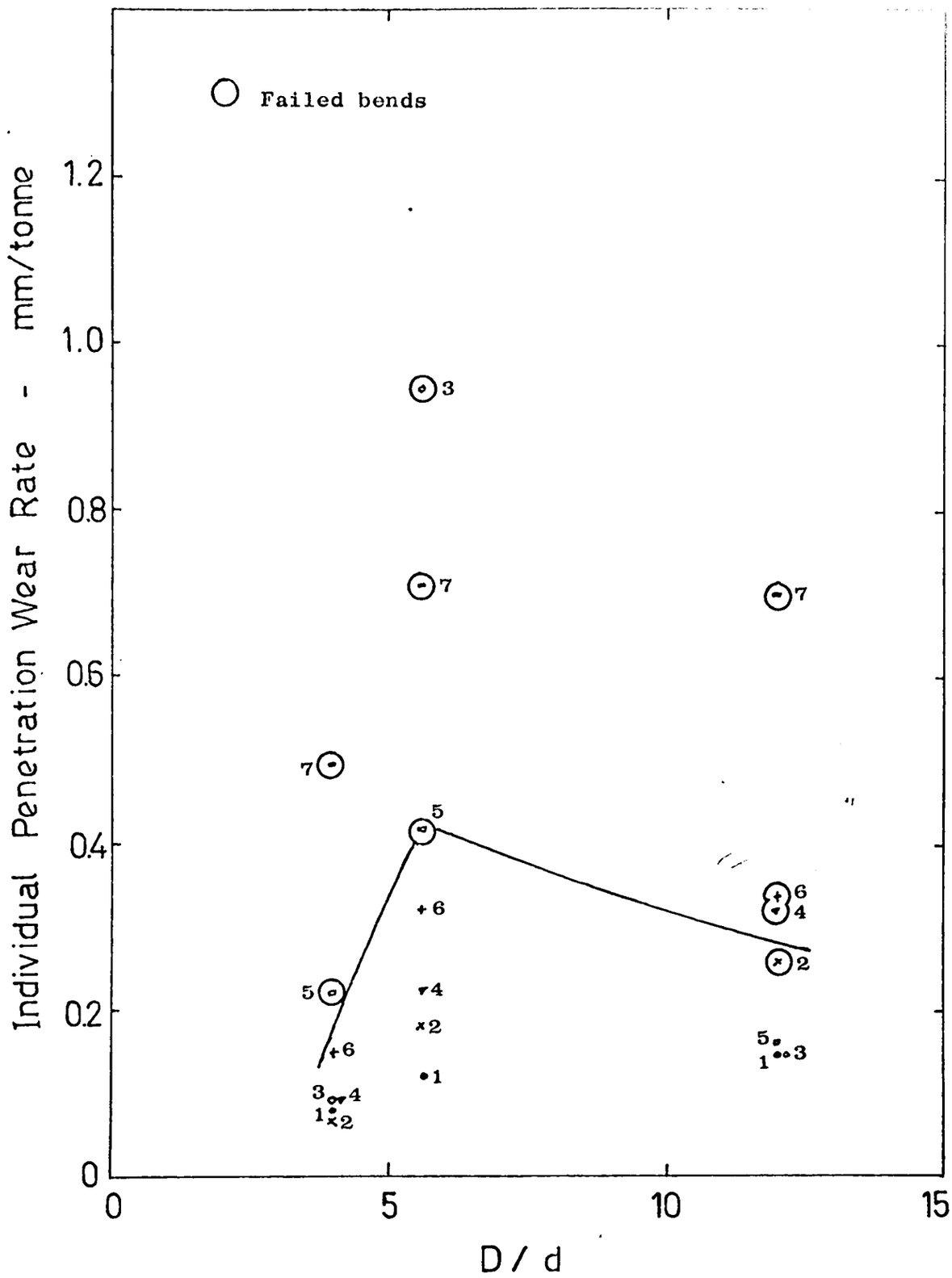

FIG. 8.13 Variation of Individual Penetration Wear Rate with Diameter Ratio

the preference is to use long radius bends rather than elbows or tight bends due to pressure drop considerations. Although it is generally recognised that pressure drop decreases as bend radius is increased, several sources (Cornish and Charity 1966, Schuchart 1968, Ghosh and Kalyanaraman 1970, Scott 1976, 1978) reported that beyond a value of D/d of about 10 no significant further decrease in pressure drop is obtained. Apart from costs, ease of installation and space limitation considerations, two important additional erosion factors must also be taken into account in the choice of a suitable value of D/d. These relate to the possibility of further erosion along the inner bend radius and along the following straight pipe runs due to the deflection of particles if the bend is too large (Mason and Smith 1972); and the potential for premature bend failure due to an increase in the scatter of results as D/d is increased, as shown in Figs. 8.7 and 8.12 in this work. Hence, in this respect, in order to avoid the rapid wear situation observed in bends with a value of D/d of 5.6, it is recommended that bends with D/d's between 10 to 20 be used.

8.4.5 Inter-relating Effects of Bend Radius and Effective Impact Angle

The experimental results presented in the preceding sections have clearly demonstrated the significant effect of bend radius, in terms of D/d, on both erosion and penetration. In Fig. 8.7 a threshold value of D/d, beyond which erosion is relatively unaffected by bend radius, is shown to exist, and this value appears to lie between 4 and 5.6. In terms of penetration wear rate (Fig. 8.12), maximum penetration is shown to occur at a D/d of 5.6. In both cases the magnitude of the dependence of these two parameters on bend radius is also considerably determined by the inter-relating effect of effective impact angle, as shown by the trend of the curves over a period of time in Figs. 8.7 and 8.12.

In this section the inter-relating effect of this variation of effective impact angle on both erosion and penetration is analysed. As mentioned earlier, after each set of tests all the bends were removed and the wear profiles of each bend were recorded. From these wear profile records the corresponding effective impact angle at various stages of erosion could be approximately estimated. However, for comparison purposes, since there is a considerable variation in

individual wear profiles, it was not possible to 'average' the wear profiles of the seven test bends at each set of tests. Therefore, in order to obtain a representative wear profile from which the effective impact angle so estimated could be considered as reasonably representative, it was necessary to select a particular test bend with individual specific erosion and penetration wear rate values which are comparable to the overall mean values corresponding to each test set. For the elbows and intermediate bends the individual erosion and penetration values which closely correspond to the respective mean values were from those of bend 6, and for the long radius bends it was those of bend 3.

Fig. 8.14 shows the individual respective wear profiles of these three bends. For the sake of clarity, the wear profiles corresponding to test set 2 (6 runs) and 4 (12 runs) are omitted from these bends. The corresponding approximate effective impact angle relative to each set of tests are given in Table 8.2. For comparison purposes, the corresponding individual specific erosion and penetration wear rates are also included in this table. Fig. 8.15 shows the corresponding pipe section wear profiles, taken along plane X-X as shown in Fig. 8.14, which is normal to the direction of the flow in the bend. On the basis of these wear profiles, quantitative comparisons of the inter-relating effects of bend radius and effective impact angle on the magnitude of both erosion and penetration can be evaluated as shown by the curves in Fig. 8.16.

The trend of the curves in this figure is remarkably similar to the characteristic ductile erosion and penetration curves (see Figs. 8.19 and 8.21), and serves to explain the results obtained in Figs. 8.7 and 8.12.

In terms of specific erosion, the lack of any substantial erosion for the elbows viz-a-viz the two larger bends, is explained by the initial high effective angle of impact, which corresponds to a decrease in erosion rate for this range of effective impact angles from about 40^{o} onwards. For the two larger bends, the initial high rate of erosion corresponds to the estimated effective impact angle of about 20 to 30^{o}, and is followed by a gradual decrease as the effective impact angle increases. In terms of D/d, the lower rate

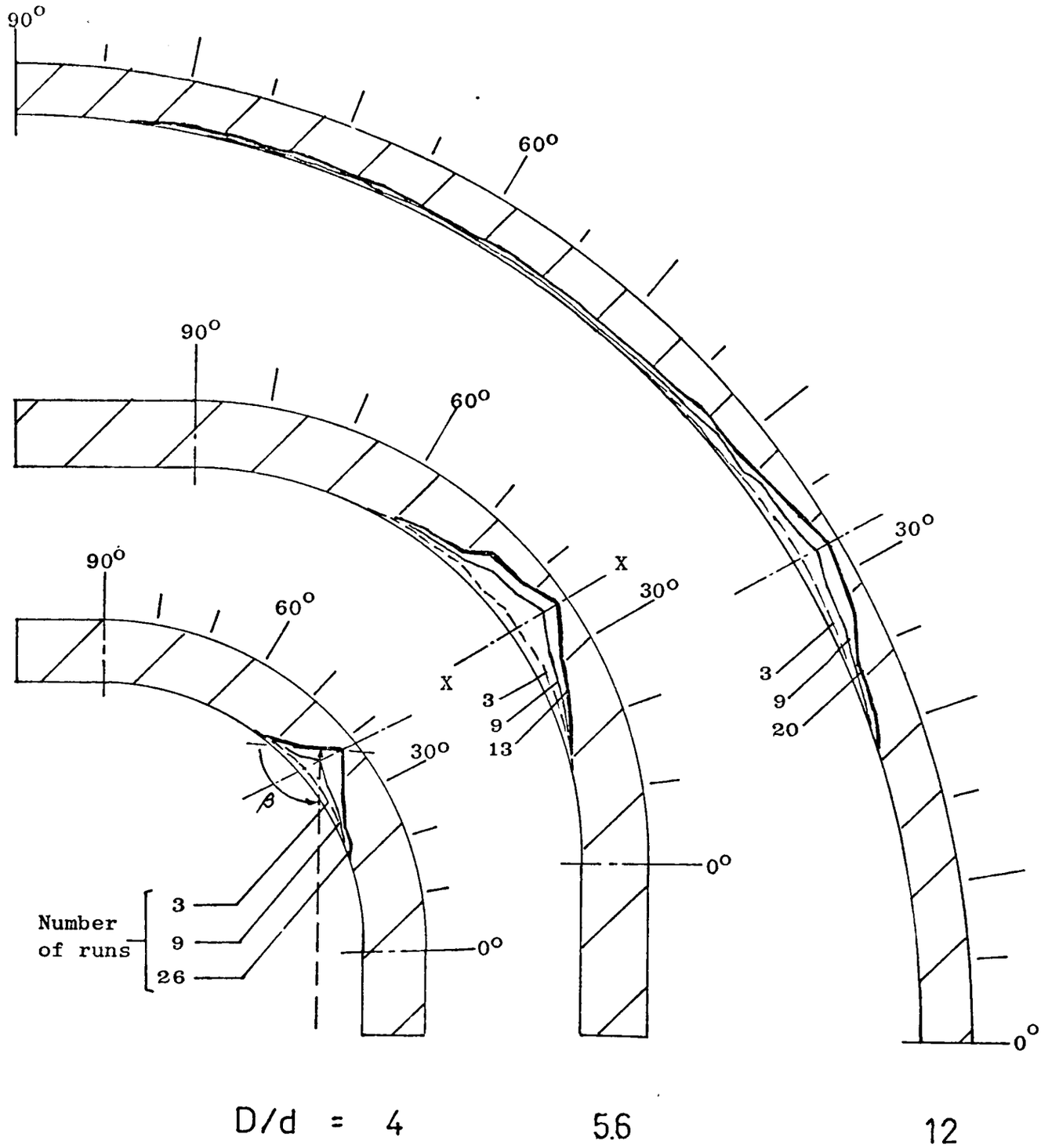

FIG. 8.14 Influence of Bend Geometry on Bend Wear Profile

TABLE 8.2 Influence of Effective Impact Angle on Specific Erosion and Penetration Wear Rate

D/d	Number of runs	Approximate Effective Impact Angle (β) degrees	Specific Erosion g/tonne	Penetration Wear Rate mm/tonne
4	3	40	2.24	0.22
	6	45	2.03	0.18
	9	65	2.08	0.19
	12	75	1.89	0.18
	26	90	1.65	0.15
5.6	3	35	12.00	0.31
	6	50	9.11	0.49
	9	55	7.83	0.41
	12	60	7.41	0.33
	13	65	6.46	0.32
12	3	20	9.78	0.22
	6	25	7.56	0.22
	9	30	6.07	0.19
	12	35	5.44	0.21
	20	40	4.00	0.14

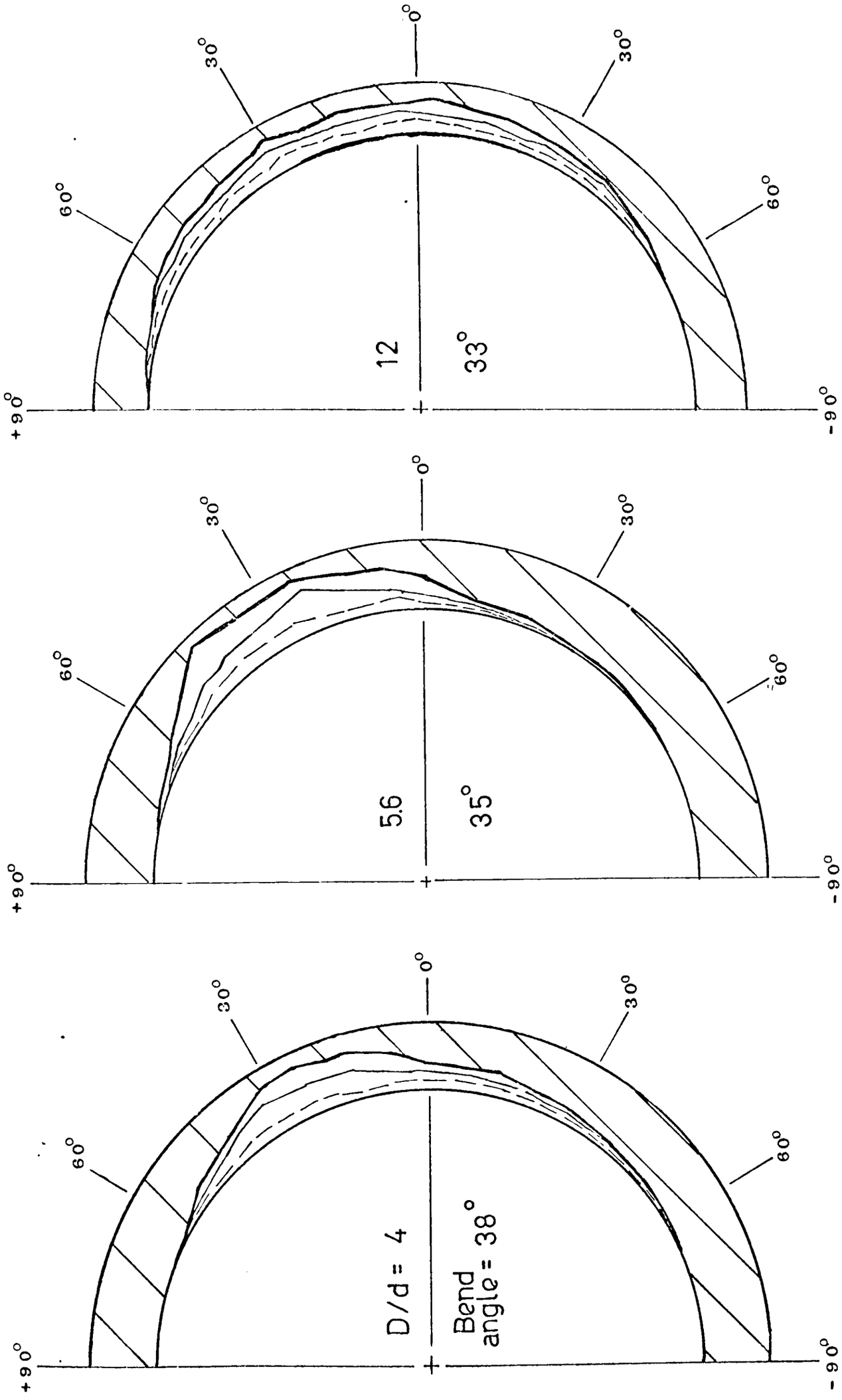

FIG. 8.15 Influence of Bend Geometry on Pipe Section Wear Profile

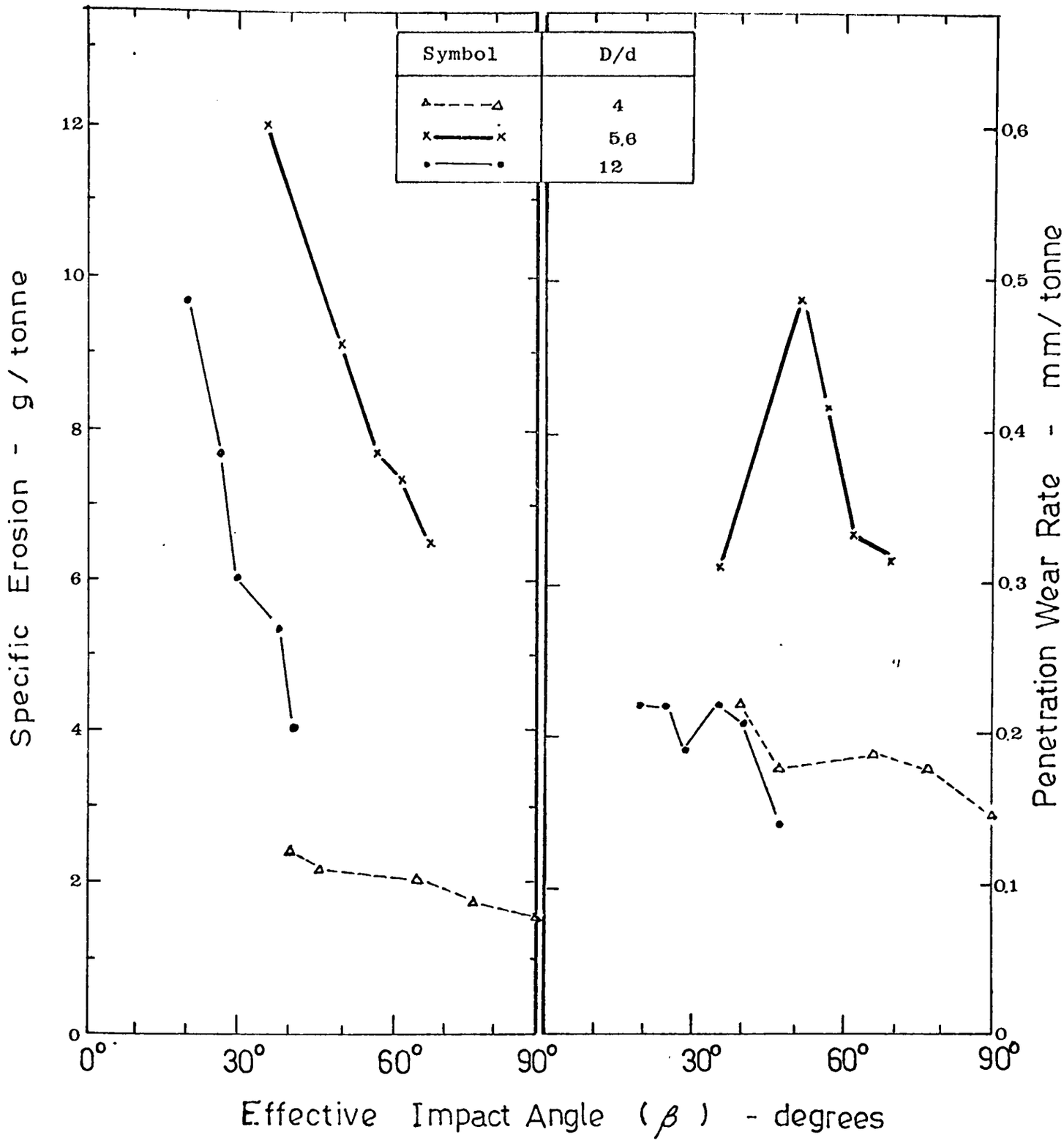

FIG. 8.16 Influence of Bend Geometry and Effective Impact Angle on Specific Erosion and Penetration Wear Rate

of erosion for the elbows is also attributed to a correspondingly smaller concentrated region of erosion per unit surface area. As bend radius is increased, the region of erosion increases and hence more mass would be eroded, as expected. However, the results for the long radius bend clearly contradict this assumption. The lower rate of erosion obtained for this particular long radius bend, compared to the intermediate bend, is apparently due to the increased tendency of the particles to slide along the outer bend surface rather than impacting directly as in the intermediate bend. The lack of any substantial decrease in erosion for the bends, particularly beyond test set 3, as shown in Fig. 8.7, is attributed to the slight increase in effective impact angle, corresponding to a similar slow rate of decrease in erosion for the two larger bends. For the elbows, the effective impact angle, and hence the corresponding erosion rate, appears to stabilise mid-way through the test series of 26 runs.

In terms of penetration wear rate a pronounced maximum is observed, corresponding to an effective impact angle of about 50^{o}, for the intermediate bend. This substantiates the results of Brauer and Kriegel (1963) and Krasnov and Zhilinskii (1973), although these were based on flat plate specimens. The rapid increase in penetration rate as the effective impact angle increases from about 35 to 50^{o}, which corresponds to test sets 1 and 2, provides an explanation for the corresponding increase in the mean value, as shown in Fig. 8.12 for the intermediate bends. For the elbows, although there is also an increase in effective impact angle from about 40 to 75^{o} over this range of test sets, no corresponding increase in penetration is observed. The lack of any increase is attributed to the over-riding effect of bend radius. As an erosion pocket is being developed, some of the impacting particles are embedded into this pocket and subsequently act as a shield against any further increase in both erosion and penetration, and hence prolong its service life. For the long radius bend, the lack of any similar increase is penetration is attributed to the combined effects of the sliding motion of the particles and the limitation of any subsequent potential increase in effective impact angle beyond 40^{o} over this range of test sets.

In both cases, bends with a D/d of 5.6 clearly correspond to the worst case in terms of specific erosion and penetration wear rates. The

three basic stages of erosion which are dependent upon effective impact angle as identified by Mills and Mason (1977 b) have been substantiated, particularly by the results obtained for the intermediate bend. An initial high rate of erosion corresponding to an effective impact angle of about 30^{o} (primary wear stage), followed by a rapid increase in penetration as the effective impact angle is increased to about 50^{o} (secondary wear stage), and a minimum as the effective impact angle increases to about 80^{o} (tertiary wear stage), is clearly exemplified by the curves of the intermediate bend. Hence, in terms of D/d, bends with a value around $5\frac{1}{2}$ should be avoided.

8.4.6 Effect of D/d in Terms of Impact Angle

In Fig. 8.16 the curves clearly showed that both erosion and penetration are influenced by the combined inter-relating effects of bend geometry and effective impact angle. In terms of magnitude, however, the effect due to bend geometry has an over-riding influence over that of effective impact angle. As reported in section 8.2.1, the potential location of impact, and hence magnitude of effective impact angle, is determined by the intersection of the particle trajectory and the outer bend radius (see Fig. 8.1) which in turn is dependent upon bend geometry. Furthermore, since the thickness of the bend is small in relation to its diameter, the magnitude of the influence due to effective impact angle is of secondary importance and plays a subsidiary role only compared to the effect of bend geometry in terms of D/d.

Although the service life of bends is determined by the rate of penetration, the location of maximum wear, and ultimately failure, is largely predetermined by its D/d ratio. To some extent the influence of bend geometry can be predicted on the basis of a correlation between the results obtained in terms of impact bend angle and a typical characteristic ductile erosion curve obtained from bench type tests over a range of impact angles.

To explain this further, it is necessary to consider once again the wear profiles shown in Fig. 8.14. Whilst the effective impact angle varies over a period of time, the location of maximum wear remains relatively constant once a crater has been established. In Table 5.3

the mean position of failure in terms of impact bend angle of the bends which failed over this range of D/ds tested, were approximately 37^{o}, 34^{o} and 33^{o} for the elbows, intermediate and long radius bends respectively. The lack of any substantial variation in the position of failure clearly indicates that the trajectory of the particles into the bend must also be taken into account, as shown in Fig. 8.17.

For ductile materials it is well recognised that maximum erosion corresponds to an impact angle of about 20 to 30^{o}, and the coincidence of a similar position in terms of impact bend angle in bend erosion, irrespective of its D/d, clearly demonstrates that particle trajectory is an important factor in determining the location of maximum wear and failure, as reported in section 8.2.2.

In Fig. 8.17 the position of failure for the elbows and intermediate bends appears to be located by the intersection of the projected path of particle trajectory along the centre line of the straight pipe and the outer bend radius. For the long radius bends it appears to be located by the trajectory along the boundary of the inner bend radius to the outer bend wall (point A). Brauer and Kriegel (1965 a,b) have extensively investigated the trajectories of particles into a bend and found that, over a range of D/ds, the position of failure can be generally described by the curve in equation 8.1, which is based on the particle trajectory along the inner bend radius only (Fig. 8.1). Glatzel (1977) found that this semi-empirical equation was applicable for perspex bends with a range of D/ds from 4 to 16.

Fig. 8.18 shows the curve based on equation 8.1 (curve A), and the results obtained in this work by the author clearly show that it coincides with the long radius bend results only. Curve B is based on the trajectory along the centre line of the preceding straight pipe. For comparison purposes, the data of Mills and Mason (1979a) and Bikbaev et al (1972, 1973) are also included in this figure. Whilst Mills and Mason have only carried out tests on bends with a single D/d of 5.6, the data of Bikbaev and co-workers was based on various alloy bends with a range of D/ds from 4.8 to 15.6. It should be noted that the plots obtained from Bikbaev and co-workers' results are based on the estimated position of maximum wear only.

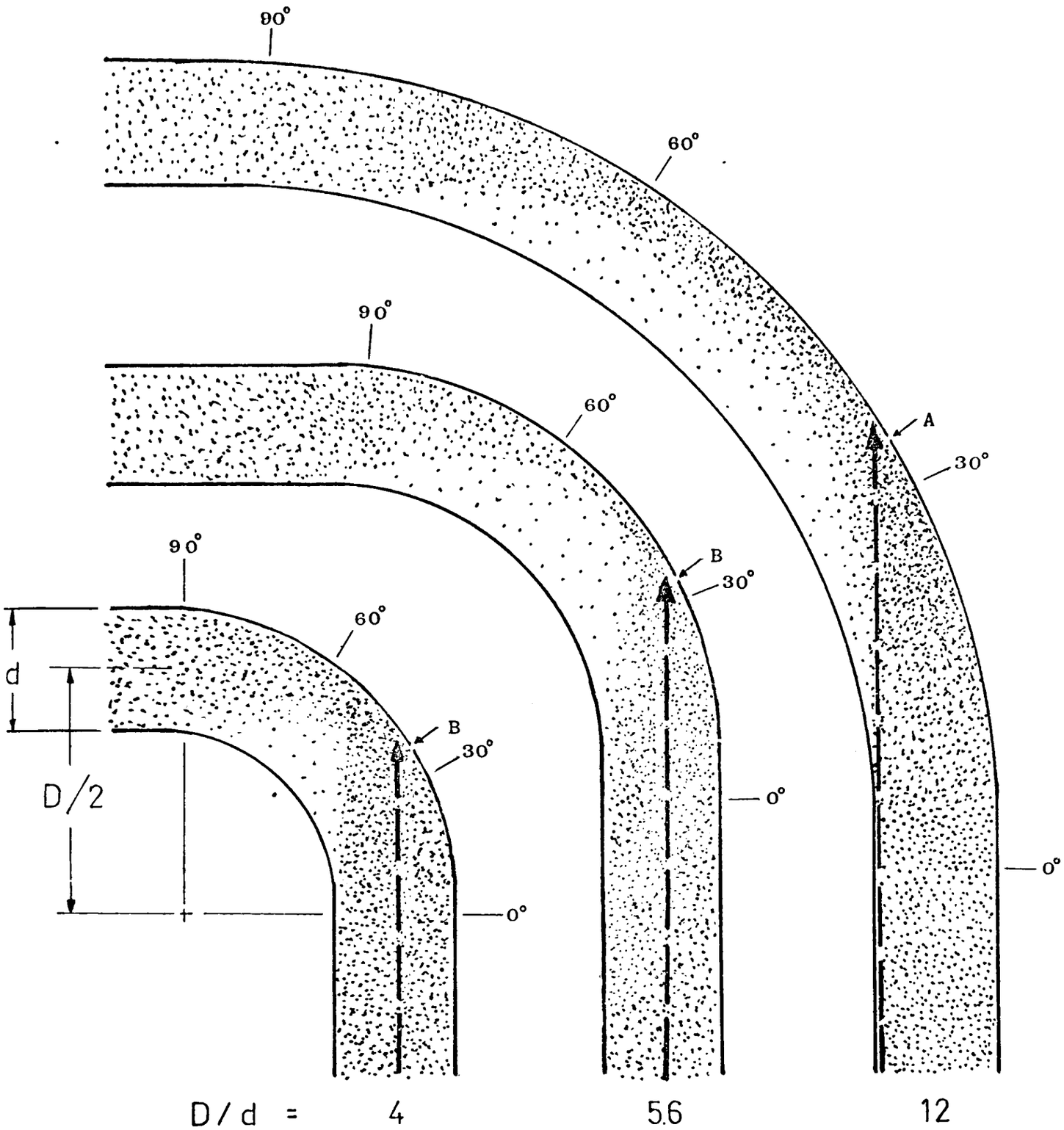

FIG. 8.17 Influence of Bend Geometry and Particle Trajectory on the Location of Maximum Wear and Failure.

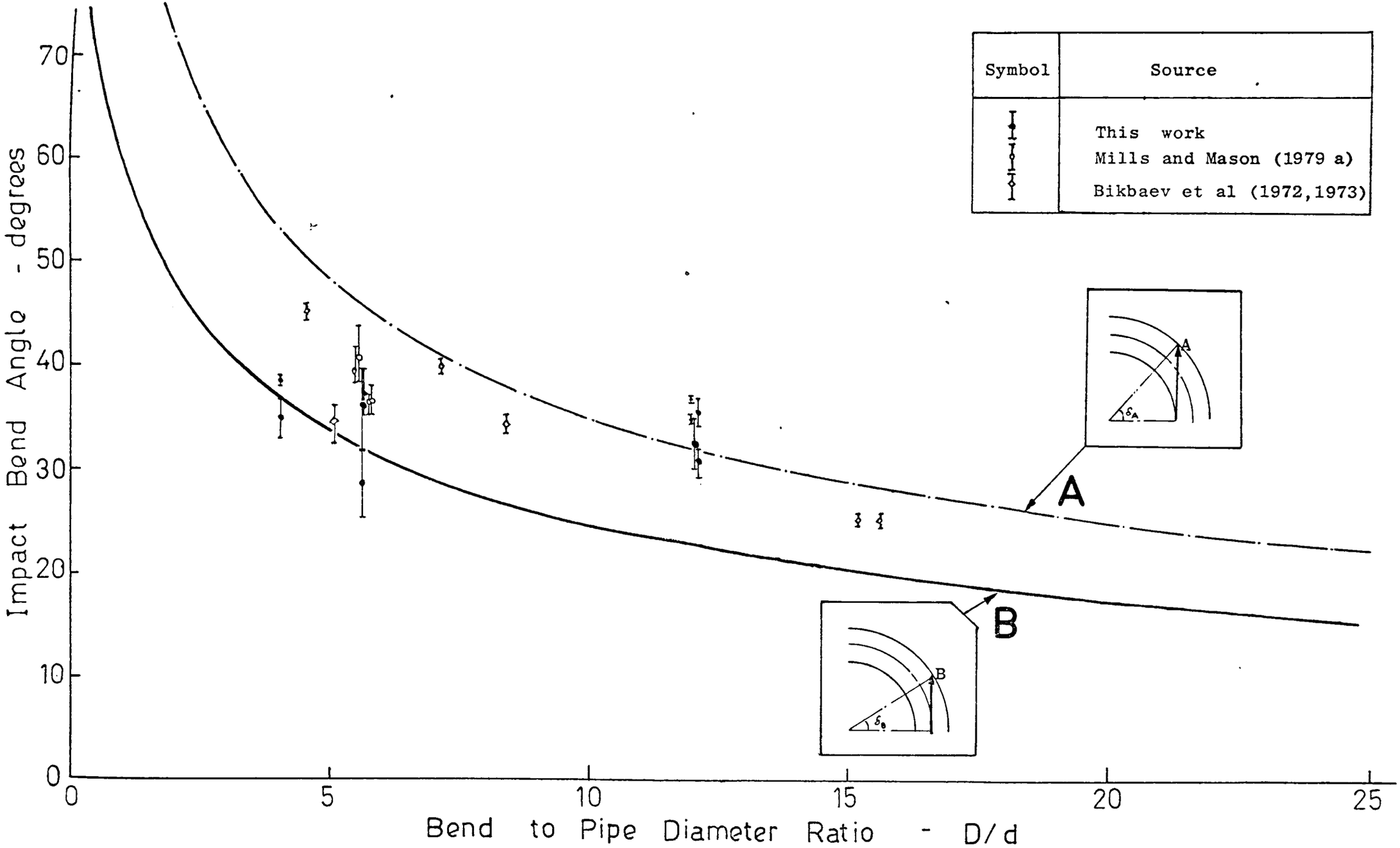

FIG. 8.18 Variation of Impact Bend Angle with D/d for Different Particle Trajectories

However, it is unlikely that the ultimate position of failure will vary appreciably. The higher value of impact bend angles over this corresponding range of D/ds tested, obtained by Glatzel, can be explained by the characteristic behaviour of the perspex bends used in his work. These behave in a semi-ductile brittle manner, with maximum erosion at an impact angle of about 45^{o} compared to about 20 to 30^{o} for ductile materials. As a result there is a tendency for maximum erosion to occur at a correspondingly higher impact bend angle for perspex bends and, in this case, it would be located by the trajectory along the boundary of the inner bend radius as described by curve A, over a similar range of D/ds considered.

However, in general it can be seen that the position of failure appears to lie within the boundary of these two curves. On the basis of the curves in this figure it is possible to predict the effect of D/d to a certain extent, by cross-correlating the impact bend angle in this figure with the impact angle based on a typical characteristic ductile erosion or penetration curve.

Fig. 8.19 shows a typical ductile erosion curve which has been normalised to a relative value of 1.0 at 30^{o} impact angle. This curve is based on a compilation of experimental data from various ductile metals and alloys, obtained from several sources by Hutchings (1979 a). For comparison purposes the actual results obtained in this work are also included. These are based on the mean specific erosion data after test set 2 or 6 runs, which has been normalised to a relative value of 1.0 at D/d of 5.6. Since there are two possible impact angles at each value of D/d due to the two trajectory curves, the two separate but identical sets of curves (a and b) are presented. Curve 'a' corresponds to the upper boundary according to curve A in Fig. 8.18, and similarly, curve 'b' corresponds to the lower boundary according to curve B. By cross-correlating the impact angles in Figs. 8.18 and 8.19, the effect of D/d in terms of relative erosion values is obtained as shown in Fig. 8.20. In this figure curves A and B are based on the typical ductile erosion curve, and relate to the two possible values of D/d due to the two trajectory curves. Curves a and b relate directly to the two separate, identical curves in the previous figures. The curves in Fig. 8.20 clearly show that the effect of D/d on relative erosion is considerably influenced by particle

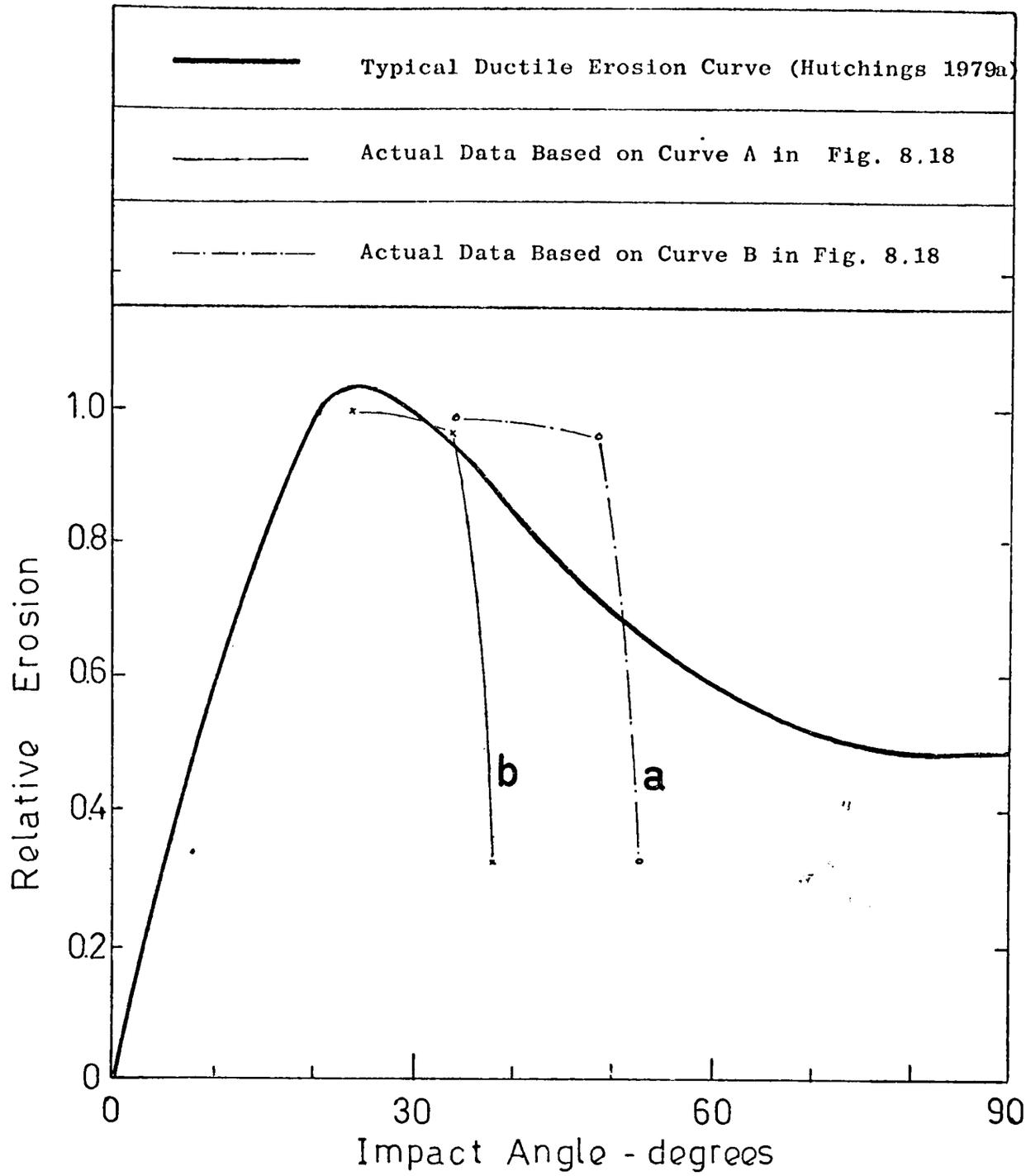

FIG. 8.19 Variation of Relative Erosion with Impact Angle

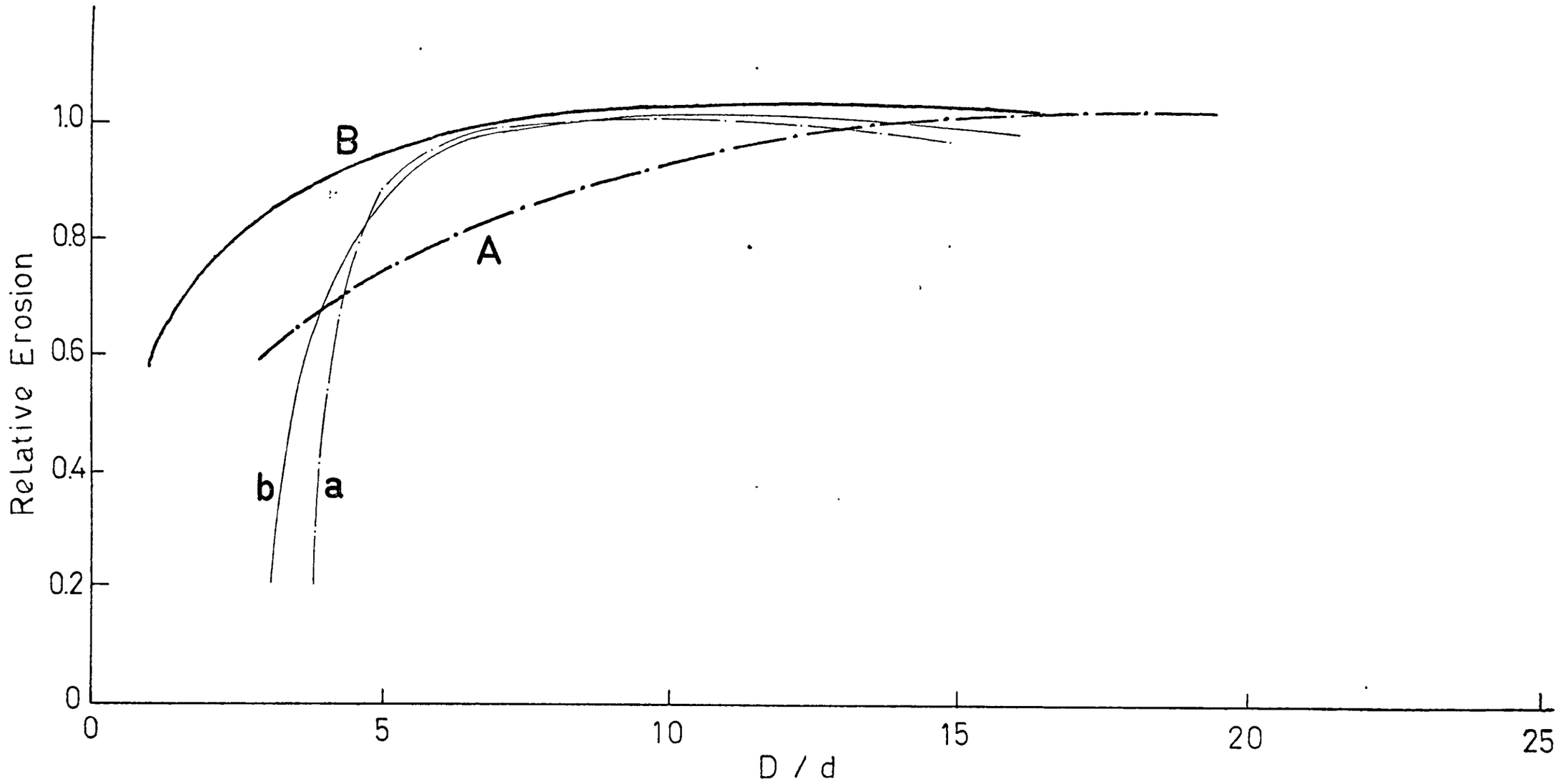

FIG. 8.20 Comparison between Actual and Predicted Data on the Effect of D/d on Erosion

trajectory. Although the curves (a and b),which are based on the actual normalised results, are comparable, there is a significant variation based on the typical erosion curve data. Although all the curves clearly indicate the existence of a threshold value beyond which erosion is unaffected by bend radius, as shown in Fig. 8.7, curve A shows that it occurs at a D/d of about 15 compared to around 6 by the other curves. In this case, curve B would give a more accurate and reliable prediction, and clearly shows that particle trajectory must also be taken into consideration.

Following a similar procedure, the influence of D/d in terms of penetration can also be predicted based on a typical ductile penetration curve as shown in Fig. 8.21. This curve have been normalised to a relative value of 1.0 at an impact angle of 50^{o}, and is based on a curve given by Krasnov and Zhilinskii (1973) from tests on mild steel specimens eroded by sand at various angles of impact. For comparison purposes, the actual results obtained in this work, which have been normalised to a relative value of 1.0 at D/d of 5.6, have also been included as indicated by curves a and b.

The results of a similar cross-correlation procedure of the respective curves in Figs. 8.21 and 8.18, are presented in Fig. 8.22. It can be seen that the trend of these curves is similar to that obtained in Fig. 8.12, although there is an appreciable degree of variation in terms of a critical value of D/d. Whilst the curves based on the actual results show maximum penetration at a D/d of about 6, curves A and B, which are based on a typical penetration data, show a maximum at about 3.5 and 2.5. Although the variation is significant, it appears that, in this case, the values of curve A are nearer to the actual results than those of curve B.

An important feature of the curves presented in Figs. 8.20 and 8.22 is the accuracy and reliability of the predicted curves based on the typical ductile erosion and penetration results. In Fig. 8.20 in terms of relative erosion, prediction based on curve B is comparable to the actual results, whilst in Fig. 8.22, in terms of penetration, it is those based on curve A instead. In both cases, although it has been clearly shown that it is feasible to predict the effect of D/d on the basis of a typical erosion or penetration curve, the inter-

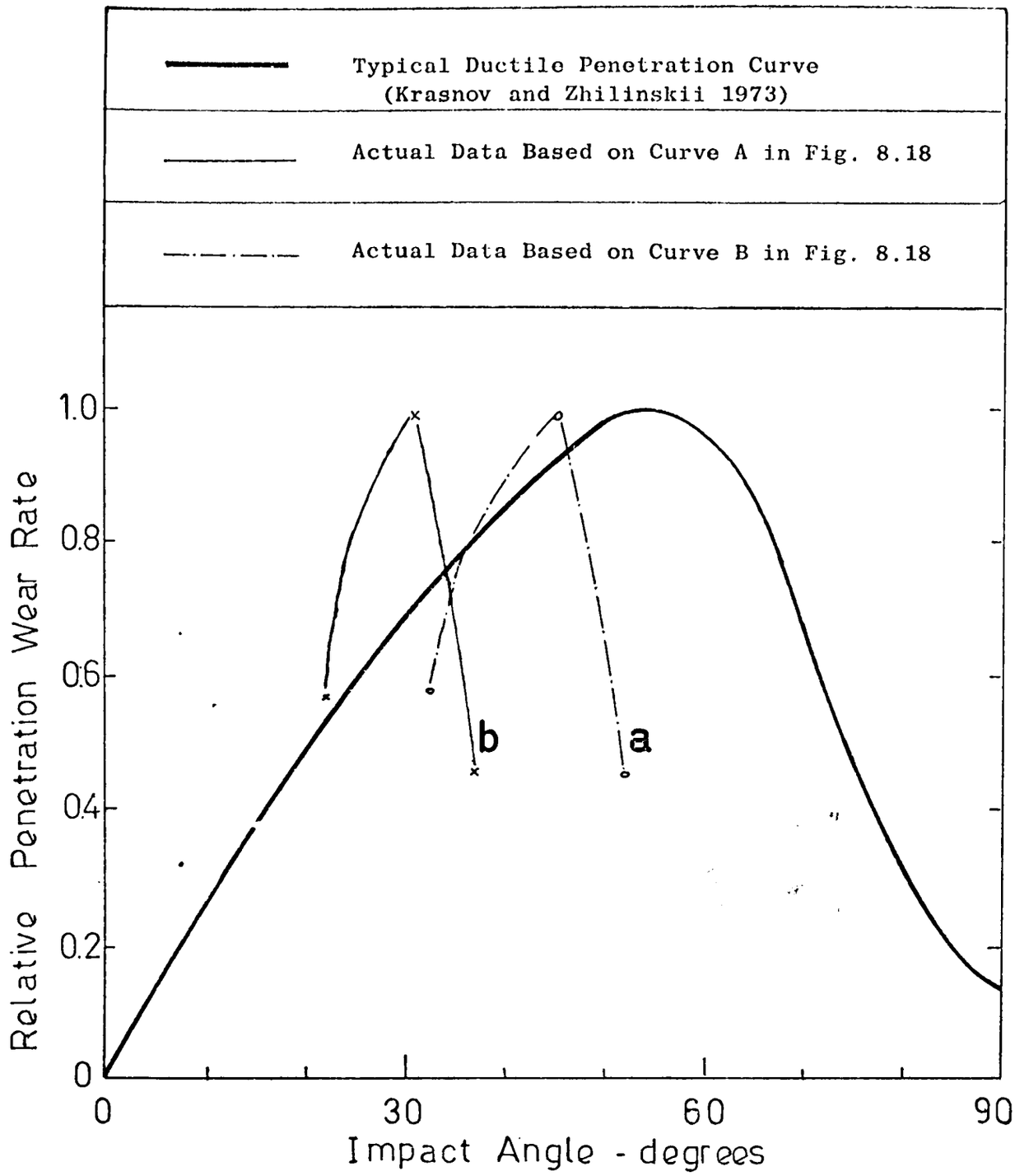

FIG. 8.21 Variation of Relative Penetration with Impact Angle

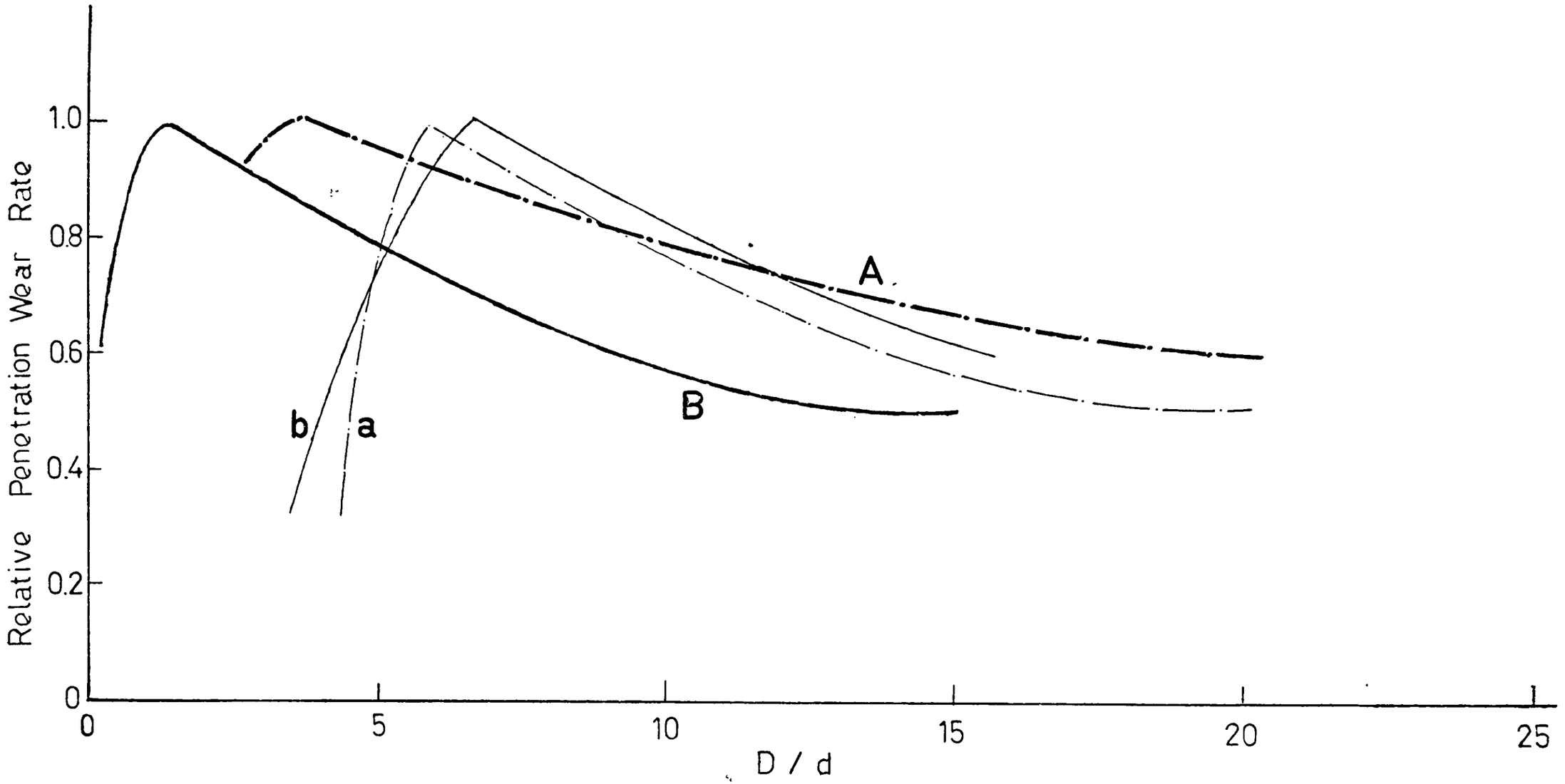

FIG. 8.22 Comparison between Actual and Predicted Data on the Effect of D/d on Penetration

relating effect of particle trajectory must also be taken into account.

8.4.7 Surface Erosion Profiles

Figs. 8.23 to 8.25 are photographs of some of the bends tested in this work. The surface erosion patterns of the two elbows which failed in this particular test series, i.e. bends 7 and 5, are shown in Fig. 8.23 (a and b). In Fig. 8.24 the eroded bend wall wear profiles of two of the intermediate bends which failed prematurely i.e. bends 3(b) and 7 (c), and their replacement bends, 3R(a) and 7R(d), are also presented. A photograph of an additional intermediate bend tested in this series was shown earlier, in Fig. 7.28 (c) (bend 6). For the long radius bends, Fig. 8.25 (a to d) shows respectively the surface erosion patterns of bends 6, 5, 3 and 2.

Since all the bends were eroded by similar sized 70 μm sand under identical conveying conditions, it can be clearly seen that a common feature of all the erosion patterns is the presence of a characteristic complex pattern of steps and ridges. These are particularly pronounced in the elbows, where a multitude of small steps is evident. Although these are mainly concentrated over a small area immediately beyond the point of maximum wear zone, the vertical depth of the steps at this point is well over 2mm. The magnitude of these steps serves to explain the rapid increase in effective impact angle over a short period of time and, consequently, a lack of any substantial increase in the amount of mass eroded and a limited penetration rate for the elbows. By contrast, for the two larger sets of bends, these steps are more widespread and indicate some amount of erosion occurring beyond a bend angle of about 40^{o} to about 80^{o}.

Another common feature of the erosion patterns in these bends is the evidence of a pronounced tracking of the erosion path across the bends. These erosion tracks are particularly prominent in the larger set of bends. As discussed in the previous chapters, the presence of these tracks is clear evidence of swirling in the flows and, combined with the presence of 'fines', the bends in every case are likely to fail prematurely. This is a characteristic feature of all the bends which failed prematurely, as shown in Fig. 8.24, where all the bends shown failed rapidly. In Fig. 8.25 a pronounced erosion tracking pattern

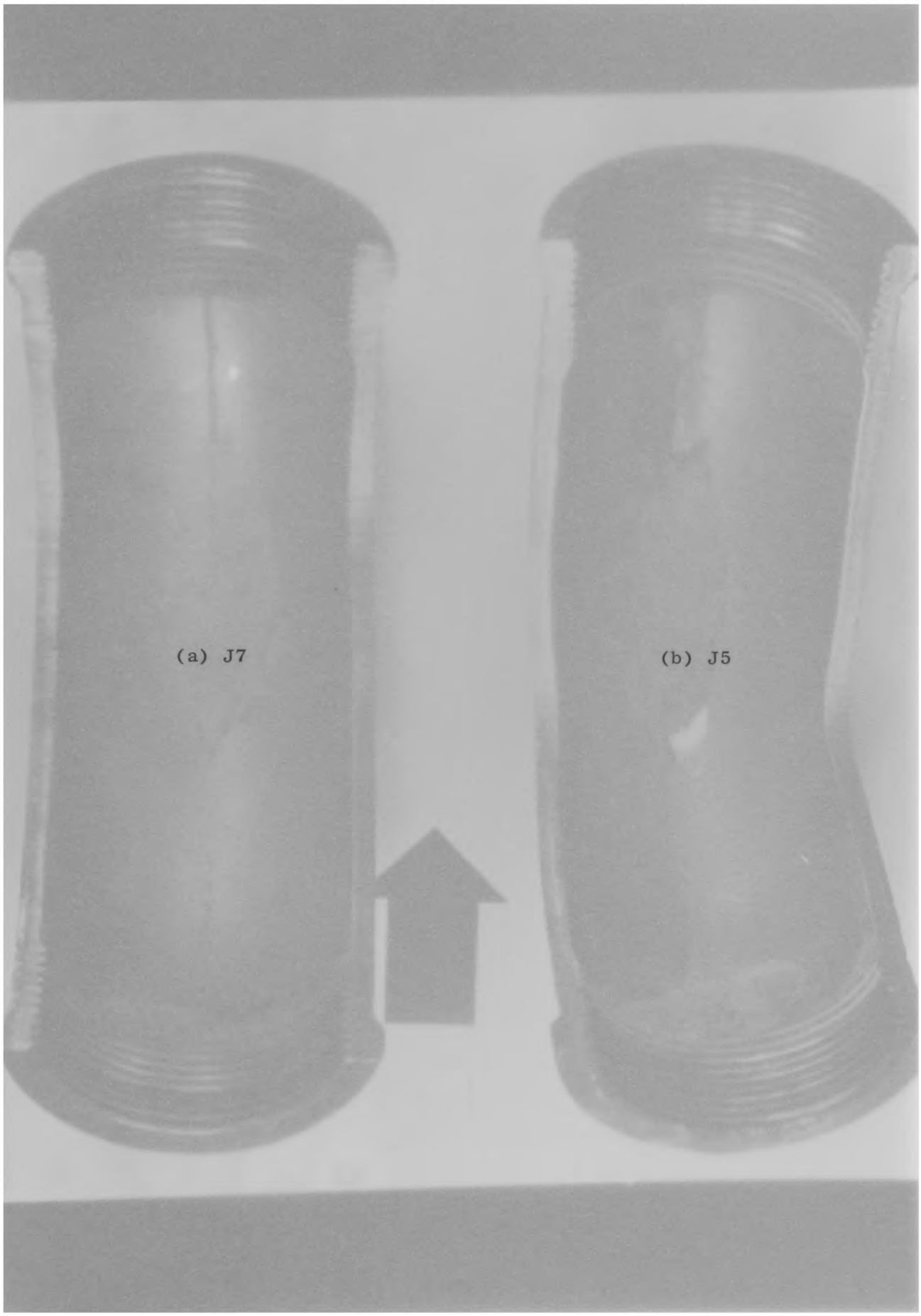

FIG. 8.23 Surface Erosion Patterns of Elbows

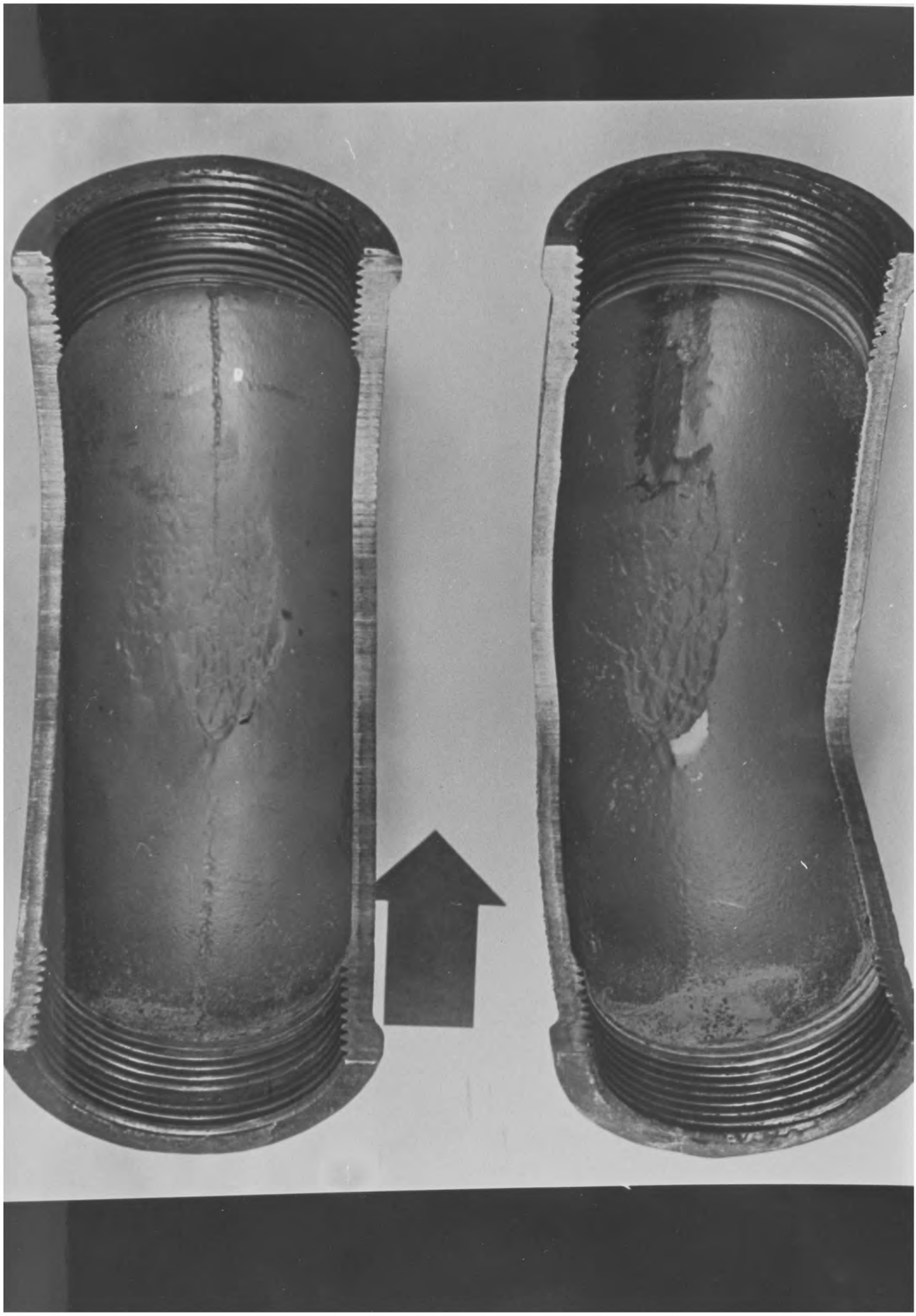

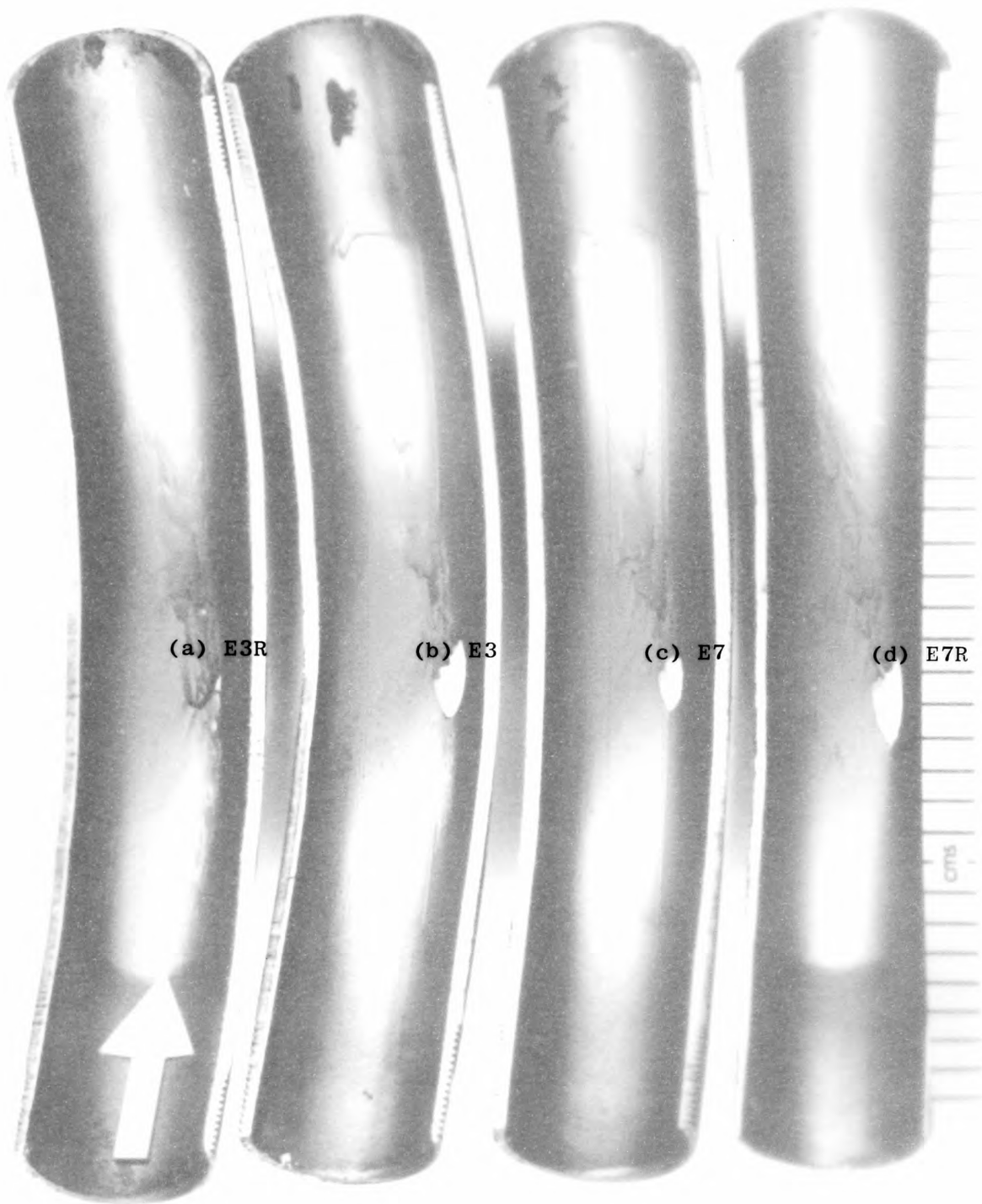

FIG. 8.24 Surface Erosion Patterns of Bends with D/d of 5.6

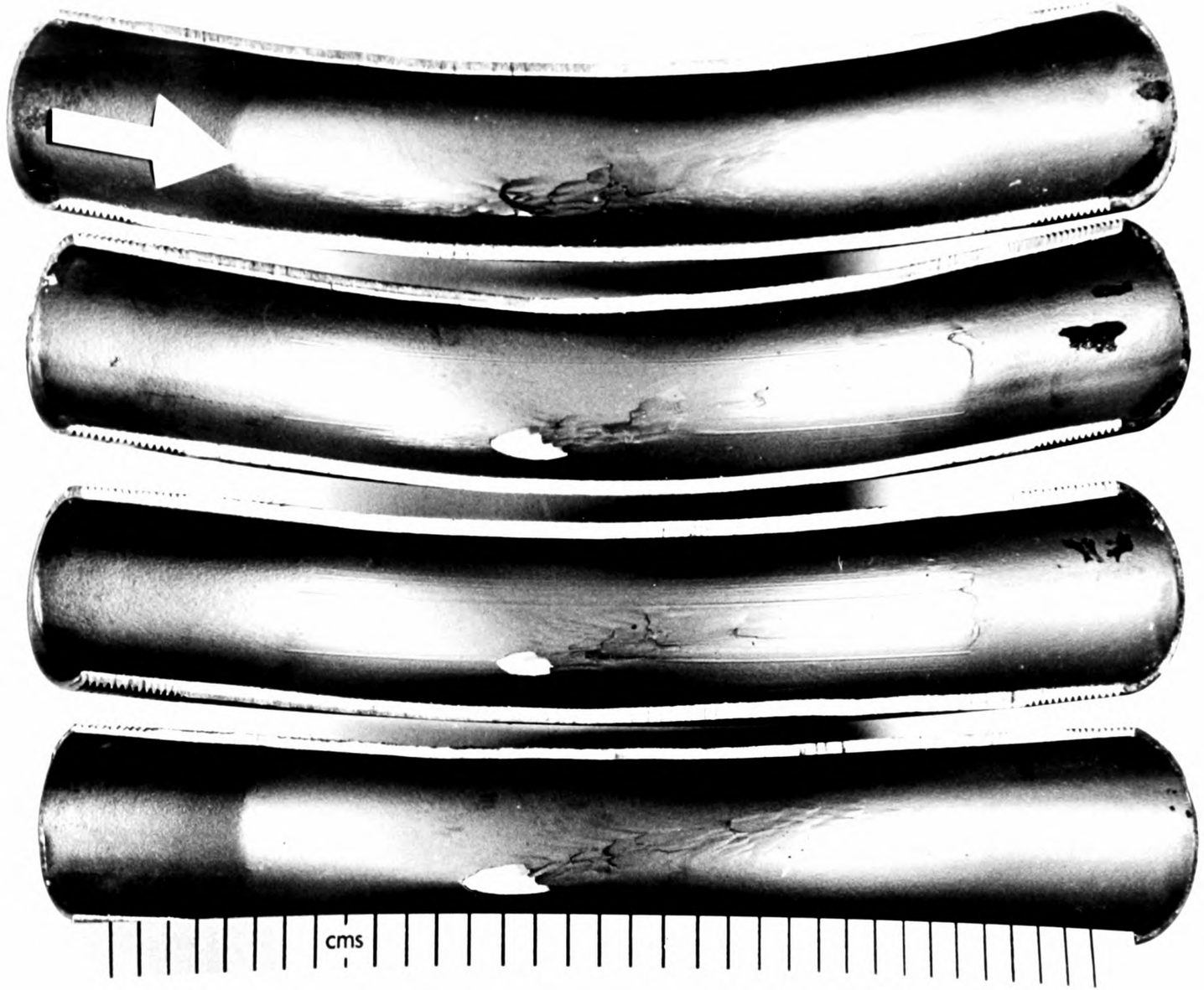
cms

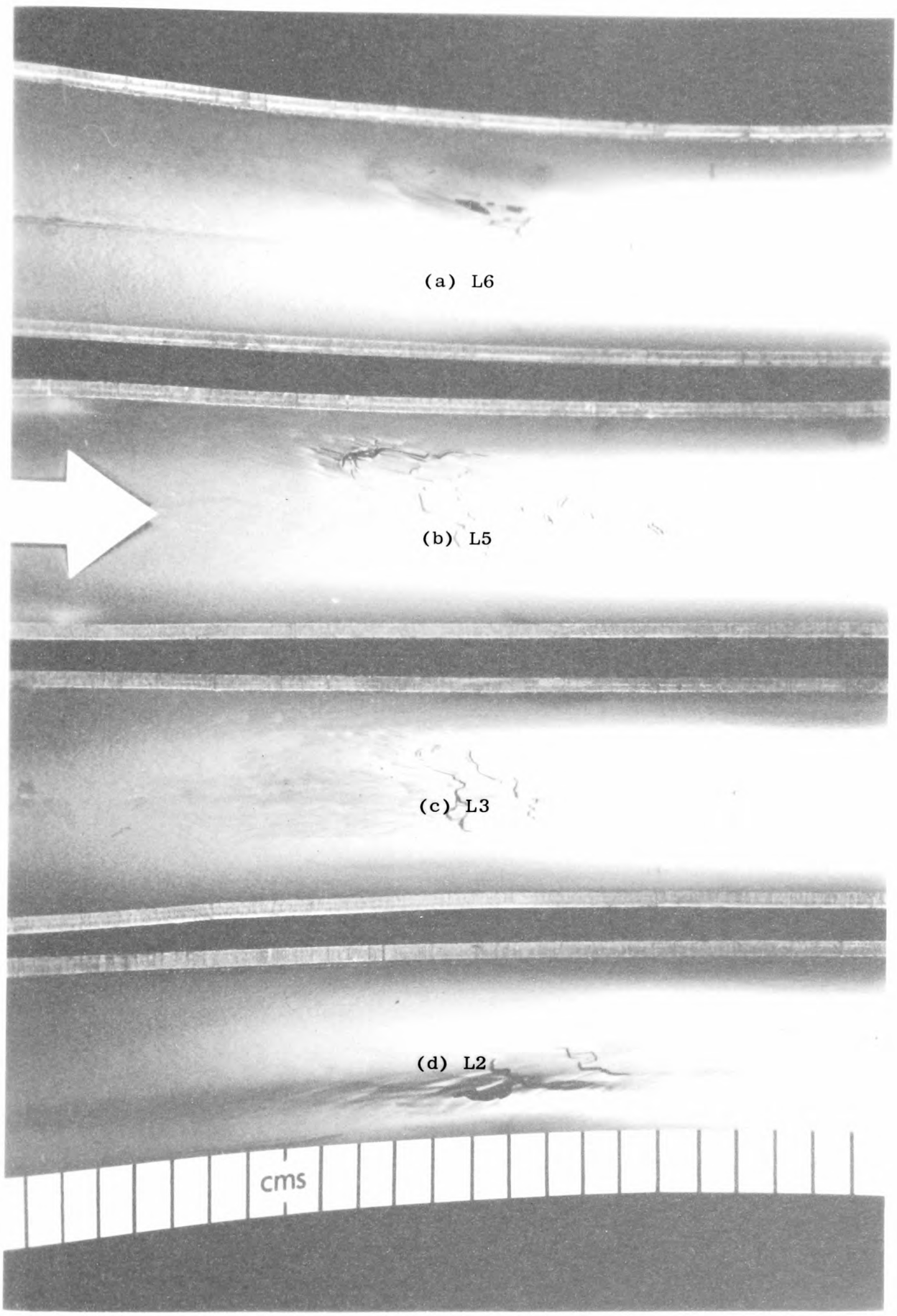

FIG. 8.25 Surface Erosion Patterns of Bends with D/d of 12

cms

is also observed, particularly in bends 6,5, and 2. With the exception of bend 5, which is attributed to misalignment, bends 6 and 2 failed after 14 and 17 runs and, when bend 6 was replaced, its replacement failed almost immediately; in fact, after 4 runs only. The lack of any substantial erosion tracking in bend 3 is probably due to its position in the test loops, which is 7 m away from the preceding bend. This particular bend was still in service after 20 runs. The corresponding erosion patterns of bends 7 and 4, and their replacement bends, are shown in the next chapter, in which the aspect of premature bend failures will be discussed in more detail.

Figs 8.26 and 8.27 are linear representations of the corresponding bend and pipe section wear profiles of Figs. 8.14 and 8.15. These show the effect of D/d on the magnitude of mass eroded and depth of penetration after a constant 6 runs. In both cases it can be clearly seen that, although the amount of mass eroded from the two larger bends are comparable in terms of penetration, an immediate rapid wear situation corresponding to the secondary wear stage is apparently well established in the intermediate bend after only a few runs. In fact, bend 3 failed after 6 runs, followed by bend 7 two runs later. By contrast, although the corresponding wear profiles for the elbows are concentrated over a smaller area, it can be seen that a distinct step is gradually being established at a bend angle of about 40^{o}. The large difference in the amount of mass eroded between the elbows and the long radius bends shown in Fig. 8.7 is explained by a correspondingly larger erosion trough for the larger bends. However, in terms of depth of wear, the lack of any substantial increase in penetration rate, particularly for the elbows, is explained by a correspondingly sharper wear profile which acts as a recess, thereby allowing some of the impacting particles to be embedded into the crater and hence preventing any further increase in penetration.

In general, the main feature in these two figures is that they show where an erosion crater is being established around the bend. In terms of bend angle the position of maximum wear and consequent failure appears to lie between 30^{o} to 40^{o} for all the bends tested in this work, and substantiate that it is independent of bend geometry. In terms of pipe angle, however, although there is no apparent distinct trend, it appears to vary over a wider range of pipe angles.

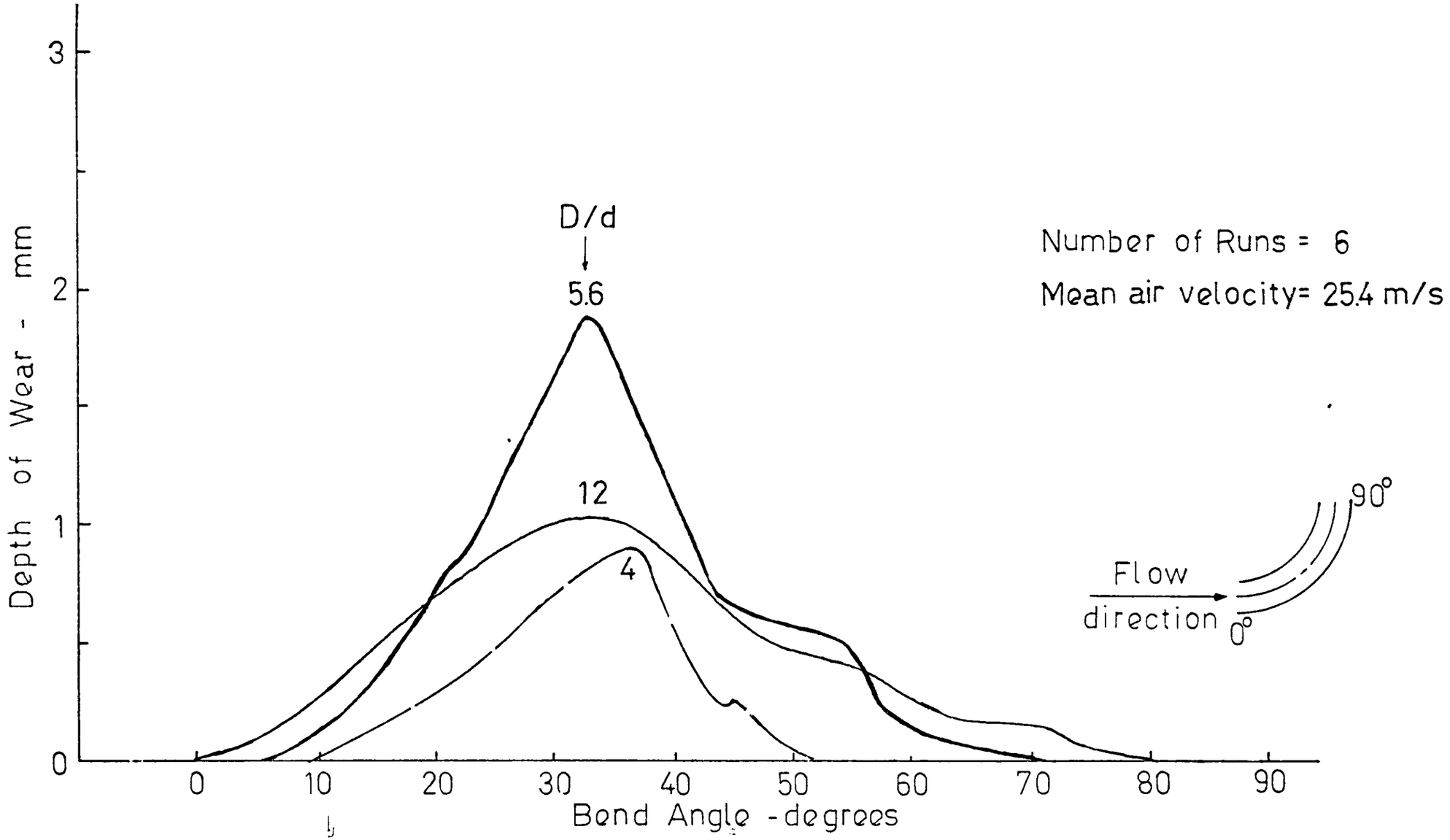

FIG. 8.26 **Influence of Diameter Ratio on Bend Wear Profile**

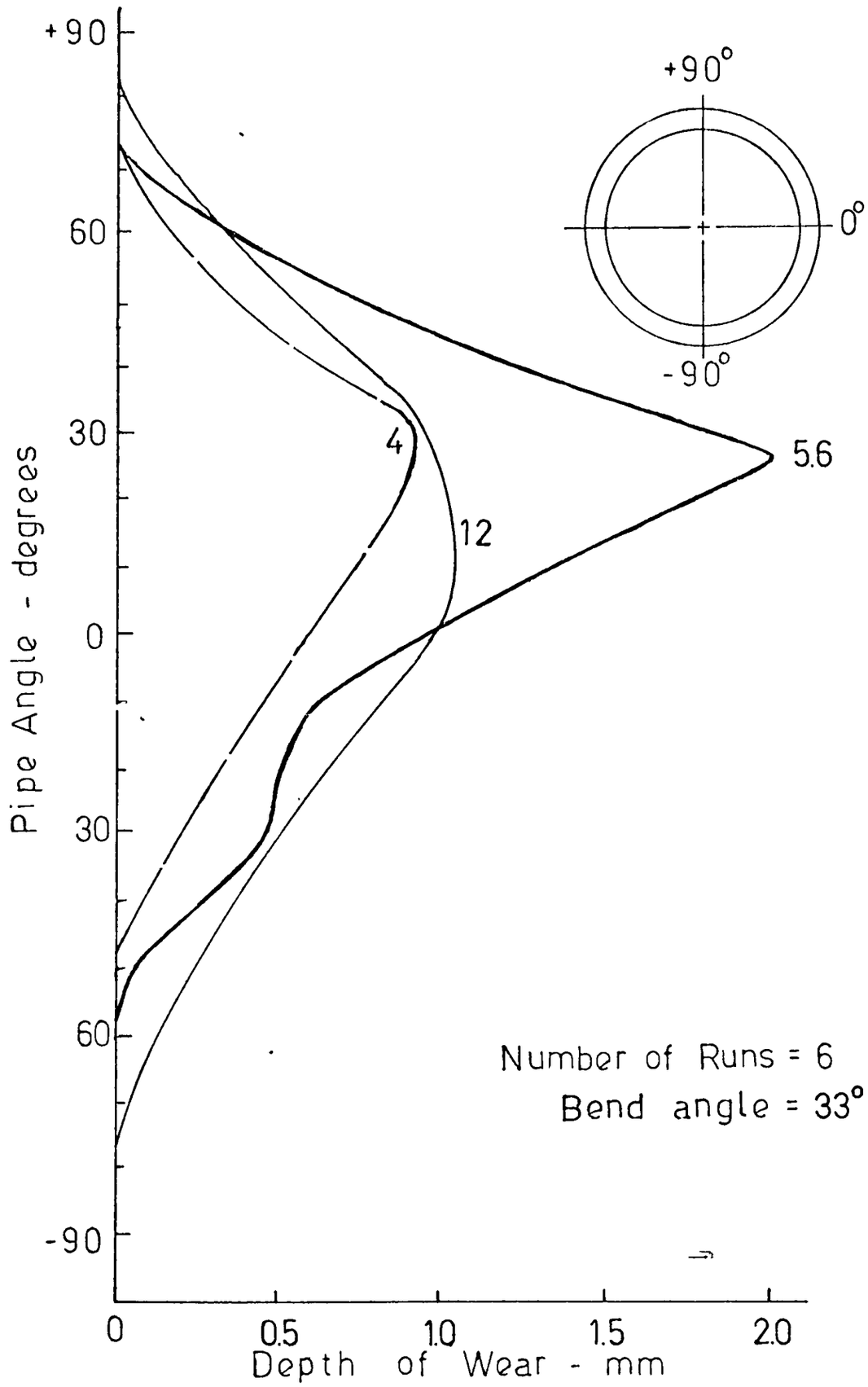

FIG. 8.27 Influence of Diameter Ratio on Pipe Wear Profile

8.5 CONCLUSIONS

The work presented here clearly demonstrates that bend radius, in terms of the D/d parameter, is a significant factor in bend erosion. From the experimental results definitive trends with regard to specific erosion and penetration wear rate have been established and, for the range of D/ds tested, a critical maximum is observed in bends with a value of D/d of about $5\frac{1}{2}$. The magnitude of both erosion and penetration have been shown to be depenent upon the inter-relating effects of bend radius and effective impact angle and both are at a maximum and coincide at this particular critical value of D/d. Hence, in order to avoid this rapid wear situation, for design purposes, the choice is to use either elbows or long radius bends. Although in terms of pressure drop, the preference is for long radius bends, the increased susceptibility to premature failure as bend radius is increased is also an important factor which must be taken into consideration.

A number of bends which failed prematurely in the course of each particular test series were replaced with similar sized bends. These replacement bends unexpectedly failed almost immediately, whilst the other original bends were still in service. The causes of this phenomenon of rapid failure of replacement bends, and its effect on bend life evaluation, are reported in the next chapter.

It has also been established that, to a certain extent, the effect of D/d can be predicted from a typical ductile erosion or penetration curve in terms of the influence of impact angle. However, the accuracy and reliability of these predictions are considerably dependent upon the inter-relating effect of particle trajectory.

Although the test conditions in this work are limited to one particular material and conveyed under constant conditions, it is unlikely that the critical value of D/d will vary substantially, since it has been shown by other workers that the effect of D/d on erosion and penetration is independent of velocity, phase density and particle size.

Chapter 9

Erosion of Replacement Bends

9.1 INTRODUCTION

One of the more prominent aspects of the work presented in the preceding chapter was the premature failure of bends. As reported in the previous chapters, premature failure of bends is a recurring feature in work of this nature, particularly when a number of bends are eroded simultaneously. Apart from its random nature, the likelihood of premature failure has been shown to be directly related to the degree of scatter of the results, and is dependent upon a critical combination of certain variables. Whilst the magnitude of the degree of scatter gives an indication of repeatability, it also indicates an element of unpredictability.

From the experimental results obtained in the course of the work on the effects of diameter ratio, an additional factor in the premature failure of bends which has not been investigated in previous erosion studies, is the effect of subsequent erosion on replacement bends A number of bends which failed prematurely were immediately replaced with similar sized new bends. As the other remaining original bends which were still in service had already been eroded to a considerable extent, it was expected that little erosion would be observed in these replacement bends. However this assumption was completely contradicted by the unexpected rapid failure of some of these replacement bends, which failed in an even shorter time period than the original bends which they were replacing. In tests with bends having a D/d of 5.6, the replacement bends failed in about half the time, and in the case of the long radius replacement bends, some failed even more rapidly (see Table 9.1).

Mills and Mason (1976 c) have analysed the various potential factors involved in the premature failure of bends such as phase density, velocity, particle size and shape, secondary flows, etc.. However, the problem of replacement bends was not considered and in the following sections a number of other factors which may be responsible for the phenomenon of rapid and premature failure of replacement bends are considered by the author.

9.2 FACTORS INVOLVED

As shown in Figs. 8.4 and 8.5 in the preceding chapter, the magnitude of the scatter of results for replacement bends in terms of the variation of

erosion with mass conveyed, is clearly demonstrated. Erosion data on the bends which failed has been presented in Table 5.3, and for comparison purposes, further detailed erosion and penetration data of all the individual bends which failed prematurely, and their respective replacement bends, is given in Table 9.1.

As reported previously, in tests with the elbows, bend 7 was the only bend which failed prematurely. The effect of subsequent erosion on replacement bends, however, was not realised at that time and so this particular elbow was replaced with a normal bend with a D/d of 5.6. As this replacement bend had been used in a previous test series it is not appropriate to equate the results of this replacement bend with the original replaced elbow and so only the data for the intermediate and long radius bends are presented in Table 9.1. In the following sections the potential factors involved in the rapid failure of replacement bends will therefore be mainly based on the basis of the intermediate and long radius bends data.

9.2.1 Effects of Particle Size and Shape

One of the major causes of premature failure reported by Mills and Mason (1976 c) is the inter-relating effects of particle size and shape. Although in terms of mass eroded, relatively fresh particles with a sharp, angular profile will cause more erosion than worn, rounded particles, in terms of depth of penetration the situation is markedly reversed (see Fig. 3.19). An additional inter-relating factor is the effect of particle degradation. As reported in the previous chapters, the degree of scatter is related to the magnitude of degradation of the particles. The resultant increase in the 'fines' combined with the effect of secondary flows, has been shown to be predominantly responsible for the premature failure of bends. In this work the percentage of 'fines' below 45 μm in tests with the elbows and long radius bends increased by a factor of about 1.4:1, whereas in tests with the intermediate bends it increased by a factor of about 1.8:1. Although this increase is not significiant, it should be noted that the sand was recirculated 26 times in tests with the elbows and 20 times for the long radius bends. For the intermediate bends the sand was recirculated only 13 times. In fact, as reported in Chapter 7, the percentage of 'fines' had already increased by a factor of about 1.5:1 after only 6 runs. The rapid failure of the replacement

D/d	Bend Number	No. of batches	Mass Eroded at Failure (g)	Mass Conveyed (tonne)	Conveying Time (h)	Specific Erosion (g/tonne)	Erosion Rate (g/h)	Maximum Depth of Penetration (mm)	Penetration Wear Rate (mm/tonne)	Penetration Rate (mm/h)
5.6	*3	6	51	4.10	5.33	12.44	9.57	3.9	0.95	0.73
	*3R	4	45	2.72	3.93	16.54	11.45	3.9	1.43	0.99
	3RR	3	+34	2.25	3.38	15.11	10.06	2.5	1.11	0.74
	*7	8	58	5.62	8.00	10.32	7.25	4.0	0.71	0.50
	*7R	5	42	3.37	4.97	12.46	8.45	3.3	0.98	0.66
12	*2	17	88	12.50	16.75	7.02	5.25	3.3	0.26	0.20
	2R	3	+36	2.25	3.03	16.00	11.88	1.5	0.67	0.50
	*4	14	81	9.99	13.43	8.11	6.01	3.2	0.32	0.24
	*4R	5	62	3.63	4.18	17.08	14.83	3.2	0.88	0.77
	4RR	1	+23	0.75	1.03	30.67	22.33	1.0	1.33	0.97
	*6	14	80	10.35	13.88	7.73	5.76	3.4	0.33	0.24
	*6R	4	60	2.55	3.38	23.53	17.75	3.4	1.33	1.01
	6RR	2	+44	1.50	2.03	29.33	21.67	1.8	1.20	0.89
	*7	7	73	4.60	6.38	15.87	11.44	3.2	0.70	0.50
	7R	13	+66	9.75	12.82	6.77	5.15	2.1	0.22	0.16

*Failed

+Total Mass Eroded

TABLE 9.1 Comparisons between the Prematurely Failed Bends and Replacement Bends

bends in tests with the intermediate bends, is attributed by the author to this particularly large increase in the 'fines', which are more susceptible to the secondary flows induced in these types of bends.

9.2.2 Effect of Bend Position

As reported in Chapter 4, in tests with the elbows and the intermediate bends, the test section in both cases was identical. It consisted of a double loop in a rectangular configuration. The random nature of the failure of bends and the comparability of the individual results confirmed that bend position was not a likely source of premature failure in both cases. However, in the case of the long radius bends, the data in Table 9.1 clearly shows that bend position is a major contributing factor. With the exception of bend 7, bends 2, 4 and 6 were sited in close proximity to the preceding bends, which were bends 1, 3 and 5 (see Fig. 4.7). Whilst bends 2, 4 and 6 failed in the course of this test series, bends 1, 3 and 5 were still in service. As explained in section 4.4, the dimensions of this new test loop were restricted by both minimum acceleration length requirements and available laboratory space limitation considerations.

From an expression given by Rose and Duckworth (1969), a minimum length of 2.3 m was considered adequate for fully established flow to be achieved, based on the given test conditions. As the minimum distance in this particular test configuration is 3 m between bends 5 and 6, it would appear that all the bends are sufficiently far apart for the particles to be fully accelerated from rest to the average conveying velocity before entering the next bend. A similar acceleration length of about 3 m was also reported to be adequate by several workers (Ito 1960, Barth 1962, Ghosh and Kalyanaraman 1970, Marcus et al 1976). However, the results obtained in Table 9.1 show that, in terms of erosion, this length is clearly inadequate. By normalising the individual results to a velocity of 25 m/s, and by summing and averaging these individual normalised values, the data based on bends 2, 4 and 6 is some 40% greater than those based on bends 1, 3, 5 and 7. The large difference between these two sets of data clearly shows that bend position is a significant factor in premature failure of bends only if the bends are sited in close

proximity to each other. To a large extent the magnitude of this effect is also considerably influenced by the inter-relating effect of secondary flows, which is considered in the next section.

9.2.3 Effect of Secondary Flows

Of all the factors involved in the premature failure of bends, Mills and Mason (1976 c) have identified that the predominant cause is due to the presence of secondary flows in the bends. A characteristic feature of all the bends which failed prematurely was the pronounced tracking of the pattern across the surface of the bend. This characteristic erosion pattern has also been observed in all the bends which failed prematurely in the course of this work. Apart from Figs. 8.23 to 8.29, Fig. 9.1 shows the erosion pattern of two more long radius bends which failed (bends 4 and 7), and their replacement bends (4R and 7R).

In tests with the long radius bends, as mentioned earlier, it has been shown that the position of the bend is also a significant factor. The pronounced erosion tracking pattern in each of the bends which failed (bends 2, 4 and 6) provides clear evidence of swirling in the flow in these bends. Although it is well established that the nature of gas-solid suspension flow in a duct is basically turbulent, it has generally been estimated that about 40 to 50 pipe diameters is adequate for the turbulence to be fully developed (Boothroyd 1971). However, an additional factor which must also be taken into consideration is the effect of bends. This relates to the fact that large scale secondary flows which are induced in the bends may persist for some considerable distance along the downstream of the straight section before the flow is fully developed again (Mason and Smith 1973). Although the presence of 'fines' may dampen the turbulence to a certain extent (Boothroyd 1971, Mason and Boothroyd 1971), it has been reported by Pfeffer and Kane (1974), based on a number of drag reduction studies, that this presence of 'fines' in the suspension does not produce a general suppression of the turbulence as expected. The surface erosion patterns of this set of bends (2,4 and 6) clearly substantiates the presence of a considerable degree of turbulence in the flow well before entering the bends.

The presence of turbulence in these long radius bends has the additional

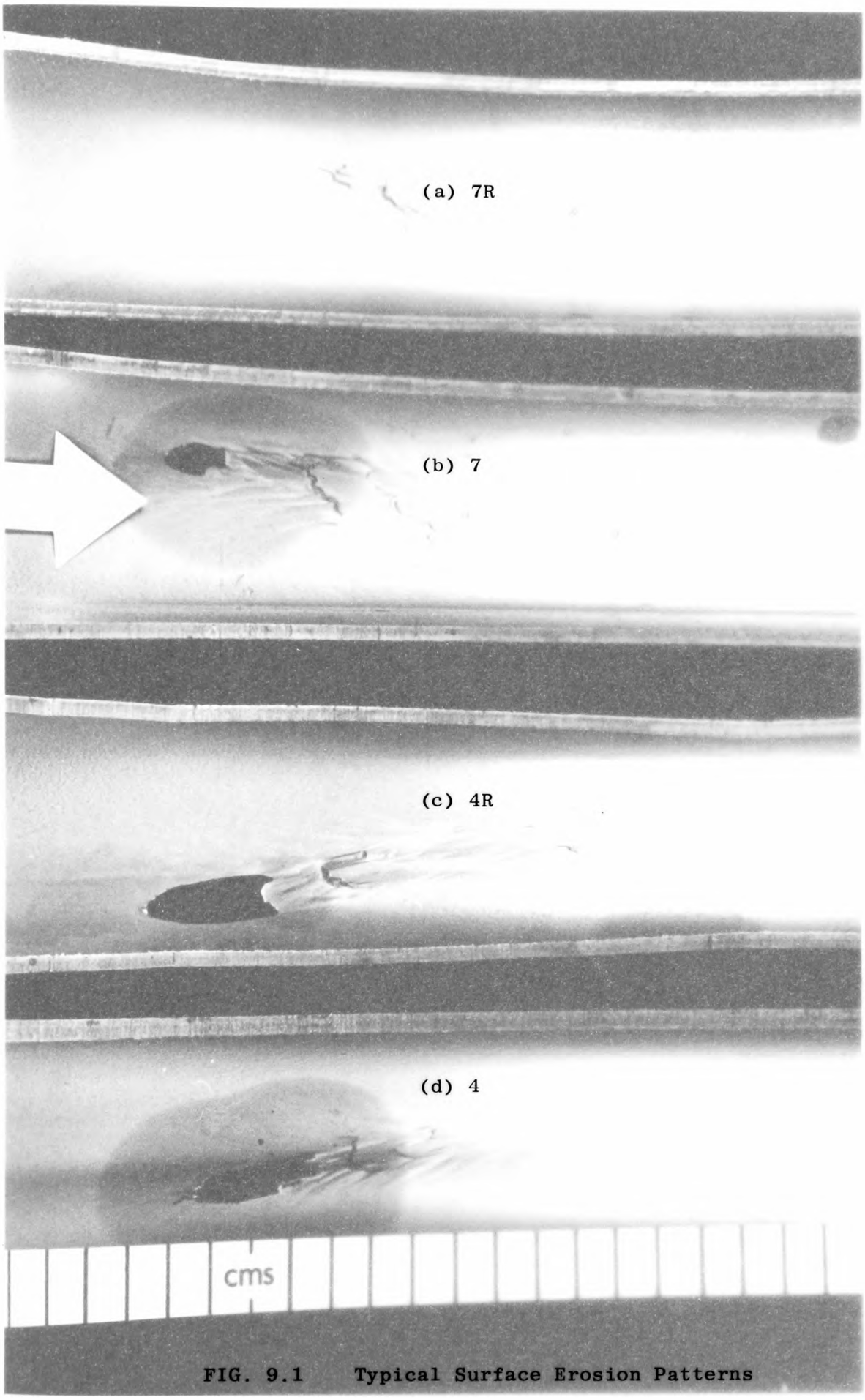

FIG. 9.1 Typical Surface Erosion Patterns

cms

effect of lowering the velocity of the particles in these bends considerably. It would be expected, therefore, that less mass would be eroded from these bends. However, Table 9.1 clearly shows that an average of about 83 g was eroded at failure for this set of bends, compared to 73 g for bend 7 and about 58 g for bends 1, 3 and 5. The higher value is probably explained by a correspondingly higher value of velocity exponent which has been observed at low velocities by Goodwin et al (1969) and attributed to transitional effects by Mills and Mason (1976 b). Above the transition velocity the bends would be eroded normally, but below the transition little wear is observed. Mills and Mason found that if tests are carried out on either side of the transition, almost any value of the exponent could be obtained. The consistently higher amount of mass eroded from this particular set of bends appears to indicate that it is considerably influenced by this transitional effect with a resultant higher velocity exponent.

In tests with the elbows, the surface erosion patterns in Fig. 8.23 show the presence of a considerable degree of swirling in the flows. Glatzel (1977) carried out tests on a range of elbows and reported that a considerable turbulence intensity is generated in these tight elbows. He attributed this to the severe multiple inter-particulate collisions between the impacting and rebounding particles observed in the elbows and consequently explained that the lack of any substantial increase in the amount of mass eroded compared with that obtained for the larger bends was partly due to this effect.

9.2.4 Effect of Effective Impact Angle

As shown in section 8.4.5, the magnitude of erosion in terms of specific erosion and penetration wear rate, is dependent upon the inter-relating effects of the D/d ratio and effective impact angle. In tests with the intermediate bends the rapid failure of the replacement bends (3R abd 7R) can be explained by considering the wear profiles shown in Fig. 8.14, together with the curves presented in Fig. 8.16. It can be seen that after 6 runs the effective impact angle has progressively increased from the primary wear stage to beyond the secondary wear state. When the replacement bends were introduced into the test section, the initial effective impact angle of these new replacement bends corresponds to the primary wear stage,

i.e. maximum erosion. However, due to the condition of the particles, which is fairly degraded and worn after a number of runs, the amount of mass eroded from these replacement bends is considerably less than the original bends which they were replacing. As an erosion crater is being created, the effective impact angle rapidly increases for secondary wear to occur. In the meantime, the effective impact angle for the other remaining original bends has already increased to the tertiary wear stage, corresponding to a decrease in both erosion and penetration. Due to the condition of the product, a rapid increase in penetration rate is observed in these replacement bends at the secondary wear stage and, as a result, these replacement bends failed even more rapidly (Table 9.1).

A similar rapid failure rate is also observed in the case of the long radius replacement bends, although the corresponding increase in effective impact angle is not as large compared to the intermediate bends. However, this is compensated by the presence of considerable turbulence in these long radius replacement bends as mentioned earlier. For the elbows, although no replacement elbow data is available, a similar situation corresponding to the intermediate bends case would be observed, although it would not be expected to fail so rapidly, due to the over-riding effectsof bend radius and turbulence intensity.

9.2.5 Other Factors

The factors which are primarily responsible for the premature failure of bends, discussed by Mills and Mason (1976 c), are operative in every case. In the rapid failure of replacement bends, therefore, the other factors, apart from bend radius (see section 8.4.3.1) such as moisture content and particle hardness, are not expected to have any significant effect.

To a considerable extent all the factors discussed in the preceding sections are inter-related and inter-dependent. As mentioned previously, due to these complex inter-relationships and the difficulty involved in isolating each respective variable, no attempt had been made to quantify to what extent each factor is responsible, suffice to say that all the factors are involved in one way or another in the premature failure of bends. An additional factor which must also be taken into account, associated with premature failure, is an element of

unpredictability. If a bend shows clear evidence of the characteristic tracking of erosion patterns across its surface, it can be conclusively ascertained that this bend is likely to fail prematurely.

As premature failure of bends is an important factor which must be taken into consideration by the pneumatic conveying engineer, further research into the specific effect of each variable is obviously needed. The need for further research is reinforced by the work shown in the preceding chapter, which shows an additional factor due to the rapid failure of some of the replacement bends.

As bends are a common feature of pneumatic conveying systems, in a practical situation a number of bends may be located close to each other. A starting point for further work is perhaps on the inter-relating effects of bend position and secondary flows. By designing a single test section with varying length it would be possible to incorporate a number of test loops with an adjustable positioning of bends. This arrangement would allow the inter-relating effects of bend position and secondary flows to be investigated properly. By careful selection of the test conditions it would be possible to control the test conditions effectively and provide detailed experimental data on the phenomenon of rapid failure in replacement bends. Although Mills and Mason (1976 c) have analysed the various potential factors involved in the premature failure of bends, it has been shown that this is a recurrent feature in this programme of work and, to a certain extent, is unavoidable when a number of bends are eroded simultaneously.

9.3 EFFECT ON BEND WEAR RESULTS

The magnitude of the effect of premature failure of bends, particularly the rapid failure of some of the replacement bends, on the overall bend performance data is clearly evident by comparing the individual test data presented in Table 8.1 (pages 176 to 178) and Table 9.1.

For instance, an extreme example is to consider the individual data of the two intermediate bends, i.e. bends 1 and 3R. For comparison purposes in terms of service life of the bends, it is the individual penetration rate in terms of mm/h of these two bends that is of interest. The individual penetration rate for bend 1 (Table 8.1) is approximately 0.09 mm/h and for bend 3R (Table 9.1) it is 0.99 mm/h. The magnitude of penetration for

the replacement bend is some ten times greater. In terms of bend life, therefore, for a constant thickness of 4 mm, bend 3R will fail in about 4 hours as confirmed by the actual results, whereas bend 1 is not expected to fail until after some 40 hours. A similar order of magnitude is also observed in the case of the long radius bends when the individual test data of bends 3 and 6R are compared.

The individual replacement bend values presented in Table 9.1 are based on the corresponding number of runs per respective replacement bend. As there is a large variation in the number of runs between these replacement bends, it was not possible to evaluate this individual test data based on a common factor of 6 runs, as in the case of the original bends. Hence, for comparison purposes it was decided by the author to consider the mean values based on four separate sets of test data, corresponding to the four erosion and penetration parameters, as presented in Table 9.2. In this table the mean value in set A is calculated on the basis of the individual results of the seven original test bends at the end of each particular test series (see Table 8.1 for individual test data).

The corresponding mean value in set B is also based on the individual test data of these seven original bends. However, the mean value calculated is based on a common factor of 6 runs or test set 2.

As no replacement elbow data is available in tests with the elbows, the mean value obtained in set C refers to the mean of the individual results of all the respective replacement bends in tests with the intermediate and long radius bends only.

Since the corresponding mean values in sets A and B are comparable, the effect of replacement bends on the overall bend performance is given in set D. This is based on the individual test results of all the bends at the end of each test series. For the intermediate bends this would include the individual test data for bends 3R, 3RR and 7R, and for the long radius bends the data of bends 2R, 4R, 4RR, 6R, 6RR and 7R. In the case of the elbows, the corresponding mean values in set D would be identical to set A.

Since the trend of the data, in terms of specific erosion and erosion rate, is similar, Fig. 9.2 shows the influence of replacement bends on the overall result in terms of specific erosion only. Fig. 9.3 similarly shows the effect in terms of penetration wear rate only.

TABLE 9.2 Influence of the Erosion and Penetration Rates of Replacement Bends on the Overall Results

Mean Value at each Set of Data	Diameter Ratio - (D/d)		
	4	5.6	12
Specific Erosion (g/tonne)			
A	1.88	6.88	7.18
B	2.48	7.30	7.24
C	-	14.70	20.56
D	(1.88)	9.23	13.36
Erosion Rate (g/h)			
A	1.33	4.92	5.31
B	1.82	5.19	5.24
C	-	9.99	15.60
D	(1.33)	6.44	10.60
Penetration Wear Rate (mm/tonne)			
A	0.17	0.42	0.29
B	0.17	0.37	0.21
C	-	1.17	0.94
D	(0.17)	0.64	0.59
Penetration Rate (mm/h)			
A	0.12	0.30	0.22
B	0.13	0.26	0.15
C	-	0.80	0.72
D	(0.12)	0.45	0.45

Note:- 'A' denotes the set of data based on the original seven test bends at the end of each test series.

'B' as in 'A' but is based on the individual test data after 6 runs.

'C' denotes the set of data based on the replacement bends only.

'D' denotes the set of data based on all the test bends in each test series.

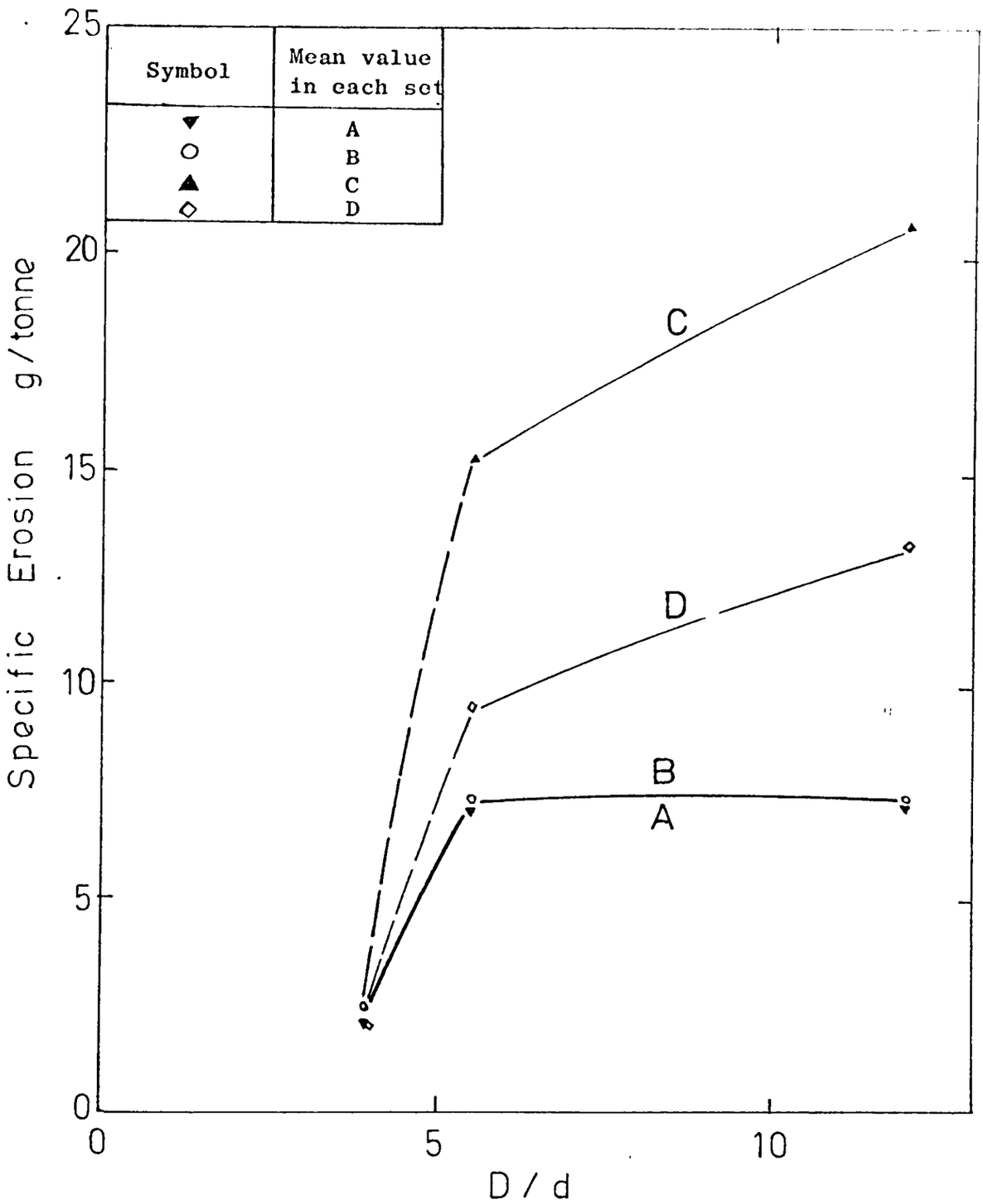

FIG. 9.2 Influence of Replacement Bends on the Variation of Specific Erosion with Diameter Ratio

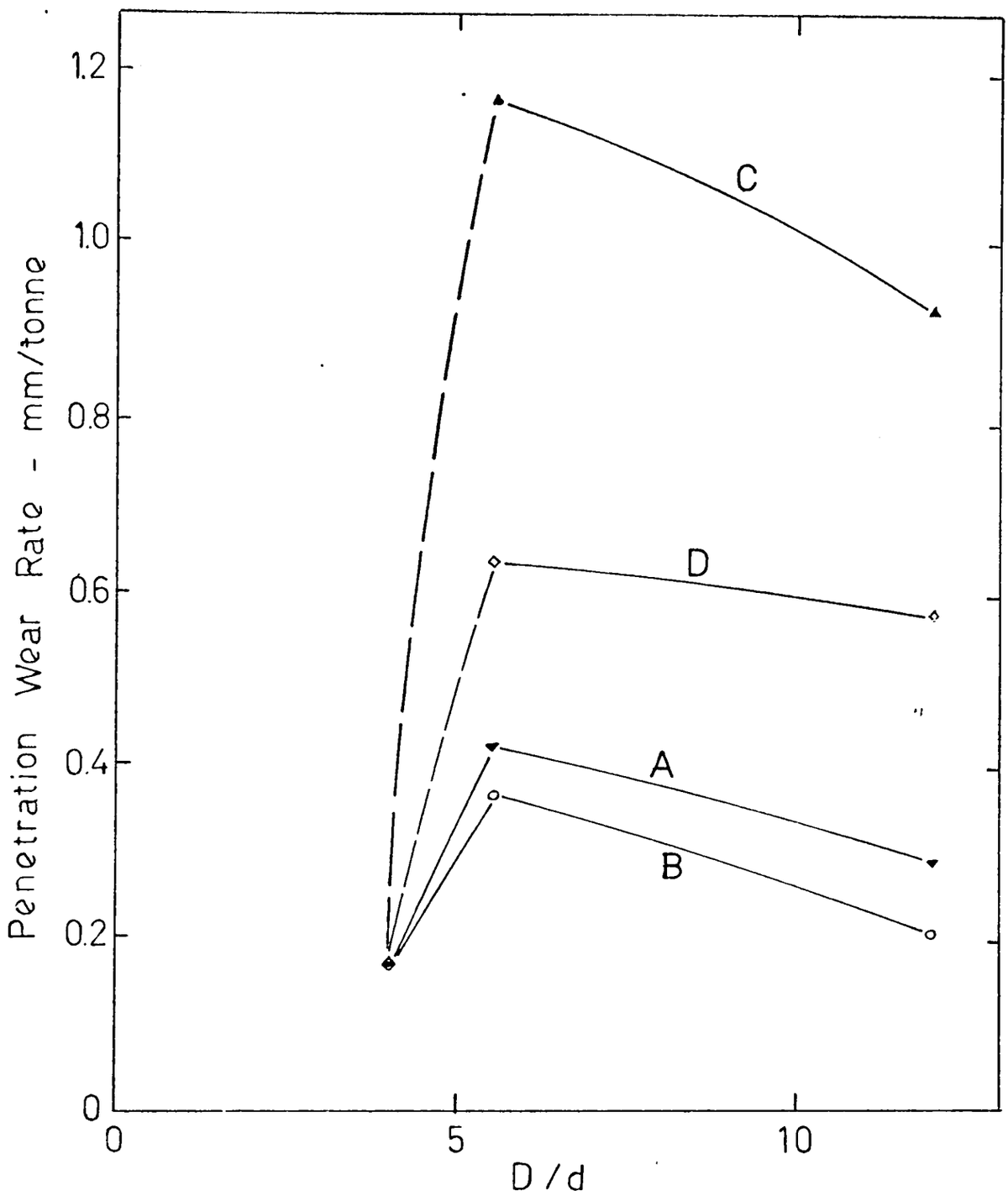

FIG. 9.3 Influence of Replacement Bends on the Variation of Penetration Wear Rate with Diameter Ratio

9.3.1 Specific Erosion Results

The magnitude of the influence of replacement bends on the overall performance of bends, in terms of specific erosion, is clearly demonstrated by the curves in Fig. 9.2. Apart from the trend of these curves, an additional feature of interest is with regard to the set of results in curves A and B. As mentioned in the preceding section, the mean set of values in curve A is based on the individual test results at the end of each particular test series, whilst the corresponding set of values in curve B is based on the results after 6 runs only. The close similarity of these two sets of data indicates that, in spite of the large degree of variation in individual values, the mean rate of erosion appears to stabilise after 6 runs, from which it then gradually decreases at a constant rate.

Taken individually, the order of magnitude of the erosion of replacement bends is clearly illustrated by curve C. Comparison of the data presented in Table 9.2 shows that a 3-fold increase in the mean specific erosion rate is obtained for the long radius replacement bends. In the case of the intermediate replacement bends a corresponding 2-fold increase is similarly observed. In terms of the overall effect, the order of magnitude is much lower, with an increase by a factor of about 1.8:1 for the long radius bends and about 1.3:1 for the intermediate bends. The consistently higher rate of increase for the long radius bends is largely due to the larger mass eroded as a result of the inter-relating effect of bend position and turbulence, as explained in sections 9.2.2 and 9.2.3 earlier. Although the net effect is an increase in the overall mean value (curve D), the trend of all the curves clearly indicates the existence of a threshold value of D/d in terms of specific erosion, and this value is around 5.6.

9.3.2 Penetration Wear Rate Results

A central feature of the curves in Fig. 9.3 is the pronounced maximum corresponding to a D/d value of about 5.6. In both figures it can be seen that the magnitude of the curves is dependent upon its D/d ratio and the different effect of the high erosion and penetration rates of replacement bends on the overall results is clearly demonstrated by the contrast in the trend of the curves. Whilst curve C

in Fig. 9.2 shows that erosion increases as the value of the D/d ratio is increased, the same curve in Fig. 9.3, in terms of penetration wear rate, shows a markedly reversed trend.

In terms of individual mean values, the increase in the order of magnitude due to the intermediate replacement bends is considerably lower than those due to the long radius replacement bends. Comparison of the mean set of values (curves A and C)shows that a similar 3-fold increase is observed when the individual penetration data of all the replacement bends in both sets of bends are considered. In terms of overall effect, however, an increase by a factor of about 1.5:1 is observed in the case of the intermediate bends, compared to a 2-fold increase in the case of the long radius bends.

The information presented in Tables 9.1 and 9.2 and Figs. 9.2 and 9.3 clearly has important implications for the pneumatic conveying system designer. Although, in a practical situation, a bend which fails is usually replaced immediately, the results obtained in this work on the erosion of replacement bends clearly show that this particular replacement bend is likely to fail again, and at a faster rate. It is perhaps surprising that, whilst the factors involved in the mechanics of the erosion process in pipe bends have been extensively investigated, virtually no information is available regarding the phenomenon of rapid failure of replacement bends. The experimental data obtained by the author in this work clearly provides an important source of information on the specific effect of the rapid rates of erosion and penetration of replacement bends. However, as mentioned earlier, further work is needed in order to quantify the net effect of all the factors involved in the rapid failure of replacement bends.

9.4 BEND LIFE ANALYSIS

In Chapter 8 the influence of bend radius, in terms of the D/d parameter, on erosion has been discussed. From the experimental results obtained, the curves presented in Figs. 8.7 and 8.12 show a definite trend with regard to specific erosion and penetration wear rates. In both cases over the range of D/ds tested, a critical maximum is observed in bends with a D/d ratio of about 5.6.

However, as reported in the preceding sections in this chapter, an additional inter-relating factor which must also be taken into consideration in the analysis of bend performance is the phenomenon of rapid failure of replacement bends. Figs. 9.2 and 9.3 clearly show that the rapid erosion of these replacement bends can have a significant effect on the magnitude of the overall results. Hence, in order to take into account the rapid erosion of replacement bends, the calculation procedure is separated into two parts.

In section 9.4.1 the analysis is solely based on the test data of the original seven test bends. As in previous bend life analyses, the set of results is based on a relatively fresh batch of materials and so, for the purpose of evaluation, the mean values in set B (Table 9.2) are taken.

In section 9.4.2 the calculation is based on the corresponding mean values in set D (Table 9.2). In this particular set of values the erosion data of all the replacement bends is included and so the following bend life analysis will include the effect of the subsequent rapid erosion of these replacement bends on the overall results. On this basis, the effect of D/d in terms of the overall bend performance could be assessed, and compared with those based on the original test data only.

9.4.1 Data Based on Original Test Bends

Fig. 9.4 is a log plot of the corresponding specific erosion data in Fig. 9.2. The relevant set of mean values (curve B) is represented by the thick solid line in this log plot. It can be clearly seen that there is a distinct change in the slope over this range of test D/ds and, for the purpose of this analysis, as the magnitude of these two slopes is substantially different, it was decided by the author to consider these two separate slopes individually, i.e. between the range of D/ds from 4 to 5.6 and from 5.6 to 12.

From a linear regression analysis of the relevant separate sets of test data, the variation of specific erosion (ε) with D/d is given by:-

$$\varepsilon_1 = 0.03\ (D/d)^{3.21} \quad \text{g/tonne} \qquad (9.1a)$$

for $4 \leq D/d \leq 5.6$, and

$$\varepsilon_2 = 7.41\ (D/d)^{-0.01} \quad \text{g/tonne} \qquad (9.2a)$$

for $5.6 \leq D/d \leq 12$.

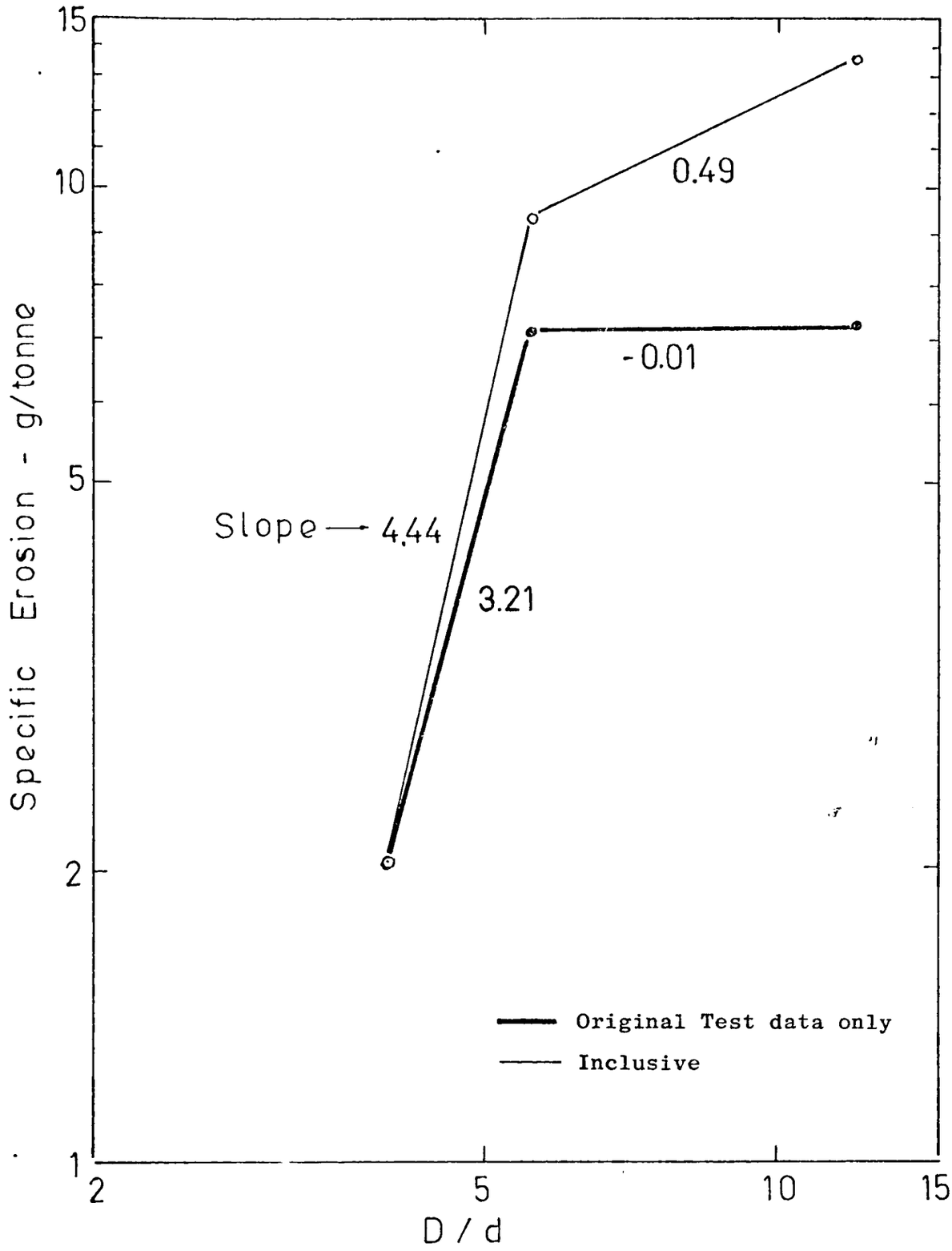

FIG. 9.4 Variation of Specific Erosion with Diameter Ratio

In both cases the subscripts 1 and 2 denote the appropriate range of D/ds considered.

As in previous bend life analyses, the relationship between the mass eroded at failure (E_{bf}) and D/d is required for the purpose of determining the conveying capacity of bends. Details of all the bends which failed have been presented in Table 5.3 (page 77), and Fig. 9.5 is a log plot of the relevant test data. The vertical line indicates the upper and lower limits and the location of the symbol its mean value. Subject to a certain degree of variation, these individual sets of plots appear to lie within a fairly straight narrow band. In this figure the original test data is represented by the thick solid plots, and the slope of these plots is approximately 0.61 over this range of D/ds tested. Hence, the variation of E_{bf} with D/d can be given by :-

$$E_{bf} = 18.2\ (D/d)^{0.61} \quad g \qquad (9.3a)$$

The mass of sand that can be conveyed before failure occurs (M_s) is given by :-

$$M_s = \frac{E_{bf}}{\varepsilon}$$

Substituting the appropriate (ε) denominator term gives -

$$M_{s1} = 627.6\ (D/d)^{-2.60} \text{ tonne} \qquad (9.4a)$$

for $4 \leq D/d \leq 5.6$, and

$$M_{s2} = 2.46\ (D/d)^{0.62} \quad \text{tonne} \qquad (9.5a)$$

for $5.6 \leq D/d \leq 12$.

Graphical representations of these two expressions are given in Fig. 9.6. These curves are identified by the corresponding equation numbers.

In terms of bend life, the conveying time to failure ($\Delta\tau$) is given by :-

$$\Delta\tau_{bf} = \frac{M_s}{\dot{m}_s} = \frac{M_s}{\phi\ \dot{m}_a} \quad h$$

Substituting the appropriate (M_s) numerator term gives :

$$\Delta\tau_{bf1} = 853.5\ (D/d)^{-2.60} \quad h \qquad (9.6a)$$

for $4 \leq D/d \leq 5.6$, and

$$\Delta\tau_{bf2} = 3.35\ (D/d)^{0.62} \quad h \qquad (9.7a)$$

for $5.6 \leq D/d \leq 12$.

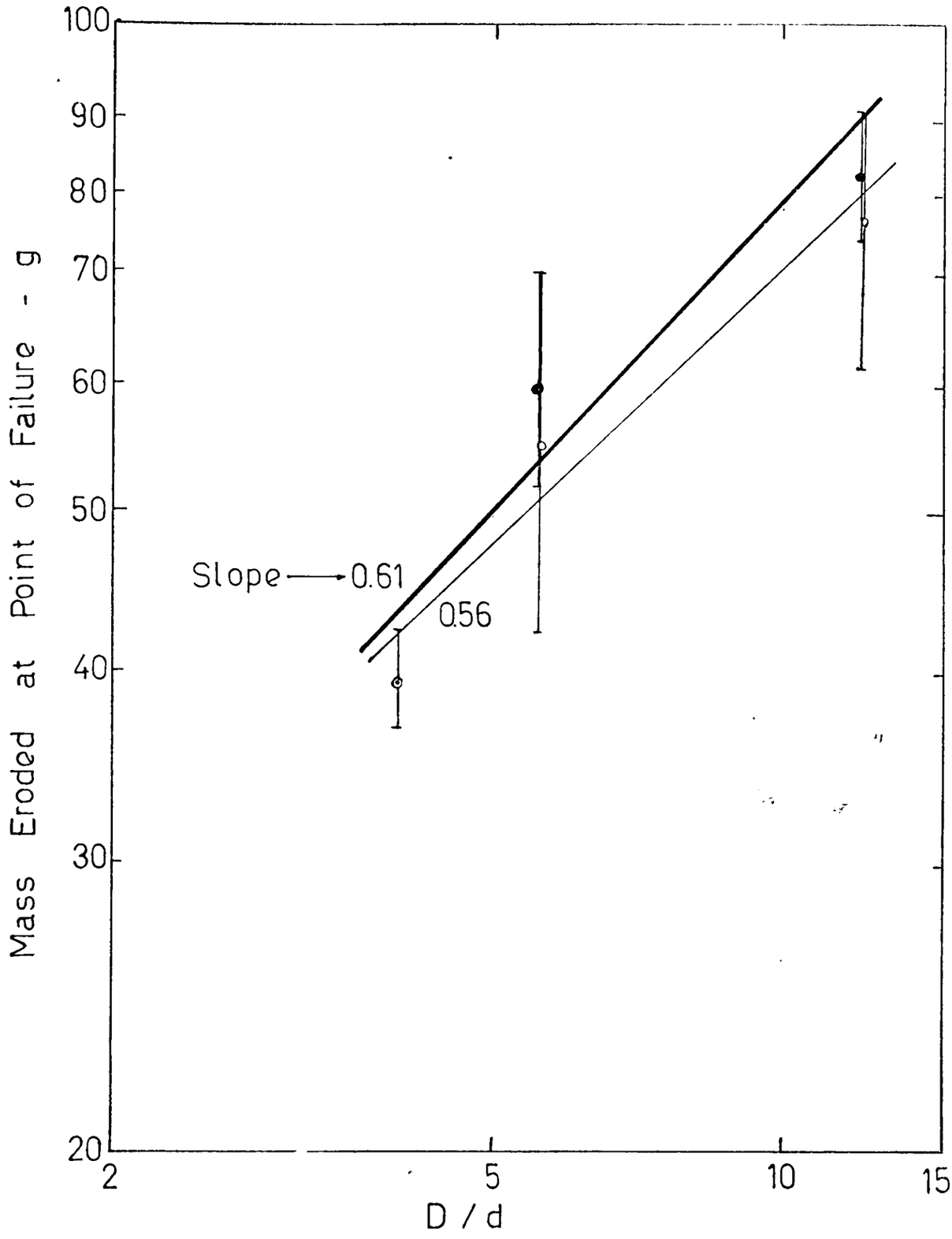

FIG. 9.5 Variation of Mass Eroded at Failure with Diameter Ratio

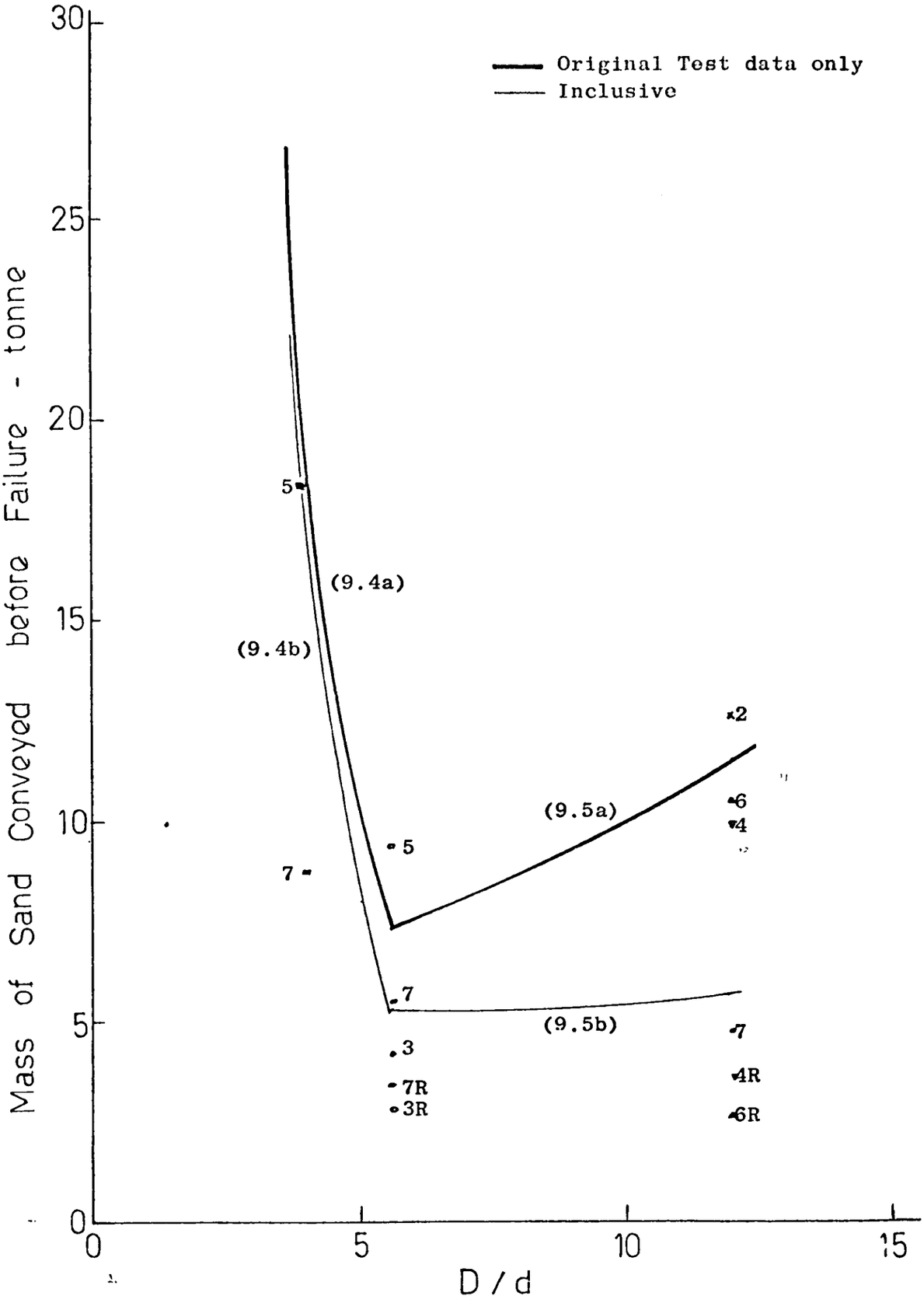

FIG. 9.6 Influence of Diameter Ratio on the Conveying Capacity of Bends

Graphical representations of these two expressions are given in Fig. 9.7. These curves are identified by the corresponding equation numbers.

9.4.2 Data Based on All Test Bends

A log plot of the relevant sets of mean specific erosion data, based on all the test bends in each test series, is also presented in Fig. 9.4. A similar distinct change in the slope is also observed as indicated by the thin solid line, and a similar separate set of analysis is also adopted in this section.

A linear regression analysis of the appropriate set of values shows that :-

$$\varepsilon_{1T} = 0.004\ (D/d)^{4.44} \quad \text{g/tonne} \qquad (9.1b)$$

for $4 \leqslant D/d \leqslant 5.6$, and

$$\varepsilon_{2T} = 3.98\ (D/d)^{0.49} \quad \text{g/tonne} \qquad (9.2b)$$

for $5.6 \leqslant D/d \leqslant 12$.

In both cases the subscripts 1 and 2 denote the similar separate range of $\bar{D}/ds$ considered as in the previous section, and T denotes the data is based on the overall results.

In Fig. 9.5 the thin vertical line of plots shows the upper and lower limits of all the bends which failed in each test series. Apart from a wider degree of variation, the slope of these individual plots can also be represented by a thin solid line as shown, with a gradient of approximately 0.56 over this range of D/ds tested.

The variation of mass eroded at failure (E_{bf}) with D/d can therefore be given by :-

$$E_{bfT} = 19.1\ (D/d)^{0.56} \quad \text{g} \qquad (9.3b)$$

Hence, the mass of sand that can be conveyed before failure occurs, (M_{sT}) is :-

$$M_{s1T} = 4762.5\ (\bar{D}/d)^{-3.88} \quad \text{tonne} \qquad (9.4b)$$

for $4 \leqslant D/d \leqslant 5.6$, and

$$M_{s2T} = 4.79\ (D/d)^{0.07} \quad \text{tonne} \qquad (9.5b)$$

for $5.6 \leqslant D/d \leqslant 12$.

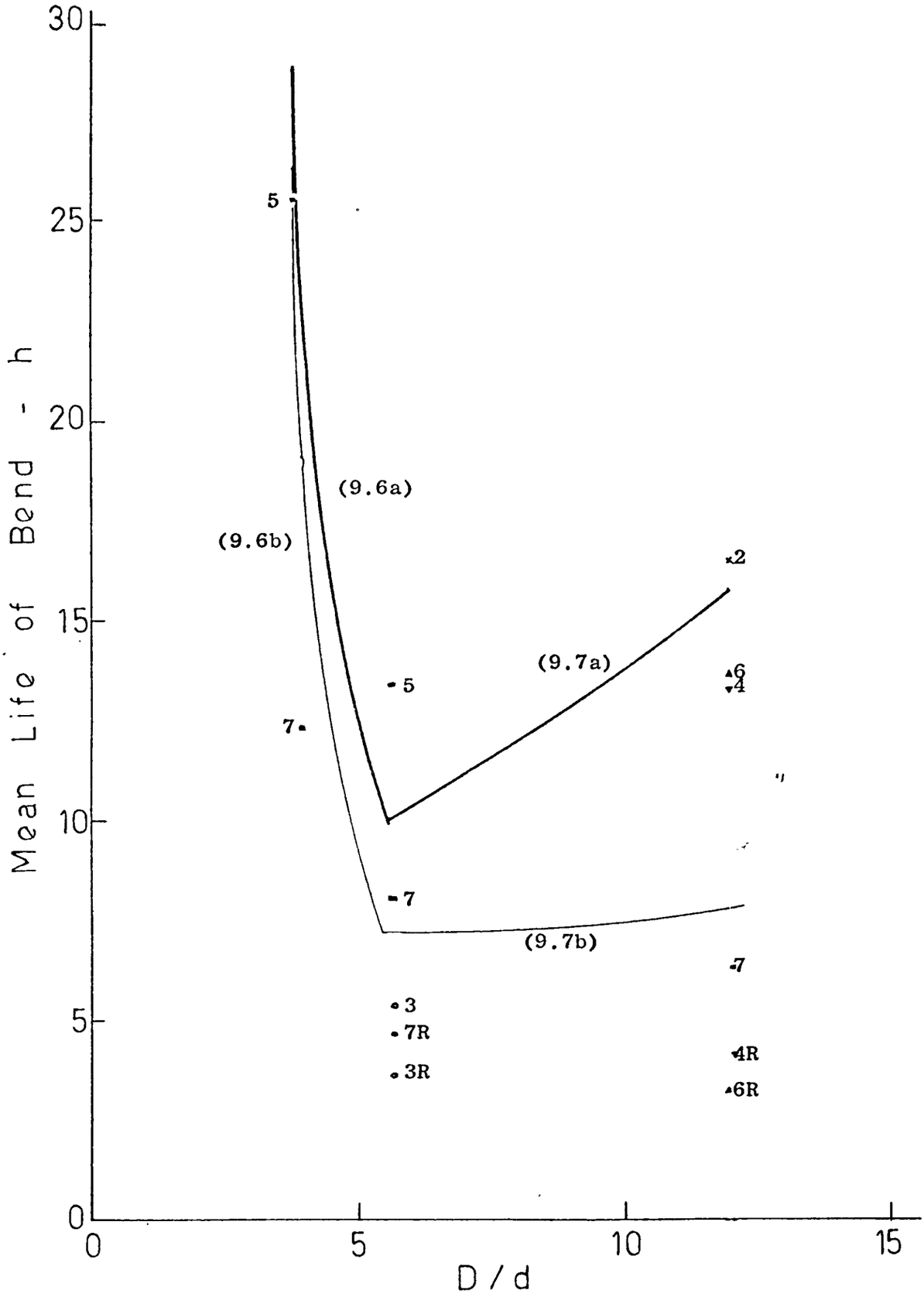

FIG. 9.7 Influence of Diameter Ratio on the Service Life of Bends

Graphical representations of these two expressions are also given in Fig. 9.6, and these are identified by the corresponding equation numbers.

In terms of bend life, the conveying time to failure is :-

$$\Delta\tau_{bf1T} = 6477\ (D/d)^{-3.88}\ h \qquad (9.6b)$$

for $4 \leqslant D/d \leqslant 5.6$, and

$$\Delta\tau_{bf2T} = 6.51\ (D/d)^{0.07}\ h \qquad (9.7b)$$

for $5.6 \leqslant D/d \leqslant 12$.

Graphical representations of these two expressions are also given in Fig. 9.7 and these are identified by the corresponding equation numbers.

9.4.3 Discussion

The curves presented in Figs. 9.6 and 9.7 show the influence of D/d on the conveying capacity and service life of bends in an actual pneumatic conveying situation. These curves also provide a real basis of comparison in terms of bend performance, the magnitude of the effect of subsequent rapid erosion and penetration of replacement bends, on the overall results.

In all cases, the trend of the curves shows a clearly defined value of D/d at which both conveying capacity and the life of the bends are at a minimum. In order to show its predictive ability, the test data of all the bends which failed in this particular programme of work (Table 5.3) is also included in both figures. On the basis of the data based on the original bends only, it can be clearly seen that, apart from the bends which failed prematurely, the actual test values for the elbows and the long radius bends appear to lie within ± 6% of the calculated values, and within ± 15% for intermediate bends. A similar comparison between the actual and calculated data of all bends tested shows a difference of about ± 10% for the two sets of bends, and about ± 20% for the elbows, in terms of conveying capacity. In terms of bend life, the difference is some ± 4% for the intermediate bends and about ± 15% for the elbows and long radius bends.

Although the actual and calculated values based on the original test data are comparable, there appears to be a substantial degree of variation when the test data of all the prematurely failed bends and replacement bends are included. This can be explained to a certain extent by the unpredictability which is inherently associated with the rapid premature failure of bends. In general, allowing for this element of unpredictability, the curves in Figs. 9.6 and 9.7 appear to be reasonably accurate.

Whilst it should be noted that these curves are based on the results of a limited range of D/ds tested, and on a particular material conveyed at a constant phase density and velocity, it is unlikely that the trend and magnitude of these curves will vary significantly. As discussed earlier, it has been recommended by the author that bends with a value of D/d of between 10 and 20 should be used in practice; therefore, the curves within the range of D/ds from 5.6 to 12 shown in Figs. 9.6 and 9.7 are of specific interest. These can be extrapolated to this recommended range of D/ds and serve as a practical guide for design purposes.

As reported earlier, Glatzel (1977) and Ryabov (1978) have also provided semi-empirical models for determining the service life of pipe bends. However, the specific effect of bend radius, in terms of the D/d parameter, is substituted by some other related factor in their formulae. Owing to the different test parameters and conveying conditions, direct comparison between these expressions is not appropriate. In addition, Glatzel's formula contains a number of highly idealised assumptions and consequently his formula is only applicable for large particle sized materials. However, Glatzel has reported that the trend and magnitude of the curves are both significantly influenced by the nature of the test material itself, as well as the shape of the velocity and particle concentration profiles in the bend (see Fig. 3.10).

9.5 CONCLUSIONS

Although premature failure of bends is a recurring feature throughout this work, an additional significant factor which has not been investigated elsewhere is the phenomenon of rapid failure of replacement bends. A number of potential variables associated with this phenomenon have been

briefly considered and it has been shown that the effects of these variables are closely inter-related and inter-dependent. Further work is necessary for a detailed, proper investigation of all the potential variables involved, and to quantify precisely to what extent each variable is responsible.

The significance of the rapid erosion of the replacement bend is demonstrated by the curves presented in Figs. 9.2 and 9.3 in terms of specific erosion and penetration wear rate. In both cases up to a two-fold increase in the overall rates is observed when the individual test data of all the long radius replacement bends are taken into account, and a $1\frac{1}{2}$-fold similar increase is observed in the case of the intermediate replacement bends.

A series of analyses on the specific influence of the D/d ratio, in terms of the conveying capacity and service life of the bends, have been presented. These curves, apart from providing a practical basis on which the performance of bends in respect of bend radius should be compared, also show the magnitude of the effect of subsequent erosion of replacement bends. In all cases the curves show a clearly defined value of D/d at which the performance of bends is at a minimum and it is found to be approximately around 5.6. Whilst there is a certain degree of variation between the measured and calculated values, the predictive ability of these curves is substantiated by the actual test results and, in the absence of any comparable expressions, these curves are the only ones available for design purposes.

Chapter 10

The Influence of Phase Density - II

10.1 INTRODUCTION

In pneumatic conveying situations it has been shown that apart from velocity the next most important parameter in terms of erosion is phase density. Although the specific effect of phase density has received comparatively little attention until recently, the general consensus of opinion has been that erosion decreases as phase density is increased, and therefore dense phase conveying is often recommended for this purpose. Mills and Mason (1977 a), however, have shown that, in terms of depth of wear, there is a corresponding increase in penetration rate, which has an over-riding influence. The net effect is not only a reduction in bend life, but also a reduction in the conveying capacity of the bends.

In addition, it has also been shown that the magnitude of the effect of phase density is considerably influenced by the inter-relating effects of velocity (Mason and Smith 1972, Mills and Mason 1976 a), and particle size (Chapter 6). Although these findings are only applicable over a limited range of phase densities investigated, the implications for dense phase conveying of abrasive materials are quite serious.

As explained in Chapters 4 and 5, the test rig used in the work reported in Chapters 6 to 9 was specifically designed for tests up to a phase density of about 10. Therefore, in order to extend the range of phase densities above 10, and to investigate the effect of dense phase conveying on erosion, a high pressure test rig capable of conveying materials well in excess of a phase density of 100, was utilised for this purpose. As explained in section 5.3, apart from the specific effect of phase density, the inter-related effects of velocity and bend radius could be investigated simultaneously in this programme of tests and so, in this chapter, the effects of these inter-related variables are also reported.

10.2 REVIEW OF PREVIOUS WORK

The influence of phase density on erosion has been briefly reviewed in Chapters 2, 3 and 6. As mentioned in these reviews, apart from the recent work of Mills and Mason (1976a, 1977a), the effect of phase density has received relatively little attention, particularly in the more general solid particle erosion studies. Although a number of studies into the specific

effect of particle concentration have been reported (see section 2.2.2), the results are often conflicting. However, on the basis of these relatively limited results, the general consensus of opinion is that erosion decreases with increase in particle concentration.

In pneumatic conveying situations, a number of studies into the specific effect of phase density on bend erosion has also been reported recently, but the range of phase densities investigated in these works has been almost exclusively limited to the dilute phase regime (see Table 3.1, p32). Apart from commercial information supplied by a number of pneumatic conveying system manufacturers, in which the benefits of conveying abrasive materials in dense phase are widely advertised, no published experimental data is available to the author's knowledge on the specific effect of dense phase conveying in terms of erosion. Hence, in this section, only the more recent experimental studies on the effect of phase density, which have some relevance to dense phase conveying, will be discussed.

Mills and Mason (1976 a) have correlated some of the published results in terms of particle concentration in mg/ m^3 units as shown in Fig. 10.1. In this figure the set of curves represented by the thin solid lines on the left, are the group of results in terms of erosion in g/kg units. The thick solid lines on the right similarly represent the group of results in terms of comparative wear rates. Although direct comparisons between these two sets of data are not appropriate, the curves nevertheless clearly show comparative trends with respect to particle concentration. Apart from a general trend towards a decrease in erosion as particle concentration is increased, two of the curves clearly indicate the existence of a critical value corresponding to maximum wear. Although the actual values differ by a factor of about 5000:1, the curve based on industrial data is of particular interest in this work, since the corresponding critical value in terms of phase density, is about 24. It should be noted that this particular curve is based on industrial information quoted in a paper by Mason and co-workers (Arundel et al 1973), in which the relative wear rate is expressed in terms of depth of wear per unit mass conveyed, i.e. penetration wear rate in mm/tonne. However, apart from this curve, no experimental information or data was given in the paper.

To a certain extent, the existence of such a critical maximum, in terms of penetration wear rate, has also been postulated in an earlier paper by Mason and Smith (1972). Apart from demonstrating the inter-relating effects

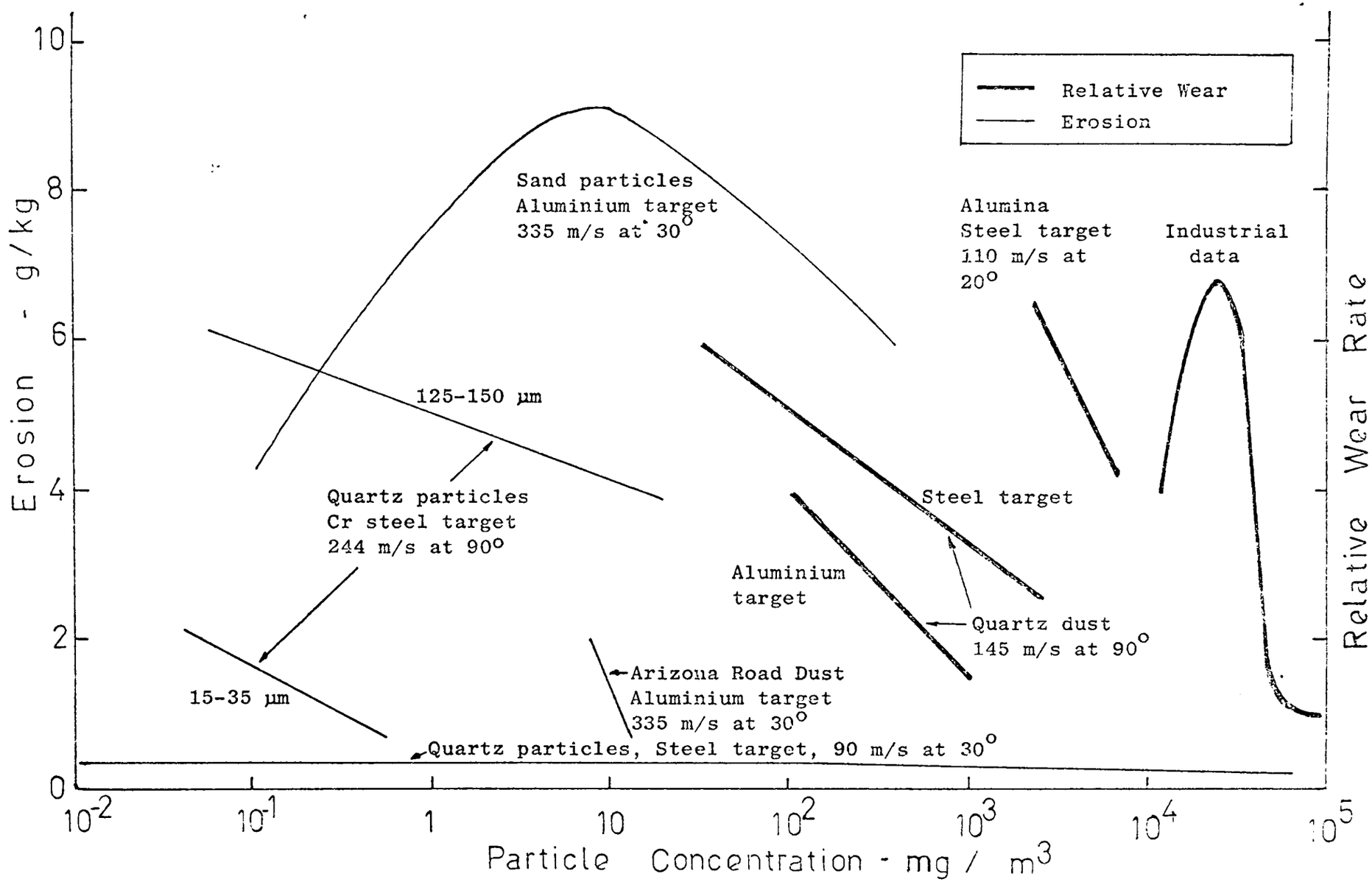

FIG. 10.1 Effect of Particle Concentration on Erosion and Relative Wear
(Source: Mills and Mason 1976 a)

of phase density and velocity, the authors showed that in terms of mass conveyed per unit depth eroded under constant velocity conditions, a critical minimum in respect of phase density is predicted.

The inter-relating effects of phase density and velocity have also been reported by Bikbaev et al (1973). Apart from showing that the location of maximum wear is independent of both phase density and velocity, the authors reported that for bends with a constant D/d ratio of about 5.1, the magnitude of penetration rate in terms of mm/h is predominantly influenced by velocity rather than by phase density (see Fig. 3.4, p35.)

Although Mills and Mason (1976 a,b,d, 1977 a) have extensively investigated the effects of phase density and velocity on bend erosion, the range of their investigations has been limited to dilute phase conveying conditions. As discussed in Chapters 3 and 6, although definitive trends in terms of both erosion and penetration with respect to phase density have been observed, the trends with regard to higher phase density remains to be established. From their limited test results, the effects of phase density and velocity were shown to be inter-related and can be given by :-

$$\text{erosion} \propto (\text{phase density})^{-0.37} \times (\text{velocity})^{4.1} \qquad (10.1)$$

However, both exponents were found to be considerably influenced by the condition of the conveyed product.

From tests with 230 μm sand, the authors found that the phase density exponent varied from -0.16 to -0.38. In terms of individual test values it varied from 0.16 to -0.73. To a certain extent, however, this large degree of variation was due to the lack of any systematic testing procedure in their work and, in order to determine the value of the phase density exponent more precisely, a series of tests with 250 μm sand was specially carried out and reported in Chapter 6. Over a similar range of phase densities, from 1 to 7, the exponent was found to vary very slightly from -0.33 to -0.47 (see Fig. 6.8, p91), and in terms of individual test values it remained remarkably consistent at about -0.42.

As the velocity exponent was much higher than the generally accepted value of about 2 to 3, the authors carried out a further series of tests over a wider range of velocities, from 15 to 31 m/s and found that it was consistently about 2.65. However, a remarkable feature in this series of tests was the presence of a transitional effect in the erosion process over this range of velocities. The magnitude of the transition velocity was

found to vary with the degree of erosiveness of the product and, within this transition region, the velocity exponent could have any value. The authors commented that, if the material is conveyed in the dense phase region the transition would be crossed due to a correspondingly lower range of velocity and the net result should be a significant reduction in erosion. However, the authors found that the true effect of velocity is much more serious than that based on specific erosion results alone. Although specific erosion was found to increase as velocity was increased, the mass which had to be eroded from the bends before failure occurred was found to decrease correspondingly. Hence, in terms of depth of penetration of the particles, bends were found to fail in an even shorter time than that predicted by specific erosion results alone. The net effect, in terms of potential service life of the bends, is an increase in the velocity exponent from 2.65 to 4.5. Previous work at low values of phase density, therefore, has shown that although mass eroded decreases slightly with increase in phase density, penetration rate has an over-riding effect. Conveying air velocity and particle shape have also been shown to have an inter-relating effect on the problem. In addition to this, the work reported in Chapter 6 demonstrated that the magnitude of the penetration rate is also influenced by particle size (see Fig. 6.10). Before any definitive conclusions can be drawn, therefore, it is quite clear that this work needs to be extended to obtain a complete picture with regard to this particular parameter.

10.3 EXPERIMENTAL PLAN

10.3.1 Introduction

As mentioned in section 10.1, in order to extend the range of phase densities to be investigated in this programme of tests and to present results of direct relevance to industry, a full scale high pressure test rig was used. This particular test rig was essentially designed to convey materials in the dense phase mode, and details of the plant, including the test section, were described in sections 4.3 and 4.4. The test programmes were briefly outlined in section 5.3 and the corresponding conveying test details were summarised in Table 5.1, p.75.

Although the parameter investigated in this work is primarily phase density, due to the large air supply pressure necessarily associated with a higher range of phase densities considered, there will be a

large pressure drop in the system. As a result there will be a substantial variation in the velocity from the first test bend to the last. Since the single test loop in this high pressure rig can be linked to the two low pressure test loops (see Fig. 4.8, p.61) with different sized test bends, the inter-relating effects of these secondary variables, i.e. velocity and diameter ratio, can also be taken into consideration. With such a number of potential inter-relating variables, however, proper control of the factors that influence erosion is of major importance if meaningful results of any value are to be obtained in this work.

10.3.2 Powder Considerations

Although with this particular high pressure test rig phase densities well in excess of 100 can be readily achieved, the actual operational range is dependent upon the type of material being conveyed and the conveying distance.

For p.f. ash the typical conveying characteristics presented in Fig. 5.1, p.72, showed that this particular material can be conveyed at a phase density of about 140 and that the conveying air velocity can be safely reduced to about 4 m/s without risk of blocking the pipeline. However, as reported in Chapter 7, only a limited amount of erosion was measurable with p.f. ash. As sand was shown to exhibit maximum erosiveness and since previous test data with similar sized sand over a lower range of phase densities was available for comparison purposes, it was decided by the author to use similar sized sand for this programme of work. The mean particle size distributions, before and after each test series, are presented in Fig. 10.2. Although the sand used in this work was Grade HH sand, similar to that used in Chapter 7, the mean particle size for this new batch was approximately 65 μm.

In order to establish the potential operational range of phase densities for sand, a series of commissioning tests was carried out over a range of conveying distances. It was found that the maximum phase density that could be achieved without blockages in the system was about 22. This substantial drop in the order of magnitude compared to about 140 for p.f. ash, restricted the possibility of carrying out tests in the dense phase region. For sand it was found that a minimum conveying

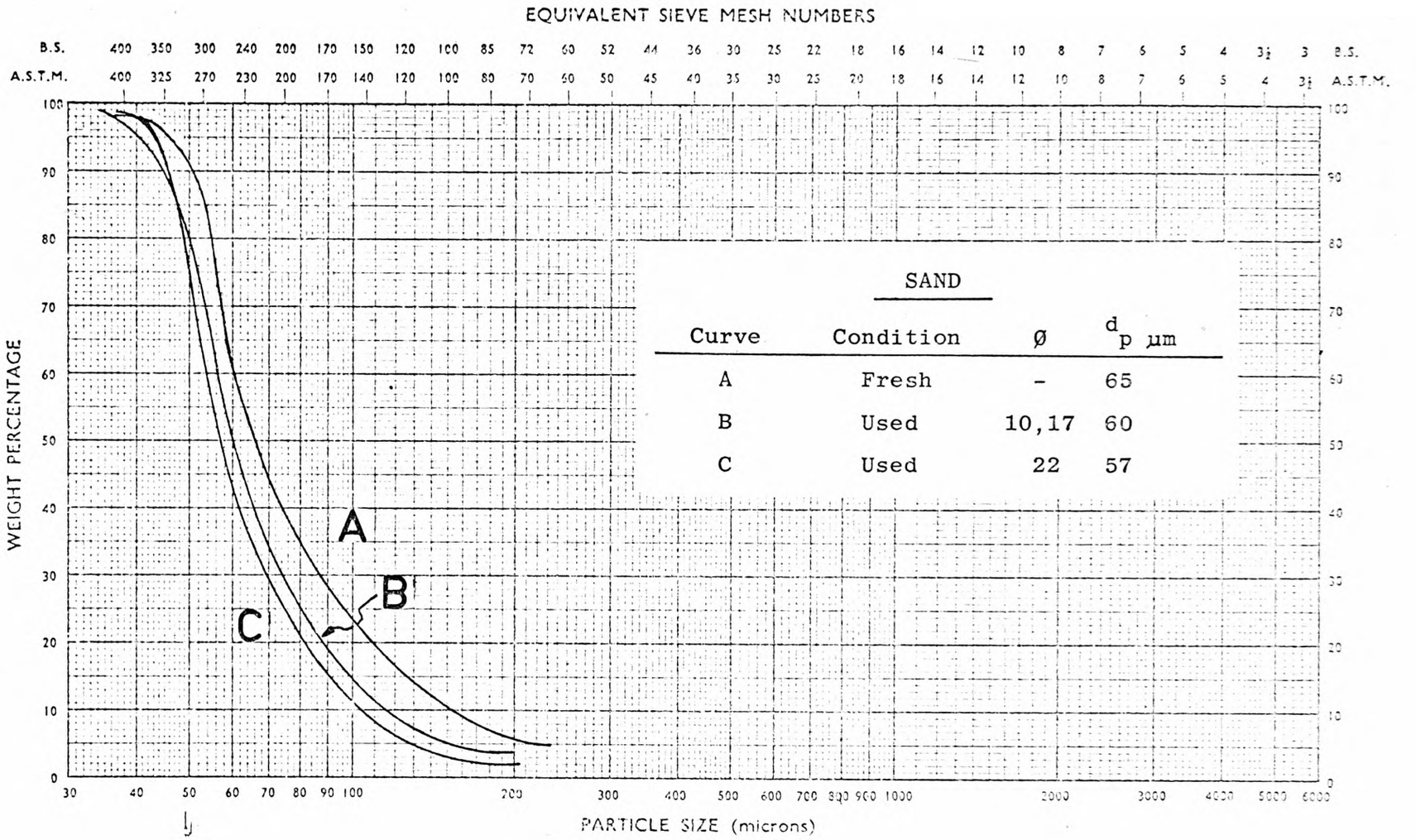

FIG. 10.2 Particle Size Distribution of Sand

air velocity of about 15 m/s was required, irrespective of conveying distance. This meant that the conveying line pressure drop in the pipeline could not be less than about 0.8 bar. As described in section 4.3, the total air supply is the sum of the air passing through the blow tank (fluidising air) and that passing directly into the conveying line (supplementary air) (see Fig. 4.4, p.56). For a given total air mass flow rate the mass flow rate of the product, and hence phase density, is proportional to the percentage of the total which passes to the blow tank.

Attempts to increase the quantity of fluidising air into the blow tank beyond about 10% of the total, however, resulted in frequent blockages of the pipeline. Visual observation of the flow showed that it was unstable, with dunes being formed on top of a moving deposited bed of particles in the lower half of the pipe. As blockage became imminent, the flow became extremely erratic. A rapid surge in the blow tank and conveying line pressure was observed, accompanied by severe vibrations in the pipeline. At this stage the vent line was opened in order to release these pressures and to stop any further flow of material into the conveying line. The blockages were subsequently removed by increasing the supplementary air flow into the pipeline.

To a certain extent the contrast in the conveying characteristics between p.f. ash and sand is due to the individual powder properties and can be explained according to Geldart's (1973) powder classification diagram in terms of minimum fluidization characteristics. Although both are essentially Group B powders, since the size distributions are comparatively similar and the particle densities are greater than 1.4 g/cm^3, according to Geldart's criteria, p.f. ash behaves as a Group A powder rather than Group B. The Group A powders exhibit dense phase expansion after minimum fluidization and retain aeration for a considerable period of time even after the gas supply is cut off. Doig (1975) and Dixon (1979) reported that Group A materials can be readily conveyed in the dense phase mode. Since Group B materials do not retain aeration when the gas supply is cut off, the flow consists of a moving layer of particles containing dunes and so these materials are usually conveyed in the medium phase regime, although Doig reported that some of these materials could be conveyed in the dense phase mode by means of a pulse phase system.

10.3.3 Velocity Considerations

A major problem associated with dense phase conveying is the requirement of a high pressure in the system. As the flow of a gas-solid suspension in a pipeline is necessarily associated with a pressure drop, the high pressure air will gradually expand along the length of a conveying line and, consequently, the air velocity will increase along the conveying line. The magnitude of the variation is dependent upon the total pressure drop of the system, which varies with phase density and conveying distance. In addition, with a number of different sized bends in the test section, the pressure drop across each bend, and hence velocity, will also be different.

Although phase density and velocity are inter-related variables in terms of erosion, velocity is a major variable in its own right and so analysis of the results will also have to take this effect into account. As in previous chapters, the velocity recorded is the conveying air velocity and is determined on the basis of the estimated pressure drop across each individual test bend in the test section.

In this work the velocity at each test bend is estimated from an empirical expression given by Schuchart (1968). This expression was based on the ratio of the pressure drop across the bend to the pressure drop in an equivalent length of straight pipe, and correlated in terms of the D/d ratio. It should be noted that, although an error of about ± 25% was associated with this particular expression, the maximum deviation in the velocity estimated in this work is only about ± 10% at the two lower phase densities and about ± 15% at a phase density of 22, and these occurred in bends 7, 4 and 5 respectively.

In a dense phase system the material does not have to be conveyed in suspension, but can be swept along the pipeline in the form of slugs by the air. The actual mechanism of the flow is, however, much more complex. As the maximum phase density that could be achieved with sand in this particular system was about 22, the flow is essentially in the medium phase range. Apart from a minimum conveying velocity of about 15 m/s, the velocity at the last test bend was consistently about 30 m/s over the range of phase densities considered. The two-fold increase in the velocity range within the test section clearly indicated that there is a transition in the flow patterns from medium phase flow at the low velocity end to dilute phase flow at the high

velocity end. This apparent change in the flow patterns is substantiated by visual observations of the flow via a short piece of sight glass at the start and end of the conveying line.

These visual observations indicated that the flow is initially in the medium phase mode, and can be basically categorised as 'degenerate dune flow' according to Wen and Galli's(1971) flow characteristics, to dilute phase suspension or 'homogenous' flow at the end of the conveying line. To a certain extent the transition in the flow patterns could also be explained in terms of the Froude number of the suspension, since the Froude number function is essentially an expression of the frequency with which particles collide with the wall in a given length of pipe (Boothroyd 1971). Barth (1962) reported that, at very high Froude numbers the particles are uniformly distributed over the entire cross-section of the pipe but, as the Froude number is reduced, some of the particles begin to drop out of suspension and form a layer of deposits along the lower part of the pipe. Since the Froude number is directly related to the velocity of the suspension, the transition in the pattern of flow will therefore correspond with a similar change in the Froude number of the suspension in the pipeline. As the Froude number provides a physical explanation of the flow, a number of expressions have been published recently (Duckworth 1971, Jones and Leung 1978), which correlate the Froude number to the phase density of the suspension, from which the minimum saltation velocity could be determined.

As explained briefly in section 4.3, the main control over the gas-solids flow in this conveying plant is basically through the air supply into the blow tank. Although the actual quantity of total air supply into the system could be varied over a wide range of choked flow nozzle combinations by regulating the upstream air supply pressure, it was not possible to preset these in order to obtain a desired product flow rate for each test run. As there was no discharge valve at the outlet from the blow tank to the conveying line, the material is not discharged into the conveying line at a steady rate until the blow tank has been pressurised to a certain steady operating pressure. Since the conveying line pressure drop is dependent upon the blow tank pressure, which in turn depends upon the fluidisation characteristics of the material, the operational range of velocities in the test section is partly determined by the test material itself. The limits are the minimum conveying velocity required, prior to blockages in the pipeline, and the maximum due to the total pressure drop in the system.

10.3.4 Test Programmes

Since the total pressure drop of the system increases approximately in proportion to the square of the velocity, in order to isolate phase density from the effect of velocity it was necessary to limit the operational velocity range such that it was the same at each test phase density. As the potential range of phase densities is effectively limited by the material and conveying distance, it was decided by the author to carry out tests at phase densities of 10, 17 and 22.

At a phase density of 10 the test section consisted of three test loops with a total conveying length of about 96 m. There were eleven test bends in this particular test section; three large radius bends with D/d ratios of 24, seven intermediate bends with 5.6 and a Booth bend with 2.4 (see Fig. 4.8, p.61). Twenty-four test runs were carried out and the mean conveying line pressure drop was about 0.86 bar gauge. The maximum and minimum velocities in this test section were about 15 and 26 m/s, corresponding to the first and last test bends.

In order to increase the conveying line pressure drop and hence phase density, and at the same time restrict the velocity range, two test loops were used in tests at phase densities of 17 and 22. The total conveying length was about 69 m and the test section consisted of three large radius bends and three intermediate bends. In tests at a phase density of 17 the Booth bend was not included. The conveying line pressure drop was about 1.06 bar at a phase density of 17 and 1.59 bar at a phase density of 22. The corresponding range of velocities was from 15 to 27 m/s and 14 to 31 m/s. Twenty-four test runs were also carried out at a phase density of 17 and thirty test runs at 22.

Although a batch of about 750 kg of similar sized sand was used at each test phase density, due to discontinuation of further supplies of fresh sand it was decided to use the same batch of sand which was previously tested at a phase density of 17 for the next series of tests at a phase density of 22. The mean particle size after twenty-four runs in tests at phase densities of 10 and 17 was similar, at about 60 μm. (Fig. 10.2, curve B) After a further thirty runs in tests at a phase density of 22 it reduced marginally to about 57 μm (curve C). The percentage of fines below 45 μm increased by about 30% after twenty-four runs in tests at the two lower phase densities and only a further 8% after fifty-four runs in tests at the higher

phase density. The lack of any substantial increase in the fines clearly provides clear evidence that particle degradation is considerably reduced if material is conveyed at higher phase densities.

Details of the respective test programmes were presented in Tables 5.1 and 5.2, and further individual erosion and conveying test data is presented in Table 10.1.

It should be noted that in this work the phase density values are based on the steady state conveying conditions over each conveying cycle, as shown by a typical conveying trace in Fig. 4.5, p.57. Steady state conditions were not reached until a blow tank pressure of at least 1.4 bar gauge had been achieved and the rate of pressurisation depends upon the quantity of fluidising air into the blow tank. In tests at a phase density of 10, the time taken to pressurise the blow tank to this operating pressure was about nine minutes, but at a phase density of 22 less than a minute was required. In order to compute the steady state conditions from which the product mass flow rate, and hence phase density could be determined, it was necessary to eliminate these start-up and shut-down effects. This was done by considering only the portion of the product mass flow rate corresponding to the steady state blow tank pressure trace (see Fig. 4.5) for each test run, and so the transient effects were thereby eliminated.

10.4 BEND WEAR RESULTS AND DISCUSSION

10.4.1 Introduction

In this programme of tests , for the range of phase densities investigated, the magnitude of erosion was expected to be very much lower than that obtained in previous dilute phase tests. The procedure, therefore, was to remove all the test bends after a number of test runs within each test series. As in previous analyses, the mass eroded and wear profiles of each individual bend were recorded and visually inspected for any sign of wear. In the case of the Booth bend, due to its fittings and location, similar readings were only taken prior to the start and at the end of the particular test series, and so no intermediate test data is available.

In order that the effects of this higher range of phase densities could be investigated thoroughly, and to enable direct comparison

Phase Density : 10

TABLE 10.1 Individual Test Data

Number of Batches : 24				Number of Test Loops : 3							Total Conveying Length : 96 m
D/d	24			5.6							2.4
Bend Number	1	2	11	3	4	5	6	7	8	9	10
Total Mass Eroded (g)	17	45	48	7	16	17	16	17	22	25	5
Mass Conveyed (tonne)	18	18	18	18	18	18	18	18	18	18	18
Conveying Time (h)	7.2	7.2	7.2	7.2	7.2	7.2	7.2	7.2	7.2	7.2	7.2
Specific Erosion (g/tonne)	0.94	2.50	2.67	0.39	0.89	0.94	0.89	0.94	1.22	1.39	0.28
Erosion Rate (g/h)	2.36	6.25	6.67	0.97	2.22	2.36	2.22	2.36	3.06	3.47	0.69
Maximum Depth of Penetration (mm)	0.2	0.5	0.7	0.3	1.2	1.1	1.3	1.2	1.7	2.0	3.2
Penetration Wear Rate (mm/tonne)	0.01	0.03	0.04	0.02	0.07	0.06	0.07	0.07	0.09	0.11	0.18
Penetration Rate (mm/h)	0.03	0.07	0.10	0.04	0.17	0.15	0.13	0.17	0.24	0.28	0.44
Velocity at Bend C_{aB} (m/s)	14.9	15.0	26.4	15.7	16.4	17.2	18.2	19.1	20.2	21.6	26.0
Pressure at Bend (bar abs)	1.85	1.84	1.04	1.76	1.68	1.60	1.52	1.44	1.36	1.28	1.06

Phase Density : 17

TABLE 10.1 Continued

Number of Batches : 24				Number of Test Loops : 2							Total Conveying Length : 69 m
D/d	24			5.6							2.4
Bend Number	1	2	11	3	4	5	6	7	8	9	10
Total Mass Eroded (g)	33	55	56	8	17	20	-	-	-	-	-
Mass Conveyed (tonne)	18	18	18	18	18	18	-	-	-	-	-
Conveying Time (h)	4.4	4.4	4.4	4.4	4.4	4.4	-	-	-	-	-
Specific Erosion (g/tonne)	1.83	3.06	3.11	0.44	0.94	1.11	-	-	-	-	-
Erosion Rate (g/h)	7.50	12.50	12.73	1.82	3.86	4.55	-	-	-	-	-
Maximum Depth of Penetration (mm)	0.4	1.9	0.4	0.4	0.9	0.9	-	-	-	-	-
Penetration Wear Rate (mm/tonne)	0.02	0.11	0.02	0.02	0.05	0.05	-	-	-	-	-
Penetration Rate (mm/h)	0.09	0.43	0.09	0.09	0.20	0.20	-	-	-	-	-
Velocity at Bend C_{aB} (m/s)	14.8	15.1	27.4	16.9	19.3	22.3	-	-	-	-	-
Pressure at Bend (bar abs)	2.03	1.99	1.09	1.77	1.58	1.35	-	-	-	-	-

Phase Density : 22

TABLE 10.1 Continued

Number of Batches : 30				Number of Test Loops : 2							Total Conveying Length : 69 m
D/d	24			5.6							2.4
Bend Number	1	2	11	3	4	5	6	7	8	9	10
Total Mass Eroded (g)	29	32	50	10	14	18	-	-	-	-	1
Mass Conveyed (tonne)	22.5	22.5	22.5	22.5	22.5	22.5	-	-	-	-	22.5
Conveying Time (h)	3.5	3.5	3.5	3.5	3.5	3.5	-	-	-	-	3.5
Specific Erosion (g/tonne)	1.29	1.42	2.22	0.44	0.62	0.80	-	-	-	-	0.04
Erosion Rate (g/h)	8.29	9.14	14.29	2.86	4.00	5.14	-	-	-	-	0.29
Maximum Depth of Penetration (mm)	0.3	0.3	0.3	0.3	0.4	0.6	-	-	-	-	0.6
Penetration Wear Rate (mm/tonne)	0.01	0.01	0.01	0.01	0.02	0.03	-	-	-	-	0.03
Penetration Rate (mm/h)	0.09	0.09	0.09	0.09	0.11	0.17	-	-	-	-	0.17
Velocity at Bend C_{aB} (m/s)	13.6	13.9	31.4	15.3	17.0	19.2	-	-	-	-	30.1
Pressure at Bend (bar abs)	2.55	2.50	1.11	2.27	2.04	1.81	-	-	-	-	1.15

with those obtained in the dilute phase range, it was necessary that sufficient results were obtained at each test phase density for data processing. For this reason a decision was taken that testing would continue until a reasonable amount of both erosion and penetration had been established in each individual test bend. Hence, as already mentioned, it was necessary to recirculate the sand some 24 times at the two lower phase densities and 30 times at a phase density of 22.

With this recorded test data, a comparison of both specific erosion and penetration wear rate, with respect to phase density as well as the secondary inter-relating effects of velocity and bend radius, was possible. By incorporating previous dilute phase test data an analysis of the influence of phase density, from dilute to medium phase, in terms of the conveying capacity and service life of the bends is produced, and definitive trends in terms of both erosion and penetration with respect to this higher range of phase densities are established.

10.4.1.1 Particle Concentration Effects

As already mentioned, although the primary objective in this work was to investigate the influence of a higher range of phase densities, it should be noted that, perhaps a more suitable parameter would be particle concentration. Whilst phase density is the ratio of the mass flow rate of the product being conveyed to the mass flow rate of air being used, particle concentration is basically the ratio of the mass of solids to the quantity of air in a given volume of the suspension. Hence, for a given suspension being conveyed, phase density will remain constant. However, particle concentration will not, since it varies with the density of the suspension, and hence the air pressure along the conveying line.

To a certain extent the magnitude of particle concentration also gives an indication of the degree of spacing between the particles. A change in particle concentration will give rise to a corresponding change in particle spacing. At low particle concentrations the particles are spaced in a uniformly dispersed suspension, but as particle concentration increases, the spacing will be more compact, i.e. the particles are more closely spaced together. Hence, for a given phase density, not only will particle concentration vary with air velocity and pressure, but there will also

be a corresponding variation in terms of particle spacing. An idea of the extent of this variation is to consider the magnitude of particle concentration at each test phase density. For a given solids mass flow rate, particle concentration is basically a function of air density. Whilst the variation in the air density from the first test bend to the last is small in relation to the range of phase densities tested in the dilute phase test rig, there is a corresponding substantial variation over the higher range of phase densities tested in this work. At a phase density of 10 it varies from 2.200 kg/m^3 in bend 1 to 1.237 kg/m^3 in bend 7, which represents a decrease of about 77%. At phase densities of 17 and 22, the corresponding variations are about 80 and 130%.

Although these variations are substantial, it should be appreciated that the mechanics of flow over this higher range of phase densities tested are not homogenous, but varies from medium to dilute phase as reported earlier. As particle concentration varies with density and hence air pressure, which in turn depends upon the mode of flow, it was felt that a more appropriate parameter would be phase density, since it is a dimensionless quantity and its value remains constant at any section in the pipeline. In addition, since both the solids and air mass flow rates are constant over each conveying cycle, in view of the large degree of variation in terms of particle concentration and for comparison purposes with previous dilute phase work, it is reasonable to consider phase density as a satisfactory substitute parameter.

10.4.1.2 Transitional Velocity Effects

An additional factor which must also be taken into consideration prior to processing the test data obtained in this work is the velocity term. As already mentioned elsewhere, the velocity considered throughout this work is the conveying air velocity. In dilute phase suspension flow it has been shown by the author that the particle velocity of fine particles approaches that of the conveying air velocity (see section 7.5, p.129), and so it was reasonably valid to consider the conveying air velocity as a satisfactory substitute parameter instead.

For this programme of tests however, due to the presence of a transition in the mode of flow, there will be a substantial degree of variation between the particle velocity and the conveying air velocity, and it is not possible to determine precisely the extent of this variation. As the pattern of flow in the first few test bends in essentially in the medium phase mode, the majority of the particles are being conveyed in the form of a moving bed and so the slip velocity ($U_g - U_p$) would be very high. Near the end of the test section, however, the flow is essentially in the form of a dilute phase suspension and so the slip velocity here is low . Hence, in this respect, due to this substantial degree of variation in terms of slip velocity effect, and for consistency and comparison purposes, it was decided to consider the conventional air velocity term as used in previous dilute phase work.

As mentioned in section 10.3.3, to a certain extent it is possible to determine the location of the transition of the mode of flow on the basis of saltation velocity. The value of saltation velocity for a given set of test conditions is the minimum velocity required to prevent the deposition and accumulation of stationary or slowly sliding bed of particles along the bottom of the pipeline. It is usually correlated in terms of phase density and the Froude number of the suspension. According to Matsumoto's correlation (1977), the saltation velocity at phase densities of 10, 17 and 22 are 15, 17 and 18 m/s respectively. On the basis of the estimated conveying air velocity in the bend in each respective test phase density (Table 10.1), it appears that at a phase density of 10 the transition in the mode of flow occurs in bend 2; similarly at a phase density of 17 it occurs in bend 3, and at a phase density of 22 it occurs somewhere between bends 4 and 5. In addition, as there is almost a two-fold increase in the velocity from the first test bend to the last, at each test phase density, a transition in the erosion process has also been reported over this velocity range (Mills and Mason, 1976 d). Hence, not only is there a transition in the mode of flow, but also a transition in respect of the erosion process over this velocity range, both of which are considerably influenced by the phase density and

the conveying velocity of the suspension. In the following analysis, therefore, it should be noted that, whilst phase density and conveying air velocity are the parameters that are considered in this work for convenience and comparison purposes, it must be appreciated that the variables under consideration in this respect are particle concentration and particle velocity.

10.4.2 Specific Erosion Analysis

The erosion history of all the bends tested at a given phase density is presented graphically in Figs. 10.3 to 10.5. The curves in these figures show the variation of accumulative mass eroded from each individual test bend. As the experimental data has not been normalised, it can be clearly observed that the magnitude of erosion within each test phase density is considerably influenced by velocity and bend radius. Hence, in the following analysis, the individual effects of these inter-related variables will also be discussed separately.

10.4.2.1 Scatter of Results

A common feature of the curves in these figures is, once again, the scatter of results. As already mentioned elsewhere, the scatter of results is a recurring feature throughout this work, especially when a number of bends are tested simultaneously. In the preceding chapters the various potential sources and causes of the scatter have been discussed, from which a number of variables responsible have been identified. Apart from the velocity effect due to the variation of velocity in the test loops, it has been shown that the scatter is also partly due to the combination and interaction of a number of factors. These are :- particle size and degradation, secondary flows, bend radius, and bend position. With regard to phase density, although Mills and Mason (1976 a, 1977 a) reported that the degree of scatter increases with phase density and attributed this increase predominantly to a corresponding increase in secondary flow effects, the magnitude of the degree of scatter is, however, considerably dependent upon particle size (Chapter 6).

With regard to the scatter of results in Figs. 10.3 to 10.5, a number of interesting features are observed. In terms of the overall order of magnitude, the degree of scatter appears to decrease over this range of phase densities. This is a direct

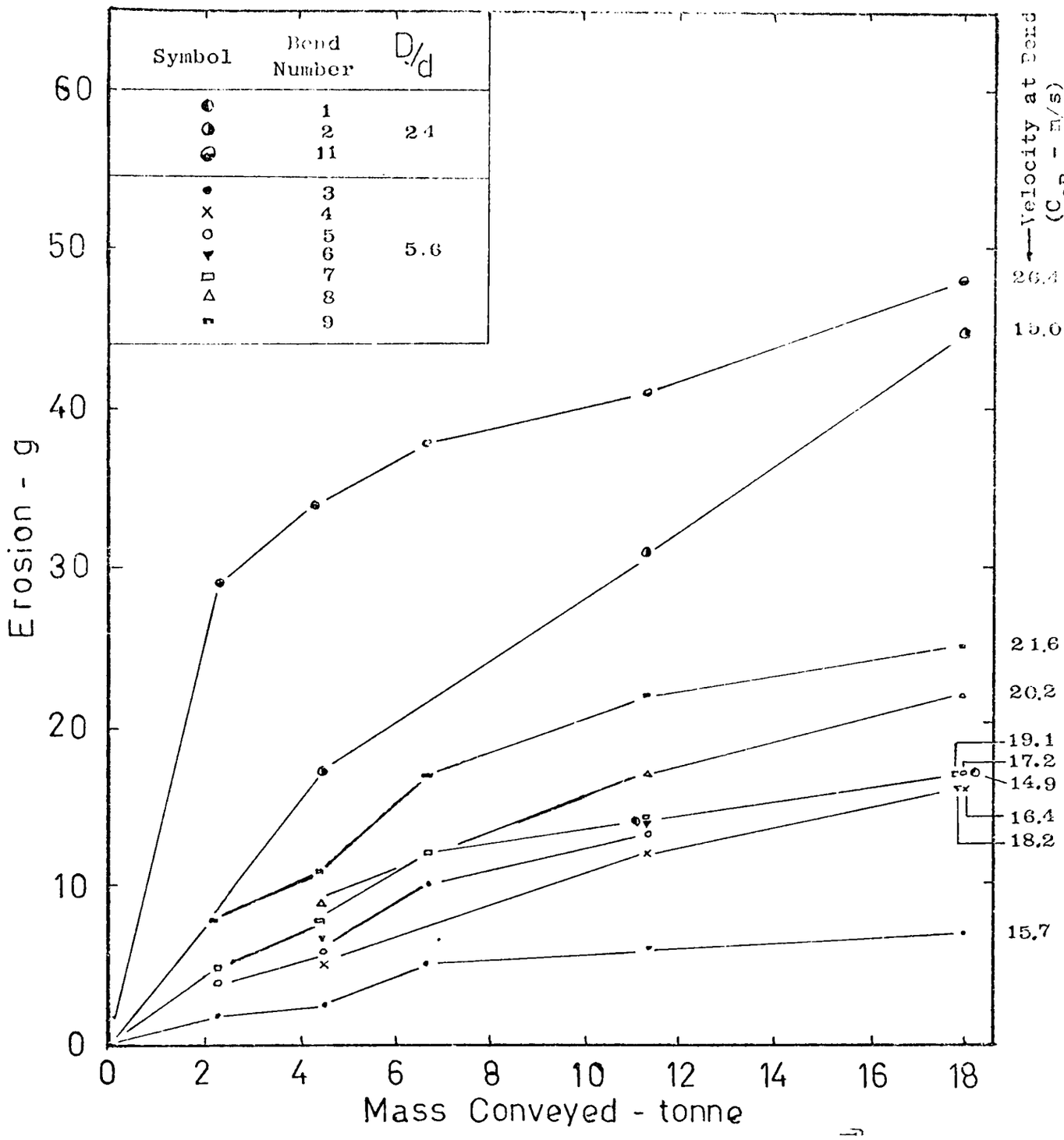

FIG. 10.3 Variation of Erosion with Mass Conveyed at a Phase Density of 10.

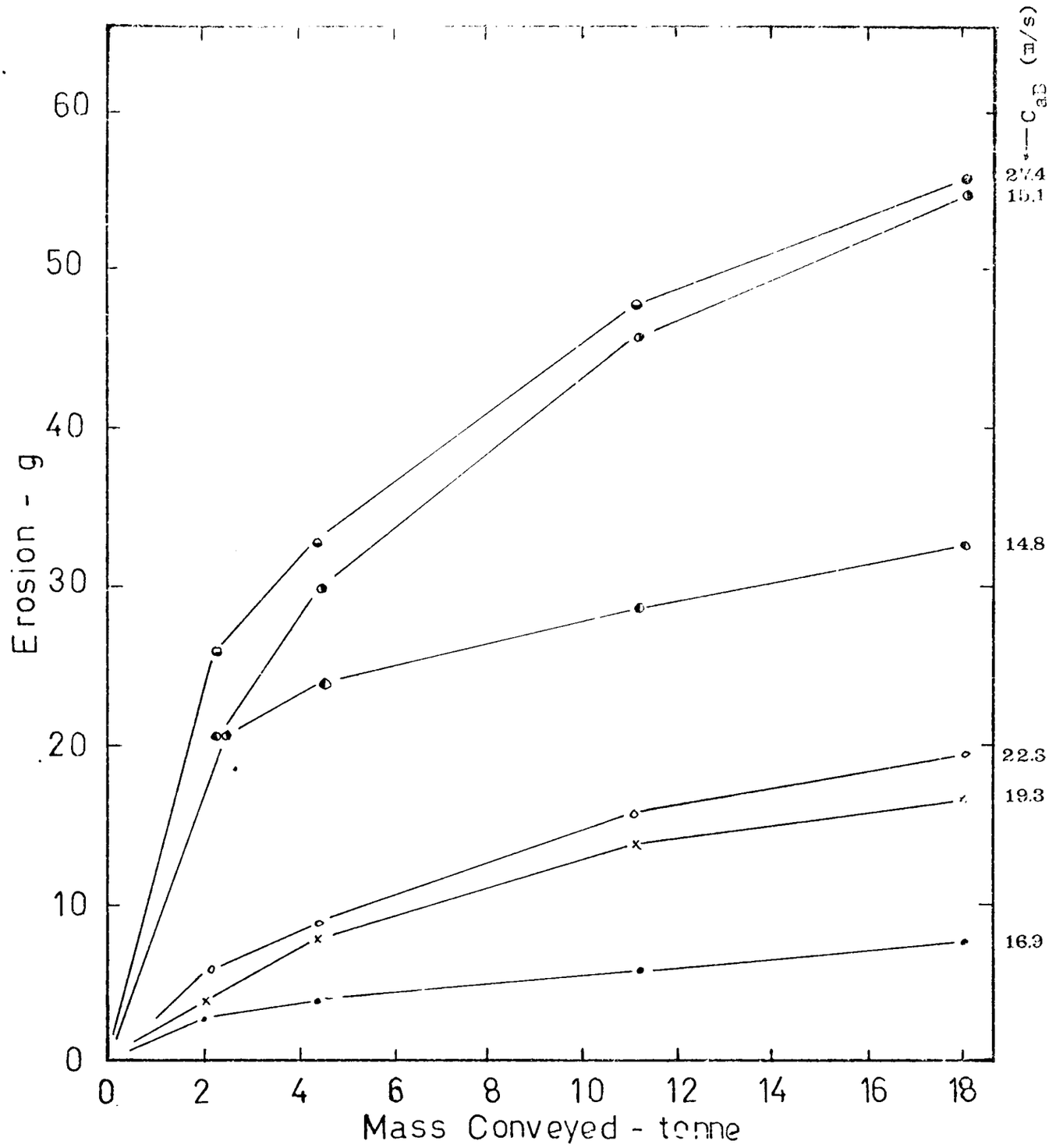

FIG. 10.4 Variation of Erosion with Mass Conveyed at a Phase Density of 17.

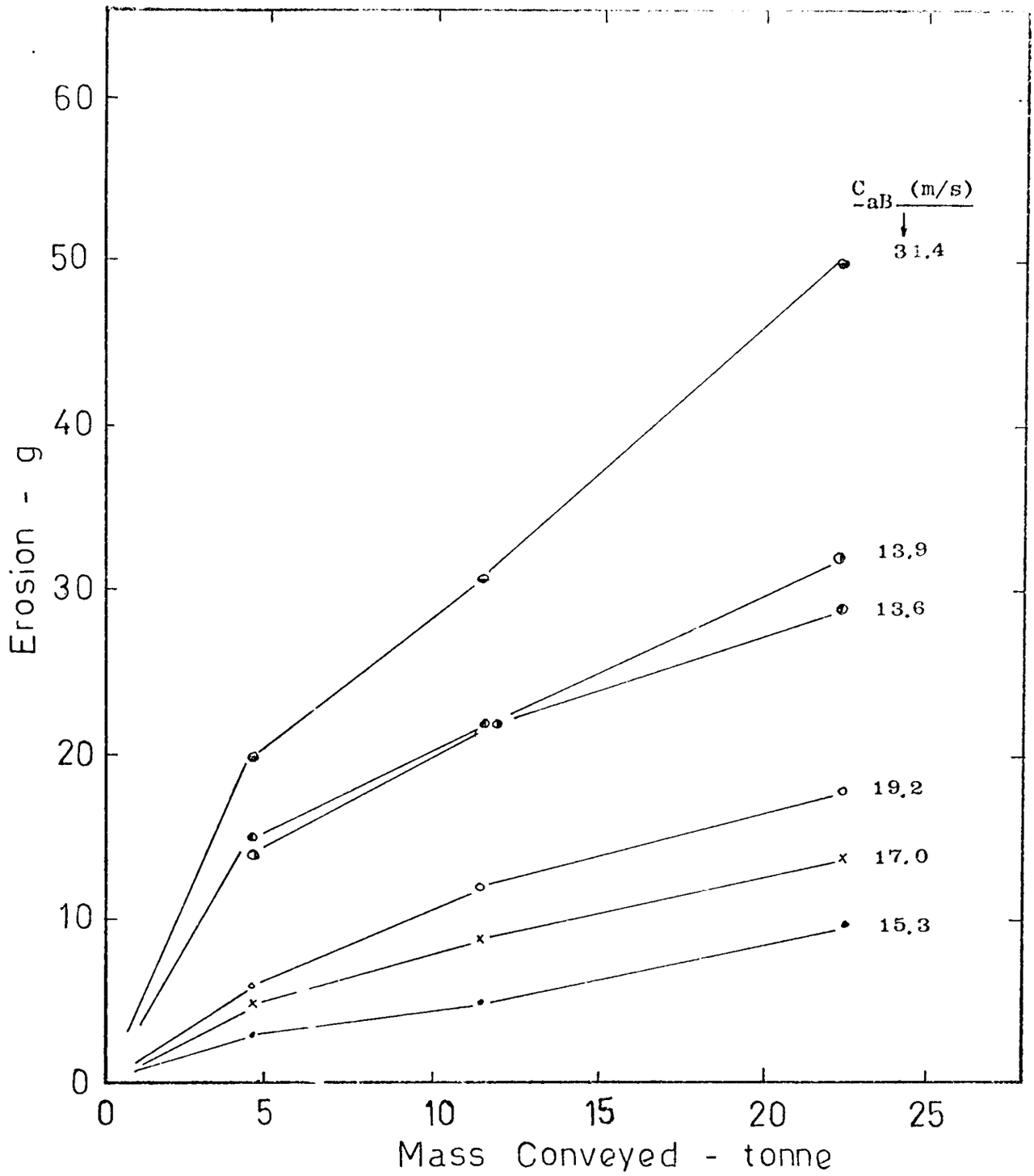

FIG. 10.5 Variation of Erosion with Mass Conveyed at a Phase Density of 22.

contrast to the trend observed by Mills and Mason (1976 a), based on dilute phase test data. To a certain extent this could be explained by the change in the nature of the flow, which consequently resulted in some fundamental transition in the mechanics of the erosion process over this range of phase densities.

This apparent transition is clearly demonstrated by the test results based on the set of large radius bends. Whilst the curves for the set of intermediate bends in Figs. 10.3 to 10.5 show that the degree of scatter due to velocity appears to be consistent and predictable, no similar predictable pattern is observed in the case of the large radius bends, particularly with regard to the individual erosion results of bend number 2 in Figs. 10.3 and 10.4.

Although the set of curves for the large radius bends at a phase density of 22 (Fig. 10.5) shows that the individual test result of bend 2 is consistent in terms of velocity and is comparable to that of bend 1, at the two lower phase densities there is a substantial degree of deviation from the expected values that would be obtained based on similar velocity projections. In fact, as shown in these figures, the individual erosion result of bend 2, particularly at a phase density of 17, is consistently comparable to that of bend 11, despite the fact that the velocity here is almost doubled.

As explained earlier, to a large extent the rapid erosion of this particular test bend is attributed to its location within the test section. Although it has been shown by the author that, on the basis of the value of minimum saltation velocity it is possible to locate the region of transition from medium to dilute phase mode, it should be noted that this transition is gradual and the process of transformation probably occurs over a certain length of pipe. Whilst the comparability of the individual erosion results of bends 1 and 2 at a phase density of 22 (Fig. 10.5) provides clear evidence that the transition process occurs well beyond bend 2, lack of any similar comparability in the corresponding set of individual results at the two lower phase densities clearly indicates that the transition occurs in the vicinity of

bend 2. Thus, it appears that the magnitude of erosion, and consequently the degree of scatter, are both significantly influenced by these inter-relating transitional effects. In addition, it should be noted that, apart from these transitional factors, those factors which were found to be responsible in previous dilute phase work are also operative over this test range. Further work is obviously necessary over a wider test range and conditions in order to investigate in more detail and to quantify to what extent these factors are responsible.

10.4.2.2 Phase Density Effects

In order to evaluate the specific effect of phase density it is necessary to isolate this parameter from velocity. For this purpose, and to provide comparability with previous dilute phase test results, all the experimental data in Figs. 10.3 to 10.5 has been normalised to a velocity of 25 m/s. The normalised data was averaged for each set of bends tested at a given phase density and the results are presented in Fig. 10.6. Apart from showing the specific effect of phase density, the curves in this figure also show more clearly the additional effect of bend radius.

From the work presented in Chapter 8 it was found that a critical value of D/d ratio exists beyond which erosion is relatively independent of bend radius. As shown by the experimental data in Fig. 8.7, the specific erosion values for bends with D/d ratios of 5.5 and 12 were comparable. However, by plotting these values in terms of average mass eroded into Fig. 10.6, the curve for these plots would lie in between the band of curves obtained in this work. Thus, it can be seen that the trend observed in Fig. 8.7 is only applicable within a certain limited low range of phase densities.

The results in Fig. 10.6 provide clear evidence that, at high phase densities, the magnitude of erosion is considerably influenced by bend radius. This apparent change in the trend, therefore, appears to substantiate that this is due to some fundamental variation in the erosion process above a phase density of about 10.

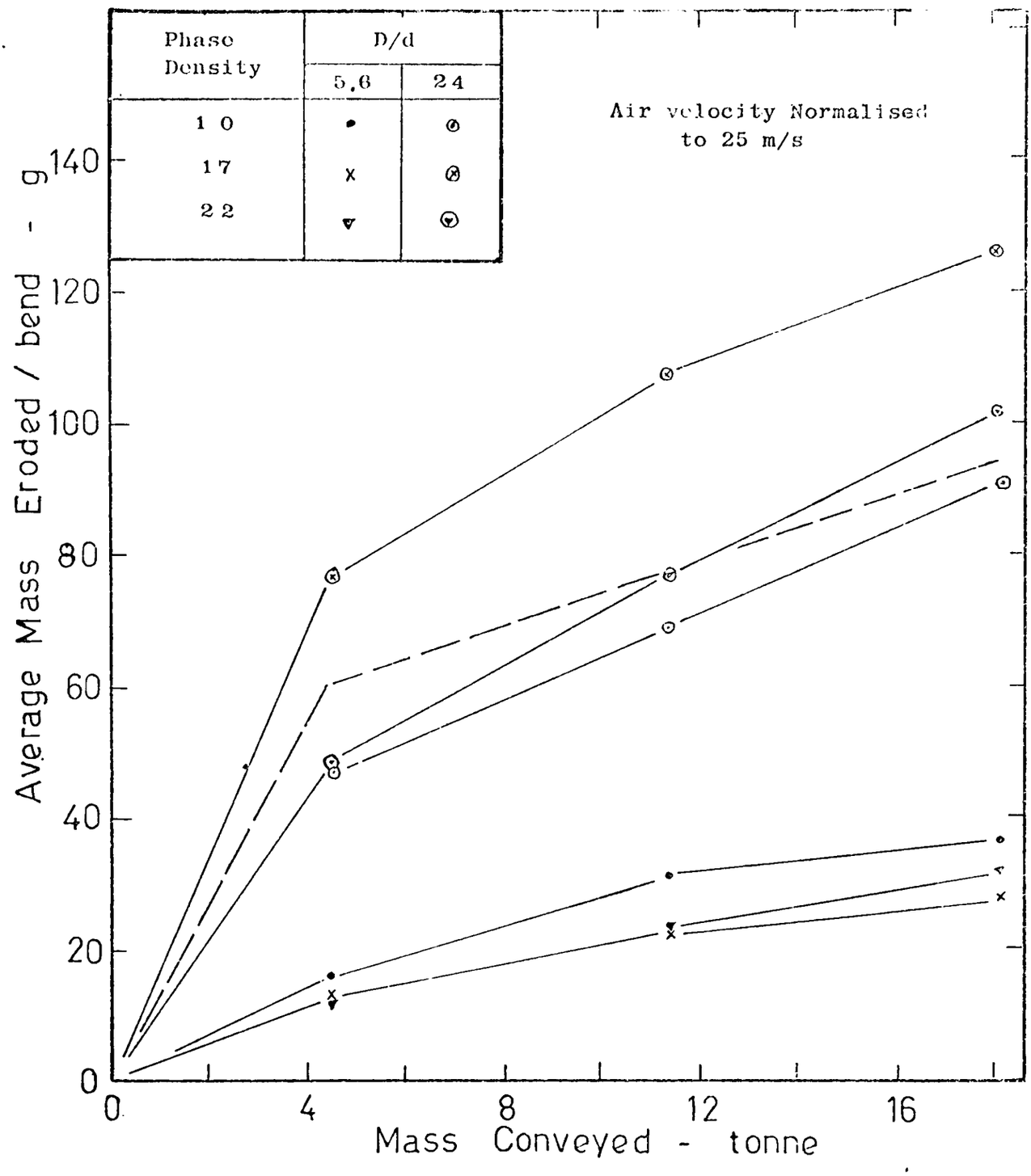

FIG. 10.6 Influence of Phase Density on the Variation of Erosion with Mass Conveyed

In terms of phase density effect, although the set of curves for the intermediate bends shows that erosion generally decreases with increase in phase density, the corresponding set of curves for the large radius bends appears to show that maximum erosion occurs at a phase density of 17. This is somewhat misleading for, as mentioned earlier, a rapid rate of erosion was observed in one particular test bend (bend 2) at this phase density. Since the curves in Fig. 10.6, for the set of large radius bends, were only based on three test bends, any substantial increase in the erosion rate of a particular bend would lead to a corresponding similar increase of magnitude in the overall mean value. By omitting the individual erosion result of this particular test bend, the net effect is a substantial decrease in the overall mean value, as represented by the dotted line in Fig. 10.6. Hence, it can be generally concluded that, in terms of phase density, no substantial variation in the magnitude of erosion is observed over this range of phase densities tested, irrespective of bend radius.

The overall magnitude of the effect of phase density is presented in Figs. 10.7 and 10.8, in terms of specific erosion. For comparison purposes three sets of test results are given. The set of results in test sets 1, 2 and 3 refer to the accumulative results after 6, 15 and 24 test runs respectively. As in previous presentations the vertical lines in both figures indicate the maximum and minimum values within each test set and the location of the symbol its mean. Fig. 10.7 shows the results based on the set of intermediate bends, whilst Fig. 10.8 shows the corresponding results based on the set of large radius bends. The dotted lines through the respective set of mean values in this figure indicate that, for the purpose of this analysis, the corresponding set of mean values at a phase density of 17 is based on the test results of bends 1 and 11 only, i.e. the individual test results of bend 2 have been excluded.

An important feature of the results presented in Figs. 10.7 and 10.8 is with regard to the trend of the curves over this range of tests. Whilst the curve in test set 1 in Fig. 10.7 shows a gradual decrease in specific erosion over this phase density test range, the corresponding curves in test sets 2 and 3 show a marked

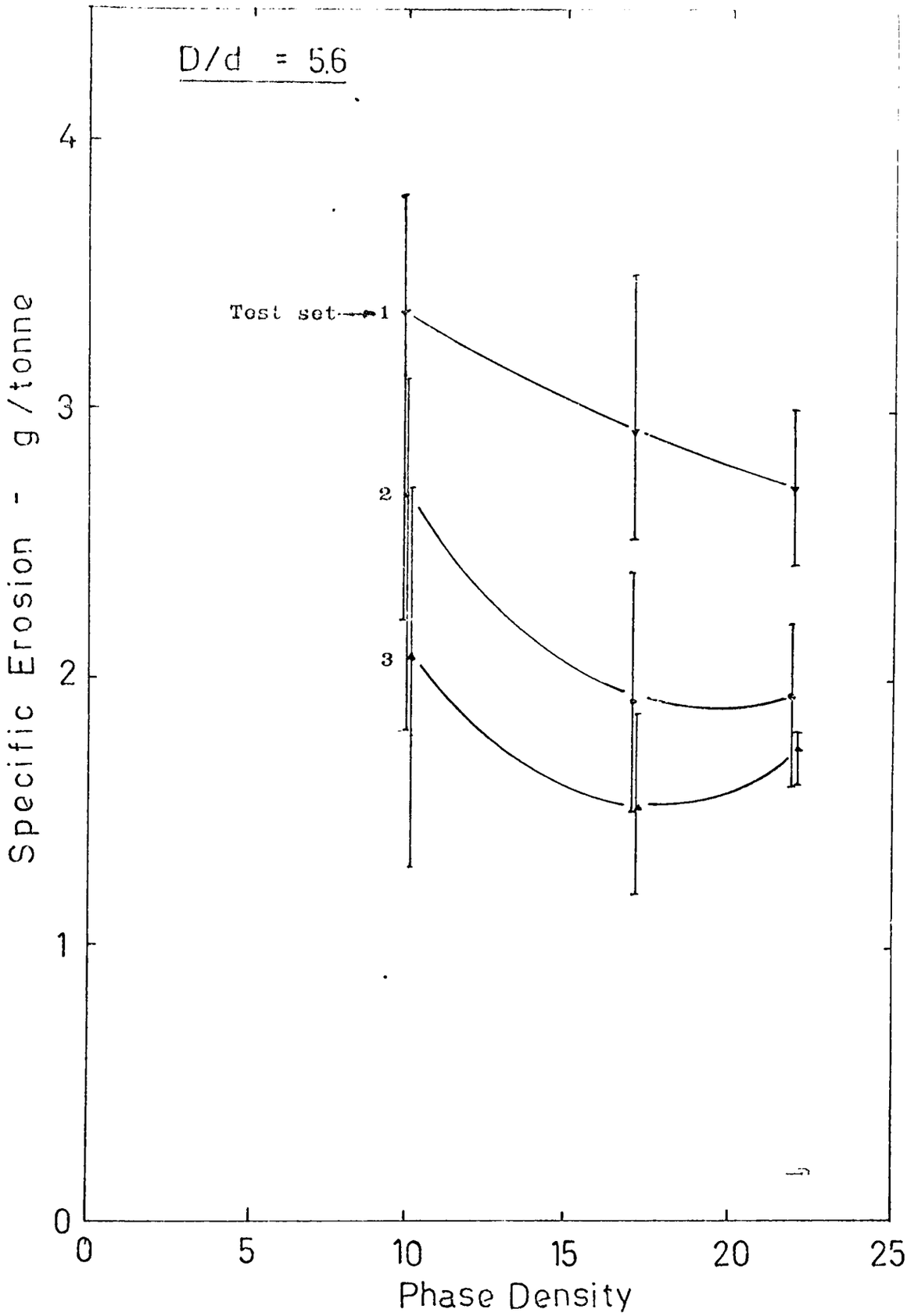

FIG. 10.7 Variation of Specific Erosion with Phase Density

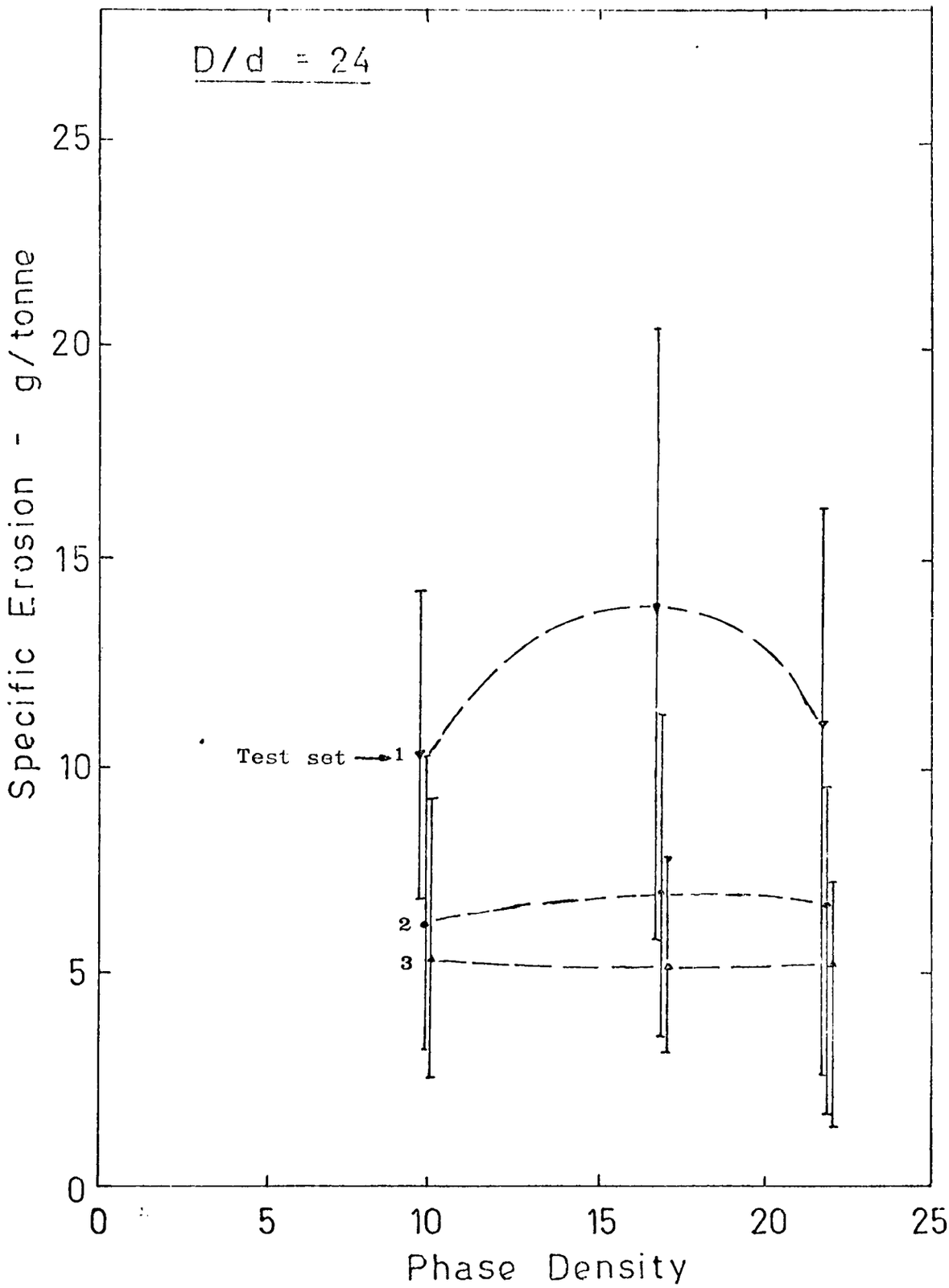

FIG. 10.8 Variation of Specific Erosion with Phase Density

decrease at a phase density of 17 compared to the corresponding values at a phase density of 22. In the case of the large radius bends (Fig. 10.8), apart from some initial variation in the mean values in test set 1, no substantial deviation is observed in the corresponding sets of mean values in test sets 2 and 3. In both figures the trend of the curves appears to provide evidence that a transition in the erosion process, similar to that in respect of velocity (see next section) is also operative over this phase density test range, and that this transition, based on the curves presented in Fig. 10.17 for the set of intermendiate bends, occurs at a phase density of about 17.

This transition is, perhaps, more clearly detected in Fig. 10.9, which is a log. plot of the mean specific erosion results presented earlier in Figs. 10.7 and 10.8. With reference to the set of mean values for the intermediate bends, although the plots through the results for test set 1 produced a perfectly straight line with a slope of -0.25, for test sets 2 and 3 it was not possible to draw continuous straight lines through all the respective sets of plots. From test set 2 onwards a distinct change in the slope occurred at a phase density of about 17 and this change in magnitude is particularly pronounced, from about -0.58 to 0.42, in test set 3. Although a gradual progressive decrease in erosion from one test set to the next is to be expected, for this instance the decrease was quite considerable. The trend of the slope in test set 1 clearly shows that erosion decreases as phase density is increased and can be explained partly as a result of fewer impacts occurring between the particles and the bend wall surface due to a corresponding decrease in particle spacing and partly as a result of particle degradation. That it should suddenly decrease by such a significant proportion below a given phase density, however, can only be attributed to a change in the nature of the erosion process below a certain transitional value of phase density.

Although a similar transition in respect of velocity has also been observed and attributed to a change in character of the product (Mills and Mason 1976 b), it should be noted that the batch of sand used in tests at a phase density of 22 had already been recirculated some 24 times previously at a phase density

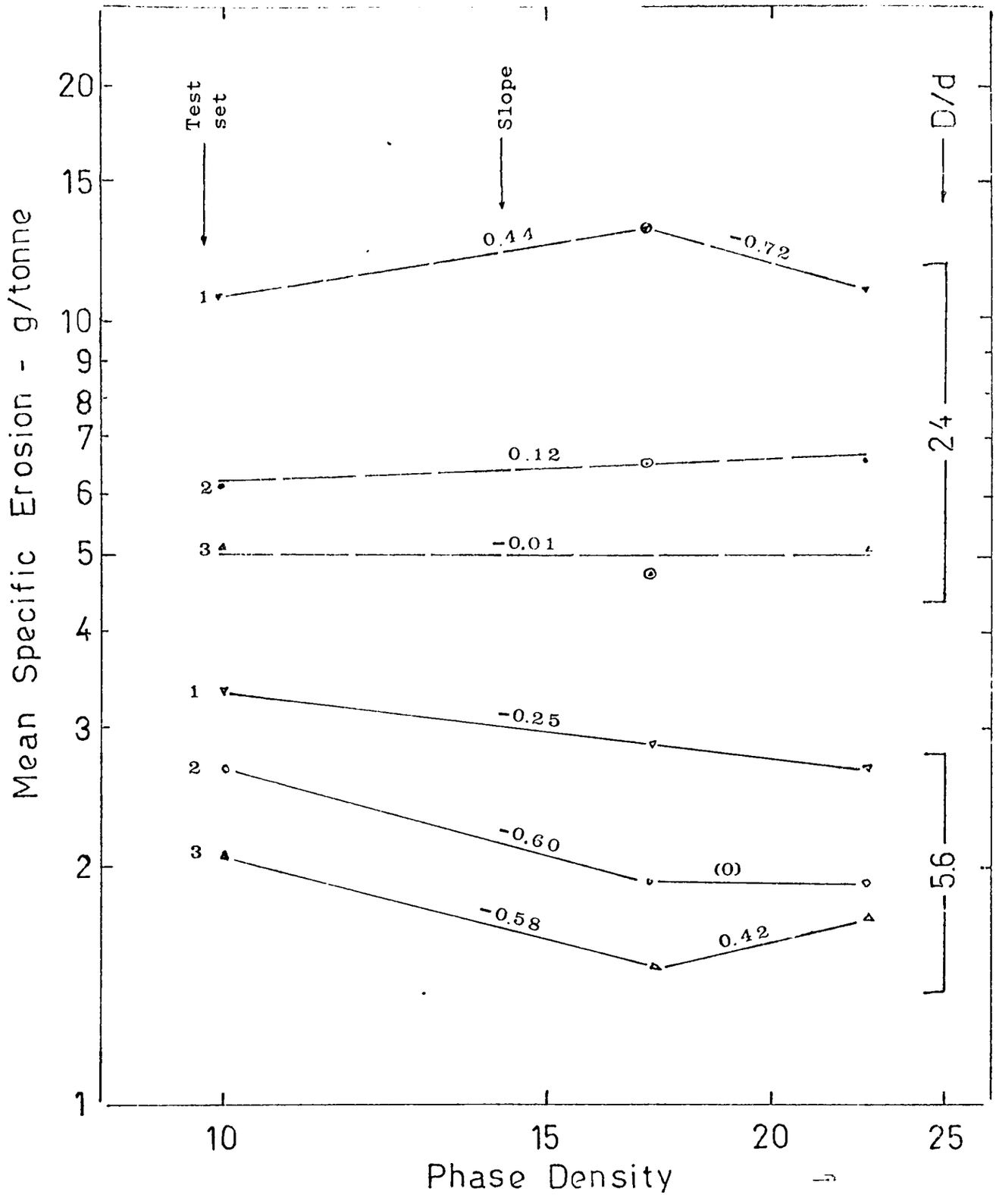

FIG. 10. 9. Variation of Specific Erosion with Phase Density

of 17. However, as reported in section 10.3.4, no substantial increase in the percentage of fines was observed after a further 30 test runs. Microscopic examination of the sand particles, in fact, revealed little noticeable difference between the fresh sand and that conveyed some 54 times. Hence, it appears that, although the sudden decrease at a phase density of 17 could be partly attributed to this limited change in particle degradation, a number of other factors, such as flow pattern, velocity, etc., are also involved. Further work, particularly above a phase density of 25 and over a wider range of test conditions, is needed in order to establish conclusively that a similar transition in respect of phase density also exists in terms of erosion.

With regard to the corresponding sets of test data for the large radius bends, the trend of the slopes appears to indicate that the transitional phase density effect is also considerably influenced by bend radius. Although the slope in test set 1 also shows a comparable change in the order of magnitude, which also occurs at a phase density of 17, it was, however, possible to draw continuous straight lines through the respective sets of erosion plots in test sets 2 and 3. In fact, the mean specific erosion values remain remarkably constant at about 6.6 and 5.1 g/tonne over this test phase density range. Whilst the comparability of the set of test results in test sets 2 and 3 provides evidence that for the set of large radius bends tested no similar transitional phase density effect is observed over this phase density test range, it should be noted that the mean values plotted at a test phase density of 17 exclude the individual test results of bend 2. If these were included in the analysis a transition would certainly be detected at this particular phase density. However, as explained earlier, due to the limited number of test bends and test range and the presence of other transitional effects, the values of the slopes obtained for the set of large radius bends tested are highly unreliable. Apart from these general observations, further work is obviously necessary in order to establish whether bend radius is also a significant factor in terms of the transitional phase density effect.

The absence of any significant decrease in erosion over this test range could also be partly explained by the peculiar nature of

flow in these large radius bends. As already mentioned, a transition in the mode of flow occurred in the vicinity of bend 2 at each test phase density. In bend 1 the mode of flow is essentially in the form of a moving bed and so no substantial erosion is therefore expected. In bend 11, due to the magnitude of velocity, the flow is essentially in the form of an homogeneous suspension, and so erosion would be substantially greater. In the case of bend 2, due to transitional effects erosion is unpredictable, as demonstrated by the individual curve in Figs. 10.3 and 10.4. Although there is a two-fold increase in velocity from bends 1 to 11, the corresponding increase in terms of erosion is only of the order of about 3:1 at a phase density of 10 and about 2:1 at the two higher phase densities. This magnitude of increase is much lower than the corresponding predicted increases based on velocity projection, particularly the measured values at a phase density of 22, which should show a nine-fold increase under similar conveying conditions. This lack of any substantial increase is largely attributed to the fact that as bend radius is increased a majority of the particles will tend to slide along the outer bend surface in the form of a loose and relatively slow moving deposit (Chapter 8). As the phase density of the suspension is increased there is a corresponding decrease in particle spacing, and this has the effect of reinforcing this deposited layer. As a result, for this set of large radius bends, apart from some limited initial variation, no appreciable decrease in erosion is observed over this test range.

10.4.2.3 Velocity Effects

In the analysis of the effect of phase density it was necessary to hold the velocity variable constant. As explained in section 10.3.3, velocity is a major variable in its own right and the significance of this variable is demonstrated by the trends of the curves presented in Figs. 10.3 to 10.5 earlier. In this section the specific effect of velocity is discussed in more detail.

Fig. 10.10 shows the effect of velocity based on the set of test results for the intermediate bends, and Fig. 10.11 for the large radius bends. These are log. plots of the individual

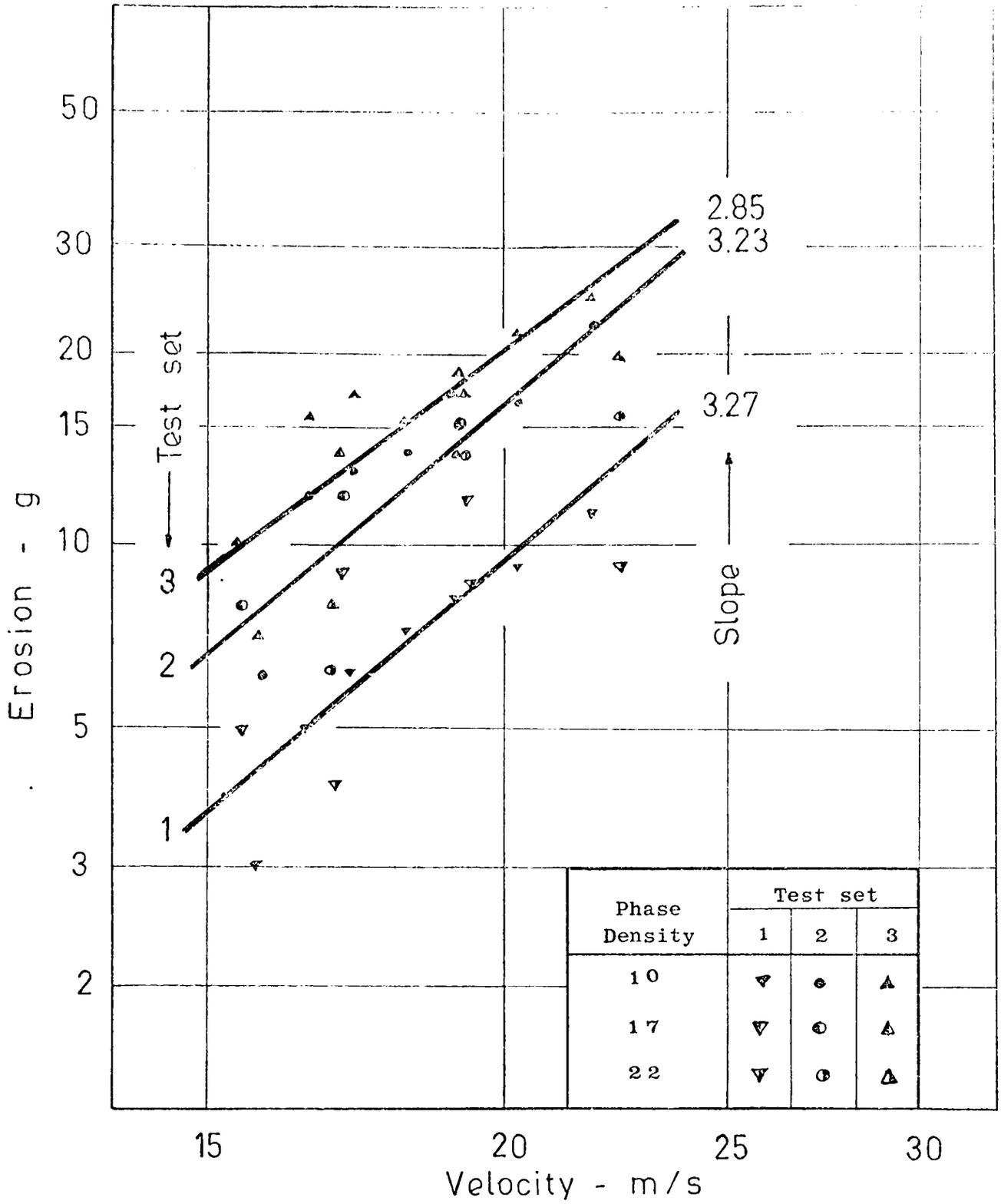

FIG. 10.10. Variation of Accumulative Erosion with Velocity

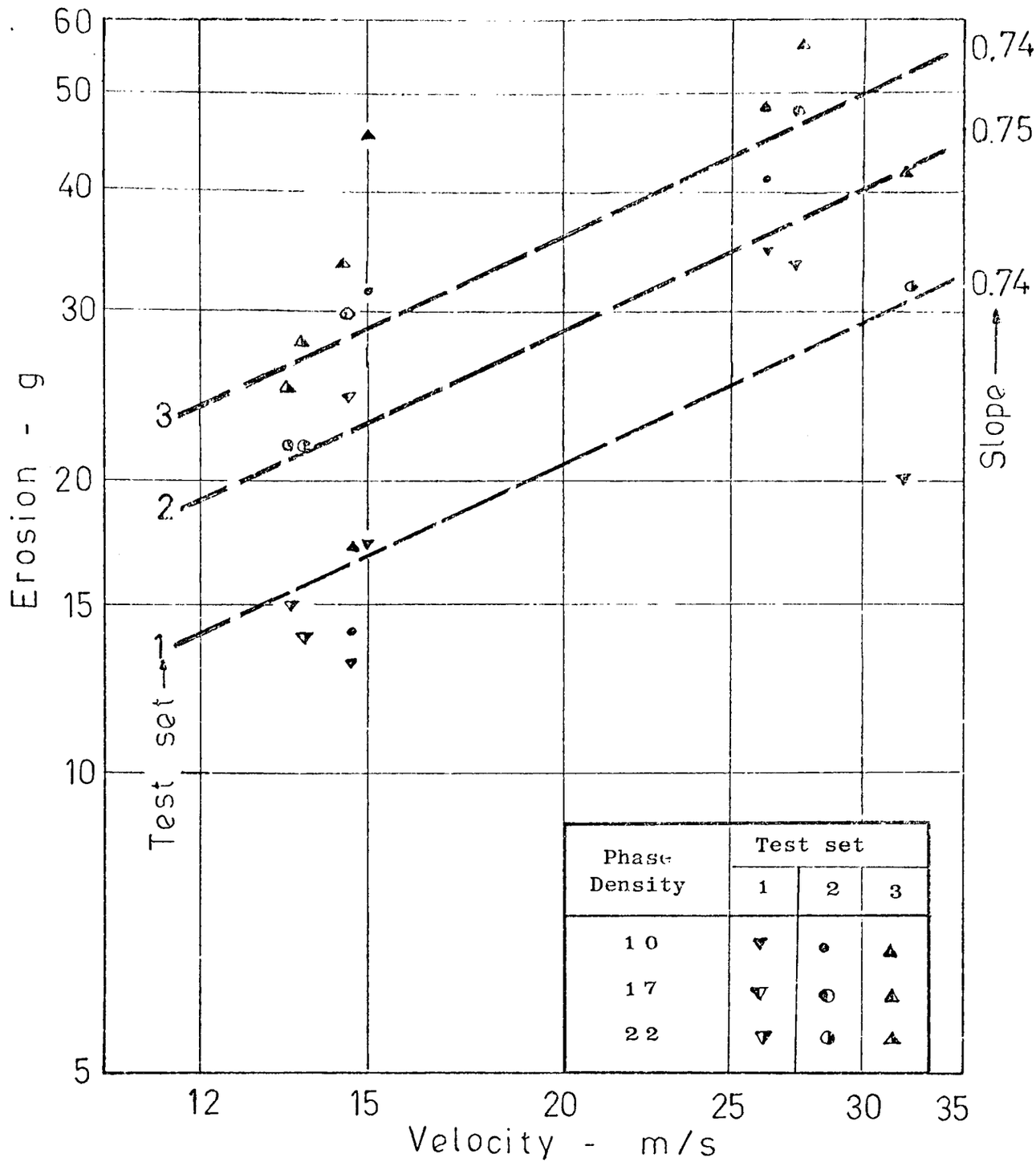

FIG. 10.11. Variation of Accumulative Erosion with Velocity

erosion values at each test phase density on an accumulative basis. Whilst the trend of the slopes in both figures clearly shows that the effect of velocity on erosion is independent of phase density, the magnitude of this effect is considerably influenced by bend radius. This is contrary to the trend of the results obtained in previous dilute phase work (see section 8.2.4, p.170), which showed that the magnitude of the effect of velocity is relatively independent of bend radius.

As discussed in the preceding section, the erosion results obtained over the range of phase densities tested clearly showed that there is some fundamental variation in the mechanics of the erosion process and, in terms of velocity effect, a similar transition in the erosion process is also observed, as shown by the sharp contrast in the magnitude of the slopes in Figs. 10,10 and 10.11.

The fact that there was a similar transition in respect of velocity has been recognised in previous studies. Goodwin et al (1969) reported that erosion results may be influenced by a threshold velocity so that there is effectively a higher exponent at low velocities, whilst Finnie (1960) postulated that below this velocity the lack of any substantial erosion is due to the particles impacting elastically with no weight loss. Mills and Mason (1976 b) found that in bend erosion situations the transition in the erosion process occurred within a narrow velocity range of about 26 to 32 m/s. Within this range an abrupt change in the velocity exponent from about 2.65 to about 4.8 was obtained, which indicated that a transitional stage in respect of erosion had been reached and that the transitional velocity at which this occurs is a function of particle shape. Mills and Mason further commented that, if tests were carried out only on either side of the transition velocity, almost any value of the velocity exponent could have been obtained.

As the velocity range for the set of intermediate bends was below this transition velocity (Fig. 10.10), it is perhaps not surprising that the velocity exponents were significantly higher than the value of 2.65. However, it is interesting to note that there is a gradual decrease in the velocity exponent and this general decrease is attributed to the limited change in the condition of the product.

In the case of the large radius bends (Fig. 10.11), although the velocity exponent remains remarkably constant at about 0.74, this value is quite meaningless. Only three large radius bends were tested within each test series, two of which were within a very narrow velocity range of about 13 to 15 m/s, and the velocity range for the third bend was about 26 to 31 m/s, which is in the region of the transition velocity range. In the absence of any intermediate erosion data between these two ranges, it was not possible to determine the actual value of the velocity exponent for this set of large radius bends.

It should be pointed out that the accuracy of the velocity exponents shown in Fig. 10.10 for the set of intermediate bends is also questionable, since no attempt was made to correct these test results at a given phase density to a given constant particle concentration. Mills and Mason (1976 a) pointed out that this correction procedure was necessary, due to the variation of particle concentration in the test section, which has an effect on the velocity term. Since there is a significant increase in both velocity and particle concentration over this test range, the individual erosion values should be normalised with respect to both these variables. This iterative normalising procedure, however, was not carried out due to the narrow range of velocities, which was below the transition velocity range, and it was felt that it would not be possible to determine the precise value of the velocity exponent with sufficient accuracy to warrant it. Suffice to conclude that the trend of the results in Fig. 10.10 provides clear evidence that an additional transition in the process in respect of the velocity has been observed over this test range. In the case of the results presented in Fig. 10.11 for the set of large radius bends, although no firm conclusions can be drawn due to the lack of sufficient test data, the magnitude of the results appears to indicate that a crossing of the transition in respect of erosion has occurred over this velocity range..

10.4.2.4 Comparison with Dilute Phase Test Data

In the preceding sections it has been shown that apart from transitional effects the magnitude of the effect of phase density on erosion is also considerably influenced by bend radius over

this test range. Owing to the unreliability of the test results and the absence of any previous corresponding dilute phase test data for this set of large radius bends, this section is mainly concerned with the test results for the set of intermediate bends. Since the velocity range is relatively limited, however, the analysis is on the specific effect of phase density only.

As shown in Fig. 10.7, although a transition in respect of erosion has been detected over this test range, the trend of the results in test set 1 clearly shows that erosion decreases slightly over this range of phase densities. From a corresponding log. plot of the curve presented in Fig. 10.9 the magnitude of the slope is -0.25, and hence for this phase density test range the effect of phase density on erosion is given by :-

$$\text{erosion} \propto (\text{phase density})^{-0.25} \qquad (10.2)$$

The value of this exponent, obtained over a relatively restricted medium phase test range, differs from those obtained in previous dilute phase work (see Fig. 6.8, p.91). As reported in Chapter 6, over a similar number of test runs, from tests with 250 μm sand the exponent was -0.43, and from tests with 230 μm and 70 μm sand, Mills and Mason (1976 a, 1977 a) reported that the exponents were -0.16 and -0.37. Although direct comparison between these exponents is not appropriate due to different test procedures, it has been shown that the exponent was also influenced by particle shape. Furthermore, at high phase densities the magnitude of this variation was shown to be dependent upon particle size. For these reasons, and in view of the associated transitional effects detected over this medium phase test range, it was decided by the author, for comparison and consistency purposes, to determine the overall effect of phase density based on the test results of 70 μm sand only.

In order to establish the overall trend it was necessary to normalise the corresponding dilute phase erosion data to a velocity of 25 m/s by a similar factor of 2.65. These normalised values, together with those obtained in this work, are presented in Fig. 10.12. From a linear regression analysis of the relevant data, the effect of phase density in terms of specific erosion

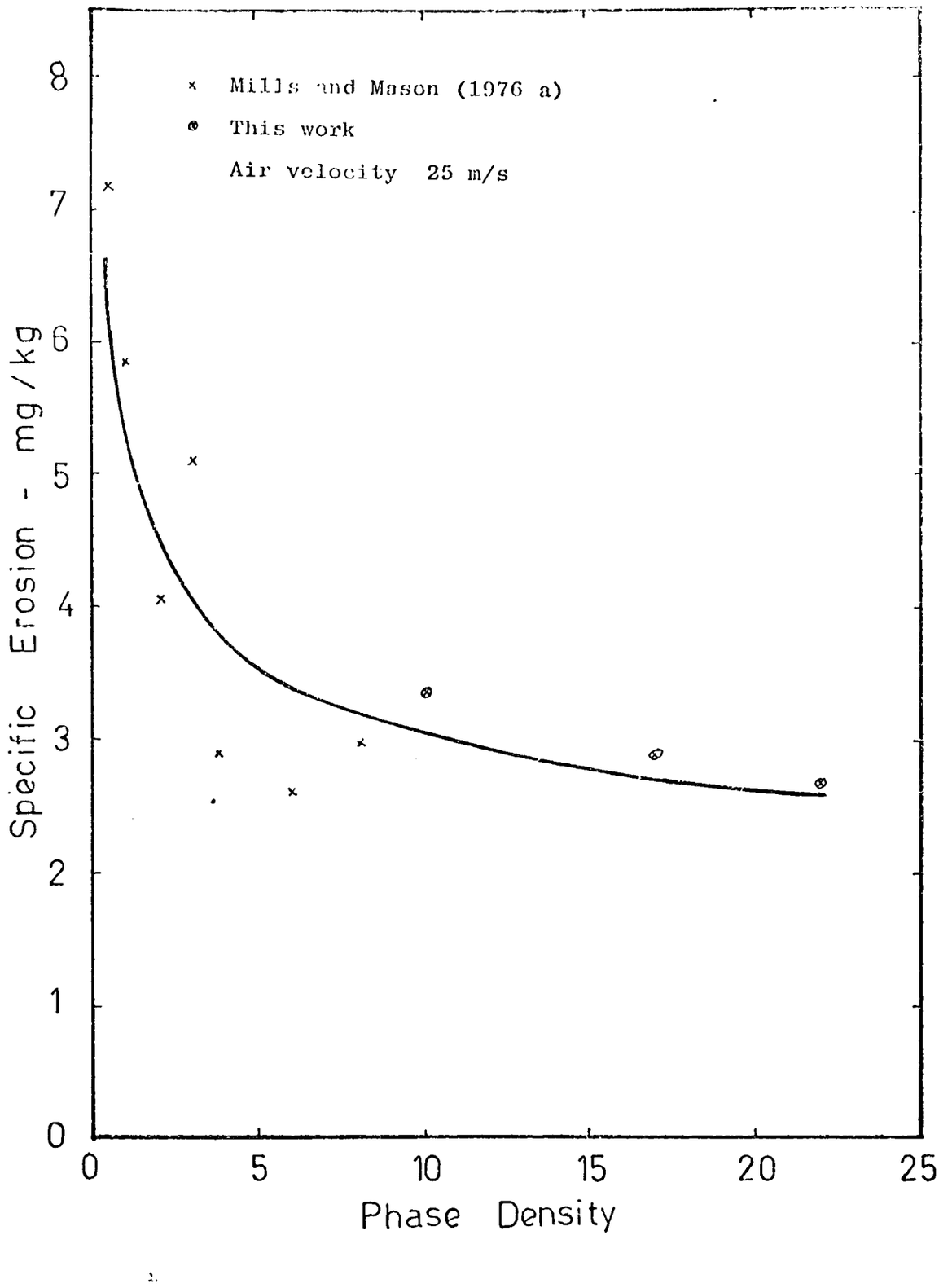

FIG. 10. 12 Influence of Phase Density on Specific Erosion

can be modelled by the expression :-

$$\text{erosion} = 5.50\ (\text{phase density})^{-0.26}\ \text{g/tonne} \qquad (10.3)$$

over both test ranges considered. Apart from some deviation between the model and the actual test results, particularly between the phase density of 3 to 6 which has been attributed to the presence of a substantial degree of scatter, the predicted and measured values are in close agreement. Although it is possible to predict the results beyond this test range by extrapolating this curve, it should be noted that the test results at a phase density of 17 and 22 were only based on three test bends. Hence, due to this relatively limited source of test data, and taking into consideration the various potential transitional effects at high phase densities, the validity of this model beyond the ranges considered here will require further work. In addition, it should also be pointed out that this model is based on the erosion of mild steel test bends with a D/d ratio of 5.6 by sand with a mean particle size of about 70 μm, and consequently the validity and applicability of this model is restricted to these test conditions.

As already discussed elsewhere, another factor which should be taken into account is the effect of bend radius. The significance of this is demonstrated by the test data presented in Fig. 10.13, which provides clear evidence that, apart from velocity, the magnitude of the effect of phase density is also considerably influenced by bend radius, particularly at high phase densities. For comparison purposes the test results based on the work reported in previous chapters are also included, together with the curves given in equation 10.3 for the set of bends with a D/d ratio of 5.6. Apart from the test data for the Booth bend (D/d of 2.4) which had been eroded by p.f. ash (Chapter 7), all the test data presented in this figure was based on similar sized 70 μm sand particles.

Although the conveying conditions vary considerably over this test range, the results do show comparative trends with respect to bend radius effect on phase density. Whilst a definitive trend with respect to the influence of bend radius is given by the curves for bends with a D/d of 5.6 and the Booth bend, the

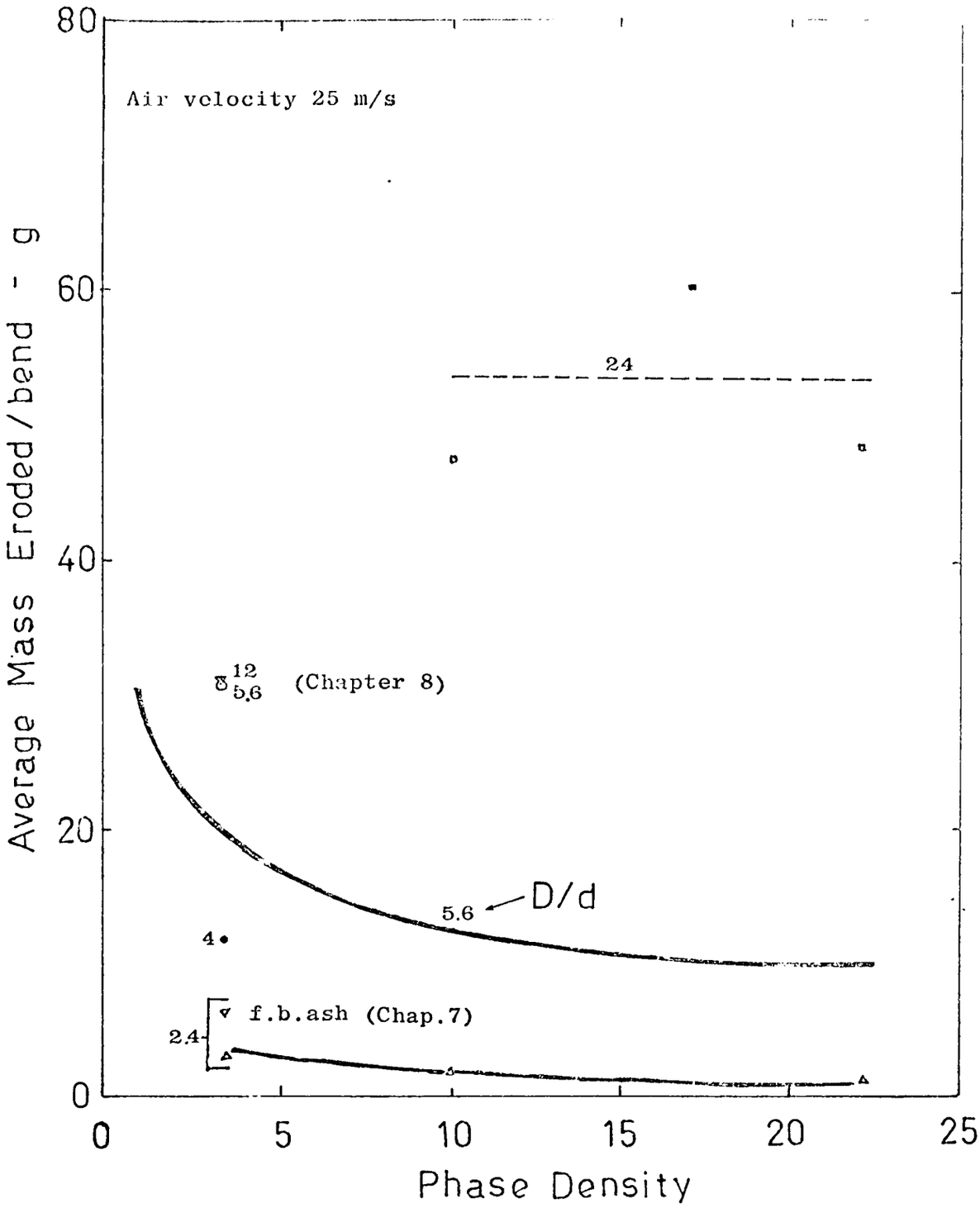

FIG.10.13 Influence of Diameter Ratio on the Variation of Phase Density with Mass Eroded

lack of any comparability of these two curves indicates that the effects of phase density and bend radius are closely interrelated. Apart from this limited observation, further work is necessary over a wider test range and bend geometry in order to determine precisely the magnitude of the effect of bend radius on phase density.

10.4.3 Penetration Rate Analysis

10.4.3.1 Introduction

In the analysis presented in the preceding section it has been clearly demonstrated that phase density has little effect in terms of specific erosion over this test range. Although this is in general agreement with the finding based on limited bench type solid particle erosion studies (see Fig. 10.1), the trend of the slopes in Fig. 10.9 appears to indicate that, in terms of bend erosion, little further effective reduction can be gained by conveying abrasive materials in the dense phase mode at a constant value of velocity. However, as explained in previous analyses in pipe bend erosion situations, since the thickness of a bend is finite it is generally the depth of penetration of the particles into the bend wall that is the important factor, as this determines the service life of the bend. In this respect the penetration rate has been shown to have an over-riding influence over that of mass eroded, although the magnitude of this penetration rate is considerably influenced by particle size.

As discussed in Chapter 6 and in section 10.2, Mills and Mason (1977 a) have found that, in terms of μm/g eroded, a marked increase in penetration rate with respect to phase density is observed (see Fig. 6.10, p.95). Whilst this relates to dilute phase conditions, the implications of this trend at higher phase densities are quite serious. In terms of penetration wear rate (mm/tonne), Mason and Smith (1972) have theoretically postulated that a critical maximum should exist with respect to phase density. In a later paper (Arundel et al 1973), they produced a curve based on industrial information which showed that it corresponds to a phase density of about 24 (see Fig. 10.1). From this relatively limited information it has been clearly demonstrated that phase density has a marked effect in terms of penetration

rate and, in order to establish whether a similar critical maximum exists over this test range, the effect of phase density on penetration is discussed in the following sections.

10.4.3.2 Phase Density Effects

Figs. 10.14 to 10.16 show the corresponding penetration results in terms of the variation of maximum depth of penetration with mass eroded at each test phase density. As in Figs. 10.3 to 10.5, the same symbols are used to identify the individual experimental points for each test bend, and so these plots show the individual penetration history at a given phase density. As the maximum depth of penetration recorded at a phase density of 22 is only 0.6 mm, compared to about 2.0 mm recorded at the two lower phase densities, the ordinate scale in Fig. 10.16 has been magnified accordingly. In the case of the Booth bend, due to the absence of any intermediate test records, it was decided not to include the test data of this particular test bend in Figs. 10.14 and 10.16. It should be noted, however, that at a phase density of 10, a maximum depth of penetration of some 3.2 mm was recorded for this particular bend. In contrast, at a phase density of 22 only a maximum depth of about 0.6mm was recorded (see Table 10.1). A number of factors which may account for this dramatic reduction are discussed in more detail in section 10.4.3.4.

In order to identify the penetration history of each individual test bend, lines were drawn through the points plotted and these curves clearly demonstrate that, in terms of penetration, bend radius is also a significant factor. However, a more important feature is with regard to the overall trend. Whilst the trend of the curves for the set of intermediate bends is remarkably consistent over this test range, in the case of the large radius bends, apart from a change in the order of magnitude, a significant transition with respect to the individual trend of the curves is clearly evident.

At phase densities of 10 (Fig. 10.14) and 22 (Fig. 10.16) the trend of the curves for bends 1 and2 is identical and clearly shows that, beyond an initial increase, no further increase in penetration is observed. In contrast, the corresponding trend of bend 11 clearly indicates a continuous progressive increase

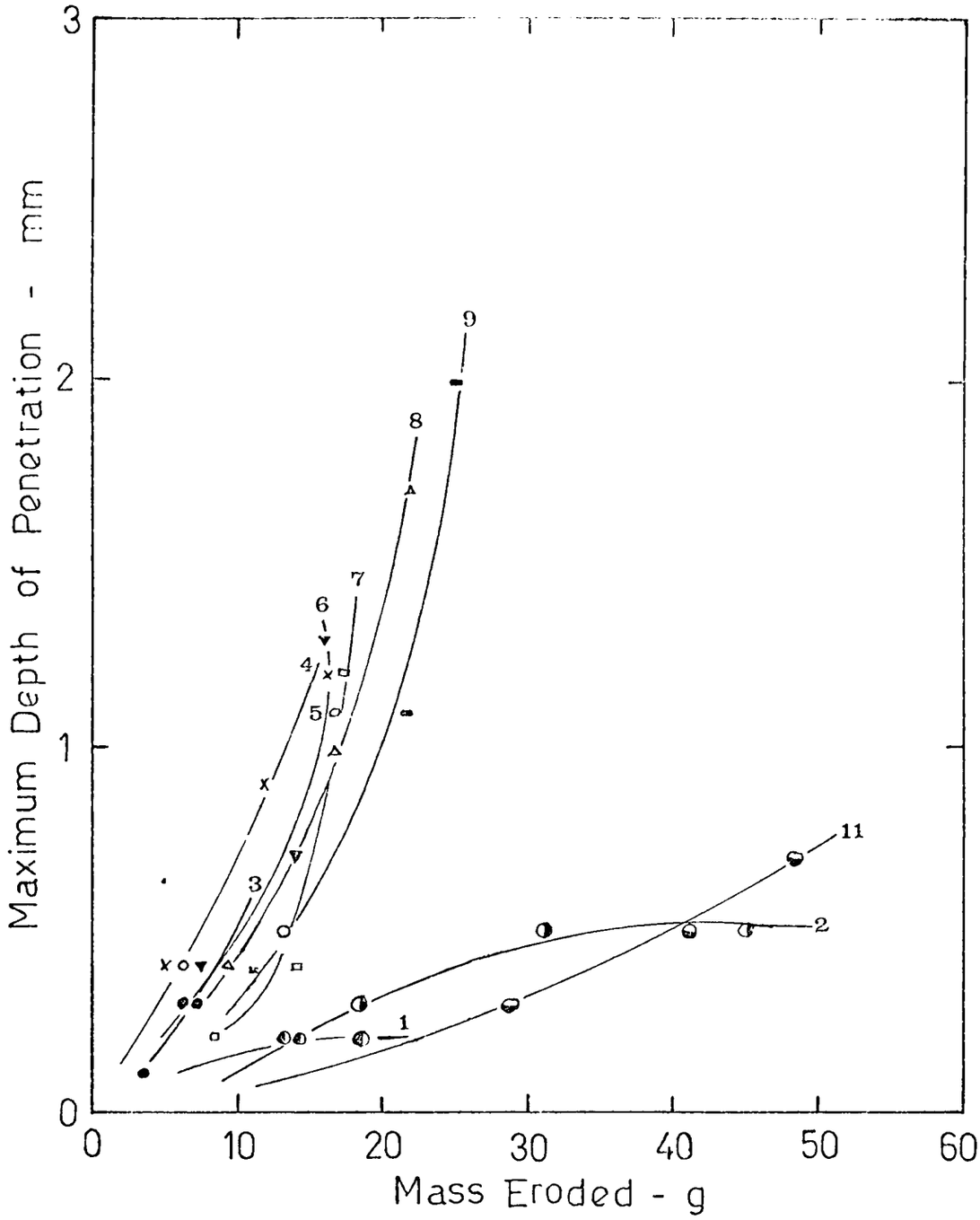

FIG. 10.14 Penetration Data for Individual Bends Tested at a Phase Density of 10

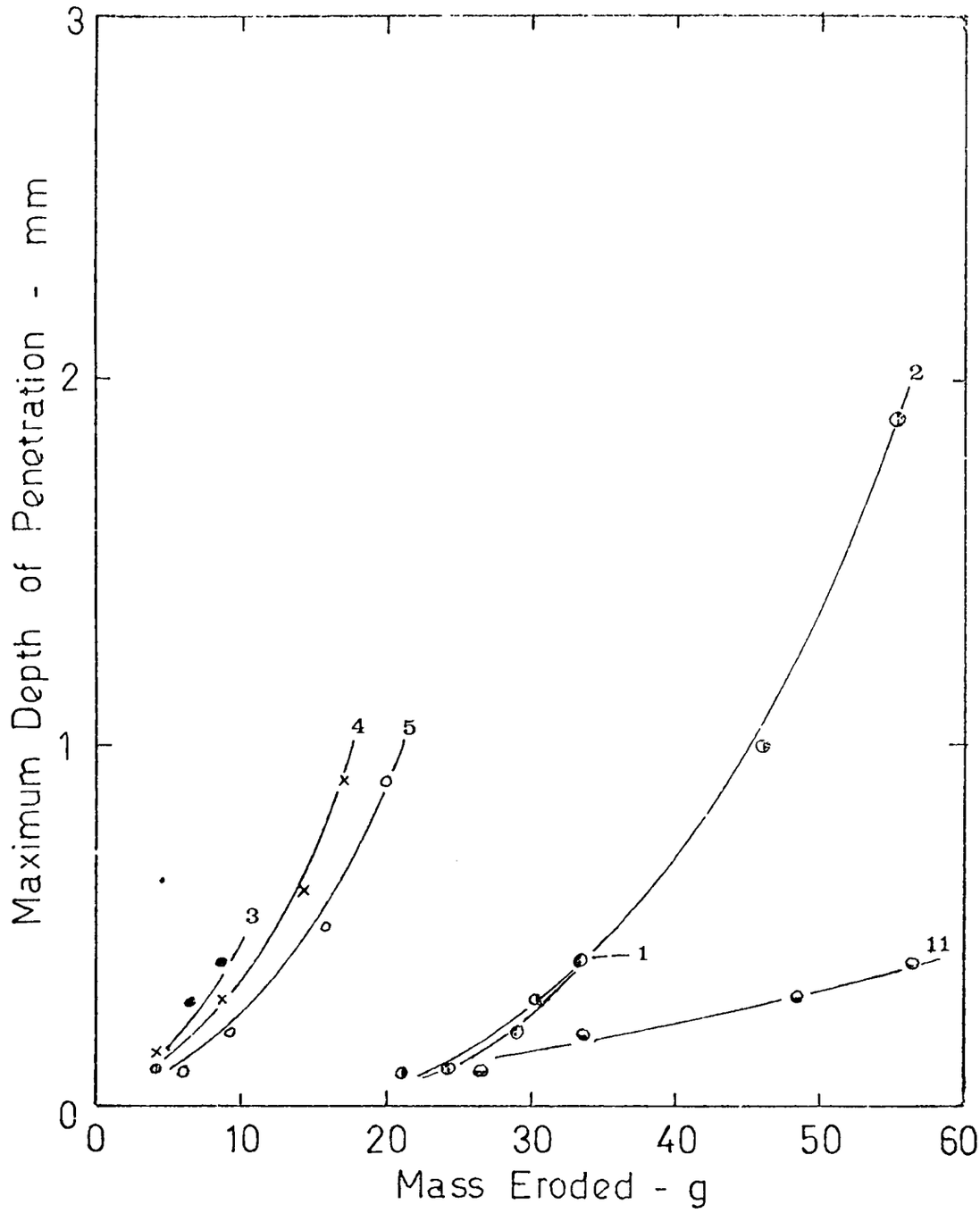

FIG. 10.15 Penetration Data for Individual Bends Tested at a Phase Density of 17

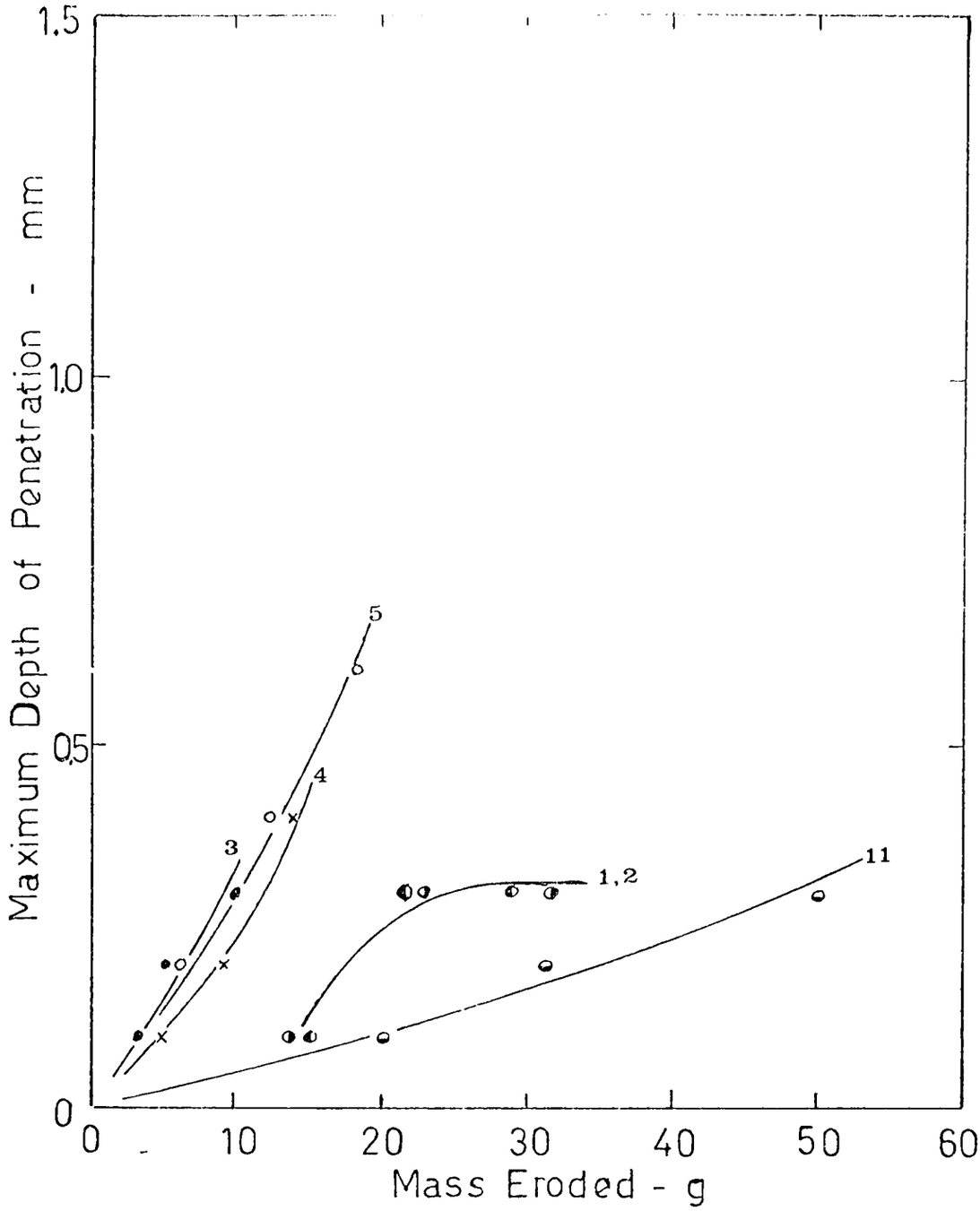

FIG. 10.16 Penetration Data for Individual Bends Tested at a Phase Density of 22

in penetration over a similar range of tests. That there should be such a distinct change in the trend between these curves clearly indicates that this is a direct result of transitional effects discussed earlier.

Comparison of the corresponding set of curves at a phase density of 17 (Fig. 10.15), however, appears to indicate that phase density might also be an additional factor. The trend of bend 2, contrary to expectations, clearly shows a rapid increase in penetration which is substantially greater than that of bend 11. Although a similar trend is also observed in bend 1, it is unlikely that a similar rapid rate of penetration would be possible in this particular test bend. The maximum depth of penetration recorded was only 0.4 mm compared to about 2.00 mm for bend 2 over a similar range of tests and in view of transitional effects the slope of this particular bend would probably level off, as indicated by the dotted line, beyond this test series. In the case of bend 11, no appreciable deviation is observed and the trend is similar to that observed at the other phase densities. In fact, the magnitude of this slope is identical to that of bend 11 at a phase density of 22 (see Fig. 10.18, p.296). Although phase density is a possible factor, perhaps a more plausible explanation for the behaviour of bend 2 is the presence of a transition in the flow pattern. As already discussed elsewhere, a transition occurred in the vicinity of bend 2 at this particular phase density and this was largely responsible for the rapid increase in respect of erosion. Although it has been shown that, for a given phase density, mass eroded is not proportional to depth of penetration (see Fig. 6.9, p.93), a rapid increase in erosion is usually followed by a similar rapid increase in penetration (Chapter 8), and so in this respect it is perhaps not surprising that a similar trend is observed in bend 2 in both cases. However, it should be noted that a similar transition also occurred in the vicinity of bend 2 at a phase density of 10, and between bends 3 and 4 at a phase density of 22. No apparent transition in respect of penetration was observed in these respective bends and it appears, therefore, that additional factors may be responsible. Visual observation of the outer bend wall surface of this particular test bend (see Fig. 10.30, p.324), shows a

clear erosion tracking pattern, which indicates the presence of a considerable degree of swirling in the flow. The presence of swirling in these bends is not unexpected, but that it should occur to such an extent is probably due to misalignment of this particular test bend. Hence, it appears that the rapid rate of wear in this particular bend is probably due to the combination and interaction of the various factors described above and further work is necessary in order to investigate in more detail this complex phenomenon.

In order to show the overall specific effect of phase density, the mean slopes of the two sets of bends tested in Figs. 10.14 to 10.16 are presented in Fig. 10.17. Since the maximum depth of penetration recorded for the majority of the test bends was relatively limited, for comparison purposes the ordinate scale is magnified accordingly.

For the set of intermediate bends, the slopes clearly show that, in terms of μm/g eroded, a definite decrease in penetration rate is observed over this test range. The overall trend of the effect of this higher range of phase densities is in complete contrast to the corresponding trend presented in Fig. 6.9, based on dilute phase test data and clearly shows that a maximum has been crossed between these two test ranges (see Fig. 10.22, p.304). It should be noted, however, that the slopes presented in Fig. 6.9 were based on tests carried out at a velocity of about 25 m/s. As the overall mean velocity is approximately 19 m/s over this test range, proper comparison between these slopes is not strictly appropriate. The test data obtained in this work will have to be normalised before accurate comparison can be made, as in the preceding analysis on specific erosion, and this will be discussed in the next section.

With respect to the corresponding mean slopes for the set of large radius bends, a similar problem also arises. As the velocity in bend 11 is approximately double that of bend 1 at each phase density, the trend of the individual curves presented in Figs. 10.14 to 10.16 is also influenced to a certain extent by this velocity difference. Apart from velocity effects it has been shown that the trend of the curves is also influenced by a number of other transitional

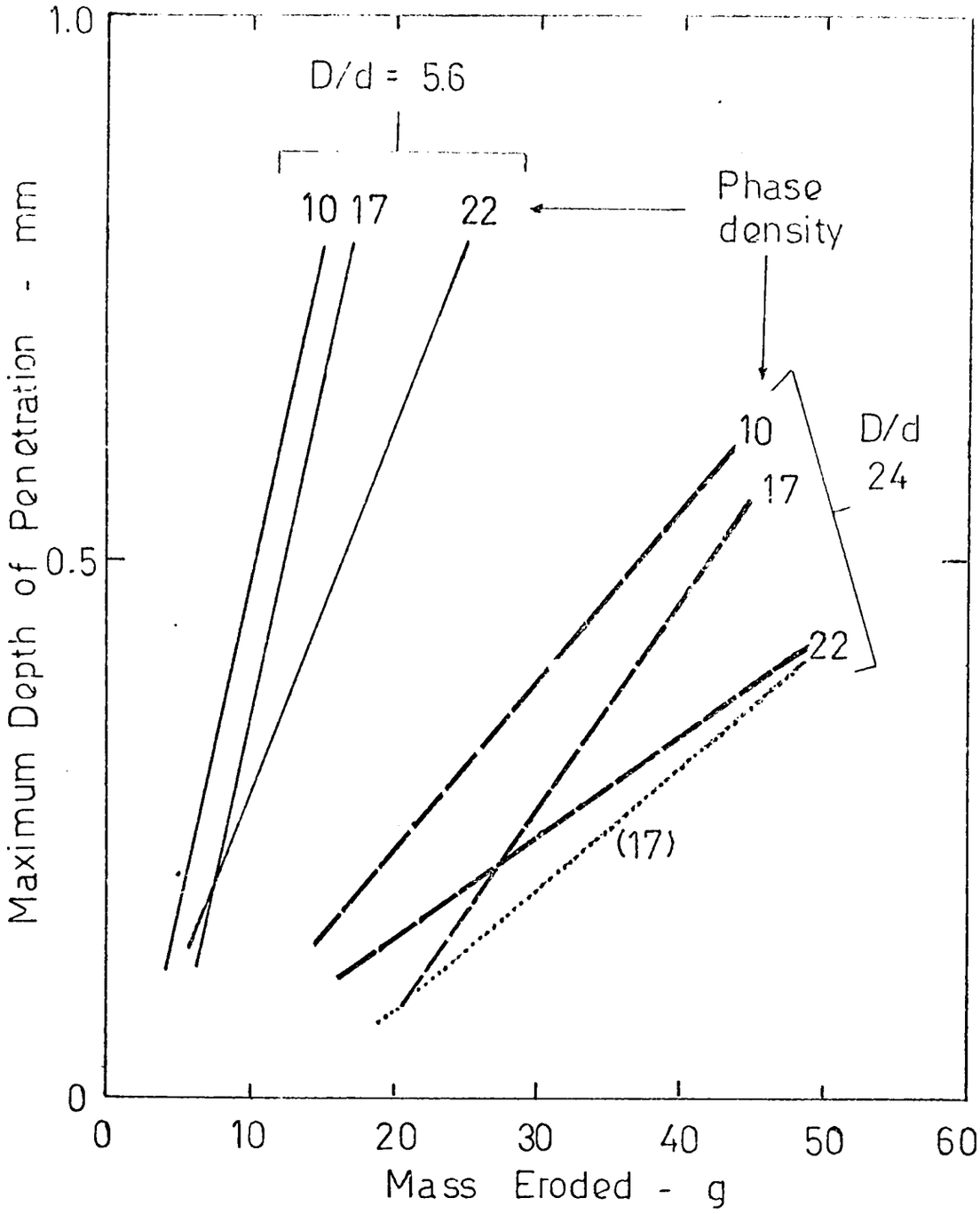

FIG. 10. 17 Influence of Phase Density on Penetration Rate

factors, and due to the limited test data accurate determination of the respective mean slopes is extremely difficult. Hence, in view of these uncertainties, the mean slopes presented in Fig. 10.17 are, at best, only approximations. Although the gradients of these slopes appear to show that maximum penetration rate occurs at a phase density of 17, it should be noted that this apparent existence of a maximum is primarily due to the rapid penetration of bend 2, as explained earlier. If the individual test results of this particular test bend are excluded from the analysis, the mean slope is subsequently represented by the dotted line and is comparable to that at a phase density of 22.

Although direct comparison between the slopes of these two sets of bends is not appropriate, the slopes do show a comparative trend in respect of phase density, and the magnitude of this is clearly influenced by bend radius. In both cases a definite trend towards a decrease in penetration rate with increasing phase density is clearly observed over this test range.

10.4.3.3 Velocity Effects

The curves presented in Figs. 10.14 to 10.16 also show the magnitude of the inter-relating effect of velocity As discussed in section 10.2, it has been reported that the magnitude of penetration is predominantly influenced by velocity (Bikbaev et al 1973), and that the rate of penetration increases with velocity (Mills and Mason 1976 d). Although these findings were based on dilute phase conveying conditions, with a correspondingly higher velocity test range, the trend of these results clearly demonstrates the paramount effect of velocity, particularly in respect of penetration.

As already discussed elsewhere, due to the essentially different operating conditions involved in this work, apart from the inter-relating effects of phase density and bend radius, it is extremely difficult to isolate velocity, particularly from transitional effects, which have been shown to be a recurring feature over this test range. Hence, in this respect analysis of the specific effect of velocity will also have to take these transitional effects into account.

To show the overall effect of velocity in terms of penetration rate, a select number of curves from Figs. 10.14 to 10.16 have been replotted and these are presented in Fig. 10.18. These curves were selected on the basis of comparability in respect of velocity such that, apart from showing the specific effect of velocity for a given phase density and bend radius and vice-versa, they also show, more importantly, the magnitude of these inter-relationships.

For the set of curves representing the intermediate bends, two important features are observed. For a given phase density a definite trend towards a decrease in penetration rate, in terms of mm/g eroded, as velocity increases, is clearly detected. Perhaps this trend is more clearly evident in Fig. 10.19, which shows in more detail the relationship based on the set of curves at a phase density of 10 (Fig. 10.14). In this figure the value of mass eroded up to a penetration depth of 1.00 mm in increments of 0.2 mm were determined and these were then plotted against the corresponding velocity appropriate to each bend. Straight lines were drawn simply to distinguish the respective groups of points and these provide experimental evidence that, for a given depth of penetration, the mass eroded from the bend increases with velocity, i.e. penetration rate decreases as velocity is increased. A similar trend is also observed over this phase density range. In terms of phase density effect, comparison of the set of curves between bends N3, P3 and Q3, and between bends N7, P4 and Q5 (Fig. 10.18), shows a similar trend in respect of phase density. In both cases this is in complete contrast to the trend reported by Mills and Mason (1976 d), based on dilute phase test data. This markedly reversed phenomenon provides additional substantial experimental evidence that a fundamental variation in the mechanics of the erosion process has been reached over this test range, and that this transition occurs between a phase density value of about 8 and 10.

For the set of large radius bends, apart from the contradictory curve of bend P2, a relatively similar trend in both cases is also clearly evident. However, it can be seen that, apart from transitional effects, the curves in Fig. 10.18 show that, over this test range the magnitude of penetration is substantially

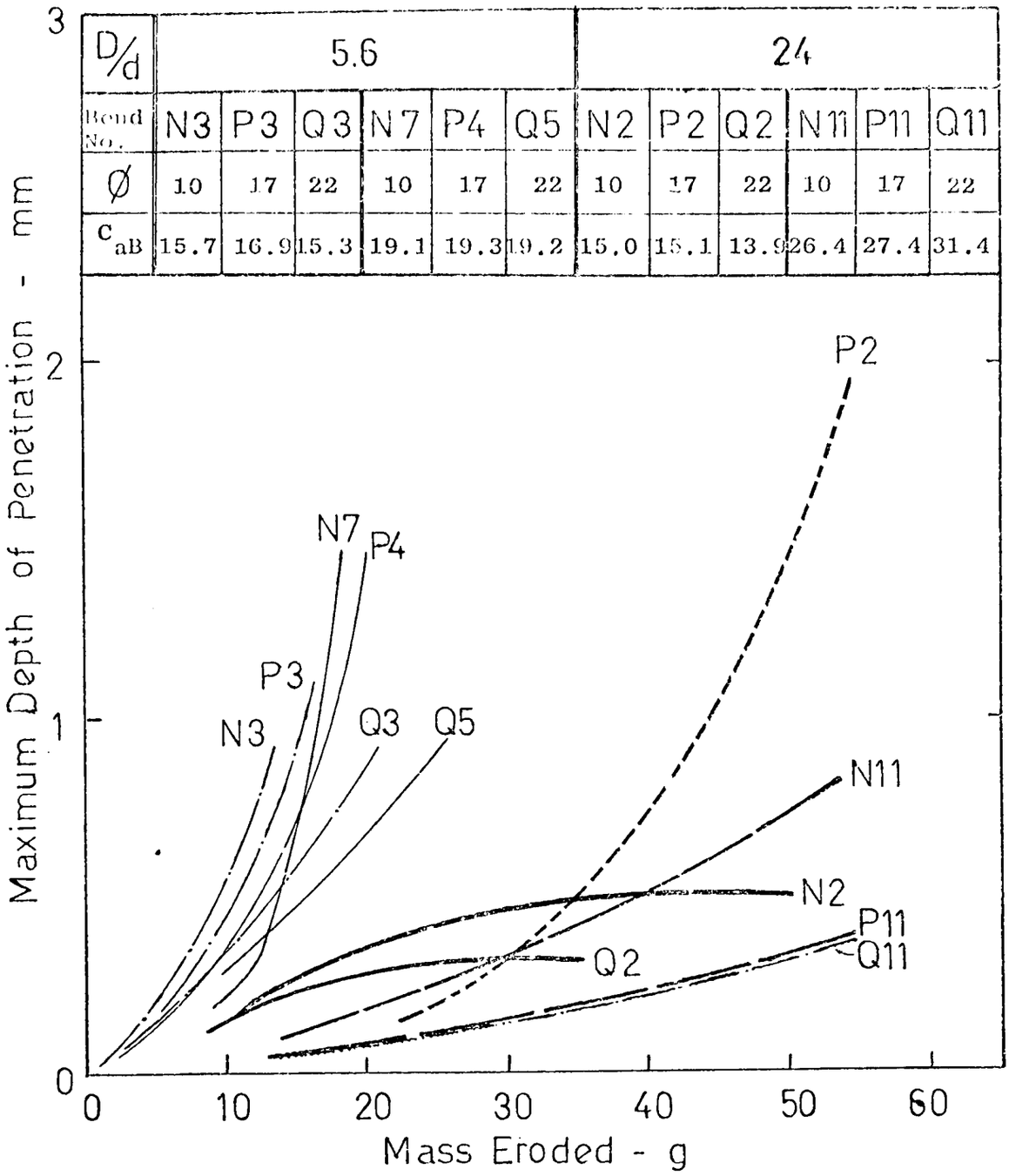

FIG. 10. 18 Variation of Maximum Depth of Penetration with Mass Eroded for a Number of Selected Test Bends

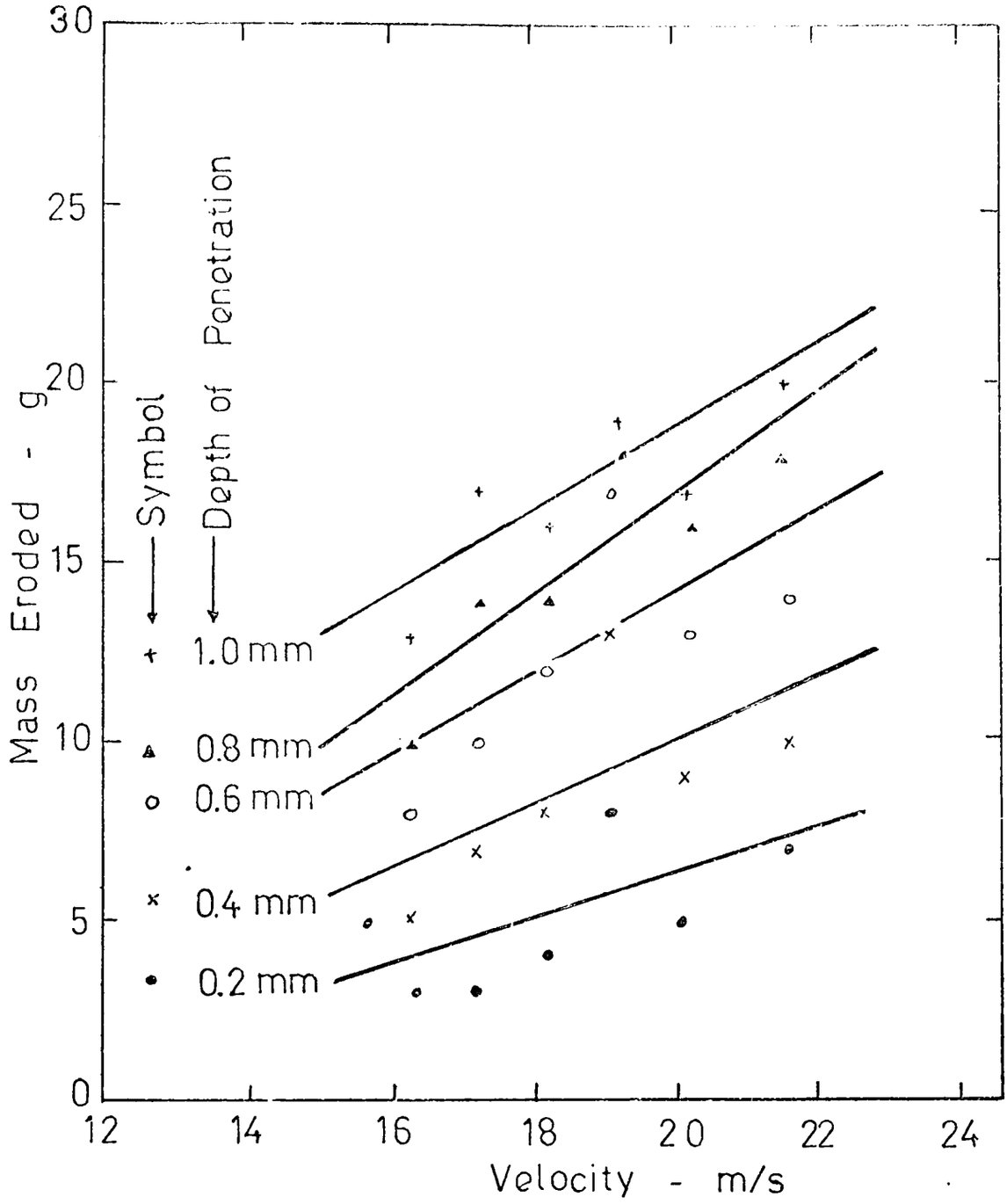

FIG. 10. 19 Influence of Velocity on Penetration in terms of Mass Eroded

influenced by the mechanics of flow which clearly has an over-riding influence over that of velocity, particularly for these large bends.

As mentioned earlier, in order to provide comparability with previous dilute phase test data, it is necessary to normalise these penetration results to a velocity of 25 m/s. To do this it is necessary to determine the relationship between depth of penetration and velocity over this test range, and these are presented in Fig. 10.20 (a to c) for the set of intermediate bends and Fig. 10.21 for the set of large radius bends. As in previous analyses, the test results corresponding to the three respective sets of tests are given.

Whilst the plots in Fig. 10.20 (a) for the set of bends tested at a phase density of 10 appear to indicate that a linear relationship exists in all cases, the corresponding sets of plots at the two higher phase densities (b and c), clearly indicate a power law relationship. However, due to the limited test data, and the lack of any overall consistent characteristic, it is not possible to determine the precise nature of this relationship and so no attempt has been made to draw lines through each respective set of plots in this figure. However, it is interesting to note that whilst the test results at the two higher phase densities appear to be comparatively consistent in terms of individual trend, at a phase density of 10 the depth of penetration appears to be initially independent of velocity but, once established, it increases rapidly as velocity increases.

For the set of large radius bends (Fig. 10.21), due to the large degree of scatter and the absence of any corresponding test data within a velocity range of about 15 to 26 m/s, it is not possible to determine a meaningful relationship over this test range, particularly when the individual test data of P2 is also taken into account. However, by excluding the test data of this particular bend and by grouping all the individual plots into the three separate test sets as indicated by the respective shaded areas, it can be seen that a linear relationship exists in all cases over this test range. From the trend of these shaded areas it appears that the depth of penetration is

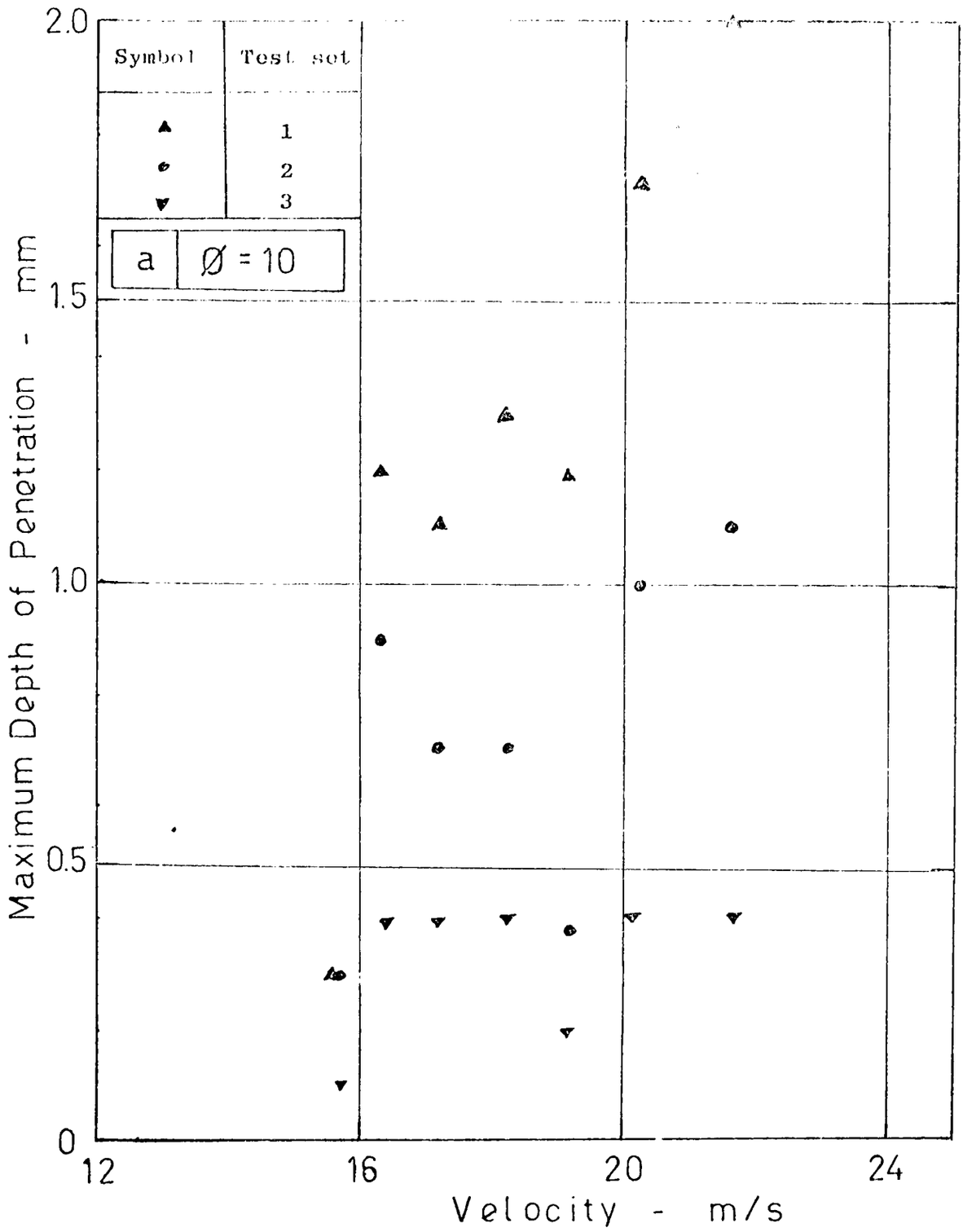

FIG. 10.20 Effect of Velocity on Maximum Depth of Penetration.
(a) at Phase Density of 10.

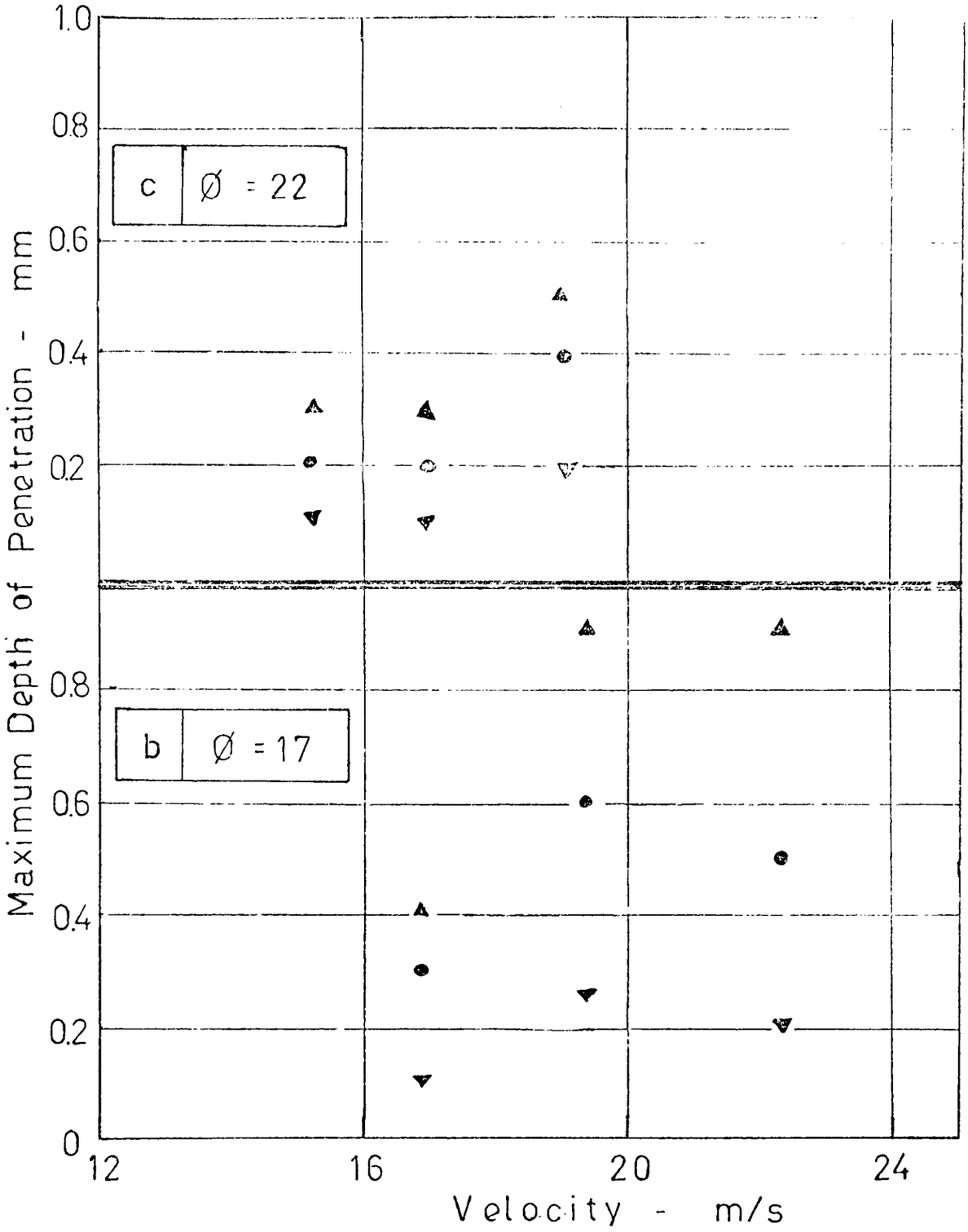

FIG. 10. 20 Effect of Velocity on Maximum Depth of Penetration
(b) at Phase Density of 17.
(c) at Phase Density of 22.

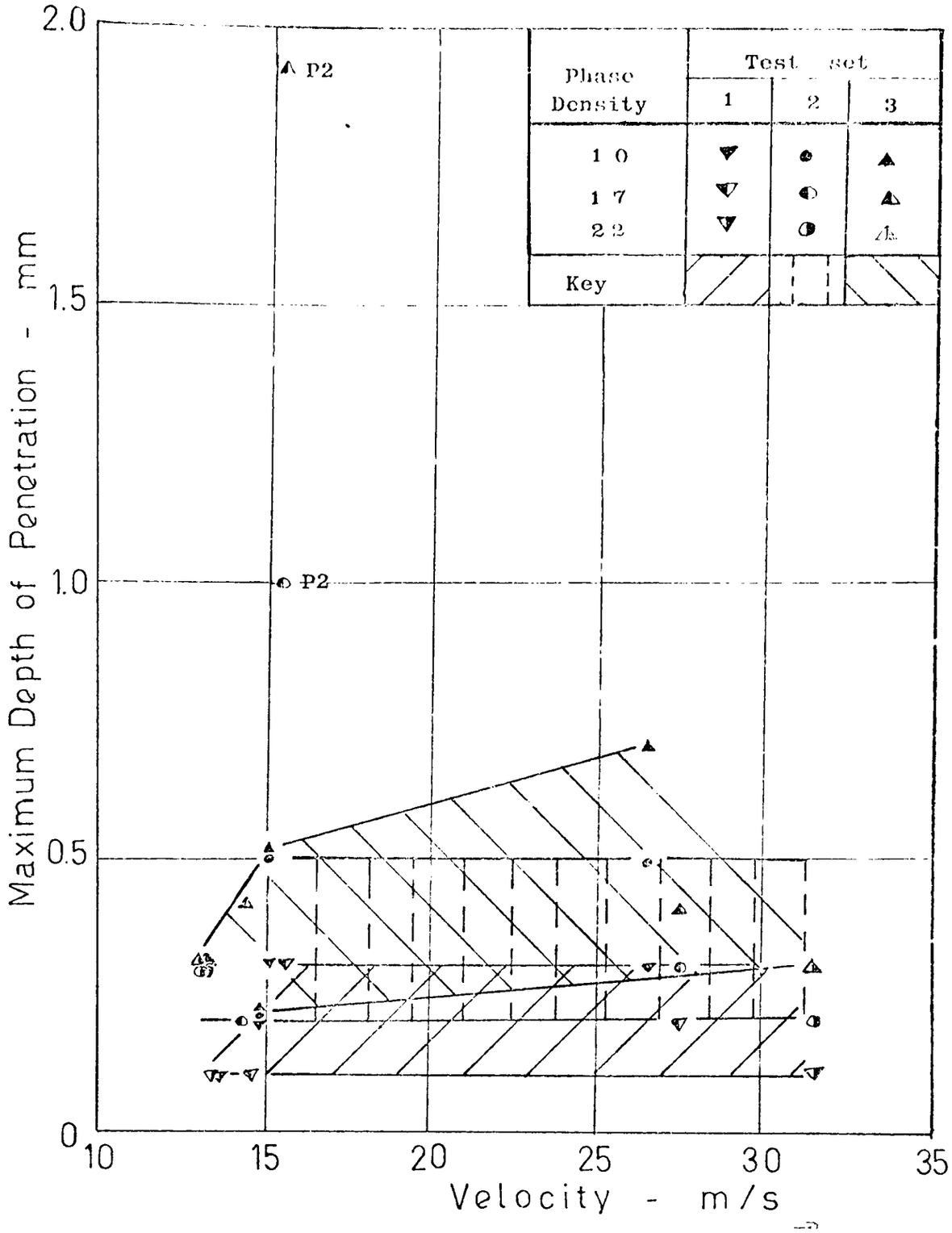

FIG. 10.21 Effect of Velocity on Maximum Depth of Penetration.

generally independent of velocity and this confirms that, for this set of large radius bends, in terms of penetration the mechanics of flow has an over-riding effect over that of velocity.

10.4.3.4 Comparison with Dilute Phase Test Data

From the graphs presented in Fig. 10.20 it has been shown that, whilst the depth of penetration is initially independent of velocity, once established, a definite trend towards an increase in penetration depth as velocity increases is clearly evident. However, the magnitude of this increase in penetration rate, apart from transitional effects, is dependent upon the inter-relating effects of phase density and bend radius.

Although it is well established that a power law relationship exists in respect of erosion, where the velocity exponent is of the order of about 2.65 in pipe bend erosion situations, apart from the recent work of Mills and Mason (1976 d) and Glatzel (1977), experimental information on the corresponding effect of velocity on penetration is relatively limited. Mills and Mason have demonstrated that, due to the over-riding influence of penetration rate in terms of μm/g eroded which increases with both velocity and phase density, an even greater power law dependence is expected, although no specific value is provided in their work. Glatzel, however, found that a velocity exponent of about 3.2 in terms of non-dimensional depth of erosion was consistently obtained over a range of impact angles and particle velocities. These were based on tests with flat perspex specimens subjected to erosion by large spherical cast shot particles over a range of velocities from about 3 to 60 m/s. Although the work of these authors clearly showed that a similar power law relationship should exist in terms of penetration wear, it should be noted that these observations were based on dilute phase conveying conditions.

In order to determine the effect of velocity on penetration in this work, a log. plot of the data presented in Fig. 10.20, based on test set 1, produced a slope of about 2.5 over this test range. It should be noted, however, that due to the limited test data and the narrow velocity range, this value is of limited usefulness for the coefficient of correlation, particularly at the two lower phase densities, is extremely low. A more accurate

determination of the relationship, particularly at a phase density of 10, is perhaps given by a linear approximation. In fact, comparison of the predicted values at a velocity of 25 m/s, based on power law and linear relationships, are in close agreement, particularly at the two higher phase densities. These were approximately 0.46 and 0.36 mm at phase densities of 22 and 17. At a phase density of 10, however, a substantial deviation is obtained, with about 0.61 mm based on power law dependency compared to about 0.40 mm based on linear extrapolation. For this analysis it was decided to consider that the value of about 0.4 mm would be more appropriate in this case. On the basis of these predicted values (see section 10.4.2.4) the normalised penetration rate in terms of μm/g eroded is, therefore, about 27, 28 and 38 at phase densities of 10, 17 and 22 respectively. These respective values are plotted in Fig. 10.22 and, for comparison purposes, the corresponding values based on dilute phase work (see Fig. 6.9, p.93) are also included.

The most significant feature of the graph presented in this figure is with respect to the overall effect of phase density over this test range. At low phase densities penetration rate increases with phase density, but beyond a phase density of about 10 a dramatic change in the trend is clearly observed. Although the range of phase densities considered in this work is relatively limited, the magnitude of penetration rate is expected to decrease gradually beyond this test range. That it should suddenly show such a markedly reversed phenomenon over this test range confirms that this is directly related to the mechanics of the erosion process, which appear to vary in some fundamental way with the phase density of the suspension, and that a transition in this process clearly occurs between a phase density of 8 and 10.

This transition is perhaps more clearly shown in Fig. 10.23, which is a graph of depth of wear against phase density, with lines of constant mass eroded plotted. The curves based on the low phase density range were plotted from test data obtained by Mills and Mason (1977 a). For the corresponding test data obtained in this work two sets of plots at each test phase density are presented.

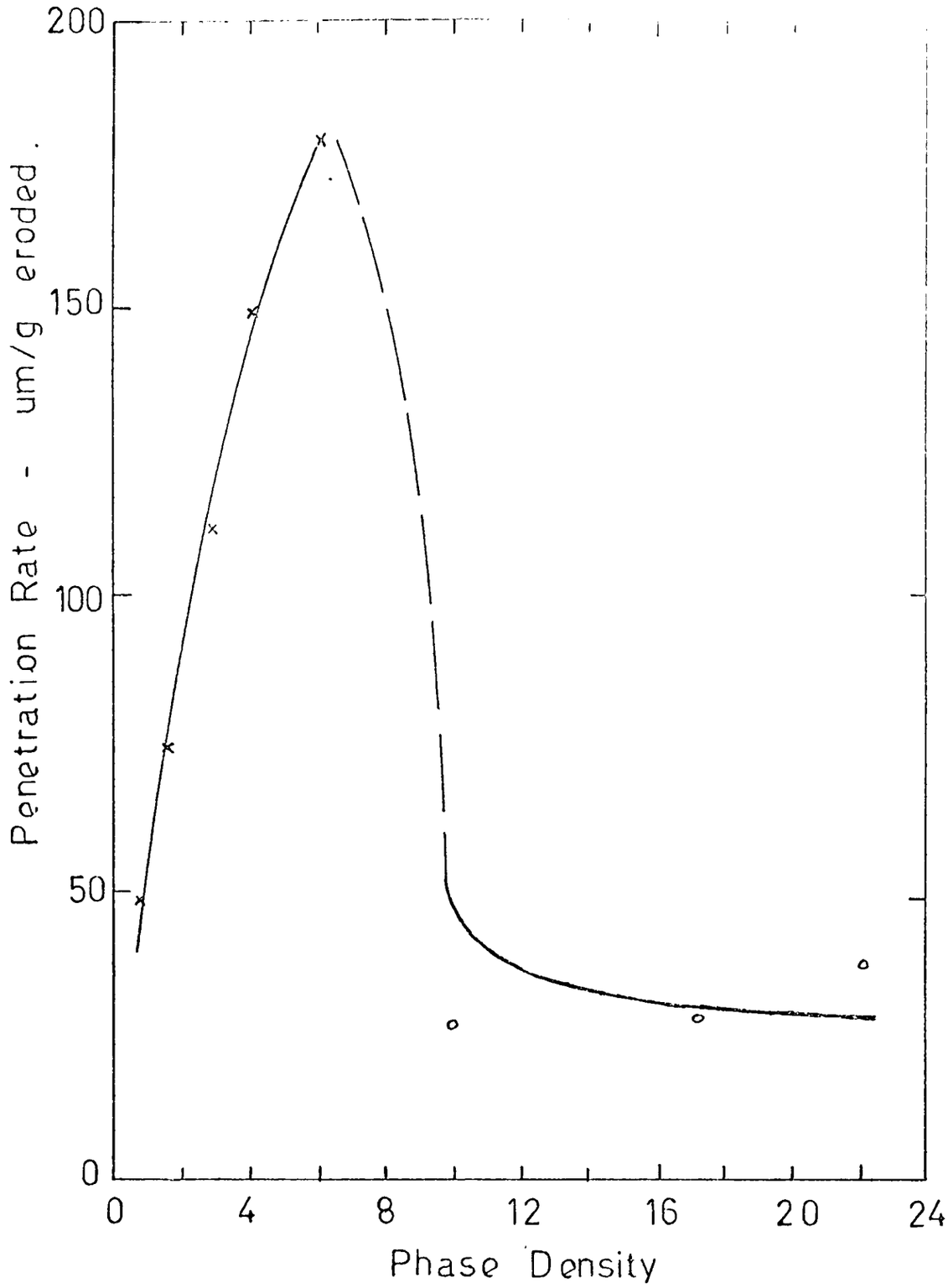

FIG. 10. 22 Influence of Phase Density on Penetration Rate

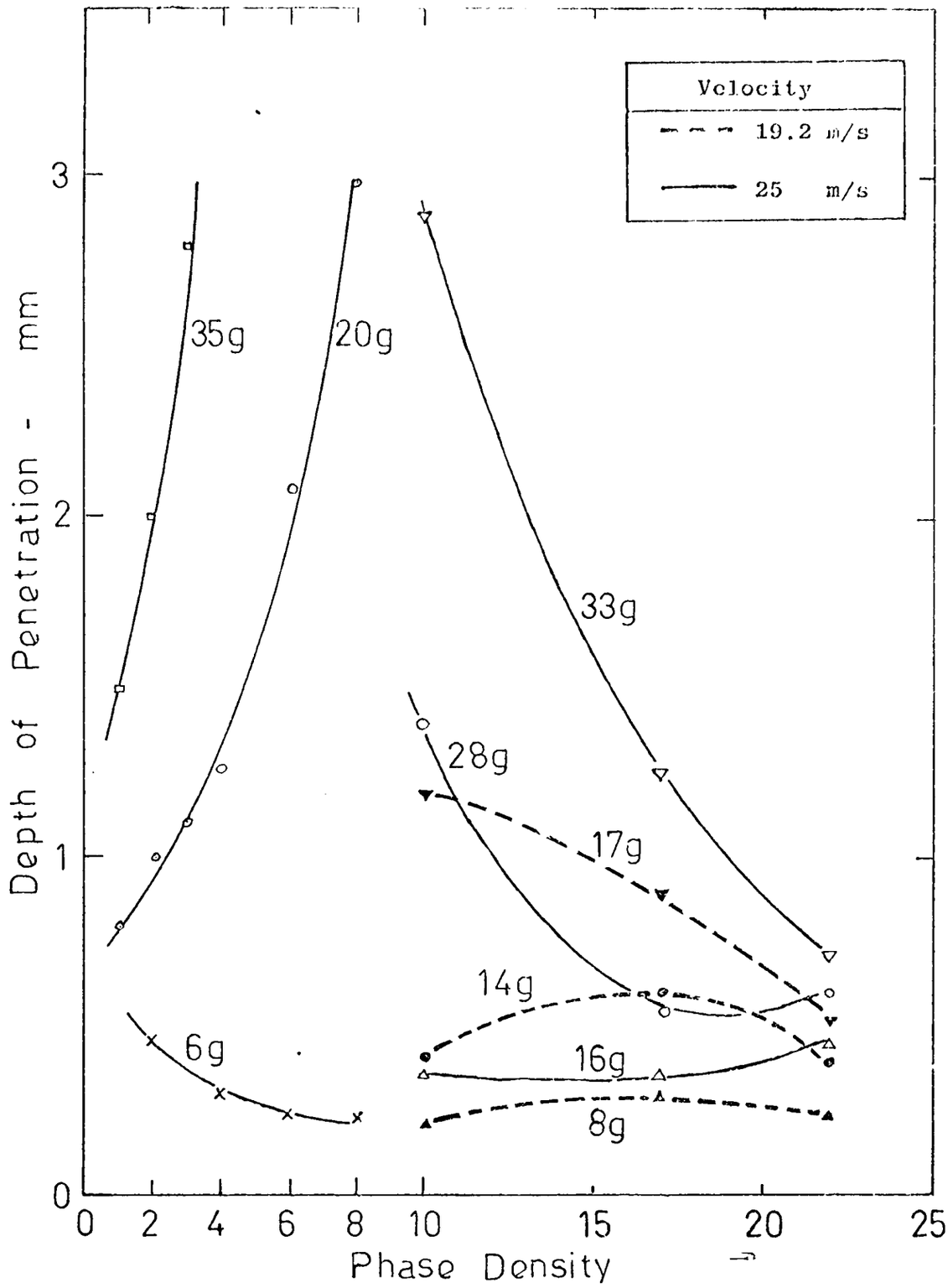

FIG. 10.23 Influence of Phase Density on Depth of Penetration for a Constant Mass Eroded

The broken lines represent the set of test results based on actual measurements, whilst the solid lines represent the corresponding values which have been normalised to a velocity of 25 m/s. In both cases these curves clearly show how the depth of wear varies with phase density and how this is influenced by mass eroded. Whilst the trend of the curves at the low phase density range shows that penetration rate increases with phase density, a markedly reversed order is clearly evident beyond a phase density of about 10. The transition between these two distinctly contrasting trends definitely occurs between the limits of these two separate test ranges, i.e. between phase densities of 8 and 10.

To a certain extent the curve presented in Fig. 10.22 also shows a very similar relationship in terms of mass conveyed, i.e. in terms of penetration wear rate, since phase density has been shown to have relatively little effect over these two separate test ranges. In fact, analysis of the test data in terms of mm/tonne (see Fig. 10.27, p.316) shows that it progressively increases to a maximum at a phase density of about 8, beyond which a markedly reversed situation is observed. This critical maximum value is significantly lower than the value of about 24 quoted by Mason and co-workers (Arundel et al 1973). As no experimental evidence was provided by these authors it was not possible to comment on this deviation. Suffice to say that, under these test conditions a maximum in terms of both penetration rate and penetration wear rate is observed at a phase density of about 8, beyond which a significant decrease in terms of magnitude in both cases is clearly evident. From this it appears that, in terms of both erosion and penetration parameters, it is therefore not necessary to convey abrasive materials solely in the dense phase mode in order to reduce erosion. From the data presented in Figs. 10.12 and 10.22, a significant reduction in erosion is already achieved by conveying the materials in the medium phase regime. Hence, in this respect an optimum value of phase density occurs at about 8, at which the potential service life and conveying capacity of the bends is clearly at the minimum.

The inter-relating effect of bend radius, in terms of penetration rate, is shown in Fig. 10.24. For comparison purposes the corresponding values, based on tests reported in the previous chapters, are also included. Apart from the curve for the set of intermediate bends (D/d ratio of 5.6) which have been tested over a range of phase densities, the only other curve available for comparison purposes is that based on the set of large radius bends (D/d of 24), which have been tested over a relatively limited phase density range. Hence, although it is not possible to determine the magnitude of the effect of bend radius over this test range, comparison of the respective penetration values shows that a substantial decrease is obtained at higher phase densities. An additional interesting feature is with respect to the curve for the set of large radius bends. In Fig. 10.13, the corresponding curve in terms of mass eroded clearly shows that over this test range erosion increases with bend radius. However, in terms of penetration rate, a reversed situation is observed.

In the case of the Booth bend (D/d of 2.4), analysis of the test data presented in Table 10.1 shows that at a phase density of 10 the penetration rate is about 640 μm/g eroded and at a phase density of 22 it is about 600 μm/g eroded. Although this is some 20 times greater than that obtained for the corresponding set of intermediate bends in identical test conditions, it should be noted that these values were based on the actual data recorded at the end of each test series. Perhaps a more useful basis of comparison would be that based on penetration wear rate. For the Booth bend the penetration wear rate values at phase densities of 10 and 22 were 0.18 and 0.03 mm/tonne. The corresponding mean values for the set of intermediate bends over a similar number of runs were 0.07 and 0.02 mm/tonne. Hence, at a phase density of 10 the penetration wear rate of the Booth bend is about $2\frac{1}{2}$ times greater than that recorded for the average intermediate bend and, similarly, about $1\frac{1}{2}$ times greater at a phase density of 22. However, comparison between the values for the Booth bend shows a 6-fold decrease at a phase density of 22. The rapid penetration of the Booth bend at a phase density of 10 is largely attributed to a combination of several interrelated factors, and these are discussed below.

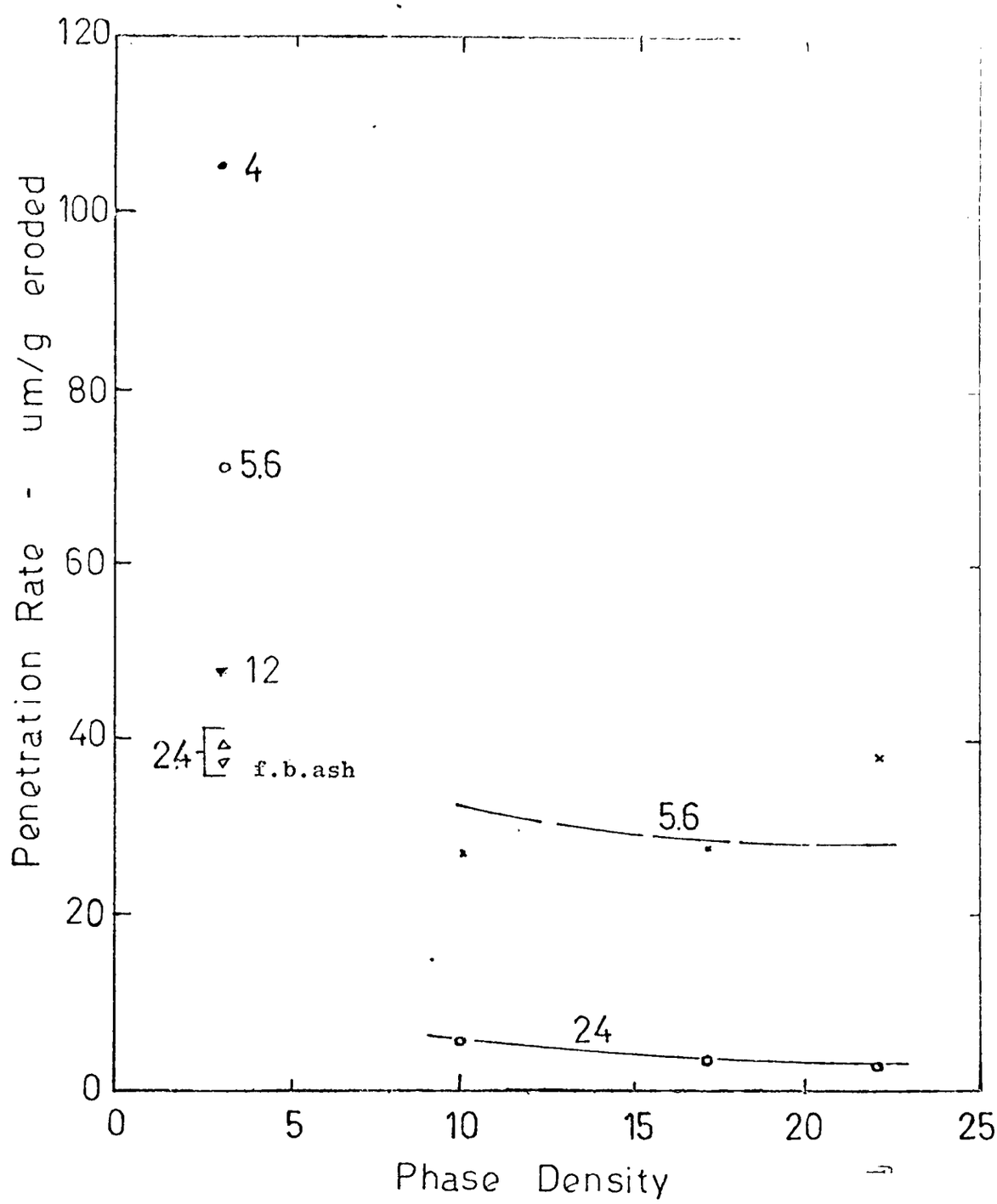

FIG. 10.24 Influence of Diameter Ratio on the Variation of Phase Density with Penetration Rate

As already discussed elsewhere, a transition in the flow from medium to dilute phase mode occurred in the test loops. Owing to its location within the test section, the mode of flow in the Booth bend is essentially in the form of an homogeneous suspension. However, due to its particular shape, some of the particles would be trapped in the recess (see Fig. 4.10, p.64) and so shield the outer bend wall surface against any further impacts by the particles into the outer surface, and consequently reduce erosion to a minimum. However, due to its tight curvature, the pressure drop in this particular bend is substantially greater than in a conventional bend, and this is accompanied by a corresponding increase in turbulence intensity as a result of a greater degree of particle-particle collisions (Chapter 9). In these tests the bend was located in a horizontal plane and so, although the recess would be filled with a layer of particles, the position and magnitude of penetration clearly indicates that only the lower half of the outer surface is effectively protected against erosion. In fact, this is confirmed by visual observation of the outer bend wall surface when it was subsequently cut into two (see Fig. 4.12, p.66). An erosion crater has been established at a bend angle of about 55^{o} and at a pipe angle of about 30^{o} above the horizontal centre line. The depth of the crater substantiated the relevant measurements presented in Table 10.1 at a phase density of 10. At a phase density of 22 the lack of any significant increase in both erosion and penetration after a further 30 test runs, and with sand that had been previously conveyed 24 times at a phase density of 17, indicated that the effective impact angle had already increased beyond the tertiary wear stage, at which both are at a minimum. Hence, although it has been shown that a significant reduction in erosion is obtained by using the Booth bend, as substantiated by the fact that some 75 tonnes of different sized materials have been conveyed through this particular bend over a range of test conditions, the effectiveness of this particular type of bend, to a certain extent, is also influenced by the combined interaction of bend location and bend orientation.

10.4.4 Bend Life Analysis

10.4.4.1 Introduction

The effect of phase density on erosion, in terms of mass eroded and depth of penetration, has been analysed and discussed in the preceding sections. Apart from the specific effect of phase density, it has been shown that the magnitude of erosion is also considerably influenced by a number of inter-relating and transitional effects. Whilst velocity and bend radius are relatively easy to isolate, it is difficult to isolate transitional effects from phase density. Since these transitional effects occur mainly in tests with the set of large radius bends, and in the absence of any corresponding dilute phase test data for this particular set of bends, this section on bend life analysis is solely based on the set of intermediate bends.

In previous bend life analyses (Chapters 6, 7 and 9), it has been shown that it was necessary to incorporate the information based on specific erosion rates with the data based on bend failures. Whilst specific erosion indicates how quickly the metal is eroded from a bend per unit tonne of material conveyed, the mass of metal which has to be eroded from a bend to cause failure provides an indication of its potential conveying capacity, and hence its working life Both parameters, however, are essentially based on mass eroded. Although previous analyses based on this particular relationship have been shown to be adequate, these were based on tests carried out at low phase densities. For this programme of tests over a higher range of phase densities, however, it was not possible to follow a similar evaluation procedure. This is entirely due to the fact that no bend failed over this programme of tests and so it was not possible to produce a relationship between the mass eroded at failure and phase density over this test range. In addition, it has been shown that a fundamental transition in the mechanics of the erosion process has occurred over this test range. Hence, not only is the analysis based on mass eroded effectively restricted to low phase density tests, at high phase densities it is necessary to produce an analysis based on another erosion parameter. In the following sections the reliability and predictive ability of these two separate evaluation procedures are discussed.

10.4.4.2 Analysis Based on Mass Eroded

As mentioned earlier, in the absence of any comparable test data in terms of bend failure over this higher phase density test range, this part of the analysis is concerned with the dilute phase range. As discussed in Chapter 6, Mills and Mason (1977 a) have already evaluated the influence of phase density in terms of bend performance, over a range of phase densities from 1 to about 8 (see Figs. 6.15 and 6.16, ps. 104 and 105). This was based on similar sized sand conveyed at a velocity of about 25 m/s and on similar sized bends. The fundamental basis of their analysis was on the relationship that specific erosion (ε) is related to phase density (ϕ) by :

$$\varepsilon \propto (\phi)^{-0.16}$$

However, as explained in Chapter 6 and in section 10.2, the phase density exponent was based on tests with 230 μm sand rather than with 70 μm sand. It has been shown that particle size has an effect in terms of specific erosion, particularly as phase density is increased, and so the validity of this expression is questionable.

In section 10.4.2.4 it has been shown that a more reliable relationship, based on the test data presented in Fig. 10.12, is given by equation 10.3, which shows that:-

$$\varepsilon \propto (\phi)^{-0.26}$$

On the basis of this relationship, and using the same expression that relates the mass eroded at failure (E_{bf}) with phase density, obtained by Mills and Mason, i.e.

$$E_{bf} \propto (\phi)^{-0.74}$$

the resultant corresponding relationships in terms of conveying capacity (M_s) and service life of the bends ($\Delta\tau_{bf}$) are therefore given by :-

$$M_s = 17.6\ (\phi)^{-0.48} \quad \text{tonne} \qquad (10.4a)$$

and

$$\Delta\tau_{bf} = 68.9\ (\phi)^{-1.48} \quad \text{h} \qquad (10.5a)$$

A graphical representation of the above two equations is given individually in Figs. 10.25 and 10.26.

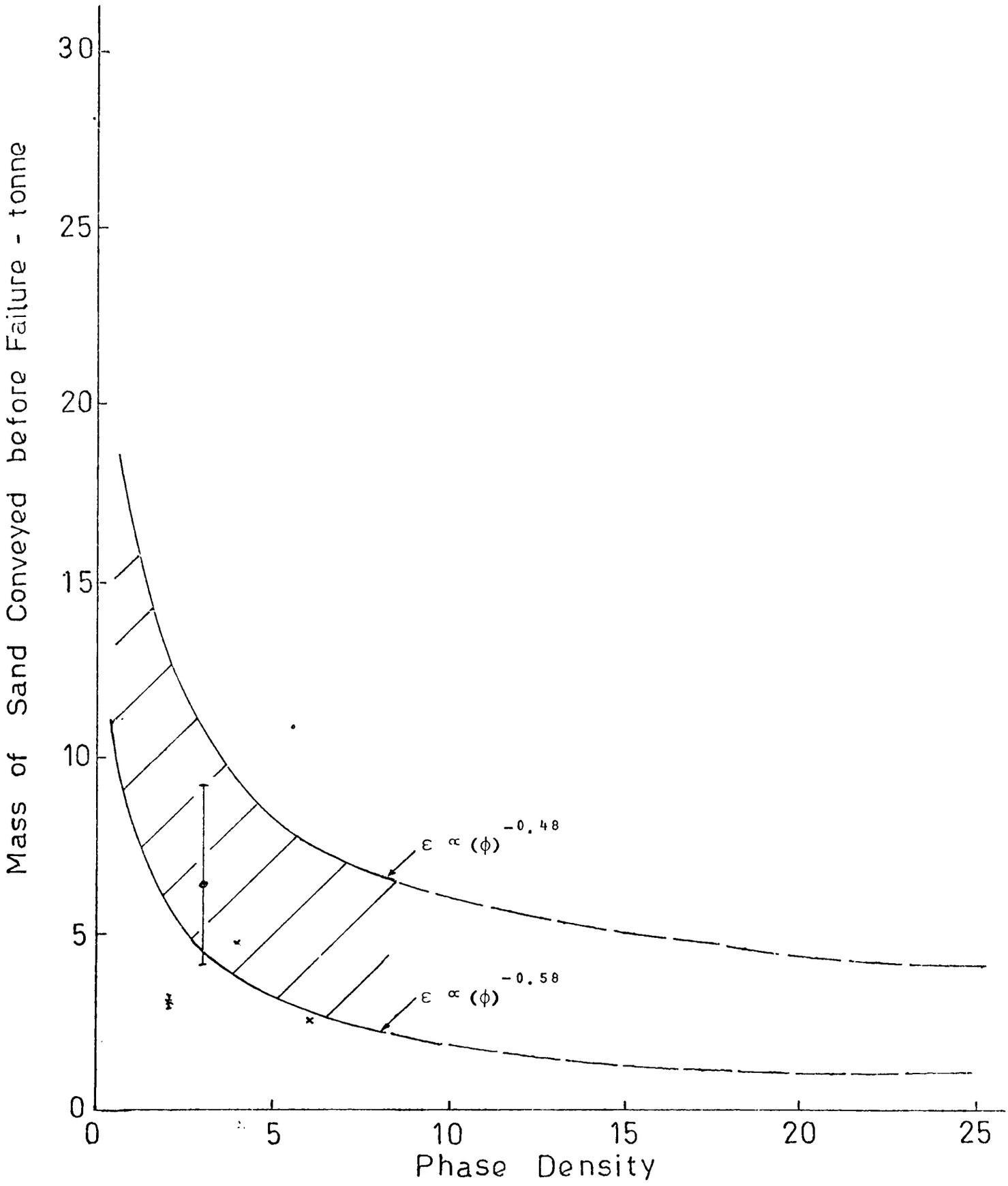

FIG. 10.25 Influence of Phase Density on the Conveying Capacity of Bends

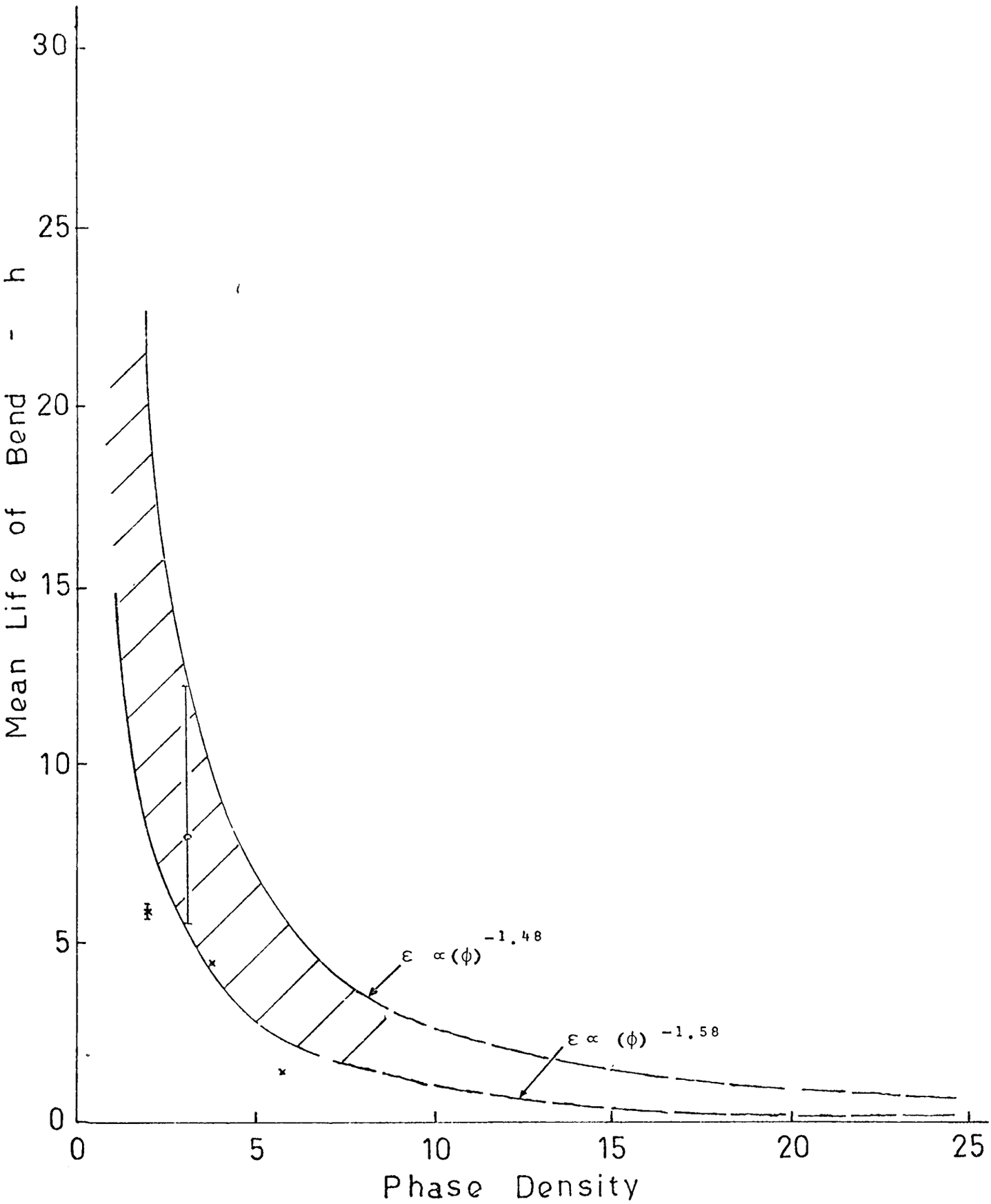

FIG. 10.26 Influence of Phase Density on the Service Life of Bends

For comparison purposes, the corresponding equations obtained by Mills and Mason were :-

$$M_s = 7.9\ (\phi)^{-0.58} \quad \text{tonne} \qquad (10.4b)$$

and

$$\Delta\tau_{bf} = 30.8\ (\phi)^{-1.58} \quad \text{h} \qquad (10.5b)$$

and are also presented graphically in Figs. 10.25 and 10.26.

To show the predictive ability of these two separate sets of equations, the actual test data of the bends which failed at phase densities of 2, 4 and 6 (Mills 1977), and 3 (Table 5.3), are also included in these figures. It should be noted, however, that the plot taken from Mills includes the bends which failed prematurely, and so it can be seen that whilst the curves based on the set of equations given by Mills and Mason appear to give a more accurate prediction, in practice the actual test data appears to lie within the boundary of these two curves, as indicated by the shaded areas. Whilst these curves, based on mass eroded, satisfactorily account for the performance of bends with a reasonable degree of accuracy, the predictive ability of these equations is clearly limited to the dilute phase range only. Extrapolation of these curves beyond a phase density of 8, as indicated by the broken lines, shows a gradual decrease in bend performance as phase density is increased, which is clearly contrary to experimental evidence.

With regard to the applicability of these equations, consider the erosion data presented in Table 5.3, p. 77, which lists the details of all the bends which failed in each respective test series. Apart from the set of test data which had already been considered (Bend Reference E), if the appropriate data of all these failed bends is also plotted in Figs. 10.25 and 10.26, it can be seen that apart from one or two isolated plots, these plots virtually lie outside the boundary of these two sets of curves. Hence, it can be generally concluded that these equations are only applicable to mild steel bends with a D/d ratio of about 5.6 eroded by 70 μm sand particles at a conveying air velocity of about 25 m/s and up to a phase density value of about 8.

10.4.4.3 Analysis Based on Depth of Penetration

As already explained, due to the relatively limited erosion obtained in tests above a phase density of 10, it was not possible to determine the influence of phase density, in respect of bend performance, over the range of phase densities investigated in this work. Although the analysis presented in the preceding section has been shown to provide a reasonably reliable prediction of bend performance, its applicability is effectively limited to a phase density value below 10. This is due to the fact that it does not take into account the transition in respect of the erosion process which occurs above this particular phase density range.

In order to produce a method of evaluation which could adequately account for this transition erosion process, an analysis based on depth of penetration is considered. This particular choice of parameter is clearly more appropriate in pipe bend erosion situations. As explained elsewhere, since the thickness of a bend is finite, it is really the rate of penetration that determines the service life of a bend. Hence, in this section an analysis based on this particular parameter is presented. As this method of evaluation has not been published elsewhere to the author's knowledge, in order to ascertain its validity it was decided to re-evaluate the dilute phase test data based on this parameter, for comparison purposes.

As specific erosion indicates how quickly the metal is eroded from a bend, the corresponding information in terms of penetration wear rate (mm/tonne), indicates the penetrative ability of the particles into the bend. From the test data given in Mills (1977), the corresponding respective penetration wear rates at phase densities of 1, 2, 3, 4 and 6 were approximately 0.31, 0.83, 0.60, 0.54 and 0.79 mm/tonne. It should be noted that these were mean values which have been estimated by the present author and were based on all the bends tested at a given phase density, including those which failed promaturely. Apart from the value at a phase density of 2, it can be seen that penetration wear rate increases with phase density over this test range. A log. plot of these values is presented in Fig. 10.27 and from a linear regression analysis of the relevant test data, the relationship between

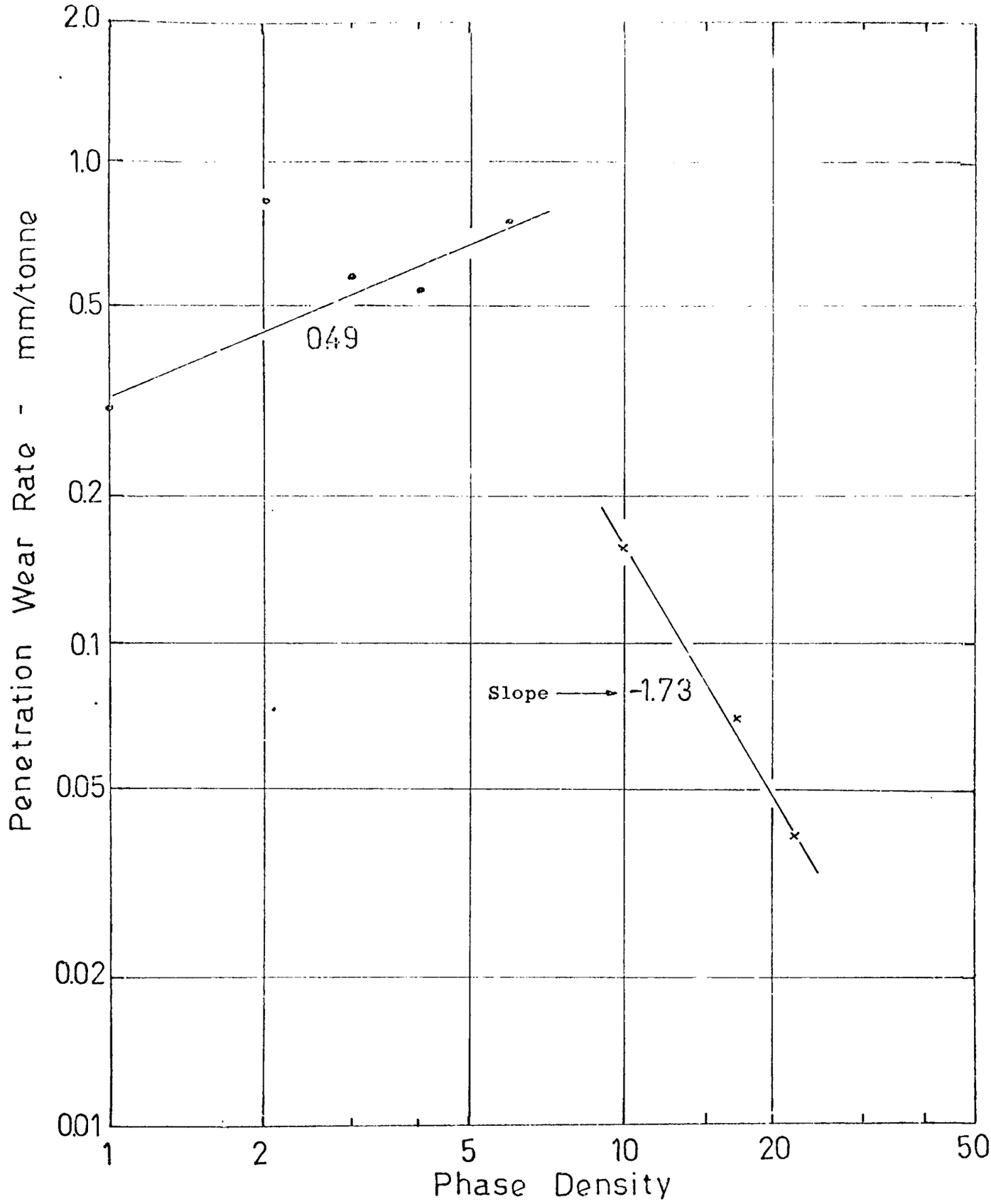

FIG. 10.27 Variation of Penetration Wear Rate with Phase Density

penetration wear rate (ω) and phase density (ϕ) can be given by:-

$$\omega = 0.32\ (\phi)^{0.49} \text{ mm/tonne} \qquad (10.6a)$$

over a range of phase densities from 1 to 6.

As the thickness of all the bends tested (s_w) is approximately 4.00 mm, the mass of sand that can be conveyed through these bends before it penetrates this thickness (M_{sp}), is given by :-

$$M_{sp} = \frac{s_w}{\omega}$$

$$= \frac{4.00}{0.32\ (\phi)^{0.49}}$$

$$= 12.5\ (\phi)^{-0.49} \text{ tonne} \qquad (10.7a)$$

In terms of bend life, the conveying time to failure ($\Delta\tau_{bfp}$) is given by :-

$$\Delta\tau_{bfp} = \frac{M_{sp}}{\dot{m}_s} = \frac{M_{sp}}{\phi\dot{m}_a}$$

In order to achieve an air velocity of 25 m/s in a 50 mm bore pipeline, an air mass flow rate of 0.071 kg/s is required. Thus,

$$\Delta\tau_{bfp} = \frac{12.5\ (\phi)^{-0.49}}{0.071 \times 3600 \times 10^{-3} \times \phi}$$

$$= 48.9\ (\phi)^{-1.49} \text{ h} \qquad (10.8a)$$

With regard to the range of phase densities considered in this work, it has been shown that it was necessary to normalise the test data in order to provide comparability with dilute phase test results. In section 10.4.3.4, the normalised depth of penetration after test set 1, at phase densities of 10, 17 and 22, were approximately 0.40, 0.36 and 0.46 mm respectively. In terms of penetration wear rate these were 0.09, 0.08 and 0.10 mm/tonne. The comparability of these values appears to indicate that phase density also has very little effect in terms of penetration wear rate, which is clearly contrary to experimental evidence, as shown in Figs. 10.22 and 10.23. As discussed in section 10.4.3.3, these normalised penetration depth values were

based on the respective set of test data presented in Fig. 10.20. As shown in this figure, although it appears that the depth of penetration is initially independent of velocity, once established it increases with velocity, particularly at a phase density of 10. Hence, in order to take this effect into consideration, and to provide a more accurate basis of determining penetration wear rate, it was decided to evaluate the respective mean values after test set 3, i.e. after 24 test runs. The corresponding normalised depth of penetration values, based on linear extrapolation in all cases, were approximately 2.9, 1.3 and 0.7 , at phase densities of 10, 17 and 22 respectively. Hence, in terms of penetration wear rate these were 0.16, 0.07 and 0.04 mm/tonne. These values are also plotted in Fig. 10.27, and from these plots it can be clearly seen that a markedly reversed trend is operative over this test range.

From a similar linear regression analysis, the effect of phase density, in terms of penetration wear rate, is given by :-

$$\omega = 8.7\ (\phi)^{-1.73} \quad \text{mm/tonne} \qquad (10.6b)$$

over a range of phase densities from 10 to 22.

Assuming a similar bend wall thickness of 4.00 mm and following a similar calculation procedure as before, the mass of sand that can be conveyed before failure occurs is therefore given by :-

$$M_{sp} = 0.46\ (\phi)^{1.73} \quad \text{tonne} \qquad (10.7b)$$

Similarly, in terms of bend life, assuming similar conveying conditions,

$$\Delta\tau_{bfp} = 1.8\ (\phi)^{0.73} \quad \text{h} \qquad (10.8b)$$

Graphical representations of equations 10.7a and b and 10.8a and b are presented in Figs. 10.28 and 10.29. To show the effect of bend thickness, the corresponding curves for s_w = 2, 8 and 16 mm are also presented in these figures.

10.4.4.4 Discussion

The most prominent feature in Figs. 10.28 and 10.29 is with respect to the trend of the curves, which clearly demonstrates the significance of the effect of phase density. The magnitude

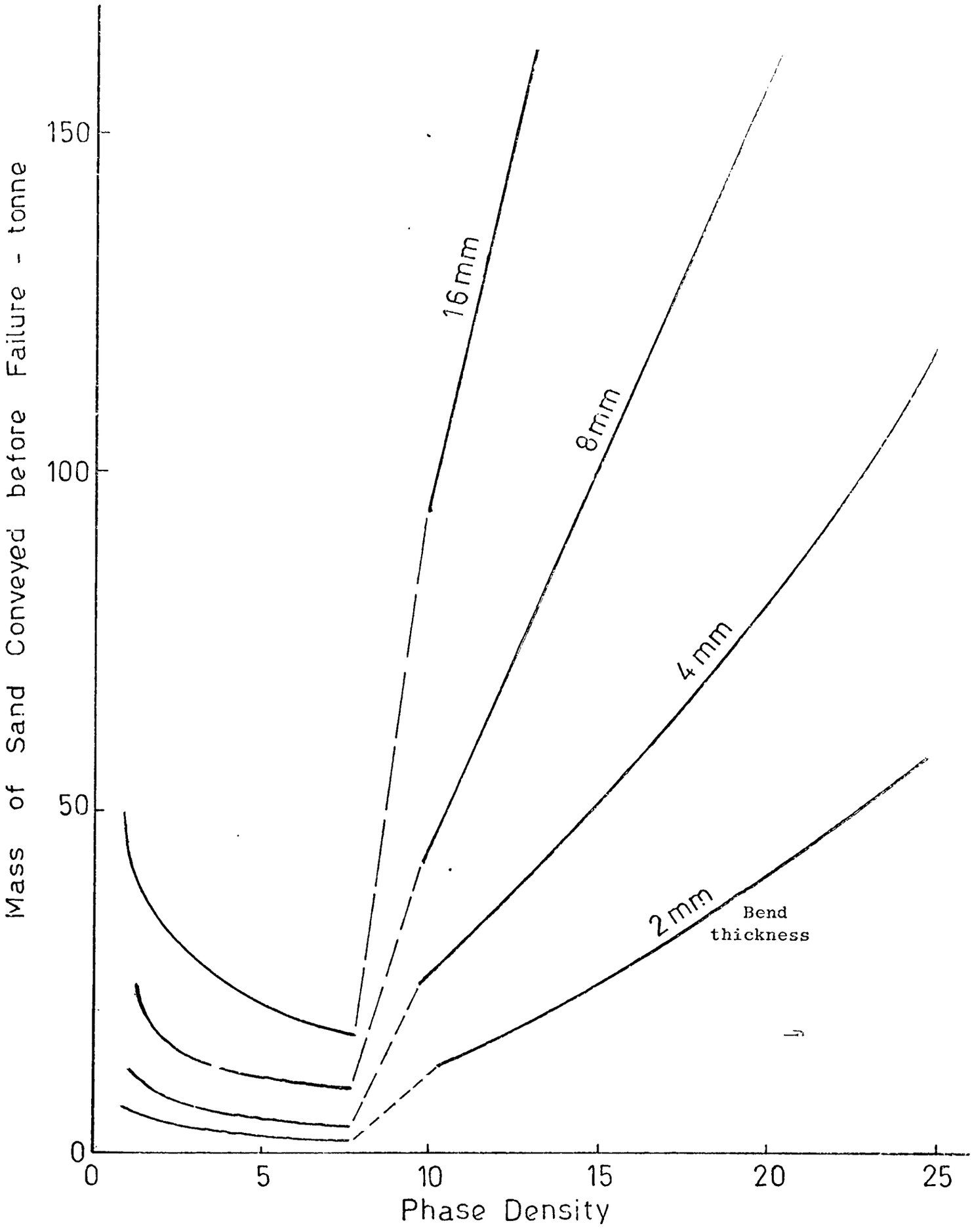

FIG.10.28 Influence of Phase Density on the Conveying Capacity of Bends

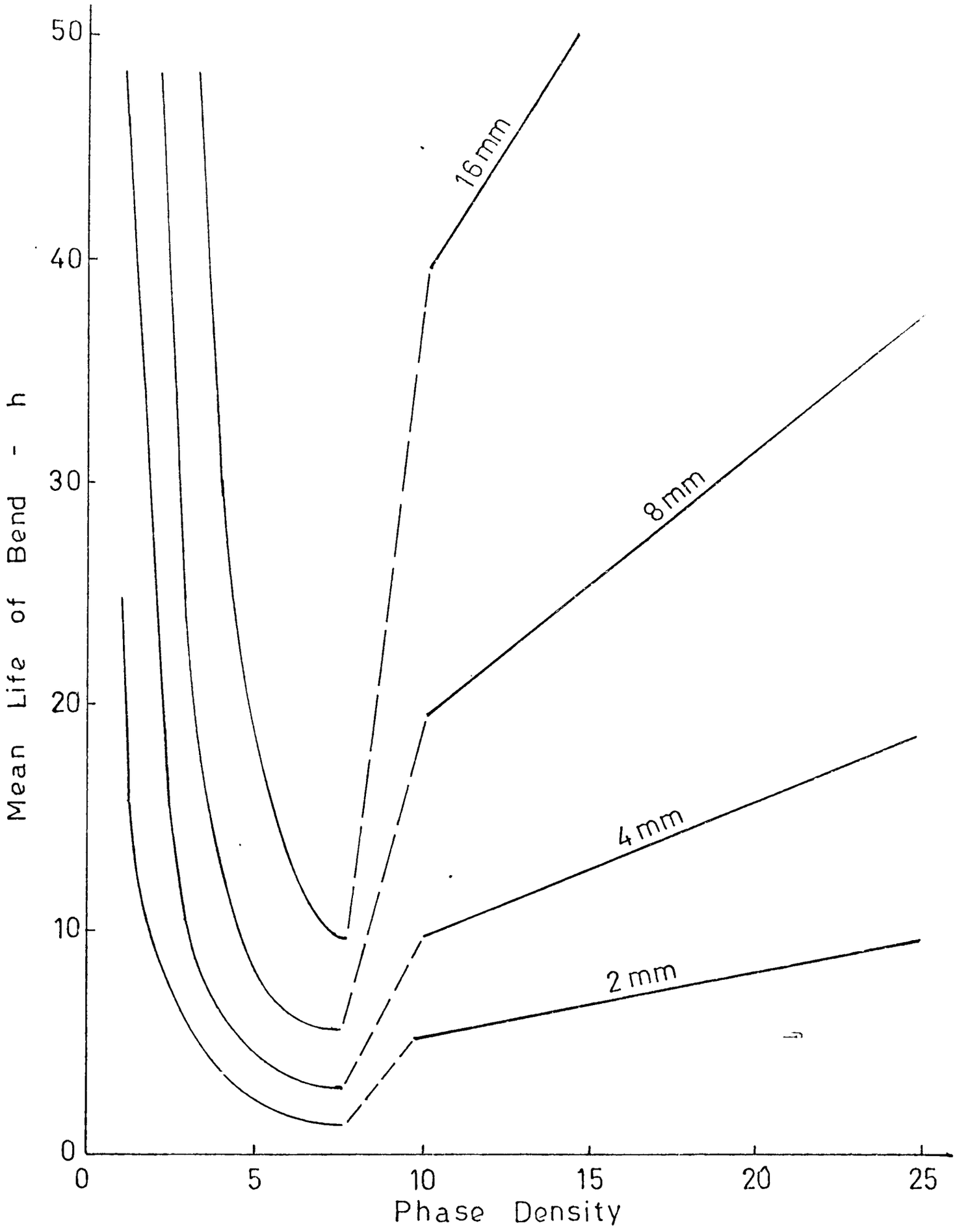

FIG.10.29 Influence of Phase Density on the Service Life of Bends

of this effect is clearly divided into two separate ranges of phase densities. Whilst the group of curves within the low phase density range shows that the performance of bends, in terms of conveying capacity and service life, decreased with phase density, above a phase density value of about 10 a markedly reversed phenomenon is observed in both cases. The distinct contrast in the overall effect of phase density over these two clearly defined test ranges provides an explanation of the presence of a fundamental variation in the mechanics of the erosion process which has been detected over this range. From the trends of these two separate groups of curves it can be clearly seen that the transition occurs between a phase density value of about 8 and 10.

In order to show the validity of this method of analysis, if the curves presented in Figs. 10.25 and 10.26 are superimposed onto Figs. 10.28 and 10.29, it can be seen that the corresponding curve, based on a bend thickness of 4.00 mm, clearly lies within the boundary of the set of curves based on mass eroded. This is perhaps not unexpected, for the analysis in terms of penetration depth is based on mean values whilst the corresponding analysis presented in section 10.4.4.2 was primarily based on the bends which failed, which in every case showed a proportionately greater rate of erosion compared to the bends which were still in service. However, that it should lie within the boundary of these curves clearly provides a more reliable method of erosion prediction and hence its validity.

For the dilute phase range a further remarkable feature with regard to the validity of the curves is the close similarity of the phase density exponent values between equations 10.4 and 10.7a, and between 10.5 and 10.8a. Apart from a difference in order of magnitude, the exponent value in terms of conveying capacity is -0.48 based on mass eroded, compared with -0.49 based on depth of penetration. In terms of bend life these are -1.48 and -1.49. These virtually identical exponent values clearly provide an additional element of legitimacy to the curves presented in these figures.

With regard to its applicability , the fact that it can also be used successfully to predict the effect of phase density beyond a value of 10 substantiates the usefulness of this particular approach.

To examine the effect of a range of phase densities above 10 in more detail, for bends with a thickness of 4.00 mm at a phase density of 10, the bends will eventually fail after some 25 tonnes of sand have been conveyed through these bends, or after some 10 hours. At a phase density of 25 the bends will eventually fail after some 120 tonnes have been conveyed, or after some 20 hours. However, if the curves are extrapolated beyond this test range, it can be observed that whilst the service life of the bends appears to increase linearly with respect to phase density, in terms of conveying capacity an exponential relationship is obtained. In terms of bend thickness, a corresponding two-fold increase is observed in every case if the thickness is increased accordingly, and a similar magnitude of increase is also achieved over the dilute phase range.

However, it should be noted that these magnitudes of increase are based on the assumption that the penetration wear rate within each test range remains constant, as defined by equations 10.6a and b. This is clearly not possible, since it has been shown that the magnitude of both erosion and penetration is considerably influenced by a number of inter-relating and transitional effects which are particularly evident above a phase density value of about 10. Further work is therefore necessary on bends with a range of thicknesses and in tests above a phase density of 25, in order to establish the validity of the curves presented in Figs. 10.28 and 10.29, before general acceptance is recommended.

It should also be pointed out that, whilst the curves presented in these two figures adequately describe the overall effect of phase density, the applicability of these curves is also limited to the given test conditions. However, since 70 μm sand particles have been shown to exhibit maximum erosiveness (Chapter 7), and as the D/d ratio of all the test bends considered in this section is 5.6 which corresponds to the worst case in terms of bend radius effect (Chapters 8 and 9), the curves presented in these

figures under-estimate the potential performance of the bend. In addition, the curves were based on test results which have been normalised to a velocity of 25 m/s. Hence, to a certain extent the curves presented in Figs. 10.28 and 10.29 indicate the minimum potential performance of the bends in a typical pneumatic conveying situation, and can therefore serve as a useful design guide for practical purposes.

10.5 SURFACE EROSION PROFILES

The surface erosion patterns of some of the bends tested in this work are shown in Fig. 10.30 for the intermediate bends, and Fig. 10.31 for the large radius bends.

Fig. 10.30 shows the wear profiles of two bends eroded at a phase density of 10 (bends N5 and N9), and one each at a phase density of 17 (P5) and 22 (Q5). As these bends were eroded by similar sized sand, a common feature of the erosion patterns is the presence of an intricate pattern of steps and ridges in each bend. Apart from bend Q5, the presence of longitudinal marks are clearly visible along the length of each bend. These are primarily score marks produced in the bending process and, as can be seen in Fig. 10.30, the presence of these marks has virtually no effect on the resultant erosion patterns.

Although there is a significant variation in velocity between these bends, it has been shown that velocity has very little effect (Mills 1977). The lack of any noticeable difference amongst the erosion patterns of these bends clearly confirms this observation.

In terms of phase density, due to the close similarity of the erosion patterns, it appears that it also has very little effect over this test range. This is in contrast to the erosion patterns observed in the dilute phase range. Mills and Mason (1977 a) reported that as phase density increased, a significant difference in the erosion pattern is observed. A pronounced stepped erosion pattern is immediately evident after only a few grammes of metal have been eroded from the bend in tests at a phase density of 6. At a phase density of 0.5 it was not until after a substantial amount of erosion had been recorded that any steps were noticed, and these were generally spread over a much wider surface area of the bend. A similar situation is also reported in tests with 250 μm sand, discussed in Chapter 6 (see Fig. 6.11, p.97).

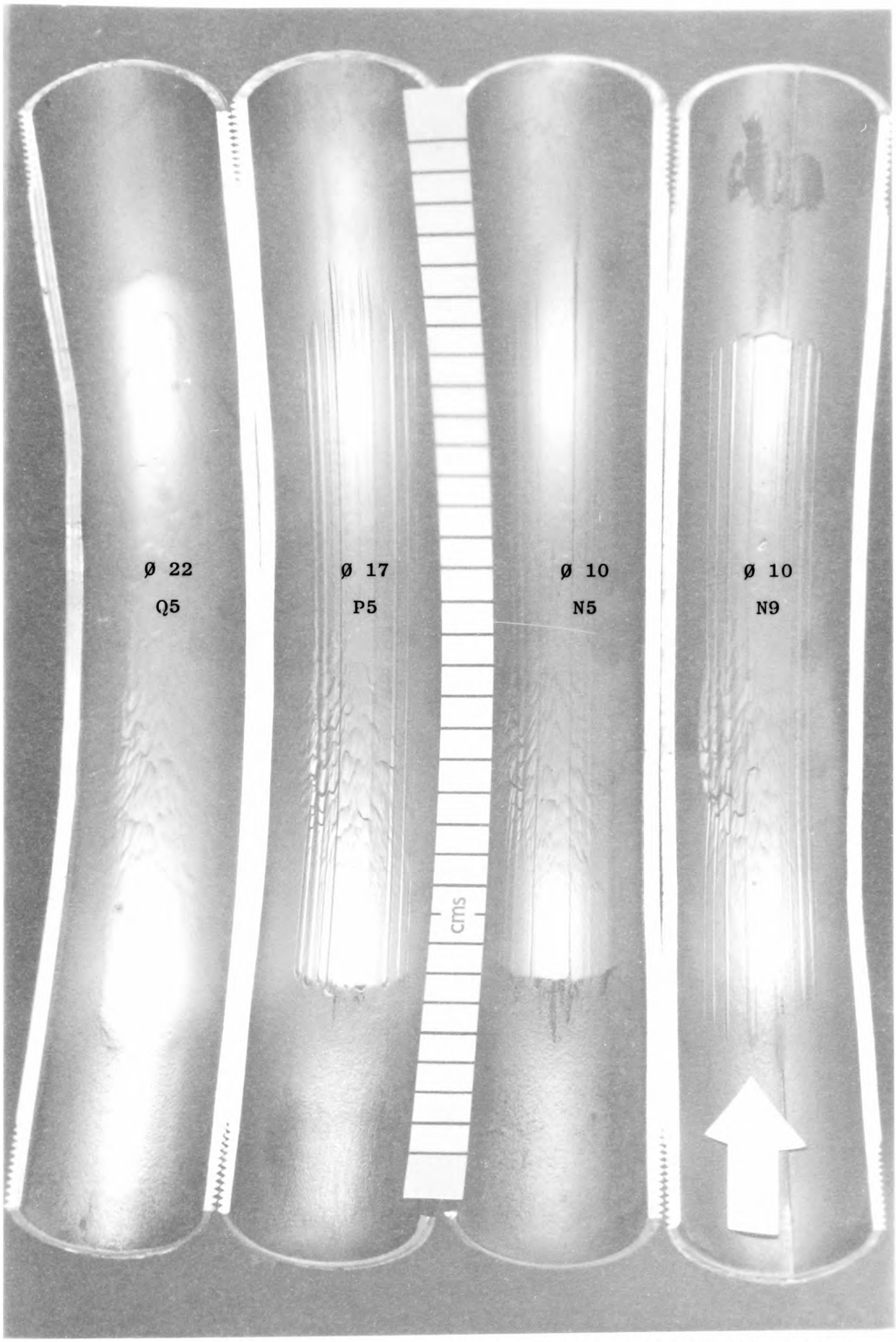

FIG. 10.30 Surface Erosion Patterns of Bends with D/d of 5.6

cms

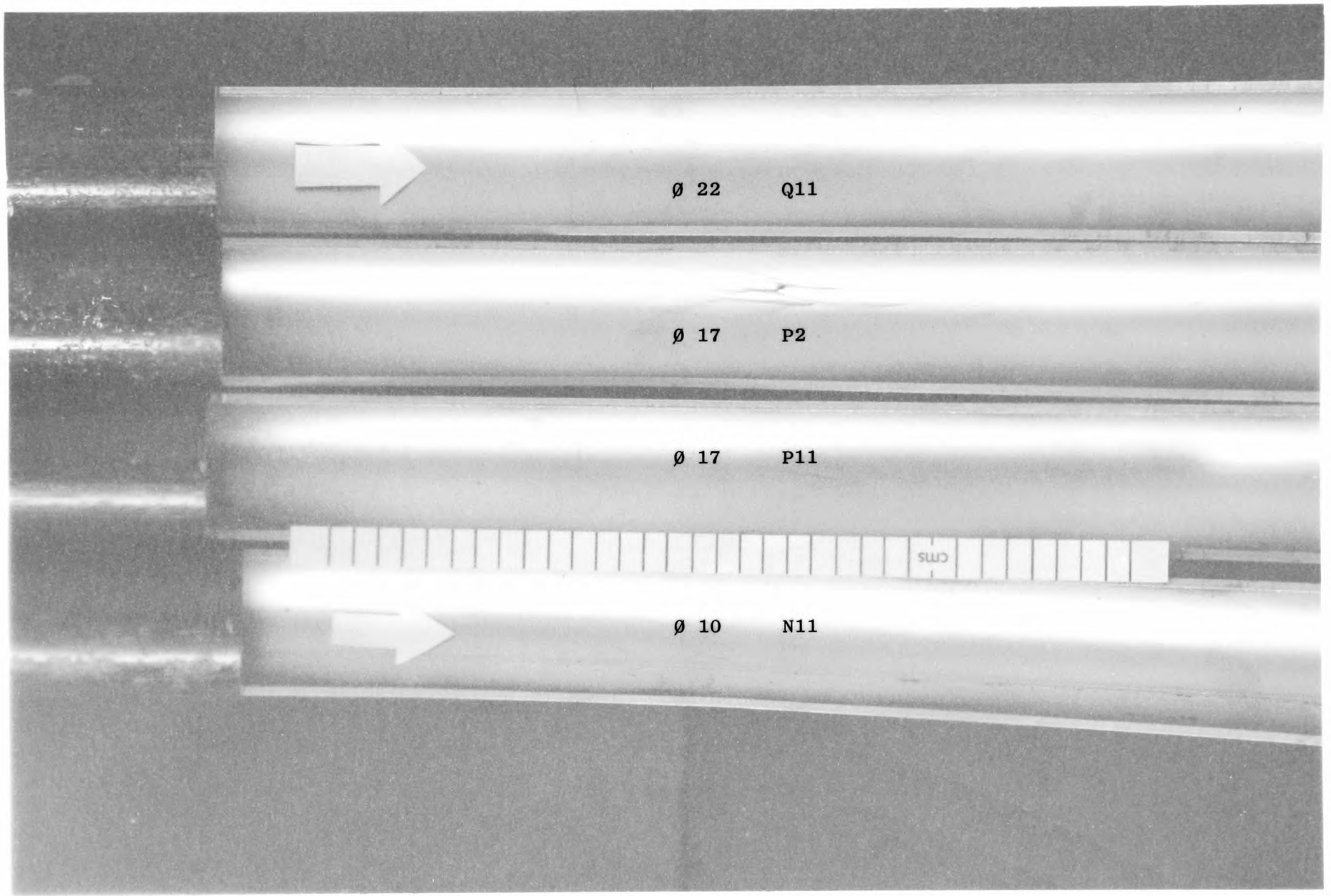

FIG. 10.31 Surface Erosion Patterns of Bends with D/d of 24

cms

As explained in section 10.3.4, the batch of sand used in tests at a phase density of 22 was previously conveyed some 24 times in tests at a phase density of 17. No significant particle degradation was observed after a further 30 test runs and, as the surface erosion patterns of these bends appear to be comparatively identical, particularly between bends P5 and Q5, it can be seen that over this range of phase densities the particles are relatively unaffected by the number of conveying cycles. Hence, in this respect it confirms that particle degradation is considerably reduced if the phase density of the suspension is increased.

For the large radius bends, Fig. 10.31 shows the erosion patterns of bend 11 at each test phase density. In addition, the erosion pattern of bend P2 at a phase density of 17 is also presented. Apart from this particular test bend, although the characteristic ripple pattern is clearly visible in the bends, no pronounced stepped pattern is observed. The contrast between the respective erosion patterns of the intermediate and large radius bends clearly confirms that, as bend radius is increased, the particles will tend to slide along the outer bend radius, as discussed in Chapter 8. The presence of this sliding layer of particles indirectly protects the outer bend surface against any direct impact by the particles, and consequently explains the lack of any pronounced stepped erosion patterns observed in Fig. 10.31.

In the case of bend P2, an erosion crater is clearly well established in the course of this particular test series. Apart from this conspicuous crater, the path of erosion appears to track across the bend. It has been shown that the presence of this tracking in the erosion pattern is a characteristic feature of premature bend failure (Chapters 8 and 9). Since a transition in the mode of flow occurred in the vicinity of this particular bend, a comparatively substantial increase in turbulence is generated in this bend, and hence a rapid erosion rate.

To show the effect of phase density in terms of mass eroded and depth of penetration, Figs. 10.32 and 10.33 are linear representations of the corresponding longitudinal and circumferential profiles of a typical intermediate test bend, taken at a given phase density. Similar linear representations for the large radius bend are also presented in Figs. 10.34 and 10.35.

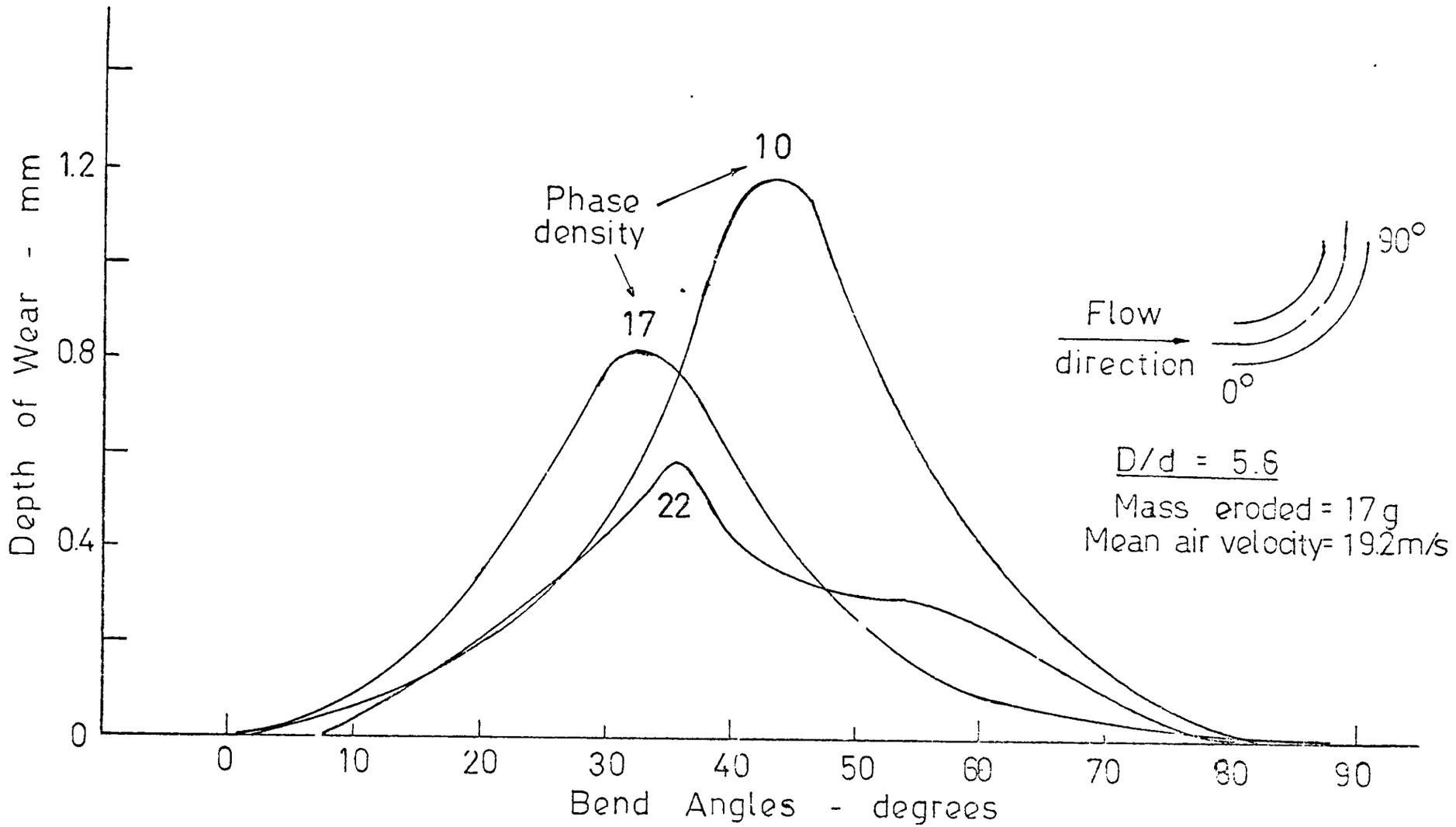

FIG. 10.32 Influence of Phase Density on Bend Wear Profile

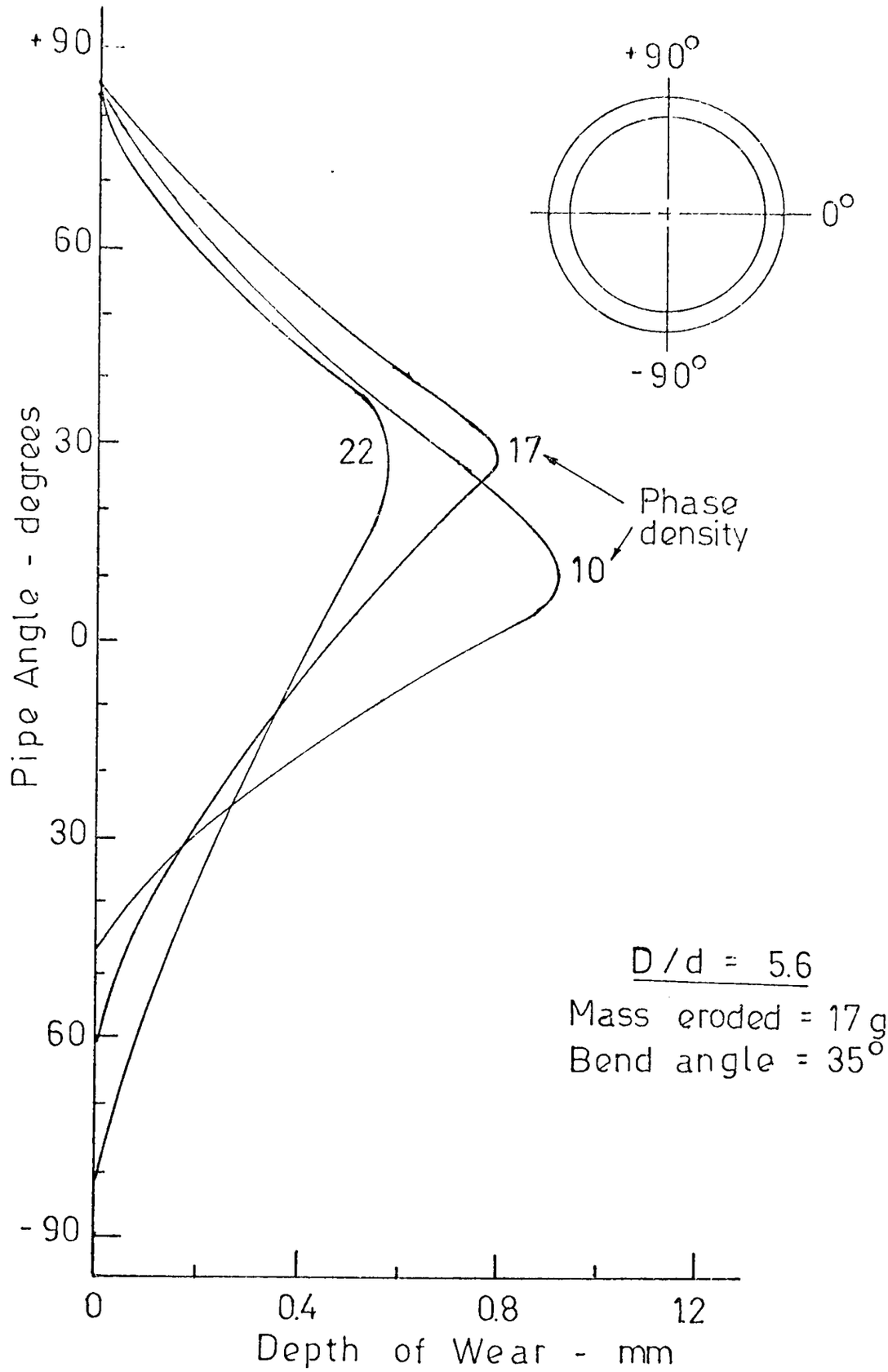

FIG. 10.33 Influence of Phase Density on Pipe Wear Profile

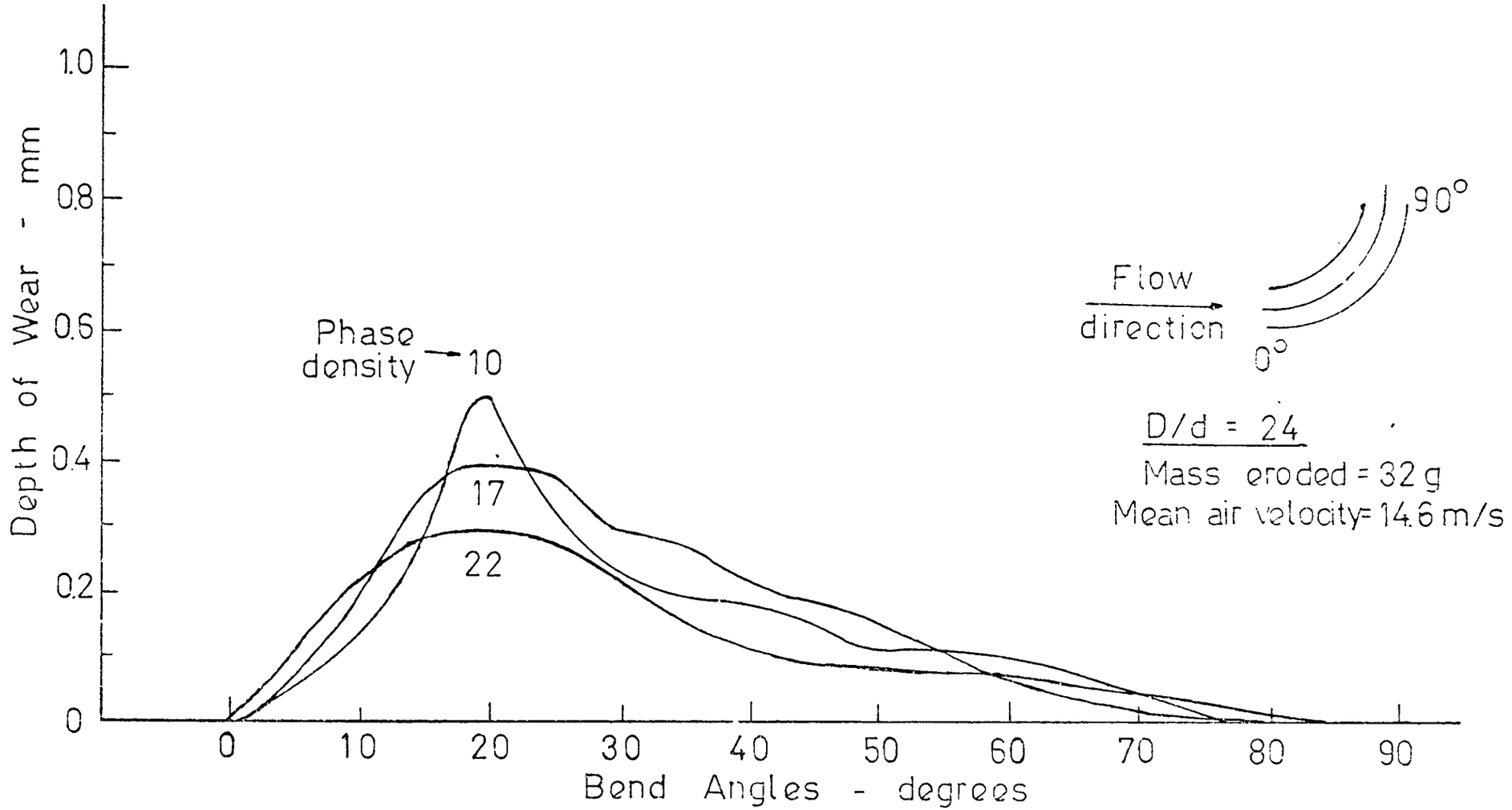

FIG. 10.34 Influence of Phase Density on Bend Wear Profile

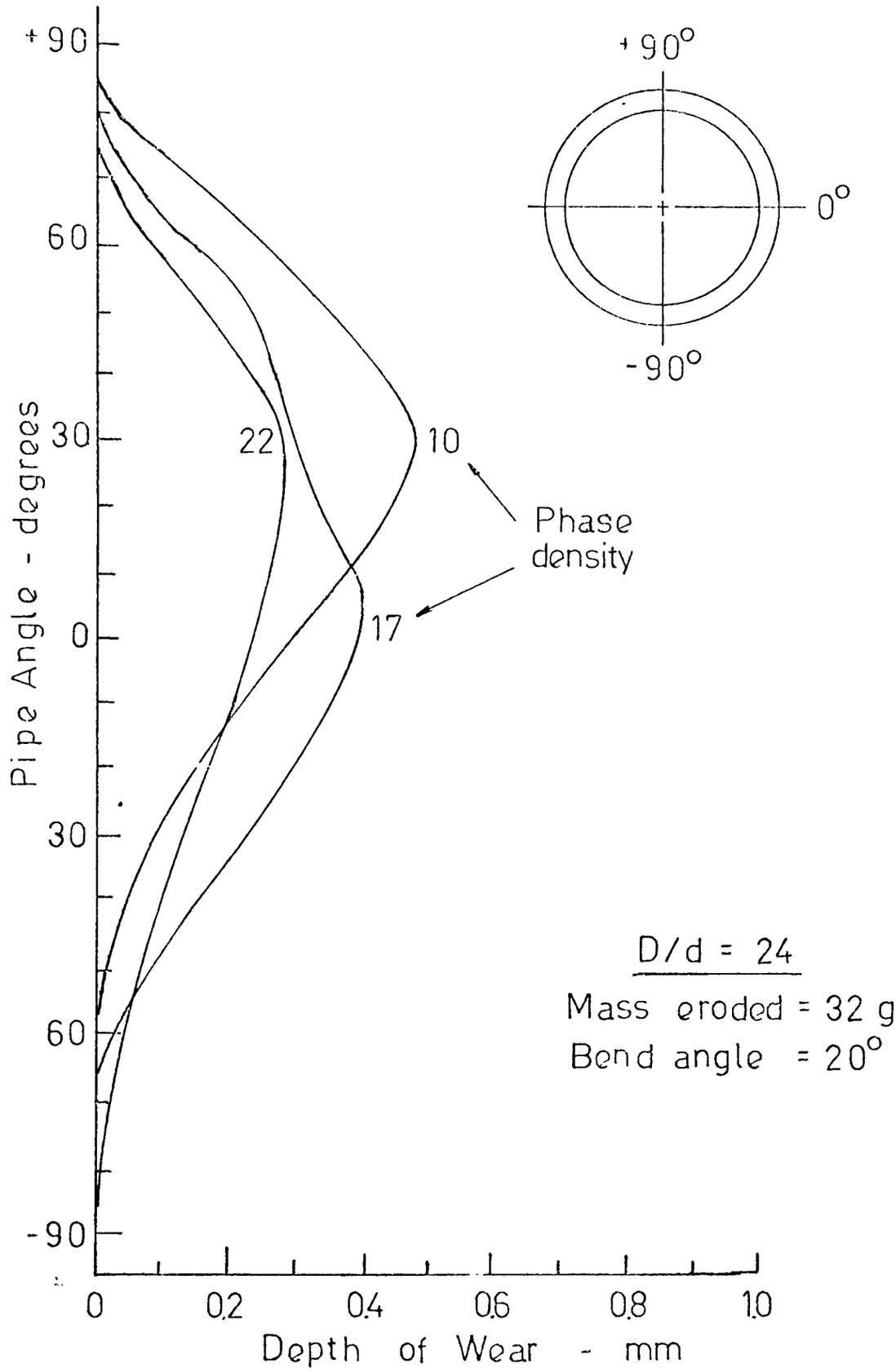

FIG. 10.35 Influence of Phase Density on Pipe Wear Profile

For comparison purposes, the wear profiles in Figs. 10.32 and 10.33 are based on bends N7, P4 and Q5. These were selected on the basis of comparability in respect of velocity. The curves in both figures clearly show that, for a given mass eroded, the depth of penetration decreases with phase density. This is in direct contrast to the trend presented in Figs. 6.12 and 6.13 (pgs. 99 and 100), based on dilute phase tests. This markedly reversed trend in terms of wear profiles provides additional experimental evidence of the presence of some fundamental variation of the mechanics of the erosion process in respect of phase density.

It is interesting to note that in both test ranges the position of maximum wear, in terms of bend angle, remains remarkably consistent at about 30 to 40^{o}. In terms of pipe angle, however, the position of maximum wear appears to vary, but within a relatively limited range of pipe angles in Fig. 10.33 compared to Fig. 6.13.

For the large radius bends the corresponding wear profiles presented in Figs. 10.34 and 10.35 are based on bends N2, P1 and Q2 respectively. In terms of phase density effect, a similar trend in respect of penetration is also observed in both figures. However, it is interesting to note that whilst the individual bend wear profiles are relatively identical, no similar pattern is observed in terms of pipe wear profiles.

As discussed in Chapter 8, it is possible to predict the potential location of maximum wear by taking into consideration the path of particle trajectory. According to the curves presented in Fig. 8.18, p. 206, for bends with a D/d ratio of 24, the predicted location should occur at a bend angle of about 25^{o}, based on curve A. This is comparable to the measured location of maximum wear, which is consistently at about 20^{o} (Fig. 10.34) for the large radius bends. The comparability between the predicted and measured values clearly demonstrates the significance of the information presented in Fig. 8.18 and shows that it is possible to predict the potential location of maximum wear in any sized bends, irrespective of test conditions. This is substantiated by the curves presented in Fig. 10.32 and Fig. 6.12 for the intermediate bends with a D/d ratio of 5.6. The position of maximum wear, as already mentioned, is consistently about 30 to 40^{o}, which is comparable to the predicted values given in Fig. 8.18, based on curve B. As the respective wear profiles were taken over a range of phase densities from 1 to 22, the comparability of these values shows that the location of maximum wear is independent of phase density, and to some extent velocity, as reported by previous workers.

To some extent the wear profiles presented in this section also indicate the magnitude of the effect of bend radius on penetration. As explained earlier, the lack of any significant depth of penetration exhibited by these large radius bends is attributed to the increased tendency of the particles to slide along the outer bend surface. Comparison between the wear profiles for both sets of bends clearly shows that in every case, apart from a difference in order of magnitude, the wear profiles for the large radius bends are generally more 'rounded' and more evenly distributed over the bend surface than the corresponding profiles for the intermediate bends (see also Figs. 8.26 and 8.27, ps. 218 and 219 on the effect of D/d). The shapes of these wear profiles consequently explain the lack of any steps or ridges in the erosion patterns presented in Fig. 10.31 for the large radius bends.

10.6 CONCLUSIONS

From the test results presented in this chapter it has been demonstrated that, apart from the specific effect of phase density, the magnitude of erosion in terms of mass eroded and depth of penetration is also considerably influenced by a number of inter-relating and transitional effects over this test range. Although the primary objective is to investigate the influence of a higher range of phase densities, the corresponding inter-relating effects of velocity and bend radius are also considered. As velocity is a major variable in its own right, in this concluding section the specific effect of velocity is therefore considered separately.

10.6.1 Phase Density

The most important feature with respect to phase density is in establishing the limits of the magnitude of the influence of this particular variable in respect of erosion. Although the range of phase densities investigated in this work is relatively limited, a number of definitive trends have been established.

In terms of mass eroded it has been shown that phase density has very little effect over this test range. Analysis of the test results over a range of phase densities from 1 to 22 shows that the influence of phase density in terms of specific erosion is given by the expression :-

$$\text{erosion} = \text{constant} \times (\text{phase density})^{-0.26}$$

In terms of depth of penetration, however, a definite trend towards a decrease in penetration rate as phase density is increased is clearly evident. This is in marked contrast to the trend reported in previous dilute phase work, which showed that penetration rate in terms of μm/g eroded, increases with phase density and has an over-riding influence over that of mass eroded. The net effect is a corresponding reduction in bend performance. However, that the penetration rate should show such a markedly reversed trend from a phase density value of 10 onwards demonstrates that some fundamental variation in the mechanics of the erosion process has occurred over these two separate test ranges. Analysis of the test data positively showed that a transition in the erosion process occurred between a phase density of 8 and 10. Although this may be a result of a combined interaction between the inter-relating effects of phase density and transitional effects, i.e. mechanics of flow, velocity, etc., further work within this transitional phase density range is obviously necessary to study in more detail this transformation process and to identify the factors responsible.

In terms of penetration wear rate (mm/tonne), a critical maximum is shown to exist at a phase density value of about 8 and hence, for bends with a given thickness, this critical phase density value represents an optimum value at which the conveying capacity and service life of the bend is at a minimum.

Apart from transitional effects, it has also been shown that over this range of phase densities the degree of scatter appears to decrease and a transition in respect of erosion has been detected which occurs at a phase density of about 17 for bends with a D/d ratio of 5.6. For bends with a D/d of 24, although no similar transition in respect of erosion has been detected, it is believed that a transition may already be crossed over this test range. However, further work over a wider test range and conditions is needed in order to establish conclusively that a similar transition in respect of phase density exists in terms of erosion.

A series of analyses on the overall effect of phase density, which encompassed both dilute and medium phase ranges, is presented. This is the range that is close to the practical limit of conveying

many products in the form of suspension flow and at a velocity that is appropriate to most conveying conditions. A significant feature of the analysis is that it is based on the concept of penetration wear rate rather than upon specific erosion, which has been shown to by only applicable up to a phase density value of about 8. The validity of this method of approach is demonstrated by the curves presented in Figs. 10.28 and 10.29, which successfully predict the actual test data based on dilute phase work within a reasonable degree of accuracy. These curves clearly show that it is not necessary to convey abrasive materials solely in the dense phase mode, for a significant reduction in erosion is achieved by conveying in the medium phase range.

In terms of bend radius it has been shown that, for a given phase density, as bend radius is increased, a corresponding increase in erosion is observed. However, in terms of penetration a reversed trend is evident. Although it has been shown that a critical value of D/d ratio exists in terms of erosion over this test range, the magnitude of the effect of bend radius is significantly influenced by transitional effects.

10.6.2 Velocity

From the analysis of the test results presented in sections 10.4.2.3 and 10.4.3.3 it has been clearly demonstrated that over this range of phase densities the effects of velocity and phase density are closely inter-related and inter-dependent. Whilst phase density has been shown to have very little effect on erosion, in terms of penetration a pronounced effect is observed. With respect to velocity, however, in both cases the magnitude of its effect, in contrast to the trend observed in previous dilute phase tests, is largely attributed to the presence of transitional effects which, combined with the inter-relating effects of phase density and bend radius, have an over-riding influence over that of velocity over this test range.

On the basis of the test data for the intermediate bends, although the velocity range is relatively narrow, a number of significant features were observed. In terms of erosion, although a power law relationship has also been established over this test range and is

shown to be independent of phase density, the magnitude of the velocity exponent is significantly higher than the value of 2.65 based on dilute phase work, and that it appears to vary with the condition of the product. This higher exponent value is not unexpected, for it has been established that a transition in the erosion process occurs at relatively low velocities, so that an effectively higher exponent value is obtained. It has been established that in pneumatic conveying situations this transition occurs within a range of velocities from about 26 to 32 m/s. As the velocity range for this set of bends tested was about 15 to 20 m/s, a crossing of the transition in respect of erosion has occured, and consequently a significant reduction of erosion by virtue of the higher velocity exponent, as substantiated by experimental evidence.

In the case of the large radius bends, due to the location of these individual bends in the test section, the velocity range is comparatively extensive, from about 15 to 30 m/s, part of which overlaps the transitional velocity range. In the absence of any intermediate test data and due to the scatter of test results, it was not possible to determine the relationship between specific erosion and velocity reliably. However, comparison between the magnitude of erosion for these two separate sets of bends showed that, over this phase density range, the effect of velocity is considerably influenced by bend radius, which is contrary to the trend reported previously which showed that it is independent of bend radius.

In terms of penetration, although a similar power law relationship is intuitively anticipated, due to the limited penetration results no firm definitive trend could be established over this test range. However, it has been demonstrated that the depth of penetration is initially relatively independent of velocity, but once established it increases with velocity. The magnitude of this increase, however, is considerably influenced by the inter-relating effects of phase density and bend radius, in addition to transitional effects. Hence, in terms of penetration rate, a definite trend towards a decrease as velocity is increased is established, and a similar trend in respect of phase density effect is also observed. In both cases this is in

direct contrast to the trend based on dilute phase tests and this markedly reversed phenomenon in respect of velocity provides additional experimental evidence that some fundamental variation in the mechanics of the erosion process has occurred over this test range.

With respect to the overall effect of bend geometry, it has been established that over this range, whilst erosion increases with bend radius, in terms of penetration a reversed trend is observed. In both cases the magnitude of this variation, apart from interrelating factors, is considerably influenced by the presence of transitional effects.

Chapter 11

Conclusions

In this final chapter, an attempt is made to collate all the work reported in this thesis. As the main features discussed in each chapter have already been presented in the respective concluding sections, in this chapter therefore, only the more pertinent central features are highlighted.

Chapter 1 Bulk solids handling is an integral part of most process industries, and of all the various forms of handling, the preference is now increasingly towards pneumatic conveying, particularly in view of its flexibility, costs and safety. However, one major limiting factor which often makes industry reluctant to install pneumatic conveying systems for handling abrasive materials, is plant erosion, particularly at pipe bends. Although recent advances in pneumatic conveying system design have largely overcome this problem by means of dense phase conveying, most materials are still conveyed in the dilute to medium phase mode, where erosion is a recurring problem, even with relatively soft materials.

Chapter 2 The general problem of solid particle erosion has been extensively investigated in recent years, but these studies have predominantly been carried out on bench-type erosion rigs. Although all the potential factors involved in the mechanics of the erosion process have been identifed, and the specific influences of some of these variables have been established, these findings are not applicable to pipe bend erosion situations. From these studies, it has been shown that the mechanics of erosion is a highly complex process. To date, no single or universal erosion mechanism has been produced which can adequately explain this phenomena, and it would appear that several mechanisms are operative simultaneously in the erosion process. Whilst much useful information has been gained from these studies, their applicability to predicting the erosion in pipe bends in pneumatic conveying conditions is, however, strictly limited.

Chapter 3 To obtain a more realistic evaluation of the erosion process in pipe bends a number of industrial and experimental studies, using full scale test rigs, have been reported recently. However, little correlation has been obtained between such service and empirical test data, since most of it has been carried out for specific purposes. Although a number of semi-empirical and theoretical models have been postulated, the predictive

ability of these models is strictly limited due to the highly idealised assumptions involved in the analysis.
Whilst Mills and Mason have probably investigated the problem of bend erosion in more detail than anyone else in this field, their work is, however, restricted to a limited number of variables only, and the results are only applicable to a limited range of test conditions.

Chapters 4 and 5 In order to widen the scope of the investigation to cover other potential variables, so that the mechanics of bend erosion could be better understood, and to present results of practical value to industry, two full scale test rigs were ultilised in this work. Details of these rigs, together with information on the test section, test bends and test materials used in the course of this work, are presented in Chapter 4. The respective test programmes are briefly outlined in Chapter 5, and the corresponding erosion test data is summarized in Tables 5.1 to 5.3.

Chapter 6 From previous work on the effect of phase density it has been shown that over a range of phase densities from 1 to about 8, specific erosion decreases with increase in phase density. In terms of penetration rate, however, a marked increase is observed, which has an over-riding effect over that of specific erosion. The net effect is that the depth of penetration by the particles into the bend wall increases with increase in phase density, with a corresponding decrease in the mass of product which can be conveyed before failure occurs.
However, from tests with larger sized 250 μm sand it has been demonstrated that over a similar range of phase densities the magnitude of the penetration rate is considerably influenced by particle size. Although a corresponding decrease in terms of bend life is observed, in terms of conveying capacity, up to a four fold increase is obtained at a phase density of about 7, when compared with the finer 70 μm sand. This was primarily due to the over-riding effect of particle size, which has been shown to be closely inter-related with phase density over this test range. Hence, it has been established that it may not be necessary to convey certain large particle sized abrasive materials in the dense phase mode in order to reduce erosion.

Chapter 7 For a given product being conveyed, the value of its hardness provides an indication of its potential erosiveness. Apart from the inter-relating effects of particle shape and size, the magnitude of erosive wear depends to a certain extent upon the difference between the conveyed product and surface material hardness values, as well as upon velocity.

From the test results presented in this chapter it has been shown that over a range of particle hardness values from about 500 to 2000 kg/mm^2, the influence of particle hardness on erosive wear can be generally represented by a power law relationship, with an exponent value of 1.57.

Although the range of particle hardness values investigated is relatively limited, a definite trend towards a threshold value of particle hardness has been detected, beyond which both erosion and penetration appear to be relatively unaffected by any further increase in particle hardness.

Among the test materials used in this programme it has been shown that the sand with a particle hardness of about 1000 kg/mm^2, represents the critical limit in terms of both erosion and penetration, and it appears that materials with hardness values well above that of sand would not necessarily be more erosive. Further work on a variety of materials with a higher range of particle hardness values is needed in order to conclusively establish this trend.

The effect of particle degradation has also been tentatively considered from tests with fluidised bed ash. It has been established that the magnitude of both erosion and penetration is directly related to the degree of degradation, but only during the initial stages. With some 50% reduction in its mean particle size, from 1350 μm to 650 μm over some 21 test runs, a rapid decrease in both specific erosion and penetration wear rate has been observed, but any further increase in degradation beyond this limit appears to have relatively little further effect on either of these parameters.

Owing to its relatively large size distribution it was not possible to assess the effect of 'fines' on the magnitude of these results. It has been recognised that the presence of 'fines' is a major cause of the scatter of results, and consequently is a major contributory factor in the premature of bends, and this is an area that warrants further detailed investigation.

Chapter 8 The effect of bend radius, in terms of the D/d parameter, has been investigated in this chapter. Over a range of D/d ratios from 4 to 12 it has been established that a critical value of D/d exists at which both erosion and penetration are at a maximum. From the test data obtained it occurs at a value of about $5\frac{1}{2}$. Although the test conditions are relatively limited, it is unlikely that this critical value will vary, for it has been reported that the magnitude of the effect of D/d is not influenced by velocity, phase density, and particle size. Hence, in order to avoid this rapid wear situation, either elbows or long radius bends should be considered. However, due to pressure drop and premature bend failure considerations it is recommended that preference should be for bends with a D/d ratio of between 10 to 20 only.
Whilst the dependence of erosion upon impact angle is well recognised, the significance of the role of effective impact angle has received comparatively little attention. In pipe bend erosion situations it has been shown that the magnitude of erosive wear is determined by the variation of effective impact angle over a period a time. The magnitude of this variation, however, is largely pre-determined by bend geometry.

It has also been established that, in order to produce an accurate prediction of the effect of D/d ratio, based on a typical erosion or penetration curve, it is necessary to take into consideration the inter-relating effect of particle trajectory.

Chapter 9 The premature failure of bends is a recurring feature throughout the course of this work. It has been reported that, apart from an element of unpredictability, the main factor responsible for the rapid failure of bends is the combined effects of fine particles being influenced by the secondary flows induced in the bends. An additional factor which has not been considered previously is bend radius, which has now been shown to have a significant effect. However, a more important aspect of premature bend failure, which has not been recognised previously, is the phenomenon of rapid failure of replacement bends. Although the factors involved in premature bend failure are also operative in every case, a number of additional potential variables, which are inter-related and inter-dependent, have also been identified. Of these, the combined inter-relating effects of the proximity of bends

and bend radius has been shown to be primarily responsible.

Further work on the premature of bends, particularly on the rapid failure of replacement bends, is recommended, for apart from these limited observations there is a need to determine and to quantify to what extent these factors are responsible.

The significance of the rapid failure of replacement bends is demonstrated by the analysis on the effect of D/d ratio on bend performance. In terms of both conveying capacity and service life, for bends with a D/d ratio of about 5½, the net effect is a 1½ fold reduction in both parameters if the rapid failure of replacement bends is taken into account. For bends with a D/d ratio of 12, a two fold reduction is similarly obtained.

Chapter 10 Whilst a number of trends with regard to the influence of phase density have already been established, these are only applicable to a low phase density range. Before any definitive conclusions can be drawn it is necessary to extent the range of phase densities, particularly above a value of 10. The results of a programme of tests over a range of phase densities from 10 to 22 have been investigated and reported in this chapter. Apart from the specific effect of phase density, a number of definitive trends with regard to the inter-relating effects of velocity and bend radius have also been established.

With regard to phase density it has been etsablished that, in terms of specific erosion, phase density indeed has very little effect over both the dilute and medium phase ranges. In terms of penetration rate, however, a marked contrast is observed. Within a dilute phase range penetration rate increases as phase density is increased. However, beyond a critical value of about 8 a markedly reversed trend is observed. This dramatic change in the trend is primarily attributed to a transition in the mechanics of the erosion process, which has been shown to vary in some fundamental way with the phase density of the suspension. This is an area that certainly warrants further work in order to identify the factors responsible for this transformation process. In terms of phase density effect, a transition in respect of erosion has also been detected at a phase density of about 17, for bends with a D/d ratio of about 5½. For the larger sized bends, although no similar transition has been detected, it is believed to have been crossed. Further work is needed, particularly

above this test range, in order to establish conclusively whether a similar transition, in respect of erosion exists in terms of phase density. A more reliable and accurate method of evaluating the overall effect of phase density, in terms of bend performance, which successfully takes into account the presence of transitional effects has been presented on the basis of the penetration depth parameter.

With regard to velocity, a similar marked contrast in the trend is also established. Whilst both erosion and penetration were shown to increase as velocity is increased, below a transitional velocity range, the magnitude of increase in both parameters, is considerably influenced by the combined interaction of transitional and bend radius effects. As bend radius is increased, the magnitude of the effect of velocity, particularly in respect of penetration, is over-riden by the presence of transitional effects. For bends with a D/d ratio of about $5\frac{1}{2}$ it has been shown that the effect of velocity on erosion is independent of phase density, but in terms of penetration it appears that the depth of penetration is initially independent of velocity, but once established, it increases with velocity. The magnitude of this increase is, however, considerably influenced by the inter-relating effects of phase density and bend radius. The net effect is that, in terms of penetration rate, a definite trend towards a decrease as velocity is increased, is observed, which is in direct contrast to the trend based on tests carried out above the transitional velocity range.

With regard to the effect of bend geometry, it has been established that bend radius has a considerable effect in terms of both mass eroded and penetration depth at higher phase densities. In terms of mass eroded, it has been shown that the magnitude of erosion increases with bend radius. In terms of penetration depth, however, a reversed trend is observed. In both cases this is in marked contrast to the trend based on the dilute phase test range, which showed that bend radius has very little effect.

Appendices

A : Nomenclature

B : References

C . : Publications

A : Nomenclature

c_a	=	Convcying air velocity	- m/s
C_{aB}	=	Velocity at bend	- m/s
d	=	Pipe bore	- mm
d_p	=	Mean particle size	- μm
D	=	Bend diameter	- mm
D/d	=	Bend to pipe diameter ratio	
E_{bf}	=	Mass eroded from bend to cause failure	- g
H_p	=	Particle Hardness	- kg/mm^2
h		Mean li. Abena	
$\dot{m}_a$	=	Mass flow rate of air	- kg/s
$\dot{m}_s$	=	Mass flow rate of solids	- kg/s
M_s	=	Mass of material conveyed through bend before failure	- tonne
M_{sp}	=	Mass of material conveyed through bend before it penetrates a given thickness	- tonne
P_{BT}	=	Blow tank pressure	- bar
s_w	=	Bend thickness	- mm
n	=	Velocity exponent	
x	=	Mass eroded at failure exponent	
y	=	Specific erosion exponent	
α	=	Angle of attack	- degree
β	=	Angle of impact	- degree
	=	Effective Impact Angle	- degree
γ	=	Bend angle	- degree
δ_A	=	Critical Impact Angle	- degree

δ_B	=	Impact Bend Angle	- degree
δ_g	=	Angle of Fracture	- degree
ε	=	Specific Erosion	- g/tonne
ρ_p	=	Particle Density	- kg/m^3
$\Delta\tau_{bf}$	=	Conveying time to failure	- h
$\Delta\tau_{bfp}$	=	Conveying time to failure based on Penetration Wear Rate	- h
ϕ	=	Phase Density	
	=	Solids Loading Ratio ($\dot{m}_s/\dot{m}_a$)	
ω	=	Penetration Wear Rate	- mm/tonne

Test Bend Symbols

Chapters 6 to 9

Symbol	Bend Ref. No.
•	1
x	2
o	3
▼	4
■	5
▲	6
▪	7
◯	indicates failed bend
R,RR	indicates Replacement Bend

Based on Low Pressure Test Rig Test Loop Configurations (Figs. 4.6 and 4.7 pgs. 59 and 60)

Chapter 10

◐	1
◍	2
◆	3
×	4
o	5
▼	6
■	7
▲	8
▪	9
◍	11

Based on High Pressure Test Rig Test Loop Configurations (Fig. 4.8 pg. 68)

B : References

Adler W.F. 1979 Assessment of the State of Knowledge Pertaining to Solid Particle Erosion
US Army Research Report No. CR79-680

Allen T. 1975 Particle Size Measurement
Chapman and Hall Ltd., London

Angus H.T. 1979 The Significance of Hardness
Wear 54 33-78

Anon. 1980 Water Jets to Cut Steel
Chartered Mechanical Engineer 27 9

Arundel P.A., Taylor I.A., Dean W., Mason J.S. & Doran T.E. 1973 The Rapid Erosion of Various Pipe Wall Materials by a Stream of Abrasive Alumina Particles
Proc. Pneumotransport 2, BHRA Paper E1

Ascarelli P. 1971 Relation between the Erosion by Solid Particles and the Physical Properties of Metals
AMMRC Technical Report No. 71-47

Bahadur S. 1978 The Economic Impact of Wear on Society
Trans. ASME 100F 145-147

Bannister H. 1959 Theory and Design of Pneumatic Transport Systems-1
Chem. & Process Engng. 40 241-244

Barth W. 1962 Flow Problems with Mixtures of Gases and Entrained Solid Particles
Engineer's Digest 23 81-85

Behrendt A. 1970 Solid Impact
Proc. 3rd Int. Conf. Rain Erosion and Associated Phenomena, RAE 2 797-820

Bikbaev F.A., Maksimenko M.Z., Berezin V.L., Krasnov V.I. & Zhilinskii I.B. 1972 Wear on Branches in Pneumatic Conveying Ducting
Chem. Petroleum Engng. 8 465-466

Bikbaev F.A., Krasnov V.I., Maksimenko M.Z., Berezin V.L., Zhilinskii I.B. & Otroshko N.T. 1973 Main Factors affecting Gas Abrasive of Elbows in Pneumatic Conveying Pipes
Chem. Petroleum Engng. 9 73-75

Bitter J.G.A. 1963 a A Study of Erosion Phenomena - Part 1
Wear 6 5-21

1963 b A Study of Erosion Phenomena - Part 2
Wear 6 169-190

Boothroyd R.G. 1971 Flowing Gas-Solids Suspensions
Chapman and Hall Ltd., London

Brauer H. & Kriegel E. 1963 Untersuchungen uber den Verschleiss von Kungstoffen Metallen
Chemie-Ing-Techn. 35 697-707

1964 Verschleiss an Rohrleitungen bei Hydraulischer Forderung von Festoffen
Stahl und Eisen 84 1313-1322

Wear on Pipes in the Hydraulic Transport of Solid Materials
CEGB Translation No. 3879

1965 a Verschleiss von Rohrkrummern beim Pneumatischen und Hydraulischen Festofftransport
Chemie-Ing-Techn. 37 265-276

1965 b Die Probleme des Verschleiss von Rohrleitungen beim Pneumatischen und Hydraulischen und Festofftransport
Maschinemart 71 20-32

Chari S.S. 1970 Pressure Drop in Horizontal Dense Phase Conveying of Air-Solid Mixtures
AIChE Symp. on Fluidization Fundamentals, Chicago, Paper 15j

Chowdury S.B., Banerjee S. & Lahiri A. 1967 Studies on Pneumatic Transport of Coal
Indian J. Technology 5 384-387

Clark R.H., Charles D.E., Richardson J.F. & Newitt D.M. 1952 Pneumatic Conveying Part I - The Pressure Drop during Pneumatic Conveyance
Trans. Inst. Chem. Engrs. 30 209-224

Cooling D.R. 1965 The Hardness of Coal and its Associated Minerals
BCURA Monthly Bulletin 29 409-435

Cornish G.K. & Charity L.F. 1966 Pressure Drops in Elbows of a Pneumatic Conveying System
Trans. ASAE 9 29-31

Craig W.N. 1980 Private Communication
Technical Consultant, BA Chemicals Ltd.

Dapkunas S.J.	1979	A Summary of Erosion Experience in the US Dept. of Energy Conversion Plants Proc. 5th Int. Conf. Erosion by Liquid and Solid Impact, Cambridge Paper 43
Dearnaley G.	1980	Ion-Implantation Improves Material Performance Part 1 - Wear Resistance Metallurgist 12 129-135
Dixon G.	1979	How do Different Powders Behave? Bulk 5 81-88
Doig I.D.	1975	Design and Performance Aspects of Dense Phase Conveying Systems SA Mech. Engr. 25 394-403
Doig I.D. & Roper G.H.	1963	Fundamental Aspects and Electrostatic Influences in Gas-Solid Transportation Aust. Chem. Engng. 4 9-17
Dolganov E.A. & Stejnberg A.M.	1966	Der Schleifverschleib an Rohrleitungen beim Pneumatischen Transport des Eisenvanadiumkontrates aus Kackanari STAL in Deutsch 6 715-717
Duckworth R.A.	1971	Pressure Gradient and Velocity Correlation and their Application to Design Proc. Pneumotransport 1, BHRA Paper R2
Duckworth R.A. & Chan T.K.	1973	The Influence of Electrostatic Charges on the Pressure Gradient during Pneumatic Transport Proc. Pneumotransport 2, BHRA Paper A5
Engel P.A.	1976	Impact Wear of Materials Elsevier Sci. Pub. Co., Amsterdam
Eyre T.S.	1978	The Mechanisms of Wear Tribology International 11 91-96
Faddick R.R. & Martin J.W.	1978	Pneumotransport of Tunnel Muck Proc. Pneumotransport 4, BHRA Paper F2
Finnie I.	1958	The Mechanism of Erosion of Ductile Metals Proc. 3rd US Nat. Cong. Appl. Mech. 527-532
	1959	An Experimental Study of Erosion Proc. Soc. Expl. Stress Analysis 17 65-70
	1960	Erosion of Surfaces by Solid Particles Wear 3 87-103
	1962	Erosion by Solid Particles in a Fluid Stream ASTM STP No. 307 70-82

	1972	Some Observations on the Erosion of Ductile Metals Wear 19 81-90
Finnie I. & Kabil Y.H.	1965	On the Formation of Surface Ripples during Erosion Wear 8 60-69
Finnie I. & McFadden D.H.	1978	On the Velocity Dependence of the Erosion of Ductile Metals by Solid Particles at Low Angles of Incidence Wear 48 181-190
Finnie I & Oh H.	1966	An Analysis of Rock Drilling by Erosion Proc. 1st Cong. Int. Soc. Rock Mech. 2 99-104
Finnie I., Wolak J. & Kabil Y.H.	1967	Erosion of Metals by Solid Particles J. Materials 2 682-700
Firstbrook J.	1980	Operation and Development of the Pneumatic Pipeline Coal Transportation System Proc. Pneumotransport 5, BHRA Paper A4
Fisher M.A. & Davies E.F.	1949	Studies on Fly Ash Erosion J. Mech. Engng. 71 481-487
Geldart D.	1973	Types of Gas Fluidization Powder Technology 7 285-292
Ghosh D.P. & Kalyanaraman K.	1970	Pressure Drops due to Solids around Horizontal Elbow Bends during Pneumatic Conveyance J. Agri. Engng. Res. 15 117-128
Glatzel W.D.	1977	Verschleiss von Rohrkrummern beim Pneumatischen Transport Ph.D. Thesis, Tech. Universitat, Berlin
Glatzel W.D. & Brauer H.	1978	Prallverschleiss Chemie-Ing-Techn. 50 487-497
Goldberg A. & Boothroyd R.G.	1969	Measurements in Flowing Gas-Solids Suspensions Br. Chemical Engng. 14 1705-1708
Goodwin J.E., Sage W. & Tilly G.P.	1969	Study of Erosion by Solid Particles Proc. I.Mech.E. 184 279-292
Grant G. & Tabakoff W.	1975	Erosion Prediction in Turbomachinery Resulting from Environmental Solid Particles J. Aircraft 12 471-478
Gulden M.E.	1979	Influence of Brittle to Ductile Transition on Solid Particle Erosion Behaviour Proc. 5th Int. Conf. Erosion by Liquid and Solid Impact, Cambridge Paper 31

Hall A.M. 1974 Coal Gasification Poses Demanding Material Requirements
Materials Engng. July 16-18

Hayden J.A. & Breidenbach A.W. 1971 The Application of Pneumatic Transport to the Collection of Solid Waste in the United States
Proc. Pneumotransport 1, BHRA Paper A3

Head W.J. & Harr M.E. 1970 The Development of a Model to Predict the Ersoion of Materials by Natural Contaminants
Wear 15 1-46

Head W.J., Lineback L.D. & Manning C.R. 1973 Modification and Extension of a Model for Predicting the Erosion of Ductile Materials
Wear 23 291-298

Hirschhorn J.S. 1969 Introduction to Powder Metallurgy
American Powder Metallurgy Institute, New York

Huff W.R. & Holden J.H. 1965 Pressure Drop in the Pneumatic Transport of Coal
Proc. Pneumatic Transportation of Solids, Morgantown, W. Virginia, 97-111

Hunter J. 1975 Pneumatic Transportation of Coal and Ash in Industrial Boiler Plant
Proc. I. Mech. E. 189 29-43

Hutchings I.M. 1974 The Erosion of Ductile Metals by Solid Particles
Ph.D. Thesis, Cambridge University

1975 Prediction of the Resistance of Metals to Erosion by Solid Particles
Wear 35 371-374

1977 Deformation of Metal Surfaces by the Oblique Impact of Square Plates
Int. J. Mech. Science 19 45-52

1979 a Mechanical and Metallurgical Aspects of the Erosion of Metals
Paper presented at the Conf. on the Corrosion/ Erosion of Coal Conversion Systems Materials, Sponsored by Nat. Assoc. Corrosion Engrs, California.

1979 b Mechanisms of the Erosion of Metals by Solid Particles
ASTM STP No. 664 59-76

Hutchings I.M. & Winter R.E. 1974 Particle Erosion of Ductile Metals: A Mechanism of Particle Removal
Wear 27 121-128

1975 The Erosion of Ductile Metals by Spherical Particles
J. Physics D8 8-14

Ito H. 1960 Pressure Losses in Smooth Pipe Bends
Trans. ASME 82D 131-143

Ives L.K. & Ruff A.W. 1978 Transmission and Scanning Electron Microscopy Studies of Deformation at Erosion Impact Sites
Wear 46 149-162

Jennings W.H., Head W.J. & Manning C.R. 1976 A Mechanistic Model for the Prediction of Ductile Erosion
Wear 40 93-112

Jones R.H. 1971 Pneumatic Transport Applied to Structural Concrete
Proc. Pneumotransport 1, BHRA Paper A5

Jones P.J. & Leung L.S. 1978 Estimation of Saltation Velocity in Horizontal Pneumatic Conveying - A Comparison of Published Correlations
Proc. Pneumotransport 4, BHRA Paper C1

Khruschov M.M. 1957 Resistance of Metals to Wear by Abrasion, as related to Hardness
Proc. Conf. Lubrication and Wear, I. Mech. E., London 546-547

1962 The Correlation between Wear Resistance in Abrasive Wear and the Strength Properties of Metals
Industrial Lab. 28 372-376

1974 Principles of Abrasive Wear
Wear 28 69-88

Kleis I.R. 1969 Probleme der Bestimmung des Strahverschleiss bei Metallen
Wear 13 199-215

Kostka K.S. 1978 Coarse Particle Erosion in Pneumatic Conveyor Bends
Proc. Pneumotransport 4, BHRA Paper F8

Krasnov V.I. & Sharafiev R.G. 1978 Gas Abrasive Wear of Inclined Pneumatic Conveyor Pipelines of Catalytic Cracking Units
Chem. Petroleum Engng. 14 366-368

Krasnov V.I. & Zhilinskii I.B. 1973 Investigation of Material Reliabilities under Gaseous Abrasive Wearing Conditions
Chem. Petroleum Engng. 9 1029-1032

Kraus M.N. 1965 Pneumatic Conveying
Chem. Engng. April 167-182

Kretz R. 1973 Physical Constants of Minerals
in Handbook of Tables for Applied Engineering Sciences CRC Press, Cleveland, Ohio

Kriegel E.	1968	Der Strahverschleiss und Werkstoffen Chemie-Ing-Techn. 40 31-36
	1970	Druckverlust und Verschleiss in Rohrkrummern bei Pneumatischen Transport Verfahrenstechnik 4 333-339
Kut S.	1971	Internal and External Pipe Coatings Proc. Pneumotransport 1, BHRA Paper D5
Laitone J.A.	1979	Aerodynamic Effects in the Erosion Process Wear 56 239-246
Larsen-Basse J.	1975	Influence of Atmospheric Humidity on Abrasive Wear - I.3-Body Abrasion Wear 31 373-379
Lehrke W.D. & Nonnen F.A.	1975	Internal Protection of Pipes against Abrasion and Corrosion by Abresist Fused-Cast Basalt Proc. 1st Int. Conf. Internal and External Protection of Pipes, BHRA Paper G2
Letson K.N.	1979	Influence of Fibre Loading on Rain Erosion Behaviour of PTFE Proc. 5th Int. Conf. Erosion by Liquid and Solid Impact, Cambridge Paper 16
Leva M.	1959	Fluidization McGraw Hill, New York
Lorenz G.C.	1970	Simulation of Erosive Effects of Multiple Particle Impacts in Hypersonic Flow J. Spacecraft 7 119-125
Marcus R.D.	1980	Recent Developments in Pipeline Conveying Proc. Conf. Solids Handling, Harrogate Paper D4
Marcus R.D., Burgess H., Fenderico D.M., Fritella A. & Vogel R.	1980	The Application of Pneumatic Conveying Techniques to the Mining Industry Proc. Pneumotransport 5, BHRA Paper H2
Marcus R.D., Dickson A.J. & Rallis C.J.	1976	Some Aspects of Dilute Phase Pneumatic Conveying of Gas-Solids Suspensions SA Mech. Engr. 26 131-136
Mason J.S.	1980	A Basis for the Selection of Pneumatic Conveyors Proc. Conf. Solids Handling, Harrogate Paper C1

Mason J.S. & Boothroyd R.G. 1971 Comparison of Friction Factors in Pneumatically Conveyed Suspensions using Different Sized Particles in Pipes of Varying Size
Proc. Pneumotransport 1, BHRA Paper C1

Mason J.S. & Smith B.V. 1972 The Erosion of Bends by Pneumatically Conveyed Suspensions of Abrasive Particles
Powder Technology 6 323-335

1973 Pressure Drop and Flow Behaviour for the Pneumatic Transport of Fine Particles around 90° Bends
Proc. Pneumotransport 2, BHRA Paper A2

Mason J.S. & Stacey R. 1975 Pneumatic Conveying - Technical Art with a Scientific Future
Bulk Nov/Dec 24-31

Matsumoto S., Kikuta K. & Maeda S. 1977 Effect of Particle Size on the Minimum Transport Velocity for Horizontal Pneumatic Conveying of Solids
J. Chem. Engng. of Japan 10 273-279

Maule B., Kleinschroth A. & Franke P.G. 1978 Pneumatic Transport of Water in Pipelines
Proc. Pneumotransport 4, BHRA Paper A6

Mehring B.F. 1971 Pneumatic Conveying Hazards
Proc. Symp. Powder Handling and Storage, Org. by PAC

Mills D. 1977 The Erosion of Pipe Bends by Pneumatically Conveyed Suspensions of Sand
Ph.D. Thesis, Thames Polytechnic

Mills D. & Mason J.S. 1975 Learning to Live with Erosion of Bends
Proc. 1st Int. Conf. Internal and External Protection of Pipes, BHRA Paper G1

1976 a The Effect of Particle Concentration on the Erosion of Pipe Bends in Pneumatic Conveying Systems
Proc. Pneumotransport 3, BHRA Paper A7

1976 b The Interaction of Particle Concentration and Conveying Velocity on the Erosive Wear of Pipe Bends in Pneumatic Conveying Lines
Paper presented at the Int. Conf. Powder and Bulk Solids Handling and Processing, Org. by PAC and IITRI, Chicago

1976 c On the Premature Failure of Pipe Bends in Pneumatic Conveying Systems
Proc. 1st Int. Conf. Bulk Solids, Storage, Handling and Flow, Org. by PAC, Stratford-upon-Avon

1976 d Conveying Velocity Effects in Bend Erosion
Proc. Int. Symp. Freight Pipeline, Org. by Univ. Penns., Washington

1977 a Particle Concentration Effects in Bend Erosion
Powder Technology 17 37-57

1977 b Particle Size Effects in Bend Erosion
Wear 44 311-328

1977 c The Influence of Particle Shape on the Erosion of Pipe Bends in Pneumatic Conveying Systems
Proc. Int. Conf. Powder and Bulk Solids Handling and Processing, Org. by Ind. & Sci. Conf. Man. Inc., Rosemont, Illinois

1978 Problems of Particle Degradation in Pneumatic Conveying Systems
Proc. Pneumotransport 4, BHRA Paper F3

1979 a The Effect of Particle Size on the Erosion of Pipe Bends in Pneumatic Conveying Systems
Proc. 6th Int.Conf. Powder Technology, Org. by I.Chem.E., Birmingham Paper H50-96

1979 b The Determination of Product Conveying Characteristics for Pneumatic Conveying Systems
Proc. Int. Conf. Pneumatic Conveying, Org. by PAC, London Paper 2

1980 The Operational Velocity Range in Pneumatic Conveying and Its Influence on Product Flow Rate
Proc. Pneumotransport 5, BHRA Paper C1

de Morton M.E. 1977 Erosion in Rocket Motor Nozzles
Wear 41 223-231

Montgomery J.E. & Clark J.M. 1962 Dust Erosion Parameters for a Gas Turbine
SAE Summer Mtg., Atlantic City Paper 538A

Mott B.W. 1956 Micro-indentation Hardness Testing
Butterworths Sci. Pub., London

Nathan G.K. & Jones W.J.D. 1966 The Empirical Relationship between Abrasive Wear and the Applied Conditions
Wear 9 300-309

Neilson J.H. & Gilchrist A. 1968 a Erosion by a Stream of Solid Particles
Wear 11 111-122

1968 b An Experimental Investigation into Aspects of Erosion in Rocket Tail Nozzles
Wear 11 123-143

Olsen E. 1976 The Role of Wear Resistance Ceramic Linings Bulk 2 48-53

Pfeffer R. & Kane R.S. 1974 A Review of Drag Reduction in Dilute Gas-Solids Suspension Flow in Tubes Proc. Int. Conf. Drag Reduction, BHRA Paper F1

Pinkus O. 1952 Pressure Drop in Pneumatic Conveyance of Solids J. Applied Mechanics 19 425-431

Preece C.M. & Macmillan N.H. 1977 Erosion Ann. Review Materials Science 7 95-121

Raask E. 1969 Tube Erosion by Ash Impaction Wear 13 301-315

1979 Impact Erosion Caused by Pulverised Coal and Ash Proc. 5th Int. Conf. Erosion by Liquid and Solid Impact, Cambridge Paper 41

Rabinowicz E. 1966 Friction and Wear of Materials John Wiley & Sons Inc., New York

Rabinowicz E., Dunn L.A. & Russel P.G. 1961 A Study of Abrasive Wear under Three Body Conditions Wear 4 345-355

Rao N.P. & Ghosh D.P. 1967 Horizontal Conveyance of Solids by Pneumatic Means J. Inst. Engrs.(India) 48 530-543

van Reimsdijk A. & Bitter J.G.A. 1959 Erosion in Gas Solid System Proc. 5th World Petroleum Congress, New York, Section VIII Paper 4

Richardson J.F. & McLeman M. 1960 Pneumatic Conveying Part II - Solids Velocities and Pressure Gradients in One-inch Horizontal Pipe Trans. Inst. Chem. Engrs. 38 257-266

Richardson R.C.D. 1967 The Wear of Metals by Hard Abrasives Wear 10 291-309

1968 The Wear of Metals by Relatively Soft Abrasives Wear 11 245-275

Riley G.S. 1977 In Search of an Easily Measurable Particle Shape Index J. Powder & Bulk Solids Tech. 1 34-39

Rose H.E. & Duckworth R.A. 1969 Transport of Solid Particles in Liquid and Gases The Engineer 227 392-396, 430-433, 478-483

Ruff A.W. & Weiderhorn S.M. 1979 Erosion by Solid Particle Impact in Treatise on Materials Science and Technology Vol. 16 69-126, Academic Press, New York

Ryabov A.U. 1978 Endurance Range of Pipe Bends in Pneumatic Transport Systems for Cast Iron Swarf and Dust Russian Engng. J. 58 58

Sage W. & Tilly G.P. 1969 The Significance of Particle Size in Sand Erosion of Small Gas Turbines Aeronaut. J. 73 427-428

Schmidt F. 1938 Neuartige Rohrkrummer fur Pneumatische und Hydraulische Forderanlangen Braunkohle 37 81-84

Schuchart P. 1968 Widerstandsgesetze beim Pneumatischen Transport in Rohrkrummern Chemie-Ing-Techn. 40 1060-1067

Scott A.M. 1976 A Full-Scale Pneumatic Conveying Test Rig: Description and Bend Effects Proc. Pneumotransport 3, BHRA Paper D10

1978 Pneumatic Conveyor Design - Art or Science? Proc. 4th Int. Conf. Powder Technology and Bulk Solids, Harrogate, 10-17

Sheldon G.L. 1970 Similarities and Differences in the Erosion Behaviour of Materials Trans. ASME 92D 619-626

1977 Effects of Surface Hardness and Other Material Properties on Erosive Wear of Metals by Solid Particles Trans. ASME 99H 133-137

Sheldon G.L. & Finnie I. 1966 a On the Ductile Behaviour of Nominally Brittle Materials during Erosive Cutting Trans. ASME 88B 387-392

1966 b The Mechanism of Metal Removal in the Erosive Cutting of Brittle Materials Trans. ASME 88B 393-400

Sheldon G.L. & Kanhere A. 1972 An Investigation of Impingement Erosion using Single Particles Wear 21 195-209

Siegelman J.I. & Pallone A. 1978 Cold Gas Injection for Erosion Protection J. Spacecraft 15 22-26

Simper J.I. Baker P.J. 1973 Pneumatic Pipeline Capsule Systems - The Future Potential Proc. Pneumotransport 2, BHRA Paper F4

Smeltzer C.E., Gulden M.E. & Compton W.A.	1970	Mechanism of Metal Removal by Impacting Dust Particles Trans. ASME 92D 639-654
Solt P.E.	1977	Bends in Pneumatic Conveying Systems Proc. Int. Conf. Powder and Bulk Solids Handling and Processing, Illinois 345-349
Soo S.L.	1977	A Note on Erosion by Moving Dust Particles Powder Technology 17 259-263
	1980	Design of Pneumatic Conveying Systems J. Powder & Bulk Solids Tech. 4 33-43
Sproson J.C., Gray W.A. & Haynes J.	1976	Pneumatic Transport of Coal Proc. Pneumotranport 3, BHRA Paper A6
Stepanoff A.J.	1969	Gravity Flow of Bulk Solids and Transport of Solids in Suspension John Wiley & Sons Inc., New York
Sterens W.D.	1949	Flyash Erosion of Boiler Surface Trans. ASME Paper 49-F-23
Stoess H.A.	1970	Pneumatic Conveying Wiley-Interscience, New York
Stoker R.L.	1949	Erosion due to Dust Particles in a Gas Stream Ind. Eng. Chem. 41 1196-1199
Tabakoff W., Kotwal R. & Hamed A.	1979	Erosion Study of Different Materials Affected by Coal Ash Particles Wear 52 161-173
Tabakoff W., Ramachandran J. & Hamed A.	1979	Temperature Effects on the Erosion of Metals used in Turbomachinery Proc. 5th Int. Conf. Erosion by Liquid and Solid Impact, Cambridge Paper 47
Tabor D.	1951	The Hardness of Metals Oxford University Press, Oxford
Thiruvengadam A.	1966	The Concept of Erosion Strength ASTM STP No. 408 22-35
Thurlow G.G.	1978	The Combustion of Coal in Fluidised Beds Proc. I. Mech. E. 192 145-156
Tilly G.P.	1969	Erosion Caused by Airborne Particles Wear 14 63-79
	1973	A Two Stage Mechanism of Ductile Erosion Wear 23 87-96

	1979	Erosion Caused by Impact of Solid Particles in Treatise on Materials Science and Technology Vol. 13 287-319, Academic Press, New York
Tilly G.P. & Sage W.	1970	The Interaction of Particle and Material Behaviour in Erosion Processes Wear 16 447-465
Truscott G.F.	1972	A Literature Survey on Abrasive Wear in Hydraulic Machinery Wear 20 29-50
	1975	A Literature Survey on Wear on Pipelines BHRA Pub. No. TN 1295
Turchaninov S.P.	1962	Rohrverschleiss bei Hydraulischer Forderung Grobkornigen Gutes Fordern und Heben 12 362-366
Uuemois U. & Kleis I.	1975	A Critical Analysis of Erosion Problems which have been little Studied Wear 31 359-371
Vaux W.G. & Newby R.A.	1978	Wear on Tubes by Jet Impingement in a Fluidised Bed Powder Technology 19 79-88
Velayudhan C.S., Inayatullah G. & Subramonium P.S.	1970	Horizontal Pneumatic Conveyance of Solids Proc. 2nd Conf. Fluid Mechanics and Fluid Power, India Vol.1 Paper K1
Vijh A.K.	1976	Resistance of Metals to Erosion by Solid Particles in Relation to the Solid State Cohesion of Metals Wear 39 173-175
	1978	Comparative Tendencies for Metal Loss by Abrasive Wear, Impact Erosion and Arc Erosion Wear 49 141-145
Waghorn D.J.W.	1977	The Performance Characteristics of a Blow Tank for Feeding a Pneumatic Conveying System Ph.D. Thesis, Thames Polytechnic
Wallis R.A.	1975	Dust Erosion of Fan Materials Proc. I.E. Aust. Mech.Chem.Eng.Trans. 33-39
Wellinger K. & Uetz H.	1963	Verschleiss durch kornige Mineralische Staffe Jerkont 143 845-904 Erosion by means of Granular Mineral Substances NEL Translation No. 1448

Wen C.Y. & Galli A.F. 1971 Dilute Phase Systems in Fluidization Ed. by Davidson and Harrison, Academic Press, London

Wheeldon J.M. & Williams J.C. 1980 The Analysis of Equilibrium Particle Velocity and Additional Pressure Drop Data for Granular Material from Horizontal and Vertical Light Phase Conveyors with Particular Reference to the Fundamental Equations of Motion and Additional Pressure Drop Proc. Pneumotransport 5, BHRA Paper B3

Winter R.E. & Hutchings I.M. 1974 Solid Particle Erosion Studies using Single Angular Particles Wear 29 181-194

1975 The Role Adiabatic Shear in Solid Particle Erosion Wear 34 141-148

Wolak J., Worm P., Patterson I. & Bodoia J. 1977 Parameters Affecting the Velocity of Particles in an Abrasive Jet Trans. ASME 99H 147-152

Wood C.D. & Espenschade P.W. 1964 Mechanisms of Dust Erosion SAE Summer Mtg., Chicago Paper 880A

Wood R.T. & Woodford D.A. 1979 Tube Erosion in Fluidised Beds Proc. 5th Int. Conf. Erosion by Liquid and Solid Impact, Cambridge Paper 42

Worster R.C. & Denny D.F. 1955 Hydraulic Transport of Solid Material in Pipes Proc. I. Mech. E. 169 563-573

Yang W.C. & Keairns D.L. 1976 Estimating the Acceleration Pressure Drop and the Particle Acceleration Length in Vertical and Horizontal Pneumatic Transport Lines Proc. Pneumotransport 3, BHRA Paper D7

Yang W.C., Keairns D.L. & Archer D.H. 1973 Estimating the Solid Particle Velocity in Horizontal Pneumatic Conveying Lines Can. J. Chem. Engng. 51 779-781

Yang W.C., Vaux W.G., Keairns D.L. & Vojnovich T. 1979 A High Temperature Pneumatic Transport Line Test Facility IEC Process Design Dev. 18 695-703

Yeung W.S. 1979 Erosion in a Curved Pipe Wear 55 91-106

Young B.B. & Millman A.P. 1964 Microhardness and Deformation Characteristics of Ore Minerals Bull. Inst. Mining Metallurgy 73 437-466

Zenz F.A. 1964 Conveyability of Materials of Mixed Particle Size
IEC Fundamentals 3 65-75

Zenz F.A. & Othmer D.F. 1960 Fluidization and Fluid Particle Systems
Reinhold, New York

C : Publications

A list of papers which have been presented at various conferences, and offered for publication. These papers are all based on various aspects of the experimental programmes carried out for this thesis.

They are all in co-authorships with:

Mills D. — First Supervisor and Director of Studies
Dip.Tech.(Eng), Ph.D., C.Eng., MIMechE., AWP

Mason J.S. — Second Supervisor and Head of School of Mechanical Engineering
BSc., Ph.D., C.Eng., FIMechE., FIMarE., MIMinE.

The Erosion of Pipe Bends in Pneumatic Conveying Systems

New Developments in the Transport of Particulate Solids. Sponsored by the Process Engineering Group of the Institution of Mechanical Engineers. Conference No. C262/79 pg. 19-26

Paper presented at the conference on 30th Oct. 1979, London.

This is a condensed paper based on Chapters 1,2 and 3 of the thesis.

The Influence of Bend Radius on the Erosion of Pipe Bends in Pneumatic Conveying Systems

International Powder and Bulk Solids Handling and Processing Conference. Sponsored by the International Powder Institute and the Fine Particle Society.

Paper presented at the conference on 14th May 1980, Chicago.

This is a condensed paper based on Chapters 8 and 9 of the thesis.

The Influence of Particle Hardness on the Erosion of Pipe Bends in Pneumatic Conveying Systems

International Powder and Bulk Solids Handling and Processing Conference. Sponsored by the International Powder Institute and the Fine Particle Society.

Paper presented at the conference on 14th May 1981, Chicago.

This paper is based on Chapter 7 of the thesis.

The Influence of Product Concentration on the Erosion of Bends in Pneumatic Conveying Lines

This paper is based on Chapter 10 of the thesis and has been submitted for presentation at an ASME conference to be held in Houston in May 1982.

PIPE BENDS IN PNEUMATIC CONVEYING SYSTEMS

by

K.N. Tong

Abstract

The main objective of this work is to determine the various fundamental parameters involved in the erosive wear process in 90° pipe bends, by a stream of pneumatically conveyed suspensions of solid particles. From appropriate analysis of the test data, a basis of correlation in terms of the respective parameters has been established, from which the likelihood of erosion can be predicted.

In order to extend the potential range of variables involved in the mechanics of the erosion process, and to present results of practical value to industry, two full scale pneumatic conveying test rigs were ultilised. A low pressure test rig enabled detailed tests to be carried out in the dilute phase range, whilst a high pressure test rig allowed tests well into the medium phase range. The potential range of variables investigated in this work was planned within the limits of each test rig.

The main variables investigated were: the inter-relating effect of particle size on phase density, particle hardness, bend to pipe diameter ratio, effect of phase density above a value of 8, and the corresponding inter-relating effects of velocity and bend radius.

In all cases, the specific effect of each variable was analysed in terms of the two primary erosion descriptors, viz mass eroded and depth of penetration. The overall magnitude of these individual variables was separately evaluated on the basis of bend performance, i.e. in terms of conveying capacity and service life of the bends, from which the potential influence of each variable, based on actual test conditions, could be assessed and compared.

Whilst the premature failure of some of the bends tested was a recurring feature throughout this work, a more significant feature, which hitherto has not been reported elsewhere, is the phenomenon of rapid failure of replacement bends. A number of potential factors have been identified. In addition, the effect of particle degradation has been briefly considered, and a number of definitive trends with regard to all the variables investigated in this work, have been established.